



**YENEPOYA**

(DEEMED TO BE UNIVERSITY)

Recognized under Sec 3(A) of the UGC Act 1956

Accredited by NAAC with 'A' Grade

### **3.1.2 The institution provides seed money to its teachers for research**

#### **Any Additional information**

<b>Sl. No.</b>	<b>Details</b>	<b>Page Number</b>
1.	Publication from seed grant projects showing acknowledgement	02 - 139
2.	Intramural grant for proteomic/genomic research under YU-IOB MoU	140 -141
3.	E-sanction letters of the seed grant projects	142 - 216



**YENEPOYA**

(DEEMED TO BE UNIVERSITY)

Recognized under Sec 3(A) of the UGC Act 1956

Accredited by NAAC with 'A' Grade

### 3.1.2. The institution provides seed money to its teachers for research

**Any other**

#### **List of selected publication from seed grant projects**

Sl. No.	Seed grant Title /(PI name)	Publication details
1.	Combination therapy strategy using antibiotics and AHL analogues for <i>Pseudomonas aeruginosa</i> infection in <i>Caenorhabditis elegans</i> model /(Dr. Rajesh Shastry)	Srinath BS, Shastry RP, Kumar SB. Role of gut-lung microbiome crosstalk in COVID-19. <i>Research on Biomedical Engineering</i> . 2020; <a href="https://doi.org/10.1007/s42600-020-00113-4">https://doi.org/10.1007/s42600-020-00113-4</a>
2.	Integrated metagenomics analysis of urine microbiome and their association with the urolithiasis /(Dr. Rekha P.D.)	Manzoor MAP, Agrawal AK, Singh B, Mujeeburahiman M, Rekha PD. Morphological characteristics and microstructure of kidney stones using synchrotron radiation $\mu$ CT reveal the mechanism of crystal growth and aggregation in mixed stones. <i>PloS One</i> . 2019; 14(3): e0214003. <a href="https://doi.org/10.1371/journal.pone.0214003">https://doi.org/10.1371/journal.pone.0214003</a>
3.	Development of bioreducible block copolymer drug conjugate nanoassemblies functionalized with noble metal nanoparticles for targeted, image guided delivery of chemotherapeutic drugs and biosensing application /(Dr. Renjith P Johnson)	Johnson RP, Preman NK. Dual and multistimuli-responsive block copolymers for drug delivery applications. <i>Advanced Nanocarriers for Therapeutics</i> . Woodhead Publishing Series in Biomaterials. Volume 2: 2019: 249-267 <a href="https://doi.org/10.1016/B978-0-08-101995-5.00011-8">https://doi.org/10.1016/B978-0-08-101995-5.00011-8</a>
4.	Development of bioreducible block copolymer drug conjugate nanoassemblies functionalized with noble metal nanoparticles for targeted, image guided delivery of chemotherapeutic drugs and biosensing application /(Dr. Renjith P Johnson)	Johnson RP, Preman NK. Responsive block copolymers for drug delivery applications. Part 2: Exogenous stimuli-responsive drug-release systems. <i>Types and Triggers</i> . Woodhead Publishing Series in Biomaterials. 2018, Pages 221-246. <a href="https://doi.org/10.1016/B978-0-08-101997-9.00010-2">https://doi.org/10.1016/B978-0-08-101997-9.00010-2</a>

5.	Development of bioreducible block copolymer drug conjugate nanoassemblies functionalized with noble metal nanoparticles for targeted , image guided delivery of chemotherapeutic drugs and biosensing application /(Dr. Renjith P Johnson)	Preman NK, Priya ES, Prabhu A, Shaikh SB, Vipin C, Barki RR, Bhnadary YP, Rekha PD, Johnson RP. Bioresponsive supramolecular hydrogels for hemostasis, infection control and accelerated dermal wound healing. <i>Journal of Material Chemistry B</i> .2020; 8: 8585-98 <a href="https://doi.org/10.1039/d0tb01468k">10.1039/d0tb01468k</a> .
6.	Development of bioreducible block copolymer drug conjugate nanoassemblies functionalized with noble metal nanoparticles for targeted , image guided delivery of chemotherapeutic drugs and biosensing application /(Dr. Renjith P Johnson)	Johnson RP, Preman NK. Responsive block copolymers for drug delivery applications. Part 1: Endogenous stimuli-responsive drug-release systems. Stimuli Responsive Polymeric Nanocarriers for Drug Delivery Applications, Volume 1. Types and Triggers. Woodhead Publishing Series in Biomaterials. 2018; 171-220 <a href="https://doi.org/10.1016/B978-0-08-101997-9_00009-6">https://doi.org/10.1016/B978-0-08-101997-9_00009-6</a>
7.	Designing and development of lab on paper device for sensng trace arsenic in ground water /(Dr. K. Sudhakar Prasad)	Swetha PDP, Manisha H, Prasad KS. Graphene and Graphene-Based Materials in Biomedical Science. <i>Particle and Particle System Characterization</i> . 2018; 35(8): 1800105. <a href="https://doi.org/10.1002/ppsc.201800105">https://doi.org/10.1002/ppsc.201800105</a>
8.	Designing and development of lab on paper device for sensing trace arsenic in ground water /(Dr. K. Sudhakar Prasad)	Manisha H, Swetha PDP, Prasad KS. Low-cost Paper Analytical Devices for Environmental and Biomedical Sensing Applications. 2018. Environmental, Chemical and Medical Sensors. Springer Nature Singapore Pte Ltd. <a href="https://doi.org/10.1007/978-981-10-7751-7_14">chapter/10.1007/978-981-10-7751-7_14</a>
9.	Designing and development of lab on paper device for sensing trace arsenic in ground water /(Dr. K. Sudhakar Prasad)	Manisha H, Swetha PDP, Shim Y-B, Prasad KS. Revisiting fluorescent carbon nanodots for environmental, biomedical applications and puzzle about fluorophore impurities. <i>Nano-Structures &amp; Nano-Objects</i> . 2019; 20: 100391. <a href="https://doi.org/10.1016/j.nanoso.2019.100391">https://doi.org/10.1016/j.nanoso.2019.100391</a>
10.	Skeletal muscle flourosis, effects on muscle cells and its associated mechanism an <i>in vitro</i> study /(Dr. Sudheer P Shenoy)	Shenoy SP, Sen U, Kapoor S, Ranade AV, Chowdhury CR, Bose B. Sodium fluoride induced skeletal muscle changes: Degradation of proteins and signaling mechanism. <i>Environmental Pollution</i> . 2019; 244: 534-48. <a href="https://doi.org/10.1016/j.envpol.2018.10.034">https://doi.org/10.1016/j.envpol.2018.10.034</a>

11.	Role of inflammatory cytokines and p53 –fibrinolytic systems in smokers with or without COPD / (Dr. Yashodhar Bhandary)	Gouda MM, Shaikh SB, Chengappa D, Kandhal F, Shetty A, Bhandary Y. Changes in the expression level of IL-17A and p53-fibrinolytic system in smokers with or without COPD. <i>Molecular Biology Reports</i> . 2018; <a href="https://doi.org/10.1007/s11033-018-4398-y">https://doi.org/10.1007/s11033-018-4398-y</a>
12.	Evaluation for the presence of CD34+/45- adult stem cells from all three germ-layers, ectoderm, mesoderm and endoderm and use of such CD34+/45- in ameliorating muscular dystrophy in mouse model system / (Dr. Bipasha Bose)	Shenoy SP, Bose B. Identification, isolation, quantification and systems approach towards CD34, a biomarker present in the progenitor/stem cells from diverse lineages. <i>Methods</i> . 2017; 131: 147-56. <a href="http://dx.doi.org/10.1016/j.ymeth.2017.06.035">http://dx.doi.org/10.1016/j.ymeth.2017.06.035</a>
13.	Determining the cause of death amongst persons treated for multidrug resistant tuberculosis / (Dr. Poonam Naik)	Naik PR, Moonan PK, Nirgude AS, Shewade HD, Satyanarayana S, Raghuvveer P, ParmarM, Ravichandra C, Singarijipura A. Use of Verbal Autopsy to Determine Underlying Cause of Death during Treatment of Multidrug-Resistant Tuberculosis, India. <i>Emerging Infectious Diseases</i> . 2018; 24(3): 478-84. <a href="https://doi.org/10.3201/eid2403.171718">https://doi.org/10.3201/eid2403.171718</a>
14.	Combination therapy strategy using antibiotics and AHL analogues for Pseudomonas aeruginosa infection in Caenorhabditis elegans model / (Dr. Rajesh P Shastry)	Shastry RP, Ghate SD, Kumar BS, Srinath BS, Kumar V. Vanillin derivative inhibits quorum sensing and biofilm formation in Pseudomonas aeruginosa: a study in a Caenorhabditis elegans infection model. <i>Natural Product Research</i> . 2021; 22: 1-6 <a href="https://doi.org/10.1080/14786419.2021.1887866">https://doi.org/10.1080/14786419.2021.1887866</a>
15.	Evaluation for the presence of CD34+/45- adult stem cells from all three germ-layers, ectoderm, mesoderm and endoderm and use of such CD34+/45- in ameliorating muscular dystrophy in mouse model system / (Dr. Bipasha Bose)	Kapoor S, Subba P, Shenoy SP, Bose B. Sc1 Cells as direct isolate (ex vivo) versus in vitro cultured exhibit differential proteomic signatures in murine skeletal muscle. <i>Stem Cell Reviews and Reports</i> . 2021; <a href="https://doi.org/10.1007/s12015-021-10134-w">10.1007/s12015-021-10134-w</a>
16.	A study on typing and detection of oncoproteins of human papilloma virus among sexually active women attending tertiary care hospital (Dr. Vidya Pai)	Varsha S, Vidya P, Rajagopal K, Abdulla M. Molecular Detection of Human Papillomavirus (HPV) in Females and Assessment of Risk Factors for HPV Infection: A Study from Coastal Karnataka. <i>Journal of Clinical and Diagnostic Research</i> . 2018,12(6): DC46-DC50. <a href="https://doi.org/10.7860/JCDR/2018/35457.11642">DOI: 10.7860/JCDR/2018/35457.11642</a>

*Uppomayan*

17.	Molecular mechanism of p53 mutations in cancer stem cells isolated from triple negative breast cancer cell lines. (Dr. Suparna Laha)	Muhseena K, Sooraj M, Shankar Prasad Das, Laha S. The repair gene BACH1 - a potential oncogene. <i>Oncology Reviews</i> 2021; Volume 15:519. <a href="https://doi.org/10.4081/oncol.2021.519">10.4081/oncol.2021.519</a>
18.	Molecular mechanism of p53 mutations in cancer stem cells isolated from triple negative breast cancer cell lines. (Dr. Suparna Laha)	Muhseena N. Katheeja, Shankar Prasad Das, Suparna Laha. The budding yeast protein Chl1p is required for delaying progression through G1/S phase after DNA damage. <i>Cell Division</i> . 2021; 16:4 <a href="https://doi.org/10.1186/s13008-021-00072-x">https://doi.org/10.1186/s13008-021-00072-x</a>
19.	Delineating the signaling mechanism involved in the neuroprotective effects of Yashtimadhu in Parkinson's disease. (Dr. Prashant Kumar Modi)	Karthikkeyan G, Najar MA, Pervaje R, Pervaje SK, Modi PK, Prasad TSK. Identification of molecular network associated with neuroprotective effect of Yashtimadhu ( <i>Glycyrrhiza glabra</i> L.) by quantitative proteomics of rotenone-induced parkinson's disease model. <i>ACS Omega</i> ; 2020; 5: 26611–26625.
20.	Delineating the signaling mechanism involved in the neuroprotective effects of Yashtimadhu in Parkinson's disease. (Dr. Prashant Kumar Modi)	Karthikkeyan G, Prasad TSK, Pervaje R, Pervaje SK, Modi PK. Prevention of MEK-ERK-1/2 hyper-activation underlines the neuroprotective effect of <i>Glycyrrhiza glabra</i> L. (Yashtimadhu) against rotenone-induced cellular and molecular aberrations. <i>Journal of Ethnopharmacology</i> . 2021; 274: 114025.
21.	Delineating the signaling mechanism involved in the neuroprotective effects of Yashtimadhu in Parkinson's disease. (Dr. Prashant Kumar Modi)	Karthikkeyan G, Pervaje R, Subbannayya Y, Patil AH, Modi PK, Prasad TSK. Plant Omics: Metabolomics and Network Pharmacology of Licorice, Indian Ayurvedic Medicine Yashtimadhu. <i>OMICS A Journal of Integrative Biology</i> . 2020; 24( 12). DOI: 10.1089/omi.2020.0156
22.	Elucidating the mechanism of piperine in enhancing the sensitivity of cisplatin treated cancers towards radiation. (Dr. Divya Lakshmanan M)	<b>Mangalath DL</b> , Mohammed SAH. Ligand binding domain of estrogen receptor alpha preserve a conserved structural architecture similar to bacterial taxis receptors. <i>Frontiers in Ecology and Evolution</i> . 2021; 9: 681913. Doi: 10.3389/fevo.2021.681913
23.	Elucidating the mechanism of piperine in enhancing the sensitivity of cisplatin treated cancers towards radiation. (Dr. Divya Lakshmanan M)	K Shaheer K, Somashekarappa HM, <b>Lakshmanan MD</b> . Piperine sensitizes radiation-resistant cancer cells towards radiation and promotes intrinsic pathway of apoptosis. <i>Journal of Food Science</i> , 2020. <a href="https://doi.org/10.1111/1750-3841.15496">Doi: 10.1111/1750-3841.15496</a>

24.	Elucidating the mechanism of piperine in enhancing the sensitivity of cisplatin treated cancers towards radiation. (Dr. Divya Lakshmanan M)	Shaheer K, <b>Lakshmanan MD</b> . Effect of piperine in combination with gamma radiation on A549 cells. <i>Journal of Health and Allied Sciences</i> . 2021; 11: 80–86. DOI <a href="https://doi.org/10.1055/s-0040-1722808">https://doi.org/10.1055/s-0040-1722808</a>
25.	Combination therapy strategy using antibiotics and AHL analogues for <i>Pseudomonas aeruginosa</i> infection in <i>Caenorhabditis elegans</i> model (Dr. Rajesh P. Shastry)	<b>Shastry RP</b> , Kanekar S, Pandial AS, Rekha PD. Isoeugenol suppresses multiple quorum sensing regulated phenotypes and biofilm formation of <i>Pseudomonas aeruginosa</i> PAO1. <i>Natural Product Research</i> . 2021 <a href="https://doi.org/10.1080/14786419.2021.1899174">https://doi.org/10.1080/14786419.2021.1899174</a>

*by Somayaj*

Registrar  
Yenepoya (Deemed to be University)  
University Road, Deralakatte  
Mangalore - 575 018



# Role of gut-lung microbiome crosstalk in COVID-19

B. S. Srinath<sup>1</sup> · Rajesh P. Shastry<sup>2</sup> · Sukesh B. Kumar<sup>2</sup>

Received: 15 June 2020 / Accepted: 17 November 2020  
© Sociedade Brasileira de Engenharia Biomedica 2020

## Abstract

**Purpose** Gut microbiota are able to generate metabolites that can alter the function of immune cells and play a major role in health and disease. Understanding the changes in gut microbiome during infections including virus may help to use novel strategies in the therapeutic interventions.

**Methods** We have reviewed recent reports on role of gut microbiome in lung infections and its possible importance in COVID-19.

**Results** Most of the studies provide an insight into the possible role of gut microbes during lung diseases including chronic obstructive pulmonary disease (COPD), cystic fibrosis, lung cancer, and other respiratory problems such as allergy and asthma. However, clinical evidence underlying gut-lung crosstalk during respiratory viral infections is limited.

**Conclusion** This review provides an overview of the role of the gut microbiome during respiratory viral infections mainly focused on COVID-19 and possible evidence for its crosstalk targeting as new therapeutics.

**Keywords** Respiratory viral infections · Microbiome · COVID-19 · Gut-lung axis

## Introduction

In December 2019, a series of cases of unsolved respiratory viral pneumonia was occurred in Wuhan, China. Primarily, most of the cases were considered to have linked with the seafood market in Wuhan. Later, it was identified that human to human transmission played a major role in the disease outbreak (Yuki et al. 2020). This disease was rapidly spread from Wuhan to other places in China and the rest of the world. To identify the causal organism of this disease, a huge number of tests were conducted. Finally, the International Committee on Taxonomy of Viruses (ICTV) named the causative virus as SARS-CoV-2 and the disease name as COVID-19 (Cui et al. 2019). This disease has been affecting a huge number of people in the worldwide, approximately more than 216 countries

and territories (Zhang et al. 2020c; Zheng 2020). As of 21st October 2020, around 40,251,950 cases have been infected and 1,116,131 deaths occurred worldwide according to the World Health Organization (WHO, 2020).

Six species of corona viruses are well known to cause diseases in human, among them the Middle East Respiratory syndrome Coronavirus (MERS-CoV) and Severe Acute Respiratory Syndrome Coronavirus (SARS-CoV) are zoonotic diseases, which caused severe respiratory illness and had higher fatality rates (Ye et al. 2020). Now, the recent pandemic COVID-19 is the seventh type of corona viruses. Phylogenetic study of its single stranded RNA viral genome (29,903 nucleotides) has revealed that the COVID-19 is almost similar (89.1% nucleotide) with SARS-like coronaviruses that had previously found in bats in China (Wu et al. 2020b). This information possibly explains the behavior of the present novel COVID-19 in human infection. Moreover, the mutational profile shows the highest mutation in the *orf1ab* gene especially the transitional mutation is much more frequent than transversion (Gupta et al. 2020). SARS-CoV-2 multifractal approach-based study concluded that structure organization linked to large fluctuations in genome imparting virulence in the virus (Mandal et al. 2020). Now, the current trend is the development of an effective vaccine and clinically efficient therapeutic treatment methods for COVID-19. Until that, we are reliant on preventative methods, such as social distancing and good hand hygiene to minimize the infection rates (WHO, 2020). An alternative addition to

---

B. S. Srinath and Rajesh P. Shastry contributed equally to this work.

✉ Rajesh P. Shastry  
rpshastry@gmail.com; rpshastry@yenepoya.edu.in

<sup>1</sup> Department of Studies and Research in Microbiology, Post Graduate Centre, Mangalore University, Jnana Kavary Campus, Kodagu, Karnataka 571232, India

<sup>2</sup> Division of Microbiology and Biotechnology, Yenepoya Research Centre, Yenepoya (Deemed to be University), University Road, Deralakatte, Mangalore 575018, India

inflammatory role (Belkaid and Hand 2014). Understanding of the gut-lung axis in respiratory disease has been recognized in recent years. Importantly, the existence of this mechanism opens up new hopes for the development of therapeutic approaches to COVID-19 and other respiratory infections (Dhar and Mohanty 2020).

## Conclusions

In viral respiratory infections, alternations in the microbial composition of the airway and intestinal microbiota are observed, commonly due to the major outgrowth of Proteobacteria and Bacteroides. A microbiome-mediated cross-talk along the gut-lung axis has been noted during lung infection specifically due to alterations in the gut microbial species and metabolites. However, clinical evidence-based mechanism by which the gut impacts the lung environment and viral infection has not yet fully understood. But, microbial metabolites such as SCFAs and probiotic microbes influence the immune responses as well as in preventing pathogen colonization. Interestingly, patients with respiratory infections and diseases generally observed with gut dysbiosis and related complications indicating gut-lung crosstalk. In COVID-19 patients, this phenomenon can also be observed. Therefore, improving gut microbiota with probiotics and other beneficial bacteria plays a major role in therapeutic applications and this could be further extended in the treatment of COVID-19 as a new therapeutic approach.

**Funding** R. P. Shastry was supported by the Yenepoya (Deemed to be University) Seed grant (YU/Seed grant/080-2019).

## Compliance with ethical standards

**Conflict of interest** The authors declare that they have no conflict of interest.

## References

- Aarnoutse R, Ziemons J, Penders J, Rensen SS, de Vos-Geelen J, Smidt ML. The clinical link between human intestinal microbiota and systemic cancer therapy. *Int J Mol Sci*. 2019;20. <https://doi.org/10.3390/ijms20174145>.
- Barcik W, Boutin RCT, Sokolowska M, Finlay BB. The role of lung and gut microbiota in the pathology of asthma. *Immunity*. 2020;52:241–55. <https://doi.org/10.1016/j.immuni.2020.01.007>.
- Bassis CM, Erb-Downward JR, Dickson RP, Freeman CM, Schmidt TM, Young VB, et al. Analysis of the upper respiratory tract microbiotas as the source of the lung and gastric microbiotas in healthy individuals. *MBio*. 2015;6:e00037. <https://doi.org/10.1128/mBio.00037-15>.
- Belkaid Y, Hand T. Role of the microbiota in immunity and inflammation. *Cell*. 2014;157:121–41. <https://doi.org/10.1016/j.cell.2014.03.011>.
- Bogaert D, van Belkum A, Sluijter M, Luijendijk A, de Groot R, Rümke HC, et al. Colonisation by *Streptococcus pneumoniae* and *Staphylococcus aureus* in healthy children. *Lancet Lond Engl*. 2004;363:1871–2. [https://doi.org/10.1016/S0140-6736\(04\)16357-5](https://doi.org/10.1016/S0140-6736(04)16357-5).
- Chavez S, Long B, Koyfman A, Liang SY. Coronavirus Disease (COVID-19): a primer for emergency physicians. *Am J Emerg Med*. 2020. <https://doi.org/10.1016/j.ajem.2020.03.036>.
- Chen L, Han X-D, Li Y-L, Zhang C-X, Xing X-Q. Severity and outcomes of influenza-related pneumonia in type A and B strains in China, 2013–2019. *Infect Dis Poverty*. 2020a;9:42. <https://doi.org/10.1186/s40249-020-00655-w>.
- Chen N, Zhou M, Dong X, Qu J, Gong F, Han Y, et al. Epidemiological and clinical characteristics of 99 cases of 2019 novel coronavirus pneumonia in Wuhan, China: a descriptive study. *Lancet Lond Engl*. 2020b;395:507–13. [https://doi.org/10.1016/S0140-6736\(20\)30211-7](https://doi.org/10.1016/S0140-6736(20)30211-7).
- Cole-Jeffrey CT, Liu M, Katovich MJ, Raizada MK, Shenoy V. ACE2 and microbiota: emerging targets for cardiopulmonary disease therapy. *J Cardiovasc Pharmacol*. 2015;66:540–50. <https://doi.org/10.1097/FJC.0000000000000307>.
- Cornuault JK, Petit M-A, Mariadassou M, Benevides L, Moncaut E, Langella P, et al. Phages infecting *Faecalibacterium prausnitzii* belong to novel viral genera that help to decipher intestinal viromes. *Microbiome*. 2018;6:65. <https://doi.org/10.1186/s40168-018-0452-1>.
- Corr SC, Li Y, Riedel CU, O’Toole PW, Hill C, Gahan CGM. Bacteriocin production as a mechanism for the anti-infective activity of *Lactobacillus salivarius* UCC118. *Proc Natl Acad Sci U S A*. 2007;104:7617–21. <https://doi.org/10.1073/pnas.0700440104>.
- Cui J, Li F, Shi Z-L. Origin and evolution of pathogenic coronaviruses. *Nat Rev Microbiol*. 2019;17:181–92. <https://doi.org/10.1038/s41579-018-0118-9>.
- Demirci M, Tokman HB, Uysal HK, Demiryas S, Karakullukcu A, Saribas S, et al. Reduced *Akkermansia muciniphila* and *Faecalibacterium prausnitzii* levels in the gut microbiota of children with allergic asthma. *Allergol Immunopathol (Madr)*. 2019;47:365–71. <https://doi.org/10.1016/j.aller.2018.12.009>.
- Dhar D, Mohanty A. Gut microbiota and Covid-19- possible link and implications. *Virus Res*. 2020:198018. <https://doi.org/10.1016/j.virusres.2020.198018>.
- Dickson RP, Erb-Downward JR, Huffnagle GB. The role of the bacterial microbiome in lung disease. *Expert Rev Respir Med*. 2013;7:245–57. <https://doi.org/10.1586/ers.13.24>.
- Dickson RP, Erb-Downward JR, Martinez FJ, Huffnagle GB. The microbiome and the respiratory tract. *Annu Rev Physiol*. 2016;78:481–504. <https://doi.org/10.1146/annurev-physiol-021115-105238>.
- Dilantika C, Sedyaningsih ER, Kasper MR, Agtini M, Listiyaningsih E, Uyeki TM, et al. Influenza virus infection among pediatric patients reporting diarrhea and influenza-like illness. *BMC Infect Dis*. 2010;10:3. <https://doi.org/10.1186/1471-2334-10-3>.
- Du J, Abdel-Razek O, Shi Q, Hu F, Ding G, Cooney RN, et al. Surfactant protein D attenuates acute lung and kidney injuries in pneumonia-induced sepsis through modulating apoptosis, inflammation and NF- $\kappa$ B signaling. *Sci Rep*. 2018;8:1–14. <https://doi.org/10.1038/s41598-018-33828-7>.
- El Feghaly RE, Stauber JL, Tarr PI, Haslam DB. Viral Co-infections are common and are associated with higher bacterial burden in children with *C. difficile* infection. *J Pediatr Gastroenterol Nutr*. 2013;57:813–6. <https://doi.org/10.1097/MPG.0b013e3182a3202f>.
- Enaud R, Prevel R, Ciarlo E, Beauflis F, Wieërs G, Guery B, et al. The gut-lung axis in health and respiratory diseases: a place for inter-organ and inter-kingdom crosstalks. *Front Cell Infect Microbiol*. 2020;10. <https://doi.org/10.3389/fcimb.2020.00009>.
- Erb-Downward JR, Thompson DL, Han MK, Freeman CM, McCloskey L, Schmidt LA, et al. Analysis of the lung microbiome in the “healthy” smoker and in COPD. *PLoS One*. 2011;6:e16384. <https://doi.org/10.1371/journal.pone.0016384>.
- Feng Z, Wang Y, Qi W. The small intestine, an underestimated site of SARS-CoV-2 Infection: from red queen effect to probiotics. 2020. <https://doi.org/10.20944/preprints202003.0161.v1>.



## RESEARCH ARTICLE

# Morphological characteristics and microstructure of kidney stones using synchrotron radiation $\mu$ CT reveal the mechanism of crystal growth and aggregation in mixed stones

Muhammed A. P. Manzoor<sup>1,2\*</sup>, Ashish K. Agrawal<sup>3</sup>, Balwant Singh<sup>3</sup>, M. Mujeeburahiman<sup>2</sup>, Punchappady-Devasya Rekha<sup>1\*</sup>

**1** Yenepoya Research Centre, Yenepoya (Deemed to be University), Mangalore, Karnataka, India, **2** Department of Urology, Yenepoya Medical College, Yenepoya (Deemed to be University), Mangalore, Karnataka, India, **3** Technical Physics Division, Bhabha Atomic Research Centre, Indore-Mumbai, India

\* Current address: ICAR–Indian Institute of Spices Research, Kozhikode, Kerala, India

\* [rekhapd@hotmail.com](mailto:rekhapd@hotmail.com), [dydirectoryrc@yenepoya.edu.in](mailto:dydirectoryrc@yenepoya.edu.in)



## OPEN ACCESS

**Citation:** Manzoor MAP, Agrawal AK, Singh B, Mujeeburahiman M, Rekha P-D (2019) Morphological characteristics and microstructure of kidney stones using synchrotron radiation  $\mu$ CT reveal the mechanism of crystal growth and aggregation in mixed stones. PLoS ONE 14(3): e0214003. <https://doi.org/10.1371/journal.pone.0214003>

**Editor:** Yogendra Kumar Mishra, Institute of Materials Science, GERMANY

**Received:** November 14, 2018

**Accepted:** March 5, 2019

**Published:** March 22, 2019

**Copyright:** © 2019 Manzoor et al. This is an open access article distributed under the terms of the [Creative Commons Attribution License](https://creativecommons.org/licenses/by/4.0/), which permits unrestricted use, distribution, and reproduction in any medium, provided the original author and source are credited.

**Data Availability Statement:** All relevant data are within the paper and its Supporting Information files.

**Funding:** The authors acknowledge the Yenepoya University for the seed grant for carrying out this study. The funder had no role in study design, data collection and analysis, decision to publish, or preparation of the manuscript.

## Abstract

Understanding the mechanisms of kidney stone formation, development patterns and associated pathological features are gaining importance due to an increase in the prevalence of the disease and diversity in the presentation of the stone composition. Based on the microstructural characteristics of kidney stones, it may be possible to explain the differences in the pathogenesis of pure and mixed types of stones. In this study, the microstructure and distribution of mineral components of kidney stones of different mineralogy (pure and mixed types) were analyzed. The intact stones removed from patients were investigated using synchrotron radiation X-ray computed microtomography (SR- $\mu$ CT) and the tomography slice images were reconstructed representing the density and structure distribution at various elevation planes. Infrared (IR) spectroscopes, X-ray diffraction (XRD) and scanning electron microscopy (SEM) were used to confirm the bulk mineral composition in the thin section stones. Observations revealed differences in the micro-morphology of the kidney stones with similar composition in the internal 3-D structure. Calcium oxalate monohydrate stones showed well-organised layering patterns, while uric acid stones showed lower absorption signals with homogenous inner structure. Distinct mineral phases in the mixed types were identified based on the differential absorption rates. The 3-D quantitative analysis of internal porosity and spatial variation between nine different types of stones were compared. The diversity among the microstructure of similar and different types of stones shows that the stone formation is complex and may be governed by both physiological and micro-environmental factors. These factors may predispose a few towards crystal aggregation and stone growth, while, in others the crystals may not establish stable attachment and/or growth.

**S2 Table. Porosity value of pure and mixed types of kidney stones.**

(DOCX)

**S1 Fig. Micro-morphology of pure calcium oxalate monohydrate.** (a & b) Different stones obtained from same patient (KS 8 and KS 16). (c & d) Different stones obtained from same patient (KS 1 and KS 2).

(TIF)

**S2 Fig. The tomographic slice image of different sections of the calcium oxalate monohydrate stone showing mineral precipitation and accumulation of minerals at different elevation plane.** (i–xx) Different sections of the stones showing mineral precipitation and accumulation of minerals at different elevation plane. Arrows indicates the nucleus.

(TIF)

**S3 Fig. Micro-tomography of mixed kidney stones.** (a) COM-COD mixed showing uniform micro-tomography and (b) COM-struvite-apatite mixed stones. Apatite showing comparatively denser structure (arrow).

(TIF)

## Acknowledgments

The authors acknowledge the Yenepoya University for the seed grant for carrying out this study and are thankful to the technical staff at Raja Ramanna Centre for Advanced Technology (RRCAT), Indore, for providing the synchrotron beam, the necessary support and infrastructure to carry out this research and their active support during data acquisition and analysis.

## Author Contributions

**Conceptualization:** Muhammed A. P. Manzoor, Ashish K. Agrawal, M. Mujeeburahiman, Punchappady-Devasya Rekha.

**Data curation:** Muhammed A. P. Manzoor, Balwant Singh.

**Formal analysis:** Muhammed A. P. Manzoor, Ashish K. Agrawal, Balwant Singh.

**Investigation:** Ashish K. Agrawal, M. Mujeeburahiman.

**Methodology:** Muhammed A. P. Manzoor, Balwant Singh.

**Resources:** Ashish K. Agrawal, M. Mujeeburahiman, Punchappady-Devasya Rekha.

**Supervision:** M. Mujeeburahiman, Punchappady-Devasya Rekha.

**Validation:** Ashish K. Agrawal, Punchappady-Devasya Rekha.

**Writing – original draft:** Muhammed A. P. Manzoor.

**Writing – review & editing:** Ashish K. Agrawal, Balwant Singh, M. Mujeeburahiman, Punchappady-Devasya Rekha.

## References

1. Daudon M, Bader CA, Jungers P. Urinary calculi: Review of classification methods and correlations with etiology. *Scanning Microsc.* 1993; 7(3):1081–106. PMID: [8146609](https://pubmed.ncbi.nlm.nih.gov/8146609/)
2. Aleighn T, Petros B. Kidney stone disease: An update on current concepts. *AdvUrol.* 2018; <https://doi.org/10.1155/2018/3068365> PMID: [29515627](https://pubmed.ncbi.nlm.nih.gov/29515627/)

# Dual and multistimuli-responsive block copolymers for drug delivery applications

9

Renjith P. Johnson, Namitha K. Preman

Polymer Nanobiomaterial Research Laboratory, Yenepoya Research Centre,  
Yenepoya University, Mangalore, India

## Abbreviations

<b>ATRP</b>	atom transfer radical polymerization
<b>BSA</b>	bovine serum albumin
<b>CA</b>	<i>cis</i> -1,2-cyclohexanedicarboxylic acid
<b>CC</b>	cytochrome <i>C</i>
<b>CPT</b>	camptothecin
<b>CUR</b>	curcumin
<b>DDS</b>	drug delivery systems
<b>DMTK</b>	dimethyl thioketal
<b>Dox</b>	doxorubicin
<b>DTT</b>	dithiothreitol
<b>FA</b>	folic acid
<b>FITC</b>	fluorescein isothiocyanate
<b>GSH</b>	glutathione
<b>HPMA</b>	<i>N</i> -(2-hydroxypropyl) methacrylamide
<b>LCST</b>	lower critical solution temperature
<b>MTT</b>	3-(4,5-dimethylthiazol-2-yl)-2,5-diphenyltetrazolium bromide
<b>NBS</b>	<i>O</i> -nitrobenzyl thioether
<b>NIPAM</b>	<i>N</i> -isopropyl acrylamide
<b>NIR</b>	near infrared
<b>PAA</b>	polyaspartamide
<b>PBS</b>	phosphate-buffered saline
<b>PEG</b>	polyethylene glycol
<b>PSI</b>	polysuccinimide
<b>PTX</b>	paclitaxel
<b>RAFT</b>	reversible addition fragmentation chain transfer
<b>ROP</b>	ring-opening polymerization
<b>SCNPs</b>	shell-cross-linked nanoparticles
<b>SS</b>	disulfide
<b>US</b>	ultrasound
<b>UV</b>	ultraviolet

## Acknowledgment

This work was supported by Seed Grant (YU/Seed-061-2017) from Yenepoya University.

## References

- [1] M.B. Yatvin, J.N. Weinstein, W.H. Dennis, R. Blumenthal, Design of liposomes for enhanced local release of drugs by hyperthermia, *Science* 202 (4374) (1978) 1290–1293.
- [2] Y. Zhong, F. Meng, C. Deng, Z. Zhong, Ligand-directed active tumor-targeting polymeric nanoparticles for cancer chemotherapy, *Biomacromolecules* 15 (6) (2014) 1955–1969.
- [3] M. Karimi, A. Ghasemi, P.S. Zangabad, R. Rahighi, S.M. Basri, H. Mirshekari, M. Amiri, Z.S. Pishabad, A. Aslani, M. Bozorgomid, D. Ghosh, Smart micro/nanoparticles in stimulus-responsive drug/gene delivery systems, *Chem. Soc. Rev.* 45 (5) (2016) 1457–1501.
- [4] J. Zhuang, M.R. Gordon, J. Ventura, L. Li, S. Thayumanavan, Multi-stimuli responsive macromolecules and their assemblies, *Chem. Soc. Rev.* 42 (17) (2013) 7421–7435.
- [5] L. Wu, Y. Zou, C. Deng, R. Cheng, F. Meng, Z. Zhong, Intracellular release of doxorubicin from core-crosslinked polypeptide micelles triggered by both pH and reduction conditions, *Biomaterials* 34 (21) (2013) 5262–5272.
- [6] W.C. Wu, C.M. Huang, P.W. Liao, Dual-sensitive and folate-conjugated mixed polymeric micelles for controlled and targeted drug delivery, *React. Funct. Polym.* 81 (2014) 82–90.
- [7] C. Gong, M. Shan, B. Li, W. G A, pH and redox dual stimuli-responsive poly (amino acid) derivative for controlled drug release, *Colloids Surf. B* 146 (2016) 396–405.
- [8] J. Chen, X. Qiu, J. Ouyang, J. Kong, W. Zhong, M.M. Xing, pH and reduction dual-sensitive copolymeric micelles for intracellular doxorubicin delivery, *Biomacromolecules* 12 (10) (2011) 3601–3611.
- [9] R.P. Johnson, Y.I. Jeong, J.V. John, C.W. Chung, D.H. Kang, M. Selvaraj, H. Suh, I. Kim, Dual stimuli-responsive poly (N-isopropylacrylamide)-b-poly (L-histidine) chimeric materials for the controlled delivery of doxorubicin into liver carcinoma, *Biomacromolecules* 14 (5) (2013) 1434–1443.
- [10] Z.Y. Qiao, R. Ji, X.N. Huang, F.S. Du, R. Zhang, D.H. Liang, Z.C. Li, Polymersomes from dual responsive block copolymers: drug encapsulation by heating and acid-triggered release, *Biomacromolecules* 14 (5) (2013) 1555–1563.
- [11] Y. Shao, C. Shi, G. Xu, D. Guo, J. Luo, Photo and redox dual responsive reversibly cross-linked nanocarrier for efficient tumor-targeted drug delivery, *ACS Appl. Mater. Interfaces* 6 (13) (2014) 10381–10392.
- [12] P. Huang, J. Liu, W. Wang, C. Li, J. Zhou, X. Wang, L. Deng, D. Kong, J. Liu, A. Dong, Zwitterionic nanoparticles constructed with well-defined reduction-responsive shell and pH-sensitive core for “spatiotemporally pinpointed” drug delivery, *ACS Appl. Mater. Interfaces* 6 (16) (2014) 14631–14643.
- [13] S. Kashyap, N. Singh, B. Surnar, M. Jayakannan, Enzyme and thermal dual responsive amphiphilic polymer core-shell nanoparticle for doxorubicin delivery to cancer cells, *Biomacromolecules* 17 (1) (2015) 384–398.
- [14] Q.N. Bui, Y. Li, M.S. Jang, D.P. Huynh, J.H. Lee, D.S. Lee, Redox- and pH-sensitive polymeric micelles based on poly ( $\beta$ -amino ester)-grafted disulfide methylene oxide poly (ethylene glycol) for anticancer drug delivery, *Macromolecules* 48 (12) (2015) 4046–4054.

# Responsive block copolymers for drug delivery applications. Part 2: Exogenous stimuli-responsive drug-release systems

*Renjith P. Johnson, Namitha K. Preman*

Polymer Nanobiomaterial Research Laboratory, Yenepoya Research Centre, Yenepoya University, Mangalore, India

## Abbreviation

<b>ADR</b>	adriamycin
<b>ATRP</b>	atom transfer radical polymerization
<b>BSA</b>	bovine serum albumin
<b>Ce6</b>	chlorin e6
<b>CPT</b>	camptothecin
<b>CUR</b>	curcumin
<b>DDS</b>	drug delivery systems
<b>Dox</b>	doxorubicin
<b>EPR</b>	enhanced permeation and retention
<b>FA</b>	folic acid
<b>HIF</b>	high-intensity focused
<b>HMS</b>	hollow mesoporous silica
<b>IC<sub>50</sub></b>	half-maximal inhibitory concentration
<b>LCST</b>	lower critical solution temperature
<b>MPC</b>	2-methacryloyloxyethyl phosphorylcholine
<b>MTT</b>	3-(4,5-dimethylthiazol-2-yl)-2,5-diphenyltetrazolium bromide
<b>NEGDM</b>	2-nitrophenyl ethylene glycol dimethacrylate
<b>NIPAM</b>	<i>N</i> -isopropyl acrylamide
<b>NIR</b>	near-infrared
<b>pNIPAM</b>	poly( <i>N</i> -isopropylacrylamide)
<b>PIC</b>	polyion complex
<b>PTX</b>	paclitaxel
<b>PVCL</b>	poly(vinyl caprolactum)
<b>RAFT</b>	reversible addition fragmentation chain transfer
<b>ROP</b>	ring opening polymerization
<b>ROS</b>	reactive singlet oxygen
<b>SP</b>	spiropyran
<b>SPIONS</b>	superparamagnetic nanoparticles
<b>US</b>	ultrasound
<b>UV</b>	ultraviolet

were used as an alternative to individual IONPs to provide enough magnetic moment; moreover, now, each and every single domain would be able to sustain their superparamagnetism and collectively they would provide enough magnetic moment to generate the necessary heat for the therapeutic purposes. However, the size of the IONPs encapsulating the pNIPAM nanoparticle needs to be fine-tuned for maintaining adequate circulation time [68]. Cui et al. fabricated magnetic nanoparticles by co-precipitation and coated with mesoporous silica for controlled as well as targeted delivery to glioma cells. They have encapsulated both Dox and PTX into the system by a process of double emulsion solid-in-oil-in water evaporation. In order to provide tumor selectivity, these particles were conjugated with transferrin, as the latter is overexpressed in glioma (U-87) cell lines. The efficacy of the final nanoparticles was evaluated both *in vivo* and *in vitro*. For *in vitro* cytotoxicity, U-87 cells were treated with the final formulation followed by application of magnetic field. The authors reported that the cytotoxicity of the nanoparticles increased when magnetic field was applied after nanoparticle injection, as compared to free drugs and control samples. They found higher efficacy of the formulation *in vivo* in U-87 tumor bearing BALB/c nude mice [69].

## 8.4 Conclusions

In the past years, significant progress has been achieved in the development of exogenous stimuli-responsive nanocarriers for drug delivery, diagnosis, and therapy. Block copolymer-based smart nanocarriers contain specific chains, ligands, or functional groups that are responsive to exogenous stimuli (temperature, light, US, magnetic field) which can be exploited for drug delivery applications, especially for the delivery of chemotherapeutic drugs. The examples discussed in this chapter have demonstrated the current status of various exogenous stimuli-responsive block copolymer-based DDS, and it was observed that the combination of manipulating exogenous stimuli-responsive nanocarriers and regulating biological processes can achieve a better therapeutic effect. It is expected that there is still a whole field to be explored in terms of existing and new delivery platforms for potential use as nanomedicine formulation in clinical settings.

## Acknowledgment

This work was supported by Seed Grant (YU/Seed-061-2017) from Yenepoya University.

## References

- [1] H. Ringsdorf, Structure and properties of pharmacologically active polymers, *J. Polym. Sci., Polym. Symp.* 51 (1975) 135–153.
- [2] Y. Matsumura, H.A. Maeda, New concept for macromolecular therapeutics in cancer chemotherapy: mechanism of tumorotropic accumulation of proteins and the antitumor agent smancs, *Cancer Res.* 4 (1986) 6387–6392.

## PAPER



Cite this: *J. Mater. Chem. B*, 2020, **8**, 8585

## Bioresponsive supramolecular hydrogels for hemostasis, infection control and accelerated dermal wound healing†

Namitha K. Preman,<sup>id</sup><sup>a</sup> Sindhu Priya E. S.,<sup>id</sup><sup>b</sup> Ashwini Prabhu,<sup>id</sup><sup>c</sup> Sadiya Bi Shaikh,<sup>id</sup><sup>c</sup> Vipin C.,<sup>id</sup><sup>de</sup> Rashmi R. Barki,<sup>id</sup><sup>c</sup> Yashodhar P. Bhandary,<sup>id</sup><sup>c</sup> P. D. Rekha<sup>id</sup><sup>d</sup> and Renjith P. Johnson<sup>id</sup><sup>\*a</sup>

Injectable, drug-releasing hydrogel scaffolds with multifunctional properties including hemostasis and anti-bacterial activity are essential for successful wound healing; however, designing ideal materials is still challenging. Herein, we demonstrate the fabrication of a biodegradable, temperature-pH dual responsive supramolecular hydrogel (SHG) scaffold based on sodium alginate/poly(*N*-vinyl caprolactam) (AG/PVCL) through free radical polymerization and the subsequent chemical and ionic cross-linking. A natural therapeutic molecule, tannic acid (TA)-incorporated SHG (AG/PVCL-TA), was also fabricated and its hemostatic and wound healing efficiency were studied. In the AG/PVCL-TA system, TA acts as a therapeutic molecule and also substitutes as an effective gelation binder. Notably, the polyphenol-arm structure and diverse bonding abilities of TA can hold polymer chains through multiple bonding and co-ordinate cross-linking, which were vital in the formation of the mechanically robust AG/PVCL-TA. The SHG formation was successfully balanced by varying the composition of SA, VCL, TA and cross-linkers. The AG/PVCL-TA scaffold was capable of releasing a therapeutic dose of TA in a sustained manner under physiological temperature-pH conditions. AG/PVCL-TA displayed excellent free radical scavenging, anti-inflammatory, anti-bacterial, and cell proliferation activity towards the 3T3 fibroblast cell line. The wound healing performance of AG/PVCL-TA was further confirmed in skin excision wound models, which demonstrated the potential application of AG/PVCL-TA for skin regeneration and rapid wound healing.

Received 11th June 2020,  
Accepted 3rd August 2020

DOI: 10.1039/d0tb01468k

rsc.li/materials-b

### 1. Introduction

Skin is the major and most susceptible organ that protects the human physique from hostile environments, microbial attacks, and also functions to prevent dehydration. Common trauma such as burns, wounds, and bruises and associated injuries

often result in acute or chronic wounds,<sup>1</sup> are always a health burden, and the loss of skin integrity often leads to disability or even death.<sup>1,2</sup> Since reconnection of injured tissues is vital in restoring their structures and functions, biological procedures initiate in re-establishing dermal functions after hemostasis. Subsequently, wound healing proceeds through sequential, correlated wound remodeling phases within weeks towards restoring the complete anatomic functions.<sup>3,4</sup> However, the dysfunction of these sequential events results in pathologically insufficient or excess wound healing, which is clinically challenging.<sup>5,6</sup> Therefore, the development of advanced wound healing materials to prevent and treat several detrimental wound healing outcomes is inevitable.

To date, a variety of wound healing materials composed of temporary dressing (gauze, thin-films, foam hydrogels, hydrocolloids, and membranes),<sup>7–12</sup> and scaffold biomaterials<sup>13,14</sup> (capable of hosting and support the growth of endogenous cells) have been employed for healing different wound types. However, many of these conventional materials have major limitations, such as limited oxygen permeability and low hydration towards wound environment, poor wound exudate management,

<sup>a</sup> Polymer Nanobiomaterial Research Laboratory, Yenepoya Research Centre, Yenepoya (Deemed to be University), Mangalore, India.

E-mail: renjithjohnson@yenepoya.edu.in; Fax: +91 8242204669;  
Tel: +91 8242204669

<sup>b</sup> Yenepoya Pharmacy College and Research Centre, Yenepoya (Deemed to be University), Mangalore, India

<sup>c</sup> Division of Cell and Molecular Biology,

Yenepoya Research Centre, Yenepoya (Deemed to be University), Mangalore, India

<sup>d</sup> Division of Biotechnology, Microbiology and Infectious Diseases,

Yenepoya Research Centre, Yenepoya (Deemed to be University), Mangalore, India

<sup>e</sup> Relicus Bio Pvt. Ltd, Technology Business Incubator, Anna University, Chennai, 600025-Tamilnadu, India

† Electronic supplementary information (ESI) available: Spectral, thermal, and rheology characterizations of hydrogels, swelling and degradation kinetics of hydrogels, anti-oxidant, anti-bacterial assays, immunofluorescence images and experimental procedures. See DOI: 10.1039/d0tb01468k

## Conflicts of interest

There are no conflicts to declare.

## Acknowledgements

This work was supported by Indian Council of Medical Research (2019-5984), Govt. of India, Seed Grant (YU/Seed-061-2017) from Yenepoya (Deemed to be University) and Core Research Grant (CRG/2018/000380-2019) from Department of Science and Technology-Science and Engineering Research Board (DST-SERB), Govt. of India.

## References

- 1 R. A. Clark, K. Ghosh and M. G. Tonnesen, *J. Invest. Dermatol.*, 2007, **127**, 1018–1029.
- 2 R. Xu, G. Luo, H. Xia, W. He, J. Zhao, B. Liu, J. Tan, J. Zhou, D. Liu, Y. Wang and Z. Yao, *Biomaterials*, 2015, **40**, 1–11.
- 3 S. Enoch and D. J. Leaper, *Surg. Oxford Int. Ed.*, 2008, **26**, 31–37.
- 4 D. Girard, B. Laverdet, V. Buhe, M. Trouillas, K. Ghazi, M. M. Alexaline, C. Egles, L. Misery, B. Coulomb, J. J. Lataillade and F. Berthod, *Tissue Eng., Part B*, 2016, **23**, 59–82.
- 5 Z. Ruzszzak, *Adv. Drug Delivery Rev.*, 2003, **55**, 1595–1611.
- 6 J. Hardwicke, E. L. Ferguson, R. Moseley, P. Stephens, D. W. Thomas and R. Duncan, *J. Controlled Release*, 2008, **130**, 275–283.
- 7 V. J. Jones, *Int. Wound J.*, 2006, **3**, 79–88.
- 8 S. Thomas, P. Loveless and N. P. Hay, *Pharm. J.*, 1988, **240**, 785–787.
- 9 H. Vermeulen, D. T. Ubbink, A. Goossens, R. De Vos and D. A. Legemate, *Br. J. Surg.*, 2005, **92**, 665–672.
- 10 K. Lay-Flurrie, *Prof. Nurse*, 2004, **19**, 269–273.
- 11 C. Dealey, *Br. J. Nurse.*, 1993, **2**, 358–365.
- 12 M. S. Khil, D. I. Cha, H. Y. Kim, I. S. Kim and N. Bhattarai, *J. Biomed. Mater. Res., Part B*, 2003, **67**, 675–679.
- 13 S. P. Zhong, Y. Z. Zhang and C. T. Lim, *Wiley Interdiscip. Rev.: Nanomed. Nanobiotechnol.*, 2010, **2**, 510–525.
- 14 D. R. Griffin, W. M. Weaver, P. O. Scumpia, D. Di Carlo and T. Segura, *Nat. Mater.*, 2015, **14**, 737–744.
- 15 R. Goldman, *Adv. Skin Wound Care*, 2004, **17**, 24–35.
- 16 A. J. Singer and R. A. Clark, *N. Engl. J. Med.*, 1999, **341**, 738–746.
- 17 B. M. Alphonsa, P. S. Kumar, G. Praveen, R. Biswas, K. P. Chennazhi and R. Jayakumar, *Pharm. Res.*, 2014, **31**, 1338–1351.
- 18 J. L. Drury and D. J. Mooney, *Biomaterials*, 2003, **24**, 4337–4351.
- 19 G. Sun, X. Zhang, Y. I. Shen, R. Sebastian, L. E. Dickinson, K. Fox-Talbot, M. Reinblatt, C. Steenbergen, J. W. Harmon and S. Gerecht, *Proc. Natl. Acad. Sci. U. S. A.*, 2011, **108**, 20976–20981.
- 20 X. Zhao, H. Wu, B. Guo, R. Dong, Y. Qiu and P. X. Ma, *Biomaterials*, 2017, **122**, 34–47.
- 21 E. Caffarel-Salvador, M. C. Kearney, R. Mairs, L. Gallo, S. A. Stewart, A. J. Brady and R. F. Donnelly, *Pharmaceutics*, 2015, **7**, 397–412.
- 22 S. Saghazadeh, C. Rinoldi, M. Schot, S. S. Kashaf, F. Sharifi, E. Jalilian, K. Nuutila, G. Giatsidis, P. Mostafalu, H. Derakhshandeh and K. A. Yue, *Adv. Drug Delivery Rev.*, 2018, **127**, 138–166.
- 23 D. W. Grainger, *Nat. Mater.*, 2015, **14**, 662–663.
- 24 A. J. Singer and A. B. Dagum, *New Engl. J. Med.*, 2008, **359**, 1037–1046.
- 25 C. Ghobril and M. W. Grinstaff, *Chem. Soc. Rev.*, 2015, **44**, 1820–1835.
- 26 N. Q. Tran, Y. K. Joung, E. Lih and K. D. Park, *Biomacromolecules*, 2011, **12**, 2872–2880.
- 27 J. Hoque, R. G. Prakash, K. Paramanandham, B. R. Shome and J. Haldar, *Mol. Pharmaceutics*, 2017, **14**, 1218–1230.
- 28 J. Hoque, B. Bhattacharjee, R. G. Prakash, K. Paramanandham and J. Haldar, *Biomacromolecules*, 2018, **19**, 267–278.
- 29 K. McKelvey, M. Xue, K. Whitmont, K. Shen, A. Cooper and C. Jackson, *Wound practice & research*, 2012, **20**, 86–89.
- 30 H. Cui, L. Cui, P. Zhang, Y. Huang, Y. Wei and X. Chen, *Macromol. Biosci.*, 2014, **14**, 440–450.
- 31 F. D. Halstead, M. Rauf, A. Bamford, C. M. Wearn, J. R. Bishop, R. Burt, A. P. Fraise, N. S. Moiemmen, B. A. Oppenheim and M. A. Webber, *Burns.*, 2015, **41**, 1683–1694.
- 32 B. Boonkaew, M. Kempf, R. Kimble, P. Supaphol and L. Cuttle, *Burns.*, 2014, **40**, 89–96.
- 33 P. Orłowski, M. Zmigrodzka, E. Tomaszewska, K. Ranošzek-Soliwoda, M. Czupryn, M. Antos-Bielska, J. Szemraj, G. Celichowski, J. Grobelny and M. Krzyzowska, *Int. J. Nanomed.*, 2018, **13**, 991–1007.
- 34 Z. Wu and Y. Hong, *ACS Appl. Mater. Interfaces*, 2019, **11**, 33734–33747.
- 35 M. V. Park, A. M. Neigh, J. P. Vermeulen, L. J. de la Fonteyne, H. W. Verharen, J. J. Briedé, H. van Loveren and W. H. de Jong, *Biomaterials*, 2011, **32**, 9810–9817.
- 36 P. V. AshaRani, G. Low Kah Mun, M. P. Hande and S. Valiyaveetil, *ACS Nano*, 2009, **3**, 279–290.
- 37 J. O. Kim, J. K. Park, J. H. Kim, S. G. Jin, C. S. Yong, D. X. Li, J. Y. Choi, J. S. Woo, B. K. Yoo, W. S. Lyoo and J. A. Kim, *Int. J. Pharm.*, 2008, **3**, 5979–5986.
- 38 A. Vijayan, A. Sabareeswaran and G. V. Kumar, *Sci. Rep.*, 2019, **9**, 19165.
- 39 L. Mi, H. Xue, Y. Li and S. Jiang, *Adv. Funct. Mater.*, 2011, **21**, 4028–4034.
- 40 Y. Li, K. N. Kumar, J. M. Dabkowski, M. Corrigan, R. W. Scott, K. Nüsslein and G. N. Tew, *Langmuir*, 2012, **28**, 12134–12139.
- 41 Y. Li, Y. Han, X. Wang, J. Peng, Y. Xu and J. Chang, *ACS Appl. Mater. Interfaces*, 2017, **9**, 16054–16062.
- 42 F. Xu, B. Weng, R. Gilkerson, L. A. Materon and K. Lozano, *Carbohydr. Polym.*, 2015, **11**, 516–524.
- 43 N. Ninan, A. Forget, V. P. Shastri, N. H. Voelcker and A. Blencowe, *ACS Appl. Mater. Interfaces*, 2016, **42**, 28511–28521.
- 44 N. Li, X. Yang, W. Liu, G. Xi, M. Wang, B. Liang, Z. Ma, Y. Feng, H. Chen and C. Shi, *Macromol. Biosci.*, 2018, 1800209.



# Responsive block copolymers for drug delivery applications. Part 1: Endogenous stimuli-responsive drug-release systems

*Renjith P. Johnson, Namitha K. Preman*

Polymer Nanobiomaterial Research Laboratory, Yenepoya Research Centre, Yenepoya University, Mangalore, India

## Abbreviations

<b>5-FU</b>	5-fluorouracil
<b>ADR</b>	adriamycin
<b>AIE</b>	aggregation-induced emission
<b>ATRP</b>	atom transfer radical polymerization
<b>BSO</b>	buthionine sulfoximine
<b>CCL</b>	core-cross-linked
<b>Ce6</b>	chlorin e6
<b>CP</b>	cisplatin
<b>CPT</b>	camptothecin
<b>CUR</b>	curcumin
<b>DDS</b>	drug delivery systems
<b>DLS</b>	dynamic light scattering
<b>Dox</b>	Doxorubicin
<b>DTT</b>	dithiothreitol
<b>DTX</b>	docetaxel
<b>EPR</b>	enhanced permeation and retention
<b>ESR</b>	endogenous stimuli-responsive
<b>FA</b>	folic acid
<b>GPC</b>	gel permeation chromatography
<b>GSH</b>	glutathione
<b>HEMA</b>	2-hydroxyethyl methacrylate
<b>IBU</b>	ibuprofen
<b>IC<sub>50</sub></b>	half-maximal inhibitory concentration
<b>MDR</b>	multidrug resistance
<b>MTT</b>	3-(4,5-dimethylthiazol-2-yl)-2,5-diphenyltetrazolium bromide
<b>MTX</b>	methotrexate
<b>NADPH</b>	nicotinamide adenine dinucleotide phosphate
<b>NIR</b>	near-infrared
<b>OPCL</b>	oxime-tethered polycaprolactone
<b>PDI</b>	polydispersity index
<b>PDT</b>	photodynamic therapy

## 7.4 Conclusions

The tremendous advances in polymer chemistry and macromolecular engineering in the past decade have brought the accessibility of new functional, responsive polymeric architectures. Combined with the advances in polymer science, materials science, and the knowledge of biology, diverse stimuli-responsive block copolymer-based nanocarriers for controlled and targeted delivery applications can be realized. Generally, block copolymer-based smart nanocarriers containing specific chains, ligands, or functional groups that are responsive to endogenous stimuli such as pH, redox potential, and enzyme can be exploited for drug delivery applications, especially in cancer chemotherapy. The examples discussed in this chapter have demonstrated the current status of various ESR block copolymer-based DDSs. It is expected that there is still a whole field to be explored in terms of existing and new ideal delivery platforms for potential use as nanomedicine in clinical settings.

## Acknowledgment

This work was supported by a Seed Grant (YU/Seed-061-2017) from Yenepoya University.

## References

- [1] K. Strebhardt, A. Ullrich, Paul Ehrlich's magical bullet concept: 100 years of progress, *Nat. Rev. Cancer* 8 (6) (2008) 473–480.
- [2] I. Brigger, C. Dubernet, P. Couvreur, Nanoparticles in cancer therapy and diagnosis, *Adv. Drug Deliv. Rev.* 54 (5) (2012) 24–36.
- [3] D. Peer, J.M. Karp, S. Hong, O.C. Farokhzad, R. Margalit, R. Langer, Nanocarriers as an emerging platform for cancer therapy, *Nat. Nanotechnol.* 2 (12) (2007) 751–760.
- [4] J.E. Kipp, The role of solid nanoparticle technology in the parenteral delivery of poorly water-soluble drugs, *Int. J. Pharm.* 284 (1–2) (2004) 109–122.
- [5] F. Alexis, E. Pridgen, L.K. Molnar, O.C. Farokhzad, Factors affecting the clearance and biodistribution of polymeric nanoparticles, *Mol. Pharm.* 5 (4) (2008) 505–515.
- [6] B.S. Pattni, V.V. Chupin, V.P. Torchilin, New developments in liposomal drug delivery, *Chem. Rev.* 115 (19) (2015) 10938–10966.
- [7] C. Argyo, V. Weiss, C. Brauchle, T. Bein, Multifunctional mesoporous silica nanoparticles as a universal platform for drug delivery, *Chem. Mater.* 26 (1) (2013) 435–451.
- [8] R.S. Navath, A.R. Menjoge, B. Wang, R. Romero, S. Kannan, R.M. Kannan, Amino acid-functionalized dendrimers with heterobifunctional chemoselective peripheral groups for drug delivery applications, *Biomacromolecules* 11 (6) (2010) 1544–1563.
- [9] N. Larson, H. Ghandehari, Polymeric conjugates for drug delivery, *Chem. Mater.* 24 (5) (2012) 840–853.
- [10] Y. Zhong, F. Meng, C. Deng, Z. Zhong, Ligand-directed active tumor-targeting polymeric nanoparticles for cancer chemotherapy, *Biomacromolecules* 15 (6) (2014) 1955–1969.
- [11] R. Langer, J. Folkman, Polymers for the sustained release of proteins and other macromolecules, *Nature* 263 (5580) (1976) 797–800.

# Graphene and Graphene-Based Materials in Biomedical Science

Poyye Dsouza Priya Swetha, Hosabettu Manisha, and Kariate Sudhakaraprasad\*

Graphene and its composite materials are very important in many disciplines of science and have been used enormously by researchers since their discovery in 2004. These are a new group of compounds, and are also wonderful model systems for quantum behavior studies. Their properties like exceptional conductivity, biocompatibility, surface area, mechanical strength, and thermal properties make them rising stars in the scientific community. Graphene and its composite compounds are utilized widely in different medical applications, for example, biosensing of biological compounds responsible for disease development, bioimaging of various cells, tissues, microorganisms, animal models, etc. In addition, they are used for enhancing and supporting the stem cell differentiation, i.e., regenerative medicine for regeneration studies of various human organs, tissue engineering in biology for the development of carrier materials, as well as in bone reformation. This review focuses on the modification procedure involved in the fabrication of graphene-based biomaterials for various applications and recent developments in research related to graphene and graphene-based materials in biosensing, optical sensing, gas sensing, drug, gene, protein delivery, tissue engineering, and bioimaging. In addition, the potential toxicological effects of graphene-based biomaterials are discussed.

## 1. Introduction

Graphene, a carbon material, has opened up another period of the investigation because of its unique properties. Graphene is made up of carbon atoms, which is atomic crystal, and these carbon atoms are formed as a hexagonal lattice which provides a structural resemblance of a honeycomb. The carbon molecules present are  $sp^2$  hybridized.<sup>[1]</sup> Graphene is the most slender (thin) and the active molecule,<sup>[2]</sup> the charge bearers available on graphene are massless; it is incredibly conductive both electrically and thermally, has wonderful adaptable nature, with high surface territory and is moreover transparent<sup>[3]</sup> and


furthermore goes about as a layer which is impermeable to any molecules,<sup>[4]</sup> this inherent nature has built up another chapter of innovative research because of its above said one of a kind properties. Consequently, more endeavours have been placed in logical analysis, especially in various fields and for other graphene-based materials for commercial and scientific applications.

Many methods can orchestrate graphene and mention few, they are, chemical vapor deposition, micromechanical method, an electrochemical method, chemical method, photocatalytic or thermal reduction, etc.<sup>[1]</sup> Wide varieties of graphene are produced using these above-said techniques, and few examples include, graphene oxide (GO) and reduced graphene oxides (rGO), which are known for their essential utilizations, the surface functionalities on GO and rGO accept a fundamental part in their catalytic activities. Graphene has some physical and substance properties which are novel, consequently can be utilized as a

standard material for various applications,<sup>[5]</sup> such as nanoelectronics,<sup>[6]</sup> composite elements,<sup>[7]</sup> energy technology (for examples, fuel cell, super capacitor, hydrogen storage),<sup>[8,9]</sup> sensors, and catalysis.<sup>[10]</sup> Typically graphene and other graphene derived compounds are applied in various types of capacitors, touch screens materials, power modules used in different appliances, in development and manufacturing of electrical gadgets, sensors for identifying multiple compounds, batteries in wide variety of applications, conductive films which are transparent for various uses, in removal of toxic compounds, high recurrence circuits, and in electronic compounds. Graphene has been as of late utilized for forms other than hardware and chemistry, that is toward biomedical applications.<sup>[11a,b]</sup> One of the most promising applications for graphene in biomedical technologies; as a perfect single-biomolecule recognition sensor stage to recognize particular target biomolecules with high affectability and selectivity, examination of blood and different samples containing specific biocompounds utilizing a graphene-based coordinated chip.<sup>[12]</sup> Because of their unique structures and exciting properties, graphene-based nanomaterials also have discovered applications in bioimaging, drug delivery, and photothermal therapies.

The initial reports on the biomedical uses of graphene ascended in 2008.<sup>[13,14]</sup> Henceforth, graphene and its substrates

P. D. Priya Swetha, H. Manisha, Dr. K. Sudhakaraprasad  
Nanomaterials Research Laboratory (NMRL)  
Nanodivison  
Yenepoya Research Centre  
Yenepoya (Deemed to be University)  
Deralakatte, Mangalore 575 018, India  
E-mail: ksprasadnair@yenepoya.edu.in

 The ORCID identification number(s) for the author(s) of this article can be found under <https://doi.org/10.1002/ppsc.201800105>.

DOI: 10.1002/ppsc.201800105

of 0.1  $\mu\text{m}$  thickness aided an inflammatory response and formation of granuloma in the lung and pleural space.<sup>[343]</sup> Also few researchers have recently found that pure and highly dispersible GO with 1–2 nm in thickness did not show any inflammatory response or granuloma formation at the mesothelial membrane after intraperitoneal injections.<sup>[344]</sup>

Though there are no sufficient number of works available regarding the cytotoxicity of graphene and graphene-based materials,<sup>[345]</sup> it is evident that different graphene and graphene-based materials will have a varying toxicological profile. There will be different conditions and effects when once exposed and also various factors are to be addressed and carefully noted before deriving to a valid conclusion. Therefore, all parameters are needed to be clearly studied and critically discussed regarding the toxic behavior of GO.

## 5. Conclusions

Major milestones have been achieved when comparing to the previous decade when seen for the improvement in graphene-based materials. Nowadays, graphene-based materials have been widely used in multiple applications in many fields of tissue engineering and regenerative pharmaceutical because of their capacity to give magnificent physical, chemical, and organic properties. The structural arrangement blesses graphene with a solid adsorbing limit with regard to use as gene/drug delivery vehicles. Graphene and its derivatives have excellent mechanical and surface properties, which is a known fact and also act as biomaterials and thus help and play a major role in inducing the cardiomyogenic, neurogenic, osteogenic, and cartilaginous capacities of undifferentiated cells. Furthermore, the high electrical conductivity of graphene and its composites is required to induce the development of cells of different lineages, for example, cardiomyocytes and neurons. Also the varying surface, chemical and mechanical properties which are excellent, can be coupled together for various patterning applications and also for making complex graphene designs, which will productively amplify their applications. In addition, not only graphene and GO but the composites of graphene and graphene biomaterials with different derivatives that have properties like wettability or adaptability make them great choice to create smart compounds with multiuse. Subsequently, the graphene composites can turn out to be ecologically delicate or can have shape–memory or self-folding properties which can broaden their biomedical applications. For instance, GO blended with a phase changing material was used to make a thermoresponsive drug delivery framework. This framework enhances drug loading or stacking efficiency alongside photothermal impacts for photodynamic treatments. Likewise, joining graphene with polydopamine can make a self-folding apparatus. Besides, consolidating the self-collapsing graphene-based materials and 3D printing innovation will help build up the future era of printing systems to apply in tissue engineering. Although, graphene and all its other derivatives have been widely utilized for important biomedical applications, still there are few issues when it comes to the cytotoxic or genotoxic impacts of these nanomaterials. There is not a highest quality level to beat the biocompatibility issues related with graphene items in living frameworks. This

requires building up graphene-based models to assess and control cellular behaviors in vitro. Surface change including protein or cytokine functionalization has pulled in a lot of thoughtfulness regarding to resolve the biocompatibility concerns. Additionally building up the testing model to comprehend the exact mechanism of graphene-based materials cytotoxicity is worth more profound examination, before graphene and all its other derivatives are utilized largely in clinics.

## 6. Perspectives

Though much research has been conducted using graphene and graphene-based materials, there are few aspects to be addressed. The toxicity of graphene and graphene-based biomaterials is a major concern and should be studied for well versed application in biological fields. As we discussed in this review, the research in graphene-related materials in biomedical application is in its infant stage, therefore more work should be carried out in developing novel and powerful tools for the diagnosis of different diseases. Even the sensitivity, specificity, and detection ranges should be improved and studies related to rapid and cost-effective modalities for detection of biomarkers should be developed. Reproducibility is another major concern and need to be addressed in the future.

## Acknowledgements

The authors are thankful to **Yenepoya (Deemed to be University)** and Department of Biotechnology (DBT—Govt. of India) **for research support.** Priya Swetha is grateful to INSPIRE doctoral fellowship from Department of Science and Technology (Govt. of India).

## Conflict of Interest

The authors declare no conflict of interest.

## Keywords

bioimaging, biosensing, drug delivery, gene delivery, graphene-based materials, stem cell differentiation, tissue engineering

Received: March 12, 2018

Revised: April 25, 2018

Published online:

- 
- [1] W. Wei, X. Qu, *Small* **2012**, *8*, 2138.  
 [2] V. B. Mohan, K. T. Lau, D. Hui, D. Bhattacharyya, *Composites, Part B* **2018**, *142*, 200.  
 [3] Y. Zhou, J. Yang, X. Cheng, N. Zhao, H. Sun, D. Li, *RSC Adv.* **2013**, *3*, 3391.  
 [4] B. Bhushan, *Springer Handbook of Nanotechnology*, Springer Science & Business Media, Germany **2010**.  
 [5] Y. Zhou, X. Jing, Y. Chen, *J. Mater. Chem. B* **2017**, *5*, 6451.  
 [6] M. A. Azam, N. N. Zulkapli, N. Dorah, R. N. Seman, M. H. Ani, M. S. Sirat, E. Ismail, F. B. Fauzi, M. A. Mohamed, B. Y. Majlis, *ECS J. Solid State Sci. Technol.* **2017**, *6*, 3035.

# Chapter 14

## Low-cost Paper Analytical Devices for Environmental and Biomedical Sensing Applications

H. Manisha, P. D. Priya Shwetha and K. S. Prasad

**Abstract** Over the last decade, the fabrication of analytical devices utilizing microfluidic structures and lab-on-a-chip platforms has shown breakthrough advancements, both for environmental and biological applications. The ASSURED criteria (affordable, sensitive, specific, user-friendly, robust, equipment-free, delivered), developed by the WHO for diagnostics devices, point towards the need of paper-based analytical devices (PAD) for diagnostics. On the other hand, cost-effective PADs owing the great advantage of affordable applicability in both resource-rich and -limited settings are recently employed for on-site environmental monitoring. In this book chapter, we will discuss about the brief history of paper analytical devices, fabrications, need, and its environmental and biomedical applications.

**Keywords** Paper analytical device · Point-of-care · Biomarkers  
Pesticides · Organic pollutants · Sensing

### 1 Paper Analytical Devices

Microfluidic devices provide innovative solutions to logistical problems, affording the advantages of high sensitivity, low cost, low reagent usage, small size, and several established fabrication techniques (Sackmann et al. 2014). Plethora of these devices has been used as a lab-on-chip type sensor for many biologically important molecules (Cate et al. 2014; Tomazelli Coltro et al. 2014). Among the developed microfluidic devices, PADs have tremendous amount of research attention due to their simplicity, capillary-based pumping ability, and low cost and easiness in

---

H. Manisha and P. D. Priya Shwetha: Equal contribution by these two authors.

---

H. Manisha · P. D. Priya Shwetha · K. S. Prasad (✉)  
Nanomaterials Research Laboratory (NMRL), Nano Division—Yenepoya Research Centre,  
Yenepoya University, Deralakatte, Mangalore 575018, India  
e-mail: ksprasadnair@yenepoya.edu.in

© Springer Nature Singapore Pte Ltd. 2018  
S. Bhattacharya et al. (eds.), *Environmental, Chemical and Medical Sensors*, Energy,  
Environment, and Sustainability, [https://doi.org/10.1007/978-981-10-7751-7\\_14](https://doi.org/10.1007/978-981-10-7751-7_14)

315

for H1 virus were found to be  $2.7 \times 10^3$  (particle forming units) pfu/assay and  $2.7 \times 10^4$  pfu/assay for H3. The as developed test was able to detect the viruses in the clinical samples and infected cell lysates (Lei et al. 2015).

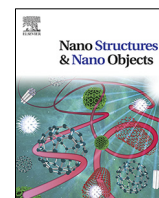
## 5 Conclusion

Since PADs are simple, cost effective, easy to handle and give on-site results, many paper sensors are fabricated for wide range of applications worldwide. These devices could be useful in rural areas and for developing countries where individuals find difficulty in bearing the cost of expensive instrumentation for diagnosis purpose as well as environmental monitoring. Researchers have shown new advantages that are obtained from paper-based hybrid microfluidic stages. Various identification systems such as colorimetric, fluorescence, chemiluminescence, ECL, and electrochemical location have been utilized as a part of microfluidic PADs investigation. Electrochemical discovery is additionally attractive for paper-based microfluidic devices, yet it is massive and costly. Albeit compact potentiostats are industrially accessible, the cost is still genuinely high. Colorimetric identification is exceptionally perfect with the way of ease to examine in resource-poor settings, yet affectability and quantitation are regularly bargained. In the most recent decades, advanced mobile phones have grown significantly. May the integration of technology and other electronic readers (e.g. glucometers) with PADs could give awesome effects on social insurance and ecological observing. For reliable PADs, it is essential to investigate the analytical performance under different test conditions (e.g. temperature, humidity, ambient light, complexity of the sample matrixes), perform stability studies (especially when sensitive reagents or materials are involved in the device architecture), and carry out interference studies.

**Acknowledgements** The authors are grateful to research grant from Department of Biotechnology, Government of India, and Yenepoya University.

## References

- Alkadir RS, Rossner A, Andreescu S (2015) Portable colorimetric paper-based biosensing device for the assessment of bisphenol A in indoor dust. *Environ Sci Technol* 49(16):9889–9897
- Apilux A, Dunchai W, Siangproh W, Praphairaksit N, Henry CS, Chailapakul O (2010) Lab-on-paper with dual electrochemical/colorimetric detection for simultaneous determination of gold and iron. *Anal Chem* 82(5):1727–1732
- Araújo AC, Song Y, Lundeberg J, Ståhl PL, Brumer H III (2012) Activated paper surfaces for the rapid hybridization of DNA through capillary transport. *Anal Chem* 84(7):3311–3317
- Badu-Tawiah AK, Lathwal S, Kaastrup K, Al-Sayah M, Christodouleas DC, Smith BS, Whitesides GM, Sikes HD (2015) Polymerization-based signal amplification for paper-based immunoassays. *Lab Chip* 15(3):655–659



# Revisiting fluorescent carbon nanodots for environmental, biomedical applications and puzzle about fluorophore impurities

H. Manisha<sup>a</sup>, P.D. Priya Swetha<sup>a</sup>, Yoon-Bo Shim<sup>b</sup>, K. Sudhakara Prasad<sup>a,\*</sup>

<sup>a</sup> Nanomaterial Research Laboratory (NMRL), Nano Division, Yenepoya Research Centre, Yenepoya (Deemed to be University), Deralakatte, Mangalore 575 018, India

<sup>b</sup> Department of Chemistry, Institute of BioPhysio Sensor Technology (IBST), Pusan National University, Busan 46241, South Korea

## ARTICLE INFO

### Article history:

Received 12 January 2019

Received in revised form 23 April 2019

Accepted 18 June 2019

### Keywords:

Photoluminescence

Biomedical

Environmental applications

Organic fluorophores

## ABSTRACT

Carbon nanodots (CNDs) are smaller nanoparticles with amorphous or crystalline core structure fabricated through easy synthesis procedures, and have advantage such as, bright luminescence, less cytotoxicity, biocompatibility, and tunable emission properties. Moreover, CNDs are found applications in environmental and biomedical sciences. Due to specific and sensitive nature, CNDs were used as a probe for detection of various metal ions, biomolecules, drug molecules etc. Because of the biocompatible nature, CNDs were used for bioimaging, targeted-drug delivery nano bio conjugates, platforms for cell differentiation, as well as in tissue engineering. But, as research focused towards the structural analysis, a doubt has been raised on the existence of CNDs. This review is focused on evaluating the recent trends in CNDs research, including CNDs synthesis, understanding of their PL properties, and also implications of organic impurities, and their influences on different applications of CND.

© 2019 Elsevier B.V. All rights reserved.

## Contents

1. Introduction.....	2
2. Synthesis.....	2
3. Formation mechanism of CNDs.....	2
4. Absorbance and PL properties.....	4
4.1. Down and Up-conversion luminescence.....	4
5. Toxicity.....	5
6. Applications.....	5
6.1. Bio imaging of cancer cells.....	5
6.1.1. Bacterial cell imaging.....	5
6.1.2. Differential staining.....	6
6.1.3. Antibacterial activity.....	6
6.2. Drug delivery mechanism.....	6
6.2.1. Passive targeting.....	6
6.2.2. Active targeting.....	6
6.3. Cell differentiation.....	7
6.4. Bone tissue engineering.....	8
6.5. Counterfeiting.....	9
6.6. Sensing.....	9
7. Perspective.....	9
7.1. Citric acid (CA) based CNDs.....	10
7.1.1. PL origin of CNDs with fluorescent by-products.....	11
7.1.2. Separation techniques for the next generation CNDs.....	11
8. Conclusion and outlook.....	11
Declaration of competing interest.....	12

\* Corresponding author.

E-mail address: [ksprasadnair@yenepoya.edu.in](mailto:ksprasadnair@yenepoya.edu.in) (K.S. Prasad).

emissive traps, edges, passivating agents, doping and also proposed as multi-chromophoric regions, cross link enhanced emission, quantum confinement effect etc. Even though, the low toxicity of CNDs is supported by many research investigations, yet the resistance to entry and aggregation of CNDs may prompt certain physiological effects. Also, CNDs were suffered from photobleaching due to cocktail of many structures, hence in this way; *in vivo* applications may require more profound examination. The prodrug and the nanocarriers combination are not completely comprehended, and the creation of CNDs with controlled size and properties are still a dream come true and it is the need of the hour to address these issue. For instance, basic methodologies to control the life-span of CNDs are not compelling by attenuating the temperature and aggregation of reactants. The detailed studies towards the reaction conditions as well as structural analysis will be required, so that avoiding of fluorophores could be achieved. The examination of properties, improvement of a novel combination and surface modification process may expand the biomedical utilizations of CNDs, which are of great interest in biosensing, bioimaging, drug delivery and advanced therapy. Fluorophore based CNDs were showed the similar properties like CNDs, which were identified at later stage of research, hence the focus as well as revisiting the applications has become necessity. Moreover, it is the need of the hour to decipher a standardized method for synthesis of CNDs to avoid erroneous conclusion with respect to the fluorescence of CNDs and to address the need for advances in the right direction with respect CNDs research. Finding new purification methods for CNDs are challenging, however recent efforts focusing on the introduction of multiple separation techniques could give significant improvement and breakthroughs for the extraction of high purity CNDs free from the so called fluorescent organic impurities. Hence, we stress for the importance of a comprehensive universal protocol for purification of CNDs to avoid the extraneous compounds.

#### Declaration of competing interest

The authors declare that they have no known competing financial interests or personal relationships that could have appeared to influence the work reported in this paper.

#### Acknowledgment

The authors are thankful to Yenepoya (Deemed to be university) for research (YU/Seed grant/060-2017) and infrastructure support.

#### References

- [1] H. Koo, M.S. Huh, J.H. Ryu, D.E. Lee, I.C. Sun, K. Choi, K. Kim, I.C. Kwon, Nanoprobes for biomedical imaging in living systems, *Nano Today* 6 (2011) 204–220.
- [2] M.K. Barman, A. Patra, Current status and prospects on chemical structure driven photoluminescence behaviour of carbon dots, *J. Photochem. Photobiol. C* 37 (2018) 1–22.
- [3] J. Chomoucka, J. Drbohlavova, V. Adam, R. Kizek, J. Hubalek, Synthesis of glutathione-coated quantum dots, in: *Electronics Technology, ISSE 2009, 32nd International Spring Seminar on 2009 May 13, IEEE, 2009*, pp. 1–5.
- [4] D. Bera, L. Qian, T.K. Tseng, P.H. Holloway, Quantum dots and their multimodal applications: a review, *Materials* 3 (2010) 2260–2345.
- [5] A.M. Bagher, Quantum dots applications, *Sensors Transducers* 198 (2016) 37–43.
- [6] A.L. Himaja, P.S. Karthik, S.P. Singh, Carbon dots: the newest member of the carbon nanomaterials family, *Chem. Rec.* 15 (2015) 595–615.
- [7] X. Wen, L. Shi, G. Wen, Y. Li, C. Dong, J. Yang, S. Shuang, Green synthesis of carbon nanodots from cotton for multicolor imaging, patterning, and sensing, *Sensors Actuators B* 221 (2015) 769–776.
- [8] W. Liu, C. Li, Y. Ren, X. Sun, W. Pan, Y. Li, J. Wang, W. Wang, Carbon dots: surface engineering and applications, *J. Mater. Chem. B* 4 (2016) 5772–5788.
- [9] K.A. Ritter, J.W. Lyding, The influence of edge structure on the electronic properties of graphene quantum dots and nanoribbons, *Nature Mater.* 8 (2009) 235–242.
- [10] S.N. Baker, G.A. Baker, Luminescent carbon nanodots: emergent nanolights, *Angew. Chem. Int. Ed.* 49 (2010) 6726–6744.
- [11] H. Li, Z. Kang, Y. Liu, S.T. Lee, Carbon nanodots: synthesis, properties and applications, *J. Mater. Chem.* 22 (2012) 24230–24253.
- [12] L. Cao, X. Wang, M.J. Meziani, F. Lu, H. Wang, P.G. Luo, Y. Lin, B.A. Harruff, L.M. Veca, D. Murray, S.Y. Xie, Carbon dots for multiphoton bioimaging, *J. Am. Chem. Soc.* 129 (2007) 11318–11319.
- [13] S.T. Yang, L. Cao, P.G. Luo, F. Lu, X. Wang, H. Wang, M.J. Meziani, Y. Liu, G. Qi, Y.P. Sun, Carbon dots for optical imaging *in vivo*, *J. Am. Chem. Soc.* 131 (2009) 11308–11309.
- [14] J. Tang, B. Kong, H. Wu, M. Xu, Y. Wang, Y. Wang, D. Zhao, G. Zheng, Carbon nanodots featuring efficient FRET for real-time monitoring of drug delivery and two photon imaging, *Adv. Mater.* 25 (2013) 6569–6574.
- [15] J. Wang, C.F. Wang, S. Chen, Amphiphilic egg-derived carbon dots: Rapid plasma fabrication, pyrolysis process, and multicolor printing patterns, *Angew. Chem. Int. Ed.* 124 (2012) 9431–9435.
- [16] L. Zhou, Y. Lin, Z. Huang, J. Ren, X. Qu, Carbon nanodots as fluorescence probes for rapid, sensitive, and label-free detection of Hg<sup>2+</sup> and biothiols in complex matrices, *Chem. Commun* 48 (2012) 1147–1149.
- [17] V. Gupta, N. Chaudhary, R. Srivastava, G.D. Sharma, R. Bhardwaj, S. Chand, Luminescent graphene quantum dots for organic photovoltaic devices, *J. Am. Chem. Soc.* 133 (2011) 9960–99603.
- [18] H. Li, X. He, Z. Kang, H. Huang, Y. Liu, J. Liu, S. Lian, C.H. Tsang, X. Yang, S.T. Lee, Water-soluble fluorescent carbon quantum dots and photocatalyst design, *Angew. Chem. Int. Ed.* 49 (2010) 4430–4434.
- [19] V. Strauss, J.T. Margraf, C. Dolle, B. Butz, T.J. Nacken, J. Walter, W. Bauer, W. Peukert, E. Spiecker, T. Clark, D.M. Guldi, Carbon nanodots: toward a comprehensive understanding of their photoluminescence, *J. Am. Chem. Soc.* 136 (2014) 17308–17316.
- [20] R. Liu, D. Wu, X. Feng, K. Müllen, Bottom-up fabrication of photoluminescent graphene quantum dots with uniform morphology, *J. Am. Chem. Soc.* 133 (2011) 15221–15223.
- [21] M.J. Krysmann, A. Kelarakis, P. Dallas, E.P. Giannelis, Formation mechanism of carbogenic nanoparticles with dual photoluminescence emission, *J. Am. Chem. Soc.* 134 (2011) 747–750.
- [22] N. Basu, D. Mandal, Fluorescence response from the surface states of nitrogen-doped carbon nanodots: evidence of a heterogeneous population of molecular-sized fluorophores, *Photochem. Photobiol. Sci.* 18 (2019) 54–63.
- [23] P.G. Luo, S. Sahu, S.T. Yang, S.K. Sonkar, J. Wang, H. Wang, G.E. Cao, L. LeCroy, Y.P. Sun, Carbon “quantum” dots for optical bioimaging, *J. Mater. Chem. B* 1 (2013) 2116–2127.
- [24] J. Tang, B. Kong, H. Wu, M. Xu, Y. Wang, Y. Wang, D. Zhao, G. Zheng, Carbon nanodots featuring efficient FRET for real-time monitoring of drug delivery and two photon imaging, *Adv. Mater.* 25 (2013) 6569–6574.
- [25] J. Wang, C.F. Wang, S. Chen, Amphiphilic egg-derived carbon dots: Rapid plasma fabrication, pyrolysis process, and multicolor printing patterns, *Angew. Chem. Int. Ed.* 124 (2012) 9431–9435.
- [26] V. Gupta, N. Chaudhary, R. Srivastava, G.D. Sharma, R. Bhardwaj, S. Chand, Luminescent graphene quantum dots for organic photovoltaic devices, *J. Am. Chem. Soc.* 133 (2011) 9960–99603.
- [27] H. Li, X. He, Z. Kang, H. Huang, Y. Liu, J. Liu, S. Lian, C.H. Tsang, X. Yang, S.T. Lee, Water-soluble fluorescent carbon quantum dots and photocatalyst design, *Angew. Chem. Int. Ed.* 49 (2010) 4430–4434.
- [28] Z.L. Wu, P. Zhang, M.X. Gao, C.F. Liu, W. Wang, F. Leng, C.Z. Huang, One-pot hydrothermal synthesis of highly luminescent nitrogen-doped amphoteric carbon dots for bioimaging from *Bombyx mori* silk–natural proteins, *J. Mater. Chem. B* 1 (2013) 2868–2873.
- [29] Q. Wang, X. Liu, L. Zhang, Y. Lv, Microwave-assisted synthesis of carbon nanodots through an eggshell membrane and their fluorescent application, *Analyst* 137 (2012) 5392–5397.
- [30] S.S. Wee, Y.H. Ng, S.M. Ng, Synthesis of fluorescent carbon dots via simple acid hydrolysis of bovine serum albumin and its potential as sensitive sensing probe for lead (II) ions, *Talanta* 116 (2013) 71–76.
- [31] Q. Wang, X. Huang, Y. Long, X. Wang, H. Zhang, R. Zhu, L. Liang, P. Teng, H. Zheng, Hollow luminescent carbon dots for drug delivery, *Carbon* 59 (2013) 192–209.
- [32] Q. Liang, W. Ma, Y. Shi, Z. Li, X. Yang, Easy synthesis of highly fluorescent carbon quantum dots from gelatin and their luminescent properties and applications, *Carbon* 60 (2013) 421–428.
- [33] D. Sun, R. Ban, P.H. Zhang, G.H. Wu, J.R. Zhang, J.J. Zhu, Hair fiber as a precursor for synthesizing of sulfur- and nitrogen-co-doped carbon dots with tunable luminescence properties, *Carbon* 64 (2013) 424–434.
- [34] A. Sachdev, I. Matai, S.U. Kumar, B. Bhushan, P. Dubey, P. Gopinath, A novel one-step synthesis of PEG passivated multicolour fluorescent carbon dots for potential biolabeling application, *RSC Adv.* 3 (2013) 16958–16961.





# Sodium fluoride induced skeletal muscle changes: Degradation of proteins and signaling mechanism<sup>☆</sup>

P. Sudheer Shenoy<sup>a,\*</sup>, Utsav Sen<sup>a,1</sup>, Saketh Kapoor<sup>a,1</sup>, Anu V. Ranade<sup>b</sup>, Chitta R. Chowdhury<sup>c,d</sup>, Bipasha Bose<sup>a,\*\*</sup>

<sup>a</sup> Stem Cells and Regenerative Medicine Centre, Yenepoya Research Centre, Yenepoya Deemed to be University, University Road, Mangalore, 575018, Karnataka, India

<sup>b</sup> College of Medicine, University of Sharjah, United Arab Emirates

<sup>c</sup> Department of Oral Biology & Genomic Studies, A.B.Shetty Memorial Institute of Dental Sciences, Nitte University, Mangalore, 575018, Karnataka, India

<sup>d</sup> School of Health and Life Sciences, Biomedical and Environmental Health Group, De Montfort University, Leicester, United Kingdom



## ARTICLE INFO

### Article history:

Received 7 June 2018

Received in revised form

4 October 2018

Accepted 5 October 2018

Available online 10 October 2018

### Keywords:

Sodium fluoride (NaF)

Parts per million (ppm)

C2C12

Myoblasts

Differentiation

Myotubes

Hypertrophy

Atrophy

## ABSTRACT

Fluoride is a well-known compound for its usefulness in healing dental caries. Similarly, fluoride is also known for its toxicity to various tissues in animals and humans. It causes skeletal fluorosis leading to osteoporosis of the bones. We hypothesized that when bones are affected by fluoride, the skeletal muscles are also likely to be affected by underlying molecular events involving myogenic differentiation. Murine myoblasts C2C12 were cultured in differentiation media with or without NaF (1 ppm–5 ppm) for four days. The effects of NaF on myoblasts and myotubes when exposed to low (1.5 ppm) and high concentration (5 ppm) were assessed based on the proliferation, alteration in gene expression, ROS production, and production of inflammatory cytokines. Changes based on morphology, multinucleated myotube formation, expression of MyHC1 and signaling pathways were also investigated. Concentrations of NaF tested had no effects on cell viability. NaF at low concentration (1.5 ppm) caused myoblast proliferation and when subjected to myogenic differentiation it induced hypertrophy of the myotubes by activating the IGF-1/AKT pathway. NaF at higher concentration (5 ppm), significantly inhibited myotube formation, increased skeletal muscle catabolism, generated reactive oxygen species (ROS) and inflammatory cytokines (TNF- $\alpha$  and IL-6) in C2C12 cells. NaF also enhanced the production of muscle atrophy-related genes, myostatin, and atrogen-1. The data suggest that NaF at low concentration can be used as muscle enhancing factor (hypertrophy), and at higher concentration, it accelerates skeletal muscle atrophy by activating the ubiquitin-proteasome pathway.

© 2018 Elsevier Ltd. All rights reserved.

## 1. Introduction

Fluorine/Fluoride (F/F) is a highly electronegative and extremely reactive compound, and its levels in drinking water should not exceed 1.0 mg/L (1 ppm- Parts per million) (WHO, 2008). However, high fluoride levels ( $\sim$ 3 ppm) are present in water in fluorosis endemic areas and it has been reported that the source of natural fluoride is rocks and granules

(Dharmagunawardhane et al., 2016; Tsunogae et al., 2003). In addition to fluoride in nature, the human population is also exposed to fluoride mainly through drinking water, fluoride rich natural foodstuffs; fluoride supplemented marketed food, fluoridated dentifrices, fluoride varnish including fluoride mouth wash. Fluoride is also considered as an important beneficial element in human health, since it has an anti-cariogenic effect and maintenance of bone density. Therefore, the diet and drinking water contributes to approximately 0.05 mg/kg daily intake for an adult individual. Such a dose (0.5 mg/kg/day) can help reduce the rate of dental caries in humans. Fluoride reportedly exerts both positive and negative effects on human health (Edmunds and Smedley, 1996; Urbansky, 2002; Bailey et al., 2006; Nielsen, 2009).

Exposure to fluoride at low concentrations causes growth, development and maintenance of the skeletal systems

<sup>☆</sup> This paper has been recommended for acceptance by Dr. D Carpenter.

\* Corresponding author.

\*\* Corresponding author.

E-mail addresses: [shenoy@yenepoya.edu.in](mailto:shenoy@yenepoya.edu.in), [shenoy2000@yahoo.com](mailto:shenoy2000@yahoo.com) (P.S. Shenoy), [Bipasha.bose@yenepoya.edu.in](mailto:Bipasha.bose@yenepoya.edu.in), [Bipasha.bose@gmail.com](mailto:Bipasha.bose@gmail.com) (B. Bose).

<sup>1</sup> Equally contributing second authors.

specific E3 ligases, such as atrogin-1 and MuRF1 and increasing intracellular ubiquitin–proteasome pathway (McFarlane et al., 2006; Lokireddy et al., 2012). In this case, we have also observed the role of high concentrations of NaF (5 ppm) leading to the expression of myostatin, upregulated muscle-specific E3 ubiquitin ligases such as atrogin-1 and MuRF1, catabolic changes, and hence atrophied myotubes. The rate of protein degradation was significantly increased when compared with control myotubes (Fig. 6). An increase in signaling of TGF $\beta$  pathway and a decrease in IGF-1/PI3K/Akt signaling pathway takes place during skeletal muscle wasting (Glass, 2005; Tisdale, 2010; Sandri et al., 2004). In the current study, our results indicated a time-dependent increase of total and phosphorylated Akt at 5 ppm concentrations of NaF in differentiating myotubes with progressive atrophy that is opposite of what has been reported by Sandri et al., (2004) (Fig. 6A). Low levels of Akt coincided with decreased protein synthesis and increase in the activity of FoxO transcription factors which further induce the expression of muscle-specific E3 ligases to enhance skeletal muscle catabolism during cancer cachexia (Sandri et al., 2004; Waddell et al., 2008).

NaF from past few decades is known for its toxic effects on human populations at higher concentrations. There are conflicting reports on the presence of fluoride (safe dose) in drinking water. Ingested fluoride is readily absorbed and gets distributed in the body; highest amount being retained in the bone and teeth (ASTDR, 2003). The occurrence of fluorosis is seen both in younger and aged individuals, the severity of fluoride intake causes changes in the musculoskeletal system such as deformity of the skeleton, degeneration of cartilage and skeletal muscle etc. Further investigations (*in vitro* and *in vivo*) are required to find out the long-term exposure of the safe dose, and exact role played by NaF on skeletal muscle and NaF toxicity reversal mechanisms.

## 5. Conclusion

Findings from our study indicate that NaF at low concentration can stimulate proliferation and differentiation of myoblasts and require a very high concentration to induce cell death and apoptosis in myoblasts. Furthermore at low concentration NaF causes excessive proliferation of myoblasts and causes hypertrophy of the myotubes during differentiation and can be possibly be used as muscle enhancing factor. At higher concentrations, NaF causes atrophy of the myotubes and can be understood as toxic for muscle growth and development.

## Acknowledgments

The authors would like to thank the Yenepoya Research Centre, Yenepoya University Mangalore for its infrastructure and core-facility support for conducting this research. This research was funded by Yenepoya Deemed to be University, India seed grant (YU/SG/059-2017) and grant from Department of Science and Technology, India (DST, EMR/2017/000591) Government of India, awarded to the principal investigator (Sudheer Shenoy P). The authors would also like to thank Dr. Harsha Gowda, Group Leader, QIMR Berghofer Medical Research Institute, University of Queensland Australia for gifting the C2C12 cell line, Anu V. Ranade (Assistant Prof University of Sharjah, UAE) for gifting four antibodies and Prof. Chitta R. Chowdhury for his support, valuable discussion, and inputs on fluoride research.

## Appendix A. Supplementary data

Supplementary data to this article can be found online at <https://doi.org/10.1016/j.envpol.2018.10.034>.

## References

- Antonio, L.S., Jeggle, P., MacVinish, L.J., et al., 2017. The effect of fluoride on the structure, function, and proteome of a renal epithelial cell monolayer. *Environ. Toxicol.* 32 (4), 1455–1467.
- Antonarakis, G.S., Moseley, R., Waddington, R.J., 2014. Differential influence of fluoride concentration on the synthesis of bone matrix glycoprotein within mineralizing bone cells *in vitro*. *Acta Odontol. Scand.* 72 (8), 1066–1069.
- Asawa, K., Singh, A., Bhat, N., Tak, M., et al., 2015. Association of temporomandibular joint signs & symptoms with dental fluorosis & skeletal manifestations in endemic fluoride areas of dungarpur district, Rajasthan, India. *J. Clin. Diagn. Res.* 9 (12), ZC18–21.
- ASTDR, 2003. Toxicological Profile for Fluorides, Hydrogen Fluoride, and Fluorine. US Department of Health and Human Services, Public Health Service, Atlanta, GA.
- Bailey, K., Chilton, J., Dahi, E., et al., 2006. Fluoride in Drinking-water. World Health Organization, Geneva.
- Berkes, C.A., Tapscott, S.J., 2005. MyoD and the transcriptional control of myogenesis. *Semin. Cell Dev. Biol.* 16 (4–5), 585–595.
- Buzalaf, M.A., Whitford, G.M., 2011. Fluoride metabolism. *Monogr. Oral Sci.* 22, 20–36.
- Carson, J.A., Baltgalvis, K.A., 2010. Interleukin 6 as a key regulator of muscle mass during cachexia. *Exerc. Sport Sci. Rev.* 38 (4), 168–176.
- Chakraborti, D., Rahman, M.M., Chatterjee, A., et al., 2016. Fate of over 480 million inhabitants living in arsenic and fluoride endemic Indian districts: magnitude, health, socio-economic effects and mitigation approaches. *J. Trace Elem. Med. Biol.* 38, 33–45.
- Chinoy, N.J., Memon, M.R., 2001. Beneficial effects of some vitamins and calcium on fluoride and aluminium toxicity on gastrocnemius muscle and liver of male mice. *Fluoride* 34 (1), 21–33.
- Dabrowska, E., Letko, R., Balunowska, M., 2006. Effect of sodium fluoride on the morphological picture of the rat liver exposed to NaF in drinking water. *Adv. Med. Sci.* 51 (Suppl. 1), 91–95.
- De Falco, M., De Luca, A., 2006. Involvement of cdk5 and cyclins in muscle differentiation. *Eur. J. Histochem.* 50 (1), 19–23.
- Denbesten, P., Li, W., 2011. Chronic fluoride toxicity: dental fluorosis. *Monogr. Oral Sci.* 22, 81–96.
- DeVol, D.L., Rotwein, P., Sadow, J.L., et al., 1990. Activation of insulin-like growth factor gene expression during work-induced skeletal muscle growth. *Am. J. Physiol.* 259 (1 Pt 1), E89–E95.
- Dharmagunawardhane, H.A., Malaviarachchi, S.P.K., Burgess, W., 2016. Fluoride content of minerals in gneissic rocks at an area of endemic dental fluorosis in Sri Lanka: estimates from combined petrographic and electron microprobe analysis. *Ceylon J Sci* 45 (1), 57–66.
- Edmunds, W.M., Smedley, P.L., 1996. Groundwater geochemistry and health: an overview. In: Appleton, Fuge, McCall (Eds.), *Environmental Geochemistry and Health*, vol. 113. Geological Society Special Publication, pp. 91–105.
- Feng, D., Huang, H., Yang, Y., et al., 2015. Ameliorative effects of N-acetylcysteine on fluoride-induced oxidative stress and DNA damage in male rats' testis. *Mutat. Res. Genet. Toxicol. Environ. Mutagen* 792, 35–45.
- Ge, Y.M., Ning, H.M., Feng, C.P., et al., 2006. Apoptosis brain cells of offspring rats exposed to high fluoride and low iodine. *Fluoride* 39 (3), 173–179.
- Glass, D.J., 2005. Skeletal muscle hypertrophy and atrophy signaling pathways. *Int. J. Biochem. Cell Biol.* 37 (10), 1974–1984.
- Gomes-Marcondes, M.C., Tisdale, M.J., 2002. Induction of protein catabolism and the ubiquitin-proteasome pathway by mild oxidative stress. *Cancer Lett.* 180 (1), 69–74.
- Gu, X., Han, D., Chen, W., et al., 2016. SIRT1-mediated FoxOs pathways protect against apoptosis by promoting autophagy in osteoblast-like MC3T3-E1 cells exposed to sodium fluoride. *Oncotarget* 7 (40), 65218.
- Hwang, S.Y., Kang, Y.J., Sung, B., et al., 2015. Folic acid promotes the myogenic differentiation of C2C12 murine myoblasts through the Akt signaling pathway. *Int. J. Mol. Med.* 36 (4), 1073–1080.
- Kale, M., Rathore, N., John, S., et al., 1999. Lipid peroxidative damage on pyrethroid exposure and alterations in antioxidant status in rat erythrocytes: a possible involvement of reactive oxygen species. *Toxicol. Lett.* 105 (3), 197–205.
- Kebede, A., Retta, N., Abuye, C., et al., 2016. Dietary fluoride intake and associated skeletal and dental fluorosis in school age children in rural Ethiopian rift valley. *Int. J. Environ. Res. Publ. Health* 13 (8).
- Kitzmann, M., Fernandez, A., 2001. Crosstalk between cell cycle regulators and the myogenic factor MyoD in skeletal myoblasts. *Cell. Mol. Life Sci.* 58 (4), 571–579.
- Krishnamachari, K.A., 1986. Skeletal fluorosis in humans: a review of recent progress in the understanding of the disease. *Prog. Food Nutr. Sci.* 10 (3–4), 279–314.
- Kumar, A., Bhatnagar, S., Paul, P.K., 2012. TWEAK and TRAF6 regulate skeletal muscle atrophy. *Curr. Opin. Clin. Nutr. Metab. Care* 15 (3), 233–239.
- Lecker, S.H., Jagoe, R.T., Gilbert, A., et al., 2004. Multiple types of skeletal muscle atrophy involve a common program of changes in gene expression. *Faseb. J.* 18 (1), 39–51.
- Li, J., Wen, C., Yang, S., et al., 1989. A preliminary analysis on the isoenzymes of SLDH from patients with endemic fluorosis. *Endem. Dis. Bull.* 4, 70–73.
- Li, Y.P., Reid, M.B., 2000. NF- $\kappa$ B mediates the protein loss induced by TNF- $\alpha$  in differentiated skeletal muscle myotubes. *Am. J. Physiol. Regul. Integr. Comp. Physiol.* 279 (4), R1165–R1170.



# Changes in the expression level of IL-17A and p53-fibrinolytic system in smokers with or without COPD

Mahesh Manjunath Gouda<sup>1</sup> · Sadiya Bi Shaikh<sup>1</sup> · Deepu Chengappa<sup>2</sup> · Irfan Kandhal<sup>2</sup> · Ashwini Shetty<sup>3</sup> · Yashodhar Bhandary<sup>1</sup>

Received: 19 July 2018 / Accepted: 19 September 2018  
© Springer Nature B.V. 2018

## Abstract

COPD is a chronic airway inflammatory disease characterized mainly by neutrophil airway infiltrations. The neutrophil airway inflammation is mainly mediated through a key player like the pro-inflammatory cytokine IL-17A which is involved in the modulation of p53-fibrinolytic system. This study was undertaken to examine the molecular changes for the expressions of IL-17A and p53-fibrinolytic system in smokers with or without COPD. Blood and serum samples were collected from ten patients of smokers having COPD and ten samples from smokers without COPD and ten healthy control subjects. Western blot analyses were performed to evaluate the expressions of IL-17A, p53 and PAI-1. Apoptosis was assessed by immunoblot for cleaved caspase-3. In addition, FEV<sub>1</sub>% was also determined of these patients. qRT-PCR was done to detect the gene expression study from the blood samples on p53-fibrinolytic components. A significant difference was found in the expression levels of IL-17A in smokers with COPD patient when compared to smokers without COPD and the control subjects. Similarly the smokers with COPD showed significant increase in the fibrinolytic component PAI-1 as well as in expression levels of p53 when compared to smokers without COPD and normal subjects. Increased cleaved caspase-3 may also promote apoptosis. The expression pattern of the IL-17A in chronic obstructive pulmonary distress syndrome samples was increased as compared of those of normal samples, and their main role in the regulation of and p53-fibrinolytic system makes these components as a predictive prominent component in smokers with COPD.

**Keywords** Chronic obstructive pulmonary disease (COPD) · Cigarette smoke · P53 · P-p53 · Urokinase plasminogen activator (uPA) · Urokinase plasminogen activator receptor (uPAR) · Plasminogen activator inhibitor-1 (PAI-I)

## Introduction

Chronic obstructive pulmonary disease (COPD) is a prime public health issue that affects universal population of about 200 million people and many more globally leading to millions of deaths every year [1, 2]. COPD is considered to

be the fourth highest leading cause of death [1] and is also said that by 2030 COPD will become the third most cause of mortality among individuals over the world [3, 4]. About 3.49% prevalence of COPD is found in India among adults of age group more than 35 years [3]. COPD is a chronic inflammatory respiratory disorder in which cigarette smoke

✉ Yashodhar Bhandary  
yash28bhandary@gmail.com;  
yashbhandary@yenepoya.edu.in

Mahesh Manjunath Gouda  
maheshmg@yenepoya.edu.in

Sadiya Bi Shaikh  
ssadiya86@gmail.com

Deepu Chengappa  
deepuchengappa@gmail.com

Irfan Kandhal  
irfan@yenepoya.edu.in

Ashwini Shetty  
drashwinishetty11@yahoo.com

<sup>1</sup> Yenepoya Research Centre, Yenepoya (Deemed to be University), Deralakatte, Mangalore, Karnataka 575 018, India

<sup>2</sup> Department of Pulmonary Medicine, Yenepoya Medical College (Deemed to be University), Deralakatte, Mangalore, Karnataka 575018, India

<sup>3</sup> Department of Anatomy, Yenepoya Medical College (Deemed to be University), Deralakatte, Mangalore, Karnataka 575018, India

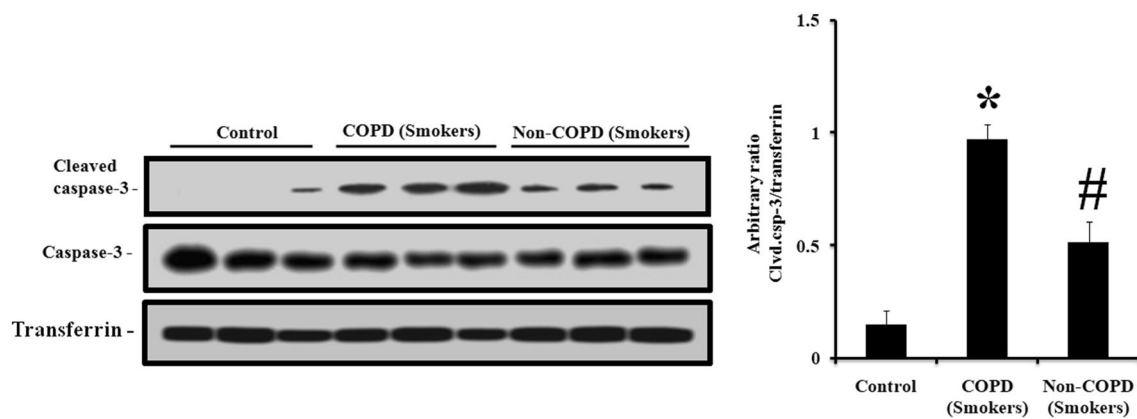


**Fig. 4** Expression levels of cleaved caspase-3 in smokers with or without COPD and healthy control subjects. Blood samples were centrifuged to collect serum. Serum samples from three different groups (control, smokers with COPD and smokers without COPD) were analyzed for western blotting to observe the expression levels of cleaved

caspase-3, caspase-3 and normalized with transferrin; representative blots are shown. Quantitative values for each treatment were obtained by densitometric analysis. \* $p < 0.01$  compared to control; # $p < 0.01$  compared to smokers with COPD (Mean  $\pm$  SD,  $n = 3$ )

**Funding** This research work received funding from Yenepoya University Seed Grant No. 050-2015.

### Compliance with ethical standards

**Conflict of interest** The authors declare that they have no conflict of interest.

### References

- Wen L, Krauss-Etschmann S, Petersen F, Yu X (2018) Autoantibodies in chronic obstructive pulmonary disease. *Front Immunol* 9:66
- Mannino DM (2002) COPD: epidemiology, prevalence, morbidity and mortality, and disease heterogeneity. *Chest* 121:121S–126S
- Kuwal A, Joshi V, Dutt N, Singh S, Agarwal KC, Purohit G (2018) A prospective study of bacteriological etiology in hospitalized acute exacerbation of COPD patients: relationship with lung function and respiratory failure. *Turk Thorax J* 19(1):19
- WHO (2007) Burden of COPD. <http://www.who.int/respiratory/copd/burden/en/>. Accessed on 7 Feb 2016
- Le Rouzic O, Pichavant M, Frealle E, Guillon A, Si-Tahar M, Gosset P (2017) Th17 cytokines: novel potential therapeutic targets for COPD pathogenesis and exacerbations. *Eur Respir J* 50:1602434
- Rovina N, Koutsoukou A, Koulouris NG (2013) Inflammation and immune response in COPD: where do we stand? *Mediators Inflamm*. <https://doi.org/10.1155/2013/412735>
- Cosio MG, Saetta M, Agusti A (2009) Immunologic aspects of chronic obstructive pulmonary disease. *N Engl J Med* 360:2396–2454
- Saetta M, Di Stefano A, Turato G, Facchini FM, Corbino L, Mapp CE, Maestrelli P, Ciaccia A, Fabbri LM (1998) CD<sup>8+</sup> T-lymphocytes in peripheral airways of smokers with chronic obstructive pulmonary disease. *Am J Respir Crit Care Med* 157:822–826
- Biernacki W, Kharitonov S, Barnes P (2003) Increased leukotriene B4 and 8-isoprostane in exhaled breath condensate of patients with exacerbations of COPD. *Thorax* 58:294–298
- Spencer S, Calverley PM, Burge PS, Jones PW (2004) Impact of preventing exacerbations on deterioration of health status in COPD. *Eur Respir J* 23:698–702
- Kessler R, Ståhl E, Vogelmeier C, Haughney J, Trudeau E, Löfdahl CG, Partridge MR (2006) Patient understanding, detection, and experience of COPD exacerbations: an observational, interview-based study. *Chest* 130:133–142
- Gompertz S, Baley DL, Hill SL, Stockley RA (2001) Relationship between airway inflammation and the frequency of exacerbations in patients with smoking related COPD. *Thorax* 56:36–41
- Boschetto P, Quintavalle S, Miotto D, Lo Cascio N, Zeni E, Mapp CE (2006) Chronic obstructive pulmonary disease (COPD) and occupational exposures. *J Occup Med Toxicol* 7:1–11
- Molano NA (2004) Genetics of COPD. *Chest* 125:1929–1940
- Singh D, Edwards L, Tal-Singer R, Rennard S (2010) Sputum neutrophils as a biomarker in COPD: findings from the ECLIPSE study. *Respir Res* 15:77
- Le Rouzic O, Pichavant M, Frealle E, Guillon A, Si-Tahar M, Gosset P (2017) Th17 cytokines: novel potential therapeutic targets for COPD pathogenesis and exacerbations. *Eur Respir J* 50:1602434
- Hansen MJ, Chan SP, Langenbach SY, Dousha LF, Jones JE, Yalmaz S, Seow HJ, Vlahos R, Anderson GP, Bozinovski S (2014) IL-17A and serum amyloid A are elevated in a cigarette smoke cessation model associated with the persistence of pigmented macrophages, neutrophils and activated NK cells. *PLoS ONE* 9:e113180
- Bhandary YP, Shetty SK, Marudamuthu AS, Midde KK, Ji HL, Shams H, Subramaniam R, Fu J, Idell S, Shetty S (2015) Plasminogen activator inhibitor-1 in cigarette smoke exposure and influenza A virus infection-induced lung injury. *PLoS ONE* 10:e0123187
- Shetty SK, Bhandary YP, Marudamuthu AS, Abernathy D, Velusamy T, Starcher B, Shetty S (2012) Regulation of airway and alveolar epithelial cell apoptosis by p53-Induced plasminogen activator inhibitor-1 during cigarette smoke exposure injury. *Am J Respir Cell Mol Biol* 47:474–483



# Identification, isolation, quantification and systems approach towards CD34, a biomarker present in the progenitor/stem cells from diverse lineages



Sudheer Shenoy P. <sup>\*,1</sup>, Bipasha Bose <sup>\*,1</sup>

Department of Stem Cell and Regenerative Medicine, Yenepoya Research Center, Yenepoya University, University Road, Mangalore 575018, Karnataka, India

## ARTICLE INFO

### Article history:

Received 1 May 2017

Received in revised form 28 June 2017

Accepted 30 June 2017

Available online 4 July 2017

### Keywords:

Mesenchymal stem cells

Skin

Skeletal muscle

Liver

CD34<sup>+</sup> cells

Isolation

Identification

Quantification

Proteomics

Mass spectrometry

## ABSTRACT

Mesenchymal stem cells (MSCs) constitute the diverse progenitor populations in almost every tissue and are of immense importance in the field of regenerative medicine. CD34 is a cell surface glycoprotein identified first as a marker for the MSCs of hematopoietic origin. CD34 is now known to be expressed in cells of diverse lineages (tissues of non-hematopoietic origin) such as ectoderm, mesoderm and endoderm and is considered as a general marker for progenitor cells. Here, we present detailed protocols to obtain pure populations of MSCs from three diverse lineages such as skeletal muscle, skin, and liver from mouse tissues. We also present here the protocol for systems biology approach (proteomic analysis) of these purified cells. This proteomic approach can elucidate key signalling pathways and proteins utilized by these CD34 positive cells in undifferentiated and differentiated conditions. Furthermore in-depth proteomic analysis can also identify the altered proteome which is responsible for their function during non-clinical and clinical conditions.

© 2017 Elsevier Inc. All rights reserved.

## 1. Introduction

Mesenchymal stem cells (MSCs) are derived exclusively from mesenchyme, the embryonic connective tissue of mesodermal origin [1,2]. However, the name MSCs has also been interchangeably used for stromal cells of mesodermal origin. Such stromal cells primarily support the epithelial tubes, sacs or tissues. Diverse cell types given rise by the mesenchyme include cartilage, smooth muscle, pericytes, mesothelium, and fibroblasts. Bone marrow-derived MSC (BM-MSC) is a classical example [3]. BM-MSCs are currently also being used for treating serious problems like spinal cord injury [4]. Other types of MSCs, which have gained impetus in research and, up to a limited extent in clinical trials/applications are adipose tissue-derived MSC [5,6], Wharton jelly MSCs from cord blood [7], umbilical cord-derived MSCs [8] dental pulp MSC [9], MSC from nasal polyps [10], skeletal muscle-derived MSCs [11], amniotic fluid MSCs [12]. MSCs have been broadly identified

by cell surface marker expression profile and have been known for simultaneous expression of the markers like CD34, CD44, CD105, CD90, CD73 [13,14].

One of the important markers expressed on various kinds of MSCs is CD34 [13,15]. CD34 is a transmembrane glycoprotein. Clinically, CD34 is associated with the selection and enrichment of MSCs from bone marrow commonly offered as a therapy for leukaemia patients [16,17]. Due to these historical and clinical associations, it is a common misconception that CD34<sup>+</sup> cells in non-hematopoietic samples represent hematopoietic contamination. Regarding the tissue distribution, cells expressing CD34 are normally found in the umbilical cord and bone marrow as hematopoietic cells, a subset of mesenchymal stem cells, endothelial progenitor cells, endothelial cells of blood vessels but not lymphatic's (except pleural lymphatics), mast cells, a sub-population dendritic cells (which are factor XIIIa-negative) in the interstitium and around the adnexa of dermis of skin, as well as cells in soft tissue tumors like dermatofibrosarcoma protuberans (DFSP), gastrointestinal stromal tumor (GIST), solitary fibrous tumor (SFT), hemangiopericytoma (HPC), and to some degree in Malignant peripheral nerve sheath tumor MPNSTs, cells of haematological malignancies [18,19] and leukemic stem cells [20]. Also,

\* Corresponding authors.

E-mail addresses: [shenoy@yenepoya.edu.in](mailto:shenoy@yenepoya.edu.in), [shenoy2000@yahoo.com](mailto:shenoy2000@yahoo.com) (P. Sudheer Shenoy), [Bipasha.bose@yenepoya.edu.in](mailto:Bipasha.bose@yenepoya.edu.in), [Bipasha.bose@gmail.com](mailto:Bipasha.bose@gmail.com) (B. Bose).

<sup>1</sup> Equally contributing.

### 3.9. Systems biology approach towards the possible applicability of CD34<sup>+</sup> cells from diverse lineages as a biomarker for progenitor cells

The isolated and sorted CD34<sup>+</sup> and CD45<sup>-</sup> cells were expanded and processed for proteomic studies.

#### 3.9.1. Cell lysis and sample preparation for proteomics

Denaturation buffer, containing protease inhibitor cocktail (500  $\mu$ l), was added to the cells in the dish. Scrape the dish using a cell scraper, mix the solution and keep it on the ice. Centrifuge the solution at 20,000 $\times$ g to remove cell debris. Store the solution at 4 °C until further use.

Protein concentration was estimated from cellular extract using the Bradford Assay kit according to the manufacturer's instructions. Total cell extract (50  $\mu$ g) was taken for protein reduction by adding 5  $\mu$ L of reduction solution and maintain the reaction at 37 °C for 1 h. Protein alkylation was performed by adding 10  $\mu$ L of the alkylating solution and maintained the reaction at room temperature for one additional hour.

Total cell extract was loaded onto SDS-PAGE in a 12% precast gel (to fractionate the complex protein mixtures) according to the manufacturer's instructions, and the gels were stained with silver stain [42]. Each gel lane can be taken individually and can perform in-gel trypsin digestion of the gel fragments. Wash the gel fragments with 200  $\mu$ L of 0.1 M ammonium bicarbonate (AB) and 50% acetonitrile (AN) solution 3 times. Discard the wash solution. Further dry gel fragments in a speed vac.

Add trypsin 20  $\mu$ L to the gel fragments to hydrate it for 15 min cover the band with approximately 100  $\mu$ L of 0.1 M AB solution. Carry out the digestion for overnight at 37 °C. Collect the solution and save. Peptides extracted from the gel pieces after washes (200  $\mu$ L of 0.1 M AB and 50% AN solution) were pooled and dried in a speed vac. Extracted peptide solutions were transferred to the mass spectrometer. High-throughput LC-MS/MS data was collected for each single fraction obtained from pooled cell extract. Sample analysis method depends upon mass spectrometer used (please see the mass spectrometer user guide for sample analysis).

LC-MS/MS files can be processed through data bank search, protein inference, and quantitative analysis [43,44] (Fig.7).

## 4. Conclusion

In conclusion, CD34<sup>+</sup> cells have found a broad range of applications in regenerative medicine, right from transplantation of CD34<sup>+</sup> bone marrow stem cells to leukemic patients, spinal cord injury, liver cirrhosis and peripheral vascular disease. However, in most of the cases, the source of such CD34<sup>+</sup> cells, for clinical applications, have been from bone marrow. Considering the invasive procedure in bone marrow collection, isolation of CD34<sup>+</sup> cells from other sources like skin, skeletal muscle and liver will be indeed advantageous. Furthermore, these tissues may be a good source for the isolation CD34<sup>+</sup> progenitor cells which can be used in regenerative therapies.

## 5. Discussion

CD34<sup>+</sup>/45<sup>-</sup> are unique cell types that have been classically reported in hematopoietic lineage. However, we have identified the presence of such cell types in tissues from all lineages of non-hematopoietic origin such as liver, skin and adipose (unpublished results). Although, CD34<sup>+</sup>/45<sup>-</sup> cells are present in the non-hematopoietic lineages, functions or developmental pathways of these cells are not elucidated. Hence, systems approach to characterise CD34<sup>+</sup>/45<sup>-</sup> from all the non-hematopoietic lineages is likely

to provide strong clues regarding origin, migration of such cells during embryonic developmental stages. Moreover, the data obtained using systems approach would also be helpful in pathway curation which can, in turn, provide clues for using such cells for cell therapy applications.

## 6. Notes (trouble shooting)

- 1) All reagents and material used must be sterile
- 2) All tissue biopsies (skeletal muscle, skin and liver) should be obtained under the relevant Institutional animal ethics committee guidelines.
- 3) Age of the mouse is critical; younger animals will yield superior and more proliferative cells. Skeletal muscle biopsies must be collected freshly either from the both hind limbs or hind limbs and forelimbs combined from the wild-type mice (C57BL/6J). Skeletal muscle and liver biopsies collected should be kept in PBS at 4 °C/ice till further processing.
- 4) Isolated mesenchymal stem cells from all the three tissues can be expanded till passage 4 and stored in LN2 until further use. Reduce repeated trypsinization of isolated cells; use (0.05% trypsin-EDTA or TrypLE).
- 5) Isolated and sorted cells from skeletal muscle will require 7–8 days to get up to 60–70% confluence and additional 1–2 weeks for expansion and cryopreservation.
- 6) Isolated cells will be positive CD34, CD44, CD90, CD73, CD105, CD146 and negative for CD45, CD31, CD56, CD14.
- 7) Always prepare fresh dithiothreitol (DTT) and acrylamide solutions, storing these solutions and using them will cause non-specific labelling.

## Acknowledgements

The project involving the isolation of CD34<sup>+</sup>/45<sup>-</sup> from all three germ layers: ectoderm, mesoderm and endoderm and studying their cellular, molecular and functional similarities/differences has been funded by the Yenepoya University Seed Grant No- YU/Seed Grant/2015-042 awarded to the Principal Investigator Dr Bipasha Bose and the Co-Principal Investigator Dr Sudheer Shenoy P. The authors earlier published the original research article that includes isolation of CD34<sup>+</sup>/45<sup>-</sup> cells from muscle corresponding to this Protocol chapter in Bose et al. [33], where the funding source was duly acknowledged.

## References

- [1] A. Porcellini, Regenerative medicine: a review, Rev. Bras. Hematol. Hemoter. 31 (Suppl 2) (2009).
- [2] M.E. Kumar, P.E. Bogard, F.H. Espinoza, D.B. Menke, D.M. Kingsley, M.A. Krasnow, Mesenchymal cells defining a mesenchymal progenitor niche at single-cell resolution, Science 346 (2014) 1258810.
- [3] C. Pontikoglou, F. Deschaseaux, L. Sensebé, H.A. Papadaki, Bone marrow mesenchymal stem cells: biological properties and their role in hematopoiesis and hematopoietic stem cell transplantation, Stem Cell Rev. 7 (2011) 569–589.
- [4] M.V. Mendonça, T.F. Larocca, B.S. Souza, C.F. Villarreal, L.F. Silva, A.C. Matos, M. A. Novaes, C.M. Bahia, A.C. Martinez, C.M. Kaneto, S.B. Furtado, G.P. Sampaio, M.B. Soares, R.R. Dos Santos, Safety and neurological assessments after autologous transplantation of bone marrow mesenchymal stem cells in subjects with chronic spinal cord injury, Stem Cell Res. Ther. 5 (2014) 126.
- [5] K.A. Chang, J.H. Lee, Y.H. Suh, Therapeutic potential of human adipose-derived stem cells in neurological disorders, J. Pharmacol. Sci. 126 (2014) 293–301.
- [6] M. García-Contreras, C.D. Vera-Donoso, J.M. Hernández-Andreu, J.M. García-Verdugo, E. Oltra, Therapeutic potential of human adipose-derived stem cells (ADSCs) from cancer patients: a pilot study, PLoS One 9 (2014) e113288.
- [7] V. Aguilera, L. Briceño, H. Contreras, L. Lamperti, E. Sepúlveda, F. Díaz-Perez, M. León, C. Veas, R. Maura, J.R. Toledo, P. Fernández, A. Covarrubias, F.A. Zuñiga, C. Radojkovic, C. Escudero, C. Aguayo, Endothelium trans differentiated from wharton's jelly mesenchymal cells promote tissue regeneration: potential role of soluble pro-angiogenic factors, PLoS One 9 (2014) e111025.

# Use of Verbal Autopsy to Determine Underlying Cause of Death during Treatment of Multidrug-Resistant Tuberculosis, India

Poonam Ramesh Naik, Patrick K. Moonan, Abhay Subhashrao Nirgude, Hemant Deepak Shewade, Srinath Satyanarayana, Pracheth Raghuv eer, Malik Parmar, Chinnappareddy Ravichandra, Anil Sing arajipura

Of patients with multidrug-resistant tuberculosis (MDR TB), <50% complete treatment. Most treatment failures for patients with MDR TB are due to death during TB treatment. We sought to determine the proportion of deaths during MDR TB treatment attributable to TB itself. We used a structured verbal autopsy tool to interview family members of patients who died during MDR TB treatment in India during January–December 2016. A committee triangulated information from verbal autopsy, death certificate, or other medical records available with the family members to ascertain the underlying cause of death. For 66% of patient deaths (47/71), TB was the underlying cause of death. We assigned TB as the underlying cause of death for an additional 6 patients who died of suicide and 2 of pulmonary embolism. Deaths during TB treatment signify program failure; accurately determining the cause of death is the first step to designing appropriate, timely interventions to prevent premature deaths.

*Mycobacterium tuberculosis* resistant to  $\geq 2$  of the most potent TB drugs, isoniazid and rifampin, is classified as multidrug-resistant tuberculosis (MDR TB). Worldwide, an estimated 580,000 MDR TB cases emerge annually (1). Unfortunately, there are substantial gaps in MDR TB detection and treatment. Approximately 1 of 5 persons needing MDR TB treatment actually receive it, and among those who do receive treatment, less than half (48%) who start

treatment finish successfully (1,2). These rates are driven by treatment failure, loss to follow-up, and premature death. In 2016, the proportion of deaths during MDR TB treatment in India was higher than the global average (20% vs. 14%) (3).

India follows the routine surveillance and reporting guidelines recommended by the World Health Organization (WHO) and considers any death that occurs during TB treatment as a TB-related death. Several studies have used all-cause mortality as a surrogate marker of mortality attributable to TB (4–6). This method of attributing all-cause mortality can overestimate TB case-fatality rates. Accurately determining the cause of death is the first step to designing appropriate and timely interventions to prevent premature deaths.

In settings with no or poorly documented vital registration and medical certification of the cause of death, verbal autopsy can be an essential public health tool for obtaining a reasonable estimation of the cause structure of mortality (7). Verbal autopsy uses systematic retrospective inquiry of family members about the symptoms and signs of illness before death to help determine the putative medical cause of death (8). The demand for and use of verbal autopsy data has rapidly gained importance and has been used to set global health priorities (9,10). Verbal autopsy data may improve surveillance and program monitoring and evaluation and could stimulate change in public health policy (11–13). In our study, we used the verbal autopsy method to determine the underlying causes of death for persons who died during MDR TB treatment (online Technical Appendix, <https://wwwnc.cdc.gov/EID/article/24/3/17-1718-Techapp1.pdf>).

## Methods

### Study Design and Population

We conducted a cross-sectional study of patients who died during MDR TB treatment during January–December

Author affiliations: Yenepoya Medical College, Yenepoya University, Mangalore, India (P.R. Naik, A.S. Nirgude, P. Raghuv eer); Centers for Disease Control and Prevention, Atlanta, Georgia, USA (P.K. Moonan); International Union Against Tuberculosis and Lung Disease, New Delhi, India (H.D. Shewade, S. Satyanarayana); World Health Organization Country Office for India, New Delhi (M. Parmar); National Tuberculosis Institute, Bangalore, India (C. Ravichandra); Department of Health and Family Welfare, Government of Karnataka, Bangalore (A. Sing arajipura)

DOI: <https://doi.org/10.3201/eid2403.171718>

TB patients consuming alcohol (26). These data reinforce the need for professional counseling and psychiatric care integration for MDR TB care (2). A recent study assessed the feasibility of integrated psychiatric and medical TB care and treatment and suggested the immediate need in India (27). Third, our finding that male sex was associated with deaths due to causes other than TB may be helpful in generating hypotheses for further research, such as risk-factor analysis in a larger, more representative cohort of patients throughout India. Finally, we acknowledge that many TB-related deaths may occur before the start of MDR treatment, after completion of MDR treatment, and among persons lost to follow-up. We are hopeful our findings will stimulate further research to document all potential TB-related deaths in the community and aid in monitoring India's progress toward reducing TB deaths by 95% by 2035 (28).

### Acknowledgments

We thank all of the proxies and families who had the courage to participate in our research during a time of mourning, grief, and personal loss. We thank the state TB officer, district TB officers, and program staff of the districts and DR-TB centers who facilitated this study. We are indebted to our independent committee members for their time and expertise during the verbal autopsy review and deliberation: Prabha Adhikari, K.M. Akshaya, Deepu Chengappa. Special thanks to Viquar Ahmed, K.R. Nischith, and Reshma Acharya for their assistance with data acquisition and local coordination and to James Tobias for cartographic assistance.

The study was conducted as a part of the National Operational Research Training Course, 2016. This training project was conceived and implemented jointly by Central TB Division, Directorate General of Health Services, Ministry of Health and Family Welfare, Government of India; the National TB Institute, Directorate General of Health Services, Ministry of Health and Family Welfare, Government of India Bangalore, India; the International Union Against Tuberculosis and Lung Diseases, South-East Asia Regional Office, New Delhi, India; and the Division of Global HIV and TB, Center for Global Health, US Centers for Disease Control and Prevention. This study was funded by the International Union Against Tuberculosis and Lung Diseases (South-East Asia Regional Office, New Delhi, India). **The travel costs associated with data collection were funded by Yenepoya University, Mangalore, Karnataka, India**

Author contributions: study conception and design, P.R.N., P.K.M., A.S.N., H.D.S., M.P., and S.S.; data collection and data entry, P.R.N., A.S.N., P.R., H.D.S.; data analysis and interpretation, P.R.N., A.S.N., P.K.M., S.S., H.D.S., P.R., C.R.; article first draft, P.R.N., P.K.M., S.S., H.D.S., A.S.N., R.C., A.S., M.P. All authors provided critical comments and approval of the final article.

### About the Author

Dr. Naik is a professor in the Department of Community Medicine, Yenepoya Medical College, Mangalore, and deputy director of the Directorate of Rural Health Care and Development, Yenepoya University. Her primary research interests include tuberculosis, noncommunicable diseases, health system research, and adolescent health.

### References


1. World Health Organization. Global tuberculosis report. Geneva: The Organization; 2016 [cited 2017 Jul 24]. [http://www.who.int/tb/publications/global\\_report/en/](http://www.who.int/tb/publications/global_report/en/)
2. Central Tuberculosis Division, Directorate General of Health Services, Ministry of Health and Family Welfare. Guidelines on programmatic management of drug resistant TB (PMDT) in India. New Delhi: The Directorate; 2012 [cited 2017 Jul 24]. <https://tbcindia.gov.in/WriteReadData/1892/8320929355Guidelines%20for%20PMDT%20in%20India%20-%20May%202012.pdf>
3. Central Tuberculosis Division, Directorate General of Health Services. TB India 2017, Revised National TB Control Programme, annual status report. New Delhi: The Directorate; 2016 [cited 2017 Jul 24]. <https://tbcindia.gov.in/WriteReadData/TB%20India%202017.pdf>
4. Lin CH, Lin CJ, Kuo YW, Wang JY, Hsu CL, Chen JM, et al. Tuberculosis mortality: patient characteristics and causes. *BMC Infect Dis.* 2014;14:5. <http://dx.doi.org/10.1186/1471-2334-14-5>
5. Rao VK, Lademarco EP, Fraser VJ, Kollef MH. The impact of co-morbidity on mortality following in-hospital diagnosis of tuberculosis. *Chest.* 1998;114:1244–52. <http://dx.doi.org/10.1378/chest.114.5.1244>
6. Hansel NN, Merriman B, Haponik EF, Diette GB. Hospitalizations for tuberculosis in the United States in 2000: predictors of in-hospital mortality. *Chest.* 2004;126:1079–86. <http://dx.doi.org/10.1378/chest.126.4.1079>
7. World Health Organization. Verbal autopsy standards: The 2012 WHO verbal autopsy instrument. Geneva: The Organization; 2012 [cited 2017 Jun 28]. [http://www.who.int/healthinfo/statistics/WHO\\_VA\\_2012\\_RC1\\_Instrument.pdf](http://www.who.int/healthinfo/statistics/WHO_VA_2012_RC1_Instrument.pdf)
8. Indian Council of Medical Research. Study on causes of death by verbal autopsy in India. New Delhi: The Council; 2009 [cited 2017 Jul 24]. [http://www.icmr.nic.in/final/causes\\_death/Contents%20NCD.pdf](http://www.icmr.nic.in/final/causes_death/Contents%20NCD.pdf)
9. Setel PW, Sankoh O, Rao C, Velkoff VA, Mathers C, Gonghuan Y, et al. Sample registration of vital events with verbal autopsy: a renewed commitment to measuring and monitoring vital statistics. *Bull World Health Organ.* 2005;83:611–7.
10. Lopez AD. Counting the dead in China. *BMJ.* 1998;317:1399–400. <http://dx.doi.org/10.1136/bmj.317.7170.1399>
11. Murray CJL, Lozano R, Flaxman AD, Serina P, Phillips D, Stewart A, et al. Using verbal autopsy to measure causes of death: the comparative performance of existing methods. *BMC Med.* 2014;12:5. <http://dx.doi.org/10.1186/1741-7015-12-5>
12. Palanivel C, Yadav K, Gupta V, Rai SK, Misra P, Krishnan A. Causes of death in rural adult population of North India (2002–2007), using verbal autopsy tool. *Indian J Public Health.* 2013;57:78–83. <http://dx.doi.org/10.4103/0019-557X.114988>
13. Jha P. Reliable direct measurement of causes of death in low- and middle-income countries. *BMC Med.* 2014;12:19. <http://dx.doi.org/10.1186/1741-7015-12-19>
14. World Health Organization. Medical certification of cause of death. Geneva: The Organization; 1979 [cited 2017 Jul 24]. <http://apps.who.int/iris/bitstream/10665/405571/9241560622.pdf>



BRIEF REPORT



## Vanillin derivative inhibits quorum sensing and biofilm formation in *Pseudomonas aeruginosa*: a study in a *Caenorhabditis elegans* infection model

 Rajesh P. Shastry<sup>a</sup> , Sudeep D. Ghate<sup>a</sup>, B. Sukesh Kumar<sup>a</sup>, B. S. Srinath<sup>b</sup> and Vasanth Kumar<sup>c</sup>

<sup>a</sup>Division of Microbiology and Biotechnology, Yenepoya Research Centre, Yenepoya (Deemed to be University), Deralakatte, Mangalore, Karnataka, India; <sup>b</sup>Department of Studies and Research in Microbiology, Post Graduate Centre, Mangalore University, Kodagu, Mangalore, Karnataka, India; <sup>c</sup>PG Department of Chemistry, Shri Dharmasthala Manjunatheshwara College (Autonomous), Ujire, Karnataka, India

### ABSTRACT

Vanillin and its derivative, (4-((E)-(4-hydroxy-2-methylphenylimino)methyl)-2-methoxyphenol (MMP) were showed clear inhibition of violacein and pyocyanin at sub-MICs indicating a possible quorum quenching effect of both the compounds. MMP was able to inhibit the biofilm formation in *Pseudomonas aeruginosa* PAO1 at 125 µg/mL ( $p < 0.05$ ), while vanillin at 250 µg/mL ( $p < 0.05$ ) indicating that they act against quorum sensing regulated biofilm formation. The inhibition of biofilm was confirmed by visualization through fluorescence microscopy followed by docking analysis of molecules against quorum sensing activator proteins. *Caenorhabditis elegans* survival assay revealed that vanillin and MMP were able to increase survival of *C. elegans* from *P. aeruginosa* PAO1 infection. The study showed that the potent features of the MMP and vanillin in inhibiting the quorum sensing regulated virulence and biofilm, which was proved in *C. elegans* infection model as well as molecular docking studies.


### ARTICLE HISTORY

Received 1 December 2020  
Accepted 3 February 2021

### KEYWORDS

Anti-quorum sensing;  
*Pseudomonas aeruginosa*;  
vanillin; *Caenorhabditis elegans*;  
biofilm

CONTACT Rajesh P. Shastry  [rps Shastry@yenepoya.edu.in](mailto:rps Shastry@yenepoya.edu.in)

 Supplemental data for this article can be accessed at <https://doi.org/10.1080/14786419.2021.1887866>.

© 2021 Informa UK Limited, trading as Taylor & Francis Group

## 2.5. Molecular docking

To understand the mechanism of interaction between quorum sensing genes and QSI (vanillin and MMP), a molecular dock program was utilized. The docking affinity of MMP with different protein complexes was compared to the docking score of vanillin (supplementary material Table S2). This inference of the MMP is better than vanillin and might inhibit the quorum sensing regulated biofilm properties through the inhibition of QS gene expression. The docking interaction between the MMP with the LasI complex had a stronger binding affinity of  $-7.8$  Kcal/mol towards the hydrogen bonding at SER66 (supplementary material Figure S7(A,B)) and CviR complex with  $-7.5$  Kcal/mol binding affinity towards the hydrogen bonding at ASP45 (supplementary material Figure S7(C,D)).

## 3. Conclusion

The significance of this study is the finding that MMP can effectively reduce *P. aeruginosa* biofilm formation and virulence which was demonstrated in *C. elegans* model. Vanillin as a natural or synthetic derived compound has been used as a food additive and generally considered a safe material. Vanillin derivative compound (MMP) looks promising as QS-antagonists for the development of novel non-antibiotic, anti-biofilm, and anti-virulent agents.

## Acknowledgement

We thank Dr. Manjunatha Thondamal, SRM University for providing *C. elegans* N2 strains and *E. coli* OP50.

## Disclosure statement



No potential conflict of interest was reported by the authors.

## Funding

The authors would like thank Yenepoya (Deemed to be University) for Seed grant support (No. YU/Seed grant/080-2019) and DST-PURSE Laboratory, Mangalore University, Mangalore for LCMS facility.

## ORCID

Rajesh P. Shastry  <http://orcid.org/0000-0001-8627-9759>

## References

- Anuradha K, Shyamala BN, Naidu MM. 2013. Vanilla-its science of cultivation, curing, chemistry, and nutraceutical properties. *Crit Rev Food Sci Nutr.* 53(12):1250–1276.
- Fitzgerald DJ, Stratford M, Gasson MJ, Ueckert J, Bos A, Narbad A. 2004. Mode of antimicrobial action of vanillin against *Escherichia coli*, *Lactobacillus plantarum* and *Listeria innocua*. *J Appl Microbiol.* 97(1):104–113.



# Sca1<sup>+</sup> Progenitor Cells (*Ex vivo*) Exhibits Differential Proteomic Signatures From the Culture Adapted Sca1<sup>+</sup> Cells (*In vitro*), Both Isolated From Murine Skeletal Muscle Tissue

Saketh Kapoor<sup>1</sup> · Pratigya Subba<sup>2</sup> · Sudheer Shenoy P<sup>1</sup> · Bipasha Bose<sup>1</sup>

Accepted: 8 February 2021

© The Author(s), under exclusive licence to Springer Science+Business Media, LLC, part of Springer Nature 2021

## Abstract

Stem cell antigen-1 (Sca-1) is a glycosyl-phosphatidylinositol-anchored membrane protein that is expressed in a sub-population of muscle stem and progenitor cell types. Reportedly, Sca-1 regulates the myogenic property of myoblasts and *Sca-1*<sup>-/-</sup> mice exhibited defective muscle regeneration. Although the role of Sca-1 in muscle development and maintenance is well-acknowledged, molecular composition of muscle derived Sca-1<sup>+</sup> cells is not characterized. Here, we applied a high-resolution mass spectrometry-based workflow to characterize the proteomic landscape of mouse hindlimb skeletal muscle derived Sca-1<sup>+</sup> cells. Furthermore, we characterized the impact of the cellular microenvironments on the proteomes of Sca-1<sup>+</sup> cells. The proteome component of freshly isolated Sca-1<sup>+</sup> cells (*ex vivo*) was compared with that of Sca-1<sup>+</sup> cells expanded in cell culture (*in vitro*). The analysis revealed significant differences in the protein abundances in the two conditions reflective of their functional variations. The identified proteins were enriched in various biological pathways. Notably, we identified proteins related to myotube differentiation, myotube cell development and myoblast fusion. We also identified a panel of cell surface marker proteins that can be leveraged in future to enrich Sca-1<sup>+</sup> cells using combinatorial strategies. Comparative analysis implicated the activation of various pathways leading to increased protein synthesis under *in vitro* condition. We report here the most comprehensive proteome map of Sca-1<sup>+</sup> cells that provides insights into the molecular networks operative in Sca-1<sup>+</sup> cells. Importantly, through our work we generated the proteomic blueprint of protein abundances significantly altered in Sca-1<sup>+</sup> cells under *ex vivo* and *in vitro* conditions. The curated data can also be visualized at <https://yenepoya.res.in/database/Sca-1-Proteomics>.

**Keywords** Stem cell antigen-1 (Sca-1) · Regenerative stem cells · Stem cells proteomics · Mass spectrometry-based proteomics

## Introduction

The stem cell antigen-1 (Sca-1), a member of *Ly6* gene family, is an 18-KDa glycosyl phosphatidylinositol-anchored protein that is localized in the lipid rafts of plasma membrane [1]. It is one of the most common markers of mouse

hematopoietic stem cells (HSCs) [2]. The expression of Sca-1 has also been identified in a variety of stem/progenitor cells from various tissues and organs [3]. In muscles, Sca-1 has been used as marker for mouse muscle-derived stem cells (MDSCs) [4] and its expression was also reported on the myogenic precursor cells [5]. The expression of Sca-1 has been reported on the muscle satellite cells and fibro/adipogenic progenitors which participate in muscle regeneration [6, 7]. However, satellite cells remain heterogeneous for the expression of Sca-1 antigen [8]. MDSCs isolated from the dystrophic *mdx* mice were shown to express Sca-1 along with early myogenic progenitor [4]. These Sca-1<sup>+</sup> MDSCs when injected into *mdx* mice, helped in the regeneration of new dystrophin positive muscle fibres [4]. Further, Sca-1<sup>+</sup> cells isolated from muscles of new-born mice enabled regeneration of muscle fibers when injected into *mdx* mice, leading to speculations on their role in therapeutic intervention in myopathies [9]. Additionally,

✉ Sudheer Shenoy P  
shenoy@yenepoya.edu.in; shenoy2000@yahoo.com

✉ Bipasha Bose  
Bipasha.bose@yenepoya.edu.in; Bipasha.bose@gmail.com

<sup>1</sup> Stem Cells and Regenerative Medicine Centre, Yenepoya Research Centre, Yenepoya (Deemed to be University), University Road, Deralakatte, Mangalore, Karnataka 575018, India

<sup>2</sup> Center for Systems Biology and Molecular Medicine, Yenepoya Research Centre, Yenepoya (Deemed to be University), Deralakatte, Mangalore, Karnataka 575018, India

condition, Sca-1<sup>+</sup> cells display increased protein synthesis. This is reflected by increased expression of Mtor, its well-characterized substrate Eif4ebp1 and multiple subunits of ribosomal protein. An important segment of our analysis is also the identification of several cell surface markers that in future may be used as additional or alternative markers to isolate Sca-1<sup>+</sup> cells. Designing such combinatorial strategies for the isolation of Sca-1<sup>+</sup> cells will provide higher validity to enrichment scores for isolation of pure cell populations.

**Acknowledgements** The authors would like to acknowledge the MASSFIITB Facility at IIT Bombay supported by the Department of Biotechnology (BT/PR13114/INF/22/206/2015) to carry out all MS-related experiments.

**Author Contributions** BB, SK and SS conceived and designed the study. SK and SS performed the animal experiments. SK carried out the MS sample preparation, analysed and performed the data analysis. SK and PS wrote the manuscript. BB and SS edited and approved the manuscript.

**Funding** The authors would like to thank the Stem Cells and Regenerative Medicine Centre of Yenepoya Research Centre, Yenepoya (Deemed to be University) for providing the infrastructure, core facility and funding in the form of Yenepoya University Seed Grant (YU/Seed Grant/2015-042) awarded to the Principal Investigator Dr Bipasha Bose to carry out this study.

**Data Availability** The MS raw files (.raw) and Proteome Discoverer search files(.msf) are available at <http://www.ebi.ac.uk/pride/archive/> with the PRIDE dataset identifier PXD022247. The curated data can also be visualized at <https://yenepoya.res.in/database/Sca-1-Proteomics>.

**Code Availability** Not applicable.

## Declarations

**Conflict of Interest** The authors declare no conflict of interest.

**Ethics Approval** This study was approved by the Institutional Animal Ethics Committee, Yenepoya (Deemed to be University) bearing number 10/4.8.2015.

**Consent to Participate** Not applicable.

**Consent for Publication** Not applicable.

## References

- Epting, C. L., King, F. W., Pedersen, A., et al. (2008). Stem cell antigen-1 localizes to lipid microdomains and associates with insulin degrading enzyme in skeletal myoblasts. *Journal of Cellular Physiology*, *217*, 250–260.
- Spangrude, G. J., Heimfeld, S., & Weissman, I. L. (1988). Purification and characterization of mouse hematopoietic stem cells. *Science*, *241*, 58–62.
- Holmes, C., & Stanford, W. L. (2007). Concise review: stem cell antigen-1: expression, function, and enigma. *Stem Cells*, *25*, 1339–1347.
- Lee, J. Y., Qu-Petersen, Z., Cao, B., et al. (2000). Clonal isolation of muscle-derived cells capable of enhancing muscle regeneration and bone healing. *The Journal of Cell Biology*, *150*, 1085–1100.
- Shen, X., Collier, J. M., Hlaing, M., et al. (2003). Genome-wide examination of myoblast cell cycle withdrawal during differentiation. *Developmental Dynamics*, *226*, 128–138.
- Zammit, P., & Beauchamp, J. (2001). The skeletal muscle satellite cell: stem cell or son of stem cell? *Differentiation*, *68*, 193–204.
- Judson, R. N., Low, M., Eisner, C., & Rossi, F. M. (2017). Isolation, culture, and differentiation of Fibro/Adipogenic Progenitors (FAPs) from skeletal muscle. *Methods in Molecular Biology*, *1668*, 93–103.
- Mitchell, P. O., Mills, T., O'Connor, R. S., et al. (2005). Sca-1 negatively regulates proliferation and differentiation of muscle cells. *Developmental Biology*, *283*, 240–252.
- Torrente, Y., Tremblay, J. P., Pisati, F., et al. (2001). Intraarterial injection of muscle-derived CD34(+)/Sca-1(+) stem cells restores dystrophin in mdx mice. *The Journal of Cell Biology*, *152*, 335–348.
- Oh, H., Bradfute, S. B., Gallardo, T. D., et al. (2003). Cardiac progenitor cells from adult myocardium: homing, differentiation, and fusion after infarction. *Proceedings of the National Academy of Sciences of the United States of America*, *100*, 12313–12318.
- Bonyadi, M., Waldman, S. D., Liu, D., et al. (2003). Mesenchymal progenitor self-renewal deficiency leads to age-dependent osteoporosis in Sca-1/Ly-6A null mice. *Proceedings of the National Academy of Sciences of the United States of America*, *100*, 5840–5845.
- Kafadar, K. A., Yi, L., Ahmad, Y., et al. (2009). Sca-1 expression is required for efficient remodeling of the extracellular matrix during skeletal muscle regeneration. *Developmental Biology*, *326*, 47–59.
- Epting, C. L., Lopez, J. E., Shen, X., et al. (2004). Stem cell antigen-1 is necessary for cell-cycle withdrawal and myoblast differentiation in C2C12 cells. *Journal of Cell Science*, *117*, 6185–6195.
- Swietlik, J. J., Sinha, A., & Meissner, F. (2020). Dissecting intercellular signaling with mass spectrometry-based proteomics. *Current Opinion in Cell Biology*, *63*, 20–30.
- Gstaiger, M., & Aebersold, R. (2009). Applying mass spectrometry-based proteomics to genetics, genomics and network biology. *Nature Reviews. Genetics*, *10*, 617–627.
- Amon, S., Meier-Abt, F., Gillet, L. C., et al. (2019). Sensitive quantitative proteomics of human hematopoietic stem and progenitor cells by data-independent acquisition mass spectrometry. *Molecular & Cellular Proteomics*, *18*, 1454–1467.
- Ohlendieck, K. (2011). Skeletal muscle proteomics: current approaches, technical challenges and emerging techniques. *Skeletal Muscle*, *1*, 6.
- Deshmukh, A. S., Murgia, M., Nagaraj, N., et al. (2015). Deep proteomics of mouse skeletal muscle enables quantitation of protein isoforms, metabolic pathways, and transcription factors. *Molecular & Cellular Proteomics*, *14*, 841–853.
- Kleinert, M., Parker, B. L., Jensen, T. E., et al. (2018). Quantitative proteomic characterization of cellular pathways associated with altered insulin sensitivity in skeletal muscle following high-fat diet feeding and exercise training. *Science Reports*, *8*, 10723.
- Ubaida-Mohien, C., Gonzalez-Freire, M., Lyashkov, A., et al. (2019). Physical activity associated proteomics of skeletal muscle: being physically active in daily life may protect skeletal muscle from aging. *Frontiers in Physiology*, *10*, 312.
- Yin, X., Mayr, M., Xiao, Q., et al. (2005). Proteomic dataset of Sca-1 + progenitor cells. *Proteomics*, *5*, 4533–4545.
- Sudheer Shenoy, P., & Bose, B. (2017). Identification, isolation, quantification and systems approach towards CD34, a biomarker present in the progenitor/stem cells from diverse lineages. *Methods*, *131*, 147–156.

# Molecular Detection of Human Papillomavirus (HPV) in Females and Assessment of Risk Factors for HPV Infection: A Study from Coastal Karnataka

VARSHA SAXENA<sup>1</sup>, VIDYA PAI<sup>2</sup>, RAJAGOPAL K<sup>3</sup>, ABDULLA MEHNAZ<sup>4</sup>

## ABSTRACT

**Introduction:** Cervical cancer is the fourth common malignancies in world and Human Papillomavirus (HPV) infection may lead to the development of the precancerous and cancerous lesions of the cervix.

**Aim:** This study was conducted to evaluate the presence of HPV in women who were admitted with cervical abnormality or attending Gynaecology OPD for any reason.

**Materials and Methods:** In this study a complete clinical history and demographic details of 90 subjects were recorded of which total 50 tissue biopsies and 40 cytobrush samples were collected. Results of histopathology and Papanicolaou (PAP) smear for biopsies and cytobrushes respectively were recorded from the medical records. Further PCR was performed for the presence or absence of HPV in all samples.

**Results:** Various risk factors for the acquisition of HPV infection were analysed in the present study. Out of 50 tissue biopsies, 15 had cervical carcinoma, 2 had Cervical Intraepithelial Neoplasia-II and 33 had chronic cervicitis. Whereas out of 40 cytobrushes, 32 were Negative for Intraepithelial Lesions/Malignancy, 2 had Atypical Squamous Cells of Undetermined Significance, 3 had Inflammatory Smear with Reactive Atypia and 3 had Inflammatory Smear. PCR results confirmed only 11 HPV positives among 50 tissue biopsies and 6 HPV positives among 40 cytobrush samples. The overall prevalence of HPV in our study was 18.8% only.

**Conclusion:** Present study shows that the occurrence of HPV is low as compared to the other studies done in other parts of India and in our region there is no awareness regarding HPV infection as well. Overall, these findings could have important implications for the preventions of cervical cancer.

**Keywords:** Awareness, Cervical cancer, Human papillomavirus, PCR, South India

## INTRODUCTION

One of the most common sexually transmitted infections is caused by HPV [1] and approximately 122,844 new cervical cancer cases are diagnosed, out of which 67,477 deaths reported annually in India [2]. HPV plays an important causative role in cervical cancer but disease can only develop when there is persistent HPV infection of the cervical epithelium [3]. It has been shown in literature that oncogenic HPV types (16, 18, 31, 33, 35, 39, 45, 51, 52, 56, 58, 59, 66, and 68) are present in up to 99.7% of cervical carcinomas [4].

Among eight HPV genes, two early genes i.e., E6 and E7 plays key role in tumor formation [5] i.e., both E6 and E7 genes interacts with the tumor suppressor genes i.e., p53 and hypophosphorylated Rb respectively [6]. These early oncogenes are invariably expressed in human cervical cancer, and their continued expression is required for maintenance of the cancerous state [7].

According to literature the sexual activity plays most important role in the acquisition of HPV infection therefore higher number of sexual partners increases the risk of HPV infection. Other risk factors includes infection with Herpes simplex virus and Chlamydia, impaired immune response, persistence of virus (HPV), smoking, extensive use of oral contraceptives and administration of steroid hormones [8,9]. The thorough understanding of the risk factors of this infection is required because this information will be helpful in implementation of future prevention strategies [8].

Cervical cancer can be prevented by early detection of abnormalities and subsequent treatment, it is important to establish cost-effective, sensitive, and accurate screening protocols within routine clinical practice [10]. Pap test is the standard method used for the screening of cervical cancer in India; however, organized screening programs

are rare. Despite the availability of Pap testing, the incidence of invasive cervical cancer remains high, especially in rural India [11]. Though HPV vaccines have been launched recently; they prevent infection by the major types of HPV only. However, cervical cancer may be caused by other genotypes of this virus as well. Hence we still need to rely on early detection of infection by screening methods and moreover there is no literature available regarding the circulating genotypes of HPV among women of our locality. Therefore, the present study has been planned to screen the women attending OBG OPD in our tertiary care hospital, with any gynaecological problem, for the presence of HPV- DNA, so as to understand the circulating genotypes of HPV among these patients.

## MATERIALS AND METHODS

For this prospective study total 90 subjects were enrolled after obtaining ethical clearance from institutional ethics committee. The sample size was calculated using the "G-Power Software, version 3.1.9.2" with the effective size of 10%. This study was conducted for a period of 11 months i.e., from November 2016 to September 2017. Data and sample collection were done at the Department of OBG and sample processing was done at the Department of Microbiology, Yenepoya Medical College, Mangalore. Informed consent was obtained from all the enrolled participants.

**Inclusion criteria:** All subjects who were married, non pregnant and had not undergone hysterectomy were included.

**Exclusion criteria:** Women who were pregnant, unmarried and refused to sign the consent were excluded.

**Data collection:** Cervical biopsies were collected from 50 subjects those who were admitted in OBG ward with cervical abnormalities

and cytobrush samples were collected from 40 subjects who came to OBG OPD and suspected to have HPV infection. Cytobrush samples were taken from the patients before Pap smear sampling during the routine examination.

Following the cervical punch biopsy, a small piece of tissue was sent for histopathology and another piece was stored in phosphate buffer saline at 2-4°C until DNA extraction for PCR. Cytobrush samples were collected using a Qiagen, Digene HC2 DNA collection device, Germany; which was after collection placed into Qiagen STM collection medium provided with the same collection kit and stored at -20°C until DNA extraction, not more than four weeks.

**Questionnaire based assessment of risk factors and awareness regarding HPV and HPV mediated malignancy:** To evaluate different aspects of knowledge and awareness of HPV and HPV mediated malignancy, all the subjects were offered a structured questionnaire from an existing interview guide from a previous study [Table/Fig-1] [12]. All subjects answered the questionnaire

Major issue	Topic Question
Awareness and knowledge of Cervical Cancer	What do you know about cervical cancer?
	What causes cervical cancer?
	Who can have cervical cancer?
	Do you think there is a possibility your daughter may have cervical cancer in the future? Why? Why not?
	Do you know the risk factors of cervical cancer?
Awareness and knowledge of HPV and HPV vaccine	Have you ever had cervical Pap smear test done?
	Have you heard about the human papillomavirus (HPV)?
	Where did you hear about it?
	Who could get HPV?
	Have you heard about the HPV vaccine?
	Have you ever had an HPV test before?

**[Table/Fig-1]:** Questionnaire used for the assessment of Knowledge about HPV and HPV mediated malignancy.

voluntarily and independently. Descriptive analysis was performed on the information collected using Microsoft Excel.

**DNA Extraction:** The tissues were cut into approximately 25 mg pieces (not more than 25 mg) and chopped into fine pieces before starting the procedure for DNA extraction. DNA was extracted from cervical tissues and from the material collected by the cytobrushes using Qiagen DNA Mini kit (Qiagen GmbH, Hilden/Germany) according to kit literature and stored at -70°C until performing PCR for HPV DNA detection. In addition, DNA was extracted from a HPV negative endometrial tissue (negative control) and from a cervical cancer tissue sample which was positive for HPV (positive control) for this study. Both the samples were obtained from the patients who were admitted in our hospital during standardisation of the PCR.

**HPV detection by Polymerase Chain Reaction (PCR):** DNA from each sample was amplified by PCR with the primer sets as given in [Table/Fig-2]. The oligonucleotide primers were procured from the EUROFINs Genomics Private India Limited, Bangalore. PCR was performed using the in-house PCR protocol in thermal cycler (applied biosystems, USA) that is routinely followed in our laboratory. A 25 µL reaction was assembled that contained 3 µL sample DNA, 12.5 µL Ampliqon Red 2X Mastermix (Tris-HCL pH 8.5, Ammonium sulphate (NH<sub>4</sub>)<sub>2</sub>SO<sub>4</sub>, 0.2 unit/ µL ampliqon Taq DNA polymerase, 0.4 mM deoxynucleotide triphosphate (dNTPs), 3 mM MgCl<sub>2</sub>, 0.2% Tween 20), 1 µL of 10 pmol of each primers (forward and reverse) and 7.5 µL molecular grade water. The PCR condition [13] for each primer set is given in [Table/Fig-3]. The amplified products were analyzed on a 2% agarose gel, stained with ethidium bromide (0.5 µL/ ml) and visualized on a UV transilluminator and photos of the bands were recorded using gel documentation system (Major

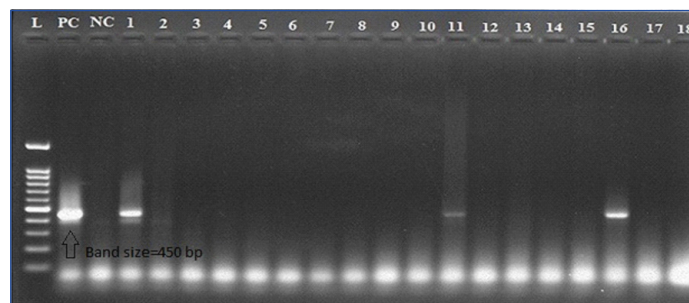
science, USA) as shown [Table/Fig-4]. The amplification was carried out in the presence of negative and positive controls; DNA from

Primer	Sequence	Target	Band size (bp)
MY09 MY11	F5'-CGTCCMARRGGAWACTGATC-3' R5'-GCMCAGGGWCATAAYATGG-3'	L1	450

**[Table/Fig-2]:** Primers used for detection of common Human papillomavirus (6, 11, 16, 18, 31 and 33).  
F-Forward, R-Rverse, bp-Base pair

Primer Name	Hot Start	Denaturation	Annealing	Extension	Final Extension
		40 cycles			
MY09/ MY11	95 °C, 5 min	94 °C, 1 min	55 °C, 1 min	72 °C, 30 s	72 °C, 5 min

**[Table/Fig-3]:** Polymerase chain reaction (PCR) conditions for primer sets.



**[Table/Fig-4]:** Agarose gel showing polymerase chain reaction on amplified product of HPV (6, 11, 16, 18, 31 and 33) common gene.  
L - 100 base pair (bp) DNA ladder (NEX-GEN, GENETICS), PC - Positive control (band size=450 bp), NC - Negative control, 1 and 16 - Strong positive, 11 - Weekly positive and 2, 10, 12, 15, 17, 18 - Negative for HPV

cervical cancer tissue sample positive for HPV was used as a positive control and a HPV negative endometrial tissue used as a negative control.

## STATISTICAL ANALYSIS

The statistical analysis was performed using the Windows program; SPSS (version 22.0). Chi square test was used and variables were compared between HPV positivity and histopathological/cytological status of the patients. p-value less than 0.05 was considered significant. Positive predictive value and negative predictive value was calculated wherever appropriate with the help of EPR-Val Test Pack 2 Web browser version.

## RESULTS

Total 90 subjects were enrolled in the present study. A complete demographic data were collected from all the participants as shown in [Table/Fig-5]. Out of 90 cervical samples, 50 were tissue biopsies and 40 were cytobrushes.

Among 50 tissue biopsies, 15 had different types of cervical carcinoma (seven Non Keratinizing Squamous Cell Carcinoma, three Keratinizing Squamous Cell Carcinoma, two Adenocarcinoma and three Moderately Differentiating Squamous Cell Carcinoma) whereas two had Cervical Intraepithelial Neoplasia-II and 33 had chronic cervicitis. Among 40 cytobrush samples, PAP smear cytology shows 32 were Negative for Intraepithelial Lesions/Malignancy, two had ASCUS, three had Inflammatory Smear with Reactive Atypia and three had Inflammatory smear as shown in [Table/Fig-6].

PCR results confirmed 11/50 (22%; p-value = 0.0004) HPV positives among tissue biopsies whereas only 6/40 (15%; p-value = 0.08) HPV positives among cytobrush sample. The distribution of HPV DNA positive samples among study participants is shown in [Table/Fig-5,6]. The occurrence of HPV in present study among invasive carcinomas was high i.e., 7/15 as compared to women with chronic cervicitis (2/33), NILM (3/32), ASCUS (1/2), IS-RA (1/3) and Inflammatory smear (1/3) ( $\chi^2 = 16.1173$ ; p-value = 0.002866).

Socio-demographic factors	n = 90	%	HPV DNA +
<b>Age group (Years)</b>			
20-30	9	10	02
30-40	25	27.8	02
40-50	36	40	05
50-60	14	15.5	05
> 60	6	6.7	03
<b>Religion</b>			
Hindu	58	64.5	10
Muslim	30	33.3	07
Christian	2	2.2	00
<b>Socioeconomic status</b>			
Below poverty line	66	73.3	13
Above poverty line	24	26.7	04
<b>Literacy</b>			
Educated	59	65.6	11
Uneducated	31	34.4	06

[Table/Fig-5]: Socio-demographic details of the participants.

Histology/Cytology of samples	Number of sample (n=90)	HPV DNA positive
<b>Invasive Cervical Cancers</b>		
NKSCC	7	4
KSCC	3	2
Adenocarcinoma	2	1
MDSCC	3	-
	} 15	
<b>CIN – II</b>	2	2
<b>Chronic Cervicitis</b>	33	2
<b>NILM</b>	32	3
<b>ASCUS</b>	2	1
<b>IS-RA</b>	3	1
<b>Inflammatory smear</b>	3	1
<b>TOTAL</b>	90	17 (18.8 %)

[Table/Fig-6]: HPV-DNA prevalence in women with different cervical abnormalities. NKSCC-Non Keratinizing Squamous Cell Carcinoma, KSCC-Keratinizing Squamous Cell Carcinoma, MDSCC-Moderately Differentiating Squamous Cell Carcinoma, CIN-II-Cervical Intraepithelial Neoplasia-II, NILM-Negative for Intraepithelial Lesion/Malignancy, ASCUS- Atypical Squamous Cells of Undetermined Significance, IS-RA-Inflammatory Smear with Reactive Atypia.

The prevalence of HPV infection in the present study is low i.e., only 18.8%.

The histopathological/cytological positive/negative results were compared with the PCR positive/negative results of both the biopsy

Total samples (n=90)	PCR positive samples	PCR negative samples	Positive predictive value	Negative predictive value	p-value
Histological positive biopsy samples (n=17)	09	08	53%	94%	0.0004
Histological negative biopsy samples (n=33)	02	31			
Cytological positive cytobrush samples (n=08)	03	05	37.5%	90.6%	0.08
Cytological negative cytobrush samples (n=32)	03	29			

[Table/Fig-7]: Comparison of histopathological/cytological findings of tissue biopsies and cytobrush samples with PCR findings.

and cytobrush samples. The positive and negative predictive values for HPV DNA from 17/50 histopathologically positive and 33/50 histopathologically negative tissue biopsies were evaluated. Similarly, the positive and negative predictive values for HPV DNA from 8/40

cytologically (PAP smear) positive and 32/40 cytologically negative cytobrush samples were evaluated as given in [Table/Fig-7].

**Assessment of Risk Factors for the Acquisition of HPV Infection:**

Patient information sheet; approved by the institutional ethics committee was provided to all the participants at the beginning of the study. With regard to age at marriage 58/90 (64.4%) had sexual debut before or at the age of 20 years however, 32/90 (35.6%) got married after the age of 21 or above. 48/90 (53.3%) women had more than three children in which some of them had even 8-10 children. Only 2/90 (2.2 %) subjects had been using oral contraceptive during last two years before participating in the present study. With regard of sexual partner, 87/90 (96.7%) were monogamous and only 3/90 (3.3%) had two or more than two partners. Upon assessment of questionnaire, it was observed in this study that even though literacy rate being 65.5%, 84/90 (93.3%) women are not aware of PAP smear screening for cervical cancer and therefore never had gone for PAP testing. Majority of women 62/90 (68.9%) used cotton cloth during menstruation whereas 28/90 (31.1%) women used sanitary pads. A 75/90 (83.3%) participants were free from any underlying conditions however, 15/90 (16.7%) participants had some underlying conditions like hypertension, diabetes etc.

**DISCUSSION**

In India, annually the incidence of cervical cancer is quite high [2] therefore, early screening of HPV and cervical cancer can be a better solution for this question. The major obstacles in India and in other developing countries for the low screening prevalence are either educational barriers or behavioral barriers [14]. Persistent high risk HPV infection increases the risk of cervical intraepithelial neoplasia or invasive cervical cancers. The distribution of HPV varies geographically however, HPV 16 found to be the commonest type followed by HPV 18 [15].

In the present study, 36/90 (40%) of the participants belonged to the 40-50 years age group followed by 25/90 (27.8%) in 30-40 years age group whereas, a study from China had maximum number of participants in the age group of 31-40 years [16]. However, study done by Vince A et al., reported maximum number of subjects from the age group (20-40 years) which was not in accordance to the present study [4]. Age specific prevalence was increased from 2.2% to 5.5% from age group 20-40 to 40-60 years, then again decreases to 3.3% from age group >60 years onwards. However, a population based survey from Bangladesh reported that the age specific prevalence was first decreased for 25-34 age group then increased for 35-44 age group and again decreased for age group above 45 years [17].

The occurrence of HPV in present study among invasive carcinomas was found to be high, being 46.7% as compared to women with chronic cervicitis and NILM being only 6.3% and 9.4%, respectively which is in accordance with a study from Pakistan [10]. In present study, the results of histopathological positive/negative and PCR positive/negative tissue biopsy samples were significantly correlated (p-value 0.0004) whereas; results of cytological positive/negative and PCR positive/negative for cytobrush samples were not significantly correlated (p-value 0.08). However, the overall prevalence of HPV in present study was low (18.8%), which is in accordance with a study from Bangladesh [17] in which the reported overall prevalence was 7.7% only. However, a study by Chakravarty J et al., from East India reported the overall prevalence of HPV among HIV positive subjects was 26.85% which according to the author was the high prevalence as compared to the general population [18]. However, results from western countries were contradictory to the present study where HPV prevalence was found to be high [19,20].

Results of the present study showed that 66/90 (73.3%) of the study participants belonged to the below poverty line status (which was considered on the basis of having a ration card), yet most of them

were educated whereas, education rate among population from the North India was found to be low [21]. After the assessment of the questionnaire given to the study participants it was analysed that even though being educated (literate and illiterate subjects were classified according to the Arora CD et al., [22]) more than 90% of the women in Mangalore region are not aware of HPV infection or HPV mediated malignancies. However, according to Ganju SA et al. the awareness regarding cervical cancer from India, Nepal and Sri Lanka was found to be 66%, 58.8% and 57.7%, respectively [14].

PAP smear is a simple, cost-effective and sensitive tool for the detection of premalignant and malignant changes in the cervix. The efficiency, sensitivity and specificity of the Pap smear depends on frequency of cervical cancer screening programs for women, adequate sample collection, and the quality of laboratory analysis [23].

A study published from north India in accordance with the present study which reported that the PAP smear had sensitivity of 80% with the positive predictive value of 48.98% and negative predictive value of 88.24% [24]. As it is well known that infection with HPV in cervix is reversible so this could be the reason for the discordance between cytology and molecular detection may also be influenced by self-clearance of the virus during the interval between PAP test and molecular assay [10].

Although vaccines are available for two major high risk oncogenic HPVs and two low risk oncogenic HPVs i.e., type 16/18 and type 6/11 respectively, the major problem in vaccinating women in developing countries is the lack of knowledge or awareness and the high cost of vaccination [25]. However, a study from North India by Hussain S et al., on the willingness of HPV vaccination after educating students about the risks of HPV infection and consequences related to this virus, it was found that the willingness was 70% among females compared to males and 64% among urban populations compared to rural populations [26].

## LIMITATION

Present study mainly focused on those HPV types which are most commonly considered as highly oncogenic, however in the recent past years some low risk oncogenic types have been emerged as a causative agent of cervical cancers. Additionally, the major drawback is that as this is a cross-sectional study and no longitudinal data is available, therefore, major conclusions cannot be drawn about causality as mere presence of HPV does not mean that patient will die of cervical cancer because in many cases the abnormal cervical cell may return to the normal state by the auto clearance of HPV from the body as a result of immune response.

## CONCLUSION

In Mangalore region, the prevalence of HPV is very low and there is absolute no awareness regarding HPV infection. Many epidemiological studies suggest that regular cervical screening in adult females is important in the reduction of HPV associated cervical malignancy. Though HPV vaccines have been launched recently; they prevent infection by the major types of HPV only. However, cervical cancer may be caused by other genotypes of this virus as well. Hence, we still need to rely on early detection methods. Therefore, molecular testing for HPV infection should additionally be used in order to identify patients who are at high risk for the development of premalignant lesions. Combination of cytology and molecular testing may help to avoid unnecessary stress and intensive follow-ups. Overall, these findings could have important implications for the preventions of cervical cancer.

## ACKNOWLEDGEMENTS

We gratefully acknowledge Dr Kishore Bhatt and Mr. Manohar K of Central Research Laboratory of Maratha Mandal Dental College, Belgaum, India for helping us in the processing of the samples and

their guidance throughout this study. We are extremely grateful to Yenepoya University for providing us seed grant for the financial support of this study and Department of Obstetrics and Gynaecology for providing tissue biopsies and cytobrush samples.

## REFERENCES

- Colon-López V, Quiñones-Avila V, Del Toro-Mejias LM, Reyes K, Rivera ME, Nieves K, et al. Oral HPV infection in a clinic-based sample of Hispanic men. *BMC Oral Health*. 2014;14(1):7.
- Sreedevi A, Javed R, Dinesh A. Epidemiology of cervical cancer with special focus on India. *Int J Womens Health*. 2015;7:405-14.
- Molijn A, Kleter B, Quint W, van Doorn LJ. Molecular diagnosis of human papillomavirus (HPV) infections. *J Clin Virol*. 2005;32:43-51.
- Vince A, Ivanisevic M, Harni V, Skalko D, Jeren T. Molecular detection of human papillomavirus in women with minor-grade cervical cytology abnormalities. *J Clin Virol*. 2001;20(1):91-94.
- Hariri S, Dunne E, Saraiya M, Unger ER, Markowitz LE. Manual for the surveillance of vaccine-preventable diseases. 5th Edition. 2011. Chapter 5: Human Papillomavirus (HPV).
- Shaikh F, Sanehi P, Rawal R. Molecular screening of compounds to the predicted Protein-Protein Interaction site of Rb1-E7 with p53-E6 in HPV. *Bioinformation*. 2012;8(13):607.
- Park S, Park JW, Pitot HC, Lambert PF. Loss of dependence on continued expression of the human papillomavirus 16 E7 oncogene in cervical cancers and precancerous lesions arising in Fanconi anemia pathway-deficient mice. *M Bio*. 2016;7(3):e00628-16.
- Jahdi F, Khademi K, Khoei EM, Haghani H, Yarandi F. Reproductive factors associated to human papillomavirus infection in Iranian woman. *J Family Reprod Health*. 2013;7(3):145.
- Stanley M. Immune responses to human papillomavirus. *Vaccine*. 2006;24:S16-22.
- Siddiqa A, Zainab M, Qadri I, Bhatti MF, Parish JL. Prevalence and genotyping of high risk human papillomavirus in cervical cancer samples from Punjab, Pakistan. *Viruses*. 2014;6(7):2762-77.
- Sowjanya AP, Jain M, Poli UR, Padma S, Das M, Shah KV, et al. Prevalence and distribution of high-risk Human Papilloma Virus (HPV) types in invasive squamous cell carcinoma of the cervix and in normal women in Andhra Pradesh, India. *BMC Infect Dis*. 2005;5(1):116.
- Fernandez ME, Le YL, Fernandez-Espada N, Calo WA, Savas LS, Verlez C, et al. Knowledge, attitudes, and beliefs about Human Papillomavirus (HPV) vaccination among puerto rican mothers and daughters, 2010: a qualitative study. *Prev Chronic Dis*. 2014;11:140171.
- Park JS, Namkoong SE, Han SK, Nha DJ, Lee HY, Kim SJ. Comparison of L1 consensus primers with E6 type specific primers for detection of human papillomaviruses in paraffin sections of cervical neoplasia. *J Korean Med Sci*. 1993;8(1):60-67.
- Ganju SA, Gautam N, Barwal V, Walla S, Ganju S. Assessment of knowledge and attitude of medical and nursing students towards screening for cervical carcinoma and HPV vaccination in a tertiary care teaching hospital. *Int J Community Med Public Health*. 2017;4(11):4186-93.
- Peedicayil A, Abraham P, Sathish N, John S, Shah K, Sridharan G, et al. Human papillomavirus genotypes associated with cervical neoplasia in India. *Int J Gynaecol Cancer*. 2006;16(4):1591-95.
- Li Z, Liu F, Cheng S, Shi L, Yan Z, Yang J, et al. Prevalence of HPV infection among 28,457 Chinese women in Yunnan Province, southwest China. *Sci rep*. 2016;6:21039.
- Nahar Q, Sultana F, Alam A, Islam JY, Rahman M, Khatun F, et al. Genital human papillomavirus infection among women in Bangladesh: findings from a population-based survey. *PLoS One*. 2014;9(10):e107675.
- Chakravarty J, Chourasia A, Thakur M, Singh AK, Sundar S, Agrawal NR. Prevalence of human papillomavirus infection & cervical abnormalities in HIV-positive women in eastern India. *Indian J Med Res*. 2016;143(1):79.
- Amrani M, Lalaoui K, El Mzibri M, Lazo P, Belabbas MA. Molecular detection of human papillomavirus in 594 uterine cervix samples from Moroccan women (147 biopsies and 447 swabs). *J Clin Virol*. 2003;27(3):286-95.
- Vorsters A, Cornelissen T, Leuridan E, Bogers J, Broeck DV, Benoy I, et al. Prevalence of high-risk human papillomavirus and abnormal pap smears in female sex workers compared to the general population in Antwerp, Belgium. *BMC Public Health*. 2016;16(1):477.
- Joseph M. Northern states versus Southern states: A Comparative analysis. Indian Centre for Research on International Economics Relations. 2004; Working Paper No. 134.
- Arora CD, Wani RJ, Kasbe A, Jain SG. Knowledge and awareness regarding cervical cancer in women with respect to risk factors, screening methods and vaccination. *EC Gastroenterology and Digestive System*. 2017;2(3):331-68.
- Cobucci RN, Maissonette MJ, Macêdo EJ, Santos Filho FC, Rodovalho PE, Nóbrega MM, et al., Pap test accuracy and severity of squamous intraepithelial lesion. *Indian J Cancer*. 2016;53(1):74.
- Kohli B, Arya SB, Goel JK, Sinha M, Kar J, Tapasvi I. Comparison of Pap smear and colposcopy in detection of premalignant lesions of cervix. *J South Asian Federation of Menopause Societies*. 2014;2(1):5.



- [25] Zaheer R, Alam N, Hussain KC, Herekar AA, Nasir H, Bhutta SZ. Awareness about human papillomavirus as a cause of cervical cancer and its prevention in the undergraduate female students of Karachi. *J Pak Med Assoc.* 2017;67(1):27-32.
- [26] Hussain S, Nasare V, Kumari M, Sharma S, Khan MA, Das BC, et al. Perception of human papillomavirus infection, cervical cancer and HPV vaccination in North Indian population. *PLoS One.* 2014;9(11):e112861.

**PARTICULARS OF CONTRIBUTORS:**

1. PhD Scholar, Department of Microbiology, Yenepoya Medical College and Hospital, Mangalore, Karnataka, India.
2. Professor and Head, Department of Microbiology, Yenepoya Medical College and Hospital, Mangalore, Karnataka, India.
3. Professor and Head, Department of OBG, Yenepoya Medical College and Hospital, Mangalore, Karnataka, India.
4. Post Graduate 2nd year, Department of OBG, Yenepoya Medical College and Hospital, Mangalore, Karnataka, India.

**NAME, ADDRESS, E-MAIL ID OF THE CORRESPONDING AUTHOR:**

Dr. Vidya Pai,  
Professor and Head, Department of Microbiology, Yenepoya Medical College and Hospital, Mangalore-575018, India.  
E-mail : micro\_vidya7417@rediffmail.com

Date of Submission: **Jan 04, 2018**Date of Peer Review: **Mar 09, 2018**Date of Acceptance: **Apr 14, 2018**Date of Publishing: **Jun 01, 2018****FINANCIAL OR OTHER COMPETING INTERESTS:** As declared above.

# The repair gene *BACH1* - a potential oncogene

Katheeja Muhseena N, Sooraj Mathukkada, Shankar Prasad Das, Suparna Laha

Yenepoya Research Centre, Yenepoya (Deemed to be University), Mangalore, Karnataka, India

## Abstract

*BACH1* encodes for a protein that belongs to RecQ DEAH helicase family and interacts with the BRCT repeats of *BRCA1*. The N-terminus of *BACH1* functions in DNA metabolism as DNA-dependent ATPase and helicase. The C-terminus consists of BRCT domain, which interacts with *BRCA1* and this interaction is one of the major regulator of *BACH1* function. *BACH1* plays important roles both in phosphorylated as well as dephosphorylated state and functions in coordination with multiple signaling molecules. The active helicase property of *BACH1* is maintained by

Correspondence: Suparna Laha, Molecular Biology Division, Yenepoya Research Centre, Yenepoya University, University Road, Derlakatte, Mangalore 575018, Karnataka, India.  
Tel.: +91.824.2203943 - Fax: +91.824.2203943.  
E-mail: suparnalaha@yenepoya.edu.in

Key words: *BACH1/BRIP1*; genomic stability; tumorigenesis; Chromatin remodeling; Chl1p.

Acknowledgements: the authors would like to acknowledge government of Karnataka for supporting the fellowship for the researcher and Yenepoya (Deemed to be) University to support my laboratory. The authors also acknowledge Yenepoya (Deemed to be) University for providing the laboratory space and infrastructure to carry out my research activities. The authors acknowledge Mr. Sandip Koyla for his helpful guidance on the bioinformatic part to Ms. Katheeja Muhseena in doing the data analysis.

Funding: this work is supported by Minority/fellowship/CR-97/2018-19 from Directorate of Minority, Government of Karnataka to K.M.N. This work has also been supported by the seed grant YU/seed grant/055/2016 from Yenepoya (Deemed to be) University, Mangalore to S.L. and by ICMR grant 5/13/2018/NCD-III.

Contributions: KMN, original draft, investigation and validation of the work; SM, formal analysis and data curation; SPD, resources, visualization, review and editing; SL, original draft, conceptualization, methodology, supervision and project administration.

Conflict of interests: the authors declare no potential conflict of interests.

Received for publication: 19 September 2020.

Revision received: 2 February 2021.

Accepted for publication: 2 March 2021.

This work is licensed under a Creative Commons Attribution NonCommercial 4.0 License (CC BY-NC 4.0).

©Copyright: the Author(s), 2021  
Licensee PAGEPress, Italy  
Oncology Reviews 2021; 15:519  
doi:10.4081/oncol.2021.519

its dephosphorylated state. Imbalance between these two states enhances the development and progression of the diseased condition. Currently *BACH1* is known as a tumor suppressor gene based on the presence of its clinically relevant mutations in different cancers. Through this review we have justified it to be named as an oncogene. In this review, we have explained the mechanism of how *BACH1* in collaboration with *BRCA1* or independently regulates various pathways like cell cycle progression, DNA replication during both normal and stressed situation, recombination and repair of damaged DNA, chromatin remodeling and epigenetic modifications. Mutation and overexpression of *BACH1* are significantly found in different cancer types. This review enlists the molecular players which interact with *BACH1* to regulate DNA metabolic functions, thereby revealing its potential for cancer therapeutics. We have identified the most mutated functional domain of *BACH1*, the hot spot for tumorigenesis, justifying it as a target molecule in different cancer types for therapeutics. *BACH1* has high potentials of transforming a normal cell into a tumor cell if compromised under certain circumstances. Thus, through this review, we justify *BACH1* as an oncogene along with the existing role of being a tumor suppressant.

## Introduction to *BACH1*

*BACH1/BRIP1/FANCD1/hCHLRI* (*BRCA1* associated C-terminal helicase 1), which is the homolog of yeast Chl1p helicase, is a phosphoprotein located on chromosome 17q22.<sup>1-3</sup> It consists of 1249 amino acid residues with the protein size of 130 KDa, the gene length of 180kb and contains 20 exons (Figure 1).<sup>1,4,5</sup> *BACH1* helicase is present in both active and inactive forms depending on the phosphorylation status at the K52 position of the protein. The dephosphorylated *BACH1* leads to the activation of helicase, which is involved in the timely progression of S-phase, repair of DNA cross-links and secondary structures formed during replication and replication induced stress.<sup>6,7</sup> Thus phosphorylated-dephosphorylated state of *BACH1* plays a major role in cell cycle regulation through activation of various pathways in *BRCA1* dependent and independent manner.<sup>4</sup> During replication stress, it acts with DNA topoisomerase-2-binding protein TOPBP1 to load replication protein A (RPA) onto the chromatin. Presence of RPA is required for activation and control of replication checkpoints and to undergo repair by homologous recombination.<sup>8,9</sup> In the case of management of DNA damage responses like interstrand crosslinks (ICLs), the helicase activity of *BACH1* and its interaction with the mismatch repair protein MLH1 provides ICL resistance.<sup>10</sup>

*BACH1* also acts as a tumor suppressor in different cancer types.<sup>7,11</sup> It maintains chromosomal integrity and prevents genomic instability by resolving the G-quadruplexes and processing replication intermediates.<sup>12-14</sup> It has the ability to recognize G-quadruplexes mostly those formed upon replication and mediates their stepwise unfolding and refolding to modulate epigenetic pro-

gramming and chromatin remodeling also.<sup>12-15</sup> *BACH1* maintains as well as preserves the chromatin structure and its epigenetic information hence facilitating the smooth progression of the replication fork when it encounters altered/ damaged/ complex DNA structures (Figure 2).<sup>11,12,14</sup> As it is involved in regulating many vital pathways, any aberration to it can cause multifactorial diseases like cancer. *BACH1/BRIP1* plays a role in hereditary breast and ovarian cancer suppression as well as instrumental in progressive bone marrow failure disorder, Fanconi anemia (FA).<sup>17</sup> Germline mutations in the *BACH1/FANCD2* gene leads to chromosomal instability which results in bone marrow failure defects, developmental abnormalities and sets up favorable conditions to develop cancer.<sup>18</sup> Clinical data analysis of *BRIP1* mutations by Seal *et al.* indicates that majority of the *BRIP1* missense mutants/variants are not linked with a risk of familial breast cancer, whereas the truncated variant of *BACH1* are more susceptible alleles of breast cancer running in the family.<sup>19</sup> The biological explanations for the differences in cancer risk for mutant variant and truncated variant are unclear. Moreover, the group identified that, biallelic *BRIP1* mutations confers less risk of breast cancer compared to the monoallelic truncated version.<sup>19</sup> Mutations in *BACH1* also lead to liver carcinogenesis, among patients with viral cirrhosis, due to impaired DNA mismatch repair pathway.<sup>20</sup> In summary to the above lines, the mutated version of *BACH1* gene leads to the development of oncogenicity (Figure 1).

*BACH1* functionally and physically interact with a bunch of proteins, like BRCA1, MUTL $\alpha$ , MLH1, PMS2, MMS19, TOPBP1, TLS polymerase, BLM, RPA1, MRE11 and FANCD2 and plays a significant role in regulating the metabolic pathways in combination with them.<sup>10,21,22</sup> The *BACH1* interactors play major and minor roles in maintenance of genomic integrity, cell cycle regulation, DNA damage detection and repair processes.<sup>11</sup> The interactors MUTL $\alpha$ , MLH1, PMS2 and RPA1 play important role in mismatch repair.<sup>21,23,24</sup> The *BACH1* homolog, *BRIP1* interacts with the mismatch repair heterodimer complex, MUTL $\alpha$ , which is composed of mismatch repair proteins MLH1 and PMS2. It also

interacts with MLH1 directly independent of BRCA1. The interaction with the single-stranded DNA-binding protein RPA (Replication Protein A) through its helicase domain enhances the DNA unwinding activities at the difficult sites of replication.<sup>25</sup> The other interactors MMS19 and TOPBP1 maintains genomic integrity with *FANCD2* in Fanconi anemia DNA damage repair pathway.<sup>24</sup> The interaction of DNA helicase *BACH1* with BLM, another helicase, coordinated with DNA damage signaling protein molecules, structure-specific nucleases, polymerases, RPA, and RAD51 imparts a delicate balance between homologous recombination (HR) and non-homologous end-joining (NHEJ) to repair double strand breaks (DSBs) and maintain genomic stability.<sup>26</sup>

The most important event is the physical interaction of *BACH1* with BRCA1 which justifies the possible role of *BACH1* in cancer development.<sup>7,11</sup> This interaction is dependent on the phosphorylation-dephosphorylation function of *BACH1*, as the interaction increases in presence of phosphatase inhibitors, whereas in the presence of  $\lambda$  phosphatase the interaction is lost,<sup>27</sup> which proves that the phosphorylated form of *BACH1* interacts with BRCA1. BRCA1 is localized to the site of DNA double strand break by forming a complex with different interacting molecules like RAP80, CTIP and FANCD2. The BRCA1-RAP80 complex comes through Abraxas ubiquitinase and follows the non-homologous end-joining at the DSBs. The parallel pathway of homologous recombination repair is followed by the BRCA1-FANCD2-CTIP complex. This complex is also regulated by heterochromatin binding protein 1 (HP1) pathway in response to DNA damage for its accumulation at the site of DNA double strand break which mediates DNA repair. FANCD2 interacts with HP1 in a BARD1 dependent manner and mediates homologous recombination.<sup>28</sup> The association of BRCA1 with *BACH1* adds on to the functioning of the G2/M checkpoint.<sup>29</sup> The BRCA1/*BACH1* complex prevents DNA breakage resulting in lowering of genomic instability.<sup>30</sup> *BACH1* status affect the recruitment of BRCA1 to double strand breaks depending on the type of damage.<sup>31</sup> Presence of change in amino acid sequence in the BRCA1 binding domain of the protein

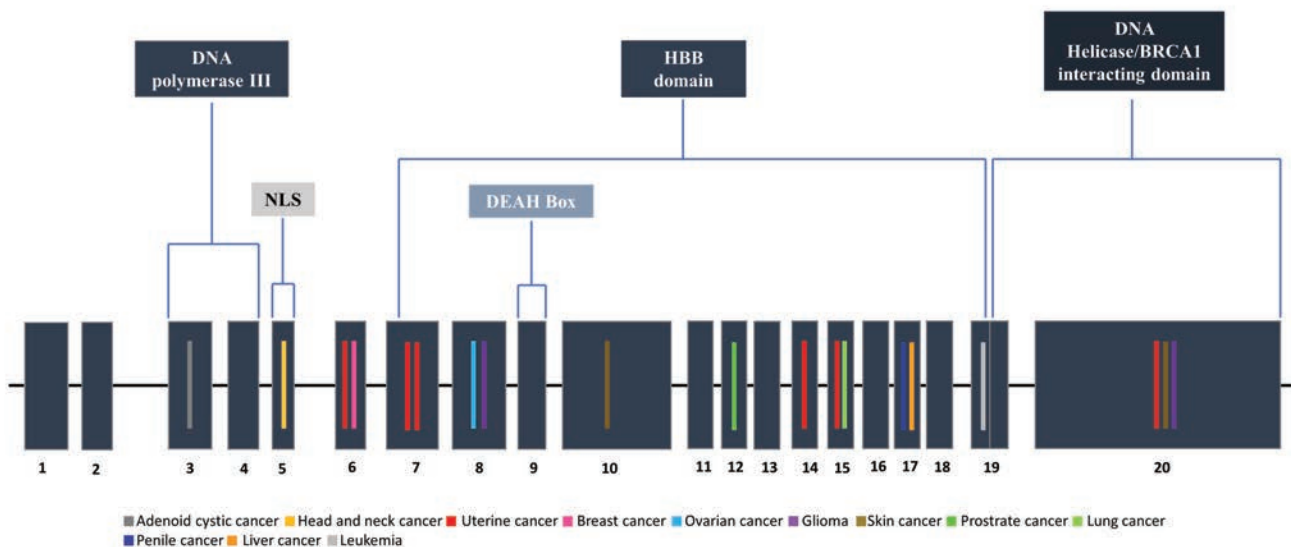


**Figure 1.** Schematic representation of *BACH1* gene with conserved domains and reported pathogenic mutations in different cancer types. The *BACH1* gene comprises of 20 exons of which exon 3&4 belongs to DNA polymerase domain (18-61aa residue), exon 5 nuclear localization signal (NLS; 158-175aa), exon7-19 HBB domain (245-881aa), exon9 DEAH box (393-396aa) and exon 19 &20 DNA helicase/*BRCA1* interacting domain (888-1063aa) respectively. The large boxes represent exons and small colored thick lines represent verified pathogenic mutations in the respective exons in different cancers (data analyzed from cBioPortal.org).

BACH1, in case of tumorigenesis, proves that recognition of BRCT phosphoprotein by BACH1 is necessary for tumor suppression activity of BRCA1.<sup>32</sup>

### **BACH1 in cell cycle regulation and replication**

The most fascinating characteristic of *BACH1* is observed during its regulation of the cell cycle through its helicase activity.<sup>33</sup> Though the expression of BACH1 protein remains the same throughout the cell cycle, its association with the chromatin increases in S-phase only.<sup>6</sup> The helicase activity of BACH1 is regulated by its phosphorylated-dephosphorylated state. The sequence of steps explaining the functioning of BACH1 in the cell cycle is represented in Figure 3. At G1-phase, BACH1 is phosphorylated leading to the interaction with BRCA complex with low ATPase/helicase activity. As a result, the movement of the replication complex slows down enhancing the proof reading of the polymerase. Adversely, during the slowdown of the fork, the nascent leading and lagging strands tend to anneal to each other due to fork

regression or reversal to form secondary structures.<sup>34</sup> The complex of BACH1/BRCA along with the combination of BLM1, a helicase with opposite polarity, resolves these difficult structural motifs encountered by the replication forks during DNA replication. Once the proofreading and resolving activity of the secondary structures are over, the de-phosphorylation of BACH1 takes place. On dephosphorylation, the BACH1/BRCA complex breaks down, leaving behind BACH1 at the fork generating the space for the replication machinery to start replication. Simultaneously dephosphorylated BACH1 regains the helicase activity to unwind the DNA for timely progression through S-phase. The helicase and translocase activities of BACH1 are also modulated by protein-protein interactions.<sup>1</sup> Replication protein A (RPA), comes with BACH1 to facilitate the removal of the DNA bound protein obstacles like the replication complex and increases the ability of BACH1 to unwind the secondary structures.<sup>35,36</sup> So BACH1 plays a major role in regulating the kinetics of replication in S-phase (Figure 3).<sup>6</sup> *BACH1* also have a role during replication stress when there is a damage to DNA or forks are blocked by blocking molecules. It resolves the blocked forks so that they can progress into S-phase and complete

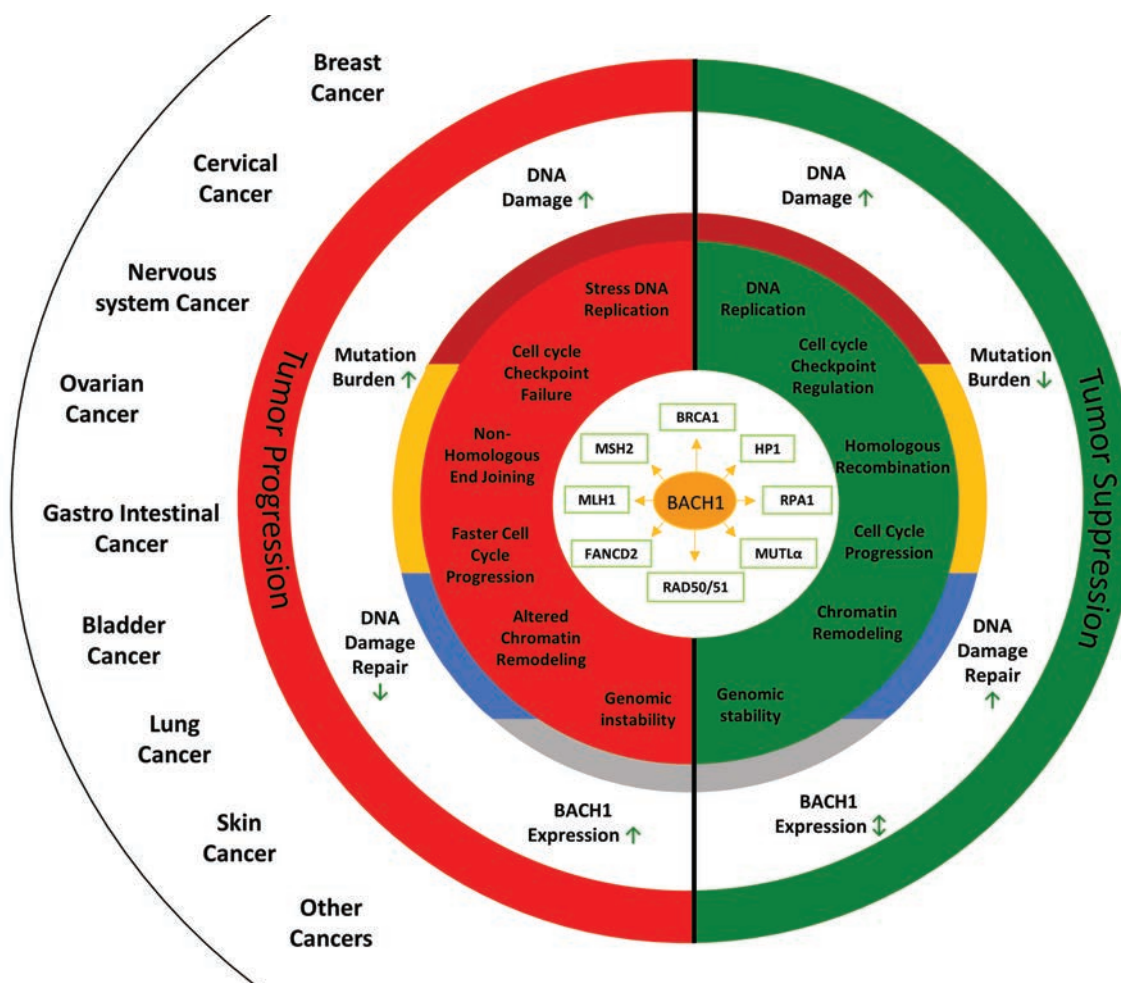


**Figure 2.** BACH1- a multifaceted protein. The schematic representation depicts the multi-functional role of BACH1. The inner circle (white) shows BACH1 and its interacting partners. The first ring represents various functions of BACH1 (half green ring) and altered function of aberrant BACH1 (half red ring). The second ring (multicolor) represents the group of functions and its correlation with different pathways where red represents DNA damage, blue represents mutation burden, yellow represents DNA damage repair and grey represents BACH1 expression. The third ring (white) represents the various pathways and its alterations, arrow represents ↑ increase, ↓ decrease and ⇕ stable functional effects. The outermost colored ring represents the collective outcome of normal and aberrant BACH1 function in cancer formation. Left outermost arc represent various cancers with significant BACH1 aberrations.

the duplication of the genome within a defined period of time.<sup>37</sup> BACH1 alone is unable to unwind partial duplex DNA structures formed due to double-strand breaks, when the strands are bound by DNA double-strand break interacting proteins or blocking molecules.<sup>8,38</sup> Similarly, as happens during replication, the presence of RPA, stimulates BACH1/FANCD1 for the displacement of the DNA interacting proteins resulting in unwinding of complex structures.<sup>39</sup> RPA also stimulates BLM1 to efficiently dislodge protein bound to duplex DNA to alleviate replication stress imposed by stalling of the replication forks.<sup>8,36,40</sup> So, during the formation of the secondary structures, these helicases, BACH1 and BLM1, displace proteins bound near double-stranded ends and resolve secondary structure or damaged DNA to enable error-free and kinetically efficient end-joining leading to the restoration of DNA replication.<sup>25</sup>

In conclusion, genomic integrity is maintained by the helicase and the phosphorylation property of BACH1. During diseased state with perturbed BRCA-BACH interaction due to dephosphorylation of BACH1, genomic instability develops by increased helicase activity and faster progression through S-phase. Accelerated S-phase leads to error-prone resolving of the secondary structures at the forks leading to genomic instability. BACH1 interacts with BRCA1, through the BRCT domain and contributes to the DNA repair function of BRCA1.<sup>41</sup> Loss in interaction also happens due to mutation in the interacting domains of the genes and so brings in less repair and helicase molecules at the damaged

sites. As a result, the secondary structures form during the replication fail to resolve, resulting in more breaks and more damage to the DNA strands. High burden of damage leads to the activation of alternate repair pathways other than homologous recombination repair which results in accumulation of mutations followed by the development of cancer.<sup>42,43</sup>

### BACH1 in DNA repair

The repair function of BACH1 along with its helicase activity maintains the genomic integrity. Unlike dephosphorylation of BACH1 for the helicase activity, the repair property is regulated through its acetylation. This acetylation of BACH1 dependent on the BRCA1-BACH1 interaction.<sup>44</sup> The BRCA1-BACH1 interaction ensures to suppress the mutation prone end-joining and promote double-strand DNA repair via the activation of homologous recombination.<sup>1,45,46</sup> Phosphorylated BACH1, interacts with BRCA1 and activates the G2/M checkpoint, results in stalled replication forks, which may signal for delayed entry into S phase which is shown in Figure 3.<sup>6,27,29</sup> On the other hand, delay in the S-phase leads to increased secondary structures and breaks resulting to activation of the DNA damage checkpoint.<sup>6,47,48</sup> This fine balance of BRCA1 interaction with phospho-BACH1 promotes a damage-free S-phase progression by activating the G2/M and damage checkpoints and ensuring error free HR repair mechanism.<sup>44,45</sup>

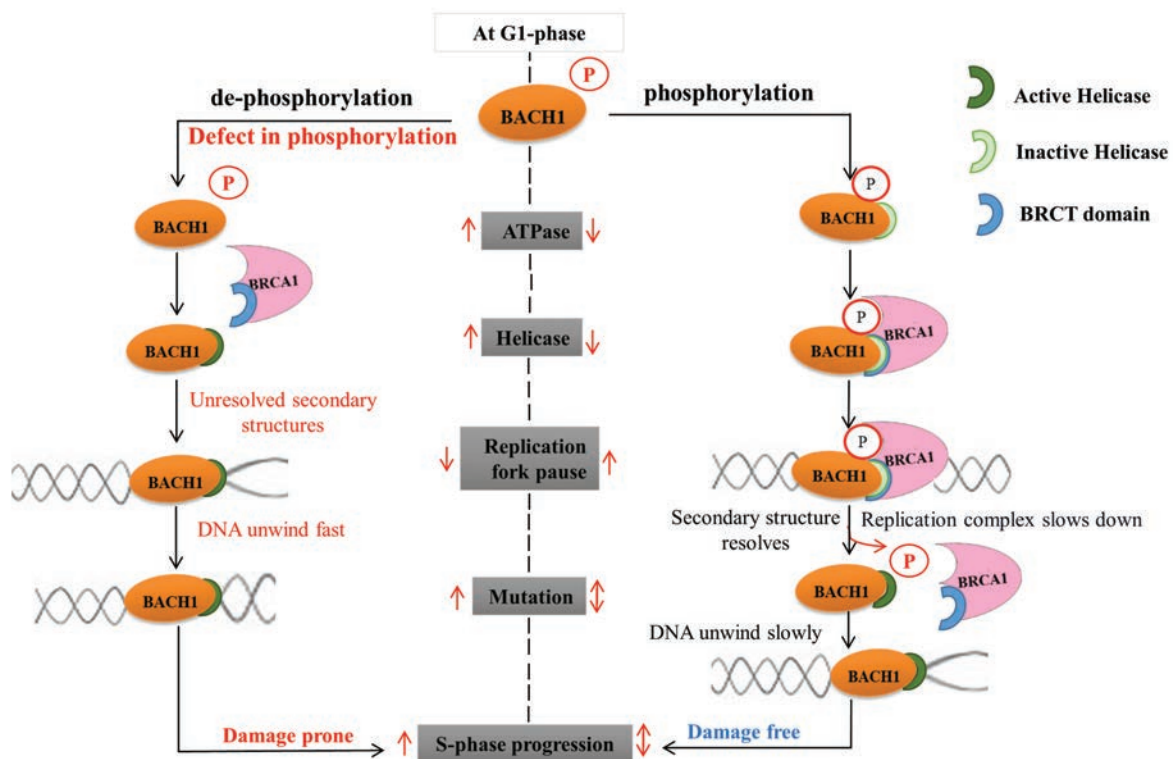


**Figure 3.** Mechanism of action of *BACH1* through its dual states. At G1-phase of the cell cycle, phosphorylated *BACH1* interacts with BRCA - complex to form the BRCA-BACH complex. This complex have low ATPase/helicase activity which results in slowdown in the S-phase progression enhancing the proof reading of the polymerase. The complex of BACH1/BRCA supports in resolving difficult structural motifs (right side of the figure). With de-phosphorylation or defect in phosphorylation, the BACH1/BRCA complex breaks down, leaving behind only BACH1 at the fork generating the space for the replication machinery to start replication. Dephosphorylated BACH1 gains the helicase activity to unwind the DNA for timely progression through S-phase (left side). Active helicase represented in dark green color, Inactive helicase-light green color and BRCT domain- blue color respectively. Arrow represents ↑ increase; ↓ decrease and ⇕ stable functional effects.

Both BRCA1 and BACH1 are recruited to the site of damage depending on the type of damage.<sup>9,11,31</sup> Recruitment of BRCA1 to laser-induced DSBs or Psoralen (Pso) Interstrand Crosslink (ICLs) is dependent on BACH1 whereas the recruitment is independent when the damage is caused by exposure to IR. Also, the recruitment of BACH1 at the damage sites is dependent on the interactor proteins to the site of damage. For laser-induced DSBs but not Psoralen (Pso)-Interstrand Crosslink (ICLs), DNA double strand break repair proteins, MRE11 and its associated nuclease activity function with or in parallel to BRCA1 for efficient BACH1 recruitment at the sites of damage.<sup>31</sup> In absence of MRE11 exonuclease, loading of another *BRCA1* interactor, CTIP, to DSBs is also delayed. CTIP is another protein associated with BRCA1 and modulates BRCA1s functions in DNA repair and/or cell cycle checkpoint control.<sup>49</sup> BRCA1 deficient cells also leads to less localization of CTIP at damage sites. This indicates that at laser induced damage sites, FANCD1/ BACH1 join hands with CTIP to remove secondary structures and helps CTIP to efficiently repair DNA ends with the help of repair protein MRE11 after interacting with BRCA1.<sup>50,51</sup> At the site of Pso-ICLs, BACH1 is also localized with the help of another mismatch repair (MMR) protein MLH1.<sup>10,33</sup> In case of UV light induced DNA crosslink, both MLH1 and upstream MMR protein MSH2 along with BACH1 is required, hence preventing aberrant DNA damage response.<sup>52</sup> So, BACH1 helps in the repair of damaged DNA through homologous recombination. In any of the situations like, absence of *BACH1*, mutation in the *BACH1* or loss of BACH1-BRCA1 interaction, the repair of damage through HR is perturbed. As a result, the alternate error-prone repair pathways like non-homologous end-joining (NHEJ) gets activated. The error-prone repair leads to mutations, which promotes the development, progression, recurrence and metastasis of cancer.

---

### ***BACH1* in chromatin remodeling**

Chromatin remodeling is another important event, which takes place in and around the replication complex or the double-strand DNA breaks aiding in genomic stability, unperturbed replication and DNA repair.<sup>53,54</sup> The proteins involved in maintaining genomic integrity bind to replication forks and damaged sites through highly organized signaling pathways.<sup>54,55</sup> BACH1 belongs to the group of human XPD-like helicases, which include XPD, RTEL1 and CHLR1, which have a role in chromatin remodeling as well as repair and regulates replication at difficult sites.<sup>56</sup> Structural and biochemical studies have proved that the XPD like helicases have an affinity towards single stranded DNA and forked DNA and plays a vital role in their arrangements.<sup>57-59</sup> BACH1 has direct interaction with BRCA1 through its BRCT domain, and also to the DNA through histone H3. This justifies that these proteins may have a role in the remodeling of chromatin along with repair, that takes place in and around the region of DNA damage.<sup>60</sup> Among the XPD like helicases, BACH1 possesses a G-quadruplex specific recognition site.<sup>13</sup> The G- quadruplexes are proven as epigenetic modulators and chromatin remodelers.<sup>15</sup> The affinity between G4s and BACH1/FANCD1 helicase strongly justify the involvement of FANCD1 in chromatin remodeling through G4s.<sup>12,13,15</sup> FANCD1 mostly recognizes the replication linked transient G4s which plays role in CpG island methylation maintenance as well as de novo CpG methylation control.<sup>15</sup> FANCD1 binds to the G4s through G4-binding peptide sequence, *RHAU18* which unwinds the branched DNA structures by repeated rounds of stepwise G4-unfolding and refolding.<sup>13</sup> It specifically binds to the 5' flaps and D-loops facilitating the fork movement through replication barriers and helps in pro-

cessing of the replication intermediates. This results in suppression of the heterochromatin spreading and proper maintenance of chromatin structure.<sup>13,14</sup> BACH1 also coordinates the functioning of polymerase REV1 and helicases WRN/BLM of opposite polarity near G4 DNA motifs to maintain epigenetic stability.<sup>12</sup> The *BACH1* sequence is significantly homologous to the DEAH helicase *CHLR1*.<sup>1</sup> CHLR1, which belongs to FANCD1 helicase family also plays a role in heterochromatin organization.<sup>3,16</sup> This helicase affects epigenetic modification of the genetic content and chromatin organization in the mammalian nucleus. In absence of CHLR1, defects in localization and organization of the chromatin have been observed. Aberrant localization of pericentric heterochromatin accompanied by perturbed centromere clustering happens in absence of CHLR1, the homolog of BACH1.<sup>16</sup> Pericentric heterochromatin is loaded with chromatin binding proteins like heterochromatin-binding protein 1 (HP1) isoforms. Epigenetic modifications like histone methylation at sites H3K9 and H4K20 also takes place at the pericentric heterochromatin.<sup>61,62</sup> *CHLR1* plays a role in the chromatin association of HP1 at the pericentric regions but it does not affect the histone modifications resulting into no alteration in the level of heterochromatin marker H3K9me3. Interestingly at the telomere regions, the association of both HP1 and histone modification is affected with depletion of FANCD1 helicase family. Therefore BACH1/FANCD1 helicase family certainly do play a role in targeting HP1 to the correct genomic regions.<sup>16</sup> Proper localization and binding of HP1 protein are required for the global organization of heterochromatin and centromere clustering. Its presence at the constitutive heterochromatin forms an obstacle for DNA replication providing a regulation to it.<sup>63,64</sup> Epigenetic modification like methylation is severely impaired at the pericentric/heterochromatin regions in absence of CHLR1, whereas the centromere/kinetochore regions are unaffected with the absence of these FANCD1 like helicase. So, BACH1/ChLR1/FANCD1 plays a heterochromatin specific role in epigenetic events.<sup>12,16</sup> Heterochromatin organization and accessibility to replication is regulated by BACH1 through HP1.<sup>28</sup> FANCD1 helicases might function in facilitating DNA replication at difficult sites, such as cohesion binding sites as well as condensed heterochromatic sites, stalled replication forks with secondary structures or at the DNA double strand breaks, by participating in both cohesion establishment and heterochromatin arrangement.<sup>12-14</sup> The *BACH1* interactor *BRCA1* is capable of functioning as a histone deacetylase.<sup>65</sup> So combination of epigenetic modifications like deacetylation and methylation at the heterochromatin or difficult to replicate regions lead to chromatin remodeling for accessibility of the DNA for repair and replication.<sup>66,67</sup> All these functions of BACH1 lead to the conclusion that *BACH1* has a role in heterochromatin organization during replication, regulation and repair of complex sites.

---

### ***BACH1* - an important player in cancer biology**

The very basic cause of cancer is the mutations in the genetic material. While mutations in tumorigenesis is very well characterized, but very little is known about the development of mutations that initiate tumorigenesis. In very simple terms cancer can develop due to genetic mutations transmitted through generations or it can be defined as a disease of ageing fueled by the accumulation of somatic mutations.<sup>68,69</sup> Mutations can develop by the variations or differential expression of the DNA damage repair molecules. Aberrations in the genetic material can also develop by the compromised proofreading activity of the replication machinery or inability to resolve the secondary structures at the difficult to repli-

cate site. In this era of cancer management, next generation sequence testing (NGS) and multi-gene ‘panel’ germline mutation testing in different cancers have identified the increase in mutations.<sup>70,71</sup> There is a rise in the number of mutations that leads to variants of uncertain significance (VUS) and needs further characterization. Characterizing these VUS will help to identify additional genes associated with an increased risk of cancer. These mutations which are till date insignificant are mostly present in the genes which play a role in DNA damage repair or cell cycle regulation pathways. Mutations in genes affecting these type of signal-

ing pathways can significantly affect the molecular pathogenesis of diseases like cancer. The helicase *BACH1*, which has a significant role in repair through homologous recombination, is instrumental in the molecular pathogenesis of cancer in different tissue types (Figure 2). Analysis from 2 different datasets, cBioPortal and COSMIC, shows a significant number of mutations in *BACH1* which are VUS. These VUS mutations significantly falls in the HBB domain, which has a role in DNA damage repair and BRCA1-BRCT interacting domain, which plays a role in helicase by considering cBioPortal and COSMIC datasets respectively

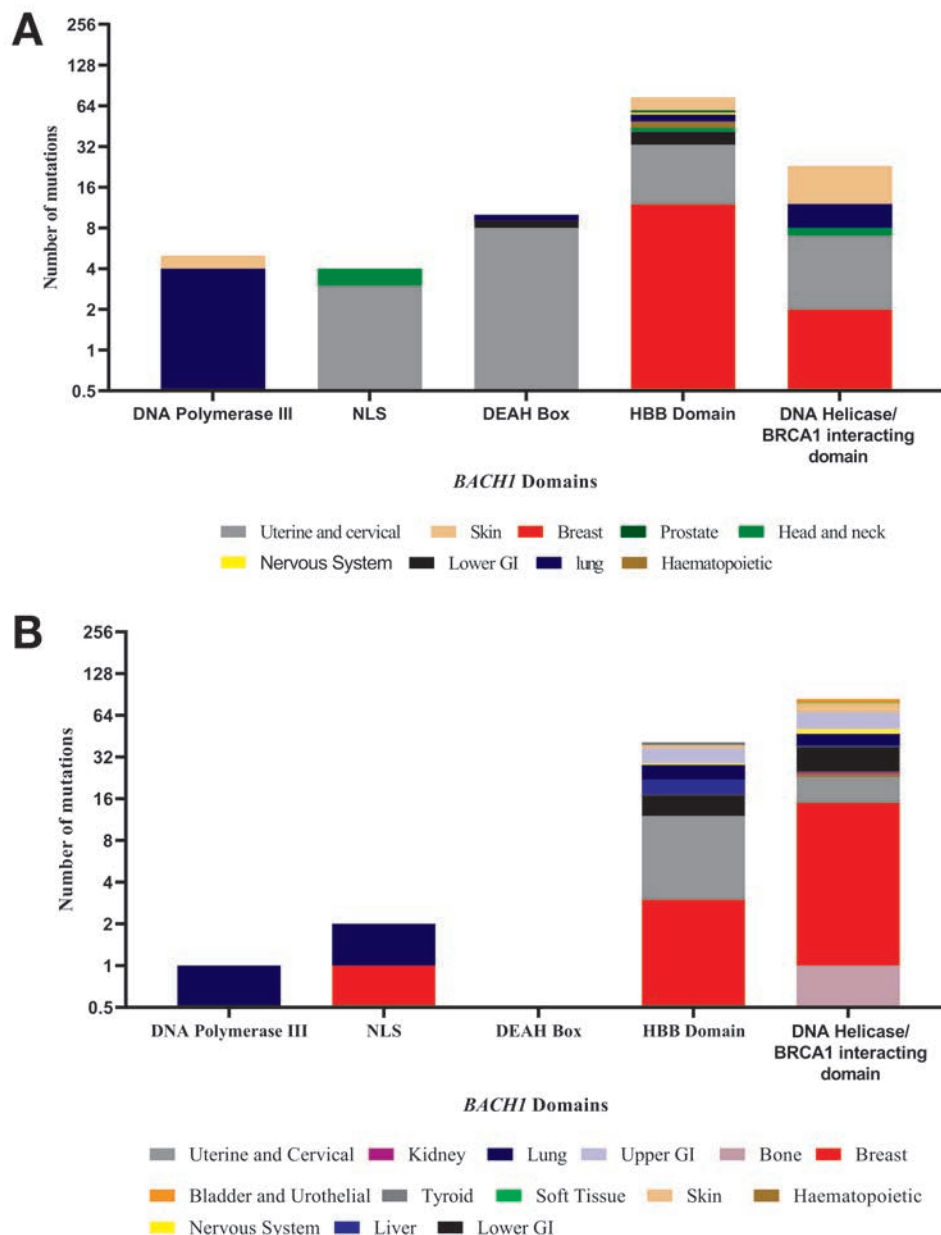


**Figure 4.** Mutation analysis of *BACH1* variants of uncertain significance, predicting its mutational hot spots. A) SNP's of *BACH1* gene were analyzed from cBioPortal. These mutations are variants of uncertain significance. The mutation position was mapped with the domains of *BACH1* respectively. X-axis represents *BACH1* domains and Y-axis represents number of mutations. Different color code is used to represent cancer types (Number of mutations= 611). B) SNP's of *BACH1* gene were analyzed from COSMIC. These mutations are variants of uncertain significance. The mutation position was mapped with the domains of *BACH1* respectively. X-axis represents *BACH1* domains and Y-axis represents number of mutations. Different color code is used to represent cancer types (Number of mutations= 560).

(Figure 4). This picture of distribution of mutation becomes clear by analyzing the characterized mutation along with the VUS. Furthermore, Analysis of mutations (SNPs) which are characterized and predicted including VUS conclude that the HBB domain of *BACH1* is the most susceptible site of mutation in different cancer types followed by the BRCT interacting domain, which is the *BRCA1* binding site (Figure 5). This conclusion justifies that *BACH1*'s repair activity significantly plays an independent role in the tumor biology of different cancer types apart from the *BRCA1* interaction. Mutational analysis reveals that the *BRIP1* locus is

strongly associated with hepatocellular carcinoma (HCC) risk in patients with hepatitis B virus (HBV) and/or hepatitis C virus (HCV)-induced liver disease.<sup>20</sup> The variants of *BACH1* which are linked with viral cirrhosis have mutations in the domains which interacts with the DSB repair protein or DNA mismatch repair protein like MRE11 or MUTL  $\alpha$  (Figure 2) [20]. Alternately, mutations in the mismatch repair proteins like MLH1 and MSH2, which regulate the localization of *BACH1* at the DSBs has been recognized as bladder cancer driver genes.<sup>72</sup> SNPs in the *BRIP1* gene influences cervical cancer susceptibility by regulating the RHOA

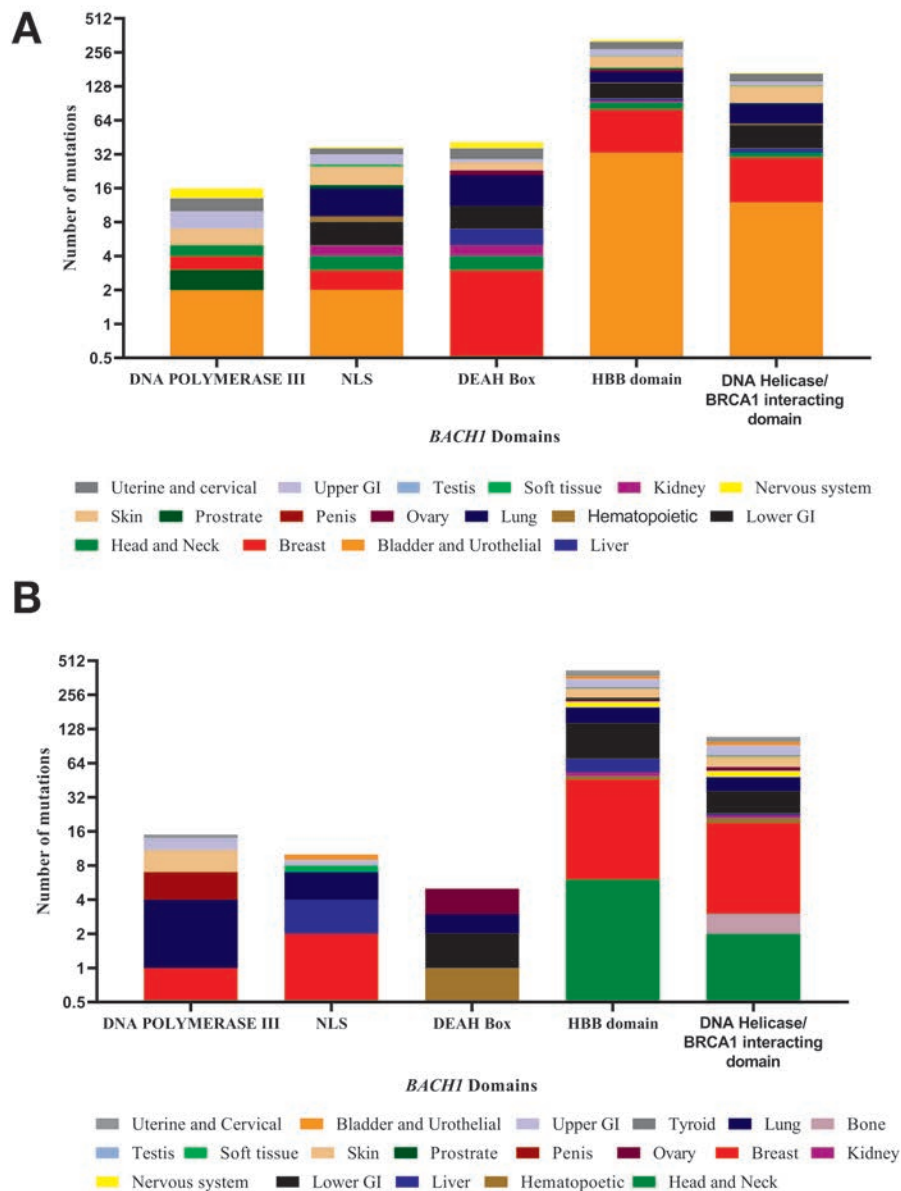


Figure 5. The bar graph represents the domain specific mutation in different cancers. A) SNP's of *BACH1* gene were analyzed from cBioPortal. These mutations are of clinical and non-clinical conditions like pathogenic, non-pathogenic and variants of uncertain significance. The mutation position was mapped with the domains of *BACH1* respectively. X-axis represents *BACH1* domains and Y-axis represents number of mutations. Different color code is used to represent cancer types (Number of mutations= 611). B) SNP's of *BACH1* gene were analyzed from COSMIC. These mutations are of clinical and non-clinical conditions like pathogenic, non-pathogenic and variants of uncertain significance. The mutation position was mapped with the domains of *BACH1* respectively. X-axis represents *BACH1* domains and Y-axis represents number of mutations. Different color code is used to represent cancer types (Number of mutations= 560).



GTPase activity, which is a player in cell proliferation, adhesion, apoptosis, cell polarity, invasion and metastasis (Figure 2).<sup>73</sup> Several somatic mutations are found in *FANCI* which are associated with skin cancer also. Mutational analysis of the melanoma candidate genes and *BRIP1* gene justifies the role of DNA damage response as an important factor in melanoma etiology (Figure 2).<sup>74</sup> Very recent case studies confirm the role of *BRIP1* in colon cancer also. Germline mutations in *BRIP1* lead to its truncated variants, which have an association with the colon cancer predisposition (Figure 2).<sup>75</sup> A brief analysis of the somatic mutations present in different cancer obtained from different databases shows an increase in *BACH1* mutation and its overexpression, confirming its involvement in different cancer type (Figure 6). Many evidences confirm the significant role of *BACH1* in the development and progression of lung cancer and most of the gynecological cancers, which are explained, in the following paragraphs.

### **BACH1 in breast cancer**

*BRCA1* gene is well established for its role in breast cancer (BC),<sup>76</sup> but recent scientific developments show that *BRCA1* interactor genes like *BRIP1* (*BACH1/FANCI*), *ATM*, *BRCC45*, *CTIP*, *MERIT40*, *NBS1*, *RAD50* and *TOPBP1* plays an important role as modifiers of breast cancer risk.<sup>77</sup> The meta-analysis study reveals that the *BACH1* polymorphism at the 919-serine position may reduce the danger of breast cancer in the Caucasian populations, mainly in postmenopausal females with a family history of breast cancer and without *BRCA1/2* mutations.<sup>78</sup> Literature shows that *BRCA1* and *TP53* are the major genetic players in case of Triple-

Negative Breast Cancer (TNBC). Though there is no significant correlation between *BRCA1* and *TP53* expression in TNBCs but their expression have a high prognostic significance.<sup>79</sup> *BRCA1*+/*TP53*+ patients had better overall survival than *BRCA1*-/*TP53*-TNBC patients.<sup>80</sup> Further research would reveal the pathways and the associated players to provide the molecular explanation behind their interactions and role in disease pathology. Low expression of *BRCA1* leads to loss of *BRCA1* protein interaction resulting in more free *BACH1* repair protein. Efficient repair is affected as *BRCA1* interactor *BACH1* cannot be loaded at the site of DNA damage. Also less damage sensing leads to less efficient homologous repair by *BACH1* and the damage is repaired through some other pathways like NHEJ, with compromised proofreading activity developing mutations.<sup>81,82</sup> Accumulation of mutations leads to favorable condition for developing transformed tumor cells which are resistant to chemotherapy-induced apoptosis. This results in the recurrence of breast cancer, which would explain why negative *BRCA1* expression is associated with poorer prognosis.<sup>83</sup> In case of *TP53*, the expression of the gene does not directly correlates with the proper function of the gene. Missense mutation of *TP53* yields a highly stable mutant *TP53* protein that can give high *TP53* expression, whereas *TP53* proteins resulting from truncating *TP53* mutations are unstable and cannot be detected.<sup>84</sup> The prevalence of *TP53* mutation types varies among different breast cancer subgroups. There is a high prevalence of missense mutations in luminal tumors whereas the prevalence of truncated mutations are there in basal tumors.<sup>85</sup> Also truncated mutations are strongly associated with poor survival and these mutations are not easy to be detected. In other words, though the mutations in checkpoints are undetected they can lead to an increase in DNA damage, which will increase the activity of repair genes like *BACH1*. Increased

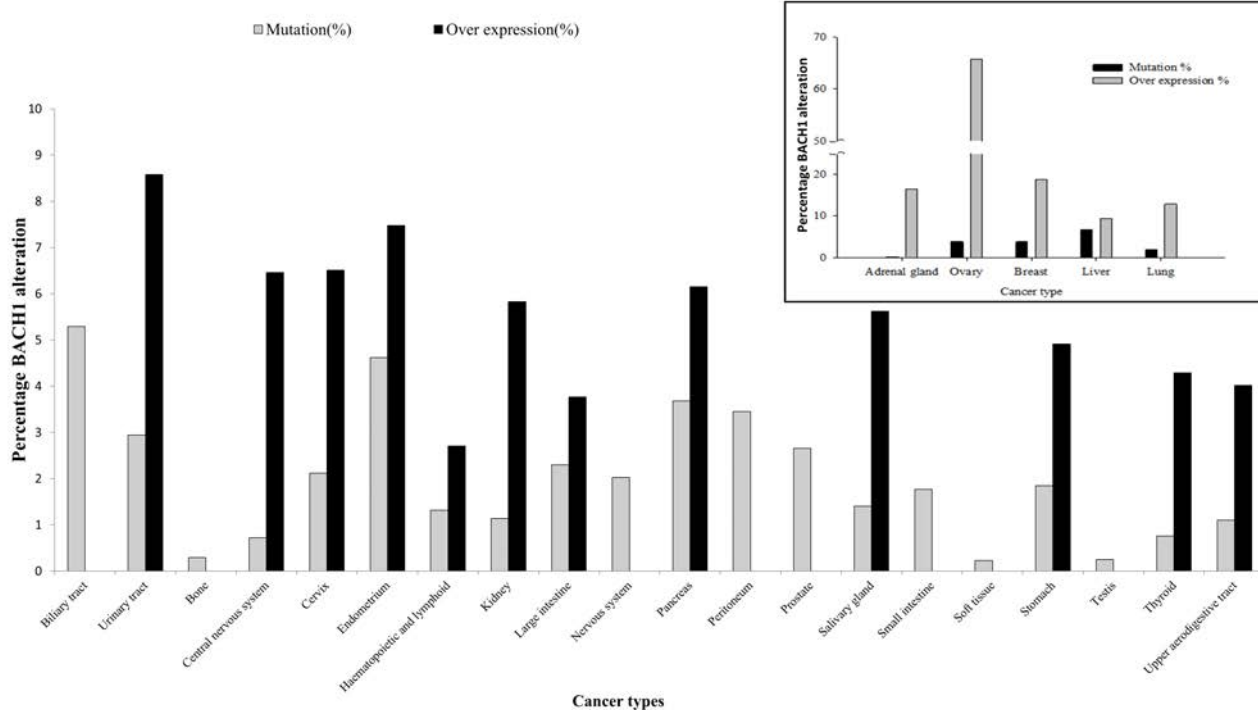


**Figure 6.** Mutation and overexpression of *BACH1* in different cancer types. The schematic bar graph represents the total percentage of samples with mutated *BACH1* and the total percentage of the sample with overexpressed *BACH1* in different cancer types. X-axis represents the type of cancer and Y-axis represents the percentage(%) of *BACH1* alteration. The data was extracted from COSMIC data base.

BACH1 transcript levels were found in tumors with an estrogen receptor-negative, progesterone receptor-negative or HER-2-positive status. BRIP1/BACH1 overexpression is also detected in primary invasive breast carcinomas.<sup>86</sup> The 2014 COSMIC data on breast cancer and case studies reports overexpression of BACH1 is 18.75% of patient samples and the mutation rate is around 3.8%, confirming the role of *BACH1* in breast cancer biology (Figure 6). The appearance of *BACH1* and its target genes was correlated to an increased risk of breast cancer reappearance in patients.<sup>87</sup> Mutations in exon 20 of *BRCA1* are identified in BC patient which alter the stability of the BRCT domain at the binding site of *BACH1*.<sup>88</sup> The male breast cancer patients are generally identified to be normal for *BRCA1/2* gene but silent mutations are found on *BACH1* tumor suppressor gene and DNA helicase.<sup>89</sup> Susceptibility towards breast cancer also develops in carriers of the C47G polymorphism and Pro-Ser genotype of *BACH1* in premenopausal women.<sup>90</sup> Deletion mutations in *BRIP1* are also identified in early-onset of breast cancer.<sup>91</sup> In conclusion, these data from different research group justifies that *BRIP1/BACH1* is a genuine target gene for breast cancer disease pathology.

### ***BACH1* in ovarian cancer**

Cancer in ovary is the leading cause of cancer associated mortality among woman.<sup>92</sup> Reproductive factors such as high parity, use of oral contraceptive, breastfeeding, removal of the uterus and tubal ligation are few ways to protect against ovarian cancer,<sup>93</sup> whereas infertility and endometriosis are the major risk factors.<sup>94</sup> The mechanism for the development of this cancer at the molecular level is not well studied and understood, but inflammation-related oxidative stress has been proposed as a unifying theory by which these risk factors could cause genomic damage leading to the development of tumorigenesis in the ovary.<sup>95</sup> In other words, the efficacy of the DNA damage repair pathway may play a major role in ovarian carcinogenesis.<sup>96</sup> The above statement is supported by the COSMIC data, which shows that in a sample size of 266 patients the percentage of BACH1 overexpression, DNA damage repair gene, is 65.75 and in 1268 patients the percentage of BACH1 mutation is 3.84 (Figure 6). Several evidences link DNA repair with ovarian cancer- most of the ovarian cancer susceptible genes, like *BRCA1* and *BRCA2* have been identified to regulate DNA repair. *TP53* is another susceptible gene, which plays a role in maintaining genomic integrity via several mechanisms including induction of cell cycle arrest in response to DNA damage, DNA repair and regulation of apoptosis.<sup>97</sup> Statistical analysis from a population-based North Carolina Ovarian Cancer Study (NCOCS) support for strong associations between ovarian cancer and polymorphisms in the repair genes. They identified two SNPs in *CHEK2*, two SNPs in *TP53*, and one SNP each in *BACH1* and *LIG4* repair genes. Few weak targets like *NBS1*, *MSH6*, *RAD52*, *XRCC5* and *GADD45B* are also identified by some other group.<sup>98</sup> As *BACH1* is a major player in HR repair pathway, it will be of great diagnostics and prognostic value to find the exact role and the underlying molecular mechanism of *BACH1* in ovarian cancer, which remains unclear. The bioinformatics data indicates that the *BACH1* SNP found in ovarian cancer patients is predicted to affect splicing and also mi-RNA binding site.<sup>99</sup> These findings reflects that *BRCA1-BACH1* interaction plays an important role in the etiology of ovarian cancer.

### ***BACH1* in lung cancer**

Lung cancer is the most commonly diagnosed cancer and it is one of the reasons for cancer death worldwide. Approximately 1.6 million case results in deaths per year.<sup>100</sup> The molecular mechanisms which play the role in malignancy are unknown. The important genes which have a role in lung cancer are the cell cycle and the repair genes like *TP53*, *RB*, *BRD7*, *PCNA* and *NFKB1*.<sup>101</sup> *BRIP1* is found to be overexpressed in lung cancer (COSMIC data, 2014, Figure 6). Homozygous deletions are observed in lung adenocarcinoma in the *BRIP1* gene (3%). Also, BRCAness, i.e. HR defects in absence of any germline mutation in *BRCA*, is usually seen in non-small cell lung cancer (NSCLC).<sup>102</sup> High transcript level expression of BRCA1 is a helpful tool for choosing NSCLC patients for individualized chemotherapy, as it is the only independent prognostic variable for NSCLC patients.<sup>103</sup> The findings of Zhang group highlights that the integrity of the FA-BRCA pathway is a determinant of sensitivity/resistance to DNA crosslinking agents in lung cancer cells and may represent a mechanism underlying the resistance to chemotherapy of DNA crosslinking agents.<sup>104</sup> Ubiquitous type of mutation having *BRIP1* variants are identified from tumor and blood sample obtained from NSCLC patients.<sup>105</sup> In lung cancer, germline mutations are observed in the *CHK1* gene which is involved in Fanconi anemia and *BRCA1/2* signaling pathways.<sup>106</sup> Methylation in *FANCF* promoter is a significant predictor for poor survival in adenocarcinoma of the lung, so inactivation of *FANCF-BRCA* pathways may result in the poorer survival rate of patients with lung cancer.<sup>107</sup> These findings justify the important role played by *FANCF/BACH1* in cancer metabolism of lungs.

### **Concluding remarks and future perspective**

Our current understanding indicates that BACH1 nuclear protein differentially participate in complex networks that regulate cell growth, cell cycle, DNA replication, DNA repair, mitotic chromatin dynamics, and also epigenetic modifications at the specific heterochromatin sites. *BACH1* functions in the replication of the difficult sites and during stress, damage and secondary structures, because of its characteristics as a helicase, repair gene and as chromatin remodeler. Cancer mutation data (COSMIC) shows the widespread mutation of this gene in different cancer types. The overexpression of this gene in different cancer types clearly explains the increase in damage in the process of tumorigenesis and the proper repair activity is highly abrogated leading to accumulation of mutations. High mutation burden provides a favorable environment for the development, progression and recurrence of tumor. Further analysis reveals that the HBB domain of *BACH1* is the most affected domain and the hot spot for characterized as well as uncharacterized mutations, explaining its role in cancer biology. Since the HBB domain has no link with BRCA1 interaction, so the effect conferred by this domain in different cancer types is independent of the *BRCA1* function. The BRCA1 binding domain or the DNA helicase comes as the second most affected region of BACH1. The analysis of variants with uncertain significance also shows HBB domain as the most susceptible sites in *BACH1* which justifies the emerging role of DNA repair through *BACH1* in cancer biology. A deep insight into the functional aspect of the HBB domain along with *BRCA1* interaction will open new avenues in the treatment of most of the deep-rooted cancers. Mutations or defect in this gene affects major molecular pathways that regulates and maintains the genomic integrity of the cells. With an aberration

in the genetic integrity tumorigenesis develops. So, *BACH1/BRIP1/FANCI/ChlR1* gene has high potentials of transforming a normal cell into a tumor cell if compromised under certain circumstances, thus justified to be named as an oncogene. Even-though *BACH1* has a substantial role in cancer biology and has a major role to play in different types of cancer, very few studies have been completed towards understanding the mechanism of how the proteins interact among themselves. In few of the cancers, *BACH1* is analyzed as the major interactor protein of *BRCA1*, so, a detailed analysis of the interaction study is required to identify its role in tumorigenesis and metastasis. Current literature and our ongoing studies indicate that *BRCA1-BACH1* interaction is lost due to diseased condition or a mutation at the interactor domain results in downregulation of DNA proofreading activity leading to more mutations, and hence increasing the risk of tumorigenesis. So, to understand *BACH1*, it is essential to explore this protein, its functional and interacting domains and critically evaluate its involvement to physiology and identify the potential roles in human pathologies, such as cancer.

## References

- Cantor SB, Bell DW, Ganesan S, et al. *BACH1*, a novel helicase-like protein, interacts directly with *BRCA1* and contributes to its DNA repair function. *Cell* 2001;105:149-60.
- Hall JM, Lee MK, Newman BM, et al. Linkage of early-onset familial breast cancer to chromosome 17q21. *Science* 1990;250:1684-9.
- Hirota Y, Lahti JM. Characterization of the enzymatic activity of hChlR1, a novel human DNA helicase. *Nucleic Acids Res* 2000;28:917-24.
- Cantor S, Drapkin R, Zhang F, et al. The *BRCA1*-associated protein *BACH1* is a DNA helicase targeted by clinically relevant inactivating mutations. *PNAS* 2004;101:2357-62.
- Levrin O, Attwooll C, Henry RT, et al. The *BRCA1*-interacting helicase *BRIP1* is deficient in Fanconi anemia. *Nat Genet* 2005;37:931-3.
- Kumaraswamy E, Shiekhhattar R. Activation of *BRCA1/BRCA2*-associated helicase *BACH1* is required for timely progression through S phase. *Mol Cell Biol* 2007;27:6733-41.
- Brosh Jr RM. DNA helicases involved in DNA repair and their roles in cancer. *Nat Rev Cancer* 2013;13:542-58.
- Gong Z, Kim JE, Leung CC, et al. *BACH1/FANCI* acts with TopBP1 and participates early in DNA replication checkpoint control. *Mol Cell* 2010;37:438-46.
- Peng M, Litman R, Jin Z, et al. *BACH1* is a DNA repair protein supporting *BRCA1* damage response. *Oncogene* 2006;25:2245-53.
- Cantor SB, Xie J. Assessing the link between *BACH1/FANCI* and *MLH1* in DNA crosslink repair. *Environ Mol Mutagen* 2010;51:500-7.
- Brosh Jr RM, Cantor SB. Molecular and cellular functions of the *FANCI* DNA helicase defective in cancer and in Fanconi anemia. *Front Genet* 2014;5:372-14.
- Sarkies P, Murat P, Phillips LG, et al. *FANCI* coordinates two pathways that maintain epigenetic stability at G-quadruplex DNA. *Nucleic Acids Res* 2012;40:1485-98.
- Wu CG, Spies M. G-quadruplex recognition and remodeling by the *FANCI* helicase. *Nucleic Acids Res* 2016;44:8742-53.
- Schwab RA, Nieminuszczy J, Shin-ya K, Niedzwiedz W. *FANCI* couples replication past natural fork barriers with maintenance of chromatin structure. *J. Cell Biol* 2013;201:33-48.
- Varizhuk A, Isaakova E, Pozmogova G. DNA G-quadruplexes (g4s) modulate epigenetic (Re) programming and chromatin remodeling. *BioEssays* 2019;41:1900091-101.
- Inoue A, Hyle J, Lechner MS, Lahti JM. Mammalian ChlR1 has a role in heterochromatin organization. *Exp Cell Res* 2011;317:2522-35.
- Wu Y, Brosh Jr RM. *FANCI* helicase operates in the Fanconi Anemia DNA repair pathway and the response to replicational stress. *Curr Mol Med* 2009;9:470-82.
- Alter BP. Diagnosis, genetics, and management of inherited bone marrow failure syndromes. *Am J Hematol* 2007;2007:29-39.
- Seal S, Thompson D, Renwick A, et al. Truncating mutations in the Fanconi anemia J gene *BRIP1* are low-penetrance breast cancer susceptibility alleles. *Nat Genet* 2006;38:1239-41.
- Oussalah A, Avogbe PH, Guyot E, et al. *BRIP1* coding variants are associated with a high risk of hepatocellular carcinoma occurrence in patients with HCV-or HBV-related liver disease. *Oncotarget* 2017;8:62842-57.
- Peng M, Litman R, Xie J, et al. The *FANCI/MutL $\alpha$*  interaction is required for correction of the cross-link response in FA-J cells. *EMBO J* 2007;26:3238-49.
- Williams SA, Wilson JB, Clark AP, et al. Functional and physical interaction between the mismatch repair and FA-*BRCA* pathways. *Hum Mol Genet* 2011;20:4395-410.
- Yeom G, Kim J, Park CJ. Investigation of the core binding regions of human Werner syndrome and Fanconi anemia group J helicases on replication protein A. *Sci Rep* 2019;9:1-10.
- Estep KN, Brosh Jr RM. RecQ and Fe-S helicases have unique roles in DNA metabolism dictated by their unwinding directionality, substrate specificity, and protein interactions. *Biochem Soc Trans* 2018;46:77-95.
- Awate S, Brosh Jr RM. Interactive roles of DNA helicases and translocases with the single-stranded DNA binding protein RPA in nucleic acid metabolism. *Int J Mol Sci* 2017;18:1-25.
- Dhar S, Brosh RM. BLM's balancing act and the involvement of *FANCI* in DNA repair. *Cell Cycle* 2018;17:2207-20.
- Yu X, Chini CC, He M, et al. The BRCT domain is a phospho-protein binding domain. *Science* 2003;302:639-42.
- Wu W, Togashi Y, Johmura Y, et al. HP1 regulates the localization of *FANCI* at sites of DNA double-strand breaks. *CANCER Sci* 2016;107:1406-15.
- Yarden RI, Pardo-Reoyo S, Sgagias M, et al. *BRCA1* regulates the G2/M checkpoint by activating Chk1 kinase upon DNA damage. *Nat Genet* 2002;30:285-9.
- Greenberg RA, Sobhian B, Pathania S, et al. Multifactorial contributions to an acute DNA damage response by *BRCA1/BARD1*-containing complexes. *Genes Dev* 2006;20:34-46.
- Suhasini AN, Sommers JA, Muniandy PA, et al. Fanconi anemia group J helicase and MRE11 nuclease interact to facilitate the DNA damage response. *Mol Cell Biol* 2013;33:2212-27.
- Shakya R, Reid LJ, Reczek CR, et al. *BRCA1* tumor suppression depends on BRCT phosphoprotein binding, but not its E3 ligase activity. *Science* 2011;334:525-8.
- Zhang X, Guo J, Wei X, et al. *Bach1*: function, regulation, and involvement in disease. *Oxid Med Cell Longev* 2018;1-8.
- Atkinson J, McGlynn P. Replication fork reversal and the maintenance of genome stability. *Nucleic Acids Res* 2009;37:3475-92.
- Wu Y, Shin-ya K, Brosh RM. *FANCI* helicase defective in

- Fanconi anemia and breast cancer unwinds G-quadruplex DNA to defend genomic stability. *Mol Cell Biol* 2008;28:4116-28.
36. Wu W, Rokutanda N, Takeuchi J, et al. HERC2 facilitates BLM and WRN helicase complex interaction with RPA to suppress G-quadruplex DNA. *Cancer Res* 2018;78:6371-85.
  37. Cantor SB, Nayak S. FANCI at the FORK. *Mutat Res* 2016;788:7-11.
  38. Gupta R, Sharma S, Sommers JA, et al. Analysis of the DNA substrate specificity of the human BACH1 helicase associated with breast cancer. *J Biol Chem* 2005;280:25450-60.
  39. Gupta R, Sharma S, Sommers JA, et al. FANCI (BACH1) helicase forms DNA damage inducible foci with replication protein A and interacts physically and functionally with the single-stranded DNA-binding protein. *Blood* 2007;110:2390-8.
  40. Sommers JA, Banerjee T, Hinds T, et al. Novel function of the Fanconi anemia group J or RECQ1 helicase to disrupt protein-DNA complexes in a replication protein A-stimulated manner. *J Biol Chem* 2014;289:19928-41.
  41. Schwartz MF, Duong JK, Sun Z, et al. Rad9 phosphorylation sites couple Rad53 to the *Saccharomyces cerevisiae* DNA damage checkpoint. *Mol Cell* 2002;9:1055-65.
  42. Xie J, Litman R, Wang S, Peng M, et al. Targeting the FANCI-BRCA1 interaction promotes a switch from recombination to pol $\eta$ -dependent bypass. *Oncogene* 2010;29:2499-508.
  43. Davis AJ, Chen DJ. DNA double strand break repair via non-homologous end-joining. *Transl. Cancer Res.* 2013;2:130-43.
  44. Xie J, Peng M, Guillemette S, et al. FANCI/BACH1 acetylation at lysine 1249 regulates the DNA damage response. *PLoS Genet* 2012;8:1-14.
  45. Savage KI, Harkin DP. BRCA1, a 'complex' protein involved in the maintenance of genomic stability. *The FEBS J* 2015;282:630-46.
  46. Dohrn L, Salles D, Siehler SY, et al. BRCA1-mediated repression of mutagenic end-joining of DNA double-strand breaks requires complex formation with BACH1. *Biochem J* 2012;441:919-28.
  47. Wang X, Lui VC, Poon RT, et al. DNA damage mediated S and G2 checkpoints in human embryonal carcinoma cells. *Stem Cells* 2009;27:568-76.
  48. Willis N, Rhind N. Regulation of DNA replication by the S-phase DNA damage checkpoint. *Cell Division* 2009;4:1-10.
  49. Yu X, Baer R. Nuclear localization and cell cycle-specific expression of CtIP, a protein that associates with the BRCA1 tumor suppressor. *J Biol Chem* 2000;275:18541-9.
  50. Anand R, Ranjha L, Cannavo E, Cejka P. Phosphorylated CtIP functions as a co-factor of the MRE11-RAD50-NBS1 endonuclease in DNA end resection. *Mol Cell* 2016;64:940-50.
  51. Wang H, Li Y, Truong LN, et al. CtIP maintains stability at common fragile sites and inverted repeats by end resection-independent endonuclease activity. *Mol Cell* 2014;54:1012-21.
  52. Peng M, Xie J, Ucher A, et al. Crosstalk between BRCA-Fanconi anemia and mismatch repair pathways prevents MSH2-dependent aberrant DNA damage responses. *The EMBO J* 2014;33:1698-712.
  53. House N, Koch MR, Freudenreich CH. Chromatin modifications and DNA repair: beyond double-strand breaks. *Front Genet* 2014;5:1-18.
  54. Lai W, Li H, Liu S, Tao Y. Connecting chromatin modifying factors to DNA damage response. *Int J Mol Sci* 2013;14:2355-69.
  55. Osley MA, Shen X. Altering nucleosomes during DNA double-strand break repair in yeast. *Trends Genet* 2006;22:671-7.
  56. White MF. Structure, function and evolution of the XPD family of iron-sulfur-containing 5'→3' DNA helicases. *Biochem Soc Trans* 2009;37:547-51.
  57. Wolski SC, Kuper J, Hanzelmann P, et al. Crystal structure of the FeS cluster-containing nucleotide excision repair helicase XPD. *PLoS Biol* 2008;6:e149.
  58. Fan L, Fuss JO, Cheng QJ, et al. XPD helicase structures and activities: insights into the cancer and aging phenotypes from XPD mutations. *Cell* 2008;133:789-800.
  59. Liu H, Rudolf J, Johnson KA, et al. Structure of the DNA repair helicase XPD. *Cell* 2008;133:801-12.
  60. Wu W, Nishikawa H, Fukuda T, et al. Interaction of BARD1 and HP1 is required for BRCA1 retention at sites of DNA damage. *Cancer Res* 2015;75:1311-21.
  61. Magaraki A, van der Heijden G, Sleddens-Linkels E, et al. Silencing markers are retained on pericentric heterochromatin during murine primordial germ cell development. *Epigenetics Chromatin* 2017;10:1-20.
  62. Muramatsu D, Singh PB, Kimura H, et al. Pericentric heterochromatin generated by HP1 protein interaction-defective histone methyltransferase Suv39h1. *J Biol Chem* 2013;288:25285-96.
  63. Yi Q, Chen Q, Liang C, et al. HP1 links centromeric heterochromatin to centromere cohesion in mammals. *EMBO reports* 2018;19:1-13.
  64. Saksouk N, Simboeck E, Déjardin J. Constitutive heterochromatin formation and transcription in mammals. *Epigenetics Chromatin* 2015;8:1-7.
  65. Yarden RI, Brody LC. BRCA1 interacts with components of the histone deacetylase complex. *PNAS* 1999;96:4983-8.
  66. Groth A, Rocha W, Verreault A, Almouzni G. Chromatin challenges during DNA replication and repair. *Cell* 2007;128:721-33.
  67. Liu J, Kim J, Oberdoerffer P. Metabolic modulation of chromatin: implications for DNA repair and genomic integrity. *Front Genet* 2013;4:1-11.
  68. Kennedy SR, Zhang Y, Risques RA. Cancer-associated mutations but no cancer: insights into the early steps of carcinogenesis and implications for early cancer detection. *Trends Cancer* 2019;5:531-40.
  69. Risques RA, Kennedy SR. Aging and the rise of somatic cancer-associated mutations in normal tissues. *PLoS Genet* 2018;14:1-12.
  70. Tate JG, Bamford S, Jubb HC, et al. COSMIC: the catalogue of somatic mutations in cancer. *Nucleic Acids Res* 2019;47:1-7.
  71. Gao J, Aksoy BA, Dogrusoz U, et al. Integrative analysis of complex cancer genomics and clinical profiles using the cBioPortal. *Sci Signal* 2013;6:1-19.
  72. Abbosh PH, Plimack ER. Molecular and clinical insights into the role and significance of mutated dna repair genes in bladder cancer. *Bladder Cancer* 2018;4:9-18.
  73. Zou W, Ma X, Hua W, et al. BRIP1 inhibits the tumorigenic properties of cervical cancer by regulating RhoA GTPase activity. *Oncol Lett* 2015;11:551-8.
  74. Guillemette S, Branagan A, Peng M, et al. FANCI localization by mismatch repair is vital to maintain genomic integrity after UV irradiation. *Cancer Res* 2014;74:932-44.
  75. Ali M, Delozier CD, Chaudhary U. BRIP-1 germline mutation and its role in colon cancer: presentation of two case reports and review of literature. *BMC Med Genet* 2019;20:1-5.
  76. Karami F, Mehdipour P. A comprehensive focus on global

- spectrum of BRCA1 and BRCA2 mutations in breast cancer. *Biomed Res Int* 2013;1-21.
77. Rebbeck TR, Mitra N, Domchek SM, et al. Modification of BRCA1-associated breast and ovarian cancer risk by BRCA1-interacting genes. *Cancer Res* 2011;71:5792-805.
  78. Shi J, Tong J, Cai S, et al. Correlation of the BACH1 Pro919Ser polymorphism with breast cancer risk: A literature based meta analysis and meta regression analysis. *Exp Ther Med* 2013;6:435-44.
  79. Yadav BS, Chanana P, Jhamb S. Biomarkers in triple negative breast cancer: a review. *World J Clin Oncol* 2015;6:252-63.
  80. Kim MC, Choi JE, Lee SJ, Bae YK. Coexistent loss of the expressions of BRCA1 and p53 predicts poor prognosis in triple-negative breast cancer. *Ann Surg Oncol* 2016;23:3524-30.
  81. Saha J, Davis AJ. Unsolved mystery: the role of BRCA1 in DNA end-joining. *J Radiat Res* 2016;57:i18-i24.
  82. Jackson SP. Sensing and repairing DNA double-strand breaks. *Carcinogenesis* 2002;23:687-96.
  83. Thangaraju M, Kaufmann SH, Couch FJ. BRCA1 facilitates stress-induced apoptosis in breast and ovarian cancer cell lines. *J Biol Chem* 2000;275:33487-96.
  84. Biganzoli E, Coradini D, Ambrogi F, et al. P53 status identifies two subgroups of triple-negative breast cancers with distinct biological features. *Jpn J Clin Oncol* 2011;41:172-9.
  85. Dumay A, Feugeas JP, Wittmer E, et al. Distinct tumor protein p53 mutants in breast cancer subgroups. *Int J Cancer* 2013;132:1227-31.
  86. Eelen G, Bempt IV, Verlinden L, et al. Expression of the BRCA1-interacting protein Brip1/BACH1/FANCL is driven by E2F and correlates with human breast cancer malignancy. *Oncogene* 2008;27:4233-41.
  87. Gupta I, Ouhitit A, Al-Ajmi A, et al. BRIP1 overexpression is correlated with clinical features and survival outcome of luminal breast cancer subtypes. *Endocr Connect* 2018;7:65-77.
  88. Chakraborty A, Katarkar A, Chaudhuri K, Mukhopadhyay A. Detection of a novel mutation in exon 20 of the BRCA1 gene. *Cell Mol Biol Lett* 2013;18:631-8.
  89. Venkateshwari A, Clark DW, Nallari P, et al. BRIP1/FANCL mutation analysis in a family with history of male and female breast Cancer in India. *J Breast Cancer* 2017;20:104-7.
  90. Pabalan N, Jarjanazi H, Ozcelik H. Association between BRIP1 (BACH1) polymorphisms and breast cancer risk: a meta-analysis. *Breast Cancer Res* 2013;137:553-8.
  91. De Nicolo A, Tancredi M, Lombardi G, et al. A novel breast cancer-associated BRIP1 (FANCL/BACH1) germ-line mutation impairs protein stability and function. *Clin Cancer Res* 2008;14:4672-80.
  92. Momenimovahed Z, Tiznobaik A, Taheri S, Salehiniya H. Ovarian cancer in the world: epidemiology and risk factors. *Int J Womens Health* 2019;11:287-99.
  93. Moorman PG, Calingaert B, Palmieri RT, et al. Hormonal risk factors for ovarian cancer in premenopausal and postmenopausal women. *Am J Epidemiol* 2008;167:1059-69.
  94. Ness RB, Cramer DW, Goodman MT, et al. Infertility, fertility drugs, and ovarian cancer: a pooled analysis of case-control studies. *Am J Epidemiol* 2002;155:217-24.
  95. Su KM, Wang PH, Yu MH, et al. The recent progress and therapy in endometriosis-associated ovarian cancer. *J Chin Med Assoc* 2020;83:227-32.
  96. Gee ME, Faraahi Z, McCormick A, Edmondson RJ. DNA damage repair in ovarian cancer: unlocking the heterogeneity. *J Ovarian Res* 2018;11:1-12.
  97. Chen CC, Feng W, Lim PX, et al. Homology-directed repair and the role of BRCA1, BRCA2, and related proteins in genome integrity and cancer. *Annu Rev Cancer Biol* 2018;2:313-36.
  98. Schildkraut JM, Iversen ES, Wilson MA, et al. Association between DNA damage response and repair genes and risk of invasive serous ovarian cancer. *PLoS One* 2010;5:1-9.
  99. Song H, Ramus SJ, Kjaer SK, et al. Tagging single nucleotide polymorphisms in the BRIP1 gene and susceptibility to breast and ovarian cancer. *PLoS One* 2007;2:1-7.
  100. Torre LA, Bray F, Siegel RL, et al. Global cancer statistics, 2012. *CA Cancer J Clin* 2015;65:87-108.
  101. Gao Y, Wang B, Gao S. BRD7 acts as a tumor suppressor gene in lung adenocarcinoma. *PLoS One* 2016;11:1-9.
  102. Waqar SN, Devarakonda SH, Michel LS, et al. BRCAness in non-small cell lung cancer (NSCLC). *J Clin Oncol* 2014;32:11033-.
  103. Bartolucci R, Wei J, Sanchez JJ, et al. XPG mRNA expression levels modulate prognosis in resected non-small-cell lung cancer in conjunction with BRCA1 and ERCC1 expression. *Clin Lung Cancer* 2009;10:47-52.
  104. Zhang J, Wang X, Lin CJ, et al. Altered expression of FANCL confers mitomycin C sensitivity in Calu-6 lung cancer cells. *Cancer Biol Ther* 2006;5:1632-6.
  105. Jamal-Hanjani M, Wilson GA, Horswell S, et al. Detection of ubiquitous and heterogeneous mutations in cell-free DNA from patients with early-stage non-small-cell lung cancer. *Ann Oncol* 2016;27:862-7.
  106. Haruki N, Saito H, Tatematsu Y, et al. Histological type-selective, tumor-predominant expression of a novel CHK1 isoform and infrequent in vivo somatic CHK2 mutation in small cell lung cancer. *Cancer Res* 2000;60:4689-92.
  107. Marsit CJ, Liu M, Nelson HH, et al. Inactivation of the Fanconi anemia/BRCA pathway in lung and oral cancers: implications for treatment and survival. *Oncogene* 2004;23:1000-4.

RESEARCH

Open Access



# The budding yeast protein Chl1p is required for delaying progression through G1/S phase after DNA damage

Muhseena N. Katheeja<sup>1</sup>, Shankar Prasad Das<sup>1,2\*</sup> and Suparna Laha<sup>1,2\*</sup>

## Abstract

**Background:** The budding yeast protein Chl1p is a nuclear protein required for sister-chromatid cohesion, transcriptional silencing, rDNA recombination, ageing and plays an instrumental role in chromatin remodeling. This helicase is known to preserve genome integrity and spindle length in S-phase. Here we show additional roles of Chl1p at G1/S phase of the cell cycle following DNA damage.

**Results:** G1 arrested cells when exposed to DNA damage are more sensitive and show bud emergence with faster kinetics in *chl1* mutants compared to wild-type cells. Also, more damage to DNA is observed in *chl1* cells. The viability falls synergistically in *rad24chl1* cells. The regulation of Chl1p on budding kinetics in G1 phase falls in line with Rad9p/Chk1p and shows a synergistic effect with Rad24p/Rad53p. *rad9chl1* and *chk1chl1* shows similar bud emergence as the single mutants *chl1*, *rad9* and *chk1*. Whereas *rad24chl1* and *rad53chl1* shows faster bud emergence compared to the single mutants *rad24*, *rad53* and *chl1*. In presence of MMS induced damage, synergistic with Rad24p indicates Chl1p's role as a checkpoint at G1/S acting parallel to damage checkpoint pathway. The faster movement of DNA content through G1/S phase and difference in phosphorylation profile of Rad53p in wild type and *chl1* cells confirms the checkpoint defect in *chl1* mutant cells. Further, we have also confirmed that the checkpoint defect functions in parallel to the damage checkpoint pathway of Rad24p.

**Conclusion:** Chl1p shows Rad53p independent bud emergence and Rad53p dependent checkpoint activity in presence of damage. This confirms its requirement in two different pathways to maintain the G1/S arrest when cells are exposed to damaging agents. The bud emergence kinetics and DNA segregation were similar to wild type when given the same damage in nocodazole treated *chl1* cells which establishes the absence of any role of Chl1p at the G2/M phase. The novelty of this paper lies in revealing the versatile role of Chl1p in checkpoints as well as repair towards regulating G1/S transition. Chl1p thus regulates the G1/S phase by affecting the G1 replication checkpoint pathway and shows an additive effect with Rad24p for Rad53p activation when damaging agents perturb the DNA. Apart from checkpoint activation, it also regulates the budding kinetics as a repair gene.

**Keywords:** Yeast, Chl1p, Checkpoint, Bud-emergence, DNA damage, G1/S phase, DNA repair

## Background

The helicase Chl1p is a nuclear protein required for sister-chromatid cohesion in mitosis and meiosis [1–3], transcriptional silencing, recombinant DNA (rDNA) recombination, ageing and plays an instrumental role in chromatin remodeling [1, 4–6]. It preserves genome integrity upon DNA damage in S-phase [7]. Chl1p

\*Correspondence: shandas76@gmail.com; suparnalaha@yenepoya.edu.in

<sup>1</sup> Cell Biology and Molecular Genetics Division, Yenepoya Research Centre, Yenepoya Medical College, Yenepoya (Deemed To Be University), University Road, 3rd floor, Academic block, Deralakatte, Mangalore 575018, India

Full list of author information is available at the end of the article



© The Author(s) 2021. **Open Access** This article is licensed under a Creative Commons Attribution 4.0 International License, which permits use, sharing, adaptation, distribution and reproduction in any medium or format, as long as you give appropriate credit to the original author(s) and the source, provide a link to the Creative Commons licence, and indicate if changes were made. The images or other third party material in this article are included in the article's Creative Commons licence, unless indicated otherwise in a credit line to the material. If material is not included in the article's Creative Commons licence and your intended use is not permitted by statutory regulation or exceeds the permitted use, you will need to obtain permission directly from the copyright holder. To view a copy of this licence, visit <http://creativecommons.org/licenses/by/4.0/>. The Creative Commons Public Domain Dedication waiver (<http://creativecommons.org/publicdomain/zero/1.0/>) applies to the data made available in this article, unless otherwise stated in a credit line to the data.

protects cells against DNA damage arising from endogenous or exogenous DNA insults which reveals the requirement of this protein in the repair of DNA damage. The three highly related human homologs of Chl1p are BACH1, hChlR1 and hChlR2. hChlR1 and hChlR2 are expressed only in proliferating human cell lines. Of these, hChlR1 shows in vitro DNA helicase activity and binds to both single- and double-stranded DNA [8, 9]. BACH1 (Breast Cancer Associated C terminal Helicase 1) is a member of the DEAH helicase family and binds to the Rad9p homolog BRCA1, contributing towards DNA repair activity [10].

In the yeast *Saccharomyces cerevisiae*, three DNA damage-inducible checkpoints have been identified that operate in G1, S, and G2 phases of the cell cycle [11–16]. Two checkpoints activate prior to S-phase checkpoints in response to DNA damage—one at G1 and the other at G1/S [12, 13] and both of them are Rad9p dependent. At low levels of drug concentrations, DNA damage activates Rad53p only in S-phase and requires the formation of replication forks [17]. When the treatment with MMS is at higher concentrations or for longer periods, DNA damage causes Rad53p activation outside S-phase, leading to G1/S or G2/M arrest [17–19]. Two genes, Mitosis Entry Checkpoint protein 1 (*MEC1/ESR1/SAD3*) and Mitosis Entry Checkpoint protein 2 (*RAD53/MEC2/SPK1/SAD1*) appear important for the performance of all three checkpoints [14, 15, 20, 21]. In case of DNA breaks due to genotoxic agents, the two phosphoinositide 3 kinase-related kinases (PI3KKs), Mec1 and Tel1, the replication factor-C (RFC) like complex consisting of RFC1-like protein Rad24p with four small RFC subunits (Rfc2– Rfc5), the proliferating cell nuclear antigen (PCNA)-like heterotrimeric ring consisting of Rad17, Ddc1 and Mec3 proteins and the MRX complex of proteins, consisting of Mre11, Rad50 and Xrs2 acts as sensors and are recruited at the site of damage to activate the downstream kinases [22–27]. They transmit the signal to the adaptor/mediator molecule, Rad9p, which is activated by phosphorylation in a Mec1/Tel1-dependent fashion. *RAD9* was the first DNA damage checkpoint gene identified in the yeast *Saccharomyces cerevisiae* and was found to play a role in ionizing radiation induced G2/M cell cycle arrest [28–33]. Throughout the cell cycle, it is required for activation of kinase Rad53p in response to DNA double stranded breaks. Another checkpoint kinase, Chk1p, in addition to Rad53p has an apparently minor role in budding yeast during M-phase and G2 phase only [34, 35]. Its activation is also dependent on Rad9p [36]. In addition to this, *RAD9*, *RAD17*, *RAD24*, and *MEC3* are involved in G1 and G2 checkpoints [12–14]. Two independent mechanisms exist for the Rad9p activity- the Tudor/BRCA1 C-terminus (BRCT) domains of Rad9p plays the

role of Rad53p activation at G1/S phase and the Cyclin Dependent Kinase (CDK) consensus sites of Rad9p activates Rad53p at G2/M [37, 38]. Rad9p homologs 53BP1, MDC1 and BRCA1 also modulates the checkpoint pathways at two phases of the cell cycle. Activation of Rad53p at G1/S depends on the association of Rad9p with the modified chromatin surrounding the double strand breaks. This is mediated by the binding of Tudor/BRCT domain of Rad9p with di-methylated histone H3 and to phosphorylated histone H2A respectively [37]. Any mutation in the pocket fail to execute the G1 checkpoint delay, but the G2/M arrest induced by Nocodazole is well maintained in presence of the same mutations. Furthermore, the binding of Rad9p to histone H2A maintains the G1 checkpoint delay instead of the phosphorylation of H2A, when challenged with xenotoxic agents [14, 37]. Thus, the delay of S-phase following treatment with DNA damaging agents is an actively regulated response that requires functional *RAD9* and *RAD24* genes [12, 13].

In this paper, we have observed the same characteristics in *chl1* mutants. Like *rad9*, *chl1* mutants also fail to execute the G1 arrest when treated with Methyl Methane Sulphonate (MMS). This study shows that Chl1p is essential for G1/S arrest in response to DNA damage and it acts in line with Rad9p. In presence of a pulse of damage, the *chl1* cells show faster kinetics of bud emergence when compared to the wild type cells indicative of a compromised checkpoint function. To understand the status of checkpoints at G1/S in presence of damage, alpha-factor treated G1 arrested cells were exposed to genotoxic agent MMS. We observed the bulk DNA accumulation along with compromised Rad53p phosphorylation in *chl1* mutant cells at G1/S phase of the cell cycle, which are the hallmark characteristics of checkpoint proteins. The above mentioned observations confirm the early entry into S-phase for *chl1* mutant cells is due to defect in checkpoints compared to wild-type cells. We also observed that apart from the checkpoint defect of Chl1p which is Rad53p dependent, it follows an additional pathway to regulate the bud emergence at G1/S upon DNA damage as the bud emergence of *rad53chl1* is additive to single mutants *rad53* and *chl1*. All these findings confirm the dual role of this protein in controlling the G1 to S transition in the cell cycle on exposure to DNA damage.

## Results

### Chl1p is required for G1/S arrest after DNA damage by MMS

Exponentially growing mutant and wild-type cells were arrested in G1 by alpha-factor for 90 min, treated with 0.2% MMS at the last 10 min of arrest and washed free of cell cycle block. MMS was quenched by 10% v/v sodium thiosulphate and released in a fresh medium. Thereafter,

at different time intervals, bud emergence was scored as a measure for functional G1/S arrest. The experiment is performed in triplicate with the same time points and nearly 150 cells were counted every time confirming the consistency of the faster bud emergence. The budding kinetics of *chl1* cells is significantly faster than the wild type cells leading us to conclude that Chl1 mutant cells were deficient in G1/S arrest when their DNA was damaged with MMS, (Fig. 1A). There was no significant difference between the WT and *chl1* cells in the kinetics of bud emergence in absence of any MMS treatment (Fig. 1A). Though the budding is slow in the initial time points for *chl1*, it catches up with WT in later time points, which is the normal behaviour of *chl1* cells as shown in Fig. 1B. Budding cells are more in *chl1* mutant cells compared to wild-type cells after 1 and 2 h of MMS treatment as shown by randomly taken representative fields (Fig. 1C). Thus, Chl1p is required for G1/S arrest in response to DNA damage at the G1 phase. The fast movement of *chl1* mutants through G1 phase indicates that the cells are spending less time for repair and may have compromised arrest at G1 due to a defective checkpoint. Faster bud emergence due to absence of a halt for repair will lead to increase fragmented DNA. 4',6-Diamidino-2-Phenylindole (DAPI) staining confirms the absence of integrity in the DNA of *chl1* cells when exposed to MMS at G1 block (Fig. 1D). To confirm the defect in G1/S arrest and justifying the progression in cell cycle of the mutant cells with more damage as a result of

compromised repair, we performed the sensitivity analysis of *chl1* cells towards the genotoxic agents. Mutant and wild-type cells were arrested in G1 using  $\alpha$ -factor for 90 min and then treated with 0.2% MMS. Aliquots of cells exposed to 0.2% MMS in presence of alpha-factor block were taken at various time intervals. Cells were counted and plated on Yeast Extract Peptone Dextrose (YEPD) plates to determine viability. Figure 1E shows nearly 75% loss in the viability of *chl1* cells after 30 min of 0.2% MMS treatment at G1/S. The loss in cell viability of *chl1* compared to wild-type cells in the presence of 0.2% MMS confirmed the accumulation of more damage due to compromised repair and checkpoint molecules.

#### Chl1p is not required at G2/M for MMS-induced DNA damage repair

In presence of DNA damage caused by MMS, G2/M-arrested wild-type cells delay nuclear division [18, 19]. To determine if Chl1p is required in this delay, mutant and wild-type cells were arrested at G2/M by nocodazole, treated with MMS, washed free of cell cycle block including MMS and released into fresh medium. The percentage of cells, which had divided their nuclei, was scored at different time intervals to measure G2/M arrest. Figure 2 shows that *chl1* mutant cells were proficient for G2/M arrest as they delayed nuclear division when their DNA was damaged with MMS. Also, the control cells did not show any significant differences in the timings of nuclear

(See figure on next page.)

**Fig. 1** Chl1p is required for G1/S after DNA damage by MMS. **A** G1-phase bud emergence kinetics of mutant and wild-type cells after MMS treatment. Wild-type (699) and mutant cell 699Dchl1 (*chl1*) were grown to exponential phase ( $\sim 0.2$  OD<sub>610nm</sub>) and arrested with 5  $\mu$ g/ml  $\alpha$ -factor for 90 min (G1 arrest) as described in materials and methods. After 80 min of  $\alpha$ -factor treatment at 30 °C, each culture was divided into two. To one half 0.2% MMS was added and the other was maintained as a control. Cells were kept shaking for a further 10 min. After treatment, MMS was inactivated by the addition of one volume of 10% sodium thiosulfate solution, cells were spun down and the pellet was washed quickly with YEPD medium at RT. The cells were released in a fresh YEPD medium at 30 °C and aliquots were removed at regular times for scoring the percentage of budded cells. The graph represents the percentage of bud emergence in WT and *chl1* cells at different time intervals after release from G1 arrest and 0.2% MMS treatment simultaneously. The black filled symbols are given for cells treated with MMS, the grey filled symbols indicates the absence of MMS. Data shown are averages of values obtained from three independent experiments and the deviations from the mean are shown as error bars. **B** Growth of WT and mutant cells on YEPD plates. Wild-type (699) and mutant cell 699Dchl1 (*chl1*), SL3 (*rad24*) and SL3Dchl1 (*rad24chl1*) were streaked for single colony on YEPD plates and incubated at 30 °C for (i) 30 h, (ii) 34 h and (iii) 60 h respectively. We could observe an initial growth difference between the WT and the mutant, *chl1* that goes of after 60 h of incubation. **C** Budding of mutant and wild-type cells after MMS treatment. The bright fields of WT and *chl1* from (A) at 40X resolution shows the budded cells in wild-type (699) and *chl1* (699Dchl1) mutant cultures after 1 and 2 h of release from MMS treatment. The budded cells are indicated with arrows. **D** *Chl1* cells have fragmented DNA at G1 phase when treated with MMS. 699 (wild-type) and 699Dchl1 (*chl1*) cells were arrested at G1 by treating the log phase cells with alpha-factor for 90 min. To these G1 blocked cells, 0.2% MMS was added to create a substantial damage. Cells were collected at different time points of MMS exposure for DAPI staining. 0' was collected just after adding 0.2% MMS to the cells with alpha-factor (G1-blocked) followed by 10', 20' and 30' of exposure to 0.2% MMS in presence of alpha-factor (G1-blocked damaged cells). Representative fields of DAPI staining of cells treated for 0' and 30' with 0.2% MMS is given for WT and *chl1* mutant cells. The corresponding bright field and merged images are also given along with the DAPI field. **E** *chl1* cells are sensitive towards killing by genotoxic agent in G1/S-phase. 699 (wild-type), 699Dchl1 (*chl1*), SL3 (*rad24*), SL3Dchl1 (*rad24chl1*), 699 $\Delta$ sgs1 (*sgs1*), 699 $\Delta$ sgs1Dchl1 (*sgs1chl1*) and SL21 (*sgs1rad24*) cells were arrested by alpha-factor in G1. To these G1 blocked cells, 0.2% MMS was added to create a substantial damage at G1. Cells were collected at different time points of MMS exposure for viability assay. 0' was collected just after adding 0.2% MMS to the cells with alpha-factor (G1-blocked) followed by 10', 20' and 30' of exposure to 0.2% MMS in presence of alpha-factor (G1-blocked damaged cells). Aliquots removed for cell viabilities at the indicated time points were washed off of both MMS and alpha-factor, resuspended in water, counted and plated after dilution on YEPD plates. The plates were incubated at 30 °C for 2–3 days and the viable colonies were counted



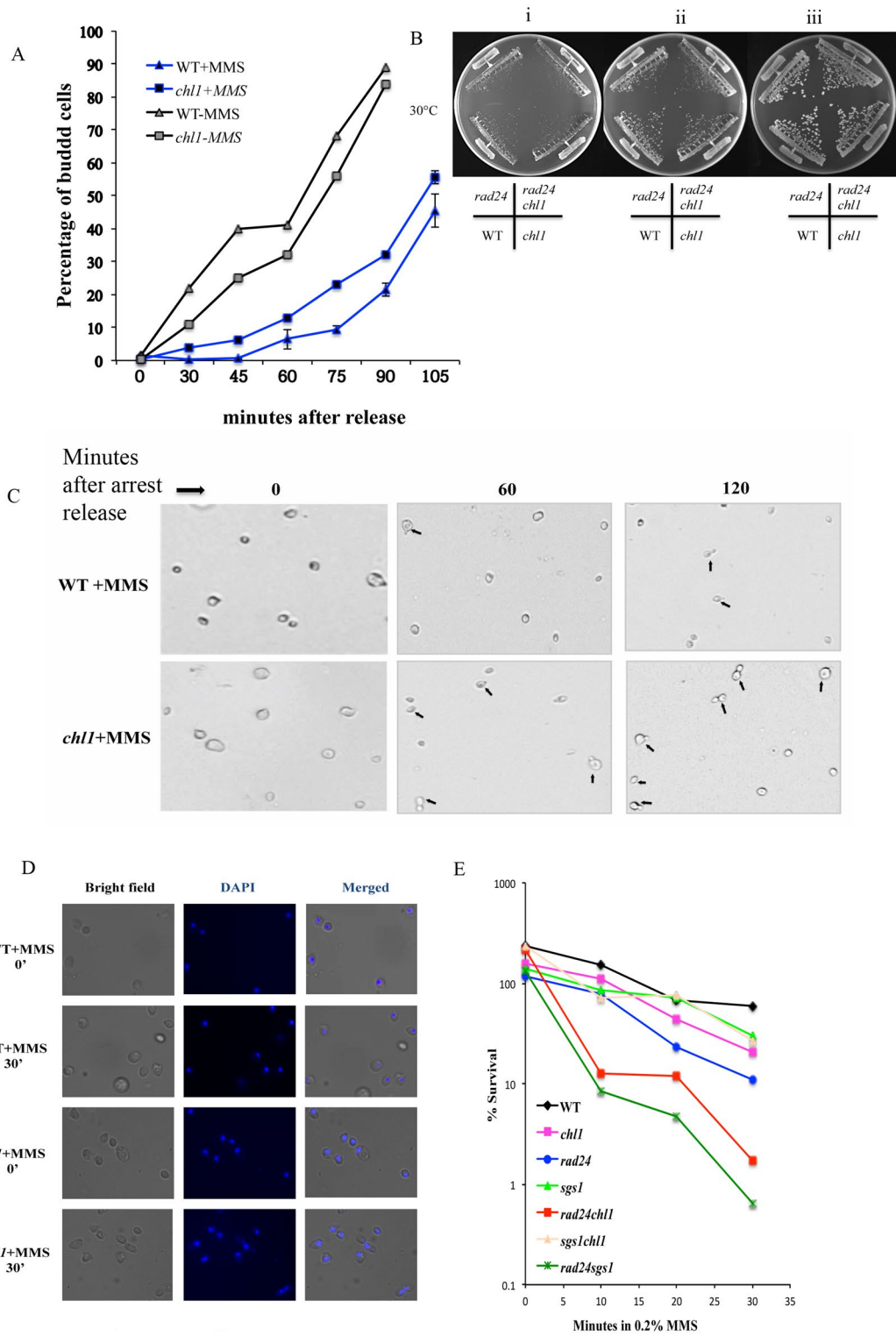
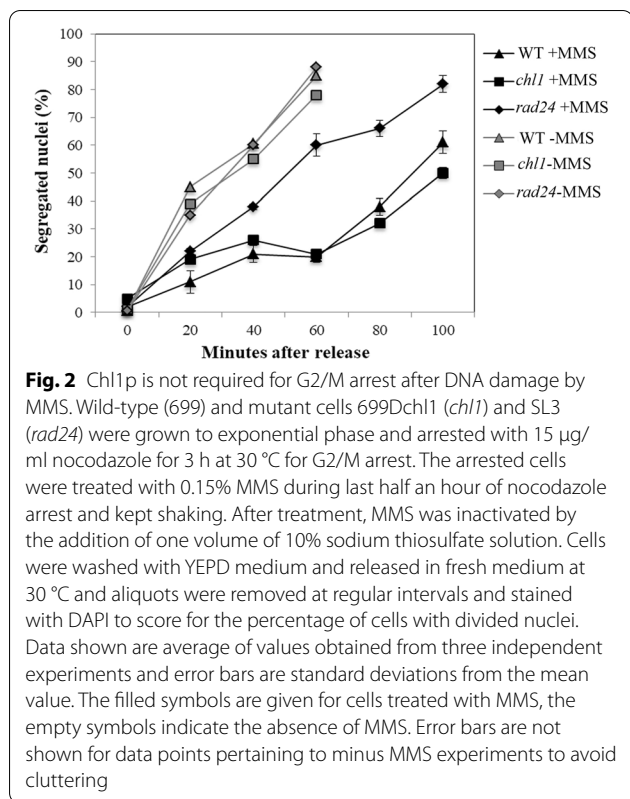


Fig.1 (See legend on previous page.)



division. Therefore, Chl1p is not required at the G2/M transition for MMS-induced DNA damage repair.

**Chl1p plays a role in regulating the checkpoints at G1/S phase of the cell cycle**

The observation that the *chl1* null mutations arrested at G1/S shows sensitivity to genotoxic agents like MMS shows its link with the surveillance mechanism on the genetic stability of the cells. The faster movement of the

cells towards bud formation in presence of damage can be an effect of perturbed checkpoint function. As the preliminary observations give a clue of compromised checkpoint function in *chl1* mutant, we decided to confirm this by more direct experiments, as described below.

The checkpoint kinase proteins inhibit the cell cycle progression in presence of damage, allowing time for DNA repair to take place [16, 39]. However, when DNA is damaged in G1/S or S-phase checkpoint mutants such as *mecl1*, *rad9*, *rad17*, *rad24* and *rad53*, S-phase appears to progress faster because of inappropriate initiation of the origins, causing additional DNA synthesis, which can be detected by flow cytometry [16, 39]. To test whether Chl1p affects the G1/S phase checkpoint function, the progression of cell cycle at G1/S was observed by monitoring the DNA content through flow-cytometry in 0.2%MMS treated G1 synchronized cells. Once the cells reaches G1 upon alpha-factor treatment for 90 min, the cells were exposed to 0.2%MMS without releasing from alpha-factor and the progression of DNA synthesis from G1 to S was monitored by flow cytometry. The *chl1* cells came out from G1 arrest by 10 min of treatment with MMS in presence of alpha-factor whereas in case of wild type the entry in S-phase from G1 was not observed (Fig. 3A). Since the G1 to S-phase progression in *chl1* was faster compared to wild-type cells in the presence of high MMS damage, it suggests that the DNA damage checkpoint pathway is perturbed in these cells. We also observed the faster movement of DNA from G1 to S phase in the known DNA damage checkpoint mutant *rad24*. Interestingly the double mutant *rad24chl1* moved fastest confirming the synergistic role of both Chl1p and Rad24p as checkpoints in presence of damage suggesting that they may follow two parallel pathways (Fig. 3A). The checkpoint mutant *sgs1* were also included along with *rad24* in the cell cycle progression studies as they

(See figure on next page.)

**Fig. 3** Chl1p plays a role in regulating the checkpoints at G1/S phase of the cell cycle. **A** G1/S-phase progression of mutant and wild-type cells in the presence of MMS. Wild-type (699) and mutant cell 699Dchl1 (*chl1*), SL3 (*rad24*) and SL3Dchl1 (*rad24chl1*) were all synchronized with alpha-factor at 30 °C and 0.2% MMS was added in presence of the G1 block. All the cultures were kept shaking at 30 °C. Aliquots were removed at various times for FACS analysis. The histogram plot at each time point are overlaid in the figure by using overlay software to understand the progression of the cells through cell cycle. The exponential cells were collected just before the addition of alpha-factor to the growing cells of 0.2 OD<sub>610nm</sub>. Arrows indicates G1 and G2 DNA contents. **B** *chl1* cells are compromised in Rad53p phosphorylation in response to MMS treatment in G1/S-phase. Wild type, CHL1 (699) and 699Dchl1 (*chl1*) cells were arrested in G1 phase and exposed to 0.2% MMS at 30 °C. Rad53p phosphorylation was detected by western blot analysis of proteins extracted from aliquots of cells removed at indicated times, using antibodies directed against the Rad53 protein. **C** *rad24chl1* cells are more compromised in Rad53p phosphorylation compared to *chl1* cells in response to MMS treatment in G1/S-phase. SL3 (*rad24*) and SL3Dchl1 (*rad24chl1*) cells were arrested in G1 phase and exposed to 0.2% MMS at 30 °C along with the cells of **B**. Rad53p phosphorylation was detected by western blot analysis of proteins extracted from aliquots of cells removed at indicated times, using antibodies directed against the Rad53 protein. **D** Quantification of Rad53p expression in *chl1* cells along with the double mutant *rad24chl1* cells. The intensity of the phosphorylated bands of Rad53p in WT (CHL1), 699Dchl1 (*chl1*), SL3 (*rad24*) and SL3Dchl1 (*rad24chl1*) cells in western blots was quantified using Image J software. The values of the Rad53p phosphorylated band intensities taken together were normalized with corresponding intensities of beta-actin to normalize the protein loading at different time points. The 0 min is just after adding 0.2% MMS followed by 10, 20 and 30 min exposure to 0.2% MMS. The graph shows the average of data obtained from 3 repeated experiments

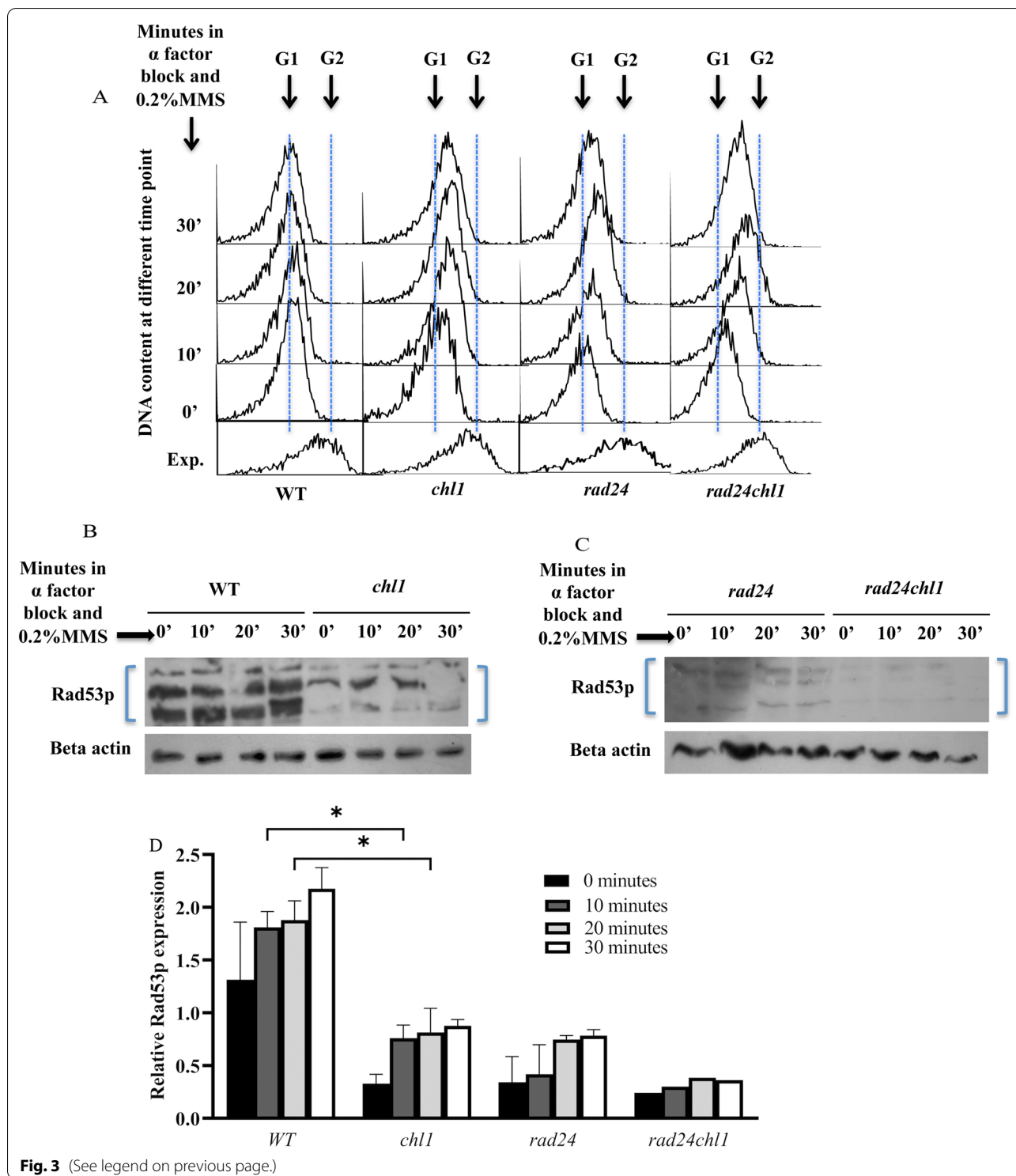


**Fig. 3** (See legend on previous page.)

have roles in replication checkpoint, like *rad24* in damage checkpoint pathways [40, 41]. In case of replication checkpoint, *sgs1* cells showed progression like WT and *Sgs1Chl1* mutant was not significantly different from *sgs1*

(Additional file 1: Fig. S1). The slow progression of *sgs1* like WT is because of the absence of any role of *Sgs1p* at G1 and also the presence of a functional repair mechanism. *Sgs1* mutants halt for repair like WT at G1 in

presence of damage. But in Chl1 mutants, due to defect in repair and checkpoint, it progresses faster in cell cycle in presence of damage. In case of *sgs1chl1* and *sgs1rad24* the progression is similar to *chl1* mutants and Rad24 mutants respectively and Sgs1 mutation plays no additive role in them.

To confirm the effect of Chl1p on checkpoints at G1/S phase, Rad53p activation was compared between wild type and *chl1* mutant cells by directly assaying for its phosphorylation in MMS-treated G1 arrested cells. Cells were synchronized with alpha-factor and treated with 0.2% MMS once all the cells reached the G1 phase. Aliquots were withdrawn at indicated times. Figure 3B and D shows that *chl1* cells had compromised Rad53p phosphorylation and which is significantly low by 10' of 0.2% MMS exposure compared to the wild type at G1/S-phase. Thus, this confirms that Chl1p is required to activate the DNA damage checkpoint pathway when cells are treated with MMS in G1/S-phase.

To further confirm that Chl1p acts in parallel to the damage checkpoint pathway, we monitored Rad53p phosphorylation both in WT, single checkpoint mutants and checkpoint mutants along with *chl1* at G1/S phase in presence of 0.2% MMS. The checkpoint mutant *rad24* was included in the Rad53p phosphorylation studies as it has a role in the damage checkpoint pathway [40, 41]. *rad24* cells, as expected, showed lower levels of Rad53p phosphorylation (Fig. 3C, D). Interestingly Rad24Chl1 mutant was even more compromised in phosphorylating Rad53p than *rad24* and *chl1* alone (Fig. 3C, D). We thus observed that the *chl1* cells started coming out from G1 arrest faster like the *rad24* checkpoint mutant cells in presence of 0.2% MMS treatment to G1 arrested cells in just 10 min. We also observed a compromised checkpoint activity of Rad53p in absence of Chl1p. The double mutant *rad24chl1* was even faster in coming out from arrest with a broader peak and had further reduced Rad53p activity. So in this section, we confirmed the role of Chl1p, in addition to Rad24p, in regulating the checkpoint pathway through Rad53p activation in G1/S.

#### Chl1p acts independently of the DNA damage checkpoint pathway

The sensitivity of *chl1* cells and damage of DNA as shown by DAPI towards xenotoxic agents, faster movement through the cell cycle in presence of damage at G1/S and compromised Rad53 activity proves the perturbed checkpoint functioning at G1 in *chl1* mutant cells. Further cell cycle progression studies with damage checkpoints and replication checkpoints confirm it to be additive to damage checkpoints rather than replication checkpoints. To confirm the pathway analysis

of Chl1p's checkpoint activity on the budding kinetics we performed the following experiments. The intra-S-phase checkpoint proteins Sgs1 and Rad24 act in parallel in the DNA replication and damage checkpoint pathways, respectively to maintain the genomic integrity. They maintain cell viability and activate Rad53p in the presence of damage through genotoxic agents [19, 42]. In the viability studies, the single mutants *sgs1* and *rad24* were included along with *chl1*. The double mutants *rad24chl1* and *sgs1chl1* were also included to determine if *chl1* showed any synergistic loss in viability with either of these two mutations at G1/S in 0.2% MMS. The results (Fig. 1E) show that there is a synergistic drop in cell viability in *rad24chl1* double mutants but not in *sgs1chl1*. The *rad24sgs1* double mutant exhibited an expected fall in cell viability. This shows that Chl1 acts in addition to the Rad24 pathway. To further confirm the pathway of Chl1p for G1-arrest we performed the bud emergence experiments with mutant genes, which regulates the effect of genetic insults on cell cycle kinetics, like *rad9*, *rad24* and the corresponding double mutants at G1. Rad9 and Rad24 epistasis group are required for efficient cell-cycle arrest after DNA damage in G1/S [12, 13] and G2/M [19, 43]. To determine if Chl1p is in Rad9p or Rad24p pathway at this phase of the cell cycle, experiments were carried out to monitor the kinetics of bud emergence. WT, *chl1*, *rad9*, *rad24*, *rad24chl1* and *rad9chl1* cells were arrested in G1 by alpha-factor, treated with 0.2% MMS, washed free of cell cycle block and MMS, and released into fresh medium to score for bud emergence. Figure 4A shows that the double mutant *rad24chl1* emerged from the arrest faster than either of the single mutants *chl1* and *rad24* and the effect appeared to be additive with *chl1* mutation. This confirms that Chl1p acts independently of Rad24p to arrest damaged cells at G1/S phase. In absence of MMS we found no significant difference in the budding kinetics after release from G1 block between *chl1*, *rad24* and *rad24chl1* cells compared to WT (Fig. 4B). On contrary to *rad24chl1* budding kinetics, Fig. 4C shows that the double mutant *rad9chl1* doesn't emerge from the arrest any faster than either of the single mutants, *rad9* and *chl1*. Thus, Chl1p acts through the Rad9 pathway. The bud emergence of the same strains also shows no significant difference compared to WT in absence of any DNA insult (Fig. 4D). Representative fields of budding cells of the single mutants *rad24*, *rad9* and the double mutants *rad24chl1*, *rad9chl1* also proves that *chl1* mutant cells have more buds compared to wild-type cells after 2 h of MMS treatment and the number of buds in case of *rad24chl1* is significantly more compared to *rad24* and *chl1* alone (Fig. 4E).

### Chl1p plays a dual role in the mode of arrest upon DNA damage in G1/S phase of the cell cycle

The pathway analysis (shown in Fig. 4), the sensitivity studies towards genotoxic agents (as shown in Fig. 1) and compromised Rad53p activity (Fig. 3) of *chl1* mutants suggests that Chl1p has a role in regulating checkpoints and acts in a synergistic way to the DNA damage checkpoint pathway. But, faster kinetics of bud emergence compared to the wild-type can also suggest that Chl1p could be involved in damage repair, and in absence of it the cells escape the time to repair the damage and hence moves faster towards budding.

Earlier we have shown that in S-phase, Chl1p plays a role in the repair pathway upon DNA damage [7]. As Chl1p acts as a repair protein in S-phase, we wanted to determine if Chl1p has some additional role at G1 phase in addition to regulating Rad53p checkpoint pathway in delaying bud emergence when exposed to damage. To reveal the additional roles of Chl1 we performed the bud emergence experiments with mutant genes *rad53*, *chl1* and the corresponding double mutants. WT, *chl1*, *rad53* and *rad53chl1* cells were arrested in G1 by alpha-factor, treated with 0.2% MMS, washed free of cell cycle block and MMS, and released into fresh medium to score for bud emergence. Figure 5A shows that the single mutants are faster than the WT and the double mutant *rad53chl1* emerges significantly faster from G1 arrest than the single mutants *chl1* and *rad53*. Figure 5B shows no significant difference in the budding kinetics of the same cells in absence of MMS. The randomly captured representative fields of budding cells of *chl1*, *rad53* and *rad53chl1* also confirm the same (Fig. 5C). The faster bud emergence of

the single mutants from WT confirms the checkpoint defect in the single mutant. But the even faster movement of the double mutant *rad53chl1* interestingly suggests that Chl1p may be following a parallel pathway for arresting cells at G1 along with Rad53p checkpoint arrest to maintain the genomic integrity on exposure to different types of genomic insults. The increase of fragmented DNA in *chl1* cells (Fig. 1D, Table 1) compared to WT also confirms the role of Chl1p in DNA repair. Literature suggests that the Chk1 checkpoint pathway acts in parallel to the Rad53p checkpoint pathway in presence of damage at G2 and M phases [34, 35]. Also, this DNA checkpoint kinase phosphorylates after MMS treatment in a Rad9-dependent and Rad53-independent manner [36]. As per our bud emergence data we can confirm that Chl1p follows a pathway in addition to Rad53p and Rad24p and goes along with Rad9p. So, Chl1p may regulate both the Rad53p and Chk1p checkpoint pathways at G1. To confirm this hypothesis we checked whether Chk1p has any role at G1 and is it linked with Chl1p. We studied the budding kinetics of single mutants *chl1* and *chk1* along with the double mutant *chl1chk1* (Fig. 5D). Though the bud emergence of *chl1* mutant's was faster than the WT, there was no additional difference of bud emergence of *chk1chl1* from *chk1* and *chl1*. Also, the budding of *chk1* cells was similar to WT. All these observations prove that Chk1p doesn't play a role in arresting at G1 in presence of damage and Chl1p doesn't act through the Chk1p pathway. The budding kinetics of WT, *chl1*, *chk1* and *chl1chk1* were almost the same in absence of any damage (Fig. 5E). So, in this section we prove that Chl1p regulates two pathways in G1 phase to delay bud emergence

(See figure on next page.)

**Fig. 4** Chl1p acts independently of the DNA damage checkpoint pathway. **A** G1-phase bud emergence kinetics of *Chl1* mutant cells are additive to *rad24* after MMS treatment. Wild-type (699) and mutant cells 699Dchl1 (*chl1*), SL3 (*rad24*), SL3Dchl1 (*rad24chl1*) were grown to exponential phase and arrested with 5 µg/ml  $\alpha$ -factor for 90 min (G1 arrest) as described in materials and methods. After 80 min of  $\alpha$ -factor treatment at 30 °C, 0.2% MMS was added. Cells were kept shaking for a further 10 min. After treatment, MMS was inactivated by the addition of one volume of 10% sodium thiosulfate solution, cells were spun down and the pellet was washed quickly with YEPD medium at RT. The cells were released in a fresh YEPD medium at 30 °C and aliquots were removed at regular times for scoring the percentage of budded cells. The graph represents the percentage of bud emergence in WT, *chl1*, *rad24* and *rad24chl1* cells at different time intervals after release from G1 arrest and 0.2% MMS treatment simultaneously. Data shown are the average of values obtained from three independent experiments. **B** G1-phase bud emergence kinetics of cells in absence of MMS treatment. Wild-type (699) and mutant cells 699Dchl1 (*chl1*), SL3 (*rad24*), SL3Dchl1 (*rad24chl1*) were simultaneously grown with the **A** cells to exponential phase and arrested with 5 µg/ml  $\alpha$ -factor for 90 min (G1 arrest). The cells were released in a fresh YEPD medium without any MMS treatment at 30 °C and aliquots were removed at regular times for scoring the percentage of budded cells. **C** G1-phase bud emergence kinetics of *Chl1* mutant cells is in line with *rad9* after MMS treatment. Wild-type (699) and mutant cells 699Dchl1 (*chl1*), SL19 (*rad9*), SL19Dchl1 (*rad9chl1*) were grown to exponential phase and follow through same experimental procedures as done in **A**. The graph represents the percentage of bud emergence in WT, *chl1*, *rad9* and *rad9chl1* cells at different time intervals after release from G1 arrest and 0.2% MMS treatment simultaneously. Data shown are average of values obtained from three independent experiments. **D** G1-phase bud emergence kinetics of cells in absence of MMS treatment. Wild-type (699) and mutant cells 699Dchl1 (*chl1*), SL19 (*rad9*), SL19Dchl1 (*rad9chl1*) were simultaneously grown with the **C** cells to exponential phase and arrested with 5 µg/ml  $\alpha$ -factor for 90 min (G1 arrest). The cells were released in a fresh YEPD medium without any MMS treatment at 30 °C and aliquots were removed at regular times for scoring the percentage of budded cells. **E** Additive and synergistic budding of mutant and wild-type cells after MMS treatment. The bright fields of WT and mutant cells from (**A**, **B**) at 40X resolution shows the budded cells in wild-type (699) and the mutant cells 699Dchl1 (*chl1*), SL3 (*rad24*), SL3Dchl1 (*rad24chl1*), SL19 (*rad9*), SL19Dchl1 (*rad9chl1*) mutant cultures after 2 h release from MMS treatment. The budded cells are indicated with arrows

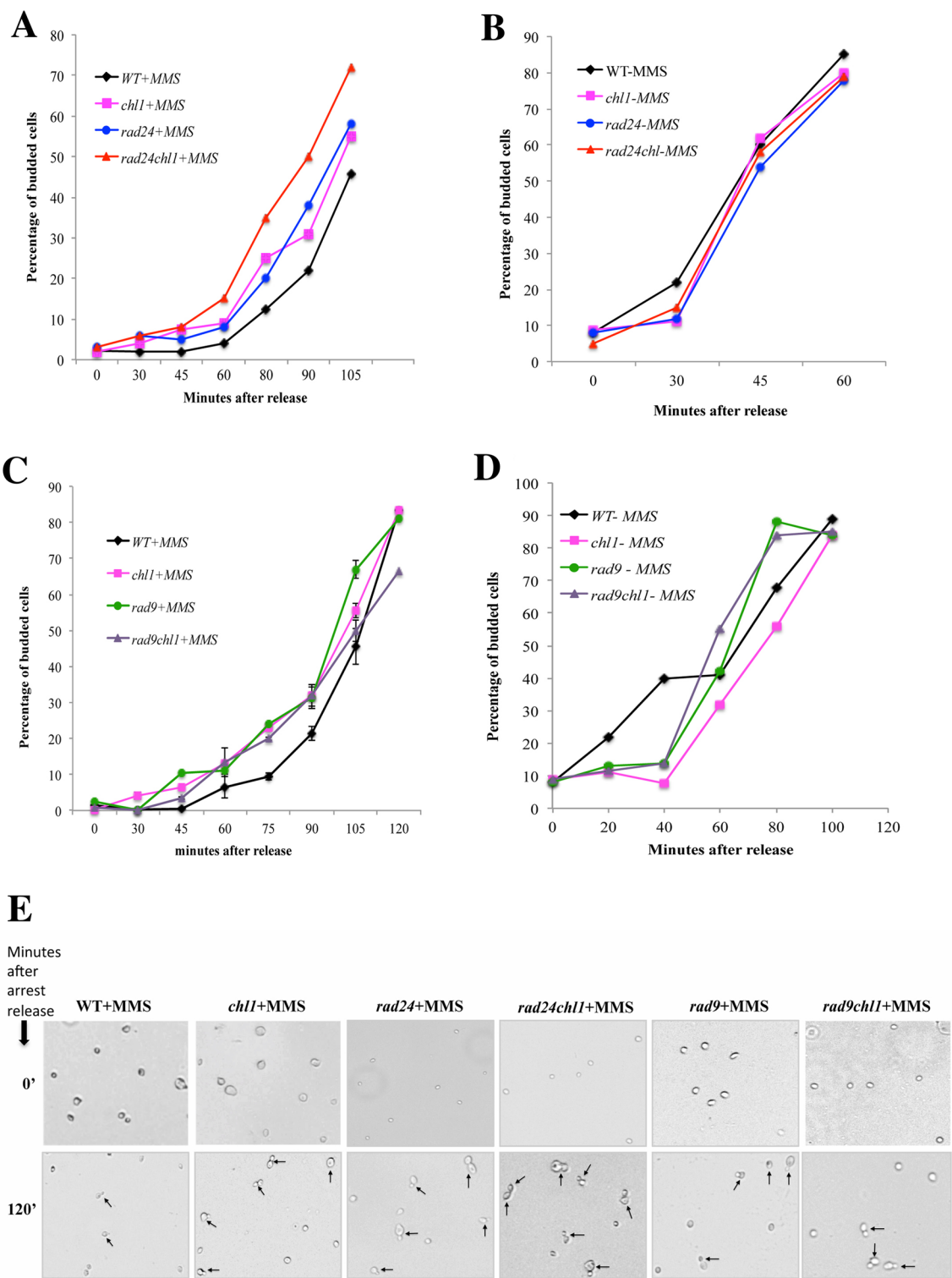


**Fig. 4** (See legend on previous page.)

in presence of damage, one is through Rad53p by modulating its phosphorylation and the other one is parallel to Rad53p but doesn't follow the Chk1p checkpoint pathway. So, the other pathway in which Chl1p has some role is the damage repair in G1 (role in repair in S phase is already known).

## Discussion

The functioning of Rad9p as G1/S checkpoint is dependent on its TUDOR and BRCT domains and is independent of its auto-phosphorylation through CDK [44]. Rad53p activation in G1 and S phase depends on the association of Rad9p with the modified chromatin adjacent to Double Standard Break (DSBs). Rad9p-chromatin association is mediated by the binding of TUDOR domains to histone di-methylated H3 and BRCT domains binding to phosphorylated histone H2A [37]. If the interaction is broken the activation of phosphorylated Rad53 is compromised in presence of a genotoxic agent like MMS and Hydroxyurea (HU). The *RAD9* BRCT mutant fails to perform the G1 checkpoint delay post DNA insult but it was proficient in checkpoint response upon DNA damage in nocodazole treated cells. So, the recruitment and retention of Rad9p at the damage sites through the BRCT domain play a vital role in the G1/S arrest. The interactor proteins of Rad9p at the BRCT domain are also instrumental in maintaining the arrest for proper repair of the damage. The human homolog of Chl1p is BACH1 and that for Rad9p is BRCA1. In mammalian system, at G1-phase, BACH1 is phosphorylated leading to the interaction with BRCA complex through BRCT domain, with low Adenosine Triphosphatase (ATPase) /helicase activity. As a result, the movement of the replication complex slows down enhancing the proof reading activity of the polymerase. Adversely, during the slow down of the fork,

the nascent leading and lagging strands tend to anneal to each other due to fork regression or reversal to form secondary structures [34]. The complex of BACH1/BRCA along with the combination of BLM1, a helicase with opposite polarity, resolves these difficult structural motifs encountered by the replication forks during DNA replication [45]. Once the proofreading and resolving activity of the secondary structures are over, the de-phosphorylation of BACH1 takes place. On de-phosphorylation, the BACH1/BRCA complex breaks down, leaving behind BACH1 at the fork generating the space for the replication machinery to start replication [45]. Simultaneously dephosphorylated BACH1 regains the helicase activity to unwind the DNA for timely progression through S-phase. So looking at the correlation and domain analogy of BACH1 and BRCA1 in mammalian system it can be concluded that Chl1p binds to Rad9p through the BRCT domain and allows Rad9p to sense the damage because of its repair and helicase activity. So, most probably the retention of Rad9p at the damage site is because of its BRCT interactor Chl1p. The recruited Rad9p activates the checkpoint Rad53p to bring in the cell cycle arrest and Chl1p gets the time to repair the damage.

In this paper, we show evidence that, like *rad9*, *chl1* mutants also fail to execute the G1 checkpoints and the delay in bud emergence is perturbed in G1-arrested cells when treated with MMS. In the presence of damage, Chl1p executes the G1/S phase arrest. In *chl1* mutants, faster kinetics of bud emergence compared to the wild-type, additionally, faster budding of *rad53chl1* cells compared to *chl1* and *rad53* suggests that Chl1p could be involved in repair, and in absence of it, the cells escape the time to repair the damage and hence moves faster towards budding with more accumulated damage and sensitive towards MMS. Compromised Rad53 activity

(See figure on next page.)

**Fig. 5** Chl1p plays role in dual mode of arrest upon DNA damage in the G1/S phase of the cell cycle. **A** *Chl1p acts independently of Rad53p at G1/S after DNA damage.* Wild-type (699) and mutant cells 699Dchl1 (*chl1*), SL7 (*rad53*) and SL7Δchl1 (*rad53chl1*) were grown to exponential phase and follow through same experimental procedures as done in 4A. The graph represents the percentage of bud emergence in WT, *chl1*, *rad53* and *rad53chl1* cells at different time intervals after release from G1 arrest and 0.2% MMS treatment simultaneously. Data shown are averages of values obtained from three independent experiments and the deviations from the mean are shown as error bars. **B** *G1-phase bud emergence kinetics of cells in absence of MMS treatment.* Wild-type (699) and mutant cells 699Dchl1 (*chl1*), SL7 (*rad53*) and SL7Δchl1 (*rad53chl1*) were simultaneously grown with Fig. 5A cells to exponential phase and arrested with 5 μg/ml α-factor for 90 min (G1 arrest). The cells were released in a fresh YEPD medium without any MMS treatment at 30 °C and aliquots were removed at regular times for scoring the percentage of budded cells. **C** *Chk1p plays no role at G1/S after MMS treatment.* Wild-type (699) and mutant cells 699Dchl1 (*chl1*), SL26 (*chk1*) and SL27 (*chk1chl1*) were grown to exponential phase and follow through the same experimental procedures as done in 4A. The graph represents the percentage of bud emergence in WT, *chl1*, *chk1* and *chk1chl1* cells at different time intervals after release from G1 arrest and 0.2% MMS treatment simultaneously. The bud emergence kinetics of *chk1* is similar to WT and *chk1chl1* is similar to the bud emergence kinetics of *chl1*. Data shown are average of values obtained from three independent experiments. **D** *G1-phase bud emergence kinetics of cells in absence of MMS treatment.* Wild-type (699) and mutant cells 699Dchl1 (*chl1*), SL26 (*chk1*) and SL27 (*chk1chl1*) were simultaneously grown with the Fig. 5C cells to exponential phase and arrested with 5 μg/ml α-factor for 90 min (G1 arrest). The cells were released in a fresh YEPD medium without any MMS treatment at 30 °C and aliquots were removed at regular times for scoring the percentage of budded cells. **E** *Budding of mutant and wild-type cells after MMS treatment.* The bright fields of WT and mutant cells from (A and C) at 40X resolution show the budded cells in different cultures after 2 h release from MMS treatment. The budded cells are indicated with arrows

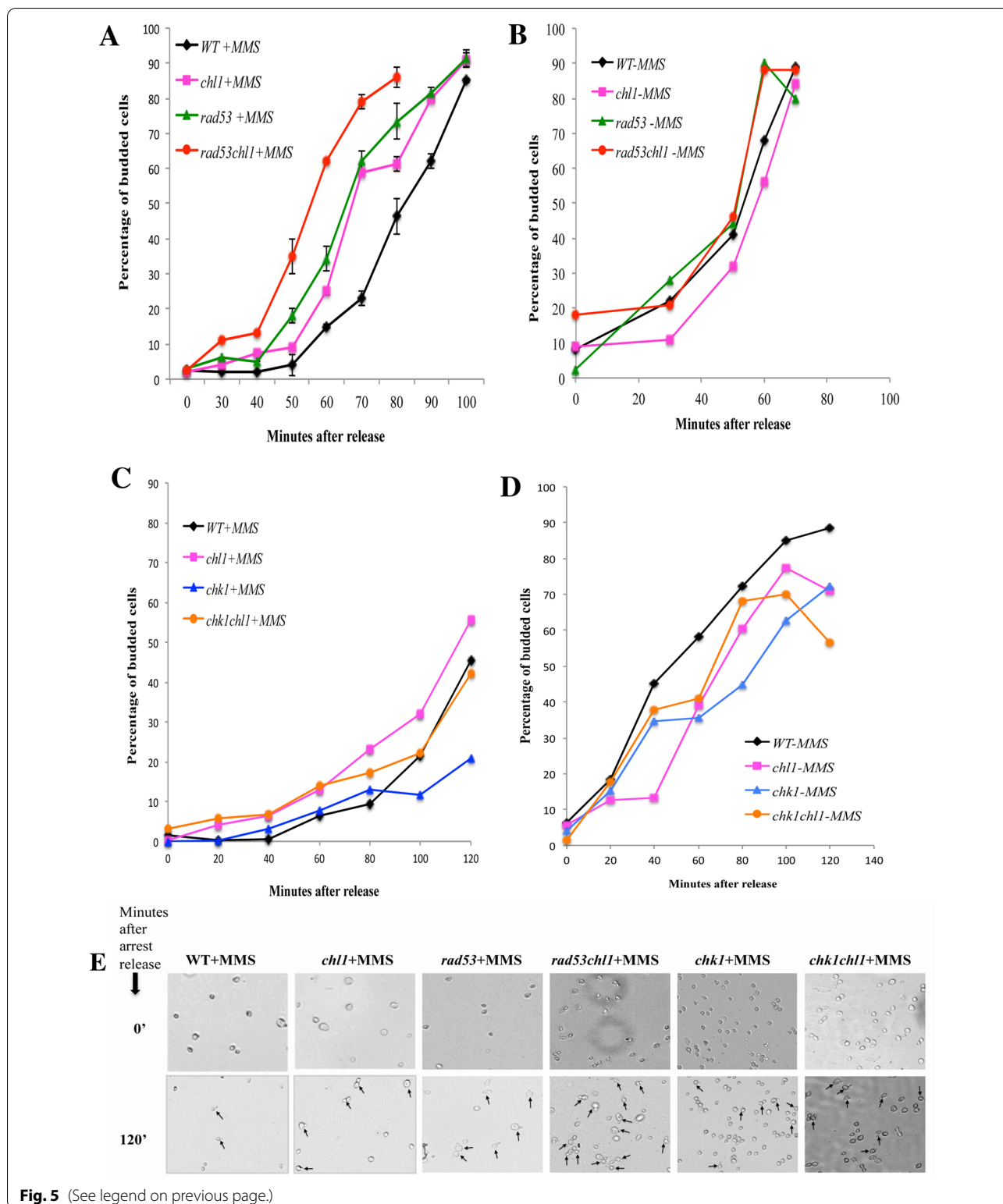


**Fig. 5** (See legend on previous page.)

of *chl1* cells at G1 in presence of MMS damage confirms its other role in regulating checkpoint pathway which also adds up in maintaining the budding kinetics at G1

after DNA damage with 0.2% MMS. It plays the checkpoint role parallel to the damage checkpoint pathway in G1 phase of the cell cycle as the Rad53p phosphorylation



**Table 1** The MMS treated cells showing percentage of DNA damage at 0 and 30 min in wild type and mutant strains

ins	MMS (Minutes')	Cells with compact DNA (%)	Cells with fragmented DNA (%)
699	0'	95.49	4.505
	30'	88.17	11.83
699chl1	0'	92.86	7.14
	30'	27.39	72.61

Rad53p activation through Rad9p and prevents bulk DNA synthesis. It regulates the repair function in addition, which is independent of Rad53p and in synchrony with Rad9p to regulate the budding kinetics following insult to the genetic material. So, in a nutshell Chl1p plays multiple roles throughout the G1 phase of the cell cycle as presented in the schematic representation of Chl1p involving pathways at G1 (Fig. 6). G2/M phase arrest is executed by the auto-phosphorylation of Rad9p and is independent of the BRCT domain [46]. Establishment of sister chromatid cohesion occurs for the repair

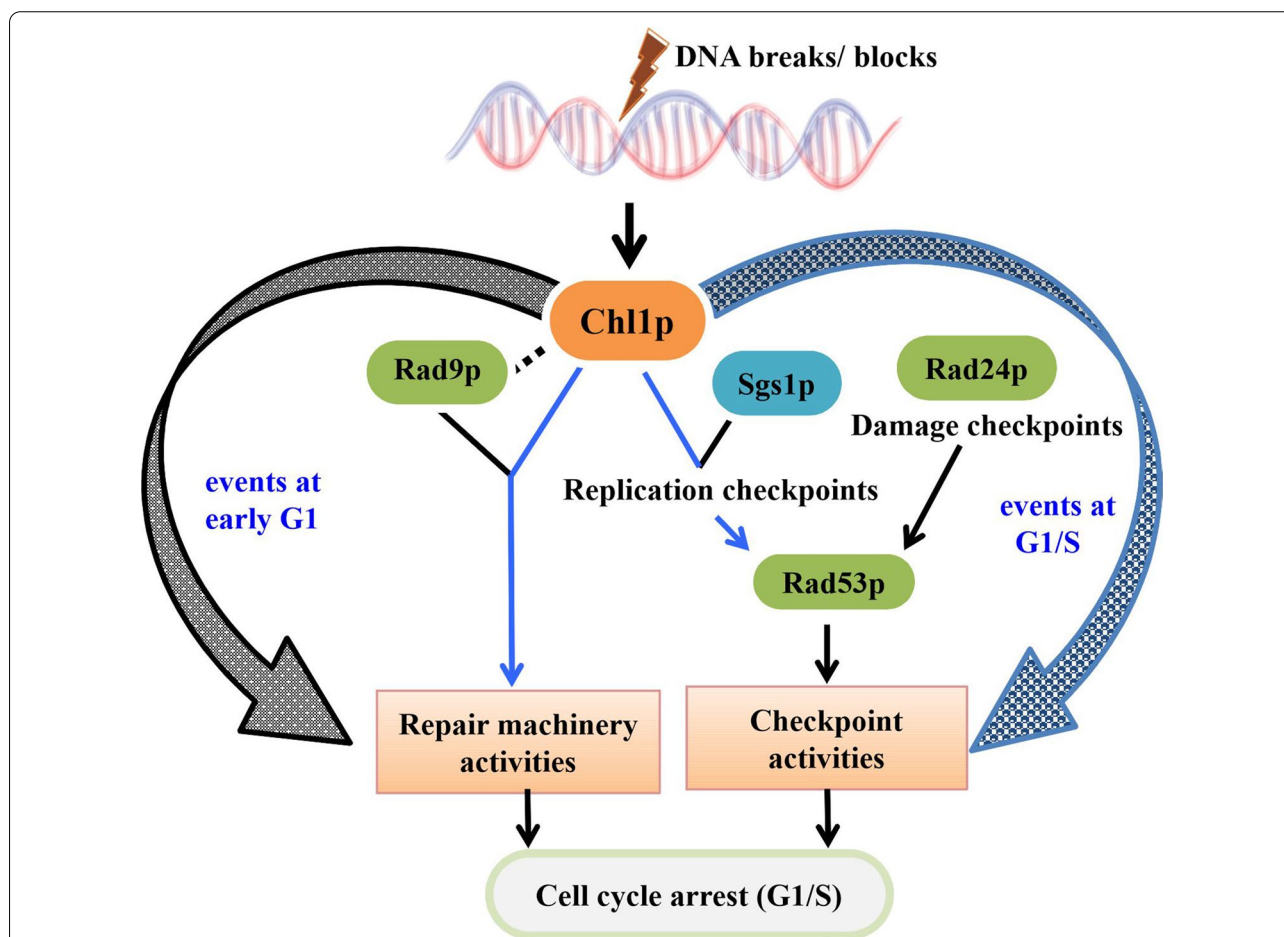


**Fig. 6** Roles of Chl1p at G1 phase of the cell cycle of budding yeast. The schematic representation depicts the multifunctional role of Chl1p at G1, once the DNA faces any insults with genotoxic agents. The wide curved grey arrow indicates the event regulated by Chl1p at early G1 phase and the blue curved one points towards the function played at G1/S. The black lines and the arrows indicate the known pathways. The blue lines and the arrows are the proposed associations explained in this paper with supporting observations. The black dotted line shows the plausible association between the two proteins, Rad9 and Chl1, which is already present in their human homologs (BRCA1 and BACH1 respectively)

of *chl1* mutants is even more compromised in absence of *rad24*. The checkpoint role through Rad53p and not through Chk1p, and the repair function in addition to Rad53 phosphorylation of Chl1p regulates the G1 phase arrest when DNA is perturbed. So Chl1p plays a role in regulating checkpoint at G1/S phase, which leads to

of double strand breaks at G2/M [47, 48]. Since Chl1p is required for the establishment of sister chromatid cohesion [1], resistance of *chl1* mutant towards faster budding kinetics and killing by MMS treatment at G2/M suggests that the repair of this damage is not critically dependent on the cohesion function of Chl1p.

## Conclusion

In summary, this paper brings to light additional role of cell cycle regulation by Chl1p in budding yeast. In presence of Chl1p, the repair and checkpoint functions are proficient in cells with double strand breaks, and so able to perform the G1/S delay in bud emergence. Chl1p leads to Rad53 activation, the major effector checkpoint kinase in presence of damage at 1. The Rad53p checkpoint activation by Chl1p at G1/S is independent of the Rad24p mediated damage checkpoint pathway. We also show that the role of Chl1p for bud emergence in G1 phase is in line with Rad9p and independent of Rad24p/ Rad53p. Sgs1p and Chk1p seem to play no role in G1 and the function of Chl1p doesn't associate with them. The, double mutant *rad9chl1* and *chk1chl1* shows similar bud emergence as the single mutants *chl1*, *rad9* and *chk1* whereas the double mutant *rad24chl1* and *rad53chl1* shows faster bud emergence than the single mutants. This budding kinetics explains an additional role of Chl1p independent of Rad53p checkpoint activation. This paper supports a model in which Chl1p plays a critical role in regulating the G1/S transition along with Rad9p when cells are compromised with DNA damaging agents. Consistent with our data and the supporting experimental findings from other groups, we predict that the helicase Chl1p plays a role in modulating the chromatin structure of the damaged DNA, aids Rad9p BRCT domain to access phosphorylated H2A S129 residue at the double strand break region followed by engagement of repair machinery. The repair process is further supported by the checkpoint activation through Chl1p. The checkpoint property further activates downstream regulators and key checkpoint proteins and keeps the cells arrested at early G1 as well as G1/S transition to provide some time for proper repair of the perturbed DNA at DSBs or blocks.

As the mammalian homologs of Rad9p (BRCA1) and Chl1p (BACH1) interacts at the BRCT domain [10], helicase Chl1p is suspected to be the Rad9p interactor and presumed to play the role of repair and remodeling of the damaged DNA along with Rad9p at the damaged sites. The findings of this paper gives a clue that the association of Rad9p to the modified chromatin at the DSB's helps to bring Chl1p repair protein through interaction with BRCT domain and repair damage by delaying G1 to S transition. During damage, the interaction between BRCT domain of Rad9p and phospho-H2A brings in the repair protein Chl1p helicase to the proximity of the damaged sites. As Chl1p also acts as a chromatin-remodeling factor [6], this in turn helps to remodel the chromatin bound Rad9p and initiate repair activity by arresting the cells at G1. The G1/S phase arrest is further supported by its Rad53p dependent checkpoint activity.

## Materials and methods

### Media and chemicals

All media, chemicals and enzymes have been described before [7, 12, 49]. DAPI, alpha-factor and goat anti-rat AP-conjugated antibody were from Sigma. Goat anti-mouse TRITC-conjugated antibody and NBT/BCIP was from Bangalore Genei Pvt. Ltd. Rad53 goat polyclonal antibody, raised against a carboxy terminus peptide of yeast Rad53p was from Abcam, and secondary HRP-conjugated anti-mouse antibody was from CST, USA. MMS was from Sigma.

### Construction of single and double mutant strains

Gene disruptions and deletions of Chl1 are described in [50]. Construction of double mutants and PCR based deletion of *CHL1* and *BARI* were carried out as described in [7, 51]. 699 and all the strains listed in Table 2 are in W303 background while the parent strains of the remaining were from G. Fink.

### Cell synchronization, bud emergence and nuclear segregation

Cells were synchronized in G1 using alpha-factor as described in [52]. Briefly, log phase cells were arrested with 0.025 µg/ml α-factor for 90 min and treated with 0.2% MMS in the last 10 min of arrest at 30 °C. MMS was quenched by 10% v/v sodium thiosulphate. Cells were washed free of cell cycle block (α-factor) and released into fresh medium. Thereafter, at different time intervals bud emergence post DNA damage was scored as a measure of G1/S arrest [53].

For G2/M arrest exponentially growing cells were treated with 15 µg/ml nocodazole for 3 h at 30 °C. The arrested cells were treated with 0.15% MMS during last half-hour of nocodazole arrest. After treatment, MMS was quenched with 10% sodium thiosulfate (v/v) and released from block. Nuclear stain was done with DAPI [54]. Around 150–200 cells were counted for nuclear morphologies, using a fluorescence microscope (Leica fitted with DC 300F camera).

### Flow cytometry

The phases of the cell cycle were determined by flow cytometry according to the protocol described in 12. Briefly, exponentially growing 1–2 X 10<sup>7</sup> cells were arrested at G1 using alpha-factor. To the arrested cells 0.2% MMS was added. Cells were collected at different time intervals in chilled 70% ethanol to do the cell cycle analysis. The cells fixed from each time point including the exponentials were spun down and fixed overnight in 70% ethanol at 4°C. Cells were washed and suspended in Tris–EDTA (pH 7.5) buffer for RNaseA treatment at

**Table 2** lists the strains used for this study

Strain	Genotype	Reference
699	<i>MATa ade2-1 trp1-1 leu2-3, 112 his 3-11, 15 ura3 can1-100</i>	[7]
699Dchl1	<i>MATa ade2-1 trp1-1 leu2-3, 112 his 3-11, 15 ura3 can1-100 chl1::HIS3</i>	[7]
US456	<i>MATa leu2 his3 trp1 ade2 rad24::URA3</i>	Uttam Surana
SL1	<i>MATa leu2 his3 trp1 ade2 rad24::URA3 chl1::HIS3</i>	This study, by crossing US456 with 699Dchl1
SL3	<i>MATa leu2 his3 trp1 ade2 rad24::URA3</i>	By crossing US456 with 699Dchl1
SL4	<i>MATa leu2 his3 trp1 ade2 rad24::URA3 chl1::HIS3</i>	By crossing US456 with 699Dchl1
US355	<i>MATa cdc13 rad9 leu2 ura3</i>	Uttam Surana
SL9	<i>MATa leu2 his3 trp1 ade2 ura3 rad9</i>	By crossing US355 with 699
SL9Dchl1	<i>MATa leu2 his3 trp1 ade2 ura3 rad9 chl1::HIS3</i>	This study, by disrupting <i>CHL1</i> in SL9
US354	<i>MATa leu2 his3 trp1 ade2 ura3 rad53-21</i>	[7]
SL7	<i>MATa leu2 his3 trp1 ade2 ura3 rad53-21</i>	[7]
SL7Dchl1	<i>MATa leu2 his3 trp1 ade2 ura3 rad53-21 chl1D::TRP1</i>	This study, by deleting <i>CHL1</i> in SL7
699Δsgs1	<i>MATa ade2-1 trp1-1 leu2-3, 112 his 3-11, 15 ura3 can1-100 sgs1Δ::LEU2</i>	This study, by deleting <i>SGS1</i> in 699
699Δsgs1 Dchl1	<i>MATa ade2-1 trp1-1 leu2-3, 112 his 311, 15 ura3 can1-100 sgs1Δ::LEU2 chl1::HIS3</i>	This study, by disrupting <i>CHL1</i> in 699Δsgs1
SL21	<i>MATa ade2-1 trp1-1 his 3-11, 15 ura3 can1-100 sgs1Δ::LEU2 rad24::URA3</i>	This study, by crossing SL1 with 699Δsgs1
SL 26	<i>MATa ade2-1 trp1-1 leu2-3, 112 his 3-11, 15 ura3 can1-100 Chk1::LEU2</i>	This study, by deleting <i>CHK1</i> in 699
SL27	<i>MATa ade2-1 trp1-1 leu2-3, 112 his 311, 15 ura3 can1-100 chl1::HIS3 Chk1::LEU2</i>	This study, by deleting <i>CHK1</i> in 699Dchl1

699 and all the strains listed are in W303 background

37 °C for 4 h. Propidium Iodide (50 µg/ml) staining was done overnight at 4 °C. Flow cytometry was done in FACS caliber (Becton Dickinson) with the sonicated samples (10 amps for 15 s).

**Protein extractions and western blot analysis**

For western blot analysis, protein extracts were prepared according to [7, 10] from cells synchronized at G1 and treated with 0.2% MMS. Proteins were separated on 8% SDS–PAGE containing an acrylamide to bis-acrylamide ratio of 80:1 and transferred to poly-vinylidene difluoride (PVDF) membrane (Millipore). Rad53 was detected using anti-Rad53 goat polyclonal antibody at 1:1000 dilution in TBS (50 mM Tris buffer pH 7.5, 150 mM NaCl) containing 0.5% BSA for 12–16 h. Secondary alkaline phosphatase-conjugated anti-goat antibody was incubated with the membrane for 2 h at 1:2500 dilution.

**Abbreviations**

ATP: Adenosine Triphosphate; BACH1: Breast Cancer Associated C-Terminal Helicase 1; BRCT: BRCA1 C Terminus; CDK: Cyclin Dependent Kinase; DAPI: 4',6-Diamidino-2-Phenylindole; DDC1: DNA Damage Checkpoint Protein 1; DSBs: Double Standard Break; HU: Hydroxy Urea; Mec: Mitosis Entry Checkpoint; MMS: Methyl Methane Sulfonate; rDNA: Recombinant DNA; RFC:

Replication Factor C; PCNA: Proliferating Cell Nuclear Antigen; PVDF: Poly-vinylidene difluoride; YEPD: Yeast Extract–Peptone–Dextrose.

**Supplementary Information**

The online version contains supplementary material available at <https://doi.org/10.1186/s13008-021-00072-x>.

Additional file 1: **Fig. S1.** Chl1p follows the replication checkpoint pathway. **A** G1/S-phase progression of single mutant and double mutant cells in the presence of MMS. Mutant cell 699Δsgs1 (*sgs1*) and the double mutants, SL21 (*rad24sgs1*) and 699Δsgs1Dchl1 (*sgs1chl1*) were arrested at G1 by treating the log phase cells with alpha factor for 90 min at 30 °C. 0.2% MMS was added in presence of the G1 block. All the cultures were kept shaking at 30 °C. Aliquots were removed at various times of MMS exposure for FACS analysis. 0' was collected just after adding 0.2% MMS to the cells with alpha factor (G1-blocked) followed by 10', 20' and 30' of exposure to 0.2% MMS in presence of alpha factor (G1-blocked damaged cells). The histogram plots at each time point are overlaid in the figure by using overlay software (Guava-Incyte) to understand the progression of the cells through cell cycle. The exponential cells were collected just before addition of alpha factor to the growing cells of 0.2 OD<sub>610nm</sub>. Arrows indicate G1 and G2 DNA contents.

**Acknowledgements**

We are very grateful to Professor Uttam Surana for providing the strains. We are thankful to Professor Pratima Sinha and our laboratory colleagues for helpful comments on the manuscript. We are thankful to the junior researchers Mr Amjad M, Ms Ameera Zulfaa and Ms Mithila Kulkarni for their supporting hands during the revision experiments. The laboratory assistance of Md. Asraf Ali Molla is gratefully acknowledged.

**Authors' contributions**

SL and SPD contributed towards design and drafting the work, analysis and interpretation of the data and gave the major contribution in writing the manuscript. KMN performed the experiments of budding index counting of different strains, imaging the strains and analyzed the data. KMN gave the major contribution in performing the revised experiments and in making the figures. All authors read and approved the final manuscript.

**Funding**

This work was supported by Grant SP/SO/DO3/2001 from the Department of Science and Technology, Government of India to P.S. and [seed grant YU/seed grant/055/2016 from Yenepoya University](#) to S.L.

**Availability of data and materials**

The datasets used and/or analyzed during the current study are available from the corresponding author on reasonable request.

**Declarations****Ethics approval and consent to participate**

Not applicable.

**Consent for publication**

Not applicable.

**Competing interests**

The authors declare that they have no financial, personal or professional competing interests that could be construed to have influenced this paper.

**Author details**

<sup>1</sup>Cell Biology and Molecular Genetics Division, Yenepoya Research Centre, Yenepoya Medical College, Yenepoya (Deemed To Be University), University Road, 3rd floor, Academic block, Deralakatte, Mangalore 575018, India. <sup>2</sup>Department of Biochemistry, Bose Institute, P1/12 CIT Scheme VII M, 700 054 Kolkata, India.

Received: 22 January 2021 Accepted: 20 August 2021

Published online: 08 September 2021

**References**

- Skibbens RV. Chl1p, a DNA helicase-like protein in budding yeast, functions in sister-chromatid cohesion. *Genetics*. 2004;166:33–42.
- Mayer ML, Pot I, Chang M, Xu H, Aneliunas V, Kwok T, Newitt R, Aebersold R, Boone C, Brown GW, Hieter P. Identification of protein complexes required for efficient sister chromatid cohesion. *Mol Biol Cell*. 2004;15:1736–45.
- Petronczki M, Chwalla B, Siomos MF, Yokobayashi S, Helmhart W, Deutschbauer AM, Davis RW, Watanabe Y, Nasmyth K. Sister-chromatid cohesion mediated by the alternative RF-C Ctf18/Dcc1/Ctf8, the helicase Chl1 and the polymerase- $\alpha$ -associated protein Ctf4 is essential for chromatid disjunction during meiosis II. *J Cell Sci*. 2004;117:3547–59.
- Holloway SL. CHL1 is a nuclear protein with an essential ATP binding site that exhibits a size-dependent effect on chromosome segregation. *Nucleic Acids Res*. 2000;28:3056–64.
- Das SP, Sinha P. The budding yeast protein Chl1p has a role in transcriptional silencing, rDNA recombination and aging. *Biochem Biophys Res Commun*. 2005;337:167–72.
- Inoue A, Hyle J, Lechner MS, Lahti JM. Mammalian ChlR1 has a role in heterochromatin organization. *Exp Cell Res*. 2011;317:2522–35.
- Laha S, Das SP, Hajra S, Sau S, Sinha P. The budding yeast protein Chl1p is required to preserve genome integrity upon DNA damage in S-phase. *Nucleic Acids Res*. 2006;34:5880–91.
- Amann J, Kidd VJ, Lahti JM. Characterization of putative human homologues of the yeast chromosome transmission fidelity gene, CHL1. *J Biol Chem*. 1997;272:3823–32.
- Hirota Y, Lahti JM. Characterization of the enzymatic activity of hChlR1, a novel human DNA helicase. *Nucleic Acids Res*. 2000;28:917–24.
- Cantor SB, Bell DW, Ganesan S, Kass EM, Drapkin R, Grossman S, Wahrer DCR, Sgroi DC, Lane WS, Haber DA, Livingston DM. BACH1, a novel helicase-like protein, interacts directly with BRCA1 and contributes to its DNA repair function. *Cell*. 2001;105:149–60.
- Hartwell LH, Weinert TA. Checkpoints: controls that ensure the order of cell cycle events. *Science*. 1989;246:629–34.
- Siede W, Friedberg AS, Friedberg EC. RAD9-dependent G1 arrest defines a second checkpoint for damaged DNA in the cell cycle of *Saccharomyces cerevisiae*. *Proc Natl Acad Sci USA*. 1993;90:7985–9.
- Siede W, Friedberg AS, Dianova I, Friedberg EC. Characterization of G1 checkpoint control in the yeast *Saccharomyces cerevisiae* following exposure to DNA-damaging agents. *Genetics*. 1994;138:271–81.
- Weinert TA, Kiser GL, Hartwell LH. Mitotic checkpoint genes in budding yeast and the dependence of mitosis on DNA replication and repair. *Genes Dev*. 1994;8:652–65.
- Paulovich AG, Hartwell LH. A checkpoint regulates the rate of progression through S phase in *S. cerevisiae* in response to DNA damage. *Cell*. 1995;82:841–7.
- Paulovich AG, Margulies RU, Garvik BM, Hartwell LH. Rad9, Rad17 and Rad24 are required for S phase regulation in *Saccharomyces cerevisiae* in response to DNA damage. *Genetics*. 1997;145:45–62.
- Tercero JA, Longhese MP, Diffley JF. A central role for DNA replication forks in checkpoint activation and response. *Mol Cell*. 2003;11:1323–36.
- Sidorova JM, Breeden LL. Rad53-dependent phosphorylation of Swi6 and down-regulation of CLN1 and CLN2 transcription occur in response to DNA damage in *Saccharomyces cerevisiae*. *Genes Dev*. 1997;11:3032–45.
- Frei C, Gasser SM. The yeast Sgs1p helicase acts upstream of Rad53p in the DNA replication checkpoint and colocalizes with Rad53p in S-phase-specific foci. *Genes Dev*. 2000;14:81–96.
- Allen JB, Zhou Z, Siede W, Friedberg EC, Elledge SJ. The SAD1/RAD53 protein kinase controls multiple checkpoints and DNA damage-induced transcription in yeast. *Genes Dev*. 1994;8:2401–15.
- Siede W, Allen JB, Elledge SJ, Friedberg EC. The *Saccharomyces cerevisiae* MEC1 gene, which encodes a homolog of the human ATM gene product, is required for G1 arrest following radiation treatment. *J Bacteriol*. 1996;178:5841–3.
- Melo J, Toczyski D. A unified view of the DNA-damage checkpoint. *Curr Opin Cell Biol*. 2002;14:237–45.
- Nyberg KA, Michelson RJ, Putnam CW, Weinert TA. Toward maintaining the genome: DNA damage and replication checkpoints. *Annu Rev Genet*. 2002;36:617–56.
- Osborn AJ, Elledge SJ, Zou L. Checking on the fork: the DNA-replication stress-response pathway. *Trends Cell Biol*. 2002;12:509–16.
- Friedberg EC. DNA damage and repair. *Nature*. 2003;421:436–40.
- Friedberg EC, McDaniel LD, Schultz RA. The role of endogenous and exogenous DNA damage and mutagenesis. *Curr Opin Genet Dev*. 2004;14:5–10.
- Cobb JA, Shimada K, Gasser SM. Redundancy, insult-specific sensors and thresholds: unlocking the S-phase checkpoint response. *Curr Opin Genet Dev*. 2004;14:292–300.
- Weinert TA, Hartwell LH. The RAD9 gene controls the cell cycle response to DNA damage in *Saccharomyces cerevisiae*. *Science*. 1988;241:317–22.
- Saka Y, Esashi F, Matsusaka T, Mochida S, Yanagida M. Damage and replication checkpoint control in fission yeast is ensured by interactions of Crb2, a protein with BRCT motif, with Cut5 and Chk1. *Genes Dev*. 1997;11:3387–400.
- Du L-L, Nakamura TM, Russell P. Histone modification-dependent and -independent pathways for recruitment of checkpoint protein Crb2 to double-strand breaks. *Genes Dev*. 2006;20:1583–96.
- Emili A. MEC1-dependent phosphorylation of Rad9p in response to DNA damage. *Mol Cell*. 1998;2:183–9.
- Vialard JE, Gilbert CS, Green CM, Lowndes NF. The budding yeast Rad9 checkpoint protein is subjected to Mec1/Tel1-dependent hyperphosphorylation and interacts with Rad53 after DNA damage. *EMBO J*. 1998;17:5679–88.
- Schwartz MF, Duong JK, Sun Z, Morrow JS, Pradhan D, Stern DF. Rad9 phosphorylation sites couple Rad53 to the *Saccharomyces cerevisiae* DNA damage checkpoint. *Mol Cell*. 2002;9:1055–65.
- Liu Y, et al. Characterization of a *Saccharomyces cerevisiae* homologue of *Schizosaccharomyces pombe* Chk1 involved in DNA-damage-induced M-phase arrest. *Mol Gen Genet*. 2000;262(6):1132–46.

35. Sanchez Y, Bachant J, Wang H, Hu F, Liu D, Tetzlaff M, Elledge SJ. Control of the DNA damage checkpoint by chk1 and rad53 protein kinases through distinct mechanisms. *Science*. 1999;286:1166–71.
36. Blankley RT, Lydall D. A domain of Rad9 specifically required for activation of Chk1 in budding yeast. *J Cell Sci*. 2003;117:601–8.
37. Chinoye C, Nnakwe MA, Jacques C, Stephen JK. Dissection of rad9 brct domain function in the mitotic checkpoint response to telomere uncapping. *DNA Repair*. 2009;8(12):1452–61.
38. Wang G, Tong X, Weng S, Zhou H. Multiple phosphorylation of Rad9 by CDK is required for DNA damage checkpoint activation. *Cell Cycle*. 2012;11:3792–800.
39. Tercero JA, Diffley JF. Regulation of DNA replication fork progression through damaged DNA by the Mec1/Rad53 checkpoint. *Nature*. 2001;412:553–7.
40. Watt PM, Hickson ID, Borts RH, Louis EJ. SGS1, a homologue of the Bloom's and Werner's syndrome genes, is required for maintenance of genome stability in *Saccharomyces cerevisiae*. *Genetics*. 1996;144:935–45.
41. Myung K, Datta A, Chen C, Kolodner RD. SGS1, the *Saccharomyces cerevisiae* homologue of BLM and WRN, suppresses genome instability and homologous recombination. *Nature Genet*. 2001;27:113–6.
42. Bjergbaek L, Cobb JA, Tsai-Pflugfelder M, Gasser SM. Mechanistically distinct roles for Sgs1p in checkpoint activation and replication fork maintenance. *EMBO J*. 2004;24:405–17.
43. Poddar A, Roy N, Sinha P. MCM21 and MCM22, two novel genes of the yeast *Saccharomyces cerevisiae* are required for chromosome transmission. *Mol Microbiol*. 1999;31:349–60.
44. Cicco GD, Bantele SCS, Reuswig KU, Pfander B. A cell cycle-independent mode of the Rad9-Dpb11 interaction is induced by DNA damage. *Sci Rep*. 2017;7:11650.
45. Muhseena KN, Mathukkada S, Das SP, Laha S. The repair gene *BACH1* - a potential oncogene. *Oncol Rev*. 2021;15(1):519.
46. Bonilla CY, Melo JA, Toczyski DP. Colocalization of sensors is sufficient to activate the DNA damage checkpoint in the absence of damage. *Mol Cell*. 2008;30:267–76.
47. Sjogren C, Nasmyth K. Sister chromatid cohesion is required for postreplicative double-strand break repair in *Saccharomyces cerevisiae*. *Curr Biol*. 2001;11:991–5.
48. Strom L, Lindroos HB, Shirahige K, Sjogren C. Post replicative recruitment of cohesin to double-strand breaks is required for DNA repair. *Mol Cell*. 2004;16:1003–15.
49. Ghosh SK, Poddar A, Hajra S, Sanyal K, Sinha P. The IML3/MCM19 gene of *Saccharomyces cerevisiae* is required for a kinetochore-related process during chromosome segregation. *Mol Genet Genomics*. 2001;265:249–57.
50. Hajra, S. (2003) Kinetochore structure of the budding yeast *Saccharomyces cerevisiae*: a study using genetic and protein–protein interactions. PhD Thesis, Jadavpur University, Kolkata.
51. Longtine MS, McKenzie A, Demarini DJ, Shah NG, Wach A, Brachat A, Philippsen P, Pringle JR. Additional modules for versatile and economical PCR-based gene deletion and modification in *Saccharomyces cerevisiae*. *Yeast*. 1998;14(10):953–61.
52. Breeden LL. Alpha-factor synchronization of budding yeast. *Methods Enzymol*. 1997;283:332–41.
53. Hammet A, Magill C, Heierhorst J, Jackson SP. Rad9 BRCT domain interaction with phosphorylated H2AX regulates the G1 checkpoint in budding yeast. *EMBO Rep*. 2007;8:851–7.
54. Ghosh SK, Sau S, Lahiri S, Lohia A, Sinha P. The Iml3 protein of the budding yeast is required for the prevention of precocious sister chromatid separation in meiosis I and for sister chromatid disjunction in meiosis II. *Curr Genet*. 2004;46:82–91.

### Publisher's Note

Springer Nature remains neutral with regard to jurisdictional claims in published maps and institutional affiliations.

Ready to submit your research? Choose BMC and benefit from:

- fast, convenient online submission
- thorough peer review by experienced researchers in your field
- rapid publication on acceptance
- support for research data, including large and complex data types
- gold Open Access which fosters wider collaboration and increased citations
- maximum visibility for your research: over 100M website views per year

At BMC, research is always in progress.

Learn more [biomedcentral.com/submissions](https://biomedcentral.com/submissions)



# Identification of Molecular Network Associated with Neuroprotective Effects of Yashtimadhu (*Glycyrrhiza glabra* L.) by Quantitative Proteomics of Rotenone-Induced Parkinson's Disease Model

Gayathree Karthikkeyan, Mohd. Altaf Najar, Ravishankar Pervaje, Sameera Krishna Pervaje, Prashant Kumar Modi,\* and Thottethodi Subrahmanya Keshava Prasad\*



Cite This: *ACS Omega* 2020, 5, 26611–26625



Read Online

ACCESS |



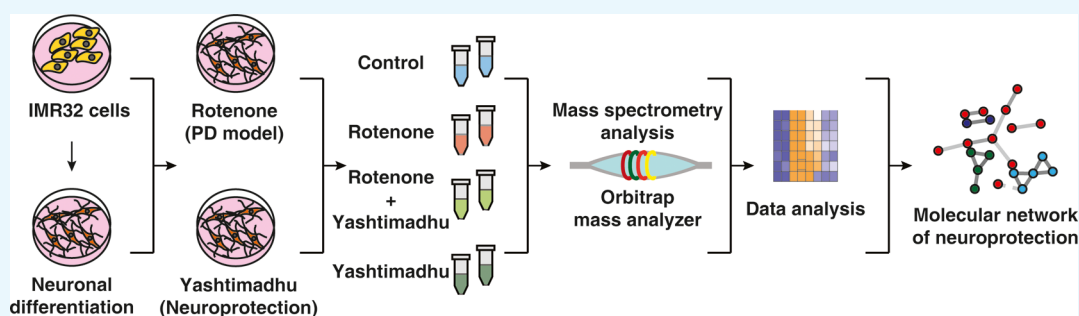
Metrics & More



Article Recommendations



Supporting Information



**ABSTRACT:** Parkinson's disease (PD) is a progressive neurodegenerative disorder, whose treatment with modern therapeutics leads to a plethora of side effects with prolonged usage. Therefore, the management of PD with complementary and alternative medicine is often pursued. In the Ayurveda system of alternative medicine, Yashtimadhu choorna, a *Medhya Rasayana* (nootropic), prepared from the dried roots of *Glycyrrhiza glabra* L. (licorice), is prescribed for the management of PD with a favorable outcome. We pursued to understand the neuroprotective effects of Yashtimadhu choorna against a rotenone-induced cellular model of PD using differentiated IMR-32 cells. Cotreatment with Yashtimadhu choorna extract rescued rotenone-induced apoptosis and hyperphosphorylation of ERK-1/2. Quantitative proteomic analysis of six peptide fractions from independent biological replicates acquired 1,561,169 mass spectra, which when searched resulted in 565,008 peptide-spectrum matches mapping to 30,554 unique peptides that belonged to 4864 human proteins. Proteins commonly identified in biological replicates and >4 PSMs were considered for further analysis, leading to a refined set of 3720 proteins. Rotenone treatment differentially altered 144 proteins (fold  $\geq 1.25$  or  $\leq 0.8$ ), involved in mitochondrial, endoplasmic reticulum, and autophagy functions. Cotreatment with Yashtimadhu choorna extract rescued 84 proteins from the effect of rotenone and an additional regulation of 4 proteins. Network analysis highlighted the interaction of proteins and pathways regulated by them, which can be targeted for neuroprotection. Validation of proteomics data highlighted that Yashtimadhu confers neuroprotection by preventing mitochondrial oxidative stress and apoptosis. This discovery will pave the way for understanding the molecular action of Ayurveda drugs and developing novel therapeutics for PD.

## INTRODUCTION

Neurodegeneration is a progressive phenomenon at old ages, which occurs as a result of neuronal loss or the inability of neurons to transmit the signals. Parkinson's disease (PD) is one such age-related progressive neurodegenerative disorder whose prevalence accounts for 3% of the population, above 65 years.<sup>1</sup> PD is caused by loss of dopaminergic neurons from the substantia nigra pars compacta (SNpc), resulting in loss of the neurotransmitter dopamine, and leads to the development of motor symptoms. The death of dopaminergic neurons is caused as a result of mitochondrial dysfunction, endoplasmic reticulum (ER) stress, neuroinflammation, and accumulation of protein aggregates.<sup>2,3</sup> The management of PD relies on the

alleviation of the symptoms, and levodopa is one of the most commonly prescribed medicines, which is useful in the early stages of the disease. However, with prolonged usage, the efficacy of PD medications decline and is reported to cause many side effects.<sup>4</sup> Thus, there is a need for the use of a sustainable alternative and complementary management

Received: July 17, 2020

Accepted: September 24, 2020

Published: October 6, 2020



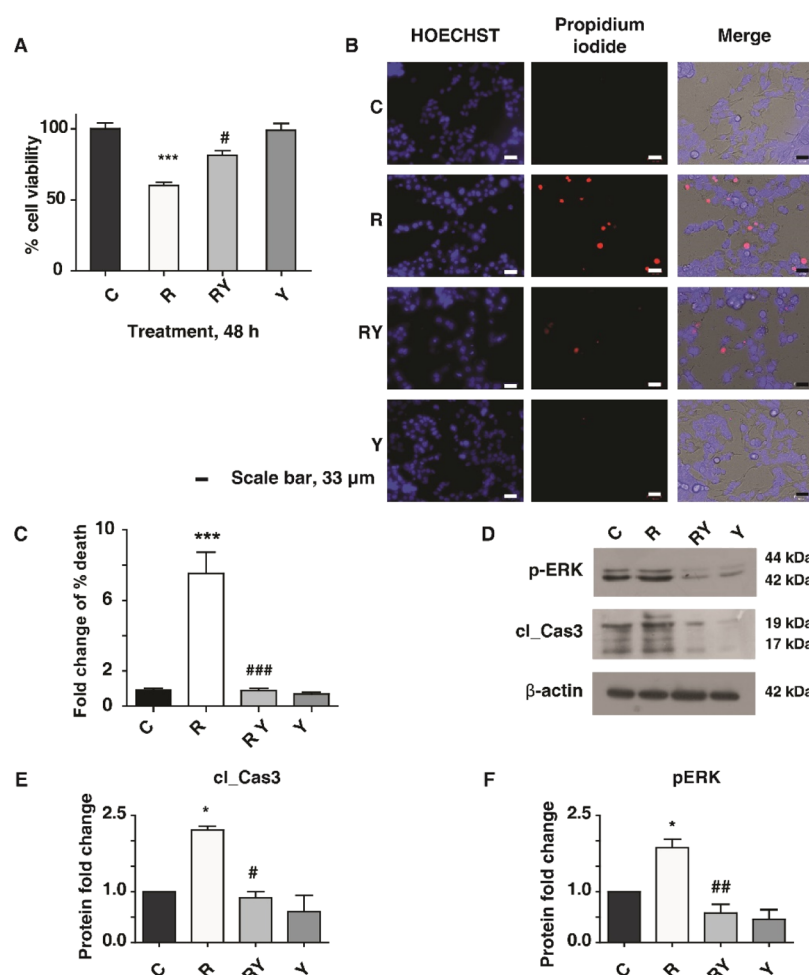


**Figure 1.** PD model validation and Yashtimadhu neuroprotection. (A) Cytotoxicity analysis showing rotenone-induced cell death and prevention of cell death by Yashtimadhu choorna extract cotreatment; (B) live–dead cell staining assay using propidium iodide (PI) (red) and HOECHST (blue) nuclear counterstain; and (C) graphical representation of cell death with respect to untreated cell control. Rotenone treatment increases cell death, encountered by Yashtimadhu choorna cotreatment, (D) immunoblot analysis of *p*-ERK-1/2 (T202/T204) and cleaved caspase-3 with  $\beta$ -actin as the loading control across control (C), rotenone (R), rotenone + Yashtimadhu choorna cotreatment (RY), and Yashtimadhu choorna extract (Y); (E) densitometry graph of cleaved caspase-3 activation, normalized with loading control, \*, with respect to control (C) and # with respect to Yashtimadhu choorna cotreatment (RY). \*,#  $p < 0.05$ , \*\*,##  $p < 0.01$ , and \*\*\*,###  $p < 0.001$ . Labels: C—untreated cells, R—rotenone treatment, RY—rotenone + Yashtimadhu choorna extract cotreatment, and Y—Yashtimadhu choorna extract treatment.

strategy of PD, which is required not only to prevent symptoms of PD but also to address the underlying molecular aberrations and improve the quality of life.

The quest for sustainable management of the disease led to the exploration of complementary and alternative medicines, which employ the use of traditional medicines and other forms of alternative treatments, including acupuncture, rhythmic therapy, and Reiki.<sup>5</sup> The Indian Ayurvedic medicinal system classifies medicinal plants with nootropic properties as *Medhya Rasayana*, which helps in improving memory and brain functions.<sup>6–8</sup> The nootropic formulations include Yashtimadhu (*Glycyrrhiza glabra*, licorice), Mandukaparni (*Centella asiatica*, Asiatic pennywort), Ashwagandha (*Withania somnifera*, Indian ginseng), and Brahmi (*Bacopa monnieri*, water hyssop).<sup>9–11</sup> Yashtimadhu choorna is prepared from the dried roots of *G. glabra* L., commonly known as licorice (<http://www.theplantlist.org/>; <http://www.ayurveda.hu/api/API-Vol-1.pdf>). Several studies have reported its effectiveness as a neuroprotectant, an antidepressant, an antioxidant, and a memory enhancer.<sup>12–18</sup> These studies highlight the neuro-

modulatory effects of Yashtimadhu; however, there exist lacunae in understanding the regulation of protein networks and the underlying molecular pathways.

PD is regarded as proteinopathy<sup>19,20</sup> because of the dysregulation of the protein dynamics, resulting in abnormal accumulation of protein aggregates. Mass spectrometry (MS)-based proteomics serves as an invaluable tool to study the alteration of proteins that drive the pathogenesis in experimental models of PD, and the counteracting neuroprotective strategies, upon the introduction of a specific drug. The experimental models of PD are generated using genetically modified *in vivo* models such as  $\alpha$ -synuclein (SNCA), parkin (PRKN), leucine-rich repeat kinases (LRRKs), or use of neurotoxins *in vitro* and *in vivo*.<sup>21</sup> The commonly used neurotoxic models of PD are generated using rotenone, MPTP (1-methyl-4-phenyl-1,2,3,6-tetrahydropyridine), paraquat, and 6-hydroxydopamine.<sup>22</sup> The establishment of an *in vitro* cellular model of PD offers advantages in monitoring and understanding the cellular mechanisms that are responsible for neurodegeneration. These proteins involved in the neuro-

degenerative mechanism can be targeted for efficient neuroprotective interventions.<sup>23,24</sup> The study of proteins altered during the progression of a disease and its recovery helps in discovering the proteins associated with a protective pathway conferred by the drug.

In this study, we sought to evaluate the neuroprotective effects of Yashtimadhu choorna extract in an *in vitro* PD model. This model was generated using rotenone (a mitochondrial complex-I inhibitor), which triggers oxidative stress and induces apoptosis,<sup>25</sup> effectively mimicking the cellular aberrations reported in PD. Quantitative proteomics was employed to identify proteins altered by rotenone and compared to their restoration by Yashtimadhu choorna extract to understand the molecular networks involved in neuroprotection.

## RESULTS AND DISCUSSION

**Yashtimadhu Choorna Extract Counteracts Rotenone-Induced Apoptosis.** We aimed to evaluate the establishment of the rotenone-induced PD model and the neuroprotection conferred by Yashtimadhu. To achieve this, we used IMR-32 cells that were differentiated with retinoic acid to yield dopaminergic neuron population.<sup>26–28</sup>

IMR-32 cells were differentiated with retinoic acid, which was confirmed with tyrosine hydroxylase (TH) expression (Supporting Information Figure S1A,B) and used to assess the neuroprotection conferred by Yashtimadhu choorna extract in a rotenone-induced PD model. Cytotoxicity assay was used to test the effective treatment doses of rotenone and Yashtimadhu choorna extract. Rotenone-induced time- and dose-dependent cell death and the IC<sub>50</sub> (50% cell death) value was observed at a 100 nM concentration for 48 h, which was used for further treatments (Supporting Information Figure S1C). At the same time, treatment with Yashtimadhu choorna extract for 48 h showed no cytotoxicity at all tested concentrations (Supporting Information Figure S1D). The cell death observed at the IC<sub>50</sub> rotenone concentration of 100 nM was prevented by cotreatment of Yashtimadhu choorna extract at a 200 μg/mL concentration, which was used for further treatments (Figure 1A). Cell death was also ascertained with the live–dead cell staining assay (Figure 1B,C). Rotenone treatment increased cell death (7.53-fold,  $p < 0.001$ ), which was rescued by Yashtimadhu choorna extract cotreatment (0.89-fold,  $p < 0.001$ ), which is in agreement with the cytotoxicity analysis.

ERK-1/2 phosphorylation and cleaved-caspase-3 activation are known to be induced by rotenone, which is also implicated in neurodegeneration.<sup>29,30</sup> Rotenone induced activation of cleaved caspase-3 (2.22-fold,  $p < 0.05$ ) and hyperphosphorylation of ERK-1/2 (1.87-fold,  $p < 0.05$ ) (Figure 1D–F). Yashtimadhu choorna extract cotreatment encountered the rotenone-induced caspase-3 activation (0.88-fold,  $p < 0.05$ ) and *p*-ERK-1/2 (0.58-fold,  $p < 0.01$ ). These observations confirm the neuroprotective effects of Yashtimadhu against rotenone-induced stress by preventing *p*-ERK-1/2 activation and subsequent apoptosis.

**Quantitative Proteomics Highlights Differentially Regulated Proteins.** Quantitative proteomics was carried out to identify the altered proteins with rotenone treatment alone and restoration of those by cotreatment with Yashtimadhu choorna extract. The data were acquired for the biological duplicates, as technical triplicates each (Figure 2A). The workflow used for filtering proteins based on their identification from the independent replicates is outlined in Figure 2B. We obtained around 1.5 million tandem mass

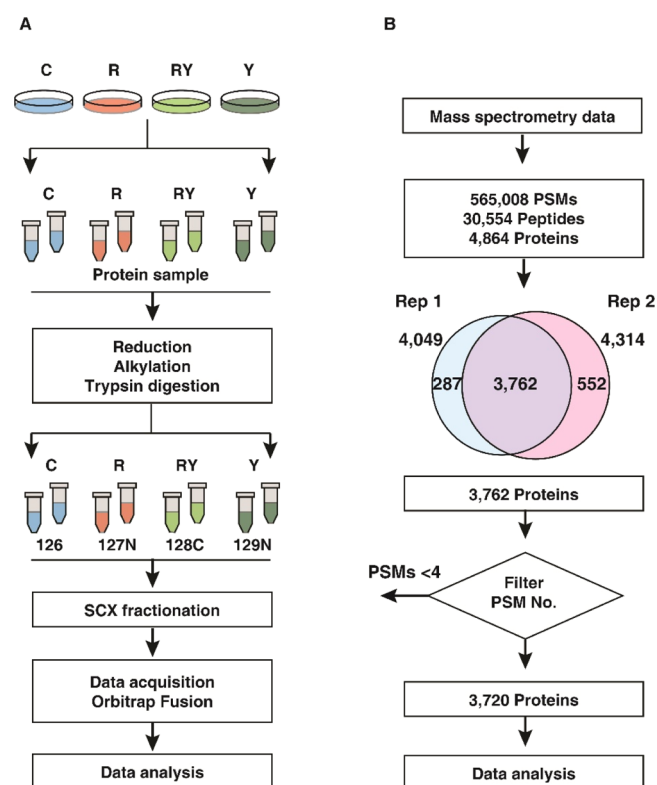


**Figure 2.** Summary of proteomics analysis. (A) Schematic of workflow employed for proteomics data acquisition. Labels: C—untreated cells, R—rotenone treatment, RY—rotenone + Yashtimadhu choorna extract cotreatment, and Y—Yashtimadhu choorna extract treatment and (B) schematic of the workflow used for proteomics data analysis.

spectrometry (MS/MS) spectra, which provided 565,008 PSMs upon searching the MS/MS data against the database (human RefSeq109). These PSMs corresponded to 30,554 nonredundant peptides, identifying 4864 protein sequences corresponding to 4783 genes. Proteins commonly identified in both the biological replicates were considered, resulting in 3762 proteins. Also, proteins with PSMs < 4 were filtered out, and a list of 3720 resultant proteins (corresponding to 3673 gene symbols) was used for subsequent analysis (Supporting Information Table S1). The fold change (FC) of these 3720 proteins, along with their respective *p*-values and *q*-values, is deposited in the PRIDE repository.

Principal component analysis (PCA) was carried out to identify the variance across the four groups. The score plot (Figure 3A) shows the clustering of the groups based on the biological replicates. Rotenone treatment showed the maximal variation in comparison with the untreated cell control group. In contrast, the Yashtimadhu choorna extract cotreatment group showed a minimum variance compared with the untreated cells, indicating the restoration of altered protein dynamics.

The FC of protein expression was calculated with respect to the untreated cell control (C) and rotenone (R). A FC cutoff of  $\geq 1.25$  for overexpression and  $\leq 0.8$  for the downregulation of proteins was selected to be biologically significant, and an adjusted *p*-value, that is,  $q \leq 0.05$ , was selected for statistical significance. A similar range of FCs has been previously reported by studies using isobaric labeling.<sup>31–35</sup> Rotenone treatment highlighted 421 differentially regulated proteins (FC



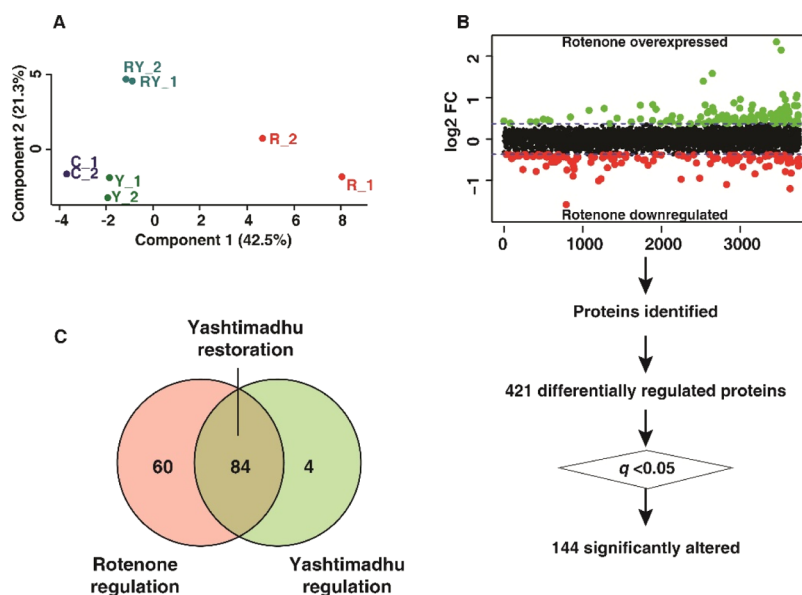


**Figure 3.** Differential regulation of proteins. (A) PCA score plot showing the variability between the groups and within the biological replicates, (B) scatter plot showing rotenone-induced differential expression, and (C) Venn diagram showing the restoration of proteins with Yashtimadhu choorna cotreatment. Labels: C—untreated cells, R—rotenone treatment, RY—rotenone + Yashtimadhu choorna extract cotreatment, and Y—Yashtimadhu choorna extract treatment.

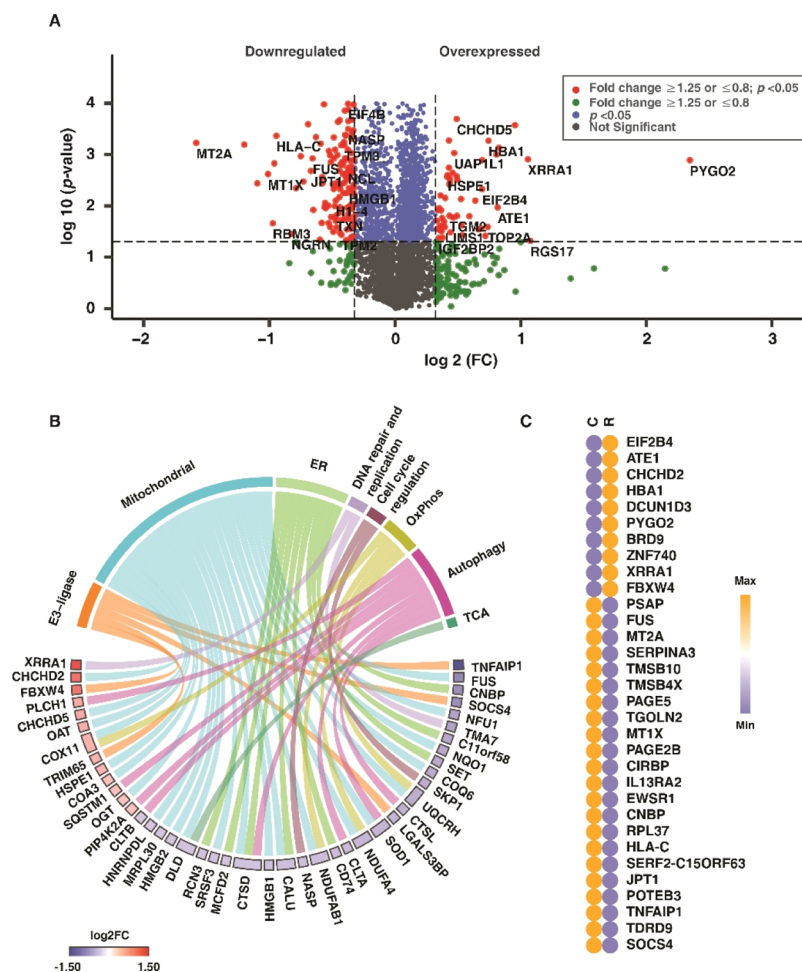


**Figure 4.** Rotenone-induced differential protein expression. (A) Volcano plot displaying the differentially altered proteins with rotenone treatment, with respect to control group (R vs C), (B) chord plot showing the classification of differentially regulated proteins and their log<sub>2</sub>FC, (C) heat map showing the differential expression of the highly upregulated (FC ≥ 1.5) and downregulated (FC ≤ 0.67) proteins, with respect to that of the control group. Labels: C—untreated cells and R—rotenone treatment.

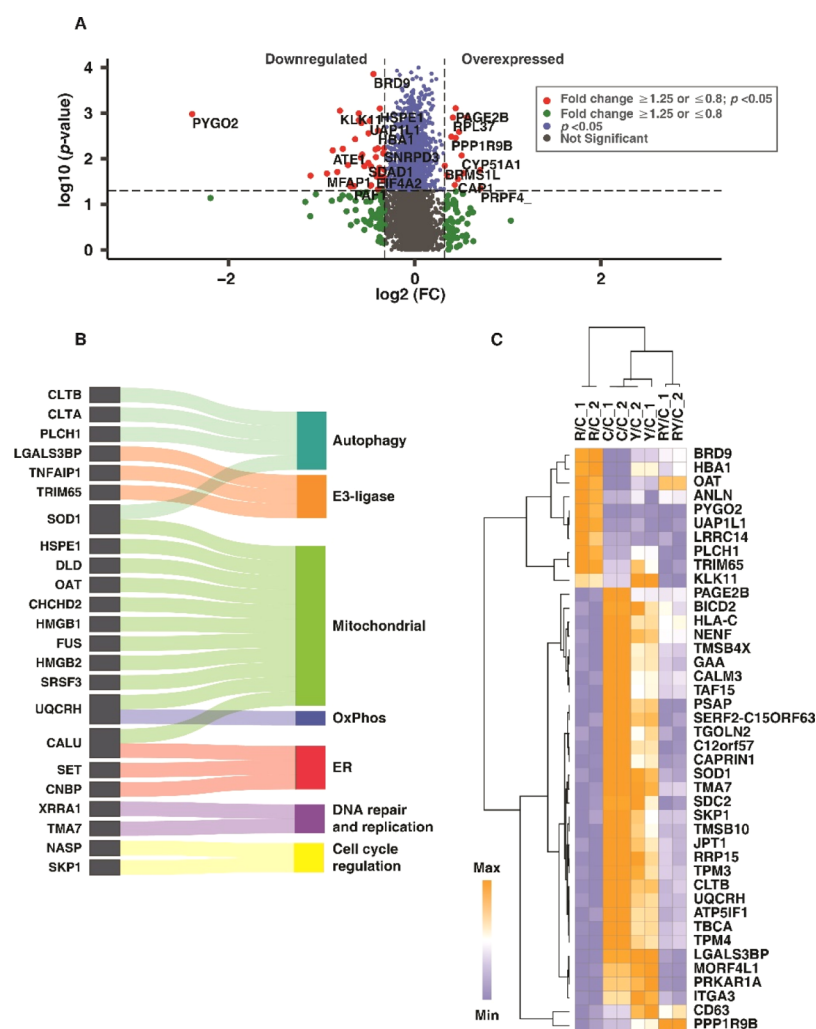


**Figure 5.** Yashtimadhu choorna extract cotreatment restores differentially regulated proteins. (A) Volcano plot displaying the differentially altered proteins with Yashtimadhu choorna extract cotreatment with rotenone, with respect to the rotenone group (RY vs R), (B) Sankey diagram showing the classification of differentially regulated proteins, and (C) heat map showing the differential expression of the proteins classified across all four groups, with respect to control. Labels: C—untreated cells, R—rotenone treatment, RY—rotenone + Yashtimadhu choorna extract cotreatment, and Y—Yashtimadhu choorna extract treatment.

$\geq 1.25$  or  $\leq 0.8$ ), of which 144 were significantly altered ( $q \leq 0.05$ , with respect to untreated cell control, Figure 3B). Yashtimadhu choorna extract cotreatment was found to significantly regulate 88 proteins ( $q \leq 0.05$ , with respect to rotenone), which included restoration of 84 proteins that were dysregulated by rotenone and an additional regulation of 4 proteins (Figure 3C).

**Classification of Identified Proteins.** Proteins were classified based on their intracellular compartmentalization and biological processes to understand the relevance of the differentially regulated proteins in the context of PD. Proteins were localized in the cytoplasm and nucleus, followed by exosomes, mitochondria, lysosomes, and ER. The proteins identified were also involved in processes such as cellular and protein metabolism, energy pathways, and cell proliferation.

Additionally, proteins were also classified using publicly available databases, such as MitoCarta, The Autophagy database, and the E3-ligases databases. The proteins regulating mitochondrial processes and energy pathways, ER function, autophagy, metabolism of proteins and lipids, cell proliferation, DNA repair, and replication were further shortlisted to

understand the effect of rotenone and rescue by Yashtimadhu choorna extract cotreatment.

**Rotenone Dysregulates Proteins Involved in Vital Functions.** The extent of cellular damage as a result of rotenone was earlier ascertained with molecular assays, and the proteomics data were used to gain deeper insights into rotenone-induced cellular stress. Rotenone treatment resulted in 30 overexpressed ( $\geq 1.25$ ,  $q < 0.05$ ) and 114 downregulated ( $\leq 0.8$ ,  $q < 0.05$ ) proteins (Figure 4A). Mitochondrial dysfunction, ER stress, and autophagy dysregulation drive neuronal cell death, leading to the onset and progression of PD.<sup>36–38</sup> Rotenone treatment altered the proteins involved in mitochondrial functions, ER functions, and autophagy. Altered mitochondrial proteins include those involved in the tricarboxylic acid (TCA) cycle and oxidative phosphorylation (OxPhos), among others (Figure 4B). The expression of these classified proteins with respect to control is also depicted in the chord diagram (Figure 4B). A heat map showing the expression of the highly overexpressed ( $FC \geq 1.5$ ,  $q \leq 0.05$ ) and downregulated ( $FC \leq 0.67$ ,  $q \leq 0.05$ ) proteins with rotenone treatment is given in Figure 4C.

Table 1. Partial List of Proteins Regulated by Yashtimadhu with Their Respective FC and *q*-Values<sup>a</sup>

description	accession	gene symbol	rotenone, FC	Yashtimadhu choorna extract cotreatment, FC
Proteins Restored by Yashtimadhu				
Proteins Overexpressed with Rotenone				
pygopus homolog 2	NP_612157.1	PYGO2	5.09,*	0.96,#
X-ray radiation resistance-associated protein 1 isoform X10	XP_011543064.1	XRRRA1	2.08,*	1.4,#
bromodomain-containing protein 9 isoform 1	NP_076413.3	BRD9	1.94,**	1.43,#
10 kDa heat shock protein, mitochondrial	NP_002148.1	HSPE1	1.34,*	1.03,#
UDP-N-acetylhexosamine pyrophosphorylase-like protein 1 isoform X1	XP_006717380.1	UAP1L1	1.39,*	0.99,#
1-phosphatidylinositol 4,5-bisphosphate phosphodiesterase eta-1 isoform X5	XP_011510867.1	PLCH1	1.41,*	0.93,#
anillin isoform X1	XP_006715809.1	ANLN	1.41,*	1.13,#
ornithine aminotransferase, mitochondrial isoform 1	NP_001309897.1	OAT	1.38,*	1.31,#
tripartite motif-containing protein 65 isoform X1	XP_006721823.1	TRIM65	1.35,*	0.89,#
kallikrein-11 isoform X1	XP_011524671.1	KLK11	1.32,*	0.76,#
Proteins Downregulated with Rotenone				
60S ribosomal protein L37	NP_000988.1	RPL37	0.67,*	0.89,#
superoxide dismutase 1 [Cu–Zn]	NP_000445.1	SOD1	0.74,*	0.77,#
zinc finger Ran binding domain-containing protein 2 isoform 1	NP_976225.1	ZRANB2	0.76,*	0.85,#
histone H1.3	NP_005311.1	H1-3	0.76,***	0.84,#
CDS9 glycoprotein	NP_001120699.1	CDS9	0.76,***	0.89,#
nucleolin	NP_005372.2	NCL	0.77,*	0.83,#
CALU isoform c	NP_001186600.1	CALU	0.77,**	0.88,#
Src substrate cortactin isoform a	NP_005222.2	CTTN	0.78,***	0.84,###
SH3 domain binding glutamic acid-rich-like protein	NP_003013.1	SH3BGRL	0.79,**	0.86,#
ashwin isoform X1	XP_024308903.1	C2orf49	0.79,**	0.89,#
Proteins Additionally Regulated by Yashtimadhu				
leucine-rich repeat-containing protein 14	NP_001258965.1	LRRC14	1.51,ns	0.97,#
pleckstrin homology-like domain family A member 3	NP_036528.1	PHLDA3	1.02,ns	0.72,#
neurabin-2	NP_115984.3	PPP1R9B	0.95,ns	1.24,#
CD63 antigen isoform A	NP_001244318.1	CD63	0.86,ns	1.16,#

<sup>a</sup>\*, significance with respect to control; #, significance with respect to rotenone. \*,#,  $q \leq 0.05$ ; \*\*,##,  $q \leq 0.01$ ; and \*\*\*,###,  $q \leq 0.005$ .

OxPhos proteins such as ubiquinol-cytochrome *c* reductase hinge protein (UQCRH), NADH: ubiquinone oxidoreductase subunit-AB1 (NDUFAB1), and TCA cycle protein, dihydro-lipoamide dehydrogenase were downregulated. Rotenone also affected the expression of ER proteins such as signal recognition particle 9 (SRP9), calumenin (CALU), eukaryotic translation initiation factor 2B subunit delta (EIF2B4), and autophagy proteins, 1-phosphatidylinositol 4,5-bisphosphate phosphodiesterase eta-1 (PLCH1) and cathepsin D (CTSD). The findings indicate mitochondrial dysfunction, autophagy dysregulation, and ER stress, which, as a result of rotenone, is reported to be a driving factor in neuronal apoptosis.<sup>25,39,40</sup>

**Yashtimadhu Restores Proteins Involved in Cellular Stress Response.** We have compared the Yashtimadhu choorna extract cotreatment group with the rotenone treatment group for differentially regulated proteins, which have been highlighted in a volcano plot (Figure 5A). The differentially regulated proteins are involved in mitochondrial functions, including the proteins in OxPhos and TCA cycle, ER and autophagy functions, cell proliferation, DNA repair, and DNA replication (Figure 5B). The proteins differentially regulated with Yashtimadhu choorna extract cotreatment are listed in Table 1 and heat map (Figure 5C).

**Yashtimadhu Regulates Pathways Essential for Neuronal Maintenance.** Protein dynamics play a crucial role in the regulation of several cellular pathways. From the pathway enrichment analysis using the Enrichr and Reactome tools, significant pathways were identified ( $p < 0.05$ ) and were

narrowed down to essential pathways, such as essential neuronal functions, metabolism of proteins, and metabolism of lipids. The proteins involved in these pathways are summarized in Table 2. Regulation of apoptosis, dopaminergic synapse, superoxide removal, mitochondrial functions, maintenance of myelin, axonal transport, and postsynaptic differentiation was enriched. In addition to this, the regulation of lipid and protein metabolism was also enriched.

**Yashtimadhu Prevents Mitochondrial Dysfunction.** Mitochondrial dysfunction is attributed to increased oxidative stress and loss of mitochondrial membrane potential and results in activation of the apoptotic cascade in neurons.<sup>41</sup> The mitochondrial OxPhos complex-III protein, cytochrome b-c1 complex subunit 6 (UQCRH), plays a vital role in ATP synthesis and maintenance of mitochondrial membrane potential. Gene expression analysis points to the reduction of UQCRH in the SNpc dopaminergic neurons of PD patients,<sup>42</sup> correlating with the observation from rotenone treatment, which was increased with Yashtimadhu choorna cotreatment. Yashtimadhu also restored ATP synthase inhibitory factor subunit 1 (ATPSIF1) and superoxide dismutase-1 (SOD1), which are reported to be downregulated with rotenone.<sup>43</sup> SOD1 quenches the reactive oxygen species (ROS) and maintaining redox balance, and ATPSIF1 inhibits mitochondrial ATP synthase, that is, complex-V and maintains the mitochondrial membrane potential.<sup>44,45</sup> The reduction in ATPSIF1 is implicated in mitochondrialopathies, while its overexpression confers neuroprotection.<sup>45,46</sup> Yashtimadhu

**Table 2. Cellular Pathways Regulated by Yashtimadhu**

pathway name	proteins
Neuronal Processes	
dopaminergic synapse	CALM3
axon guidance	SDC2; CLTB; CLTA; RPL37
transmission across chemical synapses	PRKARIA; CALM3
neurotransmitter receptors and postsynaptic signal transmission	PRKARIA; CALM3
long-term potentiation	CALM3
agrin in postsynaptic differentiation	CTTN
synaptic vesicle cycle	CLTB; CLTA
regulation of mitotic cell cycle	SKP1
regulation of cell cycle	NASP SKP1
mitochondrial transcription	SSB
ROS degradation	SOD1
apoptotic DNA fragmentation	HMGB2; HMGB1
Protein Metabolism	
protein metabolism	EIF4B; HSPE1; SRSF1; NACA; TBCA; SERPINA3; SKP1; RPL37; KLK11
translation initiation complex formation	EIF4B
cap-dependent translation initiation	RPL37; EIF4B
eukaryotic translation elongation and termination	RPL37
protein processing in the ER	SKP1
protein folding	TBCA
UPR	HDGF
activation of chaperones by IRE1 $\alpha$	HDGF
autophagy	HMGB1; PLCH1, CTLA, CTLB
neddylolation	DCUN1D3
Lipid Metabolism	
metabolism of lipids	PSAP; CYP51A1; AGPAT1
sphingolipid and glycosphingolipid metabolism	PSAP
phospholipid and glycerophospholipid metabolism	AGPAT1
CDP-diacylglycerol biosynthesis	AGPAT1
cholesterol biosynthesis	CYP51A1

also countered rotenone-induced increase of chaperonin, that is, heat shock protein-10 kDa (HSPE1) that helps in the folding of mitochondrial proteins.<sup>47</sup> Rotenone-mediated increase of HSPE1 is reported to be involved in caspase-3 activation and neuron death.<sup>48,49</sup> From these observations, it can be inferred that Yashtimadhu prevented cleaved caspase-3-mediated apoptosis by restoring the mitochondrial proteins involved in redox balance, membrane potential, and regulation of apoptosis.

**Yashtimadhu Restores Proteins Involved in Lipid Metabolism.** The differentially expressed proteins with Yashtimadhu choorna extract cotreatment were found to be involved in the metabolism of phospholipid, sphingolipid, cytidine diphosphate diacylglycerol (CDP-DAG), and cholesterol metabolism. The proteins enriched were cytochrome 1-acyl-*sn*-glycerol-3-phosphate acyltransferase 1 (AGPAT1), P450 family 51 subfamily A member 1, that is, lanosterol 14- $\alpha$  demethylase (CYP51A1), and prosaposin (PSAP). AGPAT1 is a lysophosphatidic acid acyltransferase that regulates phospholipid and triglyceride levels in the brain, while CYP51A1 is involved in cholesterol metabolism.<sup>50,51</sup>

Dysregulated lipid metabolism is associated with the cytoplasmic accumulations of SNCA with other proteins and lipids, leading to the formation of protein aggregates, that is, Lewy bodies in PD.<sup>52</sup> Lipidomic analysis of PD brains has demonstrated an increase in cholesterol metabolism and dysregulation of glycerophospholipid (CDP-DAG),<sup>53</sup> signifying the classification of PD as a lipidopathy.<sup>19</sup> The perturbations of lipid metabolism as a result of rotenone exposure in SHSY5Y cells have also been reported.<sup>54</sup> The restoration of the proteins regulating lipid metabolism highlights the protective effect of Yashtimadhu.

**Interplay between Protein Translation and Degradation Mechanisms by Yashtimadhu.** In our analysis, we also enriched the proteins involved in protein translation and degradation. ER plays a central role in protein dynamics in the cell, regulating the translation, protein folding, trafficking, and unfolded protein response (UPR).<sup>55</sup> Yashtimadhu restored ER proteins involved in translation and protein folding such as eukaryotic translation initiation factor (EIF4B) and translational regulator 60S ribosomal protein L37 (RPL37). Protein folding is a major determinant of its function, and with the accumulation of unfolded or misfolded proteins, oxidative stress and ER stress are induced. The ER stress results in the activation of UPR, which plays an essential role in PD.<sup>56,57</sup> In response to the accumulation of unfolded proteins, the UPR regulates signals that activate the protein degradation pathways, that is, autophagy and ubiquitin-proteasomal system (UPS).<sup>57,58</sup>

Autophagy is a bulk degradation mechanism that degrades proteins and damaged cell organelles. Autophagy initiation is controlled primarily by mammalian target of rapamycin (mTOR) and 5' AMP-activated protein kinase (AMPK), which in turn regulates the phosphorylation of ULK1/2.<sup>59,60</sup> UPS is involved in clearing protein aggregates, which is carried out by the 26s proteasomal system and is reported to act in close association with the autophagy mechanism.<sup>61,62</sup> Proteins that are tagged by the E3-ubiquitin ligases are selected for degradation.<sup>63</sup> Yashtimadhu regulated autophagy proteins such as 1-phosphatidylinositol-4,5-bisphosphate phosphodiesterase (PLCH1), clathrins (CTLA and CTLB), and high mobility group box 1 (HMGB1). E3-ligase-associated proteins, such as BTB/POZ domain-containing adapter for CUL3-mediated RhoA degradation (TNFAIP1), galectin-3 binding protein (LGALS3BP), and tripartite motif-containing 65 (TRIM65), were also restored by Yashtimadhu.

The enrichment analysis identified selective protein degradation pathways such as autophagy and neddylolation. Neddylolation is a degradation process similar to ubiquitination that involves the addition of a NEDD8, whose activation has been proven to be protective in PD.<sup>64</sup> Aggrephagy is a form of selective autophagy process that takes over the degradation of the accumulated proteins when the cellular UPS fails.<sup>65,66</sup> The dysregulation of the protein degradation mechanism leads to the accumulation of protein aggregates, which induce apoptosis as a result of oxidative and ER stress in PD. The regulation of the proteins involved in the translation and degradation processes makes Yashtimadhu an attractive candidate for neuroprotection.

**Regulation of Transcription Factors by Rotenone and Yashtimadhu.** We enriched the transcription factors (TFs) that control the expression of the differentially altered proteins to understand the regulation of expression at the level of transcription (Supporting Information Tables S2 and S3). The

Table 3. List of TFs Regulating the Rotenone- and Yashtimadhu-Induced Differentially Expressed Proteins

TF	no. of proteins, regulated by rotenone	no. of proteins, regulated by Yashtimadhu	representative proteins
SP1	64	39	NCL; CTTN; HMGB1; TPM3; PSAP; NASP; EIF4B; SOD1; HSPE1
KLF7	45	31	FUS; PTMS; PDCD5; CD59; CIRBP; GAA; EWSR1; UQCRH
SP4	39	21	HMGN2; HMGB2; SET; NUCKS1; CIRBP; ITGA3; CLTB
EGR1	37	20	NASP; EIF4B; SRSF1; FUS; MARCKSL1; OAT; NACA
NFYA	33	17	LRRC14; TAF15; PRKAR1A; C12orf57; CLTA; ZRANB2; XRR1
GABPA	27	16	TGOLN2; C12orf57; RPL37; CHCHD2; BICD2; C2orf49; BRD9
NRF1	22	15	PSAP; SSB; SRSF1; MARCKSL1; TBCA; PAGE5; PDCD5; GAA
YY1	22	15	CAPRIN1; TMSB4X; PRKAR1A; SRSF3; UQCRH; MORF4L1
ELK1	22	12	MT2A; TGOLN2; CLTA; RRP15; RPL37; CHCHD2; TNFAIP1
HNF4A	21	13	TPM3; HSPE1; FUS; HPCAL1; CALM3; SH3BGR1; CD59; ITGA3

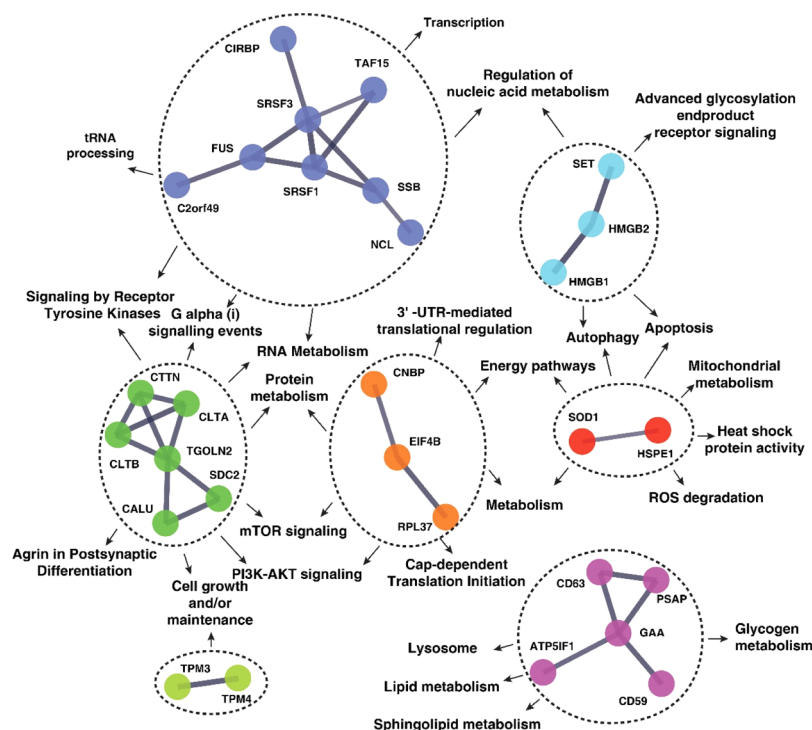


**Figure 6.** Molecular network of Yashtimadhu-mediated neuroprotection. The interaction network of Yashtimadhu-regulated proteins and interlinking pathways.

proteins altered by rotenone treatment were found to be regulated by 169 TFs. Similarly, the proteins restored by Yashtimadhu were found to be regulated by 149 TFs. A list of the top enriched TFs and the proteins regulated by them is displayed in Table 3, which includes specificity proteins-1 and 4 (SP1 and SP4), early growth response-1 (EGR1), nuclear respiratory factor-1 (NRF1), and Kruppel-like factor 7 (KLF7), to name a few. Some of the enriched TFs were previously reported to be dysregulated in PD pathogenesis, such as EGR1,<sup>67,68</sup> NRF1,<sup>69</sup> and ELK1.<sup>70</sup> These TFs were found to regulate proteins involved in autophagy, energy pathways, and metabolism of proteins and lipids. The findings show that Yashtimadhu helps in the regulation of TFs, which in turn restores the proteins impacted by rotenone.

**Molecular Network Involved in the Neuroprotective Functions of Yashtimadhu.** The functional significance of the proteins regulated by Yashtimadhu cotreatment and their cellular functions were established, and the protein–protein interaction (PPI) network was constructed with STRING

(confidence score  $\geq 0.7$ ). The PPI analysis showed the interactions between 31 out of the 84 proteins differentially regulated by Yashtimadhu (Supporting Information Table S4). We manually curated the molecular pathways that are governed by the 31 proteins and rebuilt the interaction network, highlighting the PPI and their interconnected pathways (Figure 6).

The pathways regulated by the PPI were maintenance of neuronal functions, protein translation, cellular signaling (receptor tyrosine kinases, G-protein signaling, PI3K-AKT, and mTOR signaling), ROS degradation, RNA metabolism, energy pathway, autophagy, and apoptosis regulation, while the proteins regulating lipid mechanism formed a unique cluster. The network provides a snapshot of the proteins and their functions, modulating the neuroprotective of Yashtimadhu, against the rotenone-induced *in vitro* model of PD.

**Validation of Neuroprotection Conferred by Yashtimadhu.** The MS-based analysis highlighted the proteins and pathways regulated by Yashtimadhu, which were predom-

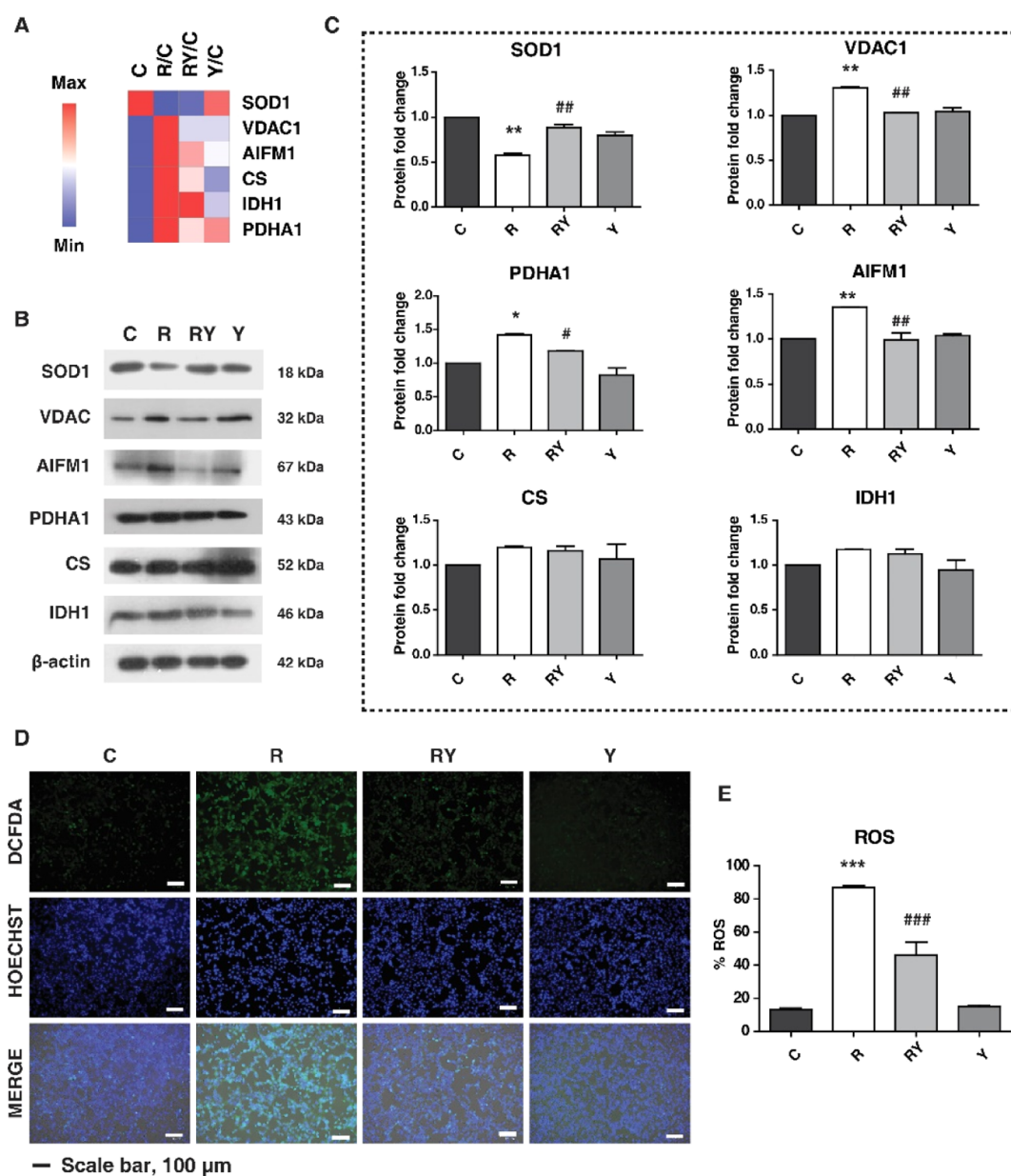


**Figure 7.** Validation of proteins and pathways regulated by Yashtimadhu. (A) Heat map showing the FC abundances of selected proteins from MS data, (B) immunoblotting analysis of proteins involved in mitochondrial health, (C) densitometry analysis showing the expression of the proteins, (D) cellular ROS staining using DCFDA (green) and counterstain HOECHST (blue), and (E) graphical representation of ROS production in the cells. \*, significant with respect to control; #, significant with respect to rotenone. \*,#,  $p \leq 0.05$ ; \*\*##,  $p \leq 0.01$ . Labels: C—untreated cells, R—rotenone treatment, RY—rotenone + Yashtimadhu choorna extract cotreatment, and Y—Yashtimadhu choorna extract treatment.

inantly involved in mitochondrial functions. As stated earlier, mitochondria regulate several cellular functions such as energy production (TCA and OxPhos), maintenance of cellular redox, and apoptosis. We validated some of the proteins and pathways regulated by Yashtimadhu, which are involved in mitochondrial homeostasis.

We selected enzymes that are involved in the regulation of cellular redox (SOD1), TCA cycle [pyruvate dehydrogenase E1 subunit  $\alpha$  1 (PDHA1), citrate synthase (CS), and isocitrate dehydrogenase 1 (IDH1)], and apoptosis [voltage-dependent anion-selective channel protein 1 (VDAC1) and apoptosis-inducing factor mitochondrial 1 (AIFM1)]. The abundance of these proteins from the MS-based proteomics is given in Figure 7A. Immunoblotting analysis correlated with the proteomics analysis and showed a decrease in SOD1 with

rotenone, which was subsequently restored by Yashtimadhu. PDHA1, AIFM1, and VDAC1 were also increased in rotenone that was restored by Yashtimadhu (Figure 7B,C). CS and IDH1 did not show significant changes in their expression patterns across the treatment conditions. VDAC is located on the mitochondrial outer membrane, forming channels for the transport of metabolites. It also plays a prime role in apoptosis by facilitating the release of proapoptotic proteins such as cytochrome-C and AIFM1, initiating apoptosis.<sup>71</sup> Rotenone-mediated increase in VDAC and AIFM1 suggests activation of apoptosis as a result of mitochondrial dysfunction, which is prevented by Yashtimadhu.

Rotenone-induced reduction in SOD1 levels was reported earlier, which also led to increased oxidative stress.<sup>43</sup> Our pathway analysis also pointed to the regulation of cellular ROS

degradation. We used 2',7'-DCFDA (2',7'-dichlorofluorescein diacetate) staining dye to observe the cellular ROS, which was increased with rotenone decreased with Yashtimadhu choorna extract cotreatment. Also, alteration in PDHA1 is implicated in ER stress before induction of mitochondrial dysfunction,<sup>72</sup> and an increase in PDHA1 is also associated with increased ROS production.<sup>73</sup> Our observations of ROS correlated with the reduced SOD1 levels with rotenone, indicating that the action of Yashtimadhu is by modulating SOD1 and PDHA1 levels and regulating cellular ROS degradation. The Yashtimadhu-mediated reduction in cellular ROS prevents cell death by preventing mitochondrial dysfunction and subsequent release of apoptotic factors.

## CONCLUSIONS

This study provides invaluable information on the neuroprotective properties of Yashtimadhu choorna against rotenone-induced PD model using quantitative proteomics. Yashtimadhu restored functions that are dysregulated in PD, such as mitochondrial function, ER health, protein, and lipid metabolism. The findings of this study enabled us to understand the proteins involved in rotenone-induced neurotoxicity that was counteracted by Yashtimadhu. Analysis of the restored proteins enabled the identification of molecular networks involved in the neuroprotective functions of Yashtimadhu. Validation of the proteins and pathways regulated by Yashtimadhu shows that it confers neuroprotection by the restoration of cellular redox potential and maintaining mitochondrial health, thereby preventing subsequent neuronal apoptosis. The identified proteins can be developed as molecular targets for neuroprotection against PD.

Our study opens new avenues in understanding and deciphering the molecular mechanisms of traditional medicine in combating neurodegenerative disorders. This omics-aided approach can be envisaged for molecularization of Indian Ayurvedic formulation-based therapeutic interventions.

## METHODS

**Reagent Procurement.** Rotenone (Cat# R8875), retinoic acid (Cat# R2625), collagen (Cat# C9791), thiazolyl blue tetrazolium bromide (MTT, Cat# M5655), bisBenzimide H 33342 (HOECHST, Cat# B2261), 2',7'-dichlorodihydrofluorescein (DCFDA, Cat# D6883), iodoacetamide (Cat# I6125), and DL-dithiothreitol (Cat# D9779) were procured from Sigma-Aldrich, St. Louis, USA. Dulbecco's modified Eagle medium (DMEM) high glucose (Cat#12100046), fetal bovine serum (FBS), and 100× antibiotic/antimycotic solution (Cat# 15240062) were purchased from Gibco. Pierce BCA protein estimation assay kit (Cat# 23225), Pierce Peptide estimation assay kit (Cat# 23275), and TMT 10plex kit (Cat# 90110) were procured from Thermo Fisher Scientific USA. Antibodies were purchased from Cell Signaling Technology, Danvers, USA, and Sigma-Aldrich, St. Louis, USA. Nitrocellulose membrane (Cat# 1620115) and Clarity ECL Substrate (Cat# 170-5061) were purchased from BioRad Laboratories, California, USA, and X-ray films from Carestream, USA. TPCK-treated trypsin (Cat# LS003741) was from Worthington Biochemical Corporation, USA. Solid-phase extraction disks, C-18 (Cat# 66883-U), and SCX (Cat# 66889-U) were procured from Empore, USA.

**Procurement of Yashtimadhu Choorna.** Yashtimadhu choorna (lot no.64) was procured from the SDP Remedies and

Research Centre, Puttur, Karnataka, India (<http://sdpayurveda.com/products/choorna/yastimadhu-choorna/>), a GMP-certified manufacturer of Ayurvedic formulations, and a specimen is maintained at the center with the identification number SDP/YM/001-2017. The industrial process includes shade-net drying and vacuum drum drying of Yashtimadhu roots, followed by pulverization of the dried roots and sieving, resulting in the fine powder, with a yield of 90%. Yashtimadhu choorna was procured, and the presence of lead molecules, glabridin (specific for *G. glabra*), glycyrrhizic acid, and licoricesaponin-G2 was confirmed using liquid chromatography–MS/MS (LC–MS/MS) analysis using QTRAP-6500, ABSCIEX. The compounds were identified based on the MS/MS fragment spectra, matched to the theoretical spectra generated using CFM-ID,<sup>74</sup> and detailed in [Supporting Information Table S5](#).

**Yashtimadhu Choorna Extract Preparation for Cell Culture Analysis.** Yashtimadhu choorna extract for cell culture treatment was prepared using an aqueous (water) extraction method. Yashtimadhu choorna, 1 g, was suspended in 10 mL of Milli-Q water (concentration, 0.1 g/mL) and incubated overnight at room temperature with continuous rotation. The extraction mixture was then centrifuged at 5000g for 10 min. The centrifugation was repeated for complete aspiration of the supernatant and transferred to a fresh tube. The aqueous extract was then dried using SpeedVac (Savant, Thermo Fisher Scientific, USA) and stored at  $-20\text{ }^{\circ}\text{C}$  until further use. The dried extract was resuspended in serum-free cell culture media before treatment.

**Cell Culture and Treatments.** IMR-32 cells (ATCC CCL-127) were procured from National Centre for Cell Science (NCCS), Pune, India. The cells were maintained in DMEM-high glucose supplemented with 10% FBS and 1× antibiotic/antimycotic solution and were incubated at  $37\text{ }^{\circ}\text{C}$  with 5%  $\text{CO}_2$ . Differentiation of cells was carried out in a collagen-coated 6-well plate, wherein the cells were seeded at a density of  $3 \times 10^4$  cells/well. The cells were treated with 10  $\mu\text{M}$  retinoic acid supplemented in 2% FBS-containing medium, for 9 days, for yielding a dopaminergic population. Differentiation was confirmed with TH expression ([Supporting Information Figure S1A,B](#)).

For MTT assay, 5000 cells/well were seeded in a 96-well plate and treated with different concentrations of rotenone (0.25, 0.5, 1, 10, 100, 200, 500, 1000, and 10000 nM) and Yashtimadhu choorna extract (50, 100, 200, 500, 1000, and 1500  $\mu\text{g}/\text{mL}$ ) for 48 h. MTT dye was added to the cells and incubated for 4 h. The resultant formazan crystals were dissolved using 50:50 of ethanol/dimethyl sulfoxide (DMSO) solution and read at 570 nm and background subtraction at 650 nm. Cell viability was calculated and represented as a percentage with respect to the untreated cells. The concentrations of rotenone and Yashtimadhu were determined from the results of the cytotoxicity assay. The differentiated cells were treated with (i) 100 nM rotenone (dissolved in DMSO), (ii) 200  $\mu\text{g}/\text{mL}$  Yashtimadhu choorna extract, and (iii) 100 nM rotenone + 200  $\mu\text{g}/\text{mL}$  Yashtimadhu choorna extract for 48 h, and untreated cells were taken as a control.

**Cell Staining Assays.** IMR-32 cells were seeded at  $1 \times 10^4$  cells/well in 12-well plates, differentiated, and treated with rotenone (100 nM), Yashtimadhu choorna extract (200  $\mu\text{g}/\text{mL}$ ), 100 nM rotenone + Yashtimadhu choorna extract cotreatment for 48 h. The untreated cells were taken as a control. Post-treatment, the medium was aspirated, and the

cells were washed with 1× phosphate-buffered saline (PBS) and treated with 20  $\mu\text{g}/\text{mL}$  of PI for dead cells and 5  $\mu\text{g}/\text{mL}$  of HOECHST as a counter nuclear stain in serum-free media for 15 min.<sup>75</sup> For staining of the intracellular ROS productions, the cells were stained with DCFDA post-treatment with rotenone, Yashtimadhu alone, and Yashtimadhu choorna extract cotreatment. The cells were washed with 1× PBS and stained with 25  $\mu\text{M}$  of DCFDA and 5  $\mu\text{g}/\text{mL}$  of HOECHST in serum-free media and stained for 15 min in the dark. Imaging was done with Zoe Imager, BioRad. The images were processed, and analysis of live–dead staining and ROS staining was measured using the ImageJ tool, NIH, USA.<sup>76</sup> Cell viability was calculated with respect to untreated cells, and % ROS was calculated with respect to nuclear counterstained cells.

**Immunoblotting Analysis.** IMR-32 cells were seeded at  $3 \times 10^4$  cells/well in collagen-coated 6-well plates and differentiated with retinoic acid. Rotenone (100 nM), Yashtimadhu choorna extract (200  $\mu\text{g}/\text{mL}$ ), and 100 nM of rotenone + Yashtimadhu choorna extract cotreatment was done for 48 h, while untreated cells were taken as a control. Post-treatment, the medium was removed, and the cells were washed with ice-cold 1× PBS. The cells were scraped and harvested in a lysis buffer containing 4% sodium dodecyl sulfate (SDS) in 50 mM triethylammonium bicarbonate (TEABC), with sodium orthovanadate (1 mM), sodium pyrophosphatase (2.5 mM), and beta-glycerophosphate (1 mM). The lysates were probe-sonicated on ice using Q-Sonica (Cole-Parmer, India) and heated at 95 °C on a dry bath for 10 min, followed by centrifugation at 12,000g for 20 min. The supernatant was aspirated into a new tube, and the protein concentration was estimated using the BCA protein estimation assay kit.

Immunoblotting was performed as described previously.<sup>77</sup> Briefly, an equal amount of protein was loaded across all treatments, electrophoretically resolved, and transferred onto the nitrocellulose membrane. The membranes were probed for the following proteins, with their dilution factors used for analysis, cleaved caspase-3 (1:1000), *p*-ERK1/2 (T202/Y204, 1:1000), TH (1:1000), SOD1 (1:1000), VDAC1 (1:1000), AIFM1 (1:1000), PDHA1 (1:1000), CS (1:1000), and IDH1 (1:1000), while  $\beta$ -actin (HRP-conjugated, 1:50,000) was used as a loading control. The blots were then incubated with the respective secondary antibodies (1:3000 dilution) and washed prior to imaging. Immunoreactive protein bands were visualized with Clarity ECL Substrate and captured onto X-ray films. The X-ray films were scanned, and densitometry analysis was carried out with ImageJ software, NIH, USA.<sup>76</sup> The area under the curve was used to calculate protein expression, normalized with  $\beta$ -actin, and expressed as FC with respect to control.

**Proteomics Sample Preparation.** IMR-32 cells were seeded at  $1 \times 10^5$  cells/plate in 10 cm collagen-coated plates and differentiated with retinoic acid. Differentiated IMR-32 cells were treated with rotenone (100 nM), rotenone (100 nM) + Yashtimadhu choorna extract (200  $\mu\text{g}/\text{mL}$ ) cotreatment, and Yashtimadhu choorna extract (200  $\mu\text{g}/\text{mL}$ ) alone. The untreated cells were taken as a control. The cells were treated as independent biological duplicates and harvested. Briefly, the cells were washed thrice in ice-cold 1× PBS and scraped-off with lysis buffer [4% SDS in 50 mM TEABC with sodium pyrophosphate (2.5 mM), sodium orthovanadate (1 mM), and  $\beta$ -glycerophosphate (1 mM)], and the lysate was prepared as mentioned above. Protein concentration was

estimated using the BCA assay, and the same was confirmed visually resolving on a 10% SDS-polyacrylamide gel electrophoresis (PAGE) gel. Based on the protein concentrations, 300  $\mu\text{g}$  of protein from each treatment was taken, reduced with dithiothreitol, and alkylated with iodoacetamide. The proteins were then precipitated with ice-cold acetone overnight at  $-20$  °C. Precipitated proteins were reconstituted in 50 mM of TEABC and digested with TPCK-trypsin overnight at a ratio of 1:20 of enzyme/protein at 37 °C.<sup>32</sup> Digestion efficiency was evaluated by resolving the samples on 10% SDS-PAGE. The peptides were dried overnight in SpeedVac and stored at  $-20$  °C until labeling.

**Tandem Mass Tag Labeling.** Peptide samples were reconstituted in 50 mM of TEABC, and their concentrations were estimated with the Pierce Peptide estimation kit. The peptide sample (50  $\mu\text{g}$ ) from each condition was used for labeling, with labels from the TMT 10plex kit. Peptides from the four different samples were labeled as follows: (i) untreated cells (C), (ii) 100 nM rotenone (R), (iii) 100 nM rotenone + 200  $\mu\text{g}/\text{mL}$  Yashtimadhu choorna extract (RY), and (iv) 200  $\mu\text{g}/\text{mL}$  Yashtimadhu choorna extract (Y), with four labels from the TMT 10plex kit, viz., 126 for C, 127N for R, 128C for RY, and 129N for Y. Both the biological replicates were independently labeled using the manufacturers' protocol. The TMT labels were reconstituted in anhydrous acetonitrile (ACN) and vortexed for dissolution. The respective TMT tags were added to both the replicates and incubated at room temperature for 1 h and quenched by adding 8  $\mu\text{L}$  of 5% hydroxylamine. The samples were pooled and dried overnight using SpeedVac. The dried samples were stored at  $-20$  °C until peptide fractionation.

**Peptide Fractionation and Clean-Up.** Peptide fractionation was carried out using a strong cation exchange (SCX) Stage Tip protocol as previously described.<sup>78</sup> Briefly, the SCX material was stacked onto 200  $\mu\text{L}$  tips and activated with 100% ACN, followed by equilibration with 2% trifluoroacetic acid (TFA). Peptides were reconstituted in 2% TFA and loaded onto the Stage Tips. The flow-through was passed twice, followed by washing with 0.2% TFA. Elution was carried out with different concentrations of ammonium acetate in ACN (50, 75, 125, 200, and 300 mM) into five separate fractions, and the sixth fraction was collected in 5% ammonium hydroxide with 80% ACN. The six fractions were collected in individual tubes and dried.

Peptide desalting was carried out with the C-18 Stage Tip method, as described previously.<sup>79</sup> The C-18 material was stacked onto 200  $\mu\text{L}$  tips, activated with 100% ACN, and equilibrated with 0.1% formic acid. Fractionated peptide samples were reconstituted in 0.1% formic acid and loaded onto the C-18 material, and the flow-through was passed twice, followed by washing with 0.1% formic acid and elution with 40% ACN in 0.1% formic acid. The dried fractions were stored at  $-20$  °C until MS analysis.

**LC–MS/MS Analysis.** LC–MS/MS analysis was carried out using an Orbitrap Fusion Tribrid mass spectrometer (Thermo Fisher Scientific, Bremen, Germany) coupled with an Easy-nl C1200 nanoflow UHPLC (Thermo Scientific, Odense, Denmark). The fractionated and dried peptides were reconstituted using 0.1% formic acid and introduced into the nanoViper trap column (75  $\mu\text{m} \times 2$  cm and 3  $\mu\text{m}$ , C18) (Thermo Fisher Scientific). Peptides were resolved on an EASY-Spray C18 Column (75  $\mu\text{m} \times 50$  cm, 275  $\mu\text{m}$ , 100 Å) maintained at a temperature of 40 °C. A gradient of 5–35%



solvent B (0.1% formic acid in 80% ACN) at a flow rate of 300 nL/min for 110 min was used for peptide resolution. A total run time of 140 min, inclusive of the column conditioning and sample loading, was used for the LC–MS/MS analysis.

The data-dependent acquisition was carried out within a mass range of 400–1600  $m/z$  in the Orbitrap mass analyzer at a resolution of 120,000 at 200  $m/z$ . Most intense precursor ions were selected for MS/MS fragmentation at a top speed data-dependent mode with a maximum cycle time of 3 s. Higher collision energy dissociation (HCD) fragmentation mode with a normalized collision energy of 35% was used in a scan range of 400–1600  $m/z$  at a resolution of 60,000 at 200  $m/z$  using the Orbitrap mass analyzer. Peptide charge states were set to 2–6, and a dynamic exclusion at 30 s, with a 10 ppm mass window, was used. Data acquisition was carried out in technical triplicates for both the biological replicates.

**Database Search for Peptide and Protein Identification.** MS raw data files were processed using Proteome Discoverer, version 2.2 (Thermo Fisher Scientific, Bremen, Germany). The data were searched against the human protein database RefSeq109 along with known contaminants (containing 81,096 entries and 116 contaminants), using SequestHT and MASCOT search algorithms. The search parameters were used as follows: a minimum peptide length of seven amino acids, with trypsin as the proteolytic enzyme and one missed cleavage. Precursor and fragment level mass tolerances were set at 10 ppm and 0.05 Da, respectively. TMT-modification at the peptide N-terminus and lysine residues and carbamidomethylation of cysteine were set as fixed modifications. Oxidation of methionine, protein N-terminal acetylation, was set as a dynamic modification. The percolator node in the consensus workflow was used to compute the false discovery rate (FDR), applied at 1% at the peptide and PSM level. Data normalization was carried out on the total peptide amount using Proteome Discoverer.

**Data Analysis.** The results file from Proteome Discoverer was used for further analysis. Perseus<sup>80</sup> was used for PCA, computing the FC, and its respective logarithmic value at base-2 ( $\log_2$  FC), which was used for calculating the  $p$ -value and Benjamini–Hochberg FDR-corrected  $p$ -value, that is, the  $q$ -value. Morpheus, Broad Institute (<https://software.broadinstitute.org/morpheus/>), was used for generating heat maps. Sankey diagram was generated using an online Sankey generator (<http://sankey-diagram-generator.acquireprocure.com/>). Proteins were classified and categorized based on Gene Ontology analysis using FunRich<sup>81</sup> and pathway analysis using Enrichr (<https://amp.pharm.mssm.edu/Enrichr/>)<sup>82</sup> and Reactome<sup>83</sup> online tools. The proteins identified were also classified based on comparison with databases such as MitoCarta, version 2.0,<sup>84</sup> The Autophagy Database,<sup>85</sup> and the E3-ligases Database.<sup>63</sup> PPI network analysis was carried out with STRING.<sup>86</sup>

**Data Records.** The MS raw data and the Proteome Discoverer-searched data were submitted to the ProteomeXchange Consortium (<http://proteomecentral.proteomexchange.org>) via the PRIDE repository<sup>87</sup> with the data set identifier PXD019672.

## ■ ASSOCIATED CONTENT

### SI Supporting Information

The Supporting Information is available free of charge at <https://pubs.acs.org/doi/10.1021/acsomega.0c03420>.

Western blotting analysis showing the expression of TH after differentiation with retinoic acid treatment, bar graph showing the densitometry analysis of tyrosine hydroxylase expression, cell cytotoxicity analysis with different concentrations of rotenone at 24 and 48 h, and cell cytotoxicity analysis with different concentrations of Yashtimadhu choorna extract at 48 h; list of proteins identified and their respective abundances; identification of transcription factors regulating proteins differentially expressed with rotenone; identification of transcription factors regulating proteins differentially expressed with Yashtimadhu choorna extract cotreatment; PPI analysis using STRING; and lead metabolites identified in Yashtimadhu choorna (PDF)

## ■ AUTHOR INFORMATION

### Corresponding Authors

**Prashant Kumar Modi** – Center for Systems Biology and Molecular Medicine, Yenepoya Research Centre, Yenepoya (Deemed to be University), Mangalore 575018, India; Email: [prashantmodi@yenepoya.edu.in](mailto:prashantmodi@yenepoya.edu.in)

**Thottethodi Subrahmanya Keshava Prasad** – Center for Systems Biology and Molecular Medicine, Yenepoya Research Centre, Yenepoya (Deemed to be University), Mangalore 575018, India; [orcid.org/0000-0002-6206-2384](https://orcid.org/0000-0002-6206-2384); Email: [keshav@yenepoya.edu.in](mailto:keshav@yenepoya.edu.in)

### Authors

**Gayathree Karthikkeyan** – Center for Systems Biology and Molecular Medicine, Yenepoya Research Centre, Yenepoya (Deemed to be University), Mangalore 575018, India

**Mohd. Altaf Najar** – Center for Systems Biology and Molecular Medicine, Yenepoya Research Centre, Yenepoya (Deemed to be University), Mangalore 575018, India

**Ravishankar Pervaje** – Sushrutha Ayurveda Hospital, Puttur 574201, India

**Sameera Krishna Pervaje** – Yenepoya Medical College, Yenepoya (Deemed to be University), Mangalore 575018, India

Complete contact information is available at: <https://pubs.acs.org/doi/10.1021/acsomega.0c03420>

### Author Contributions

T.S.K.P., R.P., and P.K.M. conceived the idea and designed and planned the experiments. G.K. performed the experiments, sample preparation, data analysis, drafting of the manuscript, and preparation of figures. M.A.N. performed the mass spectrometry data acquisition and participated in data analysis. S.K.P. participated in data analysis. R.P., a practicing Ayurveda clinician, procured the samples and authentically confirmed them. T.S.K.P. and P.K.M. critically reviewed and edited the manuscript. All authors read and approved the final version of the manuscript.

### Notes

The authors declare no competing financial interest.

## ■ ACKNOWLEDGMENTS

The authors thank Karnataka Biotechnology and Information Technology Services (KBITS), Government of Karnataka, for support to the Center for Systems Biology and Molecular Medicine at Yenepoya (Deemed to be University), Mangalore, under the Biotechnology Skill Enhancement Programme in Multiomics Technology (BiSEP GO ITD 02MDA2017). The

authors thank Yenepoya (Deemed to be University) for access to instrumentation and providing financial assistance as a seed grant (YU/Seed grant/077-2019). G.K. was a recipient of Senior Research Fellowship from the Council of Scientific & Industrial Research (CSIR), Government of India (2014-2019), and is currently a recipient of KSTePs DST-Ph.D. Fellowship from Department of Science and Technology-Karnataka Science and Technology Promotion Society, Government of Karnataka (2020-2021). M.A.N. is a recipient of Senior Research Fellowship from the University Grants Commission, Government of India.

## ABBREVIATIONS

PD	Parkinson's disease
ERK-1/2	extra cellular signal-regulated kinase-1/2
ER	endoplasmic reticulum
SNPc	substantia nigra pars compacta
SNCA	$\alpha$ -synuclein
PARK	parkin
LRRK	leucine-rich repeat kinases
MPTP	1-methyl-4-phenyl-1,2,3,6-tetrahydropyridine
cl_Cas3	cleaved caspase-3
TH	tyrosine hydroxylase
SOD1	superoxide dismutase 1
PHDA1	pyruvate dehydrogenase E1 subunit $\alpha$ 1
CS	citrate synthase
IDH1	isocitrate dehydrogenase 1
VDAC1	voltage-dependent anion-selective channel protein 1
AIFM1	apoptosis-inducing factor mitochondrial 1
OxPhos	oxidative phosphorylation
TCA	tricarboxylic acid
CDP-DAG	cytidine diphosphate diacylglycerol
UPR	unfolded protein response
ROS	reactive oxygen species
DCFDA	2',7'-dichlorodihydrofluorescein
TF	transcription factors
FC	fold change
FDR	false discovery rate
TMT	tandem mass tags
HCD	higher collision energy dissociation
LC	liquid chromatography
MS	mass spectrometry
MS/MS	tandem mass spectrometry
ACN	acetonitrile

## REFERENCES

(1) Poewe, W.; Seppi, K.; Tanner, C. M.; Halliday, G. M.; Brundin, P.; Volkman, J.; Schrag, A. E.; Lang, A. E. Parkinson disease. *Nat. Rev. Dis. Primers* **2017**, *3*, 17013.

(2) Fujita, K. A.; Ostaszewski, M.; Matsuo, Y.; Ghosh, S.; Glaab, E.; Trefois, C.; Crespo, I.; Perumal, T. M.; Jurkowski, W.; Antony, P. M. A.; Diederich, N.; Buttini, M.; Kodama, A.; Satagopam, V. P.; Eifes, S.; Del Sol, A.; Schneider, R.; Kitano, H.; Balling, R. Integrating pathways of Parkinson's disease in a molecular interaction map. *Mol. Neurobiol.* **2014**, *49*, 88–102.

(3) Maiti, P.; Manna, J.; Dunbar, G. L. Current understanding of the molecular mechanisms in Parkinson's disease: Targets for potential treatments. *Transl. Neurodegener.* **2017**, *6*, 28.

(4) Chotibut, T.; Meadows, S.; Kasanga, E. A.; McInnis, T.; Cantu, M. A.; Bishop, C.; Salvatore, M. F. Ceftriaxone reduces L-dopa-induced dyskinesia severity in 6-hydroxydopamine parkinson's disease model. *Mov. Disord.* **2017**, *32*, 1547–1556.

(5) Ghaffari, B. D.; Kluger, B. Mechanisms for alternative treatments in Parkinson's disease: acupuncture, tai chi, and other treatments. *Curr. Neurol. Neurosci. Rep.* **2014**, *14*, 451.

(6) Das, D.; Chandola, H.; Agarwal, S. Protective effect of Yashtimadhu (*Glycyrrhiza glabra*) against side effects of radiation/chemotherapy in head and neck malignancies. *Ayu* **2011**, *32*, 196–199.

(7) Payyappallimana, U.; Venkatasubramanian, P. Exploring Ayurvedic Knowledge on Food and Health for Providing Innovative Solutions to Contemporary Healthcare. *Front. Public Health* **2016**, *4*, 57.

(8) Kulkarni, R.; Girish, K.; Kumar, A. Nootropic herbs (Medhya Rasayana) in Ayurveda: An update. *Pharmacogn. Rev.* **2012**, *6*, 147–153.

(9) Singh, R. H.; Narsimhamurthy, K.; Singh, G. Neuronutrient impact of Ayurvedic Rasayana therapy in brain aging. *Biogerontology* **2008**, *9*, 369–374.

(10) Kumar, V. Potential medicinal plants for CNS disorders: an overview. *Phytother. Res.* **2006**, *20*, 1023–1035.

(11) Sarokte, A. S.; Rao, M. V. Effects of Medhya Rasayana and Yogic practices in improvement of short-term memory among school-going children. *Ayu* **2013**, *34*, 383–389.

(12) Hosseinzadeh, H.; Nassiri-Asl, M. Pharmacological Effects of *Glycyrrhiza* spp. and Its Bioactive Constituents: Update and Review. *Phytother. Res.* **2015**, *29*, 1868–1886.

(13) Hwang, I.-k.; Lim, S.-s.; Choi, K.-h.; Yoo, K.-y.; Shin, H.-k.; Kim, E.-j.; Yoon-Park, J.-h.; Kang, T.-c.; Kim, Y.-s.; Kwon, D.-y.; Kim, D.-w.; Moon, W.-k.; Won, M.-h. Neuroprotective effects of roasted licorice, not raw form, on neuronal injury in gerbil hippocampus after transient forebrain ischemia. *Acta Pharmacol. Sin.* **2006**, *27*, 959–965.

(14) Shen, B.; Truong, J.; Helliwell, R.; Govindaraghavan, S.; Sucher, N. J. An in vitro study of neuroprotective properties of traditional Chinese herbal medicines thought to promote healthy ageing and longevity. *BMC Complementary Altern. Med.* **2013**, *13*, 373.

(15) Yu, X.-Y.; Lin, S.-G.; Zhou, Z.-W.; Chen, X.; Liang, J.; Yu, X.-Q.; Chowbay, B.; Wen, J.-Y.; Duan, W.; Chan, E.; Li, X.-T.; Cao, J.; Li, C.-G.; Xue, C. C.; Zhou, S.-F. Role of P-glycoprotein in limiting the brain penetration of glabridin, an active isoflavan from the root of *Glycyrrhiza glabra*. *Pharm. Res.* **2007**, *24*, 1668–1690.

(16) Dhingra, D.; Sharma, A. Antidepressant-like activity of *Glycyrrhiza glabra* L. in mouse models of immobility tests. *Prog. Neuro-Psychopharmacol. Biol. Psychiatry* **2006**, *30*, 449–454.

(17) Martins, N.; Dueñas, L.; Santos-Buelga, C.; Ferreira, I. C. F. R. Characterization of phenolic compounds and antioxidant properties of *Glycyrrhiza glabra* L. rhizomes and roots. *RSC Adv.* **2015**, *5*, 26991–26997.

(18) Sheshagiri, S.; Patel, K.; Rajagopala, S. Randomized placebo-controlled clinical study on enhancement of Medha (intelligence quotient) in school going children with Yashtimadhu granules. *Ayu* **2015**, *36*, 56–62.

(19) Fanning, S.; Selkoe, D.; Dettmer, U. Parkinson's disease: proteinopathy or lipidopathy? *npj Parkinson's Dis.* **2020**, *6*, 3.

(20) Ganguly, G.; Chakrabarti, S.; Chatterjee, U.; Saso, L. Proteinopathy, oxidative stress and mitochondrial dysfunction: cross talk in Alzheimer's disease and Parkinson's disease. *Drug Des. Dev. Ther.* **2017**, *11*, 797–810.

(21) Konnova, E. A.; Swanberg, M. Animal Models of Parkinson's Disease. In *Parkinson's Disease: Pathogenesis and Clinical Aspects*; Stoker, T. B., Greenland, J. C., Eds.; Codon Publications: Brisbane, AU, 2018.

(22) Raza, C.; Anjum, R.; Shakeel, N. U. A. Parkinson's disease: Mechanisms, translational models and management strategies. *Life Sci.* **2019**, *226*, 77–90.

(23) Falkenburger, B. H.; Saridaki, T.; Dinter, E. Cellular models for Parkinson's disease. *J. Neurochem.* **2016**, *139*, 121–130.

(24) Ferrari, E.; Cardinale, A.; Picconi, B.; Gardoni, F. From cell lines to pluripotent stem cells for modelling Parkinson's Disease. *J. Neurosci. Methods* **2020**, *340*, 108741.

- (25) Li, N.; Ragheb, K.; Lawler, G.; Sturgis, J.; Rajwa, B.; Melendez, J. A.; Robinson, J. P. Mitochondrial complex I inhibitor rotenone induces apoptosis through enhancing mitochondrial reactive oxygen species production. *J. Biol. Chem.* **2003**, *278*, 8516–8525.
- (26) Ikram, F.; Ackermann, S.; Kahlert, Y.; Volland, R.; Roels, F.; Engesser, A.; Hertwig, F.; Kocak, H.; Hero, B.; Drexler, D.; Henrich, K.-O.; Berthold, F.; Nürnberg, P.; Westermann, F.; Fischer, M. Transcription factor activating protein 2 beta (TFAP2B) mediates noradrenergic neuronal differentiation in neuroblastoma. *Mol. Oncol.* **2016**, *10*, 344–359.
- (27) Kotapalli, S. S.; Dasari, C.; Duscharla, D.; Kami Reddy, K. R.; Kasula, M.; Ummanni, R. All-Trans-Retinoic Acid Stimulates Overexpression of Tumor Protein D52 (TPD52, Isoform 3) and Neuronal Differentiation of IMR-32 Cells. *J. Cell. Biochem.* **2017**, *118*, 4358–4369.
- (28) Chaudhari, N.; Talwar, P.; Lefebvre D'hellencourt, C.; Ravanan, P. CDDO and ATRA Instigate Differentiation of IMR32 Human Neuroblastoma Cells. *Front. Mol. Neurosci.* **2017**, *10*, 310.
- (29) Sai, Y.; Chen, J.; Wu, Q.; Liu, H.; Zhao, J.; Dong, Z. Phosphorylated-ERK 1/2 and neuronal degeneration induced by rotenone in the hippocampus neurons. *Environ. Toxicol. Pharmacol.* **2009**, *27*, 366–372.
- (30) Song, J.-X.; Choi, M. Y.-M.; Wong, K. C.-K.; Chung, W. W.-Y.; Sze, S. C.-W.; Ng, T.-B.; Zhang, K. Y.-B. Baicalein antagonizes rotenone-induced apoptosis in dopaminergic SH-SY5Y cells related to Parkinsonism. *Chin. Med.* **2012**, *7*, 1.
- (31) Thomas, S. N.; Friedrich, B.; Schnaubelt, M.; Chan, D. W.; Zhang, H.; Aebbersold, R. Orthogonal Proteomic Platforms and Their Implications for the Stable Classification of High-Grade Serous Ovarian Cancer Subtypes. *iScience* **2020**, *23*, 101079.
- (32) Kumar, S.; Kumar, M.; Ekka, R.; Dvorin, J. D.; Paul, A. S.; Madugundu, A. K.; Gilberger, T.; Gowda, H.; Duraisingh, M. T.; Keshava Prasad, T. S.; Sharma, P. PfCDPK1 mediated signaling in erythrocytic stages of Plasmodium falciparum. *Nat. Commun.* **2017**, *8*, 63.
- (33) Saul, M. J.; Hegewald, A. B.; Emmerich, A. C.; Ossipova, E.; Vogel, M.; Baumann, I.; Kultima, K.; Lenggqvist, J.; Steinhilber, D.; Jakobsson, P. J. Mass Spectrometry-Based Proteomics Approach Characterizes the Dual Functionality of miR-328 in Monocytes. *Front. Pharmacol.* **2019**, *10*, 640.
- (34) Cheng, Y.; Sun, D.; Zhu, B.; Zhou, W.; Lv, C.; Kou, F.; Wei, H. Integrative metabolic and proteomic profiling of brainstem in spontaneously hypertensive rats. *J. Proteome Res.* **2020**
- (35) Hung, C.-W.; Klein, T.; Cassidy, L.; Linke, D.; Lange, S.; Anders, U.; Bureik, M.; Heinzel, E.; Schneider, K.; Tholey, A. Comparative Proteome Analysis in Schizosaccharomyces pombe Identifies Metabolic Targets to Improve Protein Production and Secretion. *Mol. Cell. Proteomics* **2016**, *15*, 3090–3106.
- (36) Valdinocci, D.; Simoes, R. F.; Kovarova, J.; Cunha-Oliveira, T.; Neuzil, J.; Pountney, D. L. Intracellular and Intercellular Mitochondrial Dynamics in Parkinson's Disease. *Front. Neurosci.* **2019**, *13*, 930.
- (37) Colla, E. Linking the Endoplasmic Reticulum to Parkinson's Disease and Alpha-Synucleinopathy. *Front. Neurosci.* **2019**, *13*, 560.
- (38) González-Casacuberta, I.; Juárez-Flores, D. L.; Moren, C.; Garrabou, G. Bioenergetics and Autophagic Imbalance in Patients-Derived Cell Models of Parkinson Disease Supports Systemic Dysfunction in Neurodegeneration. *Front. Neurosci.* **2019**, *13*, 894.
- (39) Mader, B. J.; Pivtoraiko, V. N.; Flippo, H. M.; Klocke, B. J.; Roth, K. A.; Mangieri, L. R.; Shacka, J. J. Rotenone inhibits autophagic flux prior to inducing cell death. *ACS Chem. Neurosci.* **2012**, *3*, 1063–1072.
- (40) Goswami, P.; Gupta, S.; Biswas, J.; Sharma, S.; Singh, S. Endoplasmic Reticulum Stress Instigates the Rotenone Induced Oxidative Apoptotic Neuronal Death: a Study in Rat Brain. *Mol. Neurobiol.* **2016**, *53*, 5384–5400.
- (41) Satoh, T.; Enokido, Y.; Aoshima, H.; Uchiyama, Y.; Hatanaka, H. Changes in mitochondrial membrane potential during oxidative stress-induced apoptosis in PC12 cells. *J. Neurosci. Res.* **1997**, *50*, 413–420.
- (42) Simunovic, F.; Yi, M.; Wang, Y.; Macey, L.; Brown, L. T.; Krichevsky, A. M.; Andersen, S. L.; Stephens, R. M.; Benes, F. M.; Sonntag, K. C. Gene expression profiling of substantia nigra dopamine neurons: further insights into Parkinson's disease pathology. *Brain* **2009**, *132*, 1795–1809.
- (43) Doktor, B.; Damulewicz, M.; Pyza, E. Overexpression of Mitochondrial Ligases Reverses Rotenone-Induced Effects in a Drosophila Model of Parkinson's Disease. *Front. Neurosci.* **2019**, *13*, 94.
- (44) García-Aguilar, A.; Cuezva, J. M. A Review of the Inhibition of the Mitochondrial ATP Synthase by IF1 in vivo: Reprogramming Energy Metabolism and Inducing Mitohormesis. *Front. Physiol.* **2018**, *9*, 1322.
- (45) Shah, D. I.; Takahashi-Makise, N.; Cooney, J. D.; Li, L.; Schultz, I. J.; Pierce, E. L.; Narla, A.; Seguin, A.; Hattangadi, S. M.; Medlock, A. E.; Langer, N. B.; Dailey, T. A.; Hurst, S. N.; Faccenda, D.; Wiwczar, J. M.; Heggors, S. K.; Vogin, G.; Chen, W.; Chen, C.; Campagna, D. R.; Brugnara, C.; Zhou, Y.; Ebert, B. L.; Danial, N. N.; Fleming, M. D.; Ward, D. M.; Campanella, M.; Dailey, H. A.; Kaplan, J.; Paw, B. H. Mitochondrial Atf1f1 regulates haem synthesis in developing erythroblasts. *Nature* **2012**, *491*, 608–612.
- (46) Formentini, L.; Sánchez-Aragó, M.; Sánchez-Cenizo, L.; Cuezva, J. M. The mitochondrial ATPase inhibitory factor 1 triggers a ROS-mediated retrograde pro-survival and proliferative response. *Mol. Cell* **2012**, *45*, 731–742.
- (47) Bie, A. S.; Fernandez-Guerra, P.; Birkler, R. I.; Nisemblat, S.; Pelena, D.; Lu, X.; Deignan, J. L.; Lee, H.; Dorrani, N.; Corydon, T. J.; Palmfeldt, J.; Bivina, L.; Azem, A.; Herman, K.; Bross, P. Effects of a Mutation in the HSPE1 Gene Encoding the Mitochondrial Co-chaperonin HSP10 and Its Potential Association with a Neurological and Developmental Disorder. *Front. Mol. Biosci.* **2016**, *3*, 65.
- (48) Kennedy, D.; Jäger, R.; Mosser, D. D.; Samali, A. Regulation of apoptosis by heat shock proteins. *IUBMB Life* **2014**, *66*, 327–338.
- (49) Samali, A.; Cai, J.; Zhivotovskiy, B.; Jones, D. P.; Orrenius, S. Presence of a pre-apoptotic complex of pro-caspase-3, Hsp60 and Hsp10 in the mitochondrial fraction of jurkat cells. *EMBO J.* **1999**, *18*, 2040–2048.
- (50) Bradley, R. M.; Marvyn, P. M.; Aristizabal Henao, J. J.; Mardian, E. B.; George, S.; Aucoin, M. G.; Stark, K. D.; Duncan, R. E. Acylglycerophosphate acyltransferase 4 (AGPAT4) is a mitochondrial lysophosphatidic acid acyltransferase that regulates brain phosphatidylcholine, phosphatidylethanolamine, and phosphatidylinositol levels. *Biochim. Biophys. Acta, Mol. Cell Biol. Lipids* **2015**, *1851*, 1566–1576.
- (51) Takeuchi, K.; Reue, K. Biochemistry, physiology, and genetics of GPAT, AGPAT, and lipin enzymes in triglyceride synthesis. *Am. J. Physiol. Endocrinol. Metab.* **2009**, *296*, E1195–E1209.
- (52) Alecu, I.; Bennett, S. A. L. Dysregulated Lipid Metabolism and Its Role in alpha-Synucleinopathy in Parkinson's Disease. *Front. Neurosci.* **2019**, *13*, 328.
- (53) Cheng, D.; Jenner, A. M.; Shui, G.; Cheong, W. F.; Mitchell, T. W.; Nealon, J. R.; Kim, W. S.; McCann, H.; Wenk, M. R.; Halliday, G. M.; Garner, B. Lipid pathway alterations in Parkinson's disease primary visual cortex. *PLoS One* **2011**, *6*, No. e17299.
- (54) Worth, A. J.; Basu, S. S.; Snyder, N. W.; Mesaros, C.; Blair, I. A. Inhibition of neuronal cell mitochondrial complex I with rotenone increases lipid beta-oxidation, supporting acetyl-coenzyme A levels. *J. Biol. Chem.* **2014**, *289*, 26895–26903.
- (55) Schwarz, D. S.; Blower, M. D. The endoplasmic reticulum: structure, function and response to cellular signaling. *Cell. Mol. Life Sci.* **2016**, *73*, 79–94.
- (56) Walter, P.; Ron, D. The unfolded protein response: from stress pathway to homeostatic regulation. *Science* **2011**, *334*, 1081–1086.
- (57) Matus, S.; Lisbona, F.; Torres, M.; Leon, C.; Thielen, P.; Hetz, C. The stress rheostat: an interplay between the unfolded protein response (UPR) and autophagy in neurodegeneration. *Curr. Mol. Med.* **2008**, *8*, 157–172.
- (58) Li, H.; Chen, Q.; Liu, F.; Zhang, X.; Li, W.; Liu, S.; Zhao, Y.; Gong, Y.; Yan, C. Unfolded protein response and activated

degradative pathways regulation in GNE myopathy. *PLoS One* **2013**, *8*, No. e58116.

(59) Dunlop, E. A.; Hunt, D. K.; Acosta-Jaquez, H. A.; Fingar, D. C.; Tee, A. R. ULK1 inhibits mTORC1 signaling, promotes multisite Raptor phosphorylation and hinders substrate binding. *Autophagy* **2011**, *7*, 737–747.

(60) Kim, J.; Kundu, M.; Viollet, B.; Guan, K.-L. AMPK and mTOR regulate autophagy through direct phosphorylation of Ulk1. *Nat. Cell Biol.* **2011**, *13*, 132–141.

(61) Cohen-Kaplan, V.; Livneh, I.; Avni, N.; Fabre, B.; Ziv, T.; Kwon, Y. T.; Ciechanover, A. p62- and ubiquitin-dependent stress-induced autophagy of the mammalian 26S proteasome. *Proc. Natl. Acad. Sci. U.S.A.* **2016**, *113*, E7490–E7499.

(62) Kocaturk, N. M.; Gozuacik, D. Crosstalk Between Mammalian Autophagy and the Ubiquitin-Proteasome System. *Front. Cell. Dev. Biol.* **2018**, *6*, 128.

(63) Medvar, B.; Raghuram, V.; Pisitkun, T.; Sarkar, A.; Knepper, M. A. Comprehensive database of human E3 ubiquitin ligases: application to aquaporin-2 regulation. *Physiol. Genom.* **2016**, *48*, 502–512.

(64) Choo, Y. S.; Vogler, G.; Wang, D.; Kalvakuri, S.; Iliuk, A.; Tao, W. A.; Bodmer, R.; Zhang, Z. Regulation of parkin and PINK1 by neddylation. *Hum. Mol. Genet.* **2012**, *21*, 2514–2523.

(65) Lamark, T.; Johansen, T. Aggrephagy: selective disposal of protein aggregates by macroautophagy. *Int. J. Cell Biol.* **2012**, *2012*, 736905.

(66) Lim, J.; Yue, Z. Neuronal aggregates: formation, clearance, and spreading. *Dev. Cell* **2015**, *32*, 491–501.

(67) Yu, Q.; Huang, Q.; Du, X.; Xu, S.; Li, M.; Ma, S. Early activation of Egr-1 promotes neuroinflammation and dopaminergic neurodegeneration in an experimental model of Parkinson's disease. *Exp. Neurol.* **2018**, *302*, 145–154.

(68) Xie, B.; Wang, C.; Zheng, Z.; Song, B.; Ma, C.; Thiel, G.; Li, M. Egr-1 transactivates Bim gene expression to promote neuronal apoptosis. *J. Neurosci.* **2011**, *31*, 5032–5044.

(69) Zhang, X.; Du, L.; Zhang, W.; Yang, Y.; Zhou, Q.; Du, G. Therapeutic effects of baicalein on rotenone-induced Parkinson's disease through protecting mitochondrial function and biogenesis. *Sci. Rep.* **2017**, *7*, 9968.

(70) Iwata, A.; Miura, S.; Kanazawa, I.; Sawada, M.; Nukina, N. alpha-Synuclein forms a complex with transcription factor Elk-1. *J. Neurochem.* **2001**, *77*, 239–252.

(71) Shoshan-Barmatz, V.; De Pinto, V.; Zweckstetter, M.; Raviv, Z.; Keinan, N.; Arbel, N. VDAC, a multi-functional mitochondrial protein regulating cell life and death. *Mol. Aspect. Med.* **2010**, *31*, 227–285.

(72) Kemter, E.; Frohlich, T.; Arnold, G. J.; Wolf, E.; Wanke, R. Mitochondrial Dysregulation Secondary to Endoplasmic Reticulum Stress in Autosomal Dominant Tubulointerstitial Kidney Disease - UMOD (ADTKD-UMOD). *Sci. Rep.* **2017**, *7*, 42970.

(73) Yang, Z.; Wang, Y.; Zhang, Y.; He, X.; Zhong, C.-Q.; Ni, H.; Chen, X.; Liang, Y.; Wu, J.; Zhao, S.; Zhou, D.; Han, J. RIP3 targets pyruvate dehydrogenase complex to increase aerobic respiration in TNF-induced necroptosis. *Nat. Cell Biol.* **2018**, *20*, 186–197.

(74) Djoumbou-Feunang, Y.; Pon, A.; Karu, N.; Zheng, J.; Li, C.; Arndt, D.; Gautam, M.; Allen, F.; Wishart, D. S. CFM-ID 3.0: Significantly Improved ESI-MS/MS Prediction and Compound Identification. *Metabolites* **2019**, *9*, 72.

(75) Bose, B.; Kapoor, S.; Sen, U.; Nihad As, M.; Chaudhury, D.; Shenoy, S. Assessment of Oxidative Damage in the Primary Mouse Ocular Surface Cells/Stem Cells in Response to Ultraviolet-C (UV-C) Damage. *J. Vis. Exp.* **2020**, *156*, No. e59924.

(76) Schneider, C. A.; Rasband, W. S.; Eliceiri, K. W. NIH Image to ImageJ: 25 years of image analysis. *Nat. Methods* **2012**, *9*, 671–675.

(77) Modi, P. K.; Komaravelli, N.; Singh, N.; Sharma, P. Interplay between MEK-ERK signaling, cyclin D1, and cyclin-dependent kinase 5 regulates cell cycle reentry and apoptosis of neurons. *Mol. Biol. Cell* **2012**, *23*, 3722–3730.

(78) Subbannayya, Y.; Mir, S. A.; Renuse, S.; Manda, S. S.; Pinto, S. M.; Puttamalles, V. N.; Solanki, H. S.; Manju, H. C.; Syed, N.;

Sharma, R.; Christopher, R.; Vijayakumar, M.; Veerendra Kumar, K. V.; Keshava Prasad, T. S.; Ramaswamy, G.; Kumar, R. V.; Chatterjee, A.; Pandey, A.; Gowda, H. Identification of differentially expressed serum proteins in gastric adenocarcinoma. *J. Proteomics* **2015**, *127*, 80–88.

(79) Subbannayya, Y.; Syed, N.; Barbhuiya, M. A.; Raja, R.; Marimuthu, A.; Sahasrabudhe, N.; Pinto, S. M.; Manda, S. S.; Renuse, S.; Manju, H.; Zameer, M. A. L.; Sharma, J.; Brait, M.; Srikumar, K.; Roa, J. C.; Vijaya Kumar, M.; Kumar, K. V.; Prasad, T. K.; Ramaswamy, G.; Kumar, R. V.; Pandey, A.; Gowda, H.; Chatterjee, A. Calcium calmodulin dependent kinase kinase 2 - a novel therapeutic target for gastric adenocarcinoma. *Canc. Biol. Ther.* **2015**, *16*, 336–345.

(80) Tyanova, S.; Temu, T.; Sinitcyn, P.; Carlson, A.; Hein, M. Y.; Geiger, T.; Mann, M.; Cox, J. The Perseus computational platform for comprehensive analysis of (prote)omics data. *Nat. Methods* **2016**, *13*, 731–740.

(81) Pathan, M.; Keerthikumar, S.; Ang, C.-S.; Gangoda, L.; Quek, C. Y. J.; Williamson, N. A.; Mouradov, D.; Sieber, O. M.; Simpson, R. J.; Salim, A.; Bacic, A.; Hill, A. F.; Stroud, D. A.; Ryan, M. T.; Agbinya, J. I.; Mariadason, J. M.; Burgess, A. W.; Mathivanan, S. FunRich: An open access standalone functional enrichment and interaction network analysis tool. *Proteomics* **2015**, *15*, 2597–2601.

(82) Kuleshov, M. V.; Jones, M. R.; Rouillard, A. D.; Fernandez, N. F.; Duan, Q.; Wang, Z.; Koplev, S.; Jenkins, S. L.; Jagodnik, K. M.; Lachmann, A.; McDermott, M. G.; Monteiro, C. D.; Gundersen, G. W.; Ma'ayan, A. Enrichr: a comprehensive gene set enrichment analysis web server 2016 update. *Nucleic Acids Res.* **2016**, *44*, W90–W97.

(83) Jassal, B.; Matthews, L.; Viteri, G.; Gong, C.; Lorente, P.; Fabregat, A.; Sidiropoulos, K.; Cook, J.; Gillespie, M.; Haw, R.; Loney, F.; May, B.; Milacic, M.; Rothfels, K.; Sevilla, C.; Shamovsky, V.; Shorser, S.; Varusai, T.; Weiser, J.; Wu, G.; Stein, L.; Hermjakob, H.; D'Eustachio, P. The reactome pathway knowledgebase. *Nucleic Acids Res.* **2020**, *48*, D498–D503.

(84) Calvo, S. E.; Clauser, K. R.; Mootha, V. K. MitoCarta2.0: an updated inventory of mammalian mitochondrial proteins. *Nucleic Acids Res.* **2016**, *44*, D1251–D1257.

(85) Homma, K.; Suzuki, K.; Sugawara, H. The Autophagy Database: an all-inclusive information resource on autophagy that provides nourishment for research. *Nucleic Acids Res.* **2011**, *39*, D986–D990.

(86) Szklarczyk, D.; Gable, A. L.; Lyon, D.; Junge, A.; Wyder, S.; Huerta-Cepas, J.; Simonovic, M.; Doncheva, N. T.; Morris, J. H.; Bork, P.; Jensen, L. J.; Mering, C. V. STRING v11: protein-protein association networks with increased coverage, supporting functional discovery in genome-wide experimental datasets. *Nucleic Acids Res.* **2019**, *47*, D607–D613.

(87) Vizcaino, J. A.; Csordas, A.; del-Toro, N.; Dianes, J. A.; Griss, J.; Lavidas, I.; Mayer, G.; Perez-Riverol, Y.; Reisinger, F.; Ternent, T.; Xu, Q.-W.; Wang, R.; Hermjakob, H. 2016 update of the PRIDE database and its related tools. *Nucleic Acids Res.* **2016**, *44*, D447–D456.



## Prevention of MEK-ERK-1/2 hyper-activation underlines the neuroprotective effect of *Glycyrrhiza glabra* L. (Yashtimadhu) against rotenone-induced cellular and molecular aberrations

Gayathree Karthikkeyan<sup>a</sup>, Ravishankar Pervaje<sup>b</sup>, Sameera Krishna Pervaje<sup>c</sup>,  
Thottethodi Subrahmanya Keshava Prasad<sup>a,\*\*</sup>, Prashant Kumar Modi<sup>a,\*</sup>

<sup>a</sup> Center for Systems Biology and Molecular Medicine, Yenepoya Research Centre, Yenepoya (Deemed to be University), Mangalore 575018, India

<sup>b</sup> Sushrutha Ayurveda Hospital, Puttur 574201, India

<sup>c</sup> Yenepoya Medical College and Hospital, Yenepoya (Deemed to be University), Mangalore 575018, India

### ARTICLE INFO

#### Keywords:

Ethnopharmacology  
Nootropics  
Mitotic catastrophe  
Complementary medicine

### ABSTRACT

**Ethnopharmacological relevance:** Yashtimadhu choorna (powder) is prepared from the dried root of *Glycyrrhiza glabra* L., commonly known as licorice. The Indian Ayurvedic system classifies Yashtimadhu as a *Medhya Rasayana* that can enhance brain function, improves memory, and possess neuroprotective functions, which can be used against neurodegenerative diseases like Parkinson's disease (PD).

**Aim of the study:** We aimed to decipher the neuroprotective effects of *G. glabra* L., i.e., Yashtimadhu, in a rotenone-induced PD model.

**Materials and methods:** Retinoic acid-differentiated IMR-32 cells were treated with rotenone (PD model) and Yashtimadhu, and were assessed for cellular toxicity, live-dead staining, cell cycle, oxidative stress, protein abundance, and kinase phosphorylation.

**Results:** Yashtimadhu conferred protection against rotenone-induced cytotoxicity, countered cell death, reduced expression of pro-apoptotic proteins (cleaved-caspases-9, and 3, cleaved-PARP, BAX, and BAK) and increased anti-apoptotic protein, BCL-2. Rotenone-induced cell cycle re-entry (G2/M transition), was negated by Yashtimadhu and was confirmed with PCNA levels. Yashtimadhu countered rotenone-mediated activation of mitochondrial proteins involved in oxidative stress, cytochrome-C, PDHA1, and HSP60. Inhibition of rotenone-induced ERK-1/2 hyperphosphorylation prevented activation of apoptosis, which was confirmed with MEK-inhibitor, highlighted the action of Yashtimadhu via ERK-1/2 modulation.

**Conclusions:** We provide the evidence for neuroprotection conferred by *G. glabra* L. (Yashtimadhu) and its mechanism via inhibiting MEK-ERK-1/2 hyper-phosphorylation, prevention of mitochondrial stress, and subsequent prevention of apoptosis. The study highlights Yashtimadhu as a promising candidate with neuroprotective effects, the potential of which can be harnessed for identifying novel therapeutic targets.

### 1. Introduction

Parkinson's disease (PD) is an age-related progressive neurodegenerative motor disorder associated with selective loss of dopaminergic neurons from Substantia Nigra pars compacta (SNpc). PD is reported to affect 2–3% of the world elderly population (>65 years) of age (Poewe et al., 2017). The onset of Familial PD is generally due to genetic mutations, while sporadic PD is attributed to environmental, biochemical,

and molecular aspects that dysregulate neuron functions (Kalia and Lang, 2015; Zeng et al., 2018). The known molecular mechanisms that lead to the death of dopaminergic neurons are; protein aggregation (Lewy body formation), mitochondrial stress, oxidative stress, dopamine quinones, microglial activation, and subsequent neuroinflammation (Kalia and Lang, 2015; Poewe et al., 2017). Management of PD primarily includes levodopa, dopamine agonists, monoamine oxidase inhibitors, and deep-brain stimulation (Poewe et al., 2017; Ray Chaudhuri et al., 2016). Prolonged usage of these PD medications has been reported to

\* Corresponding author.

\*\* Corresponding author.

E-mail addresses: [gayathreek@yenepoya.edu.in](mailto:gayathreek@yenepoya.edu.in) (G. Karthikkeyan), [pervaje@rediffmail.com](mailto:pervaje@rediffmail.com) (R. Pervaje), [skperuvaje@gmail.com](mailto:skperuvaje@gmail.com) (S.K. Pervaje), [keshav@yenepoya.edu.in](mailto:keshav@yenepoya.edu.in) (T.S.K. Prasad), [prashantmodi@yenepoya.edu.in](mailto:prashantmodi@yenepoya.edu.in) (P.K. Modi).

<https://doi.org/10.1016/j.jep.2021.114025>

Received 13 March 2020; Received in revised form 7 December 2020; Accepted 10 March 2021

Available online 26 March 2021

0378-8741/© 2021 Elsevier B.V. All rights reserved.

**Abbreviations**

PD	Parkinson's disease	CAD	Collisionally activated dissociation
FBS	Fetal Bovine Serum	DP	Declustering potential
PBS	Phosphate buffered saline;	CE	Collision energy
BCA	Bicinchoninic acid	TH	tyrosine hydroxylase
ROS	Reactive oxygen species	CFM-ID	Competitive Fragmentation Modeling-ID
DMSO	dimethylsulfoxide	RRHD	Rapid Resolution High Definition
PARP	Poly-ADP-ribose-polymerase	m/z	mass to charge ratio
PCNA	Proliferating cell nuclear antigen	KEGG	Kyoto Encyclopedia of Genes and Genomes
BCL-2	B-cell lymphoma-2	MTT	(3-(4,5-dimethylthiazol-2-yl)-2,5-diphenyltetrazolium-bromide)
BAX	BCL2-associated-X protein	DCFDA	2',7'-Dichlorofluorescein diacetate (DCFDA)
BAK1	BCL2-antagonist/killer-1	SNpc	Substantia nigra pars compacta
PDHA1	Pyruvate dehydrogenase-E1 alpha-1	SNCA	$\alpha$ -synuclein
SOD1	Superoxide dismutase-1	PRKN	parkin
HSP60	Heat shock protein-60	LRRK	leucine-rich repeat kinases
ERK-1/2	Extracellular-signal-regulated kinase-1/2	JNK	c-Jun N-terminal kinase
ms	milli second	P38-MAPK	P38 mitogen-activated protein kinase
IDA	Information dependent acquisition	PI3K	phosphoinositide 3-kinase
EMS	Enhanced mass spectra	AKT	protein kinase B
EPI	Enhanced product ion	mTOR	mammalian target of rapamycin
		MPTP	1-methyl-4-phenyl-1,2,3,6-tetrahydropyridine

cause several motor and non-motor side effects, eventually compromising the quality of life of the patients (Chotibut et al., 2017; Kalinderi et al., 2019; Salat and Tolosa, 2013; Turcano et al., 2018).

The use of traditional and complementary medicines has also been explored in search of sustainable therapeutics for the management of PD. The neuroprotective efficacy of several plant extracts was reported in several *in vitro* and *in vivo* models of PD (Hu et al., 2017; Ryu et al., 2017; Silva et al., 2016).

The Indian Ayurvedic system classifies plants with nootropic and neuroprotective properties as *Medhya Rasayana*, including Yashtimadhu, *Glycyrrhiza glabra* L.; Mandukaparni, *Centella asiatica*, and Guduchi, *Tinospora cordifolia* (Sarokte and Rao, 2013). Yashtimadhu choorna (powder) is prepared from the dried root of *Glycyrrhiza glabra* L., commonly known as licorice (<http://www.theplantlist.org/>; <https://m.pns.science.kew.org/>; <http://www.ayurveda.hu/api/API-Vol-1.pdf>). The traditional uses of Yashtimadhu include several medicinal properties, such as gastro-protective effect (Asha et al., 2013; Nugroho et al., 2016), hepatoprotective (Huo et al., 2011), nephroprotective (Mohamed, 2019), expectorant (Kuang et al., 2018), antiviral (Feng Yeh et al., 2013), immunomodulatory (El-Saber Batiha et al., 2020), and anti-angiogenic and antitumor properties (Sheela et al., 2006).

Among its various benefits, Yashtimadhu is primarily known for its efficacy as a memory enhancer, neuroprotectant, and attenuating neuroinflammation (Cho et al., 2018; Cui et al., 2008; Sarokte and Rao, 2013; Sheshagiri et al., 2015). The aqueous extract of Yashtimadhu has been reported to exhibit antioxidant properties and enhance learning and memory in the *in vitro* and *in vivo* models, respectively (Chakravarthi and Avadhani, 2013; Sharifzadeh et al., 2008; Upadhyay et al., 2020). A recent study has reported the administration of Yashtimadhu (licorice root formulation) as an adjuvant for the treatment of PD, resulting in alleviation of the PD symptoms (Petramfar et al., 2020). Although various research studies have widely reported the neuroprotective attributes of Yashtimadhu, its mechanism of action remains largely unexplored.

Dysregulation in the signaling events of kinases are reported to be involved in PD, which include extracellular signal-regulated kinase-1/2 (ERK-1/2), c-Jun N-terminal kinase (JNK), P38 mitogen-activated protein kinase (P38-MAPK), phosphoinositide 3-kinase- protein kinase B (PI3K-AKT), and mammalian target of rapamycin (mTOR) (Gugliandolo et al., 2020; Ma et al., 2018; Sai et al., 2009; Wu et al., 2013). ERK-1/2 is a MAPK family member, which plays a pivotal role in memory and

synaptic plasticity (Sweatt, 2004), regulating the cellular redox potential, caspase-activation, and cell cycle, which decide the neuronal cellular fate (Modi et al., 2012; Song et al., 2020; Tang et al., 2002).

In this study, we sought to demonstrate the neuroprotective function of Yashtimadhu in the cellular model of PD generated using rotenone (Chia et al., 2020; Li et al., 2003). The neuroprotective function of Yashtimadhu was evaluated in terms of cytotoxicity, oxidative stress, apoptosis, cell cycle regulation, mitochondrial proteins, and dysregulated signaling. Our study describes the regulation of the MEK-ERK-1/2 pathway in the neuroprotective functions of Yashtimadhu against the rotenone-induced PD model.

## 2. Materials and Methods

### 2.1. Materials

Rotenone, HOECHST-33342, Propidium iodide, Collagen, MTT (3-(4,5-dimethylthiazol-2-yl)-2,5-diphenyltetrazolium-bromide), Retinoic acid, and 2',7'-Dichlorofluorescein diacetate (DCFDA), were procured from Sigma-Aldrich, St. Louis, USA. BCA assay kit, Thermo Fisher Scientific, Massachusetts, USA. MEK inhibitor U0126, Tocris Bioscience, Bristol, United Kingdom. DMEM high glucose media, fetal bovine serum (FBS), and 100X antibiotic/antimycotic solution, Gibco, ThermoFisher Scientific USA. Antibodies were procured from Cell Signaling Technology, Danvers, USA, Santa-Cruz Biotechnology, USA, and Sigma-Aldrich, St. Louis, USA. Nitrocellulose membrane and Clarity ECL Substrate, BioRad Laboratories, California, USA, and X-ray films, Carestream, USA.

### 2.2. *Glycyrrhiza glabra* L. powder (Yashtimadhu choorna) procurement and authentication

*Glycyrrhiza glabra* L. in English is known as licorice/liquorice and is commonly known in India as Yashtimadhu (<http://www.theplantlist.org/>). The root powder of Yashtimadhu (Lot No.64) was procured from SDP Remedies and Research Centre, Puttur, Karnataka, India, a GMP-certified Ayurvedic product manufacturer (<http://sdpayurveda.com/products/choorna/yastimadhu-choorna/>). *G. glabra* L. root was collected and authenticated by Dr. Harikrishna Panaje, SDP Remedies and Research Centre, and a specimen is also maintained in the centre, with the identifier SDP/YM/001–2017. The industrial process included the following steps; the roots of *G. glabra* L. were washed, dried under

shade-net, and followed by vacuum-drum drying. Dried roots were pulverized and sieved to obtain a fine powder of Yashtimadhu root, with a yield of about 90%.

### 2.3. *G. glabra* L. (Yashtimadhu) extract preparation

For cell culture treatment, 1 g of Yashtimadhu choorna was suspended in 10 ml of MilliQ-water (0.1 g/ml) and incubated overnight at room temperature, with continuous rotation. The extraction mixture was centrifuged at 5000 rpm for 10 min, twice, and the supernatant containing the soluble fraction was collected in a fresh tube. The aqueous extract was dried using SpeedVac (Savant, Thermo Fisher Scientific, USA), and the dried extract was stored at  $-20^{\circ}\text{C}$  until further use. The yield from the aqueous extraction of 1 g of Yashtimadhu powder was found to be 54% w/w. The dried *G. glabra* L. extract, hereafter referred to as Yashtimadhu extract, was dissolved in serum-free media for cell culture treatment.

### 2.4. LC-MS/MS analysis of Yashtimadhu extract

QTRAP-6500, ABSCIEX, coupled with Agilent Infinity-II 1290 liquid chromatography system was used for LC-MS/MS analysis. About 10  $\mu\text{l}$  of Yashtimadhu extract was resolved using the ZORBAX Eclipse plus C18 (Agilent), Rapid Resolution High Definition column (RRHD,  $2.1 \times 150$  mm,  $1.8 \mu\text{m}$ ) analytical column using 0.1% formic acid in MilliQ water and 0.1% formic acid in 90% LC-MS grade acetonitrile as the solvents A and B, respectively with a flow rate of 300  $\mu\text{l}/\text{min}$ . Untargeted mass spectrometry data acquisition was carried out with an information-dependent acquisition (IDA) method built with enhanced mass spectra (EMS) and enhanced product ion (EPI) scans, i.e., the EMS-IDA-EPI method (M et al., 2020; Subbannayya, 2018). Data were acquired in the low mass mode, within the mass range of 50–1000 Da, at a scan rate of 10,000 Da/s, with a dynamic fill time of 250 ms and a linear ion trap fill time of 10 ms. Top five intense precursor ions were selected using EPI (MS/MS) scan mode and fragmented with high energy collisionally activated dissociation (CAD). Data acquired in both positive and negative modes with an ion source voltage of 4500 V and  $-4500$  V respectively, a declustering potential (DP) of 100 V and  $-100$  V, and collision energy (CE) of 40 V and  $-40$  V, respectively, and the ion source was maintained at a temperature of  $450^{\circ}\text{C}$ . The data was acquired in triplicates and MZmine, version 2.31 (Pluskal et al., 2010) was used for the analysis of mass spectrometry data and visualization. The presence of the Yashtimadhu bioactive molecules such as glycyrrhizic acid, glabridin (specific for *G. glabra*), licoricesaponin-G2, and liquiritin apioside, was confirmed at MS/MS-level using the Competitive Fragmentation Modeling-ID, i.e., CFM-ID (Djombou-Feunang et al., 2019) fragmentation patterns of the molecules.

### 2.5. Cell culture and treatment

IMR-32 cells (ATCC® CCL-127™) were procured from National Centre for Cell Science, Pune, India and maintained in DMEM-high glucose medium with 10% FBS, and 1X antibiotic/antimycotic solution, at  $37^{\circ}\text{C}$ , 5%  $\text{CO}_2$ . Differentiation was carried out with  $3 \times 10^4$  cells that were seeded in collagen-coated plates and treated with 10  $\mu\text{M}$  retinoic acid in 2% FBS, for nine days. Differentiated IMR-32 cells served as a dopaminergic neuron model and validated by tyrosine hydroxylase (TH) expression and compared with undifferentiated IMR-32 cells (Ikram et al., 2016; Kotapalli et al., 2017) (Fig. S2).

Differentiated cells were treated with 100 nM rotenone (dissolved in DMSO), 200  $\mu\text{g}/\text{ml}$  of the Yashtimadhu extract, co-treatment of rotenone (100 nM), and Yashtimadhu extract (200  $\mu\text{g}/\text{ml}$ ), for 48 h. The untreated cells were taken as control. ERK1/2-inhibitor, U0126, was added to the cells 30 min prior to treatment.

### 2.6. Cell cytotoxicity assay

IMR-32 cells were seeded at 5000 cells/well, in 96-well plate, and subjected to treatment with rotenone (0.25 nM–10  $\mu\text{M}$ ) for 24 h and 48 h, Yashtimadhu (50–1500  $\mu\text{g}/\text{ml}$ ) for 48 h, and co-treatment for 48 h. The final concentration of DMSO did not exceed 2%, whose effect was also evaluated. MTT-dye was incubated for 3–4 h, and formazan crystals were dissolved using 50:50:ethanol:DMSO, read at 560 nm, and 650 nm. Cell cytotoxicity is expressed as percentage cell viability with respect to untreated control.

### 2.7. Live-dead cell staining assay

For live-dead cell staining assay, IMR-32 cells were seeded in 12-well plate coated with 1X collagen at  $1 \times 10^4$  cells/well. The cells were differentiated for 9 days using 10  $\mu\text{M}$  retinoic acid and treated with the rotenone (100 nM), Yashtimadhu (200  $\mu\text{g}/\text{ml}$ ), rotenone (100 nM) + Yashtimadhu (200  $\mu\text{g}/\text{ml}$ ) for 48 h, and untreated cells were taken as control. Treated cells were stained with 20  $\mu\text{g}/\text{ml}$  of propidium iodide (PI) and Hoechst-33342 at 5  $\mu\text{g}/\text{ml}$ , prepared in serum-free media, and incubated for 15 min (Bose et al., 2020). Cells were imaged in four different fields per well, using ZOE™ Fluorescent Cell Imager, BioRad Laboratories, California, USA. ImageJ, NIH (Schneider et al., 2012) software was used to calculate the ratio of PI to Hoechst-33342 stained cells. The percentage of cell death was calculated with respect to control and later converted to fold change.

### 2.8. Assessment of reactive oxygen species (ROS)

IMR-32 cells were seeded at  $1 \times 10^4$  cells/well in collagen-coated 12-well plates and differentiated for 9 days with 10  $\mu\text{M}$  retinoic acid and treated with the rotenone (100 nM), Yashtimadhu (200  $\mu\text{g}/\text{ml}$ ), rotenone (100 nM) + Yashtimadhu (200  $\mu\text{g}/\text{ml}$ ) for 48 h, while untreated cells were taken as control. The cells were assessed for intracellular ROS using 25  $\mu\text{M}$  DCFDA and 5  $\mu\text{g}/\text{ml}$  of Hoechst-33342, in serum-free media was added to the cells and incubated for 15 min in the dark and imaged using ZOE™ Fluorescent Cell Imager (Bose et al., 2020). ImageJ tool was used for analyzing the DCFDA-positive cells, and results were expressed as percentage ROS with respect to control.

### 2.9. Cell cycle analysis

IMR-32 cells were seeded at  $3 \times 10^4$  cells/well into the collagen-coated 6-well plate, differentiated with retinoic acid (10  $\mu\text{M}$ ) and treated with rotenone (100 nM), Yashtimadhu (200  $\mu\text{g}/\text{ml}$ ), rotenone (100 nM) + Yashtimadhu (200  $\mu\text{g}/\text{ml}$ ) for 48 h, while untreated cells were taken as control. The cells were washed with 1X PBS, trypsinized and further washed twice with 1X PBS and re-suspended in hypotonic buffer (2  $\mu\text{g}/\text{ml}$  PI, 1 mg/ml trisodium citrate, 0.1% Triton-X 100, and 100  $\mu\text{g}/\text{ml}$  RNase), incubated in the dark for 30 min, and the red fluorescence was measured using Guava® easyCyte Flow Cytometer, EMD Millipore, Massachusetts, USA. Cell cycle data analysis was carried out with FCS Express (version-6).

### 2.10. Immunoblotting

IMR-32 cells seeded in collagen-coated 6-well plates at  $3 \times 10^4$  cells/well and differentiated with 10  $\mu\text{M}$  retinoic acid for nine days. Differentiated cells were treated with rotenone (100 nM), Yashtimadhu (200  $\mu\text{g}/\text{ml}$ ), and rotenone (100 nM) + Yashtimadhu (200  $\mu\text{g}/\text{ml}$ ) co-treatment, for 48 h, and untreated cells were taken as control. Post-treatment, cells were washed thrice with 1X PBS and harvested in cell lysis buffer [4% sodium dodecyl sulfate in 50 mM triethylammonium bicarbonate, with sodium orthovanadate (1 mM), sodium pyrophosphate (2.5 mM), and beta-glycerophosphate (1 mM)]. Cells were lysed by sonication on ice, at an amplitude of 20% for 2 min of two cycles

using Q-Sonica (Cole-Parmer, India). The lysate was cleared by centrifugation at  $12000 \times g$  for 20 min at  $4^\circ\text{C}$ , and protein estimation was done by the BCA method by using BSA as standard. Following proteins were assessed: tyrosine hydroxylase for differentiation, cleaved-caspase-9 (cl-Cas-9), cleaved caspase-3 (cl-Cas-3), cleaved-Poly-ADP-ribose polymerase (PARP), proliferating cell nuclear antigen (PCNA), B-cell lymphoma-2 (BCL-2), BCL2-associated-X protein (BAX), BCL2-antagonist/killer-1 (BAK1), pyruvate dehydrogenase-E1 alpha-1 (PDHA1), cytochrome-C, superoxide dismutase-1 (SOD1), heat-shock protein-60 (HSP60), total and phosphorylated extracellular-signal-regulated kinase-1/2 (ERK-1/2), and  $\beta$ -actin (loading control). The catalog numbers and the respective dilution factors of the antibodies used are given in [Supplementary Table 2](#).

Protein concentration was estimated with BCA assay, and immunoblotting was carried out as described previously ([Modi et al., 2012](#)). Briefly, an equal amount of protein from the four conditions was loaded onto SDS-PAGE and resolved. The resolution of proteins for assessing PCNA, cleaved-caspase-9, PDHA, HSP60, p-ERK1/2, t-ERK-1/2, and  $\beta$ -actin was carried out with 10% gel. Cleaved-caspase-3, BCL-2, BAK1, BAX, cytochrome-C were resolved in 13% gel, and cleaved-PARP using 8% gel. The proteins were transferred onto nitrocellulose membrane; upon completion of the transfer, the membranes were blocked with 5% skimmed milk in 1X phosphate-buffered saline in 0.5% Tween-20 (PBST), for 1 h. Membranes were incubated in primary antibodies with the respective dilutions ([Supplementary Table 2](#)), which were diluted in 3% BSA in 1X PBST overnight at  $4^\circ\text{C}$ . Washing of membranes was carried out with 1X PBST. Membranes were further incubated with HRP-conjugated secondary antibodies in 3% BSA in 1X PBST for 2 h at room temperature. The immunoreactive bands were developed with Enhanced Chemiluminescence reagent and captured onto X-ray films. Densitometry analysis of band intensity was performed using ImageJ tool (NIH), normalized with loading-control and fold-change calculated with respect to untreated cells.

### 2.11. Statistical analysis

GraphPad Prism-5 was used for statistical analysis, and data were expressed as mean  $\pm$  SEM from three independent experiments. One-way ANOVA with Bonferroni posthoc-test was used for comparison between groups, and a  $p$ -value  $< 0.05$  was considered to be significant. The test statistics are reported as the  $F$ -value along with the degrees of freedom between and within groups from the ANOVA table, and the  $p$ -value computed from the Bonferroni post-hoc test.

## 3. Results

### 3.1. LC-MS/MS analysis of Yashtimadhu powder

Untargeted metabolomics using the tandem mass spectrometry (MS/MS) approach was used for the identification of the signature metabolites of Yashtimadhu. Data were acquired in both positive and negative modes, and the total ion chromatograms are given in [Fig. S1A](#) and [B](#). MZmine tool was used for data alignment from the technical replicates of their respective polarities, and the precursor mass to charge ratio ( $m/z$ ), retention time, fragment masses were obtained. The  $m/z$  ratio was used for metabolite assignment using the Kyoto Encyclopedia of Genes and Genomes (KEGG) database, which resulted in putative identification of over 1600 metabolites from both the positive and negative modes. We identified mono-, di-, and tri-terpenoids, alkaloids, flavanols and flavonoids, and betalains class of metabolites which includes; glycyrrhizin, limonene, ononin, apigenin, to name a few.

To confirm the presence of the bioactive compounds of *G. glabra* L. and authentication of Yashtimadhu choorna, metabolite assignment was carried out at the MS/MS fragment level. The compound mapping was carried out with the precursor masses and the fragmentation patterns (MS/MS), which was compared with the fragments generated using

CFM-ID. The precursor scan (MS1) and the fragment scan (MS/MS) of the signature compounds are given in [Fig. S1](#) and [Supplementary Table 1](#), for: Glycyrrhizic acid ([Fig. S1C-D](#)), Glabridin ([Fig. S1E-F](#)), Licoricesaponin G2 ([Fig. S1G-H](#)), and Liquiritin apioside ([Fig. S1I-J](#)). The abundance of these metabolites was calculated using the peak-area computed using MZmine software. The percentage abundance of the compounds were as follows; glycyrrhizic acid (0.234%), glabridin (0.025%), licoricesaponin G2 (0.226%) and liquiritin apioside (0.033%).

### 3.2. Cytotoxicity of rotenone and Yashtimadhu extract

IMR-32 cells were exposed to different concentrations of rotenone (0.25 nM–10  $\mu\text{M}$ ) for 24 h and 48 h, which showed time and concentration-dependent effect of rotenone, [Fig. 1A](#) and [B](#). Yashtimadhu treatment (50  $\mu\text{g/ml}$  to 1500  $\mu\text{g/ml}$ ) proved to be non-toxic at all tested concentrations, [Fig. 1C](#). The  $\text{IC}_{50}$  was observed at 10  $\mu\text{M}$  ( $p < 0.01$ ) for 24 h and 100 nM ( $p < 0.005$ ) for 48 h. Based on the MTT assay, 100 nM rotenone and 200  $\mu\text{g/ml}$  Yashtimadhu for 48 h was used for further experiments. Yashtimadhu co-treatment with rotenone protected the cells from rotenone-induced cytotoxicity ( $F(3, 8) = 25.90$ ,  $p < 0.05$ ), [Fig. 1D](#).

### 3.3. Rotenone and Yashtimadhu differentially regulate cell cycle

Cell cycle analysis ([Fig. 2](#)) revealed that the differentiated control cells had a predominant population of G0/G1 (56.1%) and S-phase (38.8%). Yashtimadhu treatment also resulted in a majority of G0/G1 (53.4%) and S-phase (45.1%); however, the G2/M-phase cells were much lesser (1.5%) than the control (5.0%). Rotenone treatment revealed a significant population of cells ( $F(3, 8) = 16.75$ ,  $p < 0.05$ ), in G2/M-phase (38.5%) and lesser in G0/G1 (40.3%) and S-phases (21.2%). The co-treatment with rotenone and Yashtimadhu, significantly ( $F(3, 8) = 16.75$ ,  $p < 0.05$ ) reversed the cells from G2/M (5.8%) to the G0/G1 (57.7%) and S-phases (36.5%). The undifferentiated cells, however, showed a distinct profile compared to the differentiated cells (G0/G1- 56.9%, S-29%, and G2/M-14.1%). PCNA, an S-phase marker was reduced with rotenone to 0.43-folds compared to control ( $F(3, 8) = 9.36$ ,  $p < 0.05$ ), which was restored with Yashtimadhu co-treatment (0.99-folds,  $p < 0.05$ , compared to rotenone). The reduction of S-phase marker with rotenone suggests a transition to G2/M-phase, in agreement with the cell cycle data.

### 3.4. Yashtimadhu counters rotenone-induced cell death and caspase activation

In addition to the cell cytotoxicity analysis, we carried out a live-dead cell staining assay ([Fig. 3A–B](#)). Increased PI (red (in the web version)) staining of cells, i.e., a 9.14-fold increase in cell death compared to control ( $F(3, 8) = 30.57$ ,  $p < 0.005$ ) in rotenone treatment, indicating cell death which is decreased with Yashtimadhu co-treatment.

We profiled the expression of cleaved-caspase-9, cleaved-caspase-3 and cleaved-PARP ([Fig. 3C–F](#)). Rotenone induced caspase-9 cleavage (Asp330) to about 1.58-folds compared to control ( $F(3, 8) = 11.96$ ,  $p < 0.05$ ), thereby activating the caspase pathway, which was significantly decreased in co-treatment with Yashtimadhu, 1.03-fold ( $p < 0.05$ , compared to rotenone). Cleaved-caspase-9, in turn, activates the caspase-3 cleavage (Asp175), increased to 2.35-folds with rotenone, compared to control ( $F(3, 8) = 10.31$ ,  $p < 0.05$ ) and decreased with Yashtimadhu co-treatment, 1.04-folds ( $p < 0.05$ , compared to rotenone). Cleaved-PARP was also significantly increased to about 1.42-folds with rotenone treatment ( $F(3, 8) = 14.76$ ,  $p < 0.05$ , compared to control) and reduced by Yashtimadhu 0.9-folds ( $p < 0.01$ , compared to rotenone).



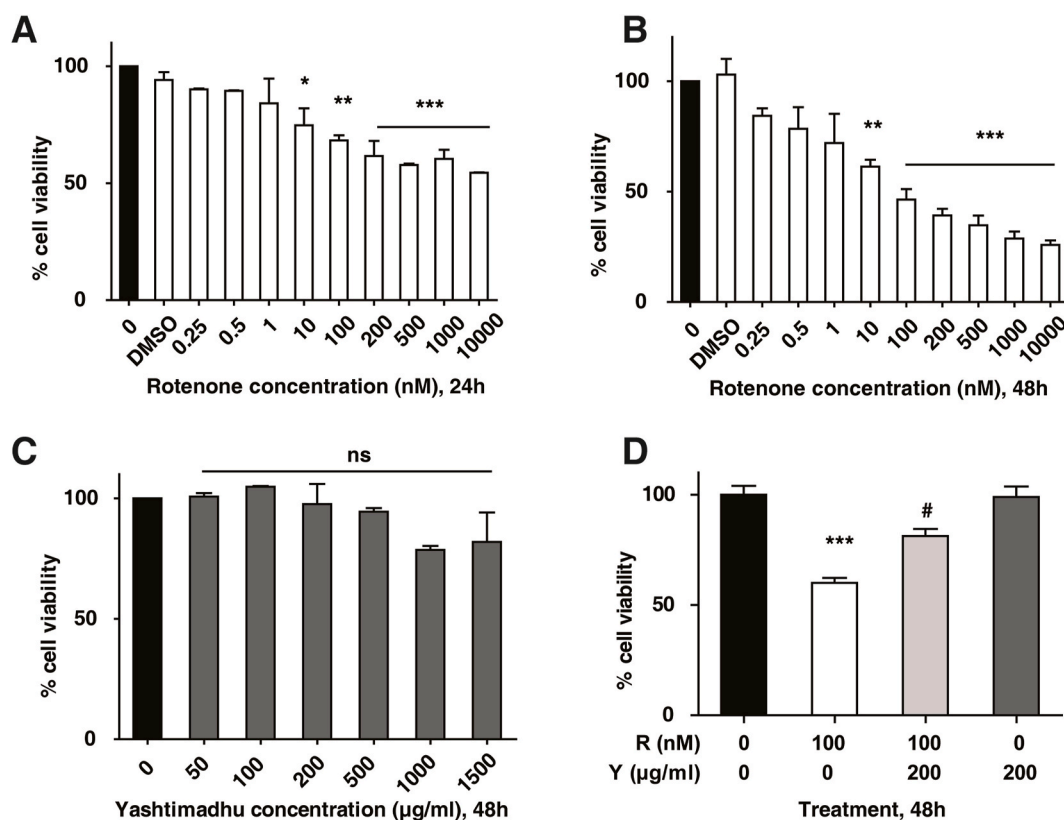


**Fig. 1.** Rotenone exerts time and dose-dependent toxicity, Yashtimadhu prevents rotenone-induced cytotoxicity. Cytotoxicity analysis of IMR-32 cells with different concentrations of rotenone, at (A) 24 h, and (B) 48 h, showing time and concentration-dependent toxicity, (C) Yashtimadhu at tested concentrations is non-toxic, (D) Co-treatment of Yashtimadhu (200 µg/ml) and rotenone (100 nM), at 48 h, showing prevention of cell death. Untreated cells were taken as control. \* $p < 0.05$ , \*\* $p < 0.01$ , \*\*\* $p < 0.001$ , compared to control and # $p < 0.05$ , compared to rotenone.

### 3.5. Yashtimadhu counters rotenone-induced ROS and mitochondrial proteins

Rotenone-mediated mitochondrial complex-I inhibition, increases ROS dramatically, resulting in cell death via caspases. Treatment with rotenone showed ROS induction (84.5%,  $F(3, 16) = 59.81$ ,  $p < 0.0001$ ), compared to control (12.7%) and Yashtimadhu (14.7%). Co-treatment with Yashtimadhu significantly reduced the ROS accumulation (48.4%,  $p < 0.0001$ , compared to rotenone), Fig. 4A–B. We also evaluated the expression of several mitochondrial proteins such as BCL-2, PDHA1, SOD1, and Cytochrome-C, Fig. 4C–J. Interestingly, the anti-apoptotic protein BCL-2 was reduced with rotenone treatment to 0.43-folds, ( $F(3, 8) = 16.44$ ,  $p < 0.01$  compared to control) and increased with Yashtimadhu co-treatment to 0.8-folds ( $p < 0.05$  compared to rotenone). The expression of Cytochrome-C and PDHA1 levels were increased with rotenone treatment at 3.78-folds ( $F(3, 8) = 91.01$ ,  $p < 0.001$ ) and 1.86-folds ( $F(3, 8) = 16.73$ ,  $p < 0.05$ ), respectively and reduced with Yashtimadhu co-treatment to 2.1-folds ( $p < 0.01$  compared to rotenone) and 0.86-folds ( $p < 0.01$  compared to rotenone), respectively. The expression of SOD1 with rotenone treatment did not show a significant change. BAX and BAK1 are mitochondrial proteins, which play a major role in apoptosis. BAX, BAK1, and HSP60, a stress-induced protein were significantly induced in rotenone to 4.56 ( $F(3, 8) = 181.7$ ,  $p < 0.05$ ), 1.44 ( $F(3, 8) = 22.19$ ,  $p < 0.05$ ) and 1.95 ( $F(3, 8) = 11.54$ ,  $p < 0.001$ ) folds respectively, compared to control, which was significantly reduced by Yashtimadhu co-treatment.

### 3.6. Yashtimadhu prevents ERK-1/2 hyper-activation

ERK-1/2 is implicated in the control of cell cycle and apoptosis; thus we evaluated its phosphorylation (Fig. 5). We observed hyper-activation

of ERK-1/2 (Thr202/Tyr204), in rotenone treatment at 2.02-folds ( $F(5, 12) = 11.60$ ,  $p < 0.05$ , compared to control) and decreased with Yashtimadhu co-treatment to 1.32-folds ( $p < 0.05$ , compared to rotenone). To further understand the role of Yashtimadhu on rotenone-induced activation of ERK-1/2, we used small-molecule MEK-inhibitor, U0126. ERK1/2 phosphorylation was successfully inhibited with 10 µM of U0126. Upon MEK-ERK-1/2 inhibition, the expression levels of cleaved-caspase-3 and cleaved-PARP were significantly reduced, correlating with Yashtimadhu mediated inactivation of ERK-1/2 and subsequent reduction of cleaved-caspase-3 and cleaved-PARP. This provides insights into ERK-1/2 modulation and prevention of apoptosis by Yashtimadhu as a central underlying scheme of neuroprotection.

## 4. Discussion

Parkinson's disease progression is attributable to mitochondrial dysfunction and oxidative stress (Poewe et al., 2017). The prolonged usage of PD medications is reported to induce numerous side effects. (Chotibut et al., 2017; Kalinderi et al., 2019; Salat and Tolosa, 2013; Turcano et al., 2018). It necessitates the need for sustainable management of PD, and therefore use of complementary and alternative traditional medicinal approaches has been explored as an additional option (Deolankar et al., 2020; Hu et al., 2017; Petramfar et al., 2020; Ryu et al., 2017). Several studies have reported the neuroprotective effects of Yashtimadhu (Karthikkeyan et al., 2020a; Petramfar et al., 2020; Sarokte and Rao, 2013; Sheshagiri et al., 2015), while little has been known about its mechanism of action. This work is aimed to decipher the molecular mechanism of the neuroprotective effects of Yashtimadhu using a rotenone-induced cellular model of PD (Li et al., 2003).

Untargeted metabolomics of Yashtimadhu extract has been reported to contain a diverse class of metabolites, including alkaloids, terpenoids,

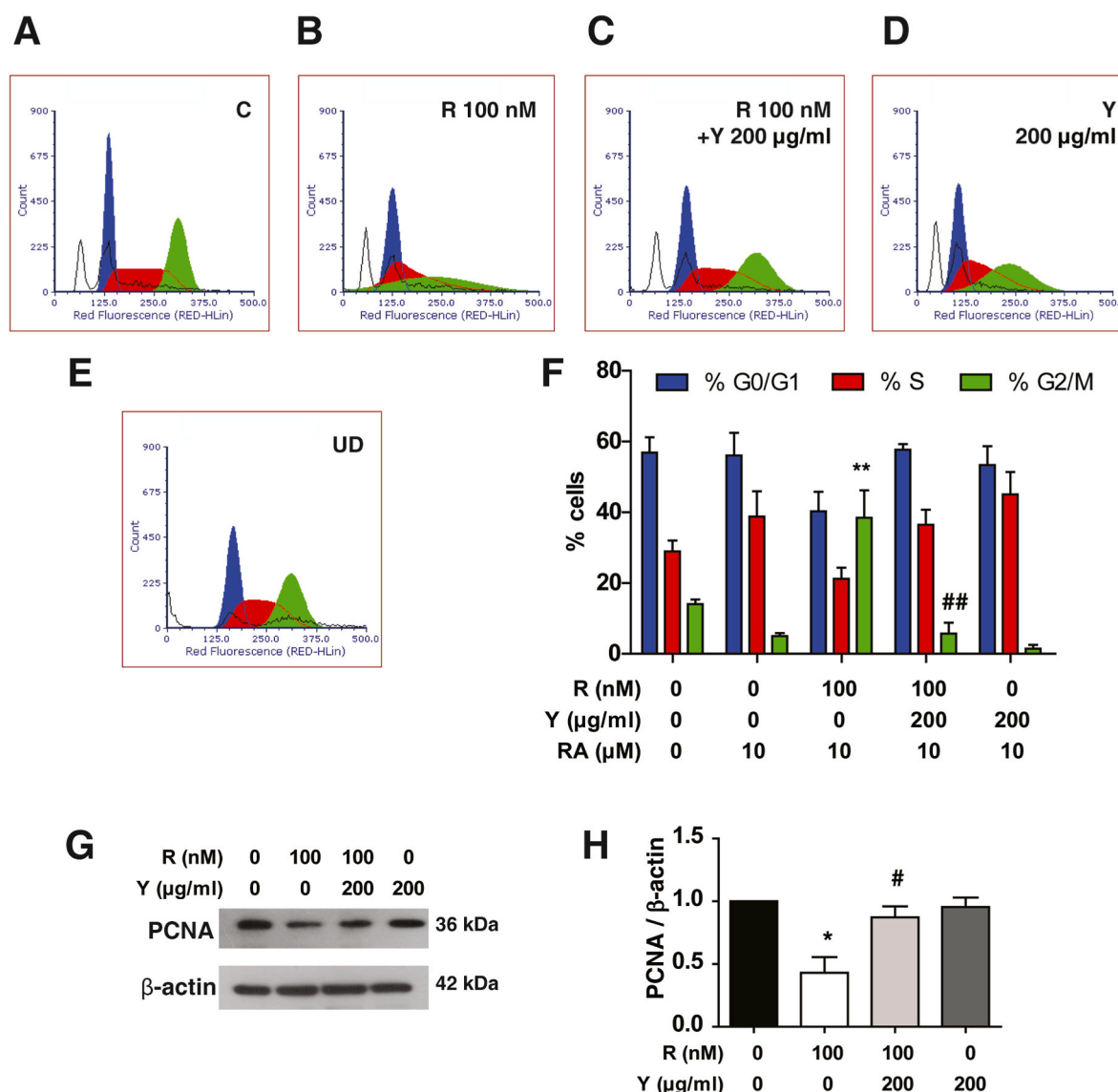


**Fig. 2.** Rotenone-induced cell cycle re-entry is countered by Yashtimadhu. Cell cycle analysis; (A) Differentiated and untreated cells control (C), (B) Rotenone (100 nM), (C) Rotenone (100 nM) with Yashtimadhu (200 μg/ml) co-treatment, (D) Yashtimadhu alone (200 μg/ml), and (E) Undifferentiated cells (UD). (F) Graphical representation of cell population across different phases. (G) Immunoblot analysis of PCNA, and (H) Graphical representation. Differentiated and untreated cells were taken as control. \* $p < 0.05$ , \*\* $p < 0.01$ , compared to control and # $p < 0.05$ , ## $p < 0.01$ , compared to rotenone.

and flavonoids, which were mapped at the precursor level (Karthikkeyan et al., 2020b). We confirmed the presence and the abundances of the lead bioactive molecules, glycyrrhizic acid, glabridin, liquiritin apioside, and licoricesaponin G2, assigned at MS/MS-level, which were similar to the abundances reported by other studies (Hayashi et al., 2016; Tian et al., 2008a, b).

Mitochondrial complex-I inhibition by rotenone causes loss of mitochondrial membrane potential and release of cytochrome-C (Condelo et al., 2011), which triggers caspase-mediated apoptosis. Procaspase-9 is the activator caspase, which promotes the cleaving of the effector procaspase-3, eventually activating cleavage of PARP-1, a DNA repair protein (Los et al., 2002). The rotenone-mediated induction of BAX and BAK1 reiterates the apoptotic signal and neurodegeneration, as previously reported (Condelo et al., 2011; Wu et al., 2013). The reduction in anti-apoptotic protein BCL-2 with rotenone predisposes the cells to apoptosis (Liu et al., 2018). Yashtimadhu mediated the inhibition of rotenone-induced activation of caspase cascade and other pro-apoptotic proteins, induced the expression of anti-apoptotic protein, and thereby provided neuroprotection.

Cell cycle analysis showed the cells from the control and Yashtimadhu groups were distributed in G0/G1 and S-phases, attributable to the G1/S-arrest by retinoic acid (Hsu et al., 2000; Seewaldt et al., 1999). Rotenone promoted the transition of cells to G2/M-phase, confirmed with reduced PCNA expression, an S-phase marker protein. As evidenced by the G2/M transition, this cell cycle re-entry leads to mitotic catastrophe by activating the caspase-3 apoptotic pathway (Wang et al., 2014). Decreased PCNA levels in dopaminergic neurons are reported to make the cells susceptible to oxidative damage and death (Li et al., 2016). The attempt for cell cycle re-entry driven by the MEK-ERK1/2 pathway leads to apoptosis under neurotoxic stress (Modi et al., 2012; Tang et al., 2002). Co-treatment with Yashtimadhu prevented the ERK-1/2 hyper-activation, preventing cell cycle re-entry and caspases-mediated cell death.

Yashtimadhu restored cellular ROS and several mitochondrial proteins, which were dysregulated by rotenone, highlighting its antioxidant potential. PDHA1 is the core enzyme in the pyruvate dehydrogenase complex, catalyzing the conversion of pyruvate to acetate. Rotenone-induced expression of PDHA1, which is known to be regulated by

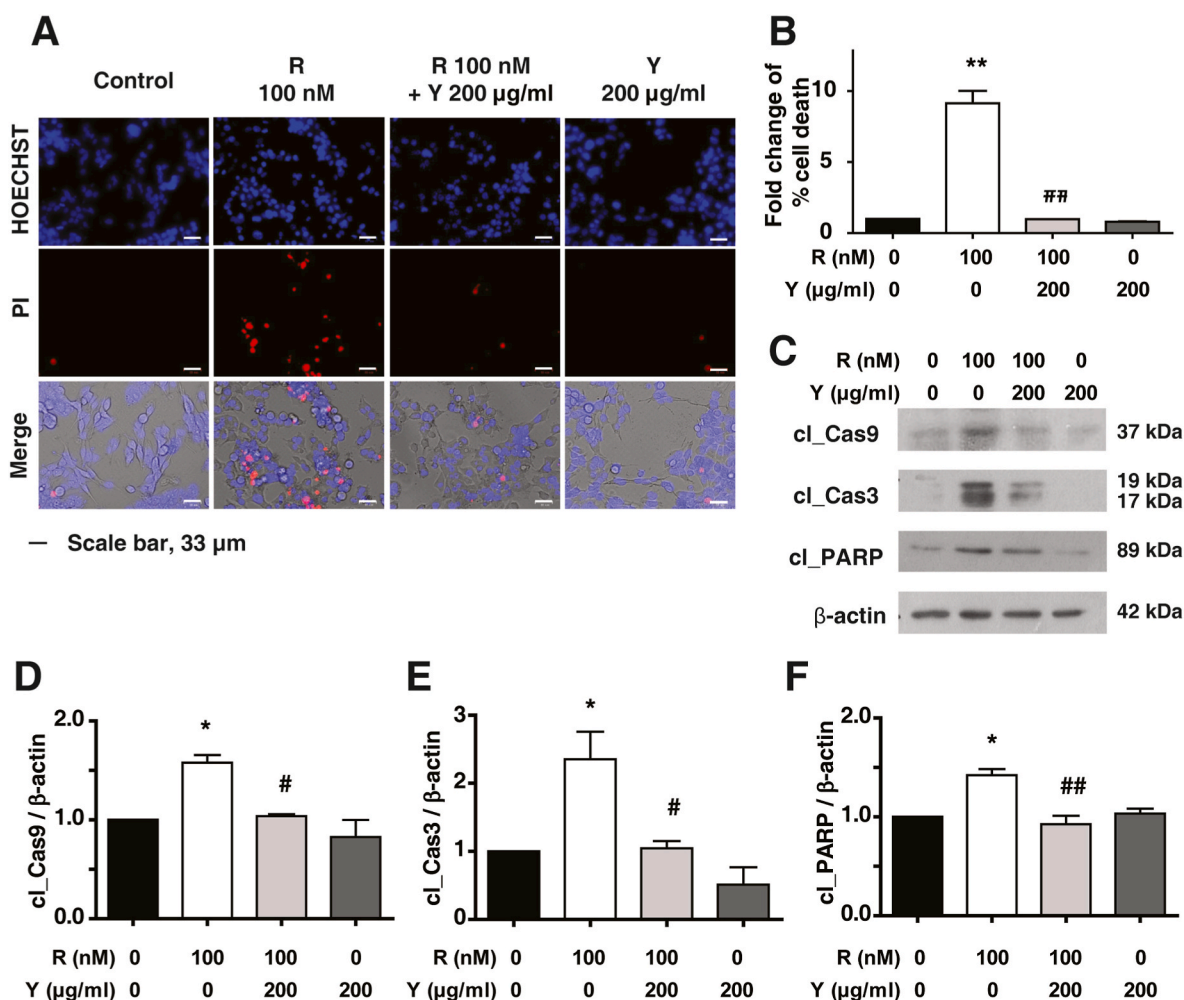


**Fig. 3.** Rotenone induces neuronal apoptosis via caspase activation, prevented by Yashtimadhu. Cells were treated with rotenone (100 nM), Yashtimadhu (200 µg/ml), their co-treatment, and untreated cells were taken as control. (A) Live/Dead cell staining assay indicating more cell death with rotenone, which is reduced by Yashtimadhu. Red channel (PI): Dead cells, Blue channel (HOECHST): nuclear counter-stain. (B) Graphical representation of fold change in % cell death, assessed by dead/live cell staining (red/blue). (C) Immunoblot analysis showing the expression of cleaved caspase-9, cleaved caspase-3 and cleaved-PARP proteins. Rotenone treatment-induced caspase-9 mediated apoptotic pathway, which is inhibited by Yashtimadhu treatment. Graphical representation of protein arbitrary units of the intensity of protein/β-actin expressed as fold-change with respect to control (D) Cleaved caspase-9 (E) Cleaved caspase-3 and (F) Cleaved-PARP. \* $p < 0.05$ , \*\* $p < 0.01$ , compared to control and # $p < 0.05$ , ## $p < 0.01$ , compared to rotenone. (For interpretation of the references to colour in this figure legend, the reader is referred to the Web version of this article.)

Receptor-interacting serine/threonine-protein kinase 3 (RIP3), increasing intracellular ROS (Li et al., 2003; Yang et al., 2018). The rotenone-mediated inhibition of complex-I and subsequent increase in cytochrome-C was reported in SHSY5Y cells (Condello et al., 2011) as an event of early mitochondrial activation during apoptosis (Chandra et al., 2002). HSP60, a mitochondrial quality control, is reported to be increased *in vitro* and the SNpc of PD patients, leading to neurodegeneration (Noelker et al., 2014).

Hyper-phosphorylation of ERK-1/2 is linked to neurodegeneration induced by rotenone in hippocampal neurons (Sai et al., 2009). Hyperactivation of MEK-ERK-1/2-induced mitotic catastrophe by regulating cell cycle, and activated apoptosis by positively regulating caspase-3 and the BCL-2 family pro-apoptotic proteins BAK and BAX (Tomiyama et al., 2010). We demonstrated the inhibition of caspase-mediated apoptosis using the small molecule MEK-inhibitor, U0126, which correlates with Yashtimadhu treatment. Together, these results suggest the role of Yashtimadhu as a neuroprotectant by inhibiting the rotenone-induced hyper-activation of the MEK-ERK-1/2 pathway, thereby preventing cell cycle re-entry and downstream apoptotic events.

## 5. Conclusions

Mitochondrial stress is a hallmark of Parkinson's disease, and we aimed to understand the neuroprotective efficacy of *Glycyrrhiza glabra* L., i.e., Yashtimadhu in the rotenone-induced stress model of PD. Our results suggest that rotenone elicits mitochondrial oxidative stress, cell cycle re-entry-mediated G2/M arrest, and subsequent activation of the caspase-3 apoptotic pathway via MEK-ERK-1/2 hyper-activation. Yashtimadhu co-treatment prevented cellular ROS and improved mitochondrial health. It also counteracted the mitotic catastrophe-mediated cell cycle re-entry and caspase activation by preventing the MEK-ERK-1/2 pathway hyper-activation. The results suggest that Yashtimadhu is protecting the cells against neurotoxic stress. Our study also paves the way for further validating the potential of Yashtimadhu and its kinase regulation in contributing to neuroprotection strategy against PD.

## Author contribution

TSKP, RP, and PKM conceived the idea, designed and planned the experiments. GK performed the experiments, analysis, and manuscript drafting. RP, an Ayurveda clinician, procured the samples and

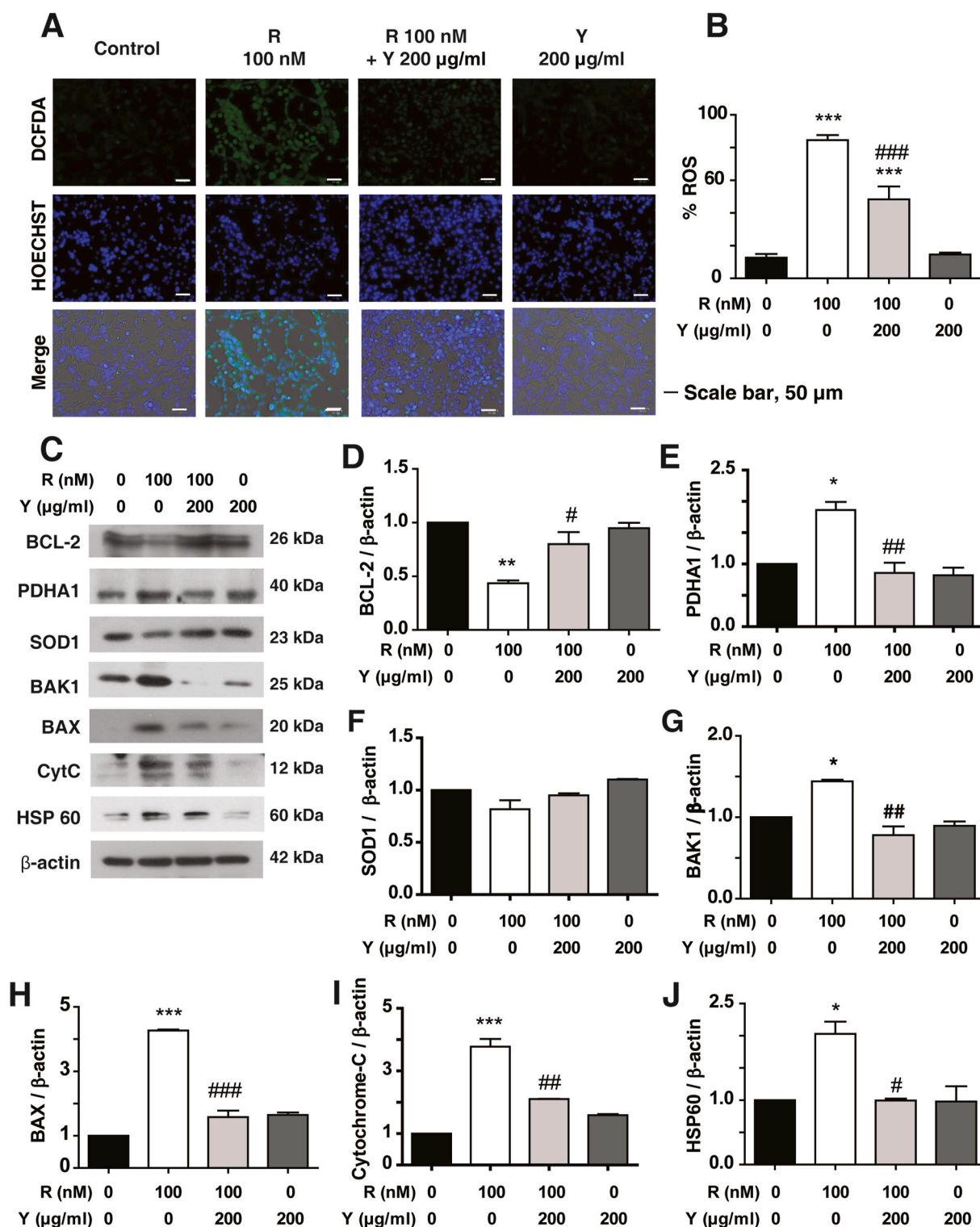


**Fig. 4.** Yashtimadhu counters ROS production and rotenone-induced mitochondrial proteins. Cells were treated with rotenone (100 nM), Yashtimadhu (200 µg/ml), their co-treatment, and untreated cells were taken as control. (A) Rotenone induces ROS production as stained by DCFDA (green) and counterstain HOECHST (blue). Yashtimadhu co-treatment reduced the ROS levels, (B) Graphical representation of ROS production, (C) Immunoblot analysis showing the expression of BCL-2, PDHA1, SOD1, BAK, BAX, cytochrome-C, and HSP60. Yashtimadhu increased BCL-2 levels and countered rotenone-induced mitochondrial key proteins such as; PDHA1, BAK, BAX, cytochrome-C and HSP60. Graphical representation of protein fold change, (D) BCL-2, (E) PDHA1, (F) SOD1, (G) BAK, (H) BAX, and (I) Cytochrome C, (J) HSP60. \* $p < 0.05$ , \*\* $p < 0.01$ , \*\*\* $p < 0.001$ , compared to control and # $p < 0.05$ , ## $p < 0.01$ , ### $p < 0.001$ , compared to rotenone. (For interpretation of the references to colour in this figure legend, the reader is referred to the Web version of this article.)

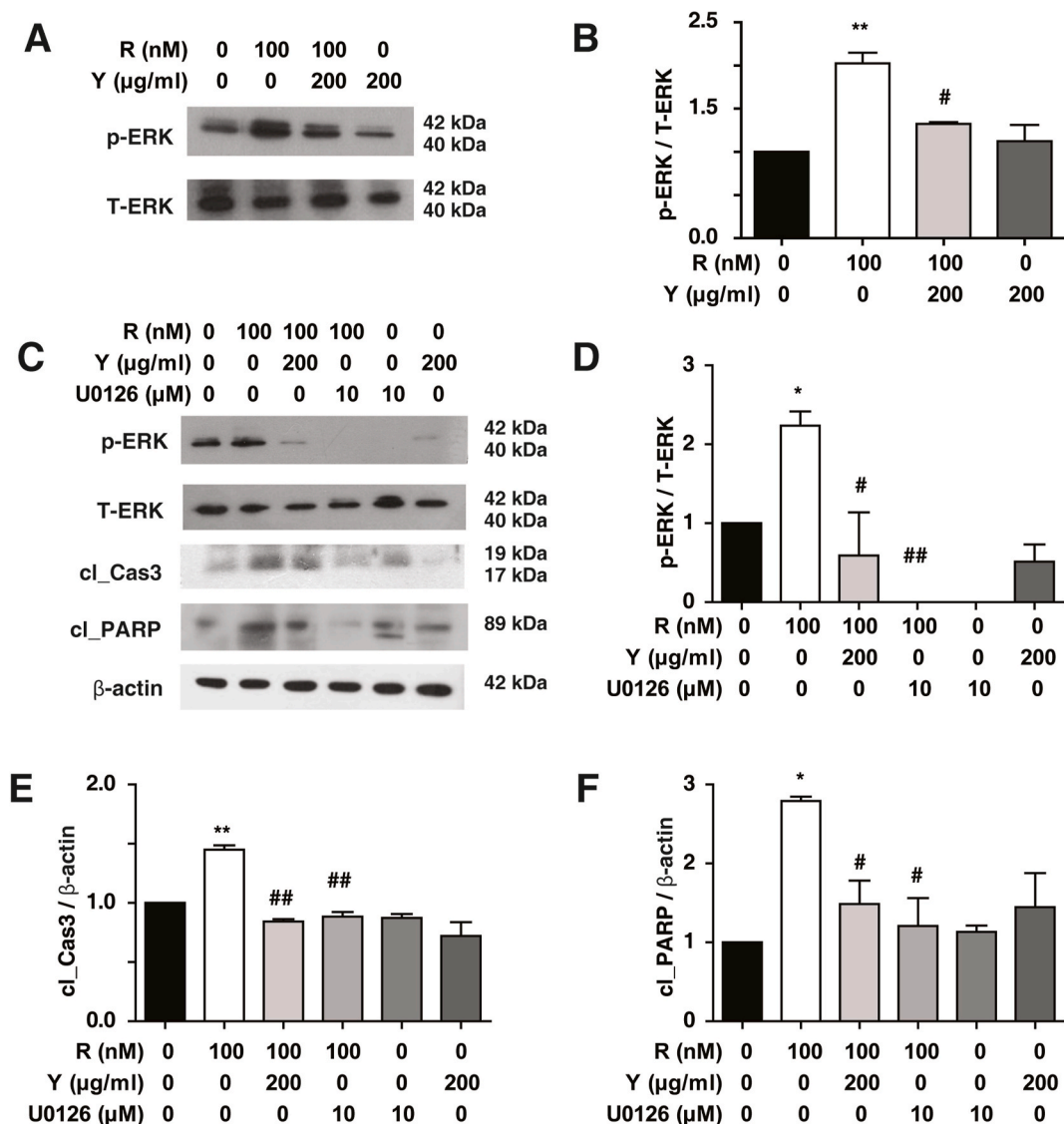


**Fig. 5.** Yashtimadhu confers neuroprotection by preventing MEK-ERK-1/2 hyper-activation. Cells were treated with rotenone (100 nM), Yashtimadhu (200 µg/ml), U0126 (10 µM), and untreated cells were taken as control. (A) Immunoblot showing rotenone-induced ERK-1/2 hyper-phosphorylation with total-ERK-1/2, (B) Graphical representation of phospho-ERK-1/2 normalized with total-ERK-1/2, (C) Immunoblot analysis after U0126 co-treatment, for pERK-1/2, T-ERK-1/2, cleaved-caspase-3, and cleaved-PARP. Graphical representation of (D) phospho-ERK-1/2,; (E) Cleaved-caspase-3 and (F) Cleaved-PARP.  $^{*}p < 0.01$ , compared to control and  $^{#}p < 0.05$ , compared to rotenone.

authentically confirmed it. PKM, SKP and TSKP participated in data analysis, critically reviewed and edited the manuscript. All authors read and approved the final version of the manuscript.

#### Acknowledgments

The authors thank Dr. Harkrishna Panaje, SDP Remedies, and Research Centre for authenticating the specimen and providing the details of Yashtimadhu choorna. The authors thank Dr. Pushkar Sharma, Staff Scientist, National Institute of Immunology, India, for providing key antibodies used in this study. The authors also thank Dr. Ashwini Prabhu, Yenepoya Research Centre, for helping with cell cycle analysis.

#### Appendix A. Supplementary data

Supplementary data to this article can be found online at <https://doi.org/10.1016/j.jep.2021.114025>.

#### Funding

The work was partially funded by Karnataka Biotechnology and Information Technology Services, Government of Karnataka, for support under the Biotechnology Skill Enhancement Programme in Multiomics Technology (BiSEP GO ITD O2MDA2017), and Yenepoya (Deemed to be University) Seed grant(YU/Seed grant/077–2019). GK was a recipient of Senior Research Fellowship from Council of Scientific & Industrial Research (CSIR), Government of India (2014–2019), and is currently a recipient of “DST-KSTePs Ph.D. Fellowship” from the Department of Science and Technology-Karnataka Science and Technology Promotion Society, Government of Karnataka (2020–2021).

#### Author disclosure

The authors declare no conflict of interest..

## References

- Asha, M.K., Debraj, D., Prashanth, D., Edwin, J.R., Srikanth, H.S., Muruganatham, N., Dethle, S.M., Anirban, B., Jaya, B., Deepak, M., Agarwal, A., 2013. In vitro anti-Helicobacter pylori activity of a flavonoid rich extract of Glycyrrhiza glabra and its probable mechanisms of action. *J. Ethnopharmacol.* 145 (2), 581–586.
- Bose, B., Kapoor, S., Sen, U., Nihad, A.S., Chaudhury, D., Shenoy, P.S., 2020. Assessment of oxidative damage in the primary mouse ocular surface cells/stem cells in response to ultraviolet-C (UV-C) damage. *J. Vis. Exp.* 156.
- Chakravarthi, K.K., Avadhani, R., 2013. Beneficial effect of aqueous root extract of Glycyrrhiza glabra on learning and memory using different behavioral models: an experimental study. *J. Nat. Sci. Biol. Med.* 4 (2), 420–425.
- Chandra, D., Liu, J.W., Tang, D.G., 2002. Early mitochondrial activation and cytochrome c up-regulation during apoptosis. *J. Biol. Chem.* 277 (52), 50842–50854.
- Chia, S.J., Tan, E.K., Chao, Y.X., 2020. Historical perspective: models of Parkinson's disease. *Int. J. Mol. Sci.* 21 (7).
- Cho, M.J., Kim, J.H., Park, C.H., Lee, A.Y., Shin, Y.S., Lee, J.H., Park, C.G., Cho, E.J., 2018. Comparison of the effect of three licorice varieties on cognitive improvement via an amelioration of neuroinflammation in lipopolysaccharide-induced mice. *Nutr. Res. Pract.* 12 (3), 191–198.
- Chotibut, T., Meadows, S., Kasanga, E.A., McInnis, T., Cantu, M.A., Bishop, C., Salvatore, M.F., 2017. Ceftriaxone reduces L-dopa-induced dyskinesia severity in 6-hydroxydopamine Parkinson's disease model. *Mov. Disord.* 32 (11), 1547–1556.
- Condello, S., Curro, M., Ferlazzo, N., Caccamo, D., Satriano, J., Ientile, R., 2011. Agmatine effects on mitochondrial membrane potential and NF-kappaB activation protect against rotenone-induced cell damage in human neuronal-like SH-SY5Y cells. *J. Neurochem.* 116 (1), 67–75.
- Cui, Y.M., Ao, M.Z., Li, W., Yu, L.J., 2008. Effect of glabridin from Glycyrrhiza glabra on learning and memory in mice. *Planta Med.* 74 (4), 377–380.
- Deolankar, S.C., Modi, P.K., Subbannayya, Y., Pervaje, R., Prasad, T.S.K., 2020. Molecular targets from traditional medicines for neuroprotection in human neurodegenerative diseases. *OMICS* 24 (7), 394–403.
- Djombou-Feunang, Y., Fiamoncini, J., Gil-de-la-Fuente, A., Greiner, R., Manach, C., Wishart, D.S., 2019. BioTransformer: a comprehensive computational tool for small molecule metabolism prediction and metabolite identification. *J. Cheminf.* 11 (1), 2.
- El-Saber Bathia, G., Magdy Beshbishy, A., El-Mleeh, A., Abdel-Daim, M.M., Prasad Devkota, H., 2020. Traditional uses, bioactive chemical constituents, and pharmacological and toxicological activities of Glycyrrhiza glabra L. (Fabaceae). *Biomolecules* 10 (3).
- Feng Yeh, C., Wang, K.C., Chiang, L.C., Shieh, D.E., Yen, M.H., San Chang, J., 2013. Water extract of licorice had anti-viral activity against human respiratory syncytial virus in human respiratory tract cell lines. *J. Ethnopharmacol.* 148 (2), 466–473.
- Gugliandolo, A., Pollastro, F., Bramanti, P., Mazzoni, E., 2020. Cannabidiol exerts protective effects in an in vitro model of Parkinson's disease activating AKT/mTOR pathway. *Fitoterapia* 143, 104553.
- Hayashi, H., Tamura, S., Chiba, R., Fujii, I., Yoshikawa, N., Fattokhov, I., Saidov, M., 2016. Field survey of Glycyrrhiza plants in central Asia (4). Characterization of G. glabra and G. Bucharica collected in Tajikistan. *Biol. Pharm. Bull.* 39 (11), 1781–1786.
- Hsu, S.L., Hsu, J.W., Liu, M.C., Chen, L.Y., Chang, C.D., 2000. Retinoic acid-mediated G1 arrest is associated with induction of p27(Kip1) and inhibition of cyclin-dependent kinase 3 in human lung squamous carcinoma CH27 cells. *Exp. Cell Res.* 258 (2), 322–331.
- Hu, X., Song, Q., Li, X., Li, D., Zhang, Q., Meng, W., Zhao, Q., 2017. Neuroprotective effects of Kukoamine A on neurotoxin-induced Parkinson's model through apoptosis inhibition and autophagy enhancement. *Neuropharmacology* 117, 352–363.
- Huo, H.Z., Wang, B., Liang, Y.K., Bao, Y.Y., Gu, Y., 2011. Hepatoprotective and antioxidant effects of licorice extract against CCl(4)-induced oxidative damage in rats. *Int. J. Mol. Sci.* 12 (10), 6529–6543.
- Ikram, F., Ackermann, S., Kahlert, Y., Volland, R., Roels, F., Engesser, A., Hertwig, F., Kocak, H., Hero, B., Dredix, D., Henrich, K.O., Berthold, F., Nurnberg, P., Westermann, F., Fischer, M., 2016. Transcription factor activating protein 2 beta (TFAP2B) mediates noradrenergic neuronal differentiation in neuroblastoma. *Mol. Oncol.* 10 (2), 344–359.
- Kalia, L.V., Lang, A.E., 2015. Parkinson's disease. *Lancet* 386 (9996), 896–912.
- Kalinderi, K., Papaliagkas, V., Fidani, L., 2019. Pharmacogenetics and levodopa induced motor complications. *Int. J. Neurosci.* 129 (4), 384–392.
- Karthikkeyan, G., Najjar, M.A., Pervaje, R., Pervaje, S.K., Modi, P.K., Prasad, T.S.K., 2020a. Identification of molecular network associated with neuroprotective effects of Yashtimadhu (Glycyrrhiza glabra L.) by quantitative proteomics of rotenone-induced Parkinson's disease model. *ACS Omega* 5 (41), 26611–26625.
- Karthikkeyan, G., Najjar, M.A., Pervaje, R., Subbannayya, Y., Patil, A.H., Modi, P.K., Prasad, T.S.K., 2020b. Plant omics: metabolomics and network pharmacology of liquorice, Indian ayurvedic medicine Yashtimadhu. *OMICS* 24 (12), 743–755.
- Kotapalli, S.S., Dasari, C., Duscharla, D., Kami Reddy, K.R., Kasula, M., Ummanni, R., 2017. All-trans-retinoic acid stimulates overexpression of tumor protein D52 (TPD52, isoform 3) and neuronal differentiation of IMR-32 cells. *J. Cell. Biochem.* 118 (12), 4358–4369.
- Kuang, Y., Li, B., Fan, J., Qiao, X., Ye, M., 2018. Antitussive and expectorant activities of licorice and its major compounds. *Bioorg. Med. Chem.* 26 (1), 278–284.
- Li, D.W., Li, G.R., Zhang, B.L., Feng, J.J., Zhao, H., 2016. Damage to dopaminergic neurons is mediated by proliferating cell nuclear antigen through the p53 pathway under conditions of oxidative stress in a cell model of Parkinson's disease. *Int. J. Mol. Med.* 37 (2), 429–435.
- Li, N., Ragheb, K., Lawler, G., Sturgis, J., Rajwa, B., Melendez, J.A., Robinson, J.P., 2003. Mitochondrial complex I inhibitor rotenone induces apoptosis through enhancing mitochondrial reactive oxygen species production. *J. Biol. Chem.* 278 (10), 8516–8525.
- Liu, J., Liu, W., Lu, Y., Tian, H., Duan, C., Lu, L., Gao, G., Wu, X., Wang, X., Yang, H., 2018. Piperlongumine restores the balance of autophagy and apoptosis by increasing BCL2 phosphorylation in rotenone-induced Parkinson disease models. *Autophagy* 14 (5), 845–861.
- Los, M., Mozulok, M., Ferrari, D., Stepczynska, A., Stroth, C., Renz, A., Herceg, Z., Wang, Z.Q., Schulze-Osthoff, K., 2002. Activation and caspase-mediated inhibition of PARP: a molecular switch between fibroblast necrosis and apoptosis in death receptor signaling. *Mol. Biol. Cell* 13 (3), 978–988.
- M, K.R., K, S.M., Nair, S.S., K, B.K., T, M.S., K, P.S., K, S., H, S., P, T.S.K., Neeli, C., Karunasagar, I., K, B.H., Karun, A., 2020. Facile coconut inflorescence sap mediated synthesis of silver nanoparticles and its diverse antimicrobial and cytotoxic properties. *Mater. Sci. Eng. C Mater. Biol. Appl.* 111, 110834.
- Ma, J., Gao, S.S., Yang, H.J., Wang, M., Cheng, B.F., Feng, Z.W., Wang, L., 2018. Neuroprotective effects of proanthocyanidins, natural flavonoids derived from plants, on rotenone-induced oxidative stress and apoptotic cell death in human neuroblastoma SH-SY5Y cells. *Front. Neurosci.* 12, 369.
- Modi, P.K., Komaravelli, N., Singh, N., Sharma, P., 2012. Interplay between MEK-ERK signaling, cyclin D1, and cyclin-dependent kinase 5 regulates cell cycle reentry and apoptosis of neurons. *Mol. Biol. Cell* 23 (18), 3722–3730.
- Mohamed, N.E., 2019. Effect of aqueous extract of Glycyrrhiza glabra on the biochemical changes induced by cadmium chloride in rats. *Biol. Trace Elem. Res.* 190 (1), 87–94.
- Noelker, C., Morel, L., Osterloh, A., Alvarez-Fischer, D., Lescot, T., Breloer, M., Gold, M., Oertel, W.H., Henze, C., Michel, P.P., Dodel, R.C., Lu, L., Hirsch, E.C., Hunot, S., Hartmann, A., 2014. Heat shock protein 60: an endogenous inducer of dopaminergic cell death in Parkinson disease. *J. Neuroinflammation* 11, 86.
- Nugroho, A.E., Wijayanti, A., Mutmainah, M., Susilowati, R., Rahmawati, N., 2016. Gastroprotective effect of combination of hot water extracts of licorice (Glycyrrhiza glabra), pulasari stem bark (Alyxia reinwardtii), and sembung leaf (blumea balsamifera) against aspirin-induced gastric ulcer model rats. *J. Evid. Based Compl. Altern. Med.* 21 (4), NP77–84.
- Petramfar, P., Hajari, F., Yousefi, G., Azadi, S., Hamed, A., 2020. Efficacy of oral administration of licorice as an adjunct therapy on improving the symptoms of patients with Parkinson's disease, A randomized double blinded clinical trial. *J. Ethnopharmacol.* 247, 112226.
- Pluskal, T., Castillo, S., Villar-Briones, A., Oresic, M., 2010. MZmine 2: modular framework for processing, visualizing, and analyzing mass spectrometry-based molecular profile data. *BMC Bioinf.* 11, 395.
- Poewe, W., Seppi, K., Tanner, C.M., Halliday, G.M., Brundin, P., Volkman, J., Schrag, A. E., Lang, A.E., 2017. Parkinson disease. *Nat. Rev. Dis. Primers* 3, 17013.
- Ray Chaudhuri, K., Qamar, M.A., Rajah, T., Loehrer, P., Sauerbier, A., Odin, P., Jenner, P., 2016. Non-oral dopaminergic therapies for Parkinson's disease: current treatments and the future. *NPJ Parkinsons Dis.* 2, 16023.
- Ryu, Y.K., Kang, Y., Go, J., Park, H.Y., Noh, J.R., Kim, Y.H., Hwang, J.H., Choi, D.H., Han, S.S., Oh, W.K., Lee, C.H., Kim, K.S., 2017. Hydrolyzed juponin prevents dopaminergic neuron death in 6-hydroxydopamine-induced models of Parkinson's disease. *J. Med. Food* 20 (2), 116–123.
- Sai, Y., Chen, J., Wu, Q., Liu, H., Zhao, J., Dong, Z., 2009. Phosphorylated-ERK 1/2 and neuronal degeneration induced by rotenone in the hippocampus neurons. *Environ. Toxicol. Pharmacol.* 27 (3), 366–372.
- Salat, D., Tolosa, E., 2013. Levodopa in the treatment of Parkinson's disease: current status and new developments. *J. Parkinsons Dis.* 3 (3), 255–269.
- Sarokte, A.S., Rao, M.V., 2013. Effects of Medhya Rasayana and Yogic practices in improvement of short-term memory among school-going children. *Ayu* 34 (4), 383–389.
- Schneider, C.A., Rasband, W.S., Eliceiri, K.W., 2012. NIH Image to ImageJ: 25 years of image analysis. *Nat. Methods* 9 (7), 671–675.
- Seewaldt, V.L., Dietze, E.C., Johnson, B.S., Collins, S.J., Parker, M.B., 1999. Retinoic acid-mediated G1-S-phase arrest of normal human mammary epithelial cells is independent of the level of p53 protein expression. *Cell Growth Differ.* 10 (1), 49–59.
- Sharifzadeh, M., Shamsa, F., Shiran, S., Karimfar, M.H., Miri, A.H., Jalalizadeh, H., Gholizadeh, S., Salar, F., Tabrizian, K., 2008. A time course analysis of systemic administration of aqueous licorice extract on spatial memory retention in rats. *Planta Med.* 74 (5), 485–490.
- Sheela, M.L., Ramakrishna, M.K., Salimath, B.P., 2006. Angiogenic and proliferative effects of the cytokine VEGF in Ehrlich ascites tumor cells is inhibited by Glycyrrhiza glabra. *Int. Immunopharm.* 6 (3), 494–498.
- Sheshagiri, S., Patel, K.S., Rajagopala, S., 2015. Randomized placebo-controlled clinical study on enhancement of Medha (intelligence quotient) in school going children with Yashtimadhu granules. *Ayu* 36 (1), 56–62.
- Silva, A.H., Fonseca, F.N., Pimenta, A.T., Lima, M.S., Silveira, E.R., Viana, G.S., Vasconcelos, S.M., Leal, L.K., 2016. Pharmacognostical analysis and protective effect of standardized extract and ziconic acid from Erythrina velutina against 6-hydroxydopamine-induced neurotoxicity in SH-SY5Y cells. *Phcog. Mag.* 12 (48), 307–312.
- Song, Z., Zhang, Y., Zhang, H., Rajendran, R.S., Wang, R., Hsiao, C.D., Li, J., Xia, Q., Liu, K., 2020. Isoliquiritigenin triggers developmental toxicity and oxidative stress-mediated apoptosis in zebrafish embryos/larvae via Nrf2-HO1/JNK-ERK/mitochondrion pathway. *Chemosphere* 246, 125727.
- Subbannayya, Y., Karthikkeyan, G., Pinto, S.M., Kapoor, S., Tyagi, A., Pervaje, S.K., Pervaje, R., Prasad, T.S.K., 2018. Global metabolite profiling and network pharmacology of Triphala identifies neuromodulatory receptor proteins as potential targets. *J. Protein Proteomics* 9 (2), 101–114.
- Sweatt, J.D., 2004. Mitogen-activated protein kinases in synaptic plasticity and memory. *Curr. Opin. Neurobiol.* 14 (3), 311–317.

- Tang, D., Wu, D., Hirao, A., Lahti, J.M., Liu, L., Mazza, B., Kidd, V.J., Mak, T.W., Ingram, A.J., 2002. ERK activation mediates cell cycle arrest and apoptosis after DNA damage independently of p53. *J. Biol. Chem.* 277 (15), 12710–12717.
- Tian, M., Yan, H., Row, K.H., 2008a. Extraction of glycyrrhizic acid and glabridin from licorice. *Int. J. Mol. Sci.* 9 (4), 571–577.
- Tian, M., Yan, H., Row, K.H., 2008b. Simultaneous extraction and separation of liquiritin, glycyrrhizic acid, and glabridin from licorice root with analytical and preparative chromatography. *Biotechnol. Bioproc. Eng.* 13 (6), 671–676.
- Tomiya, A., Tachibana, K., Suzuki, K., Seino, S., Sunayama, J., Matsuda, K.I., Sato, A., Matsumoto, Y., Nomiya, T., Nemoto, K., Yamashita, H., Kayama, T., Ando, K., Kitanaka, C., 2010. MEK-ERK-dependent multiple caspase activation by mitochondrial proapoptotic Bcl-2 family proteins is essential for heavy ion irradiation-induced glioma cell death. *Cell Death Dis.* 1, e60.
- Turcano, P., Mielke, M.M., Bower, J.H., Parisi, J.E., Cutsforth-Gregory, J.K., Ahlskog, J. E., Savica, R., 2018. Levodopa-induced dyskinesia in Parkinson disease: a population-based cohort study. *Neurology* 91 (24), e2238–e2243.
- Upadhyay, S., Mantha, A.K., Dhiman, M., 2020. Glycyrrhiza glabra (Licorice) root extract attenuates doxorubicin-induced cardiotoxicity via alleviating oxidative stress and stabilising the cardiac health in H9c2 cardiomyocytes. *J. Ethnopharmacol.* 258, 112690.
- Wang, H., Zhang, Z., Huang, J., Zhang, P., Xiong, N., Wang, T., 2014. The contribution of Cdc2 in rotenone-induced G2/M arrest and caspase-3-dependent apoptosis. *J. Mol. Neurosci.* 53 (1), 31–40.
- Wu, F., Wang, Z., Gu, J.H., Ge, J.B., Liang, Z.Q., Qin, Z.H., 2013. p38(MAPK)/p53-Mediated Bax induction contributes to neurons degeneration in rotenone-induced cellular and rat models of Parkinson's disease. *Neurochem. Int.* 63 (3), 133–140.
- Yang, Z., Wang, Y., Zhang, Y., He, X., Zhong, C.Q., Ni, H., Chen, X., Liang, Y., Wu, J., Zhao, S., Zhou, D., Han, J., 2018. RIP3 targets pyruvate dehydrogenase complex to increase aerobic respiration in TNF-induced necroptosis. *Nat. Cell Biol.* 20 (2), 186–197.
- Zeng, X.S., Geng, W.S., Jia, J.J., Chen, L., Zhang, P.P., 2018. Cellular and molecular basis of neurodegeneration in Parkinson disease. *Front. Aging Neurosci.* 10, 109.

# Plant Omics: Metabolomics and Network Pharmacology of Liquorice, Indian Ayurvedic Medicine Yashtimadhu

Gayathree Karthikkeyan,<sup>1</sup> Ravishankar Pervaje,<sup>2</sup> Yashwanth Subbannayya,<sup>1,\*</sup> Arun H. Patil,<sup>1</sup>  
Prashant Kumar Modi,<sup>1</sup> and Thottethodi Subrahmanya Keshava Prasad<sup>1</sup>

## Abstract

Plant omics is an emerging field of systems science and offers the prospects of evidence-based evaluation of traditional herbal medicines in human diseases. To this end, the powdered root of Yashtimadhu (*Glycyrrhiza glabra* L.), commonly known as liquorice, is frequently used in Indian Ayurvedic medicine with an eye to neuroprotection but its target proteins, mechanisms of action, and metabolites remain to be determined. Using a metabolomics and network pharmacology approach, we identified 98,097 spectra from positive and negative polarities that matched to ~1600 known metabolites. These metabolites belong to terpenoids, alkaloids, and flavonoids, including both novel and previously reported active metabolites such as glycyrrhizin, glabridin, liquiritin, and other terpenoid saponins. Novel metabolites were also identified such as quercetin glucosides, coumarin derivatives, beta-carotene, and asiatic acid, which were previously not reported in relation to liquorice. Metabolite–protein interaction-based network pharmacology analyses enriched 107 human proteins, which included dopamine, serotonin, and acetylcholine neurotransmitter receptors among other regulatory proteins. Pathway analysis highlighted the regulation of signaling kinases, growth factor receptors, cell cycle, and inflammatory pathways. *In vitro* validation confirmed the regulation of cell cycle, MAPK1/3, PI3K/AKT pathways by liquorice. The present data-driven, metabolomics and network pharmacology study paves the way for further translational clinical research on neuropharmacology of liquorice and other traditional medicines.

**Keywords:** liquorice, metabolomics, Ayurvedic medicine, Yashtimadhu, neuropharmacology, bioinformatics

## Introduction

**T**RADITIONAL HERBAL MEDICINES have been used in human diseases since time immemorial. Yet, their molecular mechanisms of action are not adequately characterized or remain unknown. There is a need for data-driven and evidence-based evaluation of traditional medicines and their systems scale effects.

Plant omics is an emerging field of systems science and offers veritable prospects for discovery and translational clinical research. In addition, the World Health Organization (WHO) has launched the WHO Traditional Medicine strategy 2014–2023 to strengthen and develop the role of traditional medicine practices in health. In the United States, National Center for Complementary and Alternative Medi-

cine (NCCAM) and Food and Drug Administration (FDA) are involved in the regulation of complementary and alternative medicinal (CAM) practices (Ventola, 2010), and in the European Union, CAMBrella European research network is involved in the regulation of CAM (Wiesener et al., 2012). In India, the Ministry of AYUSH acts as the regulatory body that regulates and promotes the use of Ayurvedic medicines.

The powdered root of Yashtimadhu (*Glycyrrhiza glabra* L.), commonly known as liquorice, is frequently used in Indian Ayurvedic medicine for human diseases, and in neurology and psychiatry-related clinical contexts in particular (Hosseinzadeh and Nassiri-Asl, 2015; Hwang et al., 2006; Shen et al., 2013; Yu et al., 2008). On the contrary, liquorice target proteins, mechanisms of action, and metabolites remain to be determined. Recently, we have shown that

<sup>1</sup>Center for Systems Biology and Molecular Medicine, Yenepoya Research Centre, Yenepoya (Deemed to be University), Mangalore, India.

<sup>2</sup>Sushrutha Ayurveda Hospital, Puttur, India.

\*Present address: Centre of Molecular Inflammation Research (CEMIR), Norwegian University of Science and Technology, Kunnskapssenteret, 3rd Floor Olav Kyrres Gate 10, NTNU Campus Øya, Trondheim, Norway 7030.



Yashtimadhu confers neuroprotection in rotenone-induced *in vitro* model of Parkinson's disease by restoration of dysregulated proteins, using quantitative proteomic approaches (Karthikkeyan et al., 2020).

We report here a metabolomics and network pharmacology approach to decipher the molecular correlates of liquorice at the level of metabolome that paves the way for further translational clinical research on neuropharmacology of liquorice and other traditional medicines.

## Materials and Methods

### Material procurement

This study has been approved by the Institutional Scientific Review Board (YRC SRB/028/2017).

Liquorice Ayurvedic preparation (Lot No. 64) was procured from SDP Remedies and Research Centre. The roots of liquorice were collected by SDP Remedies and Research Centre, and a specimen of it is maintained in the center with the identifier SDP/YM/001-2017.

The industrial process includes the following steps: the roots of liquorice were washed and dried under shade-net, followed by vacuum-drum drying. The dried roots were further pulverized and sieved to obtain a fine powder with a yield of ~90%. LC-MS grade solvents were used for extraction and mass spectrometry analysis; chromatographic grade methanol, acetonitrile, and formic acid were procured from Merck (Merck KGaA, Germany)

### Metabolite extraction

Metabolite extraction was carried out with a 2:2:1 ratio of methanol:acetonitrile:water in the ratios described by Lau et al. (2015), with minor modifications. The solvent mixture was added to 50 mg of liquorice root powder and incubated for 1 min at room temperature. It was sonicated for 10 min in an ultrasonic water bath and centrifuged at 12,000 *g* for 15 min at 4°C. The supernatant was collected and proceeded for liquid chromatography–tandem mass spectrometry (LC-MS/MS) analysis.

### LC-MS/MS analysis

LC-MS/MS analysis of liquorice was carried out using QTRAP-6500 mass spectrometer (AB SCIEX, USA), coupled to Agilent Infinity II 1290 liquid chromatography system (Agilent Technologies, Inc., Santa Clara, CA, USA). ZORBAX Eclipse plus C18, RRHD (rapid resolution high definition) reverse phase column (2.1 × 150 mm, 1.8 μm), was used as the analytical column. Ten-microliter metabolite extract was injected into the chromatography column, which was resolved at a flow rate of 0.3 mL/min with a 20-min gradient with solvent A (0.1% formic acid in MilliQ water) and solvent B (0.1% formic acid in 90% acetonitrile). The gradient used was  $t=0-1$  min, 2% B;  $t=10$ , 30% B;  $t=11$ , 60% B;  $t=13-17$ , 95% B,  $t=17.2-20$ , 2% B. Data acquisition was carried out with the information-dependent acquisition (IDA) method, built with the enhanced mass spectra (EMS) and enhanced product ion (EPI), that is, EMS-IDA-EPI method (Li et al., 2019; Song et al., 2012).

Data were acquired in low mass mode, with the mass range of 50–1000 Da (mass windows for each scan; 50–102.87 Da with 0.0053 s, 102.87–308.63 Da with 0.0206 s and 308.63–

1000 Da with 0.0691 s) were scanned at a rate of 10,000 Da/s and with a dynamic fill time of 250 ms and a linear ion-trap fill time of 10 ms and dynamic background subtraction. The top five ions, based on their intensity from the EMS (MS1) mode, were used for fragmentation in the EPI (MS/MS) mode. The metabolite data were acquired in both positive and negative polarities.

The source parameters were set as follows: a probe temperature of 450°C, an ion source voltage of 4500 V for positive and –4500 V for negative modes, curtain gas at 30 psi, gas I and gas II at 35 psi, each. The declustering potential was set at 100 V for positive and –100 V for negative modes. The compound parameters were set as follows: a collision energy (CE) of 40 V in positive and –40 V in negative modes, with a CE spread of ±25 V, using high-energy collisionally activated dissociation. The mass spectrometry data were acquired in two different modes, positive and negative polarities separately. The samples were run three times in each of the modes.

### Data analysis

Metabolite data analysis for identification was carried out with the MZmine 2.31 open-source framework (Pluskal et al., 2010). QTRAP-6500 raw data files were converted to .mzML format using MSConvert, Proteo Wizard (Chambers et al., 2012).

Baseline correction was carried out with a base peak chromatogram with an asymmetric factor at a value of 0.001 U and smoothing at a value of 500 U. Centroid mode mass detection with a noise-level cutoff at 1.0E5 was used. The chromatogram was reconstructed with a minimal time span of 0.05 min and a minimum peak height of 1.0E5 was used at an *m/z* tolerance of 5 parts per million (ppm). Local minima search was used for chromatogram, deconvulsion and deisotoping of peaks was carried out with isotopic peak grouper algorithm, and adducts detection was carried out using [M+H]<sup>+</sup> and [M–H]<sup>–</sup> for the positive and negative modes, respectively.

RANSAC was used for chromatogram alignment with nonlinear modeling and peak finder algorithm for the gap filling. Metabolite assignment was performed with the Kyoto Encyclopedia of Genes and Genomes (KEGG) compounds ([www.genome.jp/kegg/compound/](http://www.genome.jp/kegg/compound/)) as the back-end database provided in MZmine online search option.

Metabolite mapping was carried out with the adducts mentioned previously, based on the polarity being analyzed at a precursor *m/z* error of 0.01 Da. For selected unassigned spectra, the Human metabolomics Database (HMDB, [www.hmdb.ca/](http://www.hmdb.ca/)) version 4.0 (Wishart et al., 2018) was used for metabolite identification at fragment level, using the information from CFM-ID, that is, Competitive Fragmentation Modeling-ID (Djombou-Feunang et al., 2019).

### Bioinformatics analysis

Metabolite features from KEGG database identification were analyzed for pathway enrichment, metabolite classes, and roles using MBROLE (<http://csbg.cnb.csic.es/mbrole2/>) version 2.0 (Lopez-Ibanez et al., 2016) and Metaboanalyst ([www.metaboanalyst.ca/](http://www.metaboanalyst.ca/)) version 4.0 (Xia and Wishart, 2016). Metabolite named for SMILES ID conversion was enabled with PubChem Identifier Exchange Service ([www.pubchem.ncbi.nlm.nih.gov/idexchange/idexchange.cgi](http://www.pubchem.ncbi.nlm.nih.gov/idexchange/idexchange.cgi)). Protein

interacting partners of metabolites were identified using BindingDB ([www.bindingdb.org](http://www.bindingdb.org)), a protein–small molecule interaction database based on experimental evidence (Gilson et al., 2016). A metabolite similarity score of  $\geq 0.85$  was used to identify the interacting target proteins and those hits with a score of 1.0 are considered exact matches. UniProt IDs retrieved from BindingDB were converted to official gene symbols using the biological Database network (<https://biobdnet-abcc.ncifcrf.gov/db/db2db.php>) tool (Mudunuri et al., 2009).

Protein interaction network, Gene Ontology classification, and metabolite–protein joint pathway analysis was carried out with PANTHER, STRINGdb, and Metaboanalyst, respectively (Mi et al., 2017; Szklarczyk et al., 2019). Reactome pathway database ([www.reactome.org](http://www.reactome.org)) was used for identifying the pathways and reactions (Fabregat et al., 2018).

### Cell culture

IMR32 cells were procured from Cell Line Repository, National Centre for Cell Science (NCCS), Pune, India and cultured in Dulbecco's modified Eagle's medium (DMEM) high glucose media with 10% fetal bovine serum (FBS). For differentiation, cells were seeded onto collagen-coated plates and treated with 10  $\mu\text{M}$  retinoic acid in 2% FBS media for 7 days. Cell viability with different concentrations of liquorice treatment (50, 100, 200, 500, 1000, and 1500  $\mu\text{g}/\text{mL}$ ) for 48 h was evaluated using MTT assay.

In brief, after liquorice treatment, cells were incubated with MTT dye for 4 h and the formazan crystals were dissolved with DMSO:ethanol (50:50) and read at 570 nm and background subtraction at 650 nm. Cell viability was expressed as a percentage of control cells. For cell cycle and western blotting analysis, cells were then treated with liquorice extract at 200  $\mu\text{g}/\text{mL}$  concentration with retinoic acid for 48 h, whereas untreated cells in differentiation media served as control.

### Western blot analysis

Liquorice-treated cells were washed with phosphate-buffered saline (PBS), scraped and collected with cell lysis buffer containing sodium dodecyl sulfate (4%) in triethylammonium bicarbonate (50 mM) with sodium orthovanadate (1 mM), sodium pyrophosphatase (2.5 mM), and beta-glycerophosphate (1 mM). The lysate was sonicated and heated at 95°C and protein content was estimated with bicinchoninic acid assay (BCA; Thermo).

An equal amount of proteins from each condition was resolved in SDS-PAGE and transferred onto nitrocellulose membrane (BioRad), which was blocked and incubated with respective primary and secondary antibodies. Blots were developed using ECL clarity substrate (BioRad) and imaged using X-ray film (Carestream, Kodak). ImageJ software was used for densitometry analysis. Antibodies against pERK (T202/Y204) and pAKT (S473) were procured from Cell Signal Technology,  $\beta$ -actin horseradish peroxidase-conjugated from Sigma, and anti-rabbit secondary antibody from Merck Millipore.

### Cell cycle analysis

Liquorice-treated cells were washed with 1 $\times$ PBS and trypsinized with 0.1% trypsin–EDTA solution (Gibco). The

detached cells were further resuspended in hypotonic buffer, prepared with propidium iodide (2  $\mu\text{g}/\text{mL}$ ), trisodium citrate (1 mg/mL), Triton X-100 (1  $\mu\text{L}/\text{mL}$ ), and RNase (100  $\mu\text{g}/\text{mL}$ ) and incubated in dark. The red fluorescence from propidium iodide was measured using Guava easyCyte (Millipore). Data analysis was carried out with ModFit software.

### Statistical analysis

Cell culture experiments, western blotting, and cell cycle analysis were carried out as independent biological triplicates. GraphPad Prism was used for statistical analysis of data from western blotting and cell cycle analysis. Statistical significance of the data was tested using analysis of variance for MTT assay and Student's *t*-test was used for western blotting and cell cycle analysis. The values are represented as mean  $\pm$  standard error of the mean. For the bioinformatics and *in vitro* analysis,  $p \leq 0.05$  is considered significant.

### Data availability

The mass spectrometry data have been submitted to MetaboLights (Haug et al., 2020), the metabolomics data repository ([www.ebi.ac.uk/metabolights/index](http://www.ebi.ac.uk/metabolights/index)) with the study identifier MTBLS983.

## Results

Mass spectrometry-based untargeted metabolomics of liquorice enabled the identification of 1595 nonredundant metabolites at MS1 level corresponding to 788 metabolites in positive and 807 in negative modes, whereas other metabolic features were unassigned using the KEGG database. To aid the assignment of select unassigned metabolite features at MS/MS level, CFM-ID information from the HMDB database was used. The protein interactors of liquorice were identified using the metabolite–protein binding database.

The mass spectrometry data of liquorice were compared with previously published reports on liquorice metabolomics (Supplementary Table S1) and several lead metabolites were identified in this study, such as glycyrrhizic acid, ononin, licorice saponin, coumarins, to name a few. A schematic of the workflow applied for the study and representative total ion chromatogram from the positive mode is given in Figure 1. The identified metabolites from MZmine searched data are presented in Supplementary Tables S2 and S3. The list of unassigned features from positive and negative modes is given in Supplementary Tables S4 and S5.

### Intense liquorice metabolite features observed

Metabolite abundance was evaluated based on their peak intensities. The top five *m/z* from both positive and negative modes were unassigned; therefore, the metabolites were manually matched to the *m/z* based on their precursor and fragment masses using HMDB. The reconstructed representative extracted ion chromatograms of these features are given in Supplementary Figure S1. In positive mode, 839.52 *m/z* (fragments, 469.2 and 487.2 *m/z*) was assigned to licorice saponin G2, 983.52 *m/z* (fragments, 453.24 and 615.12 *m/z*) was assigned to triglycerides.

In negative mode, glycyrrhizinate was one of the top identifiers, with 821.16 *m/z* precursor (fragment, 351.00,

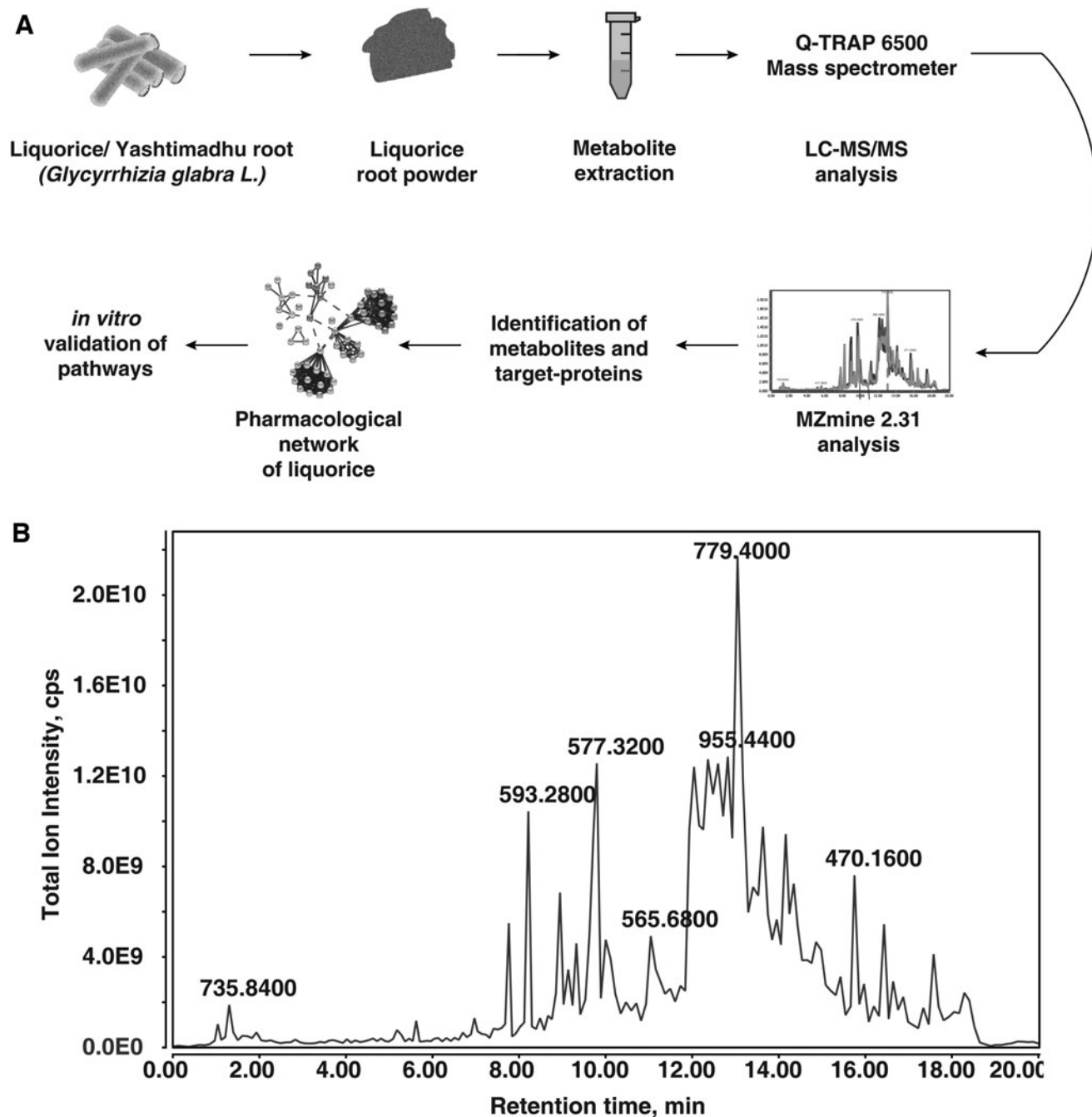


**FIG. 1.** Liquorice (Yashtimadhu) global metabolome analysis. **(A)** Schematic representation of metabolite extraction from liquorice root powder, followed by LC-MS/MS analysis using QTRAP-6500 and subsequent bioinformatics analysis. **(B)** Representative total ion chromatogram of liquorice metabolite analysis, in positive mode. LC-MS/MS, liquid chromatography–tandem mass spectrometry.

701.76 and 494.04 m/z). Precursor mass 881.52 m/z (fragments, 837.12 and 549.12 m/z) was assigned to two triterpenoid saponins with the same molecular formula and ppm error, which are elastoside E and pitheduloside B. Precursor mass 467.16 m/z (fragments, 448.9 and 367.32 m/z) was assigned to jangomolide, a steroid lactone and 778.2 m/z (fragments, 628.2 and 496.4 m/z) was assigned to various phospholipids. The list of top 20 metabolites from both assigned and unassigned metabolite features with their respective intensities and polarity is given in Table 1.

#### Signature metabolite identification

The most formulations that are used in traditional medicine have a set of signature metabolites that are specific to them based on species and geographical location. Several signature metabolites previously reported in licorice roots were identified, which include glycyrrhizinate (821.16 m/z), glabridin (324.82 m/z), isoflavone specific to *G. glabra*, liquiritin apioside (551.2 m/z), and licorice saponin G2 (839.52 m/z). Multiple putative identities were assigned for the precursor

TABLE 1. LIST OF INTENSE METABOLITES IDENTIFIED IN YASHTIMADHU

<i>m/z</i> , Da	<i>Retention time</i> , minutes	<i>Metabolite identification</i>	<i>Peak intensity</i>	<i>Polarity</i>
826.92	12.59	Cytidylyl molybdenum cofactor	5.83E+07	–
821.4	13.34	Glycyrrhizinate	6.50E+07	–
533.16	12.04	Dalpanin	6.77E+07	–
866.28	12.42	Anthemis glycoside A	6.79E+07	–
825.24	13.09	Pradimicin C	6.99E+07	–
593.16	8.2	Isoorientin 2''-O-rhamnoside	7.59E+07	–
953.4	12.42	Deltorpin A	8.16E+07	–
823.44	13.09	Yiamoloside B	1.98E+08	–
566.28	11.17	3'-Deoxydihydrostreptomycin	1.99E+08	–
563.04	8.89	UDP-3-ketoglucose	2.00E+08	–
467.16	16.34	Jangomolide	7.07E+07	–
778.2	13.35	Phospholipids	4.32E+07	–
839.52	12.34	Licorice saponin G2	2.00E+08	+
549.36	9.95	Manzamine A	1.98E+08	+
550.2	11.85	Jadomycin B	1.99E+08	+
565.32	11.13	Bonafousine	1.99E+08	+
563.4	8.93	3-Hexaprenyl-4,5-dihydroxybenzoate	1.99E+08	+
549.24	7.76	Bruceantin	1.99E+08	+
566.28	11.08	Coelichelin	1.99E+08	+
566.16	11.12	Pelargonidin 3-O-beta-D-sambubioside	1.99E+08	+
456.24	17.56	20-Hydroxyleukotriene E4	2.00E+08	+
593.28	8.24	Pheophorbide a	2.00E+08	+
983.52	12.23	Triglycerides	2.00E+08	+
881.52	12.28	Elastoside E or pitheduloside B	2.00E+08	+
837.72	12.49	Unassigned feature	1.99E+08	–
562.92	8.96	Unassigned feature	1.81E+08	–
807.96	13.21	Unassigned feature	1.99E+08	–
576.96	9.69	Unassigned feature	2.00E+08	–
566.4	11.19	Unassigned feature	1.99E+08	–
456.36	17.52	Unassigned feature	2.00E+08	–
879.72	12.41	Unassigned feature	2.00E+08	–
562.92	8.96	Unassigned feature	2.00E+08	–
880.2	12.32	Unassigned feature	2.00E+08	+
879.96	12.32	Unassigned feature	2.00E+08	+
593.4	8.2	Unassigned feature	2.00E+08	+
456.12	17.53	Unassigned feature	2.00E+08	+
576.6	9.68	Unassigned feature	2.00E+08	+
577.2	9.68	Unassigned feature	2.00E+08	+
837.48	12.61	Unassigned feature	2.00E+08	+
808.44	13.11	Unassigned feature	1.99E+08	+

418.11 *m/z* (with fragments 330.21 and 312.24 *m/z*), which were liquiritin, isoliquiritin, or barbaloin. Without targeted methods with standards, the identification could not be further assigned. Representative spectra of these signature metabolites are given in Figure 2A–E and in Table 2.

#### Unassigned metabolic features

The unidentified metabolic features cannot be ruled out as they might contain invaluable information regarding the molecular make-up of the formulation, which can be deduced by their fragment information. The representative MS/MS spectra

and the extracted ion chromatogram of these intense/abundant features from both positive and negative modes are given in Supplementary Figure S1. It is noteworthy that the reporting of the only assigned features may be equivalent to seeing the tip of the iceberg, as there are a large number of unassigned features, which may have the functions similar to the known features.

#### Metabolite classification based on chemical class and cellular compartmentalization

The metabolites were classified based on their chemical classes and subcellular localization. The identified metabolites

TABLE 2. SIGNATURE METABOLITES OF LIQUORICE

<i>Signature metabolite</i>	<i>Precursor, m/z</i>	<i>Fragments, m/z</i>	<i>Retention time, min</i>	<i>Adduct</i>	<i>Molecular formula</i>
Glabridin	324.87	183.24; 266.16	14.00	[M–H]–	C20H20O4
Licorice saponin G2	839.52	469.2; 487.2	12.55	[M+H]+	C42H62O17
Liquiritin apioside	551.2	257.04; 419.04; 135.04	11.94	[M+H]+	C26H30O13
Liquiritin	418.11	330.12; 312.24	10.06	[M–H]–	C21H22O9
Glycyrrhizinate	821.16	351.0; 701.76; 494.04	13.34	[M–H]–	C42H62O16

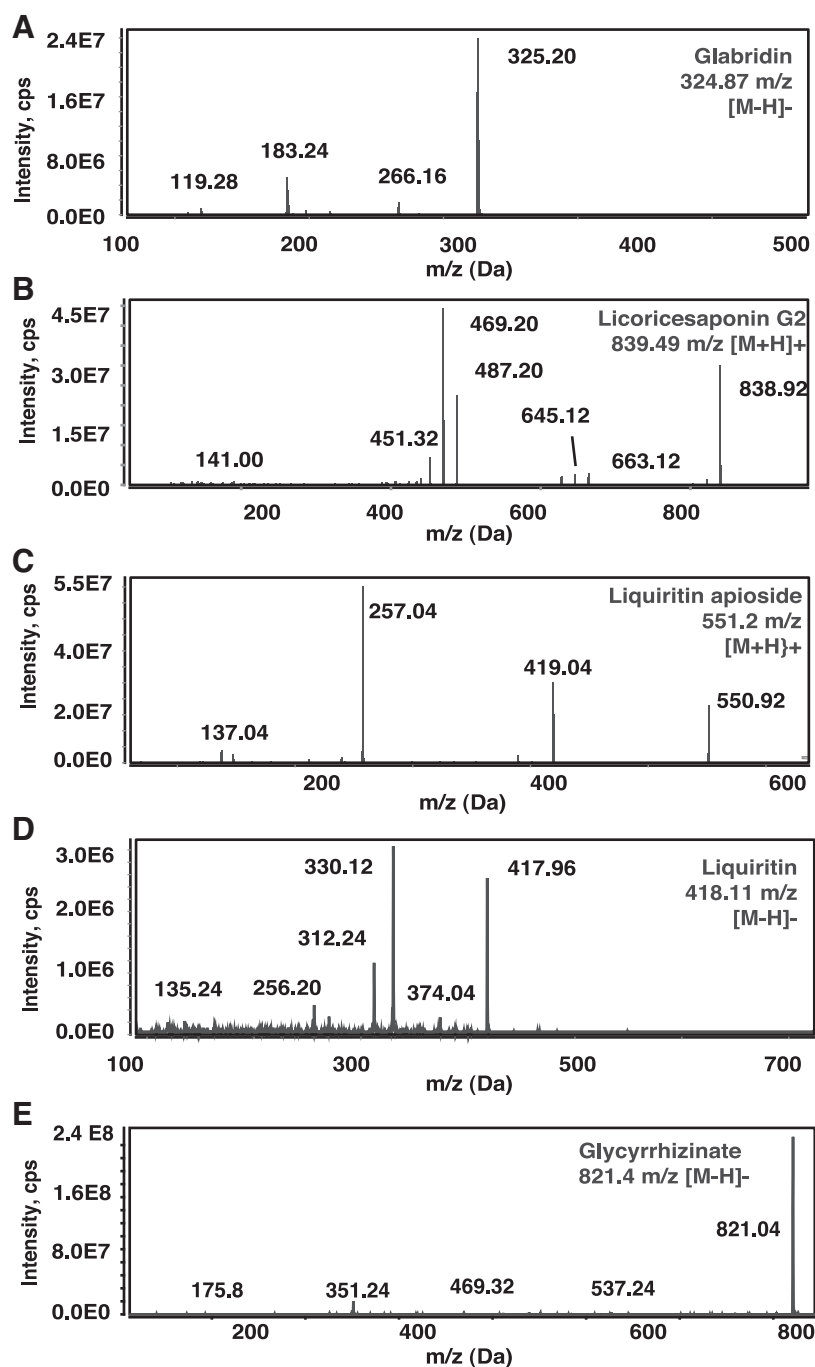


**FIG. 2.** MS/MS spectra of select lead metabolites of liquorice. (A) Glabridin, (B) licorice saponin G2, (C) liquiritin apioside, (D) liquiritin, and (E) glycyrrhizinate.

mapped to various categories, including terpenoids, diterpenoids, triterpenoids, alkaloids, phenylpropanoids, flavanols, anthocyanins, anthocyanidins, flavonoids, and betalains, to name a few, are given in Figure 3A. A select class of metabolite classification and a subset of metabolites mapped are given in Supplementary Table S6.

Assessment of cellular compartmentalization of metabolites showed enrichment of a significant number of metabolites to the intracellular space, with  $p \leq 0.05$ . The majority of the metabolites were localized to the cytoplasm, followed by the membrane, mitochondria, endoplasmic reticulum,

nucleus, peroxisome, Golgi apparatus, and lysosome represented in Figure 3B.

#### Metabolite pathway analysis

Metabolite pathway enrichment analysis was carried out with MBROLE, using *Arabidopsis thaliana* as the reference database, wherein various metabolites belonging to both primary and secondary metabolism have been described. Primary metabolism included amino acid and nucleotide metabolism, glycolysis/gluconeogenesis, oxidative phosphorylation,

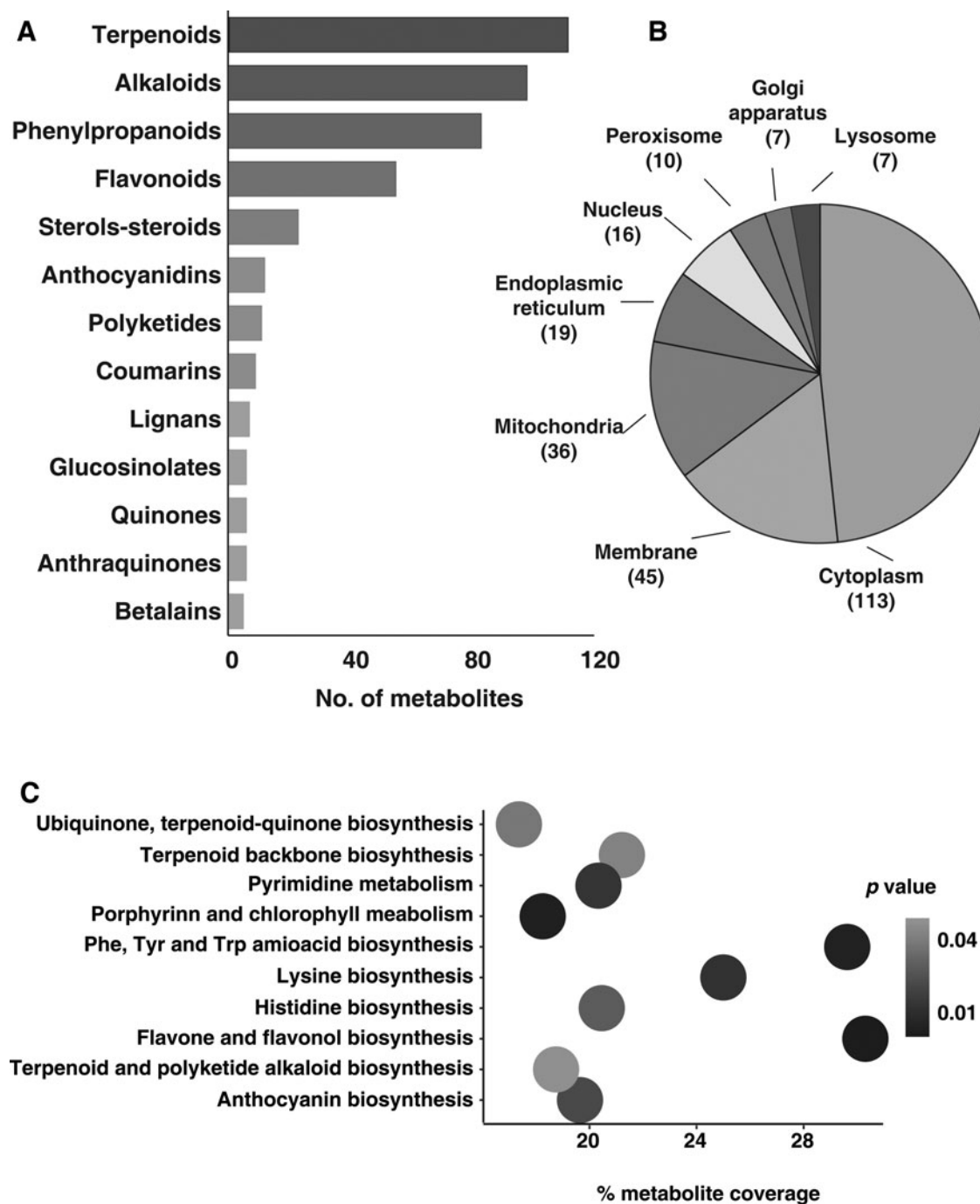


**FIG. 3.** Metabolite classification. (A) Metabolite classification based on chemical class. (B) Pie chart representing the classification of metabolite based on cellular location. (C) Bubble plot showing the metabolite pathway analysis based on % metabolite coverage, wherein the shades of the bubble represent the  $p$ -value.

and pentose pathway. Secondary metabolism enrichment with  $p \leq 0.05$  were flavones and flavonoids, isoquinoline, terpenoid, and polyketide alkaloid metabolism. Graphical representation of the pathway enrichment analysis is given in Figure 3C and Supplementary Table S7.

#### Target proteins of liquorice metabolites

Metabolites are not just the signatures of metabolism; they also influence various biochemical pathways by interacting

with different proteins involved in these pathways. Phytochemical metabolites and small molecules have been shown to interact with proteins, and the BindingDB database was used to predict the target proteins of liquorice metabolites. The BindingDB online tool provides information on protein-metabolite interaction, using the SMILES ID of the metabolite. To enable the identification of protein targets of the metabolites, they were converted to their respective SMILES ID.

The metabolite-protein interaction is based on metabolite structure and its potential or experimentally proven

interaction with a protein; a total of 107 protein interactors were identified, of which 20 were identified with exact structural matches (1.0 score) and 91 were identified with similarity matches ( $\geq 0.85$  score), given in Supplementary Table S8. The proteins included several cell surface receptors of neurotransmitters and growth factors and signaling kinases. The categorization of these proteins based on their functions and subcellular localization is given in Figure 4A.

Protein–metabolite interaction-based integrated pathway analysis was carried out to predict the pathways in humans that are induced or altered by licorice metabolites. Of the target proteins identified, receptors were found to be the dominant class of proteins, followed by the proteins with enzymatic activities such as hydrolases, isomerases, transferases, oxidoreductases, and enzyme modulators, given in Supplementary Table S9. Proteins with calcium-, chaperone-, transcription factor- and nucleic acid-binding activities were also identified, which provide an overall idea on the effect of the metabolites on cellular and molecular pathways.

Reactome pathway analysis showed enrichment of dopaminergic, serotonergic, neuropeptide, NMDA receptors, and synaptic pathways, given in Figure 4B. Apart from these, several exciting and central signaling pathways that of mitogen-activated protein kinases ERK-1/2, that is, MAPK1/3 and p38 MAPK, RAS signaling, G-protein-coupled receptor signaling (GPCR), PI3K/AKT, and cell cycle pathways were also identified, which are represented in Figure 5A.

#### *In vitro validation of licorice on differentiated IMR32 cells*

To validate the findings from the predictive analysis of licorice protein targets, retinoic acid-differentiated IMR32 cells were used. Cells were treated with different concentrations of licorice root extract from 50 to 1500  $\mu\text{g}/\text{mL}$  concentration for 48 h and evaluated cell viability using MTT assay (Supplementary Fig. S2). Treatment with licorice root extract was nontoxic at all tested concentrations and 200  $\mu\text{g}/\text{mL}$  concentration of treatment was selected to evaluate its impact on select cellular pathways such as MAPK1/MAPK3 pathway, PI3K/AKT pathway, and cell cycle on differentiated IMR32 cells given in Figure 5C–E.

The cell cycle analysis revealed that the G0/G1 population of cells to be unchanged in control (56.5%) and licorice (57%), whereas a significant increase in S-phase cells ( $p \leq 0.05$ ) and decrease in G2/M phase ( $p \leq 0.05$ ) with licorice (S-33.74%; G2/M-9.77%), compared with control (S-24.2%; G2/M-19.26). The phosphorylation status of pERK-T202/Y204 ( $p \leq 0.05$ ) and pAKT-S473 ( $p \leq 0.05$ ) were reduced with licorice treatment, compared with control, suggesting regulation of the MAPK1/MAPK3 and PI3K/AKT pathway. The *in vitro* analysis confirms the regulation of the cell cycle and signaling pathway, thereby validating the predictive regulation of protein targets of licorice.

#### *Network pharmacology of licorice metabolites and their protein targets*

To further understand the protein interacting partners of licorice metabolites, STRINGdb analysis was used to construct the protein–protein interaction network. The protein interaction network showed a prominent clustering of neurotransmitter receptors, into three sets of clusters. In addition,

several important kinases that were intertwined in the network are, signal transducer and activator of transcription-3 (STAT3), glycogen synthase kinase-3 (GSK3B), transforming protein-p21 (HRAS), proto-oncogene tyrosine-protein kinase (SRC), and cyclin-dependent kinases (CDK-1 and 2). The interaction network also features growth factors such as vascular endothelial growth factor-A (VEGFA), interleukin-1 (IL-1), fibroblast growth factor (FGF-1,2), epidermal growth factor (EGF), and its receptor (EGFR). The protein–protein interaction from STRINGdb is given in Figure 6. The network-pharmacology analysis suggests neuromodulation by interaction and regulating neurotransmitter receptors and intracellular signaling and responses mediated by licorice.

## Discussion

Licorice root formulation is widely used since time immemorial while there is a need to decipher its molecular mechanisms of action. Metabolic profiling of *G. glabra* has been reported to differ based on location, and we sought to understand the metabolome profile of the Indian origin licorice, that is, Yashtimadhu, using LC-MS/MS-based metabolomics and network pharmacology. This study focuses on two different aspects of metabolite profiling: (i) multiple solvent extraction to capture as many diverse classes of metabolites as possible, and (ii) an aqueous extraction to assess its biological effects on cell culture, which is based on its traditional usage.

This study highlights the active compounds with neuroprotective functions, including glycyrrhizic acid, liquiritin, liquiritigenin, licorice saponin G2, nononin, and glabridin, which were previously reported (Zhou et al., 2013). Glycyrrhizin is neuroprotective in the MPTP (1-methyl-4-phenyl-1,2,3,6-tetrahydropyridine) model of Parkinson's disease (PD) (Santoro et al., 2016), whereas isoliquiritigenin reportedly offers neuroprotection in a 6-hydroxydopamine model (Hwang and Chun, 2012), and while glabridin crosses the brain endothelial barrier (Hwang et al., 2006; Yu et al., 2008). The metabolomics analysis also highlighted the presence of asiatic acid, barbaloin, quercetin derivatives, coumarins, jadamycin B, dalpanin, deltropin A, jangomolide and, beta-carotene, to name a few.

This study explored the effect of licorice metabolites on the host system using bioinformatics approaches to identify and predict proteins interacting with licorice metabolites, wherein enrichment of neurotransmitter receptors and synaptic pathways were identified. These receptors included dopamine, serotonin, adenosine, and acetylcholine. Several signaling pathways were identified, including G-protein receptor signaling, MAPK1/3, PI3K/AKT, GSK-3 $\beta$ , and p38MAPK.

Studies have also suggested the role of GSK-3 $\beta$  in neuromodulation and regulation of p38MAPK by isoliquiritigenin from licorice (Chin et al., 2005; Hwang and Chun, 2012). Based on the pathway enrichment analysis, the regulation of cell cycle, phosphorylation of ERK-1/2 (MAPK1/3 pathway), and AKT (PI3K/AKT pathway) were analyzed. The involvement of the pathways, as mentioned previously, is reported to be involved normal brain functions and known to be dysregulated in neurodegeneration (Goncalves et al., 2011; Liu et al., 2014; Sai et al., 2009; Seo et al., 2014).

The regulation of basal phosphorylation of ERK-1/2 and AKT confirms the findings of the bioinformatics analysis.

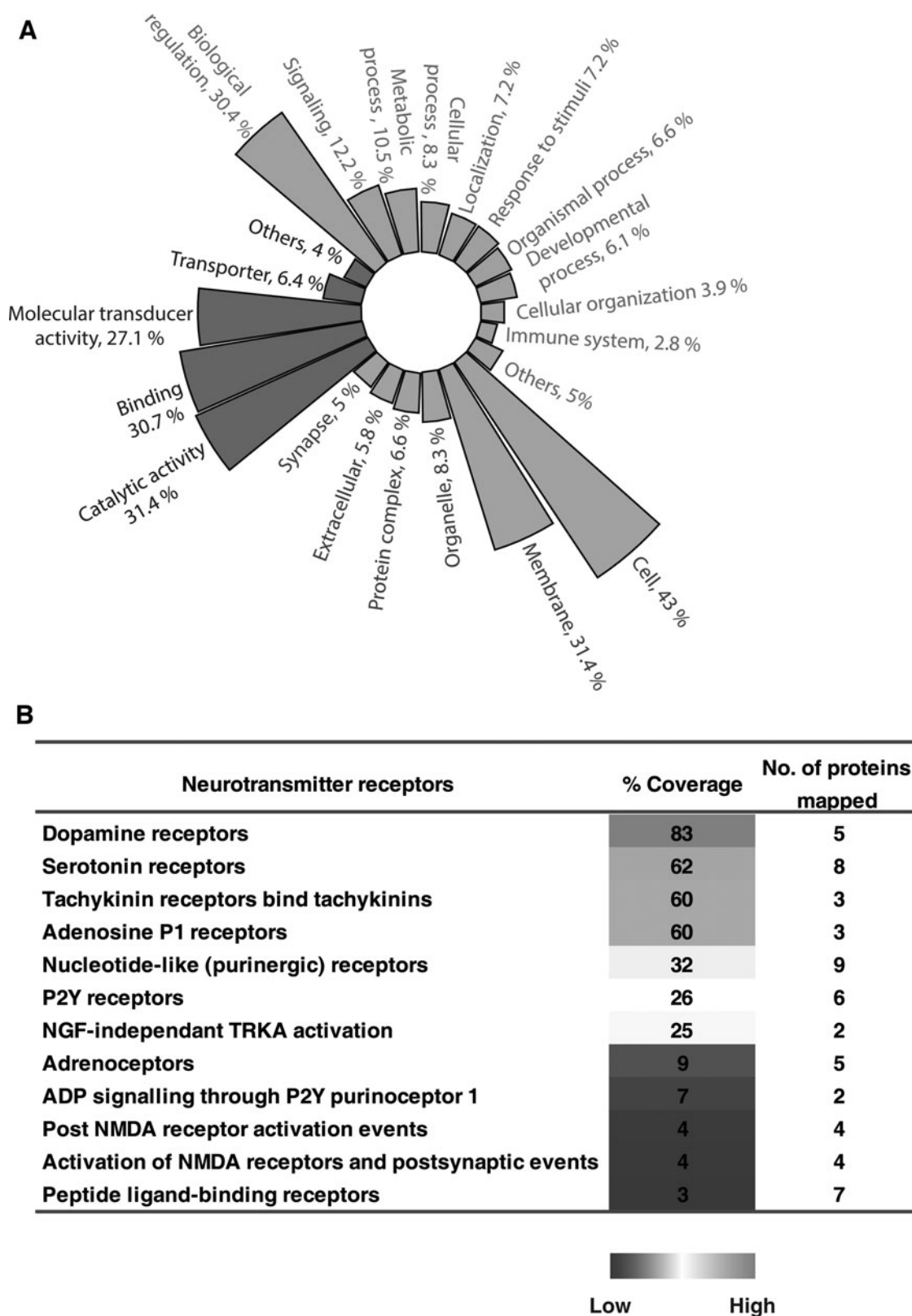


**FIG. 4.** Analysis of proteins interacting with liquorice metabolites. **(A)** Circular bar plot showing the classification of human proteins based on molecular function, biological process, and cellular localization. **(B)** Table showing coverage of different types of neurotransmitter receptors and the number of proteins identified in each type.



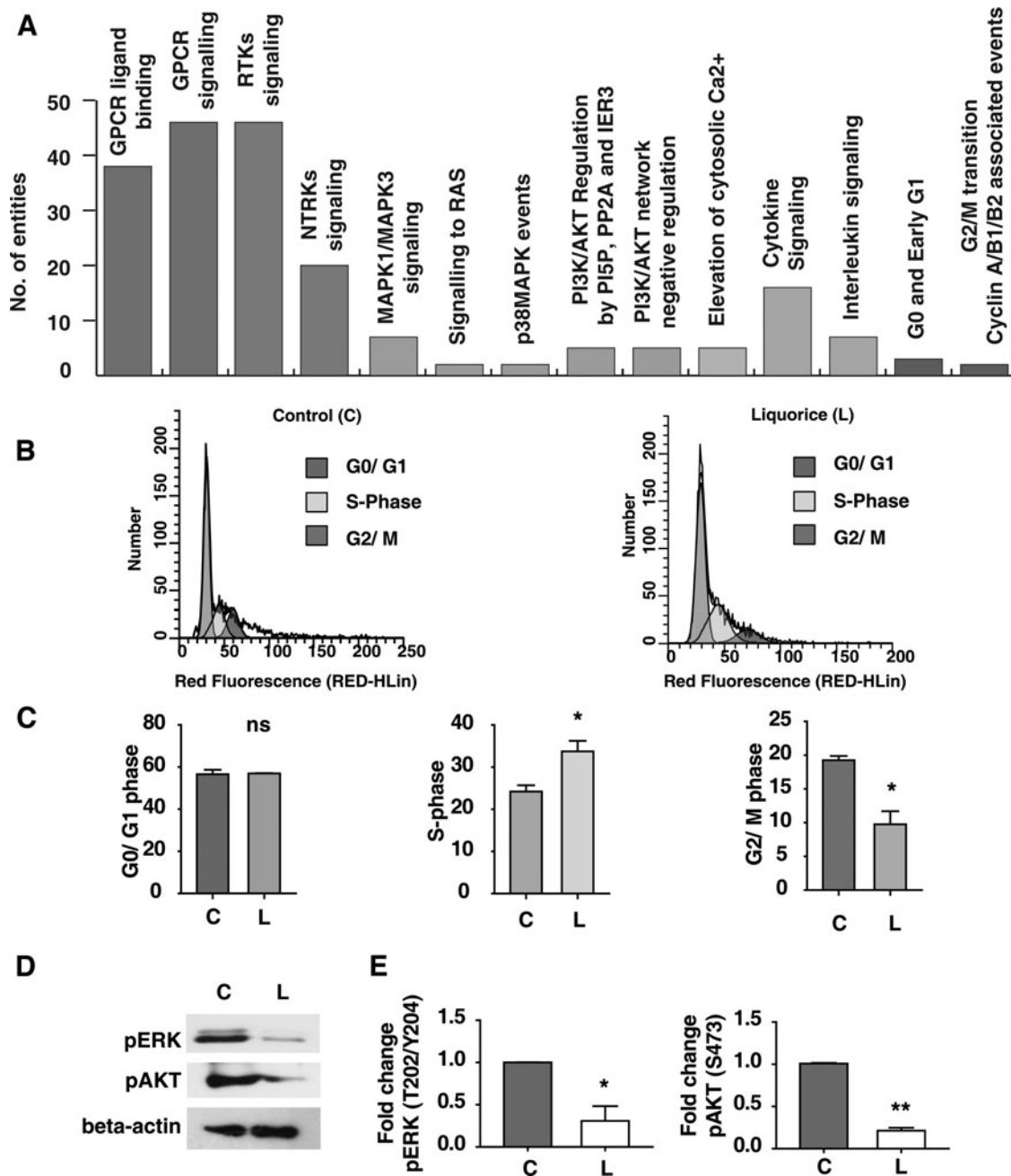


**FIG. 5.** Effect of liquorice extract on the host system processes. **(A)** Bar graph showing pathway analysis of interacting human proteins highlighting kinases, intracellular and inflammatory signaling, and cell cycle modulation. **(B)** Cell cycle analysis of untreated control cells (C) and liquorice-treated cells (L) treated with differentiated IMR32 cells. **(C)** Graphical representation of % cells in G0/G1, S, and G2/M phases. **(D)** Western blotting analysis of pERK (Thr202/Tyr204) and pAKT (Ser473), with  $\beta$ -actin as loading control. **(E)** Graphical representation of densitometry analysis and fold change of pERK and pAKT. \* $p \leq 0.05$  and \*\* $p \leq 0.01$ .

Dysregulation of cell cycle and mitotic re-entry through the ERK-1/2 pathway was reported to cause mitotic catastrophe and cell death (Modi et al., 2012). The regulation of both ERK-1/2 phosphorylation and cell cycle highlights the potential neuroprotective functions of liquorice. To the best of our knowledge, this is the first study exploring the metabolomics of liquorice and its host protein interactions using bioinformatics approaches.

This study used bioinformatics-based network pharmacology in understanding the mechanism of action of liquorice metab-

olites, and some of the pathways are validated *in vitro*; however, additional validation of the metabolite-protein interaction will prove beneficial in ascertaining the specific protein targets. In addition, the use of multiple fractionation methods of metabolite extraction will enable better coverage of metabolite classes present in traditional medicine. The characterization of the fractions will provide insights into the mechanistic actions of these metabolites and the pathways regulated by them.

The molecular components and protein interaction networks described in the study relied on the molecular features mapped

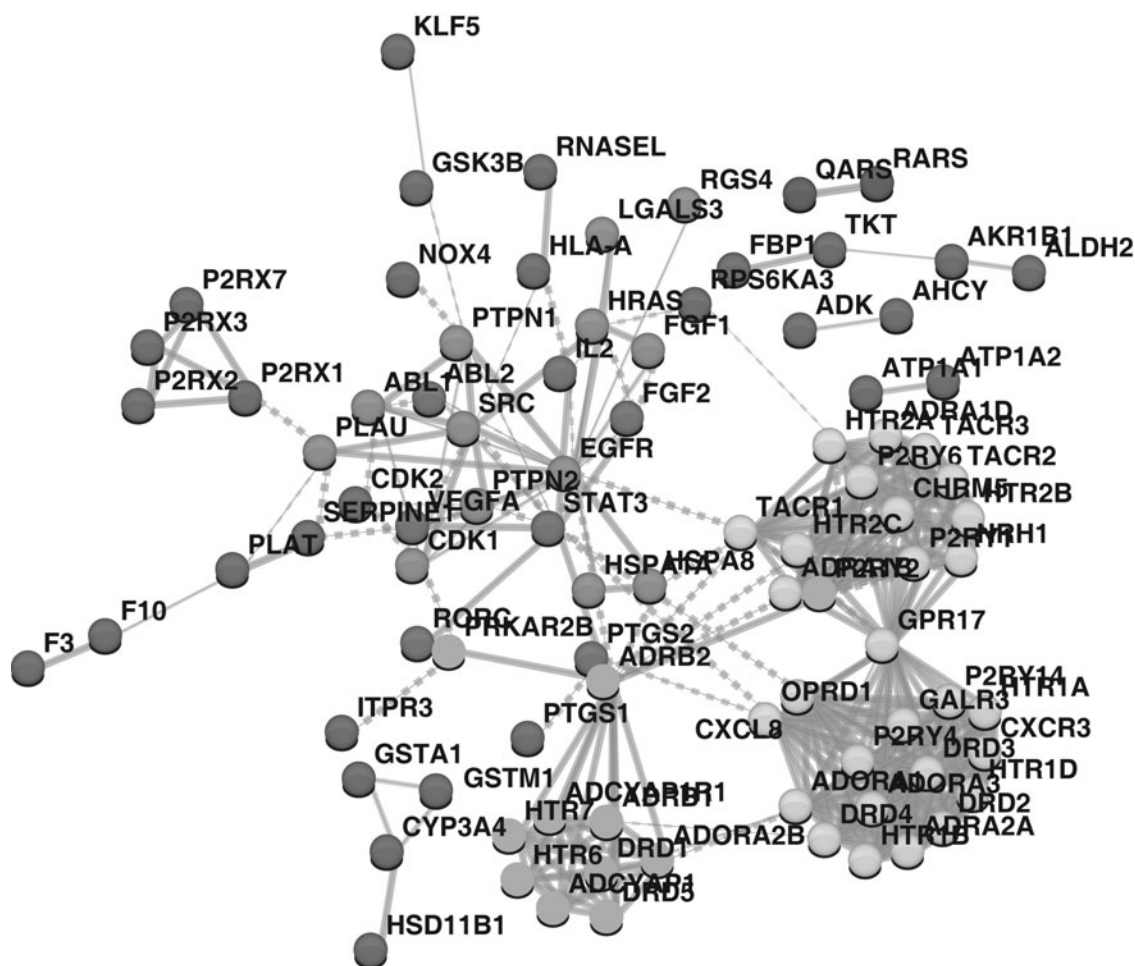


**FIG. 6.** Network pharmacology of liquorice. Protein–protein interacting network of protein targets of Yashtimadhu.

to known metabolites. There are a large number of metabolites yet to be annotated. The usage of multiple databases in addition to KEGG and HMDB, such as METLIN, PubChem, and LipidMaps (Fahy et al., 2007; Kim et al., 2019; Montenegro-Burke et al., 2020) may aid in increased putative metabolite identification; however, it may also lead to increased complexity of the data. Metabolite identification can be improved with species-specific databases that enable fragment-level identification using standards and retention time information for more efficient and confident metabolite identification.

Further work and implementation of standards/databases will allow identification of these unannotated molecular features to allow further unraveling of functional properties of traditional medicine. Our findings offer a baseline on which further discovery and translational investigations can be conducted in the field of plant omics, and with an eye to better understanding and evaluation of the neuropharmacology of liquorice and other traditional medicines.

#### Acknowledgments

The authors thank Karnataka Biotechnology and Information Technology Services (KBITS), Government of Karnataka, for support to the Center for Systems Biology and Molecular Medicine at Yenepoya (Deemed to be University), Mangalore, under the Biotechnology Skill Enhancement

Programme in Multiomics Technology (BiSEP GO ITD 02MDA2017). The authors thank Yenepoya (Deemed to be University) for access to instrumentation and providing financial assistance as a seed grant (YU/Seed grant/077–2019). G.K. was a recipient of Senior Research Fellowship from the Council of Scientific and Industrial Research (CSIR), Government of India (2014–2019), and is currently a recipient of KSTePs DST-PhD. Fellowship from the Department of Science and Technology-Karnataka Science and Technology Promotion Society, Government of Karnataka (2020–2021). All authors met the ICMJE authorship criteria and have read and approved the final version of the article.

#### Author Disclosure Statement

The authors declare they have no competing financial interests.

#### Funding Information

There was no direct funding for this work.

#### Supplementary Material

Supplementary Figure S1  
Supplementary Figure S2  
Supplementary Table S1

Supplementary Table S2  
 Supplementary Table S3  
 Supplementary Table S4  
 Supplementary Table S5  
 Supplementary Table S6  
 Supplementary Table S7  
 Supplementary Table S8  
 Supplementary Table S9

## References

- Chambers MC, Maclean B, Burke R, et al. (2012). A cross-platform toolkit for mass spectrometry and proteomics. *Nat Biotechnol* 30, 918–920.
- Chin PC, Majdzadeh N, and D’Mello SR. (2005). Inhibition of GSK3beta is a common event in neuroprotection by different survival factors. *Brain Res* 137, 193–201.
- Djoubou-Feunang Y, Pon A, Karu N, et al. (2019). CFM-ID 3.0: Significantly Improved ESI-MS/MS Prediction and Compound Identification. *Metabolites* 9, 72.
- Fabregat A, Jupe S, Matthews L, et al. (2018). The Reactome Pathway Knowledgebase. *Nucleic Acids Res* 46, D649–D655.
- Fahy E, Sud M, Cotter D, and Subramaniam S. (2007). LIPID MAPS online tools for lipid research. *Nucleic Acids Res* 35, W606–W612.
- Gilson MK, Liu T, Baitaluk M, Nicola G, Hwang L, and Chong J. (2016). BindingDB in 2015: A public database for medicinal chemistry, computational chemistry and systems pharmacology. *Nucleic Acids Res* 44, D1045–D1053.
- Goncalves AP, Maximo V, Lima J, Singh KK, Soares P, and Videira A. (2011). Involvement of p53 in cell death following cell cycle arrest and mitotic catastrophe induced by rotenone. *Biochim Biophys Acta* 1813, 492–499.
- Haug K, Cochran K, Nainala VC, Williams M, Chang J, Jayaseelan KV, O’Donovan C (2020). MetaboLights: a resource ending in response to the needs of its scientific community. *Nucleic Acids Res* 48, D440–D444.
- Hosseinzadeh H, and Nassiri-Asl M. (2015). Pharmacological Effects of Glycyrrhiza spp. and Its Bioactive Constituents: Update and Review. *Phytother Res* 29, 1868–1886.
- Hwang CK, and Chun HS. (2012). Isoliquiritigenin isolated from licorice *Glycyrrhiza uralensis* prevents 6-hydroxydopamine-induced apoptosis in dopaminergic neurons. *Biosci Biotechnol Biochem* 76, 536–543.
- Hwang IK, Lim SS, Choi KH, et al. (2006). Neuroprotective effects of roasted licorice, not raw form, on neuronal injury in gerbil hippocampus after transient forebrain ischemia. *Acta Pharmacol Sin* 27, 959–965.
- Karthikkeyan G, Najjar MA, Pervaje R, Pervaje SK, Modi PK, and Prasad TSK. (2020). Identification of Molecular Network Associated with Neuroprotective Effects of Yashtimadhu (*Glycyrrhiza glabra* L.) by Quantitative Proteomics of Rotenone-Induced Parkinson’s Disease Model. *ACS Omega* 41, 26611–26625.
- Kim S, Chen J, Cheng T, et al. (2019). PubChem 2019 update: Improved access to chemical data. *Nucleic Acids Res* 47, D1102–D1109.
- Lau SK, Lam CW, Curreem SO, et al. (2015). Identification of specific metabolites in culture supernatant of *Mycobacterium tuberculosis* using metabolomics: Exploration of potential biomarkers. *Emerg Microbes Infect* 4, e6.
- Li C, Yang J, Tong X, Zhao C, He Y, and Wan H. (2019). Precursor ion scan enhanced rapid identification of the chemical constituents of Danhong injection by liquid chromatography-tandem mass spectrometry: An integrated strategy. *J Chromatogr A* 1602, 378–385.
- Liu Q, Qiu J, Liang M, et al. (2014). Akt and mTOR mediate programmed necrosis in neurons. *Cell Death Dis* 5, e1084.
- Lopez-Ibanez J, Pazos F, and Chagoyen M. (2016). MBROLE 2.0-functional enrichment of chemical compounds. *Nucleic Acids Res* 44, W201–W204.
- Mi H, Huang X, Muruganujan A, et al. (2017). PANTHER version 11: Expanded annotation data from Gene Ontology and Reactome pathways, and data analysis tool enhancements. *Nucleic Acids Res* 45, D183–D189.
- Modi PK, Komaravelli N, Singh N, and Sharma P. (2012). Interplay between MEK-ERK signaling, cyclin D1, and cyclin-dependent kinase 5 regulates cell cycle re-entry and apoptosis of neurons. *Mol Biol Cell* 23, 3722–3730.
- Montenegro-Burke JR, Guijas C, and Siuzdak G. (2020). METLIN: A Tandem Mass Spectral Library of Standards. *Methods Mol Biol* 2104, 149–163.
- Mudunuri U, Che A, Yi M, and Stephens RM. (2009). bioDBnet: The biological database network. *Bioinformatics* 25, 555–556.
- Pluskal T, Castillo S, Villar-Briones A, and Oresic M. (2010). MZmine 2: Modular framework for processing, visualizing, and analyzing mass spectrometry-based molecular profile data. *BMC Bioinformatics* 11, 395.
- Sai Y, Chen J, Wu Q, Liu H, Zhao J, and Dong Z. (2009). Phosphorylated-ERK 1/2 and neuronal degeneration induced by rotenone in the hippocampus neurons. *Environ Toxicol Pharmacol* 27, 366–372.
- Santoro M, Maetzler W, Stathakos P, et al. (2016). In-vivo evidence that high mobility group box 1 exerts deleterious effects in the 1-methyl-4-phenyl-1,2,3,6-tetrahydropyridine model and Parkinson’s disease which can be attenuated by glycyrrhizin. *Neurobiol Dis* 91, 59–68.
- Seo HJ, Choi SJ, and Lee JH. (2014). Paraquat Induces Apoptosis through Cytochrome C Release and ERK Activation. *Biomol Ther* 22, 503–509.
- Shen B, Truong J, Helliwell R, Govindaraghavan S, and Sucher NJ. (2013). An in vitro study of neuroprotective properties of traditional Chinese herbal medicines thought to promote healthy ageing and longevity. *BMC Complement Altern Med* 13, 373.
- Song Y, Yang X, Jiang Y, and Tu P. (2012). Characterization of the metabolism of sibiricaxanthone F and its aglycone in vitro by high performance liquid chromatography coupled with Q-trap mass spectrometry. *J Pharm Biomed Anal* 70, 700–707.
- Szklarczyk D, Gable AL, Lyon D, et al. (2019). STRING v11: Protein-protein association networks with increased coverage, supporting functional discovery in genome-wide experimental datasets. *Nucleic Acids Res* 47, D607–D613.
- Ventola CL. (2010). Current Issues Regarding Complementary and Alternative Medicine (CAM) in the United States: Part 2: Regulatory and Safety Concerns and Proposed Governmental Policy Changes with Respect to Dietary Supplements. *P T* 35, 514–522.
- Wiesener S, Falkenberg T, Hegyi G, Hok J, Roberti di Sarsina P, and Fonnebo V. (2012). Legal status and regulation of complementary and alternative medicine in Europe. *Forsch Komplementmed* 2, 29–36.
- Wishart DS, Feunang YD, Marcu A, et al. (2018). HMDB 4.0: The human metabolome database for 2018. *Nucleic Acids Res* 46, D608–D617.
- Xia J, and Wishart DS. (2016). Using MetaboAnalyst 3.0 for Comprehensive Metabolomics Data Analysis. *Curr Protoc Bioinformatics* 55, 14.10.11–14.10.91.

Yu XQ, Xue CC, Zhou ZW, et al. (2008). In vitro and in vivo neuroprotective effect and mechanisms of glabridin, a major active isoflavan from *Glycyrrhiza glabra* (licorice). *Life Sci* 82, 68–78.

Zhou S, Cao J, Qiu F, Kong W, Yang S, and Yang M. (2013). Simultaneous determination of five bioactive components in radix glycyrrhizae by pressurised liquid extraction combined with UPLC-PDA and UPLC/ESI-QTOF-MS confirmation. *Phytochem Anal* 24, 527–533.

Address correspondence to:

*Thottethodi Subrahmanya Keshava Prasad, PhD*  
*Center for Systems Biology and Molecular Medicine*  
*Yenepoya Research Centre*  
*Yenepoya (Deemed to be University)*  
*Mangalore 575018*  
*India*

*E-mail: keshav@yenepoya.edu.in*

*Prashant Kumar Modi, PhD*  
*Center for Systems Biology and Molecular Medicine*  
*Yenepoya Research Centre*  
*Yenepoya (Deemed to be University)*  
*Mangalore 575018*  
*India*

*E-mail: prashantmodi@yenepoya.edu.in*

#### Abbreviations Used

AKT	=	RAC-alpha serine/threonine-protein kinase
CAM	=	complementary and alternative medicine
CE	=	collision energy
CFM-ID	=	competitive fragmentation modeling-ID
DMEM	=	Dulbecco's modified Eagle's medium
EGFR	=	epithelial growth factor receptor
EMS	=	enhanced mass spectra
EPI	=	enhanced product ion
FBS	=	fetal bovine serum
FGFR	=	fibroblast growth factor receptor
GPCR	=	G-protein-coupled receptor
GSK3B	=	glycogen synthase kinase 3 beta
HMDB	=	human metabolome database
IDA	=	information-dependent acquisition
KEGG	=	Kyoto Encyclopedia for Genes and Genomes
LC-MS/MS	=	liquid chromatography-tandem mass spectrometry
MAPK1/3	=	extracellular response kinase 1/2
MPTP	=	1-methyl-4-phenyl-1,2,3,6-tetrahydropyridine
NMDA	=	<i>N</i> -methyl-D-aspartate
PBS	=	phosphate-buffered saline
p38MAPK	=	p38-mitogen-activated protein kinase
PI3K	=	phosphoinositide 3-kinase
ppm	=	parts per million
RRHD	=	rapid resolution high definition
VEGFR	=	vascular endothelial growth factor receptor



# Ligand Binding Domain of Estrogen Receptor Alpha Preserve a Conserved Structural Architecture Similar to Bacterial Taxis Receptors

Divya Lakshmanan Mangalath<sup>1\*</sup> and Shabeer Ali Hassan Mohammed<sup>2,3</sup>

<sup>1</sup> Cancer Research and Therapeutics, Yenepoya Research Centre, Yenepoya University, Mangalore, India, <sup>2</sup> Division of Molecular Microbiology and Immunology, CSIR-Central Drug Research Institute, Lucknow, India, <sup>3</sup> Department of Biotechnology and Microbiology, Kannur University, Kannur, India

## OPEN ACCESS

### Edited by:

Ernesto Mollo,  
National Research Council (CNR), Italy

### Reviewed by:

Taisen Iguchi,  
Graduate University for Advanced  
Studies (Sokendai), Japan  
Michael Baker,  
University of California, San Diego,  
United States

### \*Correspondence:

Divya Lakshmanan Mangalath  
divyalmangalath@gmail.com;  
divya@yenepoya.edu.in

### Specialty section:

This article was submitted to  
Chemical Ecology,  
a section of the journal  
Frontiers in Ecology and Evolution

**Received:** 18 March 2021

**Accepted:** 21 June 2021

**Published:** 22 July 2021

### Citation:

Lakshmanan Mangalath D and  
Hassan Mohammed SA (2021)  
Ligand Binding Domain of Estrogen  
Receptor Alpha Preserve  
a Conserved Structural Architecture  
Similar to Bacterial Taxis Receptors.  
*Front. Ecol. Evol.* 9:681913.  
doi: 10.3389/fevo.2021.681913

It remains a mystery why estrogen hormone receptors (ERs), which are highly specific toward its endogenous hormones, are responsive to chemically distinct exogenous agents. Does it indicate that ERs are environmentally regulated? Here, we speculate that ERs would have some common structural features with prokaryotic taxis receptor responsive toward environmental signals. This study addresses the low specificity and high responsiveness of ERs toward chemically distinct exogenous substances, from an evolutionary point of view. Here, we compared the ligand binding domain (LBD) of ER alpha ( $\alpha$ ) with the LBDs of prokaryotic taxis receptors to check if LBDs share any structural similarity. Interestingly, a high degree of similarity in the domain structural fold architecture of ER $\alpha$  and bacterial taxis receptors was observed. The pharmacophore modeling focused on ligand molecules of both receptors suggest that these ligands share common pharmacophore features. The molecular docking studies suggest that the natural ligands of bacterial chemotaxis receptors exhibit strong interaction with human ER as well. Although phylogenetic analysis proved that these proteins are unrelated, they would have evolved independently, suggesting a possibility of convergent molecular evolution. Nevertheless, a remarkable sequence divergence was seen between these proteins even when they shared common domain structural folds and common ligand-based pharmacophore features, suggesting that the protein architecture remains conserved within the structure for a specific function irrespective of sequence identity.

**Keywords:** estrogen receptor, ligand binding domain, taxis receptors, domain architecture, nuclear hormone receptor

## HIGHLIGHTS

- ER-LBD shares structural folds with bacterial chemotaxis receptor LBD.
- Domain architecture is preserved by conserved structural folds, irrespective of sequence identity.
- Ligands for ER and bacterial chemotaxis receptors share common pharmacophore features.
- Ligands of bacterial chemotaxis receptors interacted with human ER and vice versa.

## INTRODUCTION

At present, the evolution of nuclear hormone receptors (NRs) is traced back up to protostomes such as plathelminths and mollusks (Kohler et al., 2007; Vogeler et al., 2014; Baker and Lathe, 2018; Wu and LoVerde, 2019). According to the present perspective, Amphioxus, a prochordate deuterostome, contains the most primitive estrogen receptor (ER) (Baker and Chandsawangbhuwana, 2008; Lecroisey et al., 2012). However, the full transcriptional function of the ER evolved hundreds of millions of years later after the evolution of early deuterostomes is reported (Kao et al., 2000; Baker and Chandsawangbhuwana, 2008; Callard et al., 2011). ER $\alpha$  is believed to be the most primitive among all the NRs reported so far. Sequence analysis indicates that the other NRs such as other ER subtypes, progesterone receptors, androgen receptors, glucocorticoid receptors, and mineralocorticoid receptors evolved from ER $\alpha$  through gene duplication and sequence divergence (Elliston and Katzenellenbogen, 1988; Thornton, 2001; Guerriero, 2009; Baker et al., 2015; Baker, 2019).

## LBD OF ESTROGEN HORMONE RECEPTORS ARE SPECIFIC TOWARD ITS ENDOGENOUS LIGAND

All the known NRs discovered so far adopts common structural and functional characteristics and consists of evolutionarily conserved, structurally and functionally distinct three to six basic domains (Lakshmanan and Shaheer, 2020). ERs are made up of an N-terminal domain, central DNA binding domain, C-terminal LBD, and two distinct, conformationally active regions designated as activation function 1 (AF-1) and activation function 2 (AF-2) (Lakshmanan and Sadasivan, 2014). DNA-binding domain (DBD) is the most conserved among the domains, and the N-terminal domain is most variable in sequence and length. ER signaling depends on the ligand/hormone and begins with the binding of ligand to LBD (Lakshmanan and Shaheer, 2020).

LBDs of nuclear hormones are specific toward its endogenous ligand and normally do not cross-interact with other non-specific endogenous hormones (Sasson and Notides, 1983; Klinge, 2001; Razandi et al., 2004; Yang et al., 2004; Morissette et al., 2008). On the other hand, they are responsive to metabolites and precursors of steroid hormones and wide variety of chemically distinct exogenous substances grouped as xenohormones. Both ER $\alpha$  and ER $\beta$  exhibits similar affinities for the endogenous hormones estradiol, estriol, and estrone (Sasson and Notides, 1983; Morissette et al., 2008).

## WHY ERs ARE RESPONSIVE TO AN ARRAY OF DIVERSE EXOGENOUS SUBSTANCES?

Estrogen hormone receptors exhibits least substrate specificity and strong binding affinities for most of the steroid/phenolic

and few of the non-phenolic/non-steroid agents classified as xenoestrogens (Cauley, 2015; Gore et al., 2015; Shafei et al., 2018; Pacyga et al., 2019; Rosenfeld and Cooke, 2019; Basak et al., 2020; Lakshmanan and Shaheer, 2020; Park et al., 2020). It is interesting to explore why a receptor that shows high specificity to its endogenous ligand can be transactivated by other hormone metabolites or chemically distinct exogenous agents. The present study was initiated to address this question through bioinformatics tools.

## LBD Structural Architecture Is Conserved Between ERs and Bacterial Taxis Receptors Irrespective of Sequence Divergence

Emergence of proteins with novel domain and/or domain combinations, generated by either homologous or non-homologous DNA repair or inserted into the genomes by transposition, is an important evolutionary mechanism, as it confers potentially diverse biological functions for the organisms (Itoh et al., 2007; Peisajovich et al., 2010; Forslund et al., 2019). Such domain accretion would have paved way in the emergence of novel proteins with specialized functions in the due course of eukaryotic evolution. While ERs are highly specific toward their endogenous hormone, they exhibit least substrate specificity and strong binding affinities toward array of exogenous ligand. This prompted us to speculate that LBD of ER alpha, the NR, would have some similarity with prokaryotic receptors responsive toward environmental signals (chemotaxis receptors). To prove this speculation, we downloaded the amino acid sequences and structures of LBDs of ER $\alpha$  and compared it with bacterial taxis receptors and sequences from other lower life forms such as protozoa and protostoma (**Table 1**) using Constraint-Based Multiple Alignment Tool (COBALT) and sequence-independent structural alignment (TM-align).

Analysis based on sequence similarity such as Basic Local Alignment Search Tool (BLAST), BLAST-Like Alignment Tool (BLAT), and CLUSTAL multiple sequence alignment tools are not reliable in detecting the homology of distantly related species if similarity of the protein sequence is <30% (Bhagwat et al., 2012; Moreno-Hagelsieb and Hudy-Yuffa, 2014; Ward and Moreno-Hagelsieb, 2014). Nevertheless, protein domain composition is anticipated to be conserved throughout the course of evolution due to functional constraints (Forslund et al., 2019; Yu et al., 2019). The function of a particular protein, to a great degree, is decided by the orderly arrangement of protein sequence to specific domains that constitutes domain architecture. Proteins with the same domain architecture may probably have similar structures and hence related cellular function (Koonin et al., 2002).

Constraint-based multiple alignment tool has advantage over other protein multiple sequence alignment tools in that it finds a set of pairwise constraints derived from conserved domain database and protein motif database and sequence similarity, using RPS-BLAST, BLASTP, and PHI-BLAST. Pairwise constraints were then integrated into a progressive multiple

alignment (Papadopoulos and Agarwala, 2007). All the protein sequences were downloaded from protein sequence database from NCBI. Protein structural files were downloaded from RCSB, protein databank, and COBALT and were used for multiple sequence alignment and prediction of common domain architecture. Molecular Evolutionary Genetics Analysis (MEGA) version X was used for constructing phylogenetic trees based on molecular evolution.

Interestingly, using COBALT, we found that LBDs of ER showed high conservation in domain architecture with all the selected sequences (Figure 1A and Supplementary Figure 1). Furthermore, we selected only the first four proteins shown in Table 1 and performed the COBALT alignment. All the four sequences, that is, LBDs of ER, nuclear receptor of *Ciona* sp., and two bacterial taxis receptors, exhibited high degree of conservation in domain architecture (Figure 1B and Supplementary Figure 2: first four sequence). As a validation to our hypothesis, we randomly selected some protein sequences (Supplementary Table 1) and repeated COBALT multiple sequence alignment. The result (Supplementary Figure 3) showed that the selected sequences have less conservation and more gaps.

The phylogenetic tree built for all the six sequences with mega gave an unrooted gene trees (Figure 1C) with clustering of genes into two separate groups. *Human ER* was clustered into a common clade with *Ciona* sp., and *Mytilus* sp. was an outgroup from this clade. Two bacterial chemoreceptors were clustered together. Tom40 of *Amoeba* was an outgroup

from the clade of bacterial receptors. Phylogenetic analysis showed that ERs and bacterial chemotactic receptors are evolutionarily unrelated.

Irrespective of their sequence and structural and functional diversity, ERs and other bacterial chemoreceptors such as taxis to serine and repellents (Tsr) and broad ligand-specific (BLS) receptor of *Pseudomonas putida* used in this study have certain common features such as a ligand binding domain (LBD) and homodimerization of the LBDs to exert their downstream signaling.

TM-align has advantage over other pairwise sequence alignment tools, as it confers sequence-independent protein structure comparison (Zhang and Skolnick, 2005). For any given two protein structures of unidentified similarity, the program uses heuristic dynamic programming iterations and initially generates optimized amino acid-to-amino acid alignment based on structural similarity. The tool then returns an optimal superposition of the two structures with a TM-score that can be used to scale the similarity. We performed TM-align to find a sequence-independent alignment based on local backbone similarity using heuristic dynamic programming iterations. The structures of LBDs of the serine receptor (Tsr) (PDB ID: 3ATP) of *Escherichia coli* with the LBD of ER-alpha (PDB ID: 1ERE) and LBDs of the chemoreceptor (BLS) (PDB ID: 6S33) of *P. putida* with the LBD of ER-alpha (PDB ID: 1ERE) were selected for TM-align.

Structural alignments with TM-align confirmed similar structural folds between LBDs of ER and LBDs of bacterial

**TABLE 1** | Sequence ID and the function for the sequences selected for COBALT analysis.

Accession ID	COBALT query	Sequence description	Organism	Protein function	Criteria for inclusion in the study
pdb 1GWQ A	10001	Ligand binding domain of ER $\alpha$ (ER $\alpha$ -LBD)	<i>Homo sapiens</i>	ER $\alpha$ is a nuclear hormone receptor that functions as a ligand-dependent transcription factor. Transactivation of the receptor is dependent on the LBD, which binds to its specific ligand to initiate the dimerization and activation of the receptors.	For understanding the low substrate specificity and strong binding affinities of ER to diverse array of exogenous ligand
pdb 3ATP A	10002	Ligand binding domain of TSR (Tsr-LBD)	<i>Escherichia coli</i>	Serine chemoreceptor (Tsr) is involved in transducing signals from a periplasmic ligand-binding site to its cytoplasmic tip and controls the activity of the CheA kinase. The functional forms of Tsr are trimers of homo dimers (TOD).	Like ERs, it has an LBD and function in dimeric form.
pdb 6S33 A	10003	Ligand binding domain of the broad ligand specific chemoreceptor (BLS-LBD)	<i>Pseudomonas putida</i>	Transmembrane protein complex that controls bacterial chemotaxis, broad substrate specific. It functions similar to Tsr .	Like ERs, it has a LBD and function in dimeric form.
NP_001087206.1	10004	Nuclear receptor	<i>Ciona intestinalis</i>	A thyroid hormone receptor playing a prominent role in a role during development and metamorphosis of <i>Ciona intestinalis</i>	To represent a primitive nuclear receptor from protostoma
CAC5376483.1	10005	Nuclear receptor	<i>Mytilus coruscus</i>	Retinoic acid receptor of <i>Mytilus coruscus</i>	To represent a primitive nuclear receptor from protostoma
AKN09692.1	10006	Tom40	<i>Amoeba proteus</i>	The translocase of the outer mitochondrial membrane (TOM) 40 functions in sorting imported protein.	Selected mainly to represent protozoa. Like ER, it translocates from cytoplasm to other organelle (ER-Nucleus, Tom-Mitochondria)

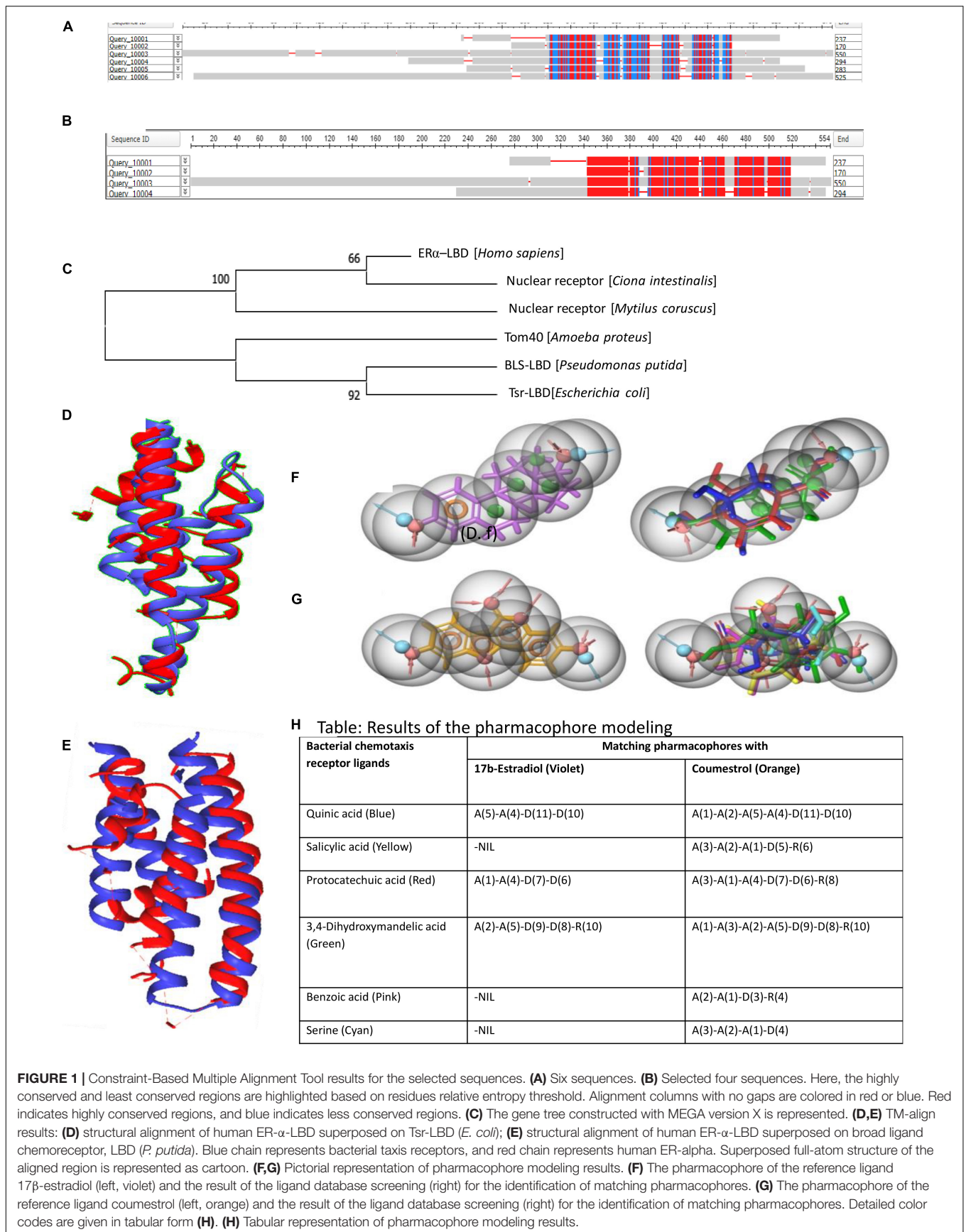


**FIGURE 1** | Constraint-Based Multiple Alignment Tool results for the selected sequences. **(A)** Six sequences. **(B)** Selected four sequences. Here, the highly conserved and least conserved regions are highlighted based on residues relative entropy threshold. Alignment columns with no gaps are colored in red or blue. Red indicates highly conserved regions, and blue indicates less conserved regions. **(C)** The gene tree constructed with MEGA version X is represented. **(D,E)** TM-align results: **(D)** structural alignment of human ER- $\alpha$ -LBD superposed on Tsr-LBD (*E. coli*); **(E)** structural alignment of human ER- $\alpha$ -LBD superposed on broad ligand chemoreceptor, LBD (*P. putida*). Blue chain represents bacterial taxis receptors, and red chain represents human ER- $\alpha$ . Superposed full-atom structure of the aligned region is represented as cartoon. **(F,G)** Pictorial representation of pharmacophore modeling results. **(F)** The pharmacophore of the reference ligand 17 $\beta$ -estradiol (left, violet) and the result of the ligand database screening (right) for the identification of matching pharmacophores. **(G)** The pharmacophore of the reference ligand coumestrol (left, orange) and the result of the ligand database screening (right) for the identification of matching pharmacophores. Detailed color codes are given in tabular form **(H)**. **(H)** Tabular representation of pharmacophore modeling results.



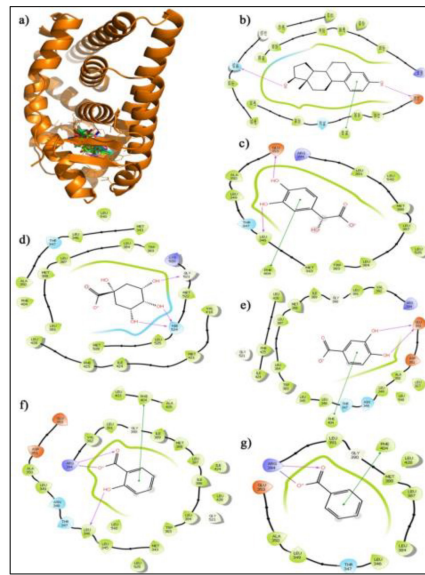
chemoreceptors (**Figures 1D,E**). The superposition of two proteins using T-align showed a clear picture on the similarity of Domain Structural architecture between Tsr and ER and between

BLS and ER, substantiating our hypothesis on preservation of common fold architecture between the LBDs between bacterial chemoreceptor and human ER $\alpha$ .

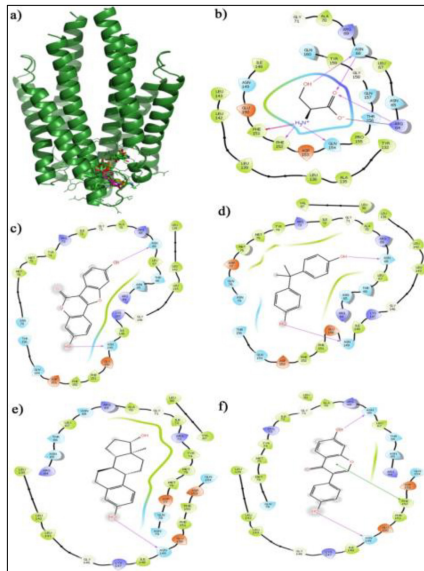
**A** Table: Detailed glide scores of ligands against corresponding receptors

Ligands	Glide score (-kCal/mol) against		
	Human ER (PDB ID 1ERE)	E.coli Tsr (PDB ID 3ATP)	P.putida PcaY_PP (PDB ID 6S33)
<b>Estrogen receptor ligands (Endogenous/synthetic/other than phytoestrogens)</b>			
17 $\beta$ -Estradiol	-11.434	-4.172	-2.986
Diethylstilbesterol	-10.251	-2.350	-4.121
Bisphenol_A	-9.216	-4.586	-4.863
DDT	-8.297	-3.765	-3.646
2,3,5,6-Tetradeuterio-4-nonylphenol	-7.275	-1.804	-2.225
2-Nonylphenol	-6.776	-1.730	-2.202
4-Nonylphenol	-6.769	-1.529	-3.401
<b>Phytoestrogens</b>			
Coumestrol	-10.121	-4.783	-4.184
Diadzein	-9.857	-4.115	-3.295
Naringenin	-9.136	-2.998	-5.902
<b>Bacterial chemotaxis receptor ligands</b>			
3,4-Dihydroxymandelic acid	-6.946	-4.750	-9.556
Quinic acid	-6.768	-7.44	-10.278
Protocatechuic acid	-5.982	-3.984	-8.133
Salicylic acid	-5.723	-4.783	-6.235
Benzoic acid	-5.288	-2.476	-5.428
Serine	-4.585	-8.604	-8.052

**B**



**C**



**D**

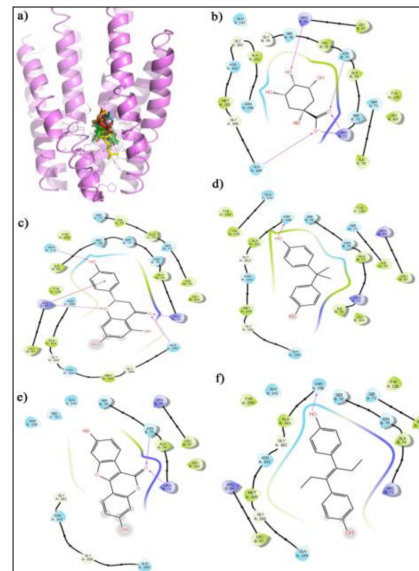


**FIGURE 2 | (A)** Table representing detailed glide scores of ligands against corresponding receptors. **(B)** Docking of human ER (PDB ID: 1ERE) with ligands of bacterial chemotaxis receptors. **(B.a)** Binding of selected ligands in the receptor cavity of human ER (orange, PDB ID 1ERE). **(B.b)** Ligand interaction diagram of the natural ER ligand 17 $\beta$ -estradiol with binding site residues of ER. **(B.c)** Ligand interaction diagrams of the top scoring bacterial chemotaxis ligands 3,4-dihydroxy mandelic acid, **(B.d)** quinic acid, **(B.e)** protocatechuic acid, **(B.f)** salicylic acid, and **(B.g)** benzoic acid. **(C)** Docking of *E. coli* chemotaxis receptor Tsr (PDB ID: 3ATP) with ligands of human ER. **(C.a)** Binding cavity in the AB chain interface of *E. coli* chemotaxis receptor Tsr (green) occupied with the reference ligand serine and ER ligands. **(C.b)** The interaction of serine, **(C.c)** coumestrol, **(C.d)** bisphenol A, **(C.e)** estradiol, and **(C.f)** diadzein. **(D)** Docking of bacterial chemotaxis receptor (PDB ID 6S33) with ligands of human ER. **(D.a)** Ligand binding domain in the AB chain interface of *P. putida* chemotaxis receptor PcaY\_PP (violet, PDB ID 6S33) occupied with the reference ligand “quinic acid” and ER ligands. The interaction of **(D.b)** quinic acid, **(D.c)** naringenin, **(D.d)** bisphenol A, **(D.e)** coumestrol, and **(D.f)** diethylstilbesterol.

## Ligands Specific for the Estrogen Receptor and Bacterial Chemotaxis Receptors Shares Common Pharmacophore Features

Pharmacophore models provide description of optimal supramolecular interactions that typically occur between small-molecule ligands and their respective protein receptor. The pharmacophores of ERs ligands and bacterial chemotaxis receptor ligands were compared to understand if these ligands shared any common pharmacophore features. Two pharmacophore hypotheses were developed in which the first hypothesis involves 17 $\beta$ -estradiol (human estrogen) as the reference ligand and the second hypothesis was focused on coumestrol (Phytoestrogen) as the reference ligand. The hypotheses were developed using the “Develop pharmacophore hypothesis” module of Maestro 11.0 Schrodinger suite. To develop the hypotheses using the reference ligands, hydrogen bond (HB) donors (D), HB acceptors (A), aromatic ring (R), hydrophobic/non-polar groups (H), and positive/negative ionizable groups were selected as the pharmacophore features. Furthermore, the ligands to be screened for matching pharmacophore features were subjected to “ligand-database pharmacophore screening” using the same software.

Interestingly, pharmacophore modeling uncovered a set of common features among the ligands specific for the ER and bacterial chemotaxis receptors (**Figures 1F–H**). All the bacterial chemotaxis receptor ligands possessed pharmacophore features that are common for 17 $\beta$ -estradiol and coumestrol (**Figures 1F–H**). The bacterial chemotaxis receptor ligands such as salicylic acid, benzoic acid, and serine exhibited matching pharmacophores with the phytoestrogen “coumestrol,” a known ER agonist.

## Natural Ligands of Bacterial Chemotaxis Receptors Exhibited Favorable Binding Affinity Toward Human Estrogen Receptor and Vice Versa

Our finding that the structural architecture was conserved between the LBD of ERs and bacterial Taxis receptors along with the existence of common pharmacophore feature between the ligands of both receptors prompted us to check for the interactions of the ligands with both receptors. The molecular docking studies were performed using Schrodinger suite 11.0. The three dimensional structures of ER (PDB ID 1ERE), *E. coli* chemotaxis receptor Tsr (PDB ID 3ATP), and *P. putida* PcaY\_PP LBD (PDB ID 6S33) were downloaded from Protein Data Bank. The downloaded protein structures were processed and energy minimized using the Protein Preparation Wizard. The protein preparation involved assigning bond orders, adding hydrogens, creating disulfide bonds, and creating zero-order bonds to metals. The het states of the proteins were generated using “Epik” at pH 7  $\pm$  2.0, and restrained minimization was performed using OPLS3 forcefield. Furthermore, a receptor grid was generated from each structure by selecting the cocrystal ligand as the centroid of the receptor. The ligand molecules (**Figure 2**) were

downloaded from NCBI-PubChem database and prepared for docking with the LigPrep module. The ligand molecules were structurally optimized at near neutral pH (7  $\pm$  1) and subjected to energy minimization using OPLS3 force field.

Furthermore, the prepared ligand sets were docked against the receptor grid of the above-mentioned target proteins. Extra precision (XP) flexible docking was performed using the GLIDE module, and the affinity of the ligands toward the target proteins were ascertained in terms of negative glide score (kcal/mol). Fifty docking poses were collected for each ligand. The binding poses were generated using Pymol software (free license). The glide score is an indirect measure of binding free energy of the ligand–receptor interaction. The more negative the glide score, the stronger the interaction.

For the molecular docking studies against human ER, 17 $\beta$ -estradiol was used as the reference ligand, and other ER ligands were used for validation of the experiment (**Figure 2A**). Similarly, quinic acid was used as the standard reference ligand for bacterial chemotaxis receptors, and other ligands specific for bacterial receptor was used for cross-validation of the experiment. The docking studies strongly support the findings of structural similarity between human ER and bacterial chemotaxis receptors that were presented in the structure alignment section. When discussing the target specificity of ER ligands against bacterial chemotaxis receptors, all the ligands exhibited thermodynamically favorable interaction (**Figure 2B**). Phytoestrogens such as coumestrol, diadzeine, and naringenin exhibited stronger interaction with high binding affinity toward bacterial chemotaxis receptors than the estradiol or synthetic ER ligands (**Figures 2C,D**). On the other hand, the natural ligands of bacterial chemotaxis receptors exhibited strong interaction with human ER (**Figures 2A,B**). The favorable interactions of all ER ligands toward bacterial receptors irrespective of their binding strength and vice versa were the key findings of this experiment.

## CONCLUSION AND PERSPECTIVE

We observed a remarkable similarity in the domain structural fold architecture of ER $\alpha$  and bacterial taxis receptors. The ligand molecules of both receptors also shared common pharmacophore features. The natural ligands of bacterial chemotaxis receptors exhibit favorable binding affinity with human ER. This holds true for ER–ligand interaction with bacterial receptors as well. However, phylogenetic analysis proves that these proteins are unrelated. Together, these results suggest that these receptors have evolved independently to respond against certain environmental agents, pointing toward a possibility of convergent molecular evolution. However, during the course of evolution, even when these sequences exhibited high divergence and acquired novel functions, the domain structural fold remained greatly preserved. Domain structural architecture for a particular acquired or specialized functions maybe conserved across species in due course of evolution even when the sequence composition varies. This hypothesis also explains the non-specific binding of the nuclear hormones toward an array of chemically distinct exogenous ligands and

at the same time maintaining its high specificity toward the respective hormones.

## DATA AVAILABILITY STATEMENT

The datasets presented in this study can be found in online repositories. The names of the repository/repositories and accession number(s) can be found in the article/**Supplementary Material**.”

## AUTHOR CONTRIBUTIONS

DL conceived the idea, developed the concept, designed the experiments, performed the experiments, and wrote the manuscript. SH contributed in doing revision experiments in the revised version of the manuscript. Both authors contributed to the article and approved the submitted version.

## FUNDING

This research was funded with **Seed grant (YU/Seed grant/065-2018), from Yenepoya (Deemed to be University)**.

## REFERENCES

- Baker, M. E. (2019). Steroid receptors and vertebrate evolution. *Mol. Cell. Endocrinol.* 496:110526. doi: 10.1016/j.mce.2019.110526
- Baker, M. E., and Chandsawangbhuwana, C. (2008). Motif analysis of amphioxus, lamprey and invertebrate estrogen receptors: toward a better understanding of estrogen receptor evolution. *Biochem. Biophys. Res. Commun.* 371, 724–728. doi: 10.1016/j.bbrc.2008.04.152
- Baker, M. E., and Lathe, R. (2018). The promiscuous estrogen receptor: evolution of physiological estrogens and response to phytochemicals and endocrine disruptors. *J. Steroid Biochem. Mol. Biol.* 184, 29–37. doi: 10.1016/j.jsbmb.2018.07.001
- Baker, M. E., Nelson, D. R., and Studer, R. A. (2015). Origin of the response to adrenal and sex steroids: roles of promiscuity and co-evolution of enzymes and steroid receptors. *J. Steroid Biochem. Mol. Biol.* 151, 12–24. doi: 10.1016/j.jsbmb.2014.10.020
- Basak, S., Das, M. K., and Duttaroy, A. K. (2020). Plastics derived endocrine-disrupting compounds and their effects on early development. *Birth Defects Res.* 112, 1308–1325. doi: 10.1002/bdr2.1741
- Bhagwat, M., Young, L., and Robison, R. R. (2012). Using BLAT to find sequence similarity in closely related genomes. *Curr. Protoc. Bioinformatics* Chapter 10:Unit 10.8.
- Callard, G. V., Tarrant, A. M., Novillo, A., Yacci, P., Ciaccia, L., Vajda, S., et al. (2011). Evolutionary origins of the estrogen signaling system: insights from amphioxus. *J. Steroid Biochem. Mol. Biol.* 127, 176–188. doi: 10.1016/j.jsbmb.2011.03.022
- Cauley, J. A. (2015). Estrogen and bone health in men and women. *Steroids* 99(Pt A), 11–15. doi: 10.1016/j.steroids.2014.12.010
- Elliston, J. F., and Katzenellenbogen, B. S. (1988). Comparative analysis of estrogen receptors covalently labeled with an estrogen and an antiestrogen in several estrogen target cells as studied by limited proteolysis. *J. Steroid Biochem.* 29, 559–569. doi: 10.1016/0022-4731(88)90152-5
- Forslund, S. K., Kaduk, M., and Sonnhammer, E. L. L. (2019). Evolution of protein domain architectures. *Methods Mol. Biol.* 1910, 469–504. doi: 10.1007/978-1-4939-9074-0\_15
- Gore, A. C., Chappell, V. A., Fenton, S. E., Flaws, J. A., Nadal, A., Prins, G. S., et al. (2015). EDC-2: the endocrine society's second scientific statement on endocrine-disrupting chemicals. *Endocr. Rev.* 36, E1–E150.
- Guerriero, G. (2009). Vertebrate sex steroid receptors: evolution, ligands, and neurodistribution. *Ann. N. Y. Acad. Sci.* 1163, 154–168. doi: 10.1111/j.1749-6632.2009.04460.x
- Itoh, M., Nacher, J. C., Kuma, K., Goto, S., and Kanehisa, M. (2007). Evolutionary history and functional implications of protein domains and their combinations in eukaryotes. *Genome Biol.* 8:R121.
- Kao, Y. C., Higashiyama, T., Sun, X., Okubo, T., Yarborough, C., Choi, I., et al. (2000). Catalytic differences between porcine blastocyst and placental aromatase isozymes. *Eur. J. Biochem.* 267, 6134–6139. doi: 10.1046/j.1432-1327.2000.01705.x
- Klinge, C. M. (2001). Estrogen receptor interaction with estrogen response elements. *Nucleic Acids Res.* 29, 2905–2919. doi: 10.1093/nar/29.14.2905
- Kohler, H. R., Kloas, W., Schirling, M., Lutz, I., Reye, A. L., Langen, J. S., et al. (2007). Sex steroid receptor evolution and signalling in aquatic invertebrates. *Ecotoxicology* 16, 131–143. doi: 10.1007/s10646-006-0111-3
- Koonin, E. V., Wolf, Y. I., and Karev, G. P. (2002). The structure of the protein universe and genome evolution. *Nature* 420, 218–223. doi: 10.1038/nature01256
- Lakshmanan, M. D., and Sadasivan, C. (2014). “Selective estrogen receptor modulators (SERMs) from plants,” in *Bioactive Natural Products: Chemistry and Biology*, ed. G. Brahmachari (Weinheim: Wiley-VCH), 375–386. doi: 10.1002/9783527684403.ch13
- Lakshmanan, M. D., and Shaheer, K. (2020). Endocrine disrupting chemicals may deregulate DNA repair through estrogen receptor mediated seizing of CBP/p300 acetylase. *J. Endocrinol. Invest.* 43, 1189–1196.
- Lecroisey, C., Laudet, V., and Schubert, M. (2012). The cephalochordate amphioxus: a key to reveal the secrets of nuclear receptor evolution. *Brief. Funct. Genomics* 11, 156–166. doi: 10.1093/bfgp/els008
- Moreno-Hagelsieb, G., and Hudy-Yuffa, B. (2014). Estimating overannotation across prokaryotic genomes using BLAST+, UBLAST, LAST and BLAT. *BMC Res. Notes* 7:651. doi: 10.1186/1756-0500-7-651
- Morissette, M., Le Saux, M., D'Astous, M., Jourdain, S., Al Sweidi, S., Morin, N., et al. (2008). Contribution of estrogen receptors alpha and beta to the effects of estradiol in the brain. *J. Steroid Biochem. Mol. Biol.* 108, 327–338. doi: 10.1016/j.jsbmb.2007.09.011
- Pacyga, D. C., Sathyanarayana, S., and Strakovsky, R. S. (2019). Dietary predictors of phthalate and bisphenol exposures in pregnant women. *Adv. Nutr.* 10, 803–815. doi: 10.1093/advances/nmz029

## ACKNOWLEDGMENTS

We would like to acknowledge Ranajith Das, Yenepoya Research Centre, for his comments and suggestions on the phylogenetic tree construction and analysis.

## SUPPLEMENTARY MATERIAL

The Supplementary Material for this article can be found online at: <https://www.frontiersin.org/articles/10.3389/fevo.2021.681913/full#supplementary-material>

**Supplementary Figure 1** | Results for Constraint-based Multiple Alignment Tool. Sequences with no gaps are colored in red or blue. Red indicates highly conserved sequence and blue indicates less conserved sequence.

**Supplementary Figure 2** | Results for Constraint-based Multiple Alignment Tool for random sequences. Sequences with no gaps are colored in red or blue. Red indicates highly conserved sequence and blue indicates less conserved sequence.

**Supplementary Figure 3** | Graphical representation of the Constraint-based Multiple Alignment for random sequences. Sequences with no gaps are colored in red or blue. Red indicates highly conserved sequence and blue indicates less conserved sequence. Line indicates gaps. **(A)** Six random sequences. **(B)** Four selected random sequences.

**Supplementary Table 1** | Sequence ID and their Function for the random sequences selected for COBALT analysis.


- Papadopoulos, J. S., and Agarwala, R. (2007). COBALT: constraint-based alignment tool for multiple protein sequences. *Bioinformatics* 23, 1073–1079. doi: 10.1093/bioinformatics/btm076
- Park, C., Song, H., Choi, J., Sim, S., Kojima, H., Park, J., et al. (2020). The mixture effects of bisphenol derivatives on estrogen receptor and androgen receptor. *Environ. Pollut.* 260:114036. doi: 10.1016/j.envpol.2020.114036
- Peisajovich, S. G., Garbarino, J. E., Wei, P., and Lim, W. A. (2010). Rapid diversification of cell signaling phenotypes by modular domain recombination. *Science* 328, 368–372. doi: 10.1126/science.1182376
- Razandi, M., Pedram, A., Merchanthaler, I., Greene, G. L., and Levin, E. R. (2004). Plasma membrane estrogen receptors exist and functions as dimers. *Mol. Endocrinol.* 18, 2854–2865. doi: 10.1210/me.2004-0115
- Rosenfeld, C. S., and Cooke, P. S. (2019). Endocrine disruption through membrane estrogen receptors and novel pathways leading to rapid toxicological and epigenetic effects. *J. Steroid Biochem. Mol. Biol.* 187, 106–117. doi: 10.1016/j.jsbmb.2018.11.007
- Sasson, S., and Notides, A. C. (1983). Estriol and estrone interaction with the estrogen receptor. II. Estriol and estrone-induced inhibition of the cooperative binding of [3H]estradiol to the estrogen receptor. *J. Biol. Chem.* 258, 8118–8122. doi: 10.1016/s0021-9258(20)82036-5
- Shafei, A., Ramzy, M. M., Hegazy, A. I., Husseny, A. K., El-Hadary, U. G., Taha, M. M., et al. (2018). The molecular mechanisms of action of the endocrine disrupting chemical bisphenol A in the development of cancer. *Gene* 647, 235–243. doi: 10.1016/j.gene.2018.01.016
- Thornton, J. W. (2001). Evolution of vertebrate steroid receptors from an ancestral estrogen receptor by ligand exploitation and serial genome expansions. *Proc. Natl. Acad. Sci. U.S.A.* 98, 5671–5676. doi: 10.1073/pnas.091553298
- Vogeler, S., Galloway, T. S., Lyons, B. P., and Bean, T. P. (2014). The nuclear receptor gene family in the pacific oyster, *Crassostrea gigas*, contains a novel subfamily group. *BMC Genomics* 15:369. doi: 10.1186/1471-2164-15-369
- Ward, N., and Moreno-Hagelsieb, G. (2014). Quickly finding orthologs as reciprocal best hits with BLAT, LAST, and UBLAST: how much do we miss? *PLoS One* 9:e101850. doi: 10.1371/journal.pone.0101850
- Wu, W., and LoVerde, P. T. (2019). Nuclear hormone receptors in parasitic platyhelminths. *Mol. Biochem. Parasitol.* 233:111218. doi: 10.1016/j.molbiopara.2019.111218
- Yang, S. H., Liu, R., Perez, E. J., Wen, Y., Stevens, S. M. Jr., Valencia, T., et al. (2004). Mitochondrial localization of estrogen receptor beta. *Proc. Natl. Acad. Sci. U.S.A.* 101, 4130–4135.
- Yu, L., Tanwar, D. K., Penha, E. D. S., Wolf, Y. I., Koonin, E. V., and Basu, M. K. (2019). Grammar of protein domain architectures. *Proc. Natl. Acad. Sci. U.S.A.* 116, 3636–3645.
- Zhang, Y., and Skolnick, J. (2005) TM-align: a protein structure alignment algorithm based on the TM-score. *Nucleic Acids Res.* 33, 2302–2309. doi: 10.1093/nar/gki524

**Conflict of Interest:** The authors declare that the research was conducted in the absence of any commercial or financial relationships that could be construed as a potential conflict of interest.

Copyright © 2021 Lakshmanan Mangalath and Hassan Mohammed. This is an open-access article distributed under the terms of the Creative Commons Attribution License (CC BY). The use, distribution or reproduction in other forums is permitted, provided the original author(s) and the copyright owner(s) are credited and that the original publication in this journal is cited, in accordance with accepted academic practice. No use, distribution or reproduction is permitted which does not comply with these terms.



# Piperine sensitizes radiation-resistant cancer cells towards radiation and promotes intrinsic pathway of apoptosis

Koniyan Shaheer, HM Somashekarappa, and M. Divya Lakshmanan 

**Abstract:** Piperine, a bioactive alkaloid, is known to have anticancer activities. Hence, in this study, the effectiveness of piperine pretreatment as a strategy for radio-sensitizing colorectal adenocarcinoma cell line (HT-29) was analyzed. For this, HT-29 cells were pretreated with piperine (12.5 and 25  $\mu\text{g}/\text{mL}$ ) and exposed to  $\gamma$ -radiation (1.25 Gy) and analyzed for various effector pathways to elucidate the possible mode of action in comparison to individual treatments. The proliferation efficiency of the cells was analyzed by trypan blue dye exclusion assay and MTT assay. The synergistic effects of the combination treatment were analyzed with compuSyn software. Downstream signaling pathways leading to apoptosis were studied using flowcytometry, immunofluorescence, and immunoblot assays. It was observed that combination treatment arrested HT-29 cells at G2/M phase nearly 2.8 folds higher than radiation treatment alone, inducing the radio-resistant cells to undergo apoptosis through mitochondria-dependent pathway. In addition, activation of caspase-3 and cleavage of poly(ADP-ribose) polymerases-1, the key molecular events in apoptotic signaling, were significantly enhanced. Activation of estrogen receptor beta ( $\text{ER}\beta$ ), a nuclear hormone transcription factor promoting tumor suppression represents a novel clinical advance towards management and prevention of cancers. Interestingly, the expression of  $\text{ER}\beta$  was increased in the cells treated with piperine. In conclusion, piperine pretreatment enhances radio-sensitization in HT-29 cells by inducing the cells to undergo apoptosis hence, can be used as a classic candidate for colon cancer sensitization towards radiotherapy.

**Keywords:** apoptosis, colon cancer, estrogen receptor, mitochondrial membrane potential, piperine, radiation sensitizer

**Practical Application:** Piperine induces enhanced radiosensitization of colon cancer cell line (HT-29) by interfering with the cancer cell line proliferation, DNA damage, and apoptosis.

## 1. INTRODUCTION

Most of the current treatment strategies for cancer show limited improvement as the patient develops resistance towards chemotherapy and radiotherapy (Hu, Li, Gao, & Cho, 2016; Kyrjiou et al., 2017). Hence, there is an urgent need to develop smarter therapeutic strategies for advanced-stage, therapy-resistant cancers. One approach to improve the efficacy and overcome the radiation resistance is to induce radiosensitization in cancer cells.

Some natural compounds such as curcumin, quercetin, genistein, (Nicholson et al., 1995) danshsensu, wortmannin, and so on, are reported for inducing radiosensitization in cancer cells (Cao et al., 2017; Javvadi, Segan, Tuttle, & Koumenis, 2008; Lagerweij et al., 2016; Ortiz, Lopez, Burguillos, Edreira, & Pinero, 2004; Tang et al., 2018). Natural products owing to their antioxidant and immune-enhancing effects may have improved effects as biological and radiation protectors for normal cells. Screening of more natural compounds may facilitate the discovery of compounds that sensitize the cancer therapy by interfering with cancer regulatory pathway and render possible treatment strategies.

Piperine is a major plant alkaloid, a phytochemical present in *Piper nigrum* Linn (black pepper) and *Piper longum* Linn (long pepper). Black pepper is one of the most common spices consumed by a large number of populations worldwide. Piperine has been reported to enhance the activity of the anticancer drugs in various drug-resistant cancer cells (Khan, Maryam, Mehmood, Zhang, & Ma, 2015; Li, Krstin, Wang, & Wink, 2018; Manayi, Nabavi, Setzer, & Jafari, 2018; Syed et al., 2017), including colorectal cancer cell line (Bolot et al., 2020). Several effector mechanism of piperine against cancer cell line such as influencing redox homeostasis, autophagy, cancer stem cell inhibition and endoplasmic reticulum modulation has been postulated earlier (Rather & Bhagat, 2018). Radiosensitizing property of piperine is yet to be understood properly. Given the need for effective therapies to treat colon cancer, we aimed to investigate the effect of piperine pretreatment on colon cancer cells to facilitate radiotherapy treatment and elucidate its molecular mechanism.

## 2. MATERIALS AND METHODS

Piperine ( $\geq 97\%$ ), poly-L-Lysine, protease inhibitor cocktail, and dimethyl sulphoxide (DMSO) were purchased from Sigma Aldrich, Bangalore, India. Chemicals such as MTT (3-(4, 5-dimethylthiazolyl-2)-2, 5-diphenyltetrazolium bromide), paraformaldehyde, bovine serum albumin (BSA), triton X 100, propidium iodide, RNase A solution, Dulbecco's Modified Eagles Medium (DMEM), fetal bovine serum (FBS), penicillin and streptomycin solution, L-glutamine, Trypan blue (0.4% solution in Dulbecco's phosphate-buffered saline) were purchased

JFDS-2020-0962 Submitted 6/7/2020, Accepted 9/18/2020. Authors Shaheer and Lakshmanan are with Molecular Biology Division, Yenepoya Research Centre, Yenepoya (deemed to be University), Deralakatte, Mangalore, Karnataka, 575018, India. Author Somashekarappa is with Centre for Application of Radioisotopes and Radiation Technology (CARRT), USIC, Mangalore University, Mangalore, Karnataka, 575018, India. Direct inquiries to author Lakshmanan (E-mail: divyalman-galath@gmail.com).

from Himedia, Mumabi, India. ER $\alpha$  (E115; ab32063) and ER $\beta$  (ab3576) specific antibodies, Goat Anti-Rabbit IgG HandL (Alexa Fluor-488; ab150077) were purchased from Abcam, Cambridge, UK. JC-1 dye was from Calbiochem, Bangalore, India (Sigma). Rabbit monoclonal antibodies  $\beta$ -actin (#4970), BAX (D2E11, #5023), BCL-2 (124, #15071), Caspase 3 (#9662) poly(ADP-ribose) polymerases-1: (PARP 1; #9541) and anti-rabbit-IgG horseradish peroxidase-conjugated secondary antibody (#7074S) were from Cell Signaling Technology (Danvers, MA, USA). Enhanced Chemi-luminescence substrate (Immobilon Forte Western HRP substrate, #WBLUF0100) was purchased from Millipore, Bangalore, India. Other chemicals used whereof analytical or molecular biology grade were procured from HiMedia, India.

## 2.1 Cell line and culture

Human colon cancer cell line- HT-29 (NCCS, Pune, India) was grown in DMEM, supplemented with 10% FBS, 1% penicillin and streptomycin, and 2 mM L-glutamine. The cell culture was maintained at 37 °C in a 5% CO<sub>2</sub> humidified atmosphere.

## 2.2 Ionizing radiation treatment and dose optimization

Exponentially growing HT-29 cells were exposed to  $\lambda$ -radiation with dose ranging from 1.25 to 10 Gy, using a Low Dose gamma Irradiator-2000 (BRIT, Mumbai, India), which is a self-shielded, irradiator with <sup>60</sup>Co. The dose rate of the instrument at the time exposure is 10.3 Gy/min. And the cells were incubated for 48 hr under normal culture conditions. After 48 hr of incubation, MTT assay was performed. Absorbance was recorded at 570 nm using the multimode reader (FLUOstar Omega, Mumbai, India). The  $\gamma$ -radiation facility was availed at Centre for Application of Radioisotopes and Radiation Technology (CARRT), Mangalore University, Mangalore, Karnataka, India.

## 2.3 Piperine treatment and dose optimization by MTT assay

The dose optimization of piperine is studied using MTT assay (Tolosa, Donato, & Gomez-Lechon, 2015). Briefly, HT-29 cells were seeded and cultured in 96-well tissue culture plate (Falcon, Corning, India) at a density of 5,000 cells/100  $\mu$ L/well for 24 hr under specified conditions mentioned earlier. Piperine was dissolved in DMSO and added into the culture at different concentrations 10 to 100  $\mu$ g/mL in triplicate, where final concentration of DMSO kept remain at 0.1% and further incubated for 48 hr under normal cell culture conditions. DMSO at a final concentration of 0.1% alone was treated as vehicle control.

## 2.4 Morphological analysis

HT-29 cells were seeded at a cell density of  $0.35 \times 10^6$  cells/mL in 35 mm dishes. After 24 hr incubation, the cells were treated with piperine for 2 hr and irradiated. Untreated and nonirradiated cells were included as control. Cell morphology was examined under magnification of 20 $\times$  by using an inverted light microscope (Zeiss Primo Vert, Mumbai, India). For fluorescent imaging, nuclei were stained with propidium iodide (0.2  $\mu$ g/mL) for 10 min. The stained cells were then analyzed under a ZOE imager (Bio-Rad, Mumbai, India).

## 2.5 Cytotoxicity assessment using Trypan blue dye exclusion assay and MTT assay

HT-29 and A549 cells were seeded and cultured in T12.5 flasks, for 24 hr under specified conditions mentioned above. Cells were treated with the piperine in two concentrations (12.5 and

25  $\mu$ g/mL) and exposed to a single dose of  $\gamma$ -radiation at a dose of 1.25 Gy. Cells (vehicle control) placed in the chamber but not irradiated were considered as sham control. The effect of piperine and radiation on HT-29 and A549 cell cytotoxicity assay was performed using MTT assay at 48 hr of incubation after radiation as described earlier (Tolosa et al., 2015). Trypan blue dye exclusion assay was performed only in HT-29 cells. Percentage of cell viability was calculated using the following formula (Stoddart, 2011).

Percentage of cell viability

$$= \frac{(\text{No. of viable cells in control} - \text{No. viable cells in test})}{\text{No. of viable cells in control}} \times 100$$

## 2.6 Analysis of the synergistic effect of the combination treatment using CompuSyn method

CompuSyn software (ComboSyn, Inc., USA) was used to quantitatively depict the effect of the combination treatment. The data from the cytotoxicity studies were taken to compute combination index (CI) values, CI plot, dose-response curve, median effect plot, and normalized isobologram. CI values were used to determine the synergism (CI < 1), additive effect (CI = 1), and/or antagonism (CI > 1) of the cotreatment (Chou, 2010; Chou & Talalay, 1984).

The combination index (CI) is calculated by using the formula:

$$CI = \frac{d1}{DX1} + \frac{d2}{DX2}$$

where Dx1 is the dose of test agent 1 (radiation) required to decrease  $\times$  percentage proliferation alone, and d1 is the dose of test agent 1 required to decrease  $\times$  percentage proliferation in combination with d2. Dx2 is similarly the dose of test agent 2 (piperine) required to decrease  $\times$  percentage proliferation alone, and d2 is the dose of test agent 2 required to decrease  $\times$  percentage proliferation in combination with d1.

## 2.7 Cell-cycle analysis

HT-29 cells were seeded in T-12.5 flasks at a density of 300,000 cells/flask and cultured for 24 hr. The cells were then treated with selected dose of piperine for 2 hr. DMSO at a final concentration of 0.1%, treated cells served as vehicle control/sham control. The cells were then exposed to 1.25 Gy of  $\lambda$ -radiation and incubated for 48 hr. Cells were trypsinized and washed with 1 $\times$  PBS (pH 7.4) fixed with chilled 75% ethanol and incubated overnight at -20 °C. Cells were washed twice with 1 $\times$  PBS (pH 7.4) and incubated with RNase A solution (50  $\mu$ g/mL) for 2 hr at 37 °C. The cells were labeled with propidium iodide (5  $\mu$ g/mL) for 10 min in dark. Cell-cycle analysis was performed using Guava easyocyte (Millipore).

## 2.8 Immunofluorescence staining

HT-29 Cells ( $0.35 \times 10^6$  cells/35mm dish) were seeded on poly-L-Lysine coated glass coverslip placed in 35 mm culture dishes. After 48 hr of combination treatment with piperine and  $\lambda$ -radiation, cells were washed with 1 $\times$  PBS (pH 7.4) and fixed with 4% paraformaldehyde and permeabilized with 0.1% Triton X-100 for 30 min at room temperature. Following blocking the cells were incubated with ER $\alpha$  (1:200) and ER $\beta$  (1:500) specific antibodies for overnight at 4 °C. The cells were then incubated with Goat Anti-Rabbit IgG HandL (Alexa Fluor-488) secondary antibody

(1:500) for 1 hr at room temperature in dark. Nuclei were counterstained with propidium iodide (0.2 µg/mL) for 10 min. The stained cells were then analyzed under a fluorescence microscope (ZOE imager; Bio-Rad).

## 2.9 Analysis of mitochondrial membrane potential (MMP)

HT-29 cells ( $3.0 \times 10^5$  cells) were seeded in a T-12.5 flask in a final volume of 3 mL and cultured for 24 h. A pretreatment of piperine in two different concentrations, was given 2 hr before  $\lambda$ -radiation (1.25 Gy) treatment and incubated for 48 hr at 37 °C. Following 48 hr of post cotreatment, the cells were treated with JC-1 dye at a final concentration of 2.5 µg/mL for 15 min. H<sub>2</sub>O<sub>2</sub> (500 µM) treated cells were taken as positive control. After incubation cells were harvested and assessed for change in the  $\Delta\Psi_m$  using Guava easycyte flow cytometer.

## 2.10 Immunoblot assay

Immunoblot of HT-29 cells pretreated with piperine (12.5 and 25 µg/mL), following  $\lambda$ - radiation (1.25 Gy) for 48 hr was performed for monoclonal antibodies such as, BCL-2, Bax, PARP-1 and Caspase 3 (1:1,000) and polyclonal antibody for ER $\beta$  (1:500). The blot was incubated with anti-rabbit-IgG-horseradish peroxidase-conjugated secondary antibody (1:10,000) for 1 hr at room temperature. The blots were probed with  $\beta$ -actin to show equal loading, and the bands were developed using enhanced chemiluminescence detection method using ECL as substrate.

## 2.11 Statistical analysis

All assays were repeated for three times and triplicate results are shown. Data were analyzed using one way ANOVA or two-way ANOVA. A *P*-value of <0.0001 was considered significant. Data were represented as mean  $\pm$  SD. All statistical analysis were done using GraphPad PRISM version 7.0.

# 3. RESULTS AND DISCUSSION

## 3.1 Synergistic effect of piperine in conjunction with radiation ameliorated the cytotoxic effects on colon cancer cell line

Prior to testing the synergetic effect of  $\lambda$ -radiation and piperine, the effective dose for each of the individual treatment were established. Based on the optimization results,  $\lambda$ -radiation dose of 1.25 Gy which led to the inhibition of HT-29 cell proliferation (15 to 25%) was chosen for further studies (Figure 1a). The effective dose of piperine was fixed at 12.5 µg/mL (IC<sub>25</sub>) and 25 µg/mL (IC<sub>50</sub>; Figure 1b).

MTT assay which measures mitochondrial succinate dehydrogenase activity was done to check the rate of cell proliferation and we found that piperine treatment in conjunction with radiation exhibited reduced cell proliferation compared to the radiation only group (Figure 1c). To find out if piperine could sensitize colon cancer cell to  $\lambda$ -radiation (IR) treatment, cells were treated with piperine, 2 hr prior to radiation with 1.25 Gy  $\lambda$ -radiation and compared the individual treatments (low-dose piperine or IR only) to a combination of treatments (low-dose piperine and IR). The cotreatment resulted in drastic cell growth inhibition compared to each agent alone. Of note, the MTT assay that is used to determine cell proliferation does not directly distinguish between induction of cell death and prevention of cell division; we further, checked the cytotoxicity by checking for cell viability using trypan blue dye exclusion assay. There was an increased cell death in combination treatment (Figure 1d). This could be correlated with

MTT results, which concludes that the piperine pretreatment augmented the effect of radiation treatment. The images of the cells stained with nucleus staining dye propidium iodide (Figure 1f) also showed considerable decrease in the cell number in the combination treatment. Anticancer effects of piperine have been studied in several cancers both *in vitro* and *in vivo*, including liver, colon, lung, prostate, and melanoma. Similar results were previously reported where piperine (40 µg/mL) and resveratrol improved the radiosensitivity ( $\approx 20\%$ ) of mouse colon carcinoma cell line CT26 and mouse melanoma cells towards  $\lambda$ -radiation (Tak, Lee, & Park, 2012). In addition to colon cancer cell line, we also checked the effect of piperine as radiosensitizer on A549 cells and we found that the combination treatment enhances the cytotoxicity in the lung adenocarcinomas cell line (Figure 1e). But HT-29 was more sensitive to the combination treatment than A549. Hence, further studies were carried out with HT-29.

To know whether the observed increase in the cytotoxicity of the combination treatment is synergistic or additive, we calculate the CI values and generated CI plot and isobologram for the equi-effective curve at two concentrations of piperine (12.5 and 25 µg/mL) against 1.25 Gy of  $\lambda$ -radiation using CompuSyn software. A dose-response curve for individual test agents were plotted as shown in the Figure 2a. Synergism is higher than an additive effect and antagonism is lower than an additive effect. As shown in Figure 2b and e for CI values and plot; CI (<1.0) obtained for both the concentrations of piperine (12.5 and 25 µg/mL) with the  $\lambda$ -radiation clearly demonstrate a synergistic effect. Interestingly, all the points (values derived from triplicate or quadruplicate experiments) in the isobologram (Figure 2c and f) plotted for the two concentrations of piperine (12.5 and 25 µg/mL) with 1.25 Gy of  $\lambda$ -radiation, fell well within the allowed region defined for synergism. Taken together these results show that pretreatment with piperine effectively sensitized colon cancer cells to the cytotoxic effects of  $\lambda$ -radiation, compared to the individual treatment.

## 3.2 Piperine enhanced the radiation induced G2/M arrest in colon cancer cells leading to mitochondria-mediated intrinsic pathway of apoptosis

Since piperine treatment in conjunction with radiation brought significant cytotoxicity in HT-29 cells, we were interested to know whether the cotreatment effected different phases of cell-cycle progression. Flow cytometric analysis with the DNA staining dye, propidium iodide was carried out to investigate, whether piperine is sensitizing HT-29 cells to radiation, through regulating cell-cycle progression. Cells followed the characteristic cell-cycle distribution pattern (Figure 3a and b) with G1 phase having  $70 \pm 1.1\%$  cells, S phase  $13.5 \pm 1.8\%$  cells, and G2/M phase with  $16.5 \pm 0.72\%$  cells. Cells treated with IC<sub>25</sub> concentration of piperine exhibited almost same cell-cycle distribution pattern similar to sham control. Interestingly, cells treated with IC<sub>25</sub> concentration of piperine along with 1.25 Gy, the percentage distribution of cells in the G2/M phase ( $43.5 \pm 0.7\%$ ) was enhanced significantly compare to that of individual agents. Since G2/M phase is arrested during DNA damage our results indicate that piperine may be potentiating the DNA damaging effects of radiation. There are other supporting data which indicate that piperine (75 to 150 µM) alone inhibited the proliferation of HT-29 cells by causing G1 phase cell-cycle arrest and apoptosis caused by endoplasmic reticulum stress (Yaffe, Power Coombs, Doucette, Walsh, & Hoskin, 2015).

G2/M arrest induces the intrinsic mitochondrial pathway which is influenced by members of the BCL family bound to

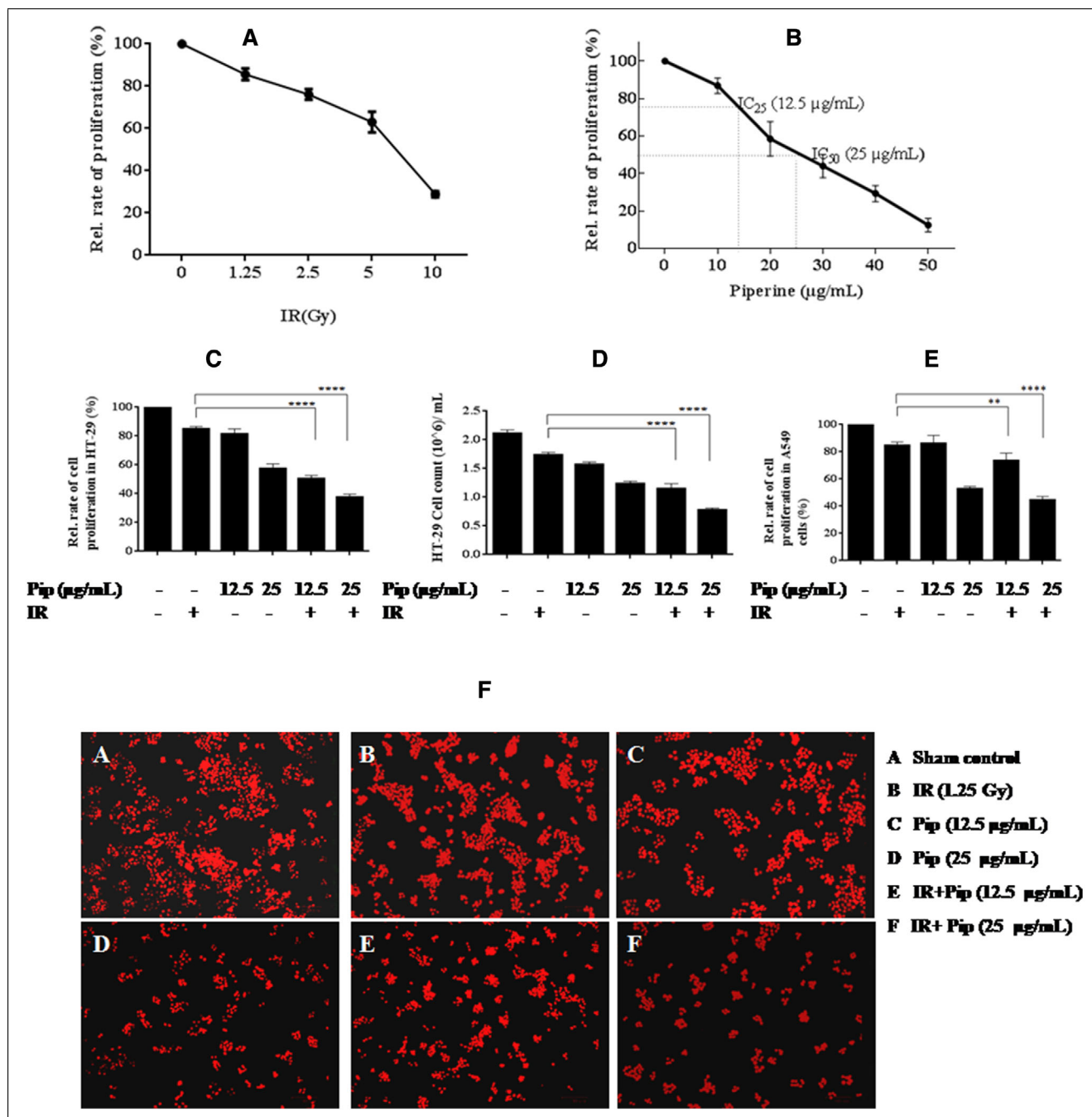


Figure 1-Piperine sensitized the colon cancer cells towards radiation. (a) Dose optimization of  $\lambda$ -radiation. Data represent mean of three repeats for each treatment (mean  $\pm$  SD). (b) Dose optimization of piperine. Dimethyl sulfoxide (DMSO) treated cells were used as vehicle control. Data represent mean of three repeats for each treatment (mean  $\pm$  SD compared). (c) Relative cell proliferation assay of the cotreatment by MTT assay in HT-29 cells. Data represent mean  $\pm$  SD, \*\*\*\* $P$  < 0.0001. The experiments were repeated three times. (d) Cytotoxicity analysis of the cotreatment by Trypan blue dye exclusion assay in HT-29 cells. Data represent mean  $\pm$  SD, \*\*\*\* $P$  < 0.0001. The experiments were repeated three times. (e) Relative cell proliferation assay of the cotreatment by MTT assay in A549 cells. (f) Representative microscopic images of the cells stained with propidium iodide showing reduction in the number of cells following treatment.

the mitochondrial membrane, including BAX and BCL-2, which act as pro- or antiapoptotic regulatory proteins, respectively (Caltabiano et al., 2013). Furthermore, upregulation of BAX and downregulation of BCL-2 is a key regulatory event during apoptosis in human cancer (Naseri et al., 2015). In piperine-treated groups, BCL-2 (26 kDa), an anti-apoptotic molecule in upstream events of intrinsic apoptosis signaling was found downregulated and BAX (20 kDa), a pro-apoptotic protein (Wei et al., 2001)

was found upregulated after 48 hr of postirradiation and piperine treatment (Figure 4c [BCL-2 and BAX] and d). Piperine is known to induce apoptosis through cell-cycle arrest, activation of caspase-3 as well as modulating the BAX and BCL-2 expression in cancer cells (Han, Liu, Yang, Cui, & Xu, 2017; Lin, Xu, Liao, Li, & Pan, 2014). BAX is a key molecular player in intrinsic pathway of apoptosis (Wei et al., 2001). Upon apoptotic stimulation, BAX forms oligomers and translocates from the cytosol to the



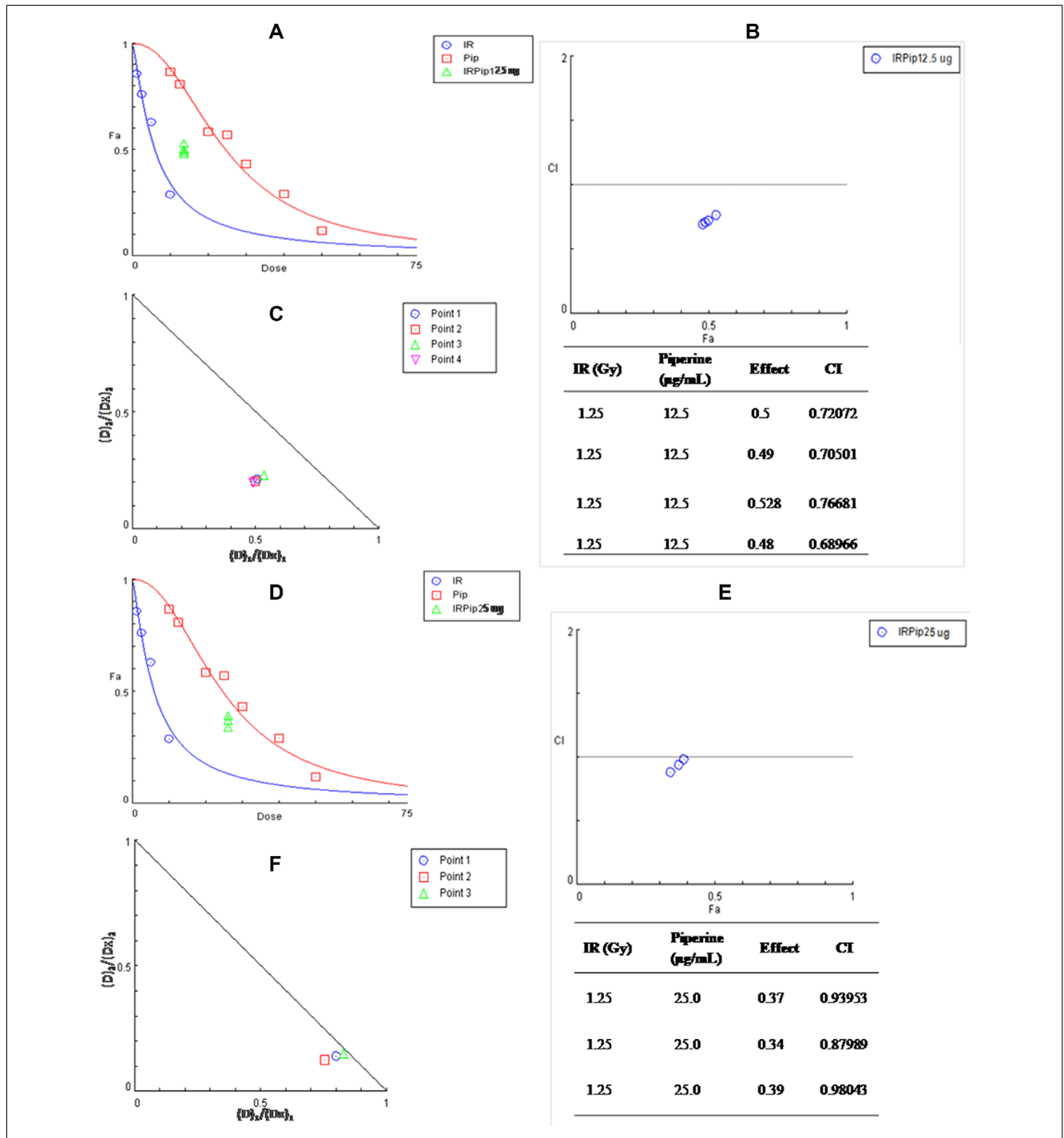


Figure 2–Determination of the synergistic effect of the treatment of piperine with ionizing radiation on cytotoxic effects. (a) Dose–response curve of piperine (Pip) and λ-radiation (IR). IRPip12.5µg indicates combination of IR (λ-radiation and piperine 12.5 µg/mL). (b) Combination index (CI) plot and CI table show that CI for the selected combination (IR+ Pip 12.5 µg/mL) is <1, indicating synergism. CI = 1 defines additive effect, CI < 1 defines synergism (super additive), whereas and CI > 1 is antagonism (sub-additive). (c) Normalized isobologram of the combination (IR+ Pip 12.5 µg/mL), where Dx1 is the dose of radiation required to decrease × percentage proliferation alone, and d1 is the dose of radiation required to decrease × percentage proliferation in combination with d2. Dx2 is the dose of piperine required to decrease × percentage proliferation alone, and d2 is the dose of piperine required to decrease × percentage proliferation in combination with d1. Each Point indicates each individual effect of the combination treatment conducted in quadruplicates. In the isobologram, the intersection of the radial line with the isobole defines the additive dose combination and, a point below indicates synergism whereas a point above indicates antagonism. (d) Dose–response curve of piperine (Pip) and λ-radiation (IR), IRPip25 µg indicates combination of IR (λ-radiation) and piperine 25 µg/mL. (e) Combination index (CI) plot and CI table show that CI for the selected combination (IR+ Pip 12.5 µg/mL) is <1, indicating synergism. (f) Normalized isobologram of the combination (IR+ Pip 25 µg/mL), where Dx1 is the dose of radiation required to decrease × percentage proliferation alone, and d1 is the dose of radiation required to decrease × percentage proliferation in combination with d2. Dx2 is the dose of piperine required to decrease × percentage proliferation alone, and d2 is the dose of piperine required to decrease × percentage proliferation in combination with d1. Each point indicates each individual effect of the combination treatment conducted in triplicates. In the isobologram, the points below the isobole indicate synergism.

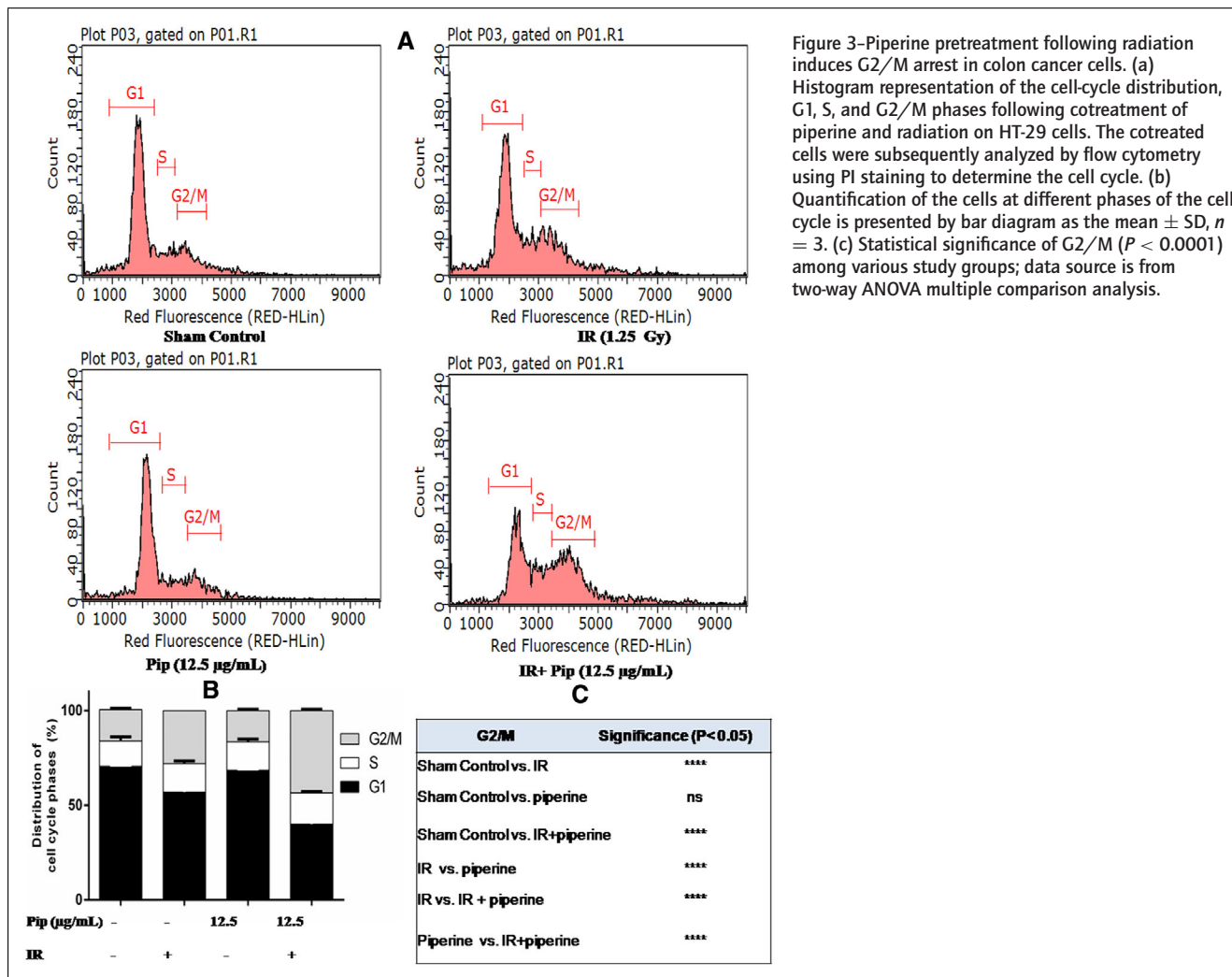


Figure 3-Piperine pretreatment following radiation induces G2/M arrest in colon cancer cells. (a) Histogram representation of the cell-cycle distribution, G1, S, and G2/M phases following cotreatment of piperine and radiation on HT-29 cells. The cotreated cells were subsequently analyzed by flow cytometry using PI staining to determine the cell cycle. (b) Quantification of the cells at different phases of the cell cycle is presented by bar diagram as the mean  $\pm$  SD,  $n = 3$ . (c) Statistical significance of G2/M ( $P < 0.0001$ ) among various study groups; data source is from two-way ANOVA multiple comparison analysis.

mitochondrial outer membrane (Jurgensmeier et al., 1998) and increases the membrane's permeability (Narita et al., 1998). Loss of mitochondrial activity is one of the key initiator signaling mechanism of cell death or apoptosis (Siddiqui, Ahamad, Jafri, Afzal, & Arshad, 2017). The MMP, associated with the opening of large pores in mitochondrial membranes, is a very important event in apoptosis. We monitored the changes in MMP ( $\Delta\Psi_m$ ) by JC-1 staining. In the cells with intact mitochondrial membrane, the dye accumulates within the mitochondria in its dimeric form and stains the mitochondria bright red, but in cells undergoing apoptosis, MMP collapses and the JC-1 remains in the cytoplasm in a green fluorescent monomeric form. Although piperine is known to induce mitochondrial dysfunction (Gunasekaran, Elangovan, & Niranjali Devaraj, 2017; Siddiqui et al., 2017; Zhang et al., 2015), its effect on cells treated with radiation is not known. As shown in Figure 4a and b, treatment of HT-29 cells with piperine and  $\lambda$ - radiation displays an increment in the population of green-fluorescence cells compared to individual agents alone, indicating that depolarization of mitochondrial membrane is enhanced in the combination treatment. The mitochondrial dysfunction may ultimately induce the cells to undergo apoptosis. The mitochondrial dysfunction results in the release of cytochrome  $c$ , which initiates the activation of cascade of caspases ultimately culminating in apoptosis.

The most prominent event involved in apoptosis signal cascade is the activation of caspases belonging to the family of cysteinyl-aspartate proteases which are naturally present in the cell as inactive zymogens. Upon activation, initiator caspases facilitates the programmed cell death through cleaving and activating the downstream effector caspases (Li & Yuan, 2008). Interestingly as shown in Figure 4c and d cotreatment increased the cleaved caspase-3 (17 kDa) level, one of the most prominent effector caspase, suggesting that piperine enhances IR induced apoptosis. Further we also investigated cleavage of PARP-1, an important molecular feature in apoptotic signaling to analyze if combination treatment enhanced the rate of apoptosis. PARP-1 helps cells to maintain their viability by promoting DNA repair in response to environmental stress (Satoh & Lindahl, 1992) and its cleavage into PARP amino-terminal DNA binding domain (24 kDa) and carboxy-terminal catalytic domain (89 kDa; Lazebnik, Kaufmann, Desnoyers, Poirier, & Earnshaw, 1994; Nicholson et al., 1995) facilitates cellular dis-assembly and serves as a molecular marker for cells undergoing apoptosis (Oliver et al., 1998). Cleavage of PARP-1 by activated caspase-3 is implicated in many cancers (Bhaskara, Panigrahi, Challa, & Babu, 2005; Do et al., 2013; Fofaria, Kim, & Srivastava, 2014). Figure 4c (cleaved PARP-1) and in Figure 4d shows the pattern of cleaved PARP-1 (89 kDa) among various treatments in HT-29 cells. The results demonstrate that

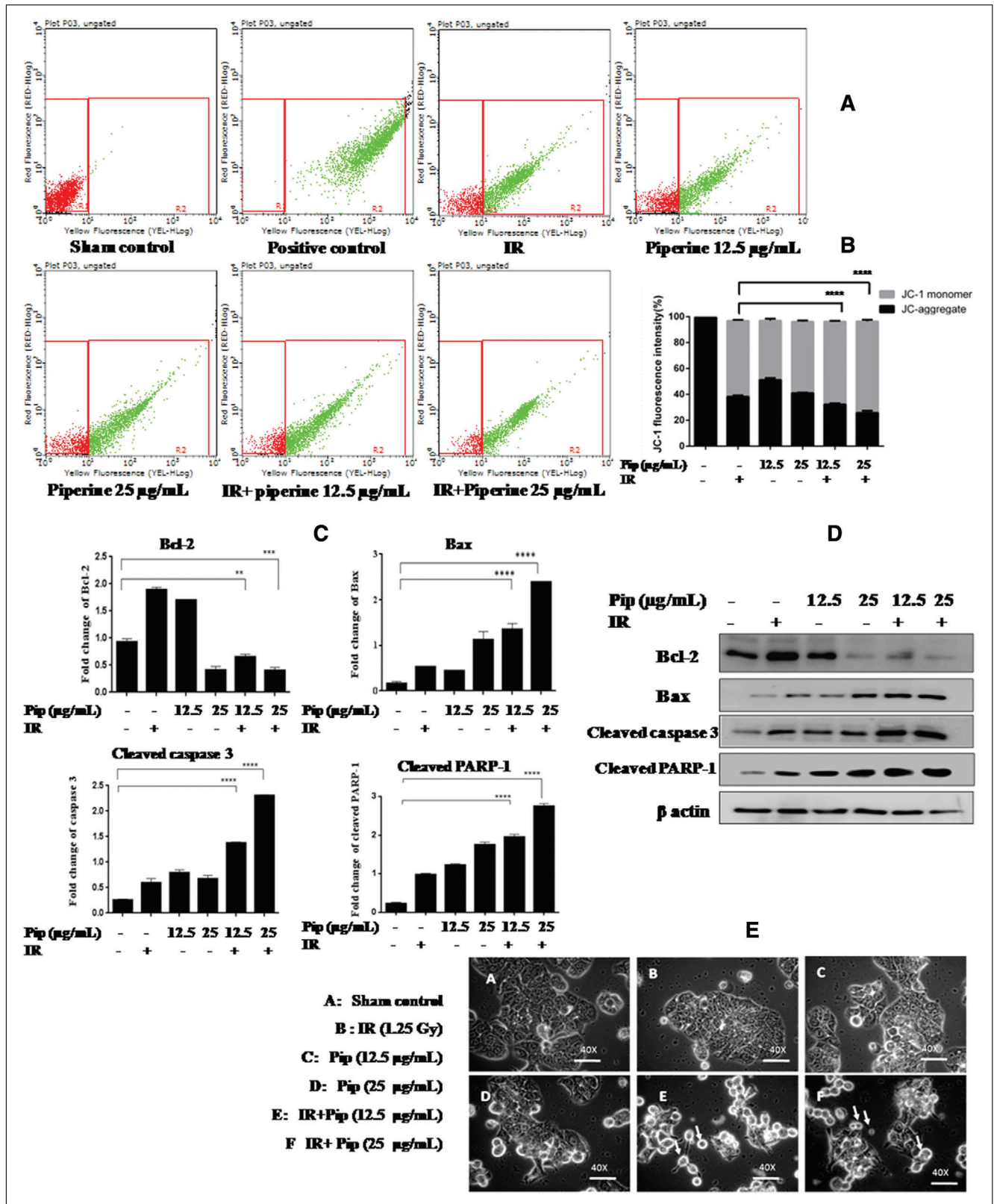
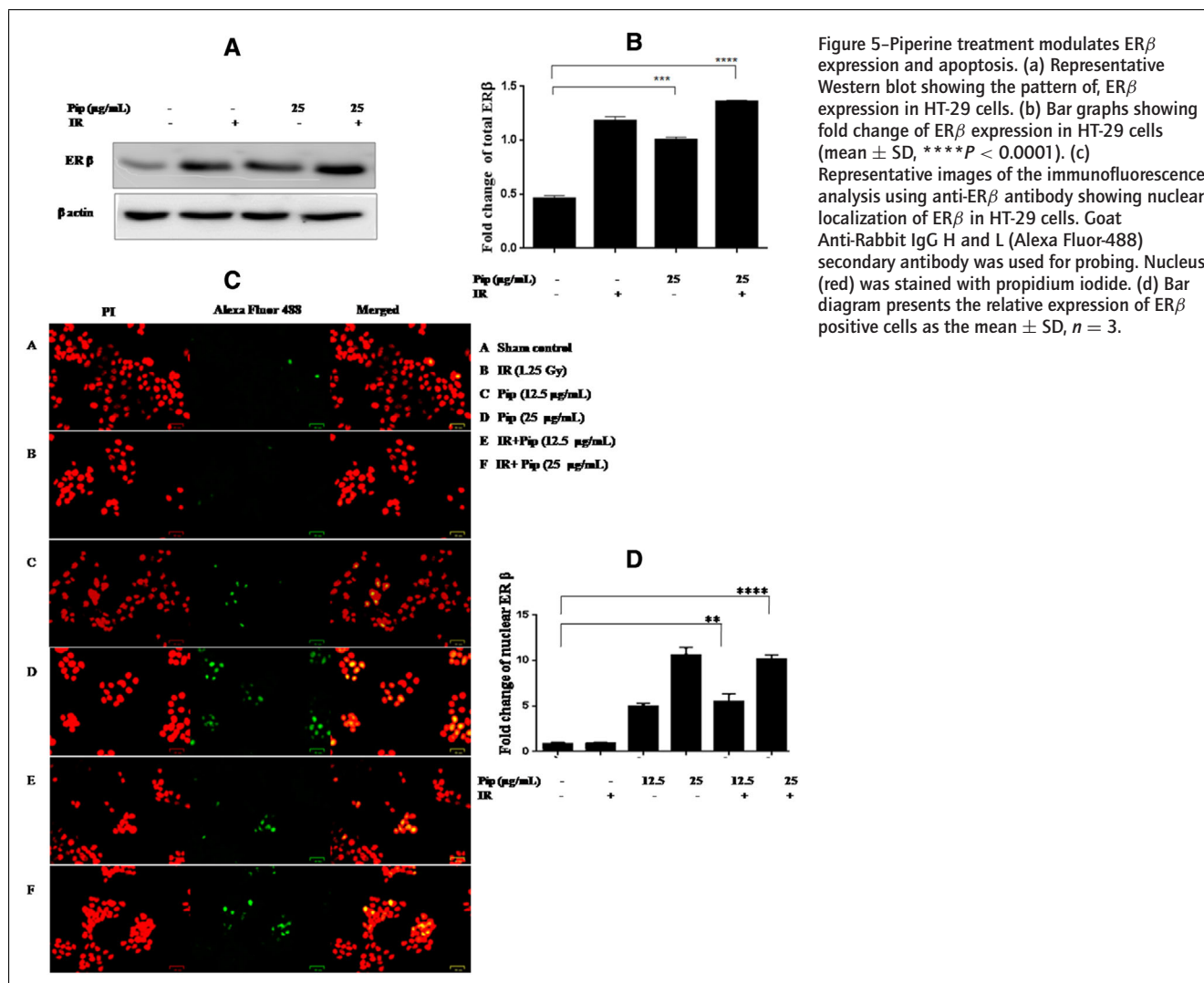


Figure 4–Piperine pretreatment following IR induces mitochondria mediated apoptosis. (a) Flowcytometric analysis of the effect of cotreatment on mitochondrial membrane potential by JC-1 staining. Dot plot shows spectral shift from red to green upon treatment. H<sub>2</sub>O<sub>2</sub> (500 µM) treated cells served as positive control. JC-red represents cells with intact membrane potential and JC-green represents cells with collapsed membrane potential. (b) Bar diagram presents the distribution of cell populations as the mean ± SD, n = 3. (c) Bar graphs showing fold change of BCL-2, BAX, cleaved caspase-3, and cleaved PARP-1 expression in HT-29 cells. (mean ± SD, \*\*\*\*P < 0.0001). (d) Representative Western blot showing the pattern of, BCL-2, BAX, cleaved caspase-3, and cleaved PARP-1 expression in HT-29 cells. (e) Effect of combination treatment (piperine [Pip] and λ-IR) on HT-29 cellular morphology. Arrows indicates cell blebbing and membrane bound apoptotic bodies



PARP-1 activity was dramatically increased ( $P$  < 0.0001) in the combination treatment, indicating that piperine may sensitize the cells to radiation and induces apoptosis.

Morphological analysis showed that piperine treatment in conjunction with radiation enhanced the apoptotic cells significantly when compared to cells treated with irradiated group. As shown in Figure 4e, the vehicle control (A) exhibited an intact colony features of colon cancer morphology, while cells with piperine followed by  $\lambda$ -radiation (Figure 4e (E) and (F)) showed morphological changes that are characteristic of apoptosis, including disappearance colony forming ability, cell shrinkage, and appearance of cell blebbing and numerous apoptotic bodies. Our results suggest that piperine pretreatment lowers the dose of radiation treatment which is needed to suppress the growth of colon cancer cells.

### 3.3 Piperine treatment upregulated the expression of estrogen receptor beta (ER $\beta$ ), a nuclear hormone-dependent transcription factor in HT-29 cells

Targeted activation of ER $\beta$  represents a novel clinical approach for management and prevention of cancers (Bolli & Marino, 2011; Williams, DiLeo, Niv, & Gustafsson, 2016) including colon cancer (Caiazza, Ryan, Doherty, Winter, & Sheahan, 2015; Maingi, Tang, Liu, Ngenya, & Bao, 2020). ER $\beta$  is a potent tumor sup-

pressor and reduces cancer metastasis (Kyriakidis & Papaioannidou, 2016; Nguyen-Vu et al., 2016; Stettner et al., 2007). Estrogen signaling pathways are regulated by a balance between the ER $\alpha$  and ER $\beta$  in target organs (Couse, Lindzey, Grandien, Gustafsson, & Korach, 1997). ER $\beta$  may have antiproliferative effects and therefore antagonistic to ER $\alpha$  function and regulates its expression in tissues expressing these receptors (Weihua et al., 2000). The expression of ER $\beta$  was found to be lowered in many cancers including colorectal carcinoma tissues (Castiglione et al., 2008; Kyriakidis & Papaioannidou, 2016; Xie, Yu, & Luo, 2004). We have investigated the expression of total ERs in HT-29 cells after 48 hr of piperine and radiation treatment. We found that ER $\beta$  expression was significantly enhanced in cells treated with both IR and piperine (Figure 5a and b). Furthermore, immunofluorescence assay was performed to validate the nuclear translocation of ER $\alpha$ / $\beta$ , a key event in genomic ER signaling pathway (Figure 5c and d). Genomic ER signaling involves ligand/hormone binding to the cytoplasmic ERs, receptor dimerization, translocation of ligand receptor complex to the cell nucleus and binding at specific DNA sequence known as estrogen responsive elements (EREs) located at the regulatory or promoter regions and which can induce activation of gene expression and recruitment of co-activators or, transcription factors lead to estrogen receptor-mediated

biological activity (Fox, Andrade, & Shupnik, 2009; Marino, Galuzzo, & Ascenzi, 2006). Immunofluorescence experiments showed ER $\beta$  translocation into the nucleus of the cells treated with piperine alone and in the cotreatment group. Although ER $\alpha$  nuclear translocation was detected in untreated control, we could not observe any detectable signals for ER $\alpha$  in treatment groups (Figure S1). Taken together, our results suggest that piperine in conjunction with  $\gamma$ -radiation arrest the HT-29 cell-cycle arrest at G2/M phase leading to alteration in the BAX/BCL-2 ratio culminating in mitochondrial depolarization and subsequent activation of effector caspase-3 and cleavage of its downstream target PARP-1 aiming to apoptosis. Piperine also induced the expression and nuclear translocation of tumor suppressor ER- $\beta$  which may result in tumor suppression.

#### 4. CONCLUSION

Piperine pretreatment increases the effectiveness of radiation treatment by increasing the sensitivity of cells to radiation induced apoptosis. Hence, pretreatment with piperine could complement radiotherapy via reducing the effective radiation dose and may also control the emergence of radioresistant cancer cells. However, further *in vivo* studies are warranted to fine-tune and establish this hypothesis.

#### ACKNOWLEDGMENT

DLM was supported by Start-up grant (YSS/2015/000987), SERB, DST, Govt. of India and Seed Seed Grant (YU/Seed grant/065-2018) from Yenepoya (deemed to be University). KS was supported by ICMR-SRF, Govt. of India.

#### AUTHOR CONTRIBUTIONS

Authors hereby declare that all authors listed in this manuscript have substantial contribution towards the work to guarantee an authorship.

#### CONFLICTS OF INTEREST

We wish to confirm that there are no known conflicts of interest associated with this publication and there has been no significant financial support for this work that could have influenced its outcome.

#### REFERENCES

Bhaskara, V. K., Panigrahi, M., Challa, S., & Babu, P. P. (2005). Comparative status of activated ERK1/2 and PARP cleavage in human gliomas. *Neuropathology*, 25(1), 48–53. <https://doi.org/10.1111/j.1440-1789.2004.00585.x>

Bolat, Z. B., Islek, Z., Demir, B. N., Yilmaz, E. N., Sahin, F., & Ucisik, M. H. (2020). Curcumin- and Piperine-Loaded Emulsomes as Combinational Treatment Approach Enhance the Anticancer Activity of Curcumin on HCT116 Colorectal Cancer Model. *Frontiers in Bioengineering and Biotechnology*, 8, 50. <https://doi.org/10.3389/fbioe.2020.00050>

Bolli, A., & Marino, M. (2011). Current and future development of estrogen receptor ligands: Applications in estrogen-related cancers. *Recent Patents on Endocrine, Metabolic & Immune Drug Discovery*, 5(3), 210–229. Retrieved from <https://doi.org/10.2174/187221411797265881>

Caiazza, F., Ryan, E. J., Doherty, G., Winter, D. C., & Sheahan, K. (2015). Estrogen receptors and their implications in colorectal carcinogenesis. *Frontiers in oncology*, 5, 19. <https://doi.org/10.3389/fonc.2015.00019>

Caltabiano, R., Leonardi, R., Musumeci, G., Bartoloni, G., Rusu, M. C., Almeida, L. E., & Loreto, C. (2013). Apoptosis in temporomandibular joint disc with internal derangement involves mitochondrial-dependent pathways. An *in vivo* study. *Acta Odontologica Scandinavica*, 71(3–4), 577–583. <https://doi.org/10.3109/00016357.2012.700060>

Cao, H. Y., Ding, R. L., Li, M., Yang, M. N., Yang, L. L., Wu, J. B., ... Wen, Q. L. (2017). Danshensu, a major water-soluble component of Salvia miltiorrhiza, enhances the radioresponse for Lewis Lung Carcinoma xenografts in mice. *Oncology letters*, 13(2), 605–612. <https://doi.org/10.3892/ol.2016.5508>

Castiglione, F., Taddei, A., Rossi Degl'Innocenti, D., Buccoliero, A. M., Bechi, P., Garbini, F., ... Gian, L. T. (2008). Expression of estrogen receptor beta in colon cancer progression. *Diagnostic Molecular Pathology*, 17(4), 231–236. <https://doi.org/10.1097/PDM.0b013e3181656d67>

Chou, T. C. (2010). Drug combination studies and their synergy quantification using the Chou-Talalay method. *Cancer Research*, 70(2), 440–446. <https://doi.org/10.1158/0008-5472.CAN-09-1947.0008-5472.CAN-09-1947>

Chou, T. C., & Talalay, P. (1984). Quantitative analysis of dose-effect relationships: The combined effects of multiple drugs or enzyme inhibitors. *Advances in Enzyme Regulation*, 22, 27–55.

Couse, J. F., Lindzey, J., Grandien, K., Gustafsson, J. A., & Korach, K. S. (1997). Tissue distribution and quantitative analysis of estrogen receptor- $\alpha$  (ER $\alpha$ ) and estrogen receptor- $\beta$  (ER $\beta$ ) messenger ribonucleic acid in the wild-type and ER $\alpha$  knock-out mouse. *Endocrinology*, 138(11), 4613–4621. <https://doi.org/10.1210/endo.138.11.5496>

Do, M. T., Kim, H. G., Choi, J. H., Khanal, T., Park, B. H., Tran, T. P., ... Jeong, H. G. (2013). Antitumor efficacy of piperine in the treatment of human HER2-overexpressing breast cancer cells. *Food Chemistry*, 141(3), 2591–2599. <https://doi.org/10.1016/j.foodchem.2013.04.125>

Fofaria, N. M., Kim, S. H., & Srivastava, S. K. (2014). Piperine causes G1 phase cell cycle arrest and apoptosis in melanoma cells through checkpoint kinase-1 activation. *Plos One*, 9(5), e94298. <https://doi.org/10.1371/journal.pone.0094298>

Fox, E. M., Andrade, J., & Shupnik, M. A. (2009). Novel actions of estrogen to promote proliferation: Integration of cytoplasmic and nuclear pathways. *Steroids*, 74(7), 622–627. <https://doi.org/10.1016/j.steroids.2008.10.014>

Gunasekaran, V., Elangovan, K., & Niranjali Devaraj, S. (2017). Targeting hepatocellular carcinoma with piperine by radical-mediated mitochondrial pathway of apoptosis: An *in vitro* and *in vivo* study. *Food and Chemical Toxicology*, 105, 106–118. <https://doi.org/10.1016/j.fct.2017.03.029>

Han, S. Z., Liu, H. X., Yang, L. Q., Cui, L. D., & Xu, Y. (2017). Piperine (PP) enhanced mitomycin-C (MMC) therapy of human cervical cancer through suppressing BCL-2 signaling pathway via inactivating STAT3/NF- $\kappa$ B. *Biomedicine & Pharmacotherapy = Biomedicine & Pharmacotherapie*, 96, 1403–1410. <https://doi.org/10.1016/j.biopha.2017.11.022>

Hu, T., Li, Z., Gao, C. Y., & Cho, C. H. (2016). Mechanisms of drug resistance in colon cancer and its therapeutic strategies. *World Journal of Gastroenterology: Wjg*, 22(30), 6876–6889. <https://doi.org/10.3748/wjg.v22.i30.6876>

Javvadi, P., Segan, A. T., Tuttle, S. W., & Koumenis, C. (2008). The chemopreventive agent curcumin is a potent radiosensitizer of human cervical tumor cells via increased reactive oxygen species production and overactivation of the mitogen-activated protein kinase pathway. *Molecular Pharmacology*, 73(5), 1491–1501. <https://doi.org/10.1124/mol.107.043554>

Jurgensmeier, J. M., Xie, Z., Deveraux, Q., Ellerby, L., Bredesen, D., & Reed, J. C. (1998). Bax directly induces release of cytochrome c from isolated mitochondria. *PNAS*, 95(9), 4997–5002. <https://doi.org/10.1073/pnas.95.9.4997>

Khan, M., Maryam, A., Mehmood, T., Zhang, Y., & Ma, T. (2015). Enhancing activity of anticancer drugs in multidrug resistant tumors by modulating P-glycoprotein through dietary nutraceuticals. *Asian Pacific Journal of Cancer Prevention*, 16(16), 6831–6839.

Kyrgiou, M., Kallila, I., Markozannes, G., Gunter, M. J., Paraskevaidis, E., Gabra, H., ... Tsilidis, K. K. (2017). Adiposity and cancer at major anatomical sites: Umbrella review of the literature. *Bmj (Clinical Research Ed.)*, 356, j477. <https://doi.org/10.1136/bmj.j477>

Kyriakidis, I., & Papaioannidou, P. (2016). Estrogen receptor beta and ovarian cancer: A key to pathogenesis and response to therapy. *Archives of Gynecology and Obstetrics*, 293(6), 1161–1168. <https://doi.org/10.1007/s00404-016-4027-8>

Lagerweij, T., Hiddingh, L., Biesmans, D., Crommentuijn, M. H., Cloos, J., Li, X. N., ... Hulleman, E. (2016). A chemical screen for medulloblastoma identifies quercetin as a putative radiosensitizer. *Oncotarget*, 7(24), 35776–35788. <https://doi.org/10.18632/oncotarget.7980>

Lazebnik, Y. A., Kaufmann, S. H., Desnoyers, S., Poirier, G. G., & Earnshaw, W. C. (1994). Cleavage of poly(ADP-ribose) polymerase by a proteinase with properties like ICE. *Nature*, 371(6495), 346–347. <https://doi.org/10.1038/371346a0>

Li, H., Krstin, S., Wang, S., & Wink, M. (2018). Capsaicin and Piperine Can Overcome Multidrug Resistance in Cancer Cells to Doxorubicin. *Molecules (Basel, Switzerland)*, 23(3). Retrieved from <https://www.mdpi.com/1420-3049/23/3/557>

Li, J., & Yuan, J. (2008). Caspases in apoptosis and beyond. *Oncogene*, 27(48), 6194–6206. <https://doi.org/10.1038/onc.2008.297>

Lin, Y., Xu, J., Liao, H., Li, L., & Pan, L. (2014). Piperine induces apoptosis of lung cancer A549 cells via p53-dependent mitochondrial signaling pathway. *Tumour Biology: The Journal of the International Society for Oncodevelopmental Biology and Medicine*, 35(4), 3305–3310. <https://doi.org/10.1007/s13277-013-1433-4>

Maingi, J. W., Tang, S., Liu, S., Ngenya, W., & Bao, E. (2020). Targeting estrogen receptors in colorectal cancer. *Molecular Biology Reports*, 47(5), 4087–4091. <https://doi.org/10.1007/s11033-020-05414-6>

Manayi, A., Nabavi, S. M., Setzer, W. N., & Jafari, S. (2018). Piperine as a potential anticancer agent: A review on preclinical studies. *Current Medicinal Chemistry*, 25(37), 4918–4928. <https://doi.org/10.2174/0929867324666170523120656>

Marino, M., Galluzzo, P., & Ascenzi, P. (2006). Estrogen signaling multiple pathways to impact gene transcription. *Current Genomics*, 7(8), 497–508. <https://doi.org/10.2174/138920206779315737>

Narita, M., Shimizu, S., Ito, T., Chittenden, T., Lutz, R. J., Matsuda, H., & Tsujimoto, Y. (1998). Bax interacts with the permeability transition pore to induce permeability transition and cytochrome c release in isolated mitochondria. *PNAS*, 95(25), 14681–14686. <https://doi.org/10.1073/pnas.95.25.14681>

Naseri, M. H., Mahdavi, M., Davoodi, J., Tackallou, S. H., Goudarzvand, M., & Neishabouri, S. H. (2015). Up regulation of Bax and down regulation of Bcl2 during 3-NC mediated apoptosis in human cancer cells. *Cancer cell international*, 15, 55. <https://doi.org/10.1186/s12935-015-0204-2>

Nguyen-Vu, T., Wang, J., Mesmar, F., Mukhopadhyay, S., Saxena, A., McCollum, C. W., ... Williams, C. (2016). Estrogen receptor beta reduces colon cancer metastasis through a novel miR-205 - PROX1 mechanism. *Oncotarget*, 7(27), 42159–42171. <https://doi.org/10.18632/oncotarget.9895>

Nicholson, D. W., Ali, A., Thornberry, N. A., Vaillancourt, J. P., Ding, C. K., Gallant, M., ... Lazebnik, Y. A. (1995). Identification and inhibition of the ICE/CED-3 protease necessary for mammalian apoptosis. *Nature*, 376(6535), 37–43. <https://doi.org/10.1038/376037a0>

Oliver, F. J., de la Rubia, G., Rolli, V., Ruiz-Ruiz, M. C., de Murcia, G., & Murcia, J. M. (1998). Importance of poly(ADP-ribose) polymerase and its cleavage in apoptosis. Lesson from an uncleavable mutant. *Journal of Biological Chemistry*, 273(50), 33533–33539. <https://doi.org/10.1074/jbc.273.50.33533>

Ortiz, T., Lopez, S., Burguillos, M. A., Edreira, A., & Pinero, J. (2004). Radiosensitizer effect of wortmannin in radioresistant bladder tumoral cell lines. *International Journal of Oncology*, 24(1), 169–175.

Rather, R. A., & Bhagat, M. (2018). Cancer Chemoprevention and Piperine: Molecular Mechanisms and Therapeutic Opportunities. *Frontiers in Cell and Developmental Biology*, 6, 10. <https://doi.org/10.3389/fcell.2018.00010>

Satoh, M. S., & Lindahl, T. (1992). Role of poly(ADP-ribose) formation in DNA repair. *Nature*, 356(6367), 356–358. <https://doi.org/10.1038/356356a0>

- Siddiqui, S., Ahamad, M. S., Jafri, A., Afzal, M., & Arshad, M. (2017). Piperine Triggers Apoptosis of Human Oral Squamous Carcinoma Through Cell Cycle Arrest and Mitochondrial Oxidative Stress. *Nutrition and Cancer*, *69*(5), 791–799. <https://doi.org/10.1080/01635581.2017.1310260>
- Stettner, M., Kaulfuss, S., Burfeind, P., Schweyer, S., Strauss, A., Ringert, R. H., & Thelen, P. (2007). The relevance of estrogen receptor-beta expression to the antiproliferative effects observed with histone deacetylase inhibitors and phytoestrogens in prostate cancer treatment. *Molecular Cancer Therapeutics*, *6*(10), 2626–2633. Retrieved from <https://doi.org/10.1158/1535-7163.MCT-07-0197>
- Stoddart, M. J. (2011). Cell viability assays: Introduction. *Methods in Molecular Biology*, *740*, 1–6. [https://doi.org/10.1007/978-1-61779-108-6\\_1](https://doi.org/10.1007/978-1-61779-108-6_1)
- Syed, S. B., Arya, H., Fu, I. H., Yeh, T. K., Periyasamy, L., Hsieh, H. P., & Coumar, M. S. (2017). Targeting P-glycoprotein: Investigation of piperine analogs for overcoming drug resistance in cancer. *Scientific Reports*, *7*(1), 7972. <https://doi.org/10.1038/s41598-017-08062-2>
- Tak, J. K., Lee, J. H., & Park, J. W. (2012). Resveratrol and piperine enhance radiosensitivity of tumor cells. *BMB Rep*, *45*(4), 242–246. <https://doi.org/10.5483/bmbrep.2012.45.4.242>
- Tang, Q., Ma, J., Sun, J., Yang, L., Yang, F., Zhang, W., ... Wang, H. (2018). Genistein and AG1024 synergistically increase the radiosensitivity of prostate cancer cells. *Oncology Reports*, *40*(2), 579–588. <https://doi.org/10.3892/or.2018.6468>
- Tolosa, L., Donato, M. T., & Gomez-Lechon, M. J. (2015). General Cytotoxicity Assessment by Means of the MTT Assay. *Methods in Molecular Biology*, *1250*, 333–348. [https://doi.org/10.1007/978-1-4939-2074-7\\_26](https://doi.org/10.1007/978-1-4939-2074-7_26)
- Wei, M. C., Zong, W. X., Cheng, E. H., Lindsten, T., Panoutsakopoulou, V., Ross, A. J., ... Korsmeyer, S. J. (2001). Proapoptotic BAX and BAK: A requisite gateway to mitochondrial dysfunction and death. *Science*, *292*(5517), 727–730. <https://doi.org/10.1126/science.1059108>
- Weihua, Z., Saji, S., Makinen, S., Cheng, G., Jensen, E. V., Warner, M., & Gustafsson, J. A. (2000). Estrogen receptor (ER) beta, a modulator of ERalpha in the uterus. *PNAS*, *97*(11), 5936–5941. Retrieved from <https://www.pnas.org/content/97/11/5936>
- Williams, C., DiLeo, A., Niv, Y., & Gustafsson, J. A. (2016). Estrogen receptor beta as target for colorectal cancer prevention. *Cancer Letters*, *372*(1), 48–56. <https://doi.org/10.1016/j.canlet.2015.12.009>
- Xie, L. Q., Yu, J. P., & Luo, H. S. (2004). Expression of estrogen receptor beta in human colorectal cancer. *World Journal of Gastroenterology: Wjg*, *10*(2), 214–217. <https://doi.org/10.3748/wjg.v10.i2.214>
- Yaffe, P. B., Power Coombs, M. R., Doucette, C. D., Walsh, M., & Hoskin, D. W. (2015). Piperine, an alkaloid from black pepper, inhibits growth of human colon cancer cells via G1 arrest and apoptosis triggered by endoplasmic reticulum stress. *Molecular Carcinogenesis*, *54*(10), 1070–1085. <https://doi.org/10.1002/mc.22176>
- Zhang, J., Zhu, X., Li, H., Li, B., Sun, L., Xie, T., ... Ye, Z. (2015). Piperine inhibits proliferation of human osteosarcoma cells via G2/M phase arrest and metastasis by suppressing MMP-2/-9 expression. *International Immunopharmacology*, *24*(1), 50–58. <https://doi.org/10.1016/j.intimp.2014.11.012>

## Supporting Information

Additional supporting information may be found online in the Supporting Information section at the end of the article.

**Figure S1.** Representative images of the immunofluorescence analysis using anti-ER alpha antibody showing nuclear localization of ER alpha in HT-29 cells. Goat Anti-Rabbit IgG HandL (Alexa Fluor 488) secondary antibody was used for probing. Nucleus (red) was stained with propidium iodide.



# Effect of Piperine in Combination with Gamma Radiation on A549 Cells

Koniyan Shaheer<sup>1</sup> M. Divya Lakshmanan<sup>1</sup>

<sup>1</sup>Molecular Biology Division, Yenepoya Research Centre, Yenepoya (Deemed to be University), Deralakatte, Mangalore, Karnataka, India

**Address for correspondence** M. Divya Lakshmanan, PhD, Molecular Biology Division, Yenepoya Research Centre, Yenepoya (deemed to be University), Deralakatte, Mangalore, Karnataka 575018, India (e-mail: divyalmangalath@gmail.com, divya@yenepoya.edu.in).

J Health Allied Sci<sup>NU</sup>:2021;11:80–86

## Abstract

**Background** Lung cancer is a major constrain that increases mortality globally. Radiotherapy is one of the treatment modalities against lung cancer. A high dose of targeted radiation is required to achieve the treatment efficacy of cell killing. After radiotherapy, eventual tumor progression and therapy resistance are still a consequence of patient who undertakes nonsurgical radiation therapy. Piperine, a plant alkaloid, has been known to enhance the action of the anticancer drugs in various drug-resistant cancer cells. The aim of the current in vitro study was to study the effect of piperine on radiosensitizing property against A549 cells.

**Methods** In vitro radiosensitizing activity of piperine was elucidated on A549 cells using MTT (3-(4, 5-dimethylthiazol-2-yl)-2,5-diphenyltetrazolium bromide) assay. CompuSyn analysis was used to compute the combination index values to analyze the combinatory effect of piperine and radiation

**Results and Conclusion** We observed that piperine increased tumor cell killing in combination with the  $\gamma$ -radiation in vitro. However, further studies are warranted to understand the molecular mechanism of the radiosensitizing action of piperine.

## Keywords

- ▶ lung cancer
- ▶ piperine
- ▶ radiosensitization
- ▶ CompuSyn analysis

## Introduction

The poor prognosis of patients with lung cancer is the major cause of cancer-related deaths.<sup>1</sup> According to GLOBOCAN 2018, lung cancer has the highest incidence rate and mortality rate.<sup>2</sup> Though the radiotherapy is a main treatment modality against lung cancer, gradual development of therapy resistance and cancer recurrence is a major constrain.<sup>3</sup> Intensive attempts to improve the outcome of radiotherapy treatment have been a remarkable challenge. One of the few achievable therapeutic strategies of lung cancer to increase the treatment efficacy demonstrated that the combination of radiosensitizer with radiation produces a significant decrease in mortality compared with irradiation group.<sup>4</sup> Because these studies use a relatively low

dose of radiation and demonstrated a reduced effect on the occurrence of cancer metastases and secondary cancer, the improvement realized by the use of radiosensitizer in therapy probably due to radiosensitization.<sup>4-6</sup> Thus, the discovery of a potent radiosensitizer against lung cancer could improve the outcome of treatment of this disease.

A most important concern about radiotherapy is that it acquires resistance by activating several alternating signaling pathways that elicit cancer and/or enhanced DNA repair pathways. Radiotherapy resistance, defined as a poor prognosis in the effectiveness of radio therapy, is a major hindrance in cancer treatment. In such cases, combinatorial approach is an effective way to augment treatment efficacy. Combinatory approach often follows three main strategies:

**published online**  
February 10, 2021

**DOI** <https://doi.org/10.1055/s-0040-1722808>  
**ISSN** 2582-4287.

© 2021. Nitte (Deemed to be University).

This is an open access article published by Thieme under the terms of the Creative Commons Attribution-NonDerivative-NonCommercial-License, permitting copying and reproduction so long as the original work is given appropriate credit. Contents may not be used for commercial purposes, or adapted, remixed, transformed or built upon. (<https://creativecommons.org/licenses/by-nc-nd/4.0/>).

Thieme Medical and Scientific Publishers Pvt. Ltd. A-12, 2nd Floor, Sector 2, Noida-201301 UP, India

(1) inhibition of possible alternative pathways, (2) targeting of the single pathway to accomplish downregulation or inhibition, or (3) targeting and downregulation or inhibition of two different pathways will lead to synergistic action on radiosensitization.<sup>7</sup>

Phytochemicals or natural based combinatorial approach may serve in the development of anticancer agents with minimal side effects and better efficacy.<sup>8-11</sup> In addition, natural compounds because of their antioxidant and anti-inflammatory effects have better effects as radiation protectors for healthy cells.<sup>12</sup> Some natural radiosensitizers are danshensu, curcumin, wortmannin, genistein, and quercetin.<sup>13-18</sup> *Piper nigrum* Linn commonly known as black pepper belongs to the spices widely consumed by a great number of people worldwide. Piperine is a bioactive compound and key alkaloid, present in *Piper nigrum* Linn and *Piper longum* Linn (long pepper). It has been found that piperine enhances the action of the anticancer drugs in various drug-resistant cancer cells.<sup>19-23</sup> Studies regarding the radiosensitizing effect of piperine on lung cancer are yet to be done. Combination index (CI) is a theorem of Chou-Talalay that defines quantitative explanation for additive effect ("CI" = 1), synergism ("CI" < 1), and antagonism ("CI" > 1) in drug combinations studies. This theory also explains algorithms for computer-based model for synergistic and/or antagonistic mechanism at any dose level and effect through isobologram and CI plot respectively.<sup>24</sup> As there is a need to develop a potent therapy to treat lung cancer, our study aimed to explore the effect of piperine pretreatment and to improve radiotherapy treatment on lung cancer cells and interpret its mechanism of action.

## Materials and Methods

The phytochemical piperine (>97%) and dimethyl sulfoxide (DMSO) were procured from Sigma-Aldrich, India. Cell culture reagents such as Dulbecco's Modified Eagles Medium (DMEM), fetal bovine serum (FBS), penicillin and streptomycin solution, L-glutamine, Trypan blue dye, 3-(4,5-dimethylthiazol-2-yl)-2,5-diphenyltetrazolium bromide (MTT), and other chemicals (analytical or molecular biology grade) were procured from HiMedia, India.

### Cell Culture

Human lung adenocarcinoma cell line-A549 (NCCS, Pune, India) was cultured in culture media (DMEM), supplemented with FBS (10%), penicillin, and streptomycin (1%) and 2 mM L-glutamine. The cells were maintained at 37°C in a 5% CO<sub>2</sub> humidified atmospheric conditions.

### Dose Optimization of Piperine on A549 Cells

Dose optimization of piperine was done using MTT assay.<sup>25,26</sup> Briefly, A549 cells (3x10<sup>3</sup> cells/well) were seeded into 96-well plate and incubated 24 hours at normal culture conditions. Piperine dissolved in DMSO was taken at concentrations of 10 to 100 µg/mL and was added into the culture plates and incubated for 48 hours and then MTT assay was

performed. The optical density readings at 570 nm were taken using the multimode plate reader (FLUOstar Omega, Mumbai, India). The experiment was performed in triplicates. The final DMSO concentration in the treatment was kept within 0.1%.

### Dose Optimization of Ionizing Gamma Radiation on A549 Cells

A549 cells were exposed to ionizing gamma (γ)-radiation (IR) at a dose ranging from 1.25 to 10 Gy, using a low-dose gamma irradiator-2000 (BRIT, Mumbai, India), with <sup>60</sup>Co source as irradiator and 10.3 Gy/min deliverable dose rate. MTT cell proliferation assay was performed after 48 hours of incubation.<sup>25,26</sup>

### Cytotoxicity Assessment Using MTT Cell Proliferation Assay

The two doses of piperine (low dose: 12.5 and high dose: 25 µg/mL) were added to A549 cells in individual flasks, 2 hours before to γ-radiation treatment (1.25 Gy) and incubated at normal culture condition for 48 hours as described previously.<sup>26</sup> Cells (vehicle control) kept in the chamber but not irradiated were considered as sham control. After 48 hours of incubation, the cytotoxic effect of piperine and γ-radiation on A549 cells was evaluated by MTT cell proliferation assay as mentioned earlier.<sup>25</sup>

$$\text{Percentage of cell viability} = \frac{(\text{No. of viable cells in control} - \text{No. viable cell in test})}{\text{No. of viable cells in control}} \times 100$$

### CompuSyn Analysis to Check the Synergistic Effect of the Combination Treatment

CompuSyn software (ComboSyn, Inc., Paramus, NJ, United States) was used to quantitatively depict the mechanistic effect of the combination treatment. The data from the cytotoxicity studies were taken to compute CI values, CI plot, dose response curve, and normalized isobologram. CI values were used to analyze the synergism ("CI" < 1), additive effect ("CI" = 1) and/or antagonism ("CI" > 1) of the co-treatment.<sup>24,27</sup>

The CI is calculated by using the formula:

$$CI = \frac{d1}{DX1} + \frac{d2}{DX2} CI$$

Where Dx1 indicates, the dose of test agent 1 (γ-radiation) needed to decrease "x" percentage of proliferation alone, and d1 indicates the dose of test agent 1 needed to decrease "x" percentage of proliferation along with d2 treatment. Similarly, Dx2 indicates the dose of test agent 2 (piperine) needed to decrease "x" percentage of proliferation alone, and d2 indicates the dose of test agent 2 needed to decrease "x" percentage of proliferation along with d1.

### Morphological Analysis

A549 cells at a cell density of 0.35 × 10<sup>6</sup> cells/mL were seeded into 35 mm dishes. After 24 hours of incubation, the cells were pretreated with piperine for 2 hours and then irradiated with γ-radiation. The cells that are untreated with piperine and



nonirradiated were taken as control. The changes in the cell morphology were observed using inverted light microscope (Zeiss Primo Vert, Mumbai, India) at a magnification of 40 $\times$ .

### Statistical Analysis

Data were represented as mean  $\pm$  standard deviation. Data analysis was done using one-way analysis of variance using GraphPad PRISM version 7.0. A *p*-value < 0.0001 was scored significant.

## Results

### Effect of Piperine and Gamma Radiation on Cell Viability or Cell Proliferation

MTT cell proliferation assay is used to check the effect of piperine and  $\gamma$ -radiation on A549 cell proliferation or cell viability indirectly that measures mitochondrial succinate dehydrogenase activity spectrophotometrically. Inhibition of A549 cell proliferation against piperine was in a

dose-dependent manner ( $\blacktriangleright$ Fig. 1A) and A549 cells show high resistance toward  $\gamma$ -radiation of selected dose ranging from 1.25 to 10 Gy. Cell killing was less than 40% (33–37%) even at 10 Gy ( $\blacktriangleright$ Fig. 1B).

### Piperine Synergistically Enhances Radiation-Induced Cell Death on A549 Cells

To analyze piperine could sensitize A549 cells to  $\gamma$ -radiation treatment (IR), two doses of piperine (low dose: 12.5 and high dose: 25  $\mu$ g/mL) were added to A549 cells in individual flasks 2 hours before to  $\gamma$ -radiation treatment (1.25 Gy) and incubated at normal culture conditions for 48 hours. We found that piperine treatment combined with  $\gamma$ -radiation exhibited enhanced inhibition of cell proliferation (~55%) compared with individual  $\gamma$ -radiation/piperine treatment alone ( $\blacktriangleright$ Fig. 1C). Significant difference among various treatment groups in the observed cytotoxicity is given in  $\blacktriangleright$ Table 1. To study whether the radiosensitization finding of the combination treatment action is synergistic

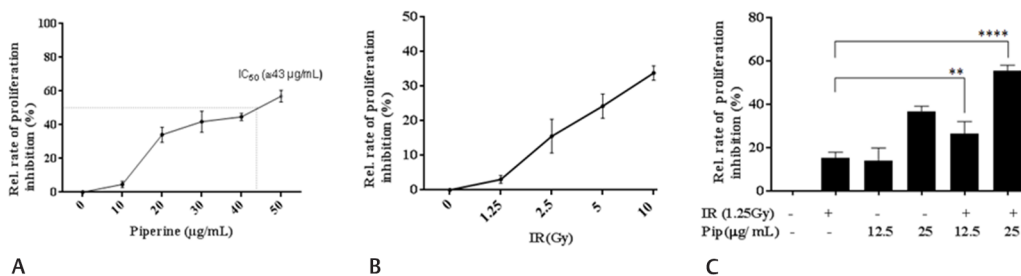


**Fig. 1** Radiosensitization effect of piperine on A549 cells. (A) Optimization of piperine dose. Piperine was taken at different concentrations 10 to 100  $\mu$ g/mL and 3-(4, 5-dimethylthiazol-2-yl)-25-diphenyltetrazolium bromide (MTT) assay was performed on A549 cells. DMSO treated cells were used as vehicle control. (B) Optimization of  $\gamma$ -radiation dose. (C) Relative cell proliferation inhibition analysis after combination treatment with piperine and  $\gamma$ -radiation by MTT assay on A549 cells. Data was represented as mean  $\pm$  standard deviation. IR, ionizing gamma radiation; Pip, piperine.

**Table 1** Multiple comparison analysis of MTT cell proliferation assay of combination experiment by post-ANOVA Bonferroni's multiple comparisons test

Comparisons among groups	Significance	Adjusted <i>p</i> -Value
Sham versus IR ( $\gamma$ )	***	0.0002
Sham versus Pip(12.5 $\mu$ g/mL)	***	0.0007
Sham versus Pip(25 $\mu$ g/mL)	****	<0.0001
Sham versus IR( $\gamma$ ) +Pip (12.5 $\mu$ g/mL)	****	<0.0001
Sham versus IR( $\gamma$ )+Pip (25 $\mu$ g/mL)	****	<0.0001
IR ( $\gamma$ ) versus Pip(12.5 $\mu$ g/mL)	ns	>0.9999
IR ( $\gamma$ ) versus Pip(25 $\mu$ g/mL)	****	<0.0001
IR ( $\gamma$ ) versus IR( $\gamma$ ) +Pip (12.5 $\mu$ g/mL)	**	0.0066
IR ( $\gamma$ ) versus IR( $\gamma$ )+Pip (25 $\mu$ g/mL)	****	<0.0001
Pip(12.5 $\mu$ g/mL) versus Pip (25 $\mu$ g/mL)	****	<0.0001
Pip(12.5 $\mu$ g/mL) versus IR( $\gamma$ ) +Pip (12.5 $\mu$ g/mL)	**	0.0019
Pip(12.5 $\mu$ g/mL) versus IR( $\gamma$ )+Pip (25 $\mu$ g/mL)	****	<0.0001
Pip(25 $\mu$ g/mL) versus IR( $\gamma$ ) +Pip (12.5 $\mu$ g/mL)	****	<0.0001
Pip(25 $\mu$ g/mL) versus IR( $\gamma$ )+Pip (25 $\mu$ g/mL)	NS	0.0801
IR( $\gamma$ ) +Pip (12.5 $\mu$ g/mL) versus IR( $\gamma$ )+Pip (25 $\mu$ g/mL)	****	<0.0001

Abbreviations: ANOVA, analysis of variance; CI, confidence interval; IR( $\gamma$ ), ionizing gamma radiation; MTT, 3-(4, 5-dimethylthiazol-2-yl)-25-diphenyltetrazolium bromide; Pip, piperine.

or additive, we computed the CI values and plotted CI plot isobologram for the two selected concentrations of piperine (low dose: 12.5 and high dose: 25 µg/mL) against exposed 1.25 Gy of  $\gamma$ -radiation using freely available CompuSyn software. This study was designed to analyze the nature of the effects of combination treatment.

A dose response curve for piperine and  $\gamma$ -radiation was generated as given in **Fig. 2A, D**. Synergism effect is higher than an additive and antagonism effect. As represented in the CI plots (**Fig. 2B, E**) and isobologram (**Fig. 2C, F**), the calculated CI values were less than 1 for the combination treatments (IR + Pip 12.5 µg/mL and IR + Pip 25 µg/mL). This clearly demonstrates a synergistic effect. Surprisingly, all the values (values computed from triplicate experiments) in the isobologram (**Fig. 2C, F**) generated for the two selected concentrations of piperine (low dose: 12.5 and high dose: 25 µg/mL) with  $\gamma$ -radiation 1.25 Gy showed well within the stipulated region of synergism. CI points of each combination study are shown in **Tables 2 and 3**, respectively. Our findings from these results show that pretreatment with piperine efficiently sensitized A549 cells toward cell killing effects of  $\gamma$ -radiation, compared with a single regime treatment.

### Cellular Morphological Analysis

Morphological assessment showed that piperine pretreatment in combination with  $\gamma$ -radiation increased the cell

death considerably when compared with A549 cells treated with piperine/ $\gamma$ -radiation alone (**Fig. 3**).

As given in **Fig. 3**, the control (**A**) exhibited colony features of A549 lung cancer morphology, while cells pretreated with piperine followed by  $\gamma$ -radiation (**Fig. 3E, F**) showed

**Table 2** CI data for combination of IR+Pip 12.5 µg/mL

IR( $\gamma$ ) (Gy)	Piperine (µg/mL)	Effect	CI
1.25	12.5	0.79	0.97832
1.25	12.5	0.75	0.84384
1.25	12.5	0.71	0.73908
1.25	12.5	0.67	0.65425

Abbreviations: CI, combination index; IR( $\gamma$ ), ionizing gamma radiation; Pip, piperine.

**Table 3** CI data for combination of IR+Pip25 µg/mL

IR( $\gamma$ ) (Gy)	Piperine (µg/mL)	Effect	CI
1.25	25.0	0.44	0.63135
1.25	25.0	0.45	0.64766
1.25	25.0	0.41	0.58435
1.25	25.0	0.47	0.68139

Abbreviations: CI, combination index; IR( $\gamma$ ), ionizing gamma radiation; Pip, piperine.

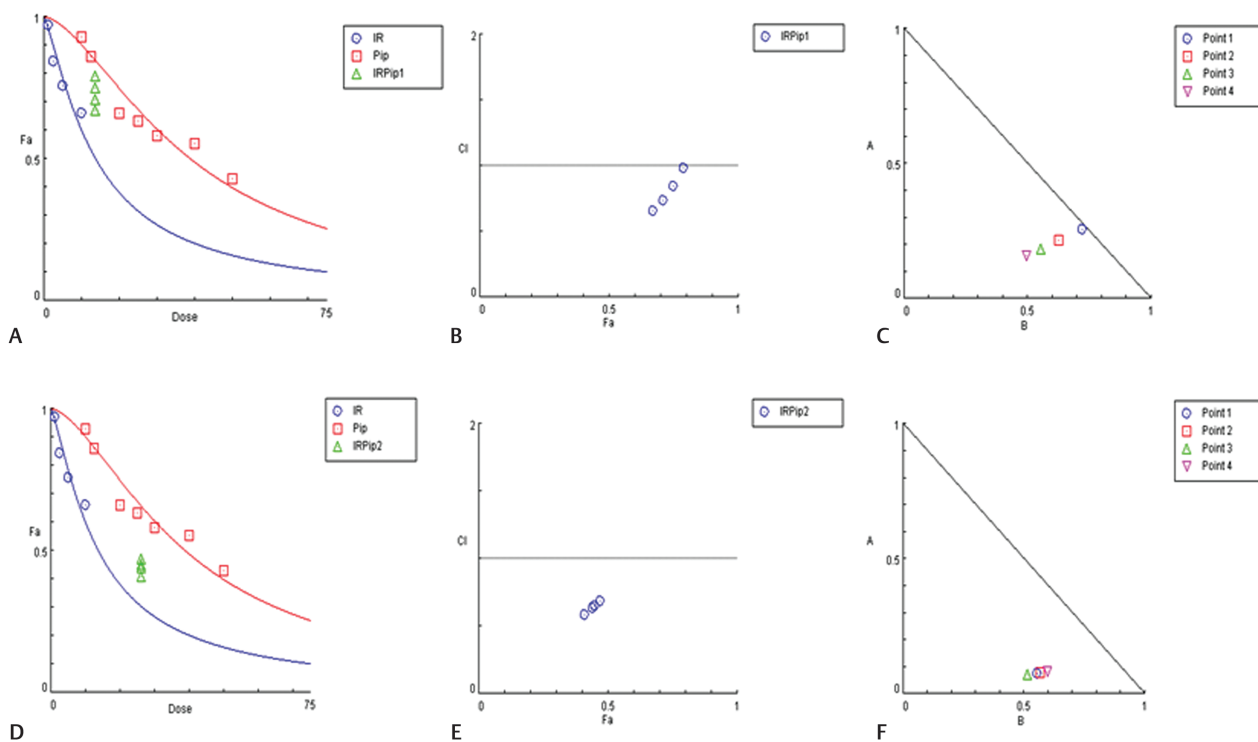


**Fig. 2** CompuSyn analysis to determine the synergistic effect of the piperine and  $\gamma$ -radiation on A549 cells. **(A)** Dose response curve of piperine (Pip) and IR (ionizing  $\gamma$ -radiation). IRPip1 indicates combination of IR (ionizing  $\gamma$ -radiation) and piperine 12.5 µg/mL. **(B)** Combination index (CI) plot and CI table depict that CI value for the chosen combination treatment (IR+ Pip 12.5 µg/mL) is <1. **(C)** Normalized isobologram of the combination treatment (IR+ Pip 12.5 µg/mL). **(D)** Dose response curve of piperine (Pip) and ionizing  $\gamma$ -radiation (IR), IRPip2 indicates combination of IR (ionizing  $\gamma$ -radiation) and piperine 25 µg/mL. **(E)** CI plot and CI table show that CI value for the chosen combination treatment (ionizing  $\gamma$ -radiation (IR)+ Pip 12.5 µg/mL) is <1. **(F)** Normalized isobologram of the combination treatment (ionizing  $\gamma$ -radiation (IR)+ Pip 25 µg/mL).

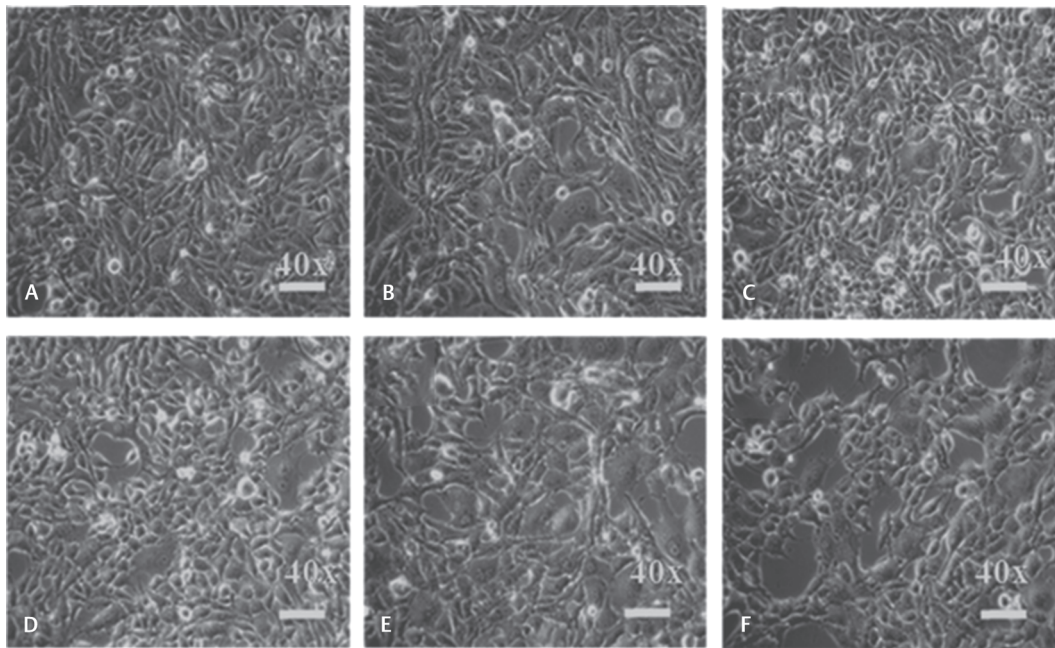


**Fig. 3** Morphological analysis of A549 cells after combination treatment with piperine (Pip) and ionizing  $\gamma$ -radiation (IR), where (A) Sham control, (B) IR, (C) Pip 12.5  $\mu\text{g}/\text{mL}$ , (D) Pip 25  $\mu\text{g}/\text{mL}$ , (E) IR+ Pip 12.5  $\mu\text{g}/\text{mL}$ , and (F) IR+ Pip 25  $\mu\text{g}/\text{mL}$ .

characteristic features of apoptosis, including disappearance colony formation and appearance of cell shrinkage. The low-dose radiation along with piperine treatment strategy results suggests that piperine pretreatment may improve the treatment strategy by decreasing the dose of radiation treatment that is necessary to suppress the augmentation of lung cancer cells.

## Discussion

Accumulating literature data on *in vitro* and *in vivo* activities of piperine show that piperine has immunomodulatory and anti-allergic, anti-inflammatory, enhanced drug bioavailability potential, antimutagenic on healthy cells.<sup>28,29</sup> Cytotoxic effect is selective toward cancer cells.<sup>30-32</sup> In the present study, we observe piperine as a new compound for reducing the lung cancer proliferation and reveal a novel radiosensitization method of lung cancer via increased inhibition of cell proliferation after piperine pretreatment prior to the radiation treatment. Furthermore, we identify the role of piperine in tumor inhibition with radiation treatment being synergistic in nature. Our results provide new strategic insight into the radiosensitization of lung cancer and suggest that piperine may be an ideal tumor suppressor compound and can be used in radiosensitization in lung cancer treatment.

Programmed cell death or apoptosis is a target of anti-tumor therapy. Chemo/radiotherapy and phytochemicals like piperine induce the generation reactive oxygen species (ROS) leading to DNA damage and cell cycle arrest. DNA damage may lead to mitochondria-mediated intrinsic pathway of apoptosis.<sup>26,33</sup> Accumulating evidence has suggested that mechanisms significance to radiosensitivity include programmed cell death or apoptosis through inhibition of cell proliferation with

characteristic morphological changes, alteration of cell cycle, inducing DNA damage and inhibition of repair pathways, and alteration of tumor immune microenvironment.<sup>26,34,35</sup> Studies have shown the targeting DNA damage response, double-strand break repair, and other molecular responses induced cell inactivation by radiation could hold a great approach for radiosensitization.<sup>36</sup> The experimental data indicate that the combination treatments augmented the cell death compared with individual regime. To study whether the combination effect is synergistic or additive, CI analysis was performed. It clearly demonstrates that the combinatorial effect is synergistic in nature for the selected dose of individual regime. The CI theorem is based on the physical, chemical, and mathematical principles of the mass-action law<sup>37,38</sup> and the CI equation.<sup>37,39</sup> Although the mechanisms of each drug are valuable to know, it is not essential to know the mechanism of each drug for studying the synergism or antagonism.<sup>37</sup> The mechanism of synergistic action after the treatment with piperine and radiation may be due to enhanced DNA damage and cell cycle arrest through induction of ROS that may alter mitochondrial membrane potential leading to apoptosis as observed in our earlier studies with colon cancer cells<sup>26</sup> and other cancer cell line studies.<sup>40</sup> These findings have unique significance, as piperine may have the potential to be developed as a radiosensitizing against lung cancer cells.

## Conclusion

The *in vitro* radiosensitization potential of piperine was elucidated on A549 lung cancer cells in combination with  $\gamma$ -radiation. Compusyn analysis shows that the combination treatment is synergistic in nature. This investigation on piperine revealed a basic knowledge on combinatory effect of piperine and  $\gamma$ -radiation on A549 cells. More studies are

warranted to understand the molecular mechanism of the radiosensitizing action of piperine.

#### Conflict of Interest

D.L.M. is supported with research grant/065–2018, Yenepoya (deemed to be University). S.K. is supported by ICMR-SRF, Govt. of India.

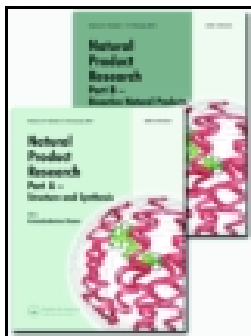
#### Acknowledgment

The authors would like to thank Prof. Somashekarappa H.M., Director, Centre for Application of Radioisotopes and Radiation Technology (CARRT), Mangalore University, Karnataka, India, for providing  $\gamma$ -radiation facility.

#### References

- Wang S, Zimmermann S, Parikh K, Mansfield AS, Adjei AA. Current diagnosis and management of small-cell lung cancer. *Mayo Clin Proc* 2019;94(8):1599–1622
- Bray F, Ferlay J, Soerjomataram I, Siegel RL, Torre LA, Jemal A. Global cancer statistics 2018: GLOBOCAN estimates of incidence and mortality worldwide for 36 cancers in 185 countries. *CA Cancer J Clin* 2018;68(6):394–424
- Spratt DE, Wu AJ, Adeseye V, et al. Recurrence patterns and second primary lung cancers after stereotactic body radiation therapy for early-stage non-small-cell lung cancer: implications for surveillance. *Clin Lung Cancer* 2016;17(3):177–183. e2, e172
- Zhao Y, Wang L, Huang Q, et al. Radiosensitization of non-small cell lung cancer cells by inhibition of TGF- $\beta$ 1 signaling with SB431542 is dependent on p53 status. *Oncol Res* 2016;24(1):1–7
- Gupta S, Koru-Sengul T, Arnold SM, Devi GR, Mohiuddin M, Ahmed MM. Low-dose fractionated radiation potentiates the effects of cisplatin independent of the hyper-radiation sensitivity in human lung cancer cells. *Mol Cancer Ther* 2011;10(2):292–302
- Kuo WT, Tsai YC, Wu HC, et al. Radiosensitization of non-small cell lung cancer by kaempferol. *Oncol Rep* 2015;34(5):2351–2356
- Morgan MA, Parsels LA, Maybaum J, Lawrence TS. Improving the efficacy of chemoradiation with targeted agents. *Cancer Discov* 2014;4(3):280–291
- Bose S, Banerjee S, Mondal A, et al. Targeting the JAK/STAT signaling pathway using phytochemicals for cancer prevention and therapy. *Cells* 2020;9(6):E1451
- Iqbal J, Abbasi BA, Batool R, et al. Potential phytochemicals for developing breast cancer therapeutics: nature's healing touch. *Eur J Pharmacol* 2018;827:125–148
- Pistollato F, Calderón Iglesias R, Ruiz R, et al. The use of natural compounds for the targeting and chemoprevention of ovarian cancer. *Cancer Lett* 2017;411:191–200
- Ho ST, Tung YT, Kuo YH, Lin CC, Wu JH. Ferruginol inhibits non-small cell lung cancer growth by inducing caspase-associated apoptosis. *Integr Cancer Ther* 2015;14(1):86–97
- Szejka M, Kołodziejczyk-Czepas J, Żbikowska HM. Radioprotectors in radiotherapy - advances in the potential application of phytochemicals. *Postepy Hig Med Dosw* 2016;70(0):722–734
- Nicholson DW, Ali A, Thornberry NA, et al. Identification and inhibition of the ICE/CED-3 protease necessary for mammalian apoptosis. *Nature* 1995;376(6535):37–43
- Cao HY, Ding RL, Li M, et al. Danshensu, a major water-soluble component of *Salvia miltiorrhiza*, enhances the radio-response for Lewis lung carcinoma xenografts in mice. *Oncol Lett* 2017;13(2):605–612
- Javvadi P, Segan AT, Tuttle SW, Koumenis C. The chemopreventive agent curcumin is a potent radiosensitizer of human cervical tumor cells via increased reactive oxygen species production and overactivation of the mitogen-activated protein kinase pathway. *Mol Pharmacol* 2008;73(5):1491–1501
- Lagerweij T, Hiddingh L, Biesmans D, et al. A chemical screen for medulloblastoma identifies quercetin as a putative radiosensitizer. *Oncotarget* 2016;7(24):35776–35788
- Ortiz T, Lopez S, Burguillos MA, Edreira A, Piñero J. Radiosensitizer effect of wortmannin in radioresistant bladder tumoral cell lines. *Int J Oncol* 2004;24(1):169–175
- Tang Q, Ma J, Sun J, et al. Genistein and AG1024 synergistically increase the radiosensitivity of prostate cancer cells. *Oncol Rep* 2018;40(2):579–588
- Khan M, Maryam A, Mehmood T, Zhang Y, Ma T. Enhancing activity of anticancer drugs in multidrug resistant tumors by modulating P-glycoprotein through dietary nutraceuticals. *Asian Pac J Cancer Prev* 2015;16(16):6831–6839
- Li H, Krstin S, Wang S, Wink M. Capsaicin and piperine can overcome multidrug resistance in cancer cells to doxorubicin. *Molecules* 2018;23(3):E557
- Manayi A, Nabavi SM, Setzer WN, Jafari S. Piperine as a potential anti-cancer agent: a review on preclinical studies. *Curr Med Chem* 2018;25(37):4918–4928
- Syed SB, Arya H, Fu IH, et al. Targeting P-glycoprotein: Investigation of piperine analogs for overcoming drug resistance in cancer. *Sci Rep* 2017;7(1):7972
- Bolat ZB, Islek Z, Demir BN, Yilmaz EN, Sahin F, Ucisik MH. Curcumin- and piperine-loaded emulsomes as combinational treatment approach enhance the anticancer activity of curcumin on HCT116 colorectal cancer model. *Front Bioeng Biotechnol* 2020;8:50
- Chou TC. Drug combination studies and their synergy quantification using the Chou-Talalay method. *Cancer Res* 2010;70(2):440–446
- Tolosa L, Donato MT, Gómez-Lechón MJ. General cytotoxicity assessment by means of the MTT assay. *Methods Mol Biol* 2015;1250:333–348
- Shaheer K, Somashekarappa HM, Lakshmanan MD. Piperine sensitizes radiation-resistant cancer cells towards radiation and promotes intrinsic pathway of apoptosis. *J Food Sci* 2020;85(11):4070–4079
- Chou TC, Talalay P. Quantitative analysis of dose-effect relationships: the combined effects of multiple drugs or enzyme inhibitors. *Adv Enzyme Regul* 1984;22:27–55
- Bang JS, Oh DH, Choi HM, et al. Anti-inflammatory and antiarthritic effects of piperine in human interleukin 1 $\beta$ -stimulated fibroblast-like synoviocytes and in rat arthritis models. *Arthritis Res Ther* 2009;11(2):R49
- Stojanović-Radić ZP, Dimitrijević M, Aleksić A, et al. Piperine-a major principle of black pepper: a review of its bioactivity and studies. *Appl Sci (Basel)* 2019;9(9):4270
- Do MT, Kim HG, Choi JH, et al. Antitumor efficacy of piperine in the treatment of human HER2-overexpressing breast cancer cells. *Food Chem* 2013;141(3):2591–2599
- Yaffe PB, Power Coombs MR, Doucette CD, Walsh M, Hoskin DW. Piperine, an alkaloid from black pepper, inhibits growth of human colon cancer cells via G1 arrest and apoptosis triggered by endoplasmic reticulum stress. *Mol Carcinog* 2015;54(10):1070–1085

- 32 Jafri A, Siddiqui S, Rais J, et al. Induction of apoptosis by piperine in human cervical adenocarcinoma via ROS mediated mitochondrial pathway and caspase-3 activation. *EXCLI J* 2019;18:154–164
- 33 Pistrutto G, Trisciuglio D, Ceci C, Garufi A, D'Orazi G. Apoptosis as anticancer mechanism: function and dysfunction of its modulators and targeted therapeutic strategies. *Aging (Albany NY)* 2016;8(4):603–619
- 34 Huang RX, Zhou PK. DNA damage response signaling pathways and targets for radiotherapy sensitization in cancer. *Signal Transduct Target Ther* 2020;5(1):60
- 35 Ozpiskin OM, Zhang L, Li JJ. Immune targets in the tumor microenvironment treated by radiotherapy. *Theranostics* 2019;9(5):1215–1231
- 36 Carrano AV. Chromosome aberrations and radiation-induced cell death. II. Predicted and observed cell survival. *Mutat Res* 1973;17(3):355–366
- 37 Chou TC. Theoretical basis, experimental design, and computerized simulation of synergism and antagonism in drug combination studies. *Pharmacol Rev* 2006;58(3):621–681
- 38 Chou TC. The mass-action law based algorithms for quantitative econo-green bio-research. *Integr Biol* 2011;3(5):548–559
- 39 Chou TC. Frequently asked questions in drug combinations and the mass-action law-based answers. *Synergy*. 2014;(1):3–21
- 40 Fofaria NM, Kim SH, Srivastava SK. Piperine causes G1 phase cell cycle arrest and apoptosis in melanoma cells through checkpoint kinase-1 activation. *PLoS One* 2014;9(5):e94298






## Isoeugenol suppresses multiple quorum sensing regulated phenotypes and biofilm formation of *Pseudomonas aeruginosa* PAO1

Rajesh P. Shastry, Saptami Kanekar, Aleema Suzna Pandial & P. D. Rekha

To cite this article: Rajesh P. Shastry, Saptami Kanekar, Aleema Suzna Pandial & P. D. Rekha (2021): Isoeugenol suppresses multiple quorum sensing regulated phenotypes and biofilm formation of *Pseudomonas aeruginosa* PAO1, Natural Product Research, DOI: [10.1080/14786419.2021.1899174](https://doi.org/10.1080/14786419.2021.1899174)



To link to this article: <https://doi.org/10.1080/14786419.2021.1899174>

 View supplementary material 

 Published online: 15 Mar 2021.

 Submit your article to this journal 

 Article views: 91


 View related articles 

 View Crossmark data 

SHORT COMMUNICATION



## Isoeugenol suppresses multiple quorum sensing regulated phenotypes and biofilm formation of *Pseudomonas aeruginosa* PAO1

Rajesh P. Shastry , Saptami Kanekar, Aleema Suzna Pandial and P. D. Rekha

Division of Microbiology and Biotechnology, Yenepoya Research Centre, Yenepoya (Deemed to be University), Deralakatte, Mangalore, India

### ABSTRACT

The potential strategy to prevent bacterial pathogenicity is disabling quorum sensing circuits with structural mimicking molecules. Here, we analyzed a synthetic molecule isoeugenol, for inhibition of quorum sensing regulated phenotype and biofilm formation. Isoeugenol was an effective inhibitor, i.e., more than 70% of virulence factors were inhibited including pyocyanin, rhamnolipid, exopolysaccharide, swarming motility and biofilm formation. Interestingly, these quorum sensing regulated phenotypes in *Pseudomonas aeruginosa* PAO1 were inhibited without affecting the planktonic cells. Moreover, the presence of isoeugenol exhibited more than 70% inhibition of biofilm formation through inhibition of the quorum sensing systems. Furthermore, docking studies suggest that isoeugenol bound to the quorum sensor regulators such as LasI, LasR PqsE and SidA with considerable binding interactions. Our results demonstrate the utility of isoeugenol as a blocker of quorum sensing, which will be functioning as an antivirulence compound.

### ARTICLE HISTORY

Received 6 January 2021  
Accepted 28 February 2021

### KEYWORDS


Isoeugenol; quorum sensing; biofilm inhibitors; *Pseudomonas aeruginosa*; antivirulence

## 1. Introduction

*P. aeruginosa* is a ubiquitous pathogen important in burn units of hospitals, immunocompromised individuals, cystic fibrosis and in implanted medical devices (Scoffone et al. 2019). To colonize and establish its pathogenicity, *P. aeruginosa* uses two major LuxI/R homologue quorum-sensing systems, the Las and Rhl systems. The LasR and RhlR regulators respond to 3-Oxo-C<sub>12</sub>-HSL and C<sub>4</sub>-HSL respectively (Chakraborty et al. 2018), which direct a large number of QS controlled virulence gene expression (Steindler et al. 2009). Therefore, the strategy is to identify small molecule inhibitors to control the expression of QS regulated virulence genes (Chakraborty et al. 2020; Shastry and Rekha 2021).

Traditional medicinal preparations from essential oils are widely used in the treatment of bacterial and fungal infections (Rajesh et al. 2015), many diseases related to

CONTACT Rajesh P. Shastry  [rps Shastry@gmail.com](mailto:rps Shastry@gmail.com)  [rps Shastry@yenepoya.edu.in](mailto:rps Shastry@yenepoya.edu.in)

 Supplemental data for this article can be accessed online at <https://doi.org/10.1080/14786419.2021.1899174>.

© 2021 Informa UK Limited, trading as Taylor & Francis Group

digestive systems and toothaches, which exhibits a large spectrum of biological activity (Topal 2019). Indeed, essential oils from many medicinal plants and spices contain isoeugenol (2-methoxy-4-propenyl-phenol) as a major component which have been used as sweetener and additives in food products (Zhang et al. 2017). Some of these essential oils and their individual chemical constituents are reported as quorum quenchers (QQ). Isoeugenol is an isomer of eugenol, however, to the best of our knowledge, it is not reported as anti-biofilm and anti-virulent agent against *P. aeruginosa*. Moreover, previous studies with eugenol rich fractions (Packiavathy et al. 2012) was conducted with crude extract rather than a purified compound. Therefore, in this study synthetic molecule isoeugenol was used to challenge on inhibition of QS-regulated virulence expression and biofilm formation in *P. aeruginosa* PAO1.

## 2. Results and discussion

Quorum sensing inhibition (QSI) by isoeugenol was initially screened using *C. violaceum* as biosensor and as model organism. Furthermore, the anti-virulence and anti-biofilm activity was established in human pathogen *P. aeruginosa* PAO1. Here, our basic idea was to reduce the selective pressure on bacterial cells by targeting the QS regulated phenotypes. This idea was extremely successful through treatment with isoeugenol which target selectively on expression of Las/Rhl QS system in *P. aeruginosa*.

### 2.1. Quorum quenching activity of isoeugenol

The effect of isoeugenol on *C. violaceum* quorum sensing was evaluated at different concentrations of isoeugenol (Supplementary material Table S1). The results revealed that at 400  $\mu$ M, violacein production was inhibited more than 70% without any significant affect on growth of the bacteria. At 200  $\mu$ M, isoeugenol did not show significant effect on the violacein production. Similarly, at 600  $\mu$ M violacein was inhibited but 50% bacterial growth was inhibited, suggesting that the optimum concentration for QSI by isoeugenol is 400  $\mu$ M (Supplementary material Figure S1). This phenomenon is necessary to avoid selective pressure on the bacteria as well as to control the development of drug resistance among the bacterial pathogens (Jiang et al. 2019). Furthermore, UV absorbance analysis (350 to 800 nm) of violacein extracted from isoeugenol treated and control bacterial cells showed significant inhibition of violacin production (Supplementary material Figure S2). Plant derived compounds provide alternative medicine or potent target molecules for treating bacterial infections. Isoeugenol, the active compound from clove (Merchán Arenas et al. 2011) and cinnamon oil (Dighe et al. 2009), is used in the food industry as well as in therapeutics.

### 2.2. Effect of isoeugenol on *P. aeruginosa* PAO1 virulence factors

To understand antivirulence strategy of isoeugenol, we estimated different QS regulated virulence phenotypes. *P. aeruginosa* has three well known QS systems (*las*, *rhl* and *pqs*), in which *las* (LasI/LasR) and *rhl* (RhlI/RhIR) systems are homologous to LuxI/LuxR respectively (Scutera et al. 2014). The growth curve analysis at different



concentrations of isoeugenol showed specific concentration dependent effect on growth of *P. aeruginosa* PAO1. As indicated by the growth curve in Figure S3 (Supplementary material), isoeugenol at concentrations  $\leq 400 \mu\text{M}$  did not significantly inhibit kinetic planktonic cell growth of *P. aeruginosa* PAO1 when compared with the control group. However, at concentration  $600 \mu\text{M}$ , the cell density of planktonic *P. aeruginosa* PAO1 was inhibited. Therefore, isoeugenol at  $400 \mu\text{M}$  was selected as the concentration for testing in the subsequent ant-virulence and anti-biofilm experiments.

The *P. aeruginosa* PAO1 virulence factors such as pyocyanin, rhamnolipid, exopolysaccharide and swarming are regulated by quorum sensing. The effect of isoeugenol on *P. aeruginosa* PAO1 virulence factors expression was investigated. The results indicated that the pyocyanin, rhamnolipid and exopolysaccharide production decreased significantly by more than 60%, 70% and 65% ( $p < 0.05$ ) respectively without affecting the growth of planktonic cells (Supplementary material Figure S4). Furthermore, the swarming motility evaluated in presence of isoeugenol revealed inhibition of dendrites (at measured length) production at  $400 \mu\text{M}$  (Supplementary material Figure S5). These results suggest that isoeugenol reduces the virulence expression regulated by quorum sensing pathway at  $400 \mu\text{M}$  concentration. Our data shows significant inhibition of pyocyanin, rhamnolipid, exopolysaccharide and swarming motility suggesting that isoeugenol inhibits *rhl* system.

### 2.3. Effect of isoeugenol on biofilm formation

The biofilm formation in *P. aeruginosa* is commonly used to test QS regulated phenotype inhibition (Rajesh and Rai 2016). *P. aeruginosa* produces two types of biofilm, one is the pellicle (Pel exopolysaccharide dependent, air-liquid interface) and surface attached (Psl exopolysaccharide) biofilms. The Psl exopolysaccharide mediated biofilm formation is regulated by QS *las* system (Lidor et al. 2015). Therefore, we examined the surface biofilm formation to estimate the effect/inhibition of QS regulated biofilm with isoeugenol. The inhibition of biofilm was quantified as per conventional crystal violet using 200, 400 and  $600 \mu\text{M}$  concentration. At  $400 \mu\text{M}$ , isoeugenol treatment was significantly effective and showed to inhibit more than 70% biofilm mode of growth (Supplementary material Figure S6) suggesting that, this molecule actively down regulates the *las* system. The results were comparable with QS inhibition assay, suggesting that higher concentration of isoeugenol inhibits the planktonic cells along with biofilm matrix. Moreover, this multiple QS system inhibition by isoeugenol makes it an ideal molecule for a non lethal to planktonic cells treatment, which are targeted at decreasing the virulence of the pathogen.

### 2.4. Molecular docking analysis

Docking analysis was performed to understand the interaction with isoeugenol and quorum sensing activator proteins. The isoeugenol anti-QS activity was replicated in the docking results. The docking results obtained for binding interaction of the molecule with protein are shown in Figure S7 (Supplementary material). The docking score was varied from  $-4.8$  to  $-6.4 \text{ kcal/mol}$  (Supplementary material Table S2) and

isoeugenol interaction showed higher binding affinity with LasI indicating efficient and stable binding. Therefore, this result suggests that the inactivation of QS activator proteins LasI and LasR can be attributed to the anti-QS activity and QS regulated anti-biofilm activity of isoeugenol in *P. aeruginosa*.

### 3. Conclusion

This study aim to exploring interference with quorum sensing regulated virulence expression, demonstrates that isoeugenol an analogue of the native *P. aeruginosa* autoinducers significantly suppresses the production of pyocyanin, rhamnolipid, exopolysaccharide, swarming motility and biofilm formation. Our data indicate that isoeugenol could serve as one of the therapeutic molecules that significantly inhibit the QS regulated virulence phenotypes including biofilm formation in Gram-negative pathogens.

### Disclosure statement

No potential conflict of interest was reported by the authors.

### Funding

R. P. Shastry was supported by the Yenepoya (Deemed to be University) Seed grant (YU/Seed grant/080-2019).

### ORCID

Rajesh P. Shastry  <http://orcid.org/0000-0001-8627-9759>

### References

- Chakraborty P, Dastidar DG, Paul P, Dutta S, Basu D, Sharma SR, Basu S, Sarker RK, Sen A, Sarkar A, et al. 2020. Inhibition of biofilm formation of *Pseudomonas aeruginosa* by caffeine: a potential approach for sustainable management of biofilm. *Arch Microbiol.* 202(3):623–635.
- Chakraborty P, Daware AV, Kumari M, Chatterjee A, Bhattacharyya D, Mitra G, Akhter Y, Bhattacharjee S, Tribedi P. 2018. Free tryptophan residues inhibit quorum sensing of *Pseudomonas aeruginosa*: a potential approach to inhibit the development of microbial biofilm. *Arch Microbiol.* 200(10):1419–1425.
- Dighe VV, Gursale AA, Charegaonkar GA. 2009. Quantitation of eugenol, cinnamaldehyde and isoeugenol from *Cinnamomum tamala* nees and Eberm. leaf powder and *Cinnamomum zeylanicum* Breyne stem bark powder by LC. *Chroma.* 70(11-12):1759–1762.
- Jiang Q, Chen J, Yang C, Yin Y, Yao K. 2019. Quorum sensing: a prospective therapeutic target for bacterial diseases. *Biomed Res Int.* 2019:2015978. <https://www.hindawi.com/journals/bmri/2019/2015978/>.
- Lidor O, Al-Quntar A, Pesci EC, Steinberg D. 2015. Mechanistic analysis of a synthetic inhibitor of the *Pseudomonas aeruginosa* LasI quorum-sensing signal synthase. *Sci Rep.* 5:16569. <https://www.ncbi.nlm.nih.gov/pmc/articles/PMC4655403/>.

- Merchán Arenas DR, Acevedo AM, Vargas Méndez LY, Kouznetsov VV. 2011. Scavenger activity evaluation of the clove bud essential oil (*Eugenia caryophyllus*) and eugenol derivatives employing ABTS decolorization. *Sci Pharm.* 79(4):779–791.
- Packiavathy IASV, Agilandeswari P, Musthafa KS, Karutha Pandian S, Veera Ravi A. 2012. Antibiofilm and quorum sensing inhibitory potential of *Cuminum cyminum* and its secondary metabolite methyl eugenol against Gram negative bacterial pathogens. *Food Res Int.* 45(1): 85–92.
- Rajesh PS, Rai VR. 2016. Inhibition of QS-regulated virulence factors in *Pseudomonas aeruginosa* PAO1 and *Pectobacterium carotovorum* by AHL-lactonase of endophytic bacterium *Bacillus cereus* VT96. *Biocatal Agric Biotechnol.* 7:154–163.
- Rajesh PS, Samaga PV, Rai VR, Rai KML. 2015. In vitro biological activity of aromadendrin-4'-methyl ether isolated from root extract of *Ventilago madraspatana* Gaertn with relevance to anticandidal activity. *Nat Prod Res.* 29(11):1042–1045.
- Scoffone VC, Trespidi G, Chiarelli LR, Barbieri G, Buroni S. 2019. Quorum sensing as antivirulence target in cystic fibrosis pathogens. *Int J Mol Sci.* 20(8). <https://www.ncbi.nlm.nih.gov/pmc/articles/PMC6515091/>.
- Scutera S, Zucca M, Savoia D. 2014. Novel approaches for the design and discovery of quorum-sensing inhibitors. *Expert Opin Drug Discov.* 9(4):353–366.
- Shastry RP, Rekha PD. 2021. Bacterial cross talk with gut microbiome and its implications: a short review. *Folia Microbiol.* 66(1):15–24..
- Steindler L, Bertani I, De Sordi L, Schwager S, Eberl L, Venturi V. 2009. LasI/R and RhII/R quorum sensing in a strain of *Pseudomonas aeruginosa* beneficial to plants. *Appl Environ Microbiol.* 75(15):5131–5140.
- Topal F. 2019. Anticholinergic and antidiabetic effects of isoeugenol from clove (*Eugenia caryophyllata*) oil. *Int J Food Prop.* 22(1):583–592.
- Zhang L-L, Zhang L-F, Xu J-G, Hu Q-P. 2017. Comparison study on antioxidant, DNA damage protective and antibacterial activities of eugenol and isoeugenol against several foodborne pathogens. *Food Nutr Res.* 61(1):1353356.

Intramural Research Expenditure  
towards Proteomics/Genomics  
Research under YU-IOB MoU



**YENEPOYA**


(DEEMED TO BE UNIVERSITY)


Recognised under Sec. 3(A) of the UGC Act 1956  
Accredited by NAAC with 'A' Grade

## **Intramural Research Expenditure towards proteomics/ Genomics research**

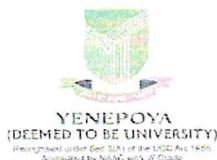
This is to certify that the following amount was utilized for the purpose of joint projects under YU - IOB MoU during 2<sup>nd</sup> July 2015 to 1<sup>st</sup> February 2018 as per the MoU terms between Yenepoya University and Institute of Bioinformatics.

<b>Year</b>	<b>Rs. in Lakhs</b>		
	<b>2015 -16</b>	<b>2016 - 17</b>	<b>2017 - 18</b>
<b>Amount spent</b>	176.56	104.49	18.39
<b>Total</b>	<b>176.56</b>	<b>104.49</b>	<b>18.39</b>

  
**Signature of the Finance Officer**  
**Finance Officer**  
Yenepoya (Deemed to be University)  
Stamp

  
**Signature of the Registrar**  
Registrar  
Yenepoya (Deemed to be University)  
University Road, Deralakatte  
Mangalore - 575 018  
Stamp

# E-Sanction letters of the Seed grant Projects



## SANCTION ORDER FOR THE SEED GRANT

YU/Seed grant/097-2021

Date: 15.04. 2021

Ref.No: YURC meeting dated 26.02.2021

Approval of the minutes of the YURC meeting in 53<sup>rd</sup> BoM meeting, dated: 23.03.2021

**Sub: R/P entitled *In vitro* evaluation of cytotoxic potential of phytochemicals from *Clitoria ternatea* against pancreatic cancer**

**Principle Investigator:** Dr. Bhagya N, Assistant Professor, Yenepoya Research Centre

On the recommendation of the Yenepoya University Research Committee Meeting held on 26.02.2021, an amount of **Rs. 2,00,000/-** has been approved for the above cited project for the first phase of the study.


Sl. no	Item	1 <sup>st</sup> Year (Rs.)
1.	Recurring: Consumables & Contingencies	2,00,000
<b>Grand Total</b>		<b>2,00,000/-</b>
<b>Rupees Two Lakhs Only</b>		

### Terms and conditions:

1. No funds will be provided directly to the Principal Investigator, all the requests for the utilization of the sanctioned funds should be through proper channel.
2. Annual progress reports should be submitted to the Registrar through proper channel.
3. On the completion of the project, a detailed report should be prepared and submitted to the Registrar within one month from the date of completion of the project.
4. **Financial utilization statement as of March 31<sup>st</sup> every year should be submitted, failing which the project will be terminated.**
5. University has all the rights to terminate the project, if the progress is not satisfactory.
6. All publications from this study should be duly acknowledge the seed grant.

### Note:


This funding is given as startup grant for the PI and should use this grant to generate the preliminary findings useful for submitting projects for funding from the external agencies.

  
Dr. K.S Gangadhara Somayaji  
REGISTRAR

**ATTESTED**

### Cc to:

1. Principle Investigator (Dr. Bhagya N)
2. Co-Investigator (Prof. K. R. Chandrashekar, Yenepoya (Deemed to be University)).
3. Finance Officer
4. Purchase and Stores/Deputy Director, YRC

  
Dr. Gangadhara Somayaji K.S.  
Registrar  
Yenepoya (Deemed to be University)  
University Road, Deralakatte  
Mangalore- 575 018, Karnataka

Page 1 of 1

**SANCTION ORDER FOR THE SEED GRANT**

YU/Seed grant/098-2021

Date: 15.04. 2021

Ref.No: YURC meeting dated 26.02.2021

Approval of the minutes of the YURC meeting in 53<sup>rd</sup> BoM meeting, dated: 23.03.2021

**Sub: R/P entitled** Application of *Calendula officinalis* in promoting granulation tissue growth in wound healing

**Principle Investigator:** Dr. A. Vincer George, Professor and HoD, Dept. of Physiology and Biochemistry, Yenepoya Homeopathic Medical College & Hospital.

On the recommendation of the Yenepoya University Research Committee Meeting held on 26.02.2021, an amount of **Rs. 1,15,000/-** has been approved for the above cited project for the period of one year.

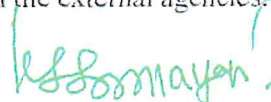
Sl. no	Item	1 <sup>st</sup> Year (Rs.)
1.	Recurring: Consumables & Contingencies	1,15,000
<b>Grand Total</b>		<b>1,15,000/-</b>
<b>Rupees One Lakh and Fifteen Thousand Only</b>		

**Terms and conditions:**

1. No funds will be provided directly to the Principal Investigator, all the requests for the utilization of the sanctioned funds should be through proper channel.
2. Annual progress reports should be submitted to the Registrar through proper channel.
3. On the completion of the project, a detailed report should be prepared and submitted to the Registrar within one month from the date of completion of the project.
4. **Financial utilization statement as of March 31<sup>st</sup> every year should be submitted, failing which the project will be terminated.**
5. University has all the rights to terminate the project if the progress is not satisfactory.
6. All publications from this study should be duly acknowledge the seed grant.

**Note:**


This funding is given as startup grant for the PI and should use this grant to generate the preliminary findings useful for submitting projects for funding from the external agencies.

  
**Dr. K.S Gangadhara Somayaji**  
Registrar

**Cc to:**

1. Principle Investigator (Dr. A. Vincer George)
2. Co-Investigator (Dr. Sushrutha K, Homeopathic Pharmacy, Dr. Melita Alva, Homeopathic Materia Medica, YHMCH, Dr. Rekha P.D., YRC)
3. Finance Officer/Purchase and Stores/Deputy Director, YRC

**ATTESTED**

  
**Dr. Gangadhara Somayaji K.S.**  
Registrar  
Yenepoya (Deemed to be University)  
University Road, Deralakatte  
Mangalore- 575 018, Karnataka  
Page 1 of 1





YENEPEYA  
(DEEMED TO BE UNIVERSITY)  
Recognized under Sec 3(A) of the UGC Act 1956  
Accredited by NAAC with A Grade

## SANCTION ORDER FOR THE SEED GRANT

YU/Seed grant/099-2021

Date: 15.04. 2021

**Sub: R/P entitled EGFR dysregulation in oral squamous cell carcinoma**

**Principle Investigator: Dr. M. Vijaya Kumar, Professor, Dept. of Surgical Oncology, YMC**

On the recommendation of the Yenepeya University Research Committee Meeting held on 26.02.2021, an amount of **Rs. 2,45,000/-** has been approved for the above cited project for the period of one year.

Sl. no	Item	1 <sup>st</sup> Year (Rs.)
1.	Recurring: Consumables & Contingencies	2,45,000
<b>Grand Total</b>		<b>2,45,000/-</b>
<b>Rupees Two Lakhs and Forty Five Thousand Only</b>		

### Terms and conditions:

1. No funds will be provided directly to the Principal Investigator, all the requests for the utilization of the sanctioned funds should be through proper channel.
2. Annual progress reports should be submitted to the Registrar through proper channel.
3. On the completion of the project, a detailed report should be prepared and submitted to the Registrar within one month from the date of completion of the project.
4. **Financial utilization statement as of March 31<sup>st</sup> every year should be submitted, failing which the project will be terminated.**
5. University has all the rights to terminate the project if the progress is not satisfactory.
6. All publications from this study should be duly acknowledge the seed grant.

### Note:

This funding is given as startup grant for the PI and should use this grant to generate the preliminary findings useful for submitting projects for funding from the external agencies.

### Cc to:

1. Principle Investigator (Dr. M. Vijaya Kumar)
2. Co-Investigator (Dr. Rohan Thomas Mathew, Dr. Rohan Shetty, Dept. of Surgical Oncology, YMC, Dr. Siddarth Biswas, Dept. of Pathology, YMC, Dr. Madan K, Dept. of Surgical Oncology, YMC, Dr. Yashodhar Bhandary, Dr. Ashwini Prabhu, YRC)
3. Finance Officer
4. Purchase and Stores
5. Deputy Director, YRC

  
Dr. K.S Gangadhara Somayaji  
Registrar  
Yenepeya (Deemed to be University)  
University Road, Deralakatte  
Mangalore - 575 018

**ATTESTED**  


Dr.Gangadhara Somayaji K.S.  
Registrar  
Yenepeya(Deemed to be University)  
University Road, Deralakatte  
Mangalore- 575 018, Karnataka

## SANCTION ORDER FOR THE SEED GRANT

YU/Seed grant/100-2021

Date: 15.04. 2021

Ref. No: YURC meeting dated 26.02.2021

Approval of the minutes of the YURC meeting in 53<sup>rd</sup> BoM meeting, dated: 23.03.2021

**Sub: R/P entitled** Analysis of metabolites of raw and commercial area extracts and their effect on fibroblastic activity

**Principle Investigator:** Dr. Sonia Adyanthaya, Dept. of Oral Pathology and Microbiology, YDC

On the recommendation of the Yenepoya University Research Committee Meeting held on 26.02.2021, an amount of **Rs. 2,10,000/-** has been approved for the above cited project for the period of one year.

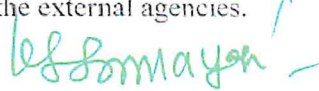
Sl. no	Item	1 <sup>st</sup> Year (Rs.)
1.	Recurring: Consumables & Contingencies	2,10,000
<b>Grand Total</b>		<b>2,10,000/-</b>
<b>Rupees Two Lakhs and Ten Thousand Only</b>		

**Terms and conditions:**

1. No funds will be provided directly to the Principal Investigator, all the requests for the utilization of the sanctioned funds should be through proper channel.
2. Annual progress reports should be submitted to the Registrar through proper channel.
3. On the completion of the project, a detailed report should be prepared and submitted to the Registrar within one month from the date of completion of the project.
4. **Financial utilization statement as of March 31<sup>st</sup> every year should be submitted, failing which the project will be terminated.**
5. University has all the rights to terminate the project if the progress is not satisfactory.
6. All publications from this study should be duly acknowledge the seed grant.

**Note:**

This funding is given as startup grant for the PI and should use this grant to generate the preliminary findings useful for submitting projects for funding from the external agencies.

  
**Dr. K.S Gangadhara Somayaji**  
**REGISTRAR**

**Cc to:**

1. Principle Investigator (Dr. Sonia Adyanthaya, Dept. of Oral Pathology and Microbiology, YDC)
2. Co-Investigator (Dr. Riaz Abdulla, Dept. of Oral Pathology and Microbiology, YDC, Dr. Keshava Prasad, YRC)
3. Finance Officer/Purchase and Stores/Deputy Director, YRC

**SANCTION ORDER FOR THE SEED GRANT**

YU/Seed grant/089-2020

Date: 13.07. 2020

**Sub: R/P entitled "Kutumba Aarogya Sarvekshana Hagu Rakshana Yojane to establish IT platform and develop health and demographic surveillance system at existing and New Surveillance sites for continuity of care"**

**Principle Investigator: PI: Dr. Abhay S Nirgude, Associate Dean and Professor of Community Medicine**

**On the recommendation of the Yenepoya University Research Committee Meeting held on 30.06.2020, an amount of Rs. 3,46,000/- has been approved for the above cited project for the first phase of the study.**

Sl. no	Item	1 <sup>st</sup> Year (Rs.)
1.	Recurring and Non recurring	3,46,000
<b>Grand Total</b>		<b>3,46,000/-</b>
<b>Rupees Three Lakhs and Forty Six Thousand only</b>		

**Terms and conditions:**

1. No funds will be provided directly to the Principal Investigator, all the requests for the utilization of the sanctioned funds should be through proper channel.
2. Annual progress reports should be submitted to the Registrar through proper channel.
3. On the completion of the project, a detailed report should be prepared and submitted to the Registrar within one month from the date of completion of the project.
4. Financial utilization statement as of March 31<sup>st</sup> every year should be submitted.
5. University has all the rights to terminate the project if the progress is not satisfactory,

**Note:**


This funding is given as startup grant for the PI and should use this grant to generate the preliminary findings useful for submitting projects for funding from the external agencies.

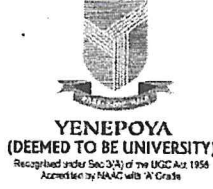
**Cc to:**

1. Principle Investigator (Dr. Abhay S Nirgude)
2. Co-Investigator (Dr. Poonam R. Naik, Dr. Akshaya K.M, Dr. Pracheth R, Dept. of community Medicine)
3. Finance Officer
4. Purchase and Stores
5. Deputy Director, YRC

  
**Dr. K.S Gangadhara Somayaji**  
**Registrar**

**ATTESTED**

  
**Dr. Gangadhara Somayaji K.S.**  
**Registrar**  
Yenepoya/Deemed to be University)  
University Road, Deralakatte  
Mangalore- 575 018, Karnataka



## SANCTION ORDER FOR THE SEED GRANT

YU/Seed grant/090-2020

Date: 13.07. 2020

**Sub: R/P entitled "Potential Biomarkers in Cervical Cancer for Early Diagnosis"**

**Principle Investigator: PI: Dr. R.C. Koumar, Associate Professor, YRC**

On the recommendation of the Yenepeya University Research Committee Meeting held on 30.06.2020, an amount of Rs. 2,00,000/- has been approved for the above cited project for the period of one year.

Sl. no	Item	1 <sup>st</sup> Year (Rs.)
1.	Recurring and Non recurring	2,00,000
<b>Grand Total</b>		<b>2,00,000/-</b>
Rupees Two Lakhs only		

### Terms and conditions:

1. No funds will be provided directly to the Principal Investigator, all the requests for the utilization of the sanctioned funds should be through proper channel.
2. Annual progress reports should be submitted to the Registrar through proper channel.
3. On the completion of the project, a detailed report should be prepared and submitted to the Registrar within one month from the date of completion of the project.
4. Financial utilization statement as of March 31<sup>st</sup> every year should be submitted.
5. University has all the rights to terminate the project if the progress is not satisfactory.

### Note:


This funding is given as startup grant for the PI and should use this grant to generate the preliminary findings useful for submitting projects for funding from the external agencies.

### Cc to:

1. Principle Investigator (PI: Dr. R.C. Koumar, YRC)
2. Co-Investigator (Dr. Jalalluddin Akbar, Professor and HOD Oncology, YMC, Dr. Shruthi Kanthaje, PDF, YRC)
3. Finance Officer
4. Purchase and Stores
5. Deputy Director, YRC

  
**Dr. K.S Gangadhara Somayaji**  
Registrar

**ATTESTED**

  
Dr.Gangadhara Somayaji K.S.  
Registrar  
Yenepeya(Deemed to be University)  
University Road, Deralakatte  
Mangalore- 575 018, Karnataka

**SANCTION ORDER FOR THE SEED GRANT**

YU/Seed grant/091-2020

Date: 13.07. 2020

**Sub: R/P entitled "Determination of the mechanism of action of a novel antimicrobial peptide with an objective to decipher new epitope for drug designing"**

**Principle Investigator: PI: Dr. Sebanti Gupta, Assistant Professor, YRC**

**On the recommendation of the Yenepoya University Research Committee Meeting held on 30.06.2020, an amount of Rs. 2,00,000/- has been approved for the above cited project for the period of one year.**

Sl. no	Item	1 <sup>st</sup> Year (Rs.)
1.	Recurring Consumables & Contingencies	2,00,000
<b>Grand Total</b>		<b>2,00,000/-</b>
<b>Rupees Two Lakhs only</b>		

**Terms and conditions:**

1. No funds will be provided directly to the Principal Investigator, all the requests for the utilization of the sanctioned funds should be through proper channel.
2. Annual progress reports should be submitted to the Registrar through proper channel.
3. On the completion of the project, a detailed report should be prepared and submitted to the Registrar within one month from the date of completion of the project.
4. Financial utilization statement as of March 31<sup>st</sup> every year should be submitted.
5. University has all the rights to terminate the project if the progress is not satisfactory.

**Note:**

This funding is given as startup grant for the PI and should use this grant to generate the preliminary findings useful for submitting projects for funding from the external agencies.

**Cc to:**

1. Principle Investigator (Dr. Sebanti Gupta, YRC)
2. Finance Officer
3. Purchase and Stores
4. Deputy Director, YRC

  
**Dr. K.S Gangadhara Somayaji**  
**Registrar**

**ATTESTED**  
  
**Dr. Gangadhara Somayaji K.S.**  
**Registrar**  
**Yenepoya (Deemed to be University)**  
**University Road, Deralakatte**  
**Mangalore- 575 018, Karnataka**

**SANCTION ORDER FOR THE SEED GRANT**

YU/Seed grant/092-2020

Date: 13.07. 2020

**Sub: R/P entitled "Understanding the cell signaling in an *in vitro* penumbral model of ischemic stroke"**

**Principle Investigator: PI: Dr. Arnab Datta, Assistant Professor, YRC**

**On the recommendation of the Yenepoya University Research Committee Meeting held on 30.06.2020, an amount of Rs. 2,00,000/- has been approved for the above cited project for the period of one year.**

Sl. no	Item	1 <sup>st</sup> Year (Rs.)
1.	Recurring Consumables & Contingencies	2,00,000
<b>Grand Total</b>		<b>2,00,000/-</b>
<b>Rupees Two Lakhs only</b>		

**Terms and conditions:**

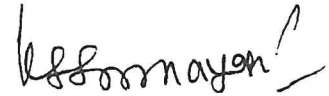
1. No funds will be provided directly to the Principal Investigator, all the requests for the utilization of the sanctioned funds should be through proper channel.
2. Annual progress reports should be submitted to the Registrar through proper channel.
3. On the completion of the project, a detailed report should be prepared and submitted to the Registrar within one month from the date of completion of the project.
4. Financial utilization statement as of March 31<sup>st</sup> every year should be submitted.
5. University has all the rights to terminate the project if the progress is not satisfactory.

**Note:**

This funding is given as startup grant for the PI and should use this grant to generate the preliminary findings useful for submitting projects for funding from the external agencies.


**Cc to:**

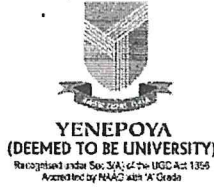
1. Principle Investigator (Dr. Arnab Datta, YRC)
2. Finance Officer
3. Purchase and Stores
4. Deputy Director, YRC



**Dr. K.S Gangadhara Somayaji**  
**Registrar**

**ATTESTED**

  
Dr.Gangadhara Somayaji K.S.  
Registrar  
Yenepoya(Deemed to be University)  
University Road, Deralakatte  
Mangalore- 575 018, Karnataka



## SANCTION ORDER FOR THE SEED GRANT

YU/Seed grant/093-2020

Date: 13.07.2020

**Sub: R/P entitled Unravelling the population history and assessing the genomic profile of Koraga an aboriginal tribe from Dakshina kannada and Udupi district, Karnataka”.**

**PI: Dr. Ranajit Das, Assistant Professor, YRC**

On the recommendation of the Yenepeya University Research Committee Meeting held on 30.06.2020, an amount of Rs. **2,50,000/-** has been approved for the above cited project for the first phase of the study.

Sl. no	Item	1 <sup>st</sup> Year (Rs.)
1.	Consumables & Sequencing cost	2,50,000
<b>Grand Total</b>		<b>2,50,000/-</b>
<b>Rupees Two Lakhs and Fifty Thousand only</b>		

### Terms and conditions:

1. No funds will be provided directly to the Principal Investigator, all the requests for the utilization of the sanctioned funds should be through proper channel.
2. Annual progress reports should be submitted to the Registrar through proper channel.
3. On the completion of the project, a detailed report should be prepared and submitted to the Registrar within one month from the date of completion of the project.
4. Financial utilization statement as of March 31<sup>st</sup> every year should be submitted.
5. University has all the rights to terminate the project if the progress is not satisfactory.

### Note:


This funding is given as startup grant for the PI and should use this grant to generate the preliminary findings useful for submitting projects for funding from the external agencies.

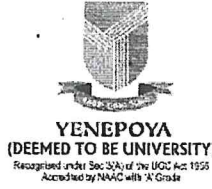
### Cc to:

1. Principle Investigator (Dr. Ranajit Das, YRC)
2. Finance Officer
3. Purchase and Stores
4. Deputy Director, YRC

  
**Dr. K.S Gangadhara Somayaji**  
Registrar

**ATTESTED**

  
Dr. Gangadhara Somayaji K.S.  
Registrar  
Yenepeya (Deemed to be University)  
University Road, Derlak, He  
Mangalore- 575 018, Karnataka



## SANCTION ORDER FOR THE SEED GRANT

YU/Seed grant/094-2020

Date: 13.07. 2020

**Sub: R/P entitled "Participatory community health development of Koraga Tribes in Mnagalore Taluk of Karnataka, South India".**

**PI: Dr. Mohammed Guthigar, HOD, Dept. of Medical Social Work, YMC**

On the recommendation of the Yenepeya University Research Committee Meeting held on 30.06.2020, an amount of Rs. 1,25,000/- has been approved for the above cited project for the first phase of the study.

Sl. no	Item	1 <sup>st</sup> Year (Rs.)
1.	Recurring Consumables & Contingencies	1,25,000
<b>Grand Total</b>		<b>1,25,000/-</b>
<b>Rupees One Lakhs and Twenty Five Thousand only</b>		

### Terms and conditions:

1. No funds will be provided directly to the Principal Investigator, all the requests for the utilization of the sanctioned funds should be through proper channel.
2. Annual progress reports should be submitted to the Registrar through proper channel.
3. On the completion of the project, a detailed report should be prepared and submitted to the Registrar within one month from the date of completion of the project.
4. Financial utilization statement as of March 31<sup>st</sup> every year should be submitted.
5. University has all the rights to terminate the project if the progress is not satisfactory.

### Note:

This funding is given as startup grant for the PI and should use this grant to generate the preliminary findings useful for submitting projects for funding from the external agencies.

### Cc to:

1. Principle Investigator (Dr. Mohammed Guthigar)
2. Finance Officer
3. Purchase and Stores
4. Deputy Director, YRC

**Dr. K.S Gangadhara Somayaji**  
Registrar

**ATTESTED**

Dr.Gangadhara Somayaji K.S.  
Registrar  
Yenepeya(Deemed to be University)  
University Road, Derlakatte  
Mangalore- 575 018, Karnataka



**SANCTION ORDER FOR THE SEED GRANT**

YU/Seed grant/095-2020

Date: 13.07. 2020

**Sub: R/P entitled** "A study to assess the occurrence of nutritional anaemia and effect of multimodel nurse lead interventions on knowledge, attitude, self reported practice and Haemoglobin levels of anaemic women of reproductive age in selected community areas of Mangaluru".

PI: Mr. Anand S, Assistant Professor, Dept. of Community Health Nursing, YNC.

On the recommendation of the Yenepoya University Research Committee Meeting held on 30.06.2020, an amount of **Rs. 1,50,000/-** has been approved for the above cited project for the period of one year.

Sl. no	Item	1 <sup>st</sup> Year (Rs.)
1.	Recurring Consumables & Contingencies	1,50,000
<b>Grand Total</b>		<b>1,50,000/-</b>
<b>Rupees One Lakhs and Fifty Thousand only</b>		

**Terms and conditions:**


1. No funds will be provided directly to the Principal Investigator, all the requests for the utilization of the sanctioned funds should be through proper channel.
2. Annual progress reports should be submitted to the Registrar through proper channel.
3. On the completion of the project, a detailed report should be prepared and submitted to the Registrar within one month from the date of completion of the project.
4. Financial utilization statement as of March 31<sup>st</sup> every year should be submitted.
5. University has all the rights to terminate the project if the progress is not satisfactory.

**Note:**

This funding is given as startup grant for the PI and should use this grant to generate the preliminary findings useful for submitting projects for funding from the external agencies.


**Cc to:**

1. Principle Investigator (Mr. Anand S)
2. Co-investigator (Dr. Leena K C, Mrs. Shycil Mathew, Mrs. Navya, Dept. of Community Health Nursing, YNC)
3. Finance Officer
4. Purchase and Stores
5. Deputy Director, YRC



**Dr. K.S Gangadhara Somayaji**  
Registrar

**ATTESTED**

  
Dr Gangadhara Somayaji K.S.,  
Registrar  
Yenepoya (Deemed to be University)  
University Road, Deralakatte  
Mangalore- 575 018, Karnataka

**SANCTION ORDER FOR THE SEED GRANT**

YU/Seed grant/096-2020

Date: 13.07. 2020

**Sub: R/P entitled** "Assessment of physical and bacterial parameters of the well and well water located at selected rural households of Mangalore".

**PI: Mrs. Nithyashree B V, Assistant Professor, Dept of Community Health Nursing, Yenepoya Nursing College.**

On the recommendation of the Yenepoya University Research Committee Meeting held on 30.06.2020, an amount of **Rs. 50,000/-** has been approved for the above cited project for the first phase of the study.

Sl. no	Item	1 <sup>st</sup> Year (Rs.)
1.	Recurring & Non recurring	50,000
<b>Grand Total</b>		<b>50,000/-</b>
<b>Rupees Fifty Thousand only</b>		

**Terms and conditions:**


1. No funds will be provided directly to the Principal Investigator, all the requests for the utilization of the sanctioned funds should be through proper channel.
2. Annual progress reports should be submitted to the Registrar through proper channel.
3. On the completion of the project, a detailed report should be prepared and submitted to the Registrar within one month from the date of completion of the project.
4. Financial utilization statement as of March 31<sup>st</sup> every year should be submitted.
5. University has all the rights to terminate the project if the progress is not satisfactory.

**Note:**


This funding is given as startup grant for the PI and should use this grant to generate the preliminary findings useful for submitting projects for funding from the external agencies.

**Cc to:**

1. Principle Investigator (Mrs. Nithyashree B V)
2. Co-investigator (Dr. Leena K C, Dept. of Community Health Nursing, YNC)
3. Finance Officer
4. Purchase and Stores
5. Deputy Director, YRC

  
**Dr. K.S Gangadhara Somayaji**  
Registrar

**ATTESTED**

  
**Dr.Gangadhara Somayaji K.S.**  
Registrar  
Yenepoya(Deemed to be University)  
University Road, Derlakatte  
Mangalore- 575 018, Karnataka

**SANCTION ORDER FOR THE SEED GRANT**

YU/Seed grant/088-2020

Date: 13.07. 2020

**Sub: R/P entitled "Knee osteoarthritis and its association with spine, hip, Knee and ankle"**

**Principle Investigator: PI: Ms. Veena Pais, Associate Professor, YPC**

On the recommendation of the Yenepoya University Research Committee Meeting held on 30.06.2020, an amount of **Rs. 1,10,000/-** has been approved for the above cited project for the period of one year.

Sl. no	Item	1 <sup>st</sup> Year (Rs.)
1.	Recurring/ Consumables, Contingencies	1,10,000
<b>Grand Total</b>		<b>1,10,000/-</b>
<b>Rupees One Lakhs and Ten Thousand Only</b>		

**Terms and conditions:**

1. No funds will be provided directly to the Principal Investigator, all the requests for the utilization of the sanctioned funds should be through proper channel.
2. Annual progress reports should be submitted to the Registrar through proper channel.
3. On the completion of the project, a detailed report should be prepared and submitted to the Registrar within one month from the date of completion of the project.
4. Financial utilization statement as of March 31<sup>st</sup> every year should be submitted.
5. University has all the rights to terminate the project if the progress is not satisfactory.

**Note:**

This funding is given as startup grant for the PI and should use this grant to generate the preliminary findings useful for submitting projects for funding from the external agencies.


**Cc to:**

1. Principle Investigator (Ms. Veena Pais)
2. Co-Investigator (Dr. Devadasa Acharya, HOD of Radiodiagnosics, YMCH, Dr. Imthiaz Ahammed, Professor, Dept. of Orthopaedics)
3. Finance Officer
4. Purchase and Stores
5. Deputy Director, YRC



**Dr. K.S Gangadhara Somayaji**  
Registrar

**ATTESTED**

  
**Dr. Gangadhara Somayaji K.S.**  
Registrar  
Yenepoya (Deemed to be University)  
University Road, Deralakatte  
Mangalore- 575 018, Karnataka



**YENEPOYA**  
(DEEMED TO BE UNIVERSITY)  
Recognised under Sec 3(A) of the UGC Act 1956  
Accredited by NAAC with 'A' Grade

## SANCTION ORDER FOR THE SEED GRANT

YU/Seed grant/080-2019

Date: 09.12.2019

**Sub: R/P entitled "Combination therapy strategy using antibiotics and AHL analogues for *Pseudomonas aeruginosa* infection in *Caenorhabditis elegans* model"**

**Principle Investigator: Dr.Rajesh P Shastry, Assistant Professor, YRC.**

On the recommendation of the Yenepoya University Research Committee Meeting held on 27.11.2019, an amount of **Rs. 2,00,000/-** has been approved for the above cited project for the period of one year.

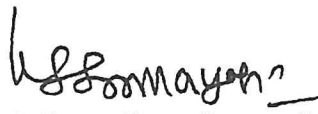
Sl. no	Item	1 <sup>st</sup> Year (Rs.)
1.	Recurring/ Consumables	2,00,000
<b>Grand Total</b>		<b>2,00,000/-</b>
<b>Rupees Two lakhs only</b>		

### Terms and conditions:

1. No funds will be provided directly to the Principal Investigator, all the requests for the utilization of the sanctioned funds should be through proper channel.
2. Annual progress reports should be submitted to the Registrar through proper channel.
3. On the completion of the project, a detailed report should be prepared and submitted to the Registrar within one month from the date of completion of the project.
4. Financial utilization statement as of March 31<sup>st</sup> every year should be submitted.
5. University has all the rights to terminate the project if the progress is not satisfactory.
6. This funding is given as startup grant for the PI and should use this grant to generate the preliminary findings useful for submitting projects for funding from the external agencies.

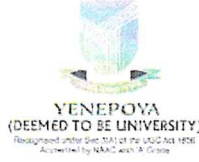
### Cc to:

1. Principle Investigator (Dr.Rajesh P Shastry)
2. Finance Officer
3. Purchase and Stores
4. Deputy Director, YRC

  
**Dr. K.S Gangadhara Somayaji**  
Registrar

**ATTESTED**

**Dr.Gangadhara Somayaji K.S.**  
Registrar  
Yenepoya(Deemed to be University)  
University Road, Derlakatte  
Mangalore- 575 018, Karnataka



YU/Seed grant/080-2019

Date: 06.01.2021

To,

Dr. Rajesh P Shastry  
Assistant Professor  
Yenepoya Research Centre  
Yenepoya (Deemed to be University)

Sub: Seed grant project No.YU/Seed grant/080-2019, "Combination therapy Strategy using antibiotics and AHL analogues for Pseudomonas aeruginosa infection in Caenorhabditis elegans model"


Ref: i) YU/Seed grant/080-2019

ii) Your report on work plan and activities to be carried out in the 1<sup>st</sup> year dated: 21.12.2020

With reference to the above, based on the recommendation on the progress, Second year grant of Rs. 1,50,000/- is sanctioned in order to complete the pending work of the project. You should submit the final report after the completion of 2<sup>nd</sup> year of the project along with the statement of accounts and copies of publications and patents made from the project as of 31<sup>st</sup> December 2021.

  
**REGISTRAR**

**ATTESTED**

  
Dr.Gangadhara Somayaji K.S.  
Registrar  
Yenepoya(Deemed to be University)  
University Road, Deraiakatte  
Mangalore- 575 018, Karnataka



YENEPOYA  
(DEEMED TO BE UNIVERSITY)  
Recognised under Sec 3(A) of the UGC Act 1956  
Accredited by NAAC with 'A' Grade

**SANCTION ORDER FOR THE SEED GRANT**

YU/Seed grant/081-2019

Date: 09.12.2019

**Sub: R/P entitled** "Comparison of the efficacy of the infra-zygomatic crest/Buccal Shelf screws for the retraction of the anterior teeth to the conventional method of retraction"

**Principle Investigator:** Dr. Sandeep Shetty, Professor, Department of Orthodontics and Dentofacial Orthopaedics, YDC.

On the recommendation of the Yenepoya University Research Committee Meeting held on 27.11.2019, an amount of Rs. 2,00,000/- has been approved for the above cited project for the period of one year.


Sl. no	Item	1 <sup>st</sup> Year (Rs.)
1.	Recurring/ Consumables	2,00,000
<b>Grand Total</b>		<b>2,00,000/-</b>
Rupees Two lakhs only		

**Terms and conditions:**


1. No funds will be provided directly to the Principal Investigator, all the requests for the utilization of the sanctioned funds should be through proper channel.
2. Annual progress reports should be submitted to the Registrar through proper channel.
3. On the completion of the project, a detailed report should be prepared and submitted to the Registrar within one month from the date of completion of the project.
4. Financial utilization statement as of March 31<sup>st</sup> every year should be submitted.
5. University has all the rights to terminate the project if the progress is not satisfactory.
6. This funding is given as startup grant for the PI and should use this grant to generate the preliminary findings useful for submitting projects for funding from the external agencies.

**Cc to:**

1. Principle Investigator (Dr. Sandeep Shetty)
2. Finance Officer
3. Purchase and Stores
4. Deputy Director, YRC

  
Dr. K.S Gangadhara Somayaji  
Registrar

ATTESTED

  
Dr. Gangadhara Somayaji K.S.  
Registrar  
Yenepoya (Deemed to be University)  
University Road, Deralakatte  
Mangalore- 575 018, Karnataka



**YENEPOYA**  
(DEEMED TO BE UNIVERSITY)  
Recognised under Sec 3(A) of the UGC Act 1956  
Accredited by NAAC with 'A' Grade

## SANCTION ORDER FOR THE SEED GRANT

YU/Seed grant/082-2019

Date: 09.12.2019

**Sub: R/P entitled** "Inflammatory and fibrinolytic changes in patients with Sepsis and ARDS"

**Principle Investigator:** Dr. Prabha Adhikari M.R, Professor and HOD of Geriatrics Medicine, YMCH.

On the recommendation of the Yenepoya University Research Committee Meeting held on 27.11.2019, an amount of Rs. 2,00,000/- has been approved for the above cited project for the period of one year.

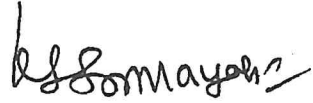
Sl. no	Item	1 <sup>st</sup> Year (Rs.)
1.	Recurring/ Consumables	2,00,000
<b>Grand Total</b>		<b>2,00,000/-</b>
<b>Rupees Two lakhs only</b>		

### Terms and conditions:

1. No funds will be provided directly to the Principal Investigator, all the requests for the utilization of the sanctioned funds should be through proper channel.
2. Annual progress reports should be submitted to the Registrar through proper channel.
3. On the completion of the project, a detailed report should be prepared and submitted to the Registrar within one month from the date of completion of the project.
4. Financial utilization statement as of March 31<sup>st</sup> every year should be submitted.
5. University has all the rights to terminate the project if the progress is not satisfactory.
6. This funding is given as startup grant for the PI and should use this grant to generate the preliminary findings useful for submitting projects for funding from the external agencies.

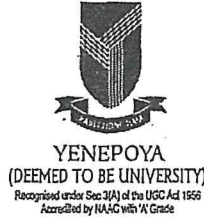
### Cc to:

1. Principle Investigator (Dr. Prabha Adhikari M.R)
2. Co-Investigator (Dr.Rashmi YMC, Dr. Shruthi S YMC, Dr. Yashodhar Bhandary and Dr. Ashwini Prabhu, YRC)
3. Finance Officer
4. Purchase and Stores
5. Deputy Director, YRC

  
Dr. K.S Gangadhara Somayaji  
Registrar

**ATTESTED**

Dr.Gangadhara Somayaji K.S.  
Registrar  
Yenepoya(Deemed to be University)  
University Road, Deralakatta  
Mangalore- 575 018, Karnataka



YENEPLOYA  
(DEEMED TO BE UNIVERSITY)  
Recognized under Sec 3(A) of the UGC Act 1956  
Accredited by NAAC with 'A' Grade

### SANCTION ORDER FOR THE SEED GRANT

YU/Seed grant/083-2019

Date: 07.12.2019

Sub: R/P entitled "Role of Thymoquinone in Sepsis induced acute kidney injury"

Principle Investigator: Mr. Anwar A.S. Lecturer Department of Physiology, YMC.

On the recommendation of the Yenepoya University Research Committee Meeting held on 27.11.2019, an amount of Rs. 2,00,000/- has been approved for the above cited project for the period of one year.


Sl. no	Item	1 <sup>st</sup> Year (Rs.)
1.	Recurring/ Consumables	2,00,000
<b>Grand Total</b>		<b>2,00,000/-</b>
Rupees Two lakhs only		

#### Terms and conditions:


1. No funds will be provided directly to the Principle Investigator, all the requests for the utilization of the sanctioned funds should be through proper channel.
2. Annual progress reports should be submitted to the Registrar through proper channel.
3. On the completion of the project, a detailed report should be prepared and submitted to the Registrar within one month from the date of completion of the project.
4. Financial utilization statement as of March 31<sup>st</sup> every year should be submitted.
5. University has all the rights to terminate the project if the progress is not satisfactory.
6. This funding is given as startup grant for the PI and should use this grant to generate the preliminary findings useful for submitting projects for funding from the external agencies.

#### Cc to:

1. Principle Investigator (Mr. Anwar A.S.)
2. Co-Investigator (Dr. Ramadas Nayak, YMC)
3. Finance Officer
4. Purchase and Stores
5. Deputy Director, YRC

  
Dr. K.S Gangadhara Somayaji  
Registrar

ATTESTED

  
Dr. Gangadhara Somayaji K.S.  
Registrar  
Yenepoya (Deemed to be University)  
University Road, Derlakatte  
Mangalore- 575 018, Karnataka





YENEPOYA  
(DEEMED TO BE UNIVERSITY)  
Recognised under Sec 3(A) of the UGC Act 1956  
Accredited by NAAC with 'A' Grade

## SANCTION ORDER FOR THE SEED GRANT

YU/Seed grant/084-2019.

Date: 09.12.2019

**Sub: R/P entitled "Evaluation of Cardio-Protective effect of *Crataeva Magna* against Isoproterenol induced myocardial injury"**

**Principle Investigator:** Dr. Manodeep Chakroborty, Associate Professor Department of Pharmacology, YPCRC.

On the recommendation of the Yenepoya University Research Committee Meeting held on 27.11.2019, an amount of Rs. 2,00,000/- has been approved for the above cited project for the period of one year.

Sl. no	Item	1 <sup>st</sup> Year (Rs.)
1.	Recurring/ Consumables	2,00,000
<b>Grand Total</b>		<b>2,00,000/-</b>
<b>Rupees Two lakhs only</b>		

### Terms and conditions:

1. No funds will be provided directly to the Principal Investigator, all the requests for the utilization of the sanctioned funds should be through proper channel.
2. Annual progress reports should be submitted to the Registrar through proper channel.
3. On the completion of the project, a detailed report should be prepared and submitted to the Registrar within one month from the date of completion of the project.
4. Financial utilization statement as of March 31<sup>st</sup> every year should be submitted.
5. University has all the rights to terminate the project if the progress is not satisfactory.
6. This funding is given as startup grant for the PI and should use this grant to generate the preliminary findings useful for submitting projects for funding from the external agencies.

### Cc to:

1. Principle Investigator (Dr. Manodeep Chakroborty)
2. Co-Investigator (Dr. Mohammed Gulzar Ahmed, YPCRC)
3. Finance Officer
4. Purchase and Stores
5. Deputy Director, YRC

Dr. K.S Gangadhara Somayaji

Registrar

ATTESTED

Dr. Gangadhara Somayaji K.S.  
Registrar  
Yenepoya (Deemed to be University)  
University Road, Deralakatte  
Mangalore- 575 018, Karnataka



YENEPOYA  
(DEEMED TO BE UNIVERSITY)  
Recognised under Sec 3(A) of the UGC Act 1956  
Accredited by NAAC with 'A' Grade

## SANCTION ORDER FOR THE SEED GRANT

YU/Seed grant/085-2019

Date: 09.12.2019

**Sub: R/P entitled "Targeted drug delivery of bevacizumab nanoparticle for ovarian cancer"**

**Principle Investigator:** Dr. Mobeen Shaik, Associate Professor Department of Pharmaceutics YPCRC.

On the recommendation of the YenepoYa University Research Committee Meeting held on 27.11.2019, an amount of Rs. 2,00,000/- has been approved for the above cited project for the period of one year.

Sl. no	Item	1 <sup>st</sup> Year (Rs.)
1.	Recurring/ Consumables	2,00,000
<b>Grand Total</b>		<b>2,00,000/-</b>
<b>Rupees Two lakhs only</b>		

### Terms and conditions:

1. No funds will be provided directly to the Principal Investigator, all the requests for the utilization of the sanctioned funds should be through proper channel.
2. Annual progress reports should be submitted to the Registrar through proper channel.
3. On the completion of the project, a detailed report should be prepared and submitted to the Registrar within one month from the date of completion of the project.
4. Financial utilization statement as of March 31<sup>st</sup> every year should be submitted.
5. University has all the rights to terminate the project if the progress is not satisfactory.
6. This funding is given as startup grant for the PI and should use this grant to generate the preliminary findings useful for submitting projects for funding from the external agencies.

### Cc to:

1. Principle Investigator (Dr. Mobeen Shaik)
2. Co-Investigator (Dr. Mohammed Gulzar Ahmed, YPCRC)
3. Finance Officer
4. Purchase and Stores
5. Deputy Director, YRC

**Dr. K.S Gangadhara Somayaji**  
Registrar

ATTESTED

Dr. Gangadhara Somayaji K.S.  
Registrar  
YenepoYa (Deemed to be University)  
University Road, Deralakatte  
Mangalore- 575 018, Karnataka

**SANCTION ORDER FOR THE SEED GRANT**

YU/Seed grant/086-2019

Date: 09.12.2019

**Sub: R/P entitled "A Comparative study of hydrogels containing Anastrozole alone & with the combination of flax seed extract for breast cancer"**

**Principle Investigator: Ms. Sanjana A, Assistant Professor, Department of Pharmaceutics, YPCRC.**

On the recommendation of the Yenepoya University Research Committee Meeting held on 27.11.2019, an amount of Rs. 2,00,000/- has been approved for the above cited project for the period of one year.

Sl. no	Item	1 <sup>st</sup> Year (Rs.)
1.	Recurring/ Consumables	2,00,000
<b>Grand Total</b>		<b>2,00,000/-</b>
<b>Rupees Two lakhs only</b>		

**Terms and conditions:**


1. No funds will be provided directly to the Principal Investigator, all the requests for the utilization of the sanctioned funds should be through proper channel.
2. Annual progress reports should be submitted to the Registrar through proper channel.
3. On the completion of the project, a detailed report should be prepared and submitted to the Registrar within one month from the date of completion of the project.
4. Financial utilization statement as of March 31<sup>st</sup> every year should be submitted.
5. University has all the rights to terminate the project if the progress is not satisfactory.
6. This funding is given as startup grant for the PI and should use this grant to generate the preliminary findings useful for submitting projects for funding from the external agencies.

**Cc to:**

1. Principle Investigator (Ms. Sanjana A)
2. Co-Investigator (Dr.Mohammed Gulzar Ahmed, YPCRC)
3. Finance Officer
4. Purchase and Stores
5. Deputy Director, YRC

  
**Dr. K.S Gangadhara Somayaji**  
Registrar

**ATTESTED**

  
Dr.Gangadhara Somayaji K.S.  
Registrar  
Yenepoya(Deemed to be University)  
University Road, Deralakatte  
Mangalore- 575 018, Karnataka

**SANCTION ORDER FOR THE SEED GRANT**

YU/Seed grant/087-2019

Date: 09.12.2019

**Sub: R/P entitled "Detection of early potential biomarkers for different Kidney Stone diseases by Proteomic and Metabolomic study"**

**Principle Investigator: Dr. Altaf Khan, Associate Professor Department of Urology, YMCH.**

On the recommendation of the Yenepoya University Research Committee Meeting held on 27.11.2019, an amount of Rs. 2,00,000/- has been approved for the above cited project for the period of one year.


Sl. no	Item	1 <sup>st</sup> Year (Rs.)
1.	Recurring/ Consumables	2,00,000
<b>Grand Total</b>		<b>2,00,000/-</b>
Rupees Two lakhs only		

**Terms and conditions:**


1. No funds will be provided directly to the Principal Investigator, all the requests for the utilization of the sanctioned funds should be through proper channel.
2. Annual progress reports should be submitted to the Registrar through proper channel.
3. On the completion of the project, a detailed report should be prepared and submitted to the Registrar within one month from the date of completion of the project.
4. Financial utilization statement as of March 31<sup>st</sup> every year should be submitted.
5. University has all the rights to terminate the project if the progress is not satisfactory.
6. This funding is given as startup grant for the PI and should use this grant to generate the preliminary findings useful for submitting projects for funding from the external agencies.

**Cc to:**

1. Principle Investigator (Dr. Altaf Khan)
2. Co-Investigator (Dr.TS Keshava Prasad and Dr. Shobha D, CSBMM, YRC)
3. Finance Officer
4. Purchase and Stores
5. Deputy Director, YRC

  
**Dr. K.S Gangadhara Somayaji**  
Registrar

**ATTESTED**

  
Dr.Gangadhara Somayaji K.S.  
Registrar  
Yenepoya(Deemed to be University)  
University Road, Deralakatte  
Mangalore- 575 018, Karnataka



**YENEPOYA**  
**(DEEMED TO BE UNIVERSITY)**  
Recognised under Sec 3(A) of the UGC Act 1956  
Accredited by NAAC with 'A' Grade

**SANCTION ORDER FOR THE SEED GRANT**

YU/Seed grant/076-2019

Date: 29.04.2019

**Sub: R/P entitled** "Identification of diagnostic and prognostic determinants derived from renal cell carcinoma (RCC) circulating tumour cells (CTCs) using proteomic approach"

**Principle Investigator:** Dr. Mujeebu Rahiman Professor Dept. of Urology Yenepoya Medical College Hospital Mangalore

On the recommendation of the Yenepoya University Research Committee Meeting held on 23.04.2019, an amount of Rs. 2,00,000/- has been approved for the above cited project for a period of one year.

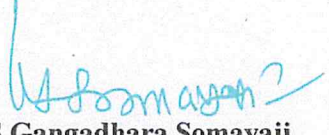
Sl. no	Item	1 <sup>st</sup> Year (Rs.)
1.	• Recurring/ Consumables	2,00,000
<b>Grand Total</b>		<b>2,00,000/-</b>
<b>Rupees Two lakhs only</b>		

**Terms and conditions:**


1. No funds will be provided directly to the Principal Investigator, all the requests for the utilization of the sanctioned funds should be through proper channel.
2. Annual progress reports should be submitted to the Registrar through proper channel.
3. On the completion of the project, a detailed report should be prepared and submitted to the Registrar within one month from the date of completion of the project.
4. University has all the rights to terminate the project if the progress is not satisfactory.
5. This funding is given as startup grant for the PI and should use this grant to generate the preliminary findings useful for submitting projects for funding from the external agencies.

**Cc to:**

1. Principal Investigator (Dr. Mujeebu Rahiman)
2. Co-Investigator (Dr. Keshava Prasad, Dr. Shobha & Dr. Prashant Kumar Modi CSBMM, YRC)
3. Finance Officer
4. Purchase and Stores
5. Deputy Director, YRC

  
**Dr. K.S Gangadhara Somayaji**  
Registrar 2/5

**ATTESTED**

  
**Dr. Gangadhara Somayaji K.S.**  
Registrar  
Yenepoya (Deemed to be University)  
University Road, Derlakatte  
Mangalore- 575 018, Karnataka



**YENEPOYA**  
(DEEMED TO BE UNIVERSITY)  
Recognised under Sec 3(A) of the UGC Act 1956  
Accredited by NAAC with 'A' Grade

**SANCTION ORDER FOR THE SEED GRANT**

YU/Seed grant/077-2019

Date: 29.04.2019

**Sub: R/P entitled** “Delineating the signaling mechanism involved in the neuroprotective effects of Yashtimadhu in Parkinson’s disease”

**Principle Investigator:** Dr. Prashant Kumar Modi, Senior Scientific Officer, CSBMM, Yenepoya Research Centre

On the recommendation of the Yenepoya University Research Committee Meeting held on 23.04.2019, an amount of **Rs. 2,00,000/-** has been approved for the above cited project for a period of one year.


Sl. no	Item	1 <sup>st</sup> Year (Rs.)
1.	• Recurring/ Consumables	2,00,000
<b>Grand Total</b>		<b>2,00,000/-</b>
<b>Rupees Two lakhs only</b>		

**Terms and conditions:**

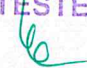
1. No funds will be provided directly to the Principal Investigator, all the requests for the utilization of the sanctioned funds should be through proper channel.
2. Annual progress reports should be submitted to the Registrar through proper channel.
3. On the completion of the project, a detailed report should be prepared and submitted to the Registrar within one month from the date of completion of the project.
4. University has all the rights to terminate the project if the progress is not satisfactory.
5. This funding is given as startup grant for the PI and should use this grant to generate the preliminary findings useful for submitting projects for funding from the external agencies.

**Cc to:**

1. Principle Investigator (Dr. Prashant Kumar Modi)
2. Co-Investigator (Dr. TS Keshava Prasad Professor Department & Deputy Director CSBMM, YRC)
3. Finance Officer
4. Purchase and Stores
5. Deputy Director, YRC

  
**Dr. K.S Gangadhara Somayaji**  
Registrar 2/5

**ATTESTED**

  
**Dr. Gangadhara Somayaji K.S.**  
Registrar  
Yenepoya (Deemed to be University)  
University Road, Deralakatte  
Mangalore- 575 018, Karnataka



**YENEPOYA**  
(DEEMED TO BE UNIVERSITY)  
Recognised under Sec 3(A) of the UGC Act 1956  
Accredited by NAAC with 'A' Grade

**SANCTION ORDER FOR THE SEED GRANT**

YU/Seed grant/079-2019 .

Date: 29.04.2019

**Sub: R/P entitled** “Study of G6PD deficiency in patients with Malaria in endemic region of Dakshina Kannada including the study of the relapse pattern”

**Principle Investigator:** Dr. Sahana K.S Associate Professor, Yenepoya Medical College Hospital.

On the recommendation of the Yenepoya University Research Committee Meeting held on 23.04.2019, an amount of Rs. 2,00,000/- has been approved for the above cited project for the period of one year.

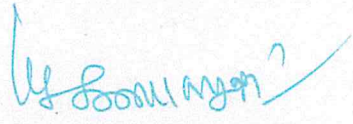
Sl. no	Item	1 <sup>st</sup> Year (Rs.)
1.	• Recurring/ Consumables	2,00,000
<b>Grand Total</b>		<b>2,00,000/-</b>
<b>Rupees Two lakhs only</b>		

**Terms and conditions:**


1. No funds will be provided directly to the Principal Investigator, all the requests for the utilization of the sanctioned funds should be through proper channel.
2. Annual progress reports should be submitted to the Registrar through proper channel.
3. On the completion of the project, a detailed report should be prepared and submitted to the Registrar within one month from the date of completion of the project.
4. University has all the rights to terminate the project if the progress is not satisfactory.
5. This funding is given as startup grant for the PI and should use this grant to generate the preliminary findings useful for submitting projects for funding from the external agencies.

**Cc to:**

1. Principle Investigator (Dr. Sahana K.S)
2. Co-Investigator (Dr. Prabha Adhikari, Professor and HOD & Dr. Shankar Prasad Das, Associate Professor)
3. Finance Officer
4. Purchase and Stores
5. Deputy Director, YRC

  
**Dr. K.S Gangadhara Somayaji**  
Registrar

**ATTESTED**

  
**Dr. Gangadhara Somayaji K.S.**  
Registrar  
Yenepoya (Deemed to be University)  
University Road, Deralakatte  
Mangalore- 575 018, Karnataka



**YENEPOYA**  
(DEEMED TO BE UNIVERSITY)  
Recognised under Sec 3(A) of the UGC Act 1956  
Accredited by NAAC with 'A' Grade

### SANCTION ORDER FOR THE SEED GRANT

YU/Seed grant/078-2019

Date: 29.04.2019

**Sub: R/P entitled** "Interaction of human Wharton's jelly mesenchymal stem cells (WJ-MSCs) with cancer stem cells in vitro: Cellular, molecular and functional aspects"

**Principle Investigator:** Dr. Vidhyashree Kamath C, Dept. of OBG, Yenepoya Medical College Hospital.

On the recommendation of the Yenepoya University Research Committee Meeting held on 23.04.2019, an amount of Rs. 2,00,000/- has been approved for the above cited project for a period of one year.

Sl. no	Item	1 <sup>st</sup> Year (Rs.)
1.	• Recurring/ Consumables	2,00,000
<b>Grand Total</b>		<b>2,00,000/-</b>
<b>Rupees Two lakhs only</b>		

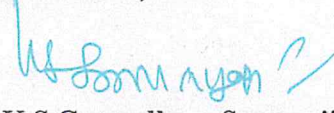
- ❖ The cost requested for the overseas training shall be reimbursed upon successful completion of the training period with a maximum limit of Rs. 2,00,000/-.

**Terms and conditions:**


1. No funds will be provided directly to the Principal Investigator, all the requests for the utilization of the sanctioned funds should be through proper channel.
2. Annual progress reports should be submitted to the Registrar through proper channel.
3. On the completion of the project, a detailed report should be prepared and submitted to the Registrar within one month from the date of completion of the project.
4. University has all the rights to terminate the project if the progress is not satisfactory.
5. This funding is given as startup grant for the PI and should use this grant to generate the preliminary findings useful for submitting projects for funding from the external agencies.

**Cc to:**

1. Principle Investigator (Dr. Vidhyashree Kamath C)
2. Co-Investigator (Dr. Bipasha Bose, SCRMC, Yenepoya Research Centre)
3. Finance Officer
4. Purchase and Stores
5. Deputy Director, YRC

  
**Dr. K.S Gangadhara Somayaji**  
Registrar 2/5

**ATTESTED**

  
Dr. Gangadhara Somayaji K.S.  
Registrar  
Yenepoya (Deemed to be University)  
University Road, Deralakatte  
Mangalore- 575 018, Karnataka





**YENEPOYA**  
(Deemed to be University)  
Recognized under Sec 3(A) of UGC Act 1956  
Accredited by NAAC with 'A' Grade

**SANCTION ORDER FOR THE SEED GRANT**

YU/YRC/Seed grant/068-2018

Date: 18.09.2018

**Sub: R/P entitled** "Effect of quercetin on cardio-protective effect of resveratrol against isoproterenol induced myocardial injury"

**Principle Investigator:** Dr. Mohammed Gulzar Ahmed, Pharmaceutics Dept., Yenepoia Pharmacy College and Research Centre

On the recommendation of the Yenepoia University Research Committee Meeting held on 21.08.2018, an amount of **Rs. 2,00,000/-** has been approved for the above cited project for the period of one year.

Sl. no	Item	1 <sup>st</sup> Year (Rs.)
1.	<b>Recurring:</b> <ul style="list-style-type: none"><li>• Consumables</li><li>• Travel</li></ul>	1,80,000 20,000
<b>Grand Total</b>		<b>2,00,000/-</b>
<b>Rupees Two lakhs only</b>		

**Terms and conditions:**

1. No funds will be provided directly to the Principal Investigator, all the requests for the utilization of the sanctioned funds should be through proper channel.
2. Annual progress reports should be submitted to the Registrar through proper channel.
3. On the completion of the project, a detailed report should be prepared and submitted to the Registrar within one month from the date of completion of the project.
4. University has all the rights to terminate the project if the progress is not satisfactory.
5. This funding is given as startup grant for the PI and should use this grant to generate the preliminary findings useful for submitting projects for funding from the external agencies.

**Cc to:**

1. Co-Investigator ( Dr. Manodeep Chakraborty, Associate Professor, Dept. of Pharmacology)
2. Finance Officer
3. Purchase and Stores
4. Deputy Director, YRC

  
**Dr. Shreekumar Menon**  
Registrar

**ATTESTED**

Dr.Gangadhara Somayaji K.S.  
Registrar  
Yenepoia(Deemed to be University)  
University Road, Deralakatte  
Mangalore- 575 018, Karnataka



**YENEPOYA**  
(Deemed to be University)  
Recognized under Sec 3(A) of UGC Act 1956  
Accredited by NAAC with 'A' Grade

**SANCTION ORDER FOR THE SEED GRANT**

YU/Seed grant/069-2018

Date: 18.09.2018

**Sub: R/P entitled** "Comparative proteomic analysis of serum to identify underlying molecular mechanism of Psoriasis"

**Principle Investigator:** Dr. Saiqa R Shah, Assistant Professor, Dept. of Bio chemistry, Yenepoya Research Centre

---

On the recommendation of the Yenepoya University Research Committee Meeting held on 21.08.2018, an amount of **Rs. 2,00,000/-** has been approved for the above cited project for the period of one year towards the cost of consumables.

**Terms and conditions:**

1. No funds will be provided directly to the Principal Investigator, all the requests for the utilization of the sanctioned funds should be through proper channel.
2. Annual progress reports should be submitted to the Registrar through proper channel.
3. On the completion of the project, a detailed report should be prepared and submitted to the Registrar within one month from the date of completion of the project.
4. University has all the rights to terminate the project if the progress is not satisfactory.
5. This funding is given as startup grant for the PI and should use this grant to generate the preliminary findings useful for submitting projects for funding from the external agencies.

**Cc to:**

1. Co-Investigator (Dr. Manjunath Shenoy M, Professor and HOD Department of Dermatology, YMC Yenepoya)
2. Finance Officer
3. Purchase and Stores
4. Deputy Director, YRC

**Dr. Shreekumar Menon**  
Registrar

**ATTESTED**

Dr. Gangadhara Somayaji K.S.  
Registrar  
Yenepoya (Deemed to be University)  
University Road, Derlakatte  
Mangalore- 575 018, Karnataka



YU/Seed grant/069-2018

24.06.2020

To,

Dr. Saiqa Rasool Shah  
Assistant Professor  
Dept. of Biochemistry, YMC  
Yenepoya (Deemed to be University)

**Sub: Seed grant project No. YU/Seed grant/069-2018, Title: "Comparative proteomic analysis of serum to identify underlying molecular mechanisms of psoriasis"**

**Ref:** i) YU/Seed grant/069-2018

ii) Your report on work plan and activities to be carried out in the 1<sup>st</sup> year dtd: 07.02.2020

With reference to the above, based on the recommendation on the progress, second year grant of Rs. 1,00,000/- is sanctioned in order to complete the pending work of the project. You should submit the final report after the completion of the project along with the statement of accounts and copies of publications made from the project on or before 31<sup>st</sup> March 2021.

  
Registrar

ATTESTED  


Dr. Gangadhara Somayaji K.S.  
Registrar  
Yenepoya (Deemed to be University)  
University Road, Deralakatte  
Mangalore- 575 018, Karnataka



**YENEPOYA**  
(Deemed to be University)  
Recognized under Sec 3(A) of UGC Act 1956  
Accredited by NAAC with 'A' Grade

**SANCTION ORDER FOR THE SEED GRANT**

YU/Seed grant/070-2018

Date: 18.09.2018

**Sub: R/P entitled** "Identification and evaluation of potential biomarkers for early diagnosis of liver cirrhosis using high-resolution mass spectrometry "

**Principle Investigator:** Dr. B. Sudheesh Shetty, Associate Professor, Dept. Of Medicine, Yenepoya Research Centre

---


On the recommendation of the Yenepoya University Research Committee Meeting held on 21.08.2018, an amount of **Rs. 2,00,000/-** has been approved for the above cited project for the period of one year towards the cost of consumables.

**Terms and conditions:**

1. No funds will be provided directly to the Principal Investigator, all the requests for the utilization of the sanctioned funds should be through proper channel.
2. Annual progress reports should be submitted to the Registrar through proper channel.
3. On the completion of the project, a detailed report should be prepared and submitted to the Registrar within one month from the date of completion of the project.
4. University has all the rights to terminate the project if the progress is not satisfactory.
5. This funding is given as startup grant for the PI and should use this grant to generate the preliminary findings useful for submitting projects for funding from the external agencies.

**Cc to:**

1. Co-Investigator (Dr. Prashant Kumar Modi, Senior Scientific Officer centre for systems Biology & Molecular Medicine, Yenepoya Research Centre)
2. Finance Officer
3. Purchase and Stores
4. Deputy Director, YRC

  
**Dr. Shreekumar Menon**  
Registrar

**ATTESTED**  


Dr.Gangadhara Somayaji K.S.  
Registrar  
Yenepoya(Deemed to be University)  
University Road, Derlakatta  
Mangalore- 575 018, Karnataka



**YENEPOYA**  
(Deemed to be University)  
Recognized under Sec 3(A) of UGC Act 1956  
Accredited by NAAC with 'A' Grade

**SANCTION ORDER FOR THE SEED GRANT**

YU/Seed grant/071-2018

Date: 18.09.2018

**Sub: R/P entitled** "Understanding the role and function of Non-coding RNAs during myogenic and osteogenic differentiations and its impact on skeletal muscle diseases"

**Principle Investigator:** Dr. Raghu Bhushan, Assistant Professor, Yenepoya Research Centre.

On the recommendation of the Yenepoya University Research Committee Meeting held on 21.08.2018, an amount of **Rs. 3,00,000/-** has been approved for the above cited project for the period of one year towards the cost of consumables.

**Terms and conditions:**

1. No funds will be provided directly to the Principal Investigator, all the requests for the utilization of the sanctioned funds should be through proper channel.
2. Annual progress reports should be submitted to the Registrar through proper channel.
3. On the completion of the project, a detailed report should be prepared and submitted to the Registrar within one month from the date of completion of the project.
4. University has all the rights to terminate the project if the progress is not satisfactory.
5. This funding is given as startup grant for the PI and should use this grant to generate the preliminary findings useful for submitting projects for funding from the external agencies.

**Cc to:**

1. Co-Investigator (Dr. R. M. Shenoy, Yenepoya Research Centre and Yenepoya Medical College)
2. Finance Officer
3. Purchase and Stores
4. Deputy Director, YRC

**Dr. Shreekumar Menon**  
Registrar

**ATTESTED**

**Dr. Gangadhara Somayaji K.S.**  
Registrar  
Yenepoya (Deemed to be University)  
University Road, Deralakatte  
Mangalore- 575 018, Karnataka



**YENEPOYA**  
(Deemed to be University)  
Recognized under Sec 3(A) of UGC Act 1956  
Accredited by NAAC with 'A' Grade

**SANCTION ORDER FOR SEED GRANT**

YU/Seed grant/065-2018

Date: 14.03.2018

**Sub: R/P entitled "Investigating the Genetics of Deep vein Thrombosis among South Indian adults"**

**Principal Investigator: Dr. Shankar Prasad Das, Assistant Professor, Yenepoya Research Centre**

On the recommendation of the Yenepoya University Research Committee Meeting held on 22.02.2018, an amount of Rs. 3,00,000/- has been approved for the above cited project for the period of one year.

Sl. no	Item	1 <sup>st</sup> Year (Rs.)
1.	<b>Recurring:</b> <ul style="list-style-type: none"><li>• Consumables</li><li>• Gilson pipetteman set</li><li>• Electrophoresis unit</li></ul>	2,00,000 1,00,000
<b>Grand Total</b>		<b>3,00,000/-</b>
<b>Three lakhs only</b>		

**Terms and conditions:**

1. No funds will be provided directly to the Principal Investigator, all the requests for the utilization of the sanctioned funds should be through proper channel.
2. Annual progress reports should be submitted to the Registrar through proper channel.
3. On the completion of the project, a detailed report should be prepared and submitted to the Registrar within one month from the date of completion of the project.
4. University has all the rights to terminate the project if the progress is not satisfactory.
5. This funding is given as startup grant for the PI and should use this grant to generate the preliminary findings useful for submitting projects for funding from the external agencies.

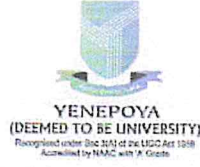
**Cc to:**

1. Finance Officer
2. Purchase and Stores
3. Deputy Director, YRC

**Dr. Shree Kumar Menon**

**Registrar**  
**Dr. Shree Kumar Menon**  
**Registrar**

**Yenepoya University**  
Dr. Gangadhara Somayaji K.S.  
Registrar  
Yenepoya (Deemed to be University)  
University Road, Derattahalli  
Mangalore-575 019, Karnataka



YU/Seed grant/065-2018

16.11.2020

To,

Dr. Shankar Prasad Das  
Assistant Professor  
Yenepoya Research Centre  
Yenepoya (Deemed to be University)

Sub: Seed grant project No. YU/Seed grant/065-2018, "Investigating the Genetics of Deep Vein Thrombosis among South Indian adults"

Ref: i) YU/Seed grant/065-2018

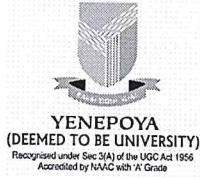
ii) Your report on work plan and activities to be carried out in the 1<sup>st</sup> year dated: 05.11.2020

With reference to the above, based on the recommendation on the progress, Second year grant of Rs. 1,50,000/- is sanctioned in order to complete the pending work of the project. You should submit the final report after the completion of the project along with the statement of accounts and copies of publications and patents made from the project as of 31<sup>st</sup> October 2021.

Registrar

ATTESTED

Dr. Gangadhara Somayaji K.S.  
Registrar  
Yenepoya (Deemed to be University)  
University Road, Derlakutti  
Mangalore- 575 018, Karnataka



## SANCTION ORDER FOR THE SEED GRANT

YU/Seedgrant/074-2018

Date: 18.09. 2018

**Sub: R/P titled** “Identification of blood and urinary markers to predict severity of neonatal asphyxia using high resolution mass spectrometry”

**Principal Investigator:** Dr. Arun A.B, Professor, Yenepoya Research Centre


On the recommendation of the Yenepoya University Research Committee Meeting held on 21.08.2018, an amount of **Rs. 3,00,000/-** has been approved for the above cited project for a period of one year towards the cost of consumables.

### **Terms and conditions:**


1. No funds will be provided directly to the Principal Investigator, all the requests for the utilization of the sanctioned funds should be through proper channel.
2. Annual progress reports should be submitted to the Registrar through proper channel.
3. On the completion of the project, a detailed report should be prepared and submitted to the Registrar within one month from the date of completion of the project.
4. University has all the rights to terminate the project if the progress is not satisfactory.
5. This funding is given as startup grant for the PI and should use this grant to generate the preliminary findings useful for submitting projects for funding from the external agencies.

### **Cc to:**

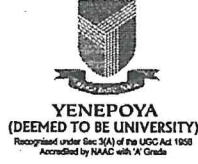
1. Co-Investigator (Dr. Sneha Pinto, DST-INSPIRE Faculty, CSBMM, YRC)
2. Finance Officer
3. Purchase and Stores
4. Deputy Director, YRC

  
**Dr. Shreekumar Menon**  
Registrar

**ATTESTED**

  
Dr.Gangadhara Somayaji K.S.  
Registrar  
Yenepoya(Deemed to be University)  
University Road, Deralakatte  
Mangalore- 575 018, Karnataka





YU/Seed grant/074-2018

03.10.2020

To,

Dr. Arun A B  
Professor  
Yenepoya Research Centre  
Yenepoya (Deemed to be University)

Sub: Seed grant project No. YU/Seed grant/074-2018, "Identification of blood and urinary markers to predict severity of neonatal asphyxia using high resolution mass spectrometry"

Ref: i) YU/Seed grant/074-2018

ii) Your report on work plan and activities to be carried out in the 1<sup>st</sup> year dated: 31.08.2020

\*\*\*\*\*

With reference to the above, based on the recommendation on the progress, Second year grant of Rs. 1,00,000/- is sanctioned in order to complete the pending work of the project. You should submit the final report after the completion of the project along with the statement of accounts and copies of publications and patents made from the project as of 30<sup>th</sup> July 2021.

*Dr. Somayaji K.S.*

REGISTRAR

ATTESTED

*Dr. Somayaji K.S.*

Dr. Gangadhara Somayaji K.S.  
Registrar  
Yenepoya (Deemed to be University)  
University Road, Deralakatte  
Mangalore- 575 018, Karnataka



**YENEPOYA**  
(Deemed to be University)  
Recognized under Sec 3(A) of UGC Act 1956  
Accredited by NAAC with 'A' Grade

**SANCTION ORDER FOR THE SEED GRANT**

YU/Seed grant/073-2018

Date: 18.09.2018

**Sub: R/P entitled** "Fucoidan beads containing hydroxyapatite and grapheme oxide for bone tissue repair and regeneration"

**Principle Investigator:** Dr. Jayachandran Venkatesan, Assistant Professor, Yenepoya Research Centre

On the recommendation of the Yenepoya University Research Committee Meeting held on 21.08.2018, an amount of Rs. 2,00,000/- has been approved for the above cited project for the period of one year.

Sl. no	Item	1 <sup>st</sup> Year (Rs.)
1.	<b>Recurring:</b> <ul style="list-style-type: none"><li>• Consumables</li><li>• Travel</li></ul>	1,90,000 10,000
<b>Grand Total</b>		<b>2,00,000/-</b>
<b>Rupees Two lakhs only</b>		

**Terms and conditions:**

1. No funds will be provided directly to the Principal Investigator, all the requests for the utilization of the sanctioned funds should be through proper channel.
2. Annual progress reports should be submitted to the Registrar through proper channel.
3. On the completion of the project, a detailed report should be prepared and submitted to the Registrar within one month from the date of completion of the project.
4. University has all the rights to terminate the project if the progress is not satisfactory.
5. This funding is given as startup grant for the PI and should use this grant to generate the preliminary findings useful for submitting projects for funding from the external agencies.

**Cc to:**

1. Finance Officer
2. Purchase and Stores
3. Deputy Director, YRC

**Dr. Shreekumar Menon**  
Registrar

**ATTESTED**

Dr. Gangadhara Somayaji K.S.  
Registrar  
Yenepoya (Deemed to be University)  
University Road, Deralakatte  
Mangalore- 575 018, Karnataka



**YENEPOYA**

(Deemed to be University)

Recognized under Sec 3(A) of UGC Act 1956

Accredited by NAAC with 'A' Grade

**SANCTION ORDER FOR SEED GRANT**

YU/YRC/Seed grant/062-2018

Date: 14/03/2018

**Sub: R/P entitled "Evaluation of Inflammatory Mediators and Magnetic Resonance Imaging Changes in Temporomandibular Joint Disorders following Arthrocentesis with Sodium Hyaluronate Injection"**

**Principal Investigator: Dr. Joyce Sequeria, Professor, Dept. of Oral & Maxillofacial Surgery, Yenepoya Dental College**

On the recommendation of the Yenepoya University Research Committee Meeting held on 22.02.2018, an amount of Rs. 3,23,000/- has been approved for the above cited project for the period of one year.

Sl. no	Item	1 <sup>st</sup> Year (Rs.)
1.	<b>Recurring:</b> <ul style="list-style-type: none"><li>• Chemical analysis of synovial fluid</li><li>• MRI imaging cost</li><li>• Sodium hyaluronate injection</li><li>• Fabrication of needle appliance</li><li>• Miscellaneous expenses</li></ul>	1,00,000 1,80,000 33,000 5,000 5,000
<b>Grand Total</b>		<b>3,23,000/-</b>
<b>Three lakhs twenty three thousand only</b>		

**Terms and conditions:**

1. No funds will be provided directly to the Principal Investigator, all the requests for the utilization of the sanctioned funds should be through proper channel.
2. Annual progress reports should be submitted to the Registrar through proper channel.
3. On the completion of the project, a detailed report should be prepared and submitted to the Registrar within one month from the date of completion of the project.
4. University has all the rights to terminate the project if the progress is not satisfactory.
5. This funding is given as startup grant for the PI and should use this grant to generate the preliminary findings useful for submitting projects for funding from the external agencies.

**Cc to:**

1. Co-Investigator ( Dr. Varsha Upadya, Dept. of Oral & Maxillofacial Surgery)
2. Finance Officer
3. Purchase and Stores
4. Deputy Director, YRC

  
**ATTESTED**  
  
**Dr. Shree Kumar Menon**  
Registrar  
Yenepoya University  
Dental College  
Mangalore - 575 018, Karnataka  
Yenepoya University



**YENEPOYA**

(Deemed to be University)

Recognized under Sec 3(A) of UGC Act 1956  
Accredited by NAAC with 'A' Grade

**SANCTION ORDER FOR SEED GRANT**

YU/Seed grant/064-2018

Date: 14.03.2018

**Sub: R/P entitled "Development of PCR based assay for scrub typhus at Yenepoya Medical College and identification and evaluation of potential biomarkers for diagnosis of scrub typhus in patients with acute undifferentiated febrile illnesses"**

**Principal Investigator: Dr. Anurag Bhargava, Professor, Dept. of Medicine, Yenepoya Medical College**

On the recommendation of the Yenepoya University Research Committee Meeting held on 22.02.2018, an amount of Rs. 3,00,000/- has been approved for the above cited project for the period of one year.

Sl. no	Item	1 <sup>st</sup> Year (Rs.)
1.	<b>Recurring:</b> <ul style="list-style-type: none"><li>• PCR reagents</li><li>• Solvents for mass spectrometry</li><li>• HILIC column for LC-MS analysis</li><li>• Metabolite standards</li><li>• Synthetic heavy peptides for MRM</li><li>• Plasticware, glassware &amp; chemicals</li><li>• Stationary expenses</li><li>• Serum lipase</li></ul>	40,000 30,000 60,000 70,000 30,000 35,000 25,000 10,000
<b>Grand Total</b>		<b>3,00,000/-</b>
<b>Three lakhs only</b>		

**Terms and conditions:**

1. No funds will be provided directly to the Principal Investigator, all the requests for the utilization of the sanctioned funds should be through proper channel.
2. Annual progress reports should be submitted to the Registrar through proper channel.
3. On the completion of the project, a detailed report should be prepared and submitted to the Registrar within one month from the date of completion of the project.
4. University has all the rights to terminate the project if the progress is not satisfactory.
5. This funding is given as startup grant for the PI and should use this grant to generate the preliminary findings useful for submitting projects for funding from the external agencies.

**Cc to:**

1. Co-Investigator (Dr. Yashwanth Subbannayya, Scientific Officer, YRC)
2. Finance Officer
3. Purchase and Stores
4. Deputy Director, YRC

  
**ATTESTED**

**Dr. Shreekumar Menon**  
Registrar  
Yenepoya University, Deemed to be University  
University Road, Deralakatte  
Karnataka - 575 018



**YENEPOYA**  
(Deemed to be University)  
Recognized under Sec 3(A) of UGC Act 1956  
Accredited by NAAC with 'A' Grade

**SANCTION ORDER FOR SEED GRANT**

YU/Seed grant/065-2018

Date: 14.03.2018

**Sub: R/P entitled "Elucidating the mechanism of piperine in enhancing the sensitivity of cisplatin treated cancers towards radiation"**

**Principal Investigator: Dr. Divya Lakshmanan M, DST-YSS Faculty, Yenepoya Research Centre**

On the recommendation of the Yenepoya University Research Committee Meeting held on 22.02.2018, an amount of Rs. 2,00,000/- has been approved for the above cited project for the period of one year.

Sl. no	Item	1 <sup>st</sup> Year (Rs.)
1.	<b>Recurring:</b> <ul style="list-style-type: none"><li>• Mouse restrainer, Gamma H2Ax antibody (primary and secondary), Comet assay reagents, Polylysine, Paraformaldehyde, Propidium Iodide, Hoest stain, DABCO Disposable plastic wares, Tissue culture wares</li></ul>	2,00,000
<b>Grand Total</b>		<b>2,00,000/-</b>
<b>Two lakhs only</b>		

**Terms and conditions:**

1. No funds will be provided directly to the Principal Investigator, all the requests for the utilization of the sanctioned funds should be through proper channel.
2. Annual progress reports should be submitted to the Registrar through proper channel.
3. On the completion of the project, a detailed report should be prepared and submitted to the Registrar within one month from the date of completion of the project.
4. University has all the rights to terminate the project if the progress is not satisfactory.
5. This funding is given as startup grant for the PI and should use this grant to generate the preliminary findings useful for submitting projects for funding from the external agencies.

**Cc to:**

1. Finance Officer
2. Purchase and Stores
3. Deputy Director, YRC

ATTESTED

**Dr. Shreekumar Menon**  
Dr. G. Shreekanth Registrar  
Yenepoya (Deemed to be University)  
University Road, Deralakatte  
Yenepoya University - 575 015, Karnataka



**YENEPOYA**  
(Deemed to be University)  
Recognized under Sec 3(A) of UGC Act 1956  
Accredited by NAAC with 'A' Grade

**SANCTION ORDER FOR SEED GRANT**

YU/Seed grant/067-2018

Date: 14.03.2018

**Sub: R/P entitled "Identification of metabolomic markers for prediction of disease progression in mild-to-moderate COPD"**

**Principal Investigator: Dr. Sneha M. Pinto, DST-INSPIRE Faculty, Yenepoya Research Centre**

On the recommendation of the Yenepoya University Research Committee Meeting held on 22.02.2018, an amount of **Rs. 2,80,000/-** has been approved for the above cited project for the period of one year.

Sl. no	Item	1 <sup>st</sup> Year (Rs.)
1.	<b>Recurring:</b> <ul style="list-style-type: none"><li>• Solvents for mass spectrometry, 35,000</li><li>• Column &amp; HPLC accessories 1,00,000</li><li>• Metabolite standards, 1,00,000</li><li>• Plasticware, glassware &amp; chemicals 35,000</li><li>• Serum lipase test 10,000</li></ul>	
<b>Grand Total</b>		<b>2,80,000/-</b>
<b>Two lakhs eighty thousand only</b>		

**Terms and conditions:**

1. No funds will be provided directly to the Principal Investigator, all the requests for the utilization of the sanctioned funds should be through proper channel.
2. Annual progress reports should be submitted to the Registrar through proper channel.
3. On the completion of the project, a detailed report should be prepared and submitted to the Registrar within one month from the date of completion of the project.
4. University has all the rights to terminate the project if the progress is not satisfactory.
5. This funding is given as startup grant for the PI and should use this grant to generate the preliminary findings useful for submitting projects for funding from the external agencies.

**Cc to:**

1. Finance Officer
2. Purchase and Stores
3. Deputy Director, YRC

  
**ATTESTED**

**Dr. Shreekumar Menon**  
Dr. Gangadhara Somayaji K.S.  
Registrar  
Yenepoya (Deemed to be University)  
Mangalagiri Road, Umalakatte  
Mangalore - 575 001, Karnataka  
Yenepoya University



**YENEPOYA**  
(Deemed to be University)  
Recognized under Sec 3(A) of UGC Act 1956  
Accredited by NAAC with 'A' Grade

**SANCTION ORDER FOR SEED GRANT**

YU/Seed grant/063-2018

Date: 14.03.2018

**Sub: R/P entitled "Early detection of idiopathic scoliosis through school based screening"**  
**Principal Investigator: Ms. Mudasir Rashid Baba, Assistant Professor, Yenepoya Physiotherapy College**

On the recommendation of the Yenepoya University Research Committee Meeting held on 22.02.2018, an amount of Rs. 1,00,000/- has been approved for the above cited project for the period of one year.

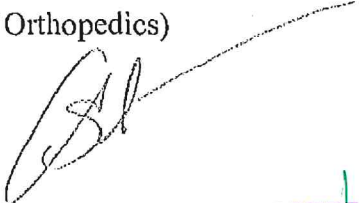
Sl. no	Item	1 <sup>st</sup> Year (Rs.)
1.	<b>Recurring:</b> <ul style="list-style-type: none"><li>• Scoliometer</li><li>• X-ray imaging</li><li>• Scolioscreen</li><li>• Local travel</li></ul>	14,000 75,000 1,000 10,000
<b>Grand Total</b>		<b>1,00,000/-</b>
<b>One lakhs only</b>		


**Terms and conditions:**

1. No funds will be provided directly to the Principal Investigator, all the requests for the utilization of the sanctioned funds should be through proper channel.
2. Annual progress reports should be submitted to the Registrar through proper channel.
3. On the completion of the project, a detailed report should be prepared and submitted to the Registrar within one month from the date of completion of the project.
4. University has all the rights to terminate the project if the progress is not satisfactory.
5. This funding is given as startup grant for the PI and should use this grant to generate the preliminary findings useful for submitting projects for funding from the external agencies.

**Cc to:**

1. Co-Investigator (Dr. R.M. Shenoy, Professor, Dept. of Orthopedics)
2. Finance Officer
3. Purchase and Stores
4. Deputy Director, YRC

  
**ATTESTED**  
**Dr. Shree Kumar Menon**  
Registrar  
Yenepoya University  
University Road, Deralakatte  
Mangalore- 575 018, Karnataka

  
**Dr. Sangadhara Somayaji K.S.**  
Registrar  
Yenepoya University  
University Road, Deralakatte  
Mangalore- 575 018, Karnataka



YENEPOYA  
UNIVERSITY

Recognized under Sec 3(A) of UGC Act 1956  
Accredited by NAAC with 'A' Grade

**SANCTION ORDER FOR THE SEED GRANT**

YU/Seed grant/059-2017

Date: 18.03.2017

**Sub: R/P entitled "Skeletal muscle fluorosis: effects on skeletal muscle cells and its associated mechanisms an in vitro study"**

**Principle Investigator: Dr. Sudheer Shenoy, Assistant Professor, Yenepoya Research Centre**

On the recommendation of the Yenepoya University Research Committee Meeting held on 09.03.2017, an amount of **Rs. 1,00,000/-** has been approved for the towards the purchase of antibodies and consumables needed for the initial phase of the study. Subsequent sanction will be made based on the outcome of the project.

Sl. No	Item	1 <sup>st</sup> Year (Rs.)
1	Consumables	1,00,000
<b>Grand Total</b>		<b>1,00,000</b>

**Terms and conditions:**

1. No funds will be provided directly to the Principal Investigator. all the requests for the utilization of the sanctioned funds should be through proper channel.
2. Progress reports on the completion of **every six months** should be submitted to the Registrar through proper channel.
3. On the completion of the project, a detailed report should be prepared and submitted to the Registrar within one month from the date of completion of the project.
4. University has all the rights to terminate the project if the progress is not satisfactory.
5. This funding is given as startup grant for the PI and should use this grant to generate the preliminary findings useful for submitting projects for funding from the external agencies.

**Cc to:**

1. Co-Investigator
2. Finance Officer
3. Purchase and Stores
4. Deputy Director, YRC

**Dr. Shree Kumar Menon**  
Registrar

**ATTESTED**

**Dr. Gangadhara Somayaji K.S.**  
Registrar  
Yenepoya (Deemed to be University)  
University Road, Deralakatte  
Mangalore- 575 018, Karnataka





Office of the Registrar  
University Road,  
Deralakatte  
Mangalore - 575018  
Ph: 0824-2204667/68/69/71  
Fax: 0824-2203943

No.YU/YRC/Seed Grant/2017

09.12.2017

Dr. Sudheer Shenoy P  
A/P & Principal Investigator  
Stem Cell and Regenerative Medicine Centre  
Yenepoya Research Centre  
Yenepoya University

---

Sub: Sanction of additional funds of Rs.60,000/- for seed grant project.

Ref: Your letter dated 22.11.2017

\*\*\*\*\*

Sanction is herewith accorded for the additional funds of Rs.60,000/- for the seed grant project titled "Skeletal muscle fluorosis: effect on skeletal muscle cells and its associated mechanisms an in vitro study".

  
(Dr. G. Shreekumar Menon)  
REGISTRAR

Cc to:

1. Dy. Director, YRC
2. Finance Officer
3. Academic Section

  
Registrar  
Yenepoya University

ATTESTED  


Dr.Gangadhara Somayaji K.S.  
Registrar  
Yenepoya(Deemed to be University)  
University Road, Deralakatte  
Mangalore- 575 018, Karnataka



Recognized under Sec 3(A) of UGC Act 1956  
Accredited by NAAC with 'A' Grade

**SANCTION ORDER FOR THE SEED GRANT**

YU/Seed grant/057-2017

Date: 18.03.2017

**Sub: R/P entitled "Determining the cause of death amongst persons treated for multidrug resistant tuberculosis, Karnataka, India 2016"**

**Principle Investigator: Dr. Poonam R Naik, Professor, Dept. of Community Medicine, Yenepoya Medical College**

On the recommendation of the Yenepoya University Research Committee Meeting held on 09.03.2017, an amount of Rs. 2,16,200/- has been approved for the above cited project for the period of one year.

Sl. no	Item	1 <sup>st</sup> Year (Rs.)
1	<b>Recurring:</b> 1. Manpower (one month for data collection) 2. Travel and daily allowance 3. Contingencies	25,000 1,77,000 10,000
2	<b>Non – Recurring:</b> (study tools, stationary)	4,200
<b>Grand Total (A+B)</b>		<b>2,16,200</b>

**Terms and conditions:**

1. No funds will be provided directly to the Principal Investigator, all the requests for the utilization of the sanctioned funds should be through proper channel.
2. Progress reports on the completion of every six months should be submitted to the Registrar through proper channel.
3. On the completion of the project, a detailed report should be prepared and submitted to the Registrar within one month from the date of completion of the project.
4. University has all the rights to terminate the project if the progress is not satisfactory.
5. This funding is given as startup grant for the PI and should use this grant to generate the preliminary findings useful for submitting projects for funding from the external agencies.

**Cc to:**

1. Co-Investigator
2. Finance Officer
3. Purchase and Stores
4. Deputy Director, YRC

**Dr. Shreckumar Menon**

Registrar

**ATTESTED**

Dr.Gangadhara Somayaji K.S.  
Registrar  
Yenepoya(Deemed to be University)  
University Road, Deralakatte  
Mangalore- 575 018, Karnataka



Recognized under Sec 3(A) of UGC Act 1956  
Accredited by NAAC with 'A' Grade

**SANCTION ORDER FOR THE SEED GRANT**

YU/Seed grant/060-2017

Date: 18.03.2017

**Sub: R/P entitled** "Designing and development of lab-on-paper device for sensing trace arsenic in ground water"

**Principle Investigator:** Dr. K. Sudhakaraprasad, Assistant Professor, Yenepoya Research Centre

On the recommendation of the Yenepoya University Research Committee Meeting held on 09.03.2017, an amount of Rs. 2,50,000/- sanctioned towards the consumables needed for the project. Subsequent sanction will be made only after evaluating the progress of the project.

Sl. No	Item	1 <sup>st</sup> Year (Rs.)
I	Consumables	2,50,000
<b>Grand Total</b>		<b>2,50,000</b>

**Terms and conditions:**

1. No funds will be provided directly to the Principal Investigator, all the requests for the utilization of the sanctioned funds should be through proper channel.
2. Progress reports on the completion of every six months should be submitted to the Registrar through proper channel.
3. On the completion of the project, a detailed report should be prepared and submitted to the Registrar within one month from the date of completion of the project.
4. University has all the rights to terminate the project if the progress is not satisfactory.
5. This funding is given as startup grant for the PI and should use this grant to generate the preliminary findings useful for submitting projects for funding from the external agencies.

**Cc to:**

1. Co-Investigator
2. Finance Officer
3. Purchase and Stores
4. Deputy Director, YRC

**Dr. Shree Kumar Menon**

Registrar  
**ATTESTED**

Dr. Gangadhara Somayaji K.S.  
Registrar  
Yenepoya (Deemed to be University)  
University Road, Derlakatte  
Mangalore- 575 018, Karnataka

YU/YRC/Seed grant/060-2017

16.08.2018

To,

Dr. Sudhakara Prasad  
Assistant Professor  
Yenepoya Research Centre  
Yenepoya (Deemed to be University)

Sub: Seed grant project No. YU/YRC/Seed grant/060-2017

Ref: i) Your report on work plan and activities to be carried out in the 3<sup>rd</sup> year  
dtd: 01.08.2018


ii) Recommendation by Dr. B.S. Rao

With reference to your letter dated: 01.08.2018, for extension of the seed grant project titled: "Designing and development of lab-on-paper device for sensing trace arsenic in ground water", based on the progress you are granted extension of tenure by one year with a grant of Rs. 2,00,000/- in order to complete the pending work of the project. You should submit the final report after the completion of the project along with the statement of accounts.



Dr. G. Shreekumar Menon  
Registrar

ATTESTED

  
Dr. Gangadhara Somayaji K.S.  
Registrar  
Yenepoya (Deemed to be University)  
University Road, Deralakatte  
Mangalore- 575 018, Karnataka

YU/Seed grant/060-2017

26.06.2020

To,

Dr. Sudhakara Prasad  
Senior Scientific Officer (Assistant Professor, AP (ii))  
Yenepoya Research Centre  
Yenepoya (Deemed to be University)

Sub: Seed grant project No. YU/ Seed grant/060-2017, "Designing and development of lab-on-paper device for sensing trace arsenic in ground water"

Ref: i) YU/ Seed grant/060-2017

ii) Your report on work plan and activities to be carried out in the 2<sup>nd</sup> year  
dtd: 21.02.2020

With reference to the above, based on the recommendation on the progress, third year grant of Rs. 1,00,000/- is sanctioned in order to complete the pending work of the project. You should submit the final report after the completion of the project along with the statement of accounts and copies of publications and patents made from the project as of 31<sup>st</sup> March 2021.

  
Registrar

ATTESTED

Dr. Gangadhara Somayaji K.S.  
Registrar  
Yenepoya (Deemed to be University)  
University Road, Deralakatte  
Mangalore- 575 018, Karnataka



YENEPOYA  
UNIVERSITY

Recognized under Sec 3(A) of UGC Act 1956  
Accredited by NAAC with 'A' Grade

**SANCTION ORDER FOR THE SEED GRANT**

YU/Seed grant/061-2017

Date: 18.03.2017

**Sub: R/P entitled** "Development of bioreducible block copolymer drug conjugate nanoassemblies functionalized with noble metal nanoparticles for targeted, image guided delivery of chemotherapeutic drugs and biosensing applications"

**Principle Investigator:** Dr. Renjith P. Johnson, Assistant Professor, Yenepoya Research Centre

On the recommendation of the Yenepoya University Research Committee Meeting held on 09.03.2017, an amount of Rs. 2,50,000/- sanctioned towards the consumables needed for the project. Subsequent sanction will be made only after evaluating the progress of the project.

Sl. No	Item	1 <sup>st</sup> Year (Rs.)
1	Consumables	2,50,000
<b>Grand Total</b>		<b>2,50,000</b>

**Terms and conditions:**

1. No funds will be provided directly to the Principal Investigator, all the requests for the utilization of the sanctioned funds should be through proper channel.
2. Progress reports on the completion of every six months should be submitted to the Registrar through proper channel.
3. On the completion of the project, a detailed report should be prepared and submitted to the Registrar within one month from the date of completion of the project.
4. University has all the rights to terminate the project if the progress is not satisfactory.
5. This funding is given as startup grant for the PI and should use this grant to generate the preliminary findings useful for submitting projects for funding from the external agencies.

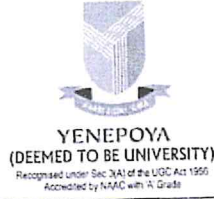
**Cc to:**

1. Co-Investigator
2. Finance Officer
3. Purchase and Stores
4. Deputy Director, YRC

**Dr. Shreeekumar Menon**  
Registrar

ATTESTED

Dr.Gangadhara Somayaji K.S.  
Registrar  
Yenepoya(Deemed to be University)  
University Road, Deralakatte  
Mangalore- 575 018, Karnataka



20.06.2018

YU/YRC/Seed grant/061-2017

To,

Dr. Renjith P. Johnson  
Assistant Professor  
Yenepoya Research Centre  
Yenepoya (Deemed to be University)

Sub: Seed grant project No. YU/YRC/Seed grant/061-2017

Ref: Your report on work plan and activities to be carried out in the 2<sup>nd</sup> year dtd:  
02.04.2018

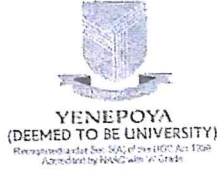
With reference to your letter dated: 02.04.2018, for extension of the seed grant project titled: "Development of bio-reducible block copolymer drug conjugate nanoassemblies functionalized with noble metal nanoparticles for targeted, image guided delivery of chemotherapeutic drugs and biosensing applications", based on the progress made so far you are granted an extension of tenure by one year with a grant of Rs. 2,00,000/- in order to complete the pending work of the project. You should submit the final report after the completion of the project along with the statement of accounts.

Dr. G. Shree Kumar Menon  
Registrar

Registrar  
Yenepoya (Deemed to be University)  
University Road, Deralakatte  
Mangalore 575 018

ATTESTED

Dr. Gangadhara Somayaji K.S.  
Registrar  
Yenepoya (Deemed to be University)  
University Road, Deralakatte  
Mangalore- 575 018, Karnataka



YU/Seed grant/061-2017

24.06.2020

To,

Dr. Renjith P Johnson  
Assistant Professor  
Yenepoya Research Centre  
Yenepoya (Deemed to be University)

**Sub: Seed grant project No. YU/Seed grant/061-2017, Title: "Development of bioreducible block copolymer drug conjugate nanoassemblies functionalized with noble metal nanoparticles for targeted, image guided delivery of chemotherapeutic drugs and biosensing applications"**

**Ref:** i) YU/Seed grant/061-2017  
ii) Your report on work plan and activities to be carried out in the 2<sup>nd</sup> year dtd: 08.02.2020

With reference to the above, based on the recommendation on the progress, third year grant of Rs. 50,000/- is sanctioned in order to complete the pending work of the project. You should submit the final report after the completion of the project along with the statement of accounts and copies of publications made from the project on or before 31<sup>st</sup> December 2020.

Registrar

ATTESTED

Dr. Gangadhara Somayaji K.S.  
Registrar  
Yenepoya (Deemed to be University)  
University Road, Deralakatti  
Mangalore- 575 018, Karnataka





YENEPOYA  
UNIVERSITY

Recognized under Sec 3 (A) of UGC Act 1956  
Accredited by NAAC with 'A' Grade

### SANCTION ORDER FOR THE SEED GRANT

No: YU/Seedgrant/035-2014

Date: 12.04.2017

R/P titled: A comparative study of level of HbA1c in normal and diabetic patients of rural population of South India-A pilot study.

**Principal Investigator:** Dr. R.N. Sujeer, Director, Dept of Rural Health care and Development, Yenepoya Medical College Hospital.

**Co-PI:** Dr. Mukhtar Ahmed B. Professor, Dept. of Internal Medicine, Yenepoya Medical College Hospital.

An amount of Rs. 70,000 has been approved towards consumables for the above cited project for the year 2017-18 with the terms and conditions listed herein.

**Terms and conditions:**

1. This funding is given as startup grant and based on the preliminary findings from the study the investigators should submit a detailed proposal for funding from the external agencies.
2. No funds will be provided directly to the Principal Investigator, all the requests for the utilization of the sanctioned funds should be through proper channel.
3. Progress reports on the completion of every six months shall be submitted to the Registrar through proper channel.
4. On the completion of the project, a detailed report should be prepared and submitted to the Registrar within one month from the date of completion of the project.
5. University has all the rights to terminate the project if the progress is not satisfactory.

**Cc to:**

1. Co-Investigator
2. Principal, Yenepoya Medical College
3. Finance Officer
4. Purchase and Stores
5. Director R&F
6. Academic Section
7. Deputy Director, YRC

Registrar

ATTESTED

Dr. Gangadhara Somayaji K.S.  
Registrar  
Yenepoya (Deemed to be University)  
University Road, Deralakatte  
Mangalore- 575 018, Karnataka



YENEPOYA  
UNIVERSITY

Recognized under Sec 3 (A) of UGC Act 1956  
Accredited by NAAC with 'A' Grade

### SANCTION ORDER FOR THE SEED GRANT

No: YU/Seedgrant/2012-019

Date: 23.04.2017

R/P titled: "A study of urinary stones in Dakshina Kannada and North Kerala: An analysis of risk factors, metabolic evaluation, prevention".

**Principal Investigator:** Dr. Mujeeburahiman, Professor Dept. of Urology, Yenepoya Medical College.

With reference to the above, based on the recommendation on the progress, a grant of Rs. 70,000/- is sanctioned in order to complete the proposed objectives of the project.

You should submit the progress report along with statement of accounts and copies of publications, presentations and patents if any made from the project.

#### ***Terms and Conditions***


1. No funds will be provided directly to the Principal Investigator, all the requests for the utilization of the sanctioned funds should be through proper channel.
2. Progress reports should be submitted to the Registrar through proper channel.
3. For the release of second year grant, a detailed expenditure certificate should be submitted to the Registrar, Yenepoya University duly verified by the Finance Officer.
4. On the completion of the project, a detailed report should be prepared and submitted to the Registrar within one month from the date of completion of the project.
5. University has all the rights to terminate the project if the progress is not satisfactory.
6. This funding is given as startup grant and based on the preliminary findings from the study the investigators should submit a detailed proposal for funding from the external agencies.

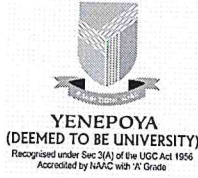
#### **Cc to:**

1. Co-Investigator
2. Dean, Yenepoya Medical College
3. Finance Officer
4. Purchase and Stores
5. Deputy Director, YRC

  
Registrar

**ATTESTED**

  
Dr.Gangadhara Somayaji K.S.  
Registrar  
Yenepoya(Deemed to be University)  
University Road, Oeralakatte  
Mangalore- 575 018, Karnataka



## SANCTION ORDER FOR THE SEED GRANT

No: YU/Seedgrant/2012-019

Date: 18.04.2018

R/P titled: "A study of urinary stones in Dakshina Kannada and North Kerala: An analysis of risk factors, metabolic evaluation, prevention"

**Principal Investigator:** Dr. Mujeeburahiman, Professor Dept. of Urology, Yenepoya Medical College.

With reference to the above, based on the recommendation on the progress, a grant of Rs. 20,000/- is sanctioned in order to complete the proposed objectives of the project.

You should submit the progress report along with statement of accounts and copies of publications, presentations and patents if any made from the project.

### ***Terms and Conditions***

1. No funds will be provided directly to the Principal Investigator, all the requests for the utilization of the sanctioned funds should be through proper channel.
2. Progress reports should be submitted to the Registrar through proper channel.
3. For the release of second year grant, a detailed expenditure certificate should be submitted to the Registrar, Yenepoya University duly verified by the Finance Officer.
4. On the completion of the project, a detailed report should be prepared and submitted to the Registrar within one month from the date of completion of the project.
5. University has all the rights to terminate the project if the progress is not satisfactory.
6. This funding is given as startup grant and based on the preliminary findings from the study the investigators should submit a detailed proposal for funding from the external agencies.

### **Cc to:**

1. Co-Investigator
2. Dean, Yenepoya Medical College
3. Finance Officer
4. Purchase and Stores
5. Deputy Director, YRC

  
Registrar

**ATTESTED**  


Dr. Gangadhara Somayaji K.S.  
Registrar  
Yenepoya (Deemed to be University)  
University Road, Derlakatte  
Mangalore- 575 018, Karnataka



Recognized under Sec 3(A) of UGC Act 1956  
Accredited by NAAC with 'A' Grade

**SANCTION ORDER FOR THE SEED GRANT**

YU/Seed grant/055-2016

Date: 05.08.2016

**Sub: R/P entitled "Molecular mechanism of p53 mutations in cancer stem cells isolated from triple negative breast cancer cell lines"**

**Principle Investigator: Dr. Suparna Laha, Assistant Professor, Yenepoya Research Centre**

On the recommendation of the Yenepoya Research Committee Meeting held on 14.07.2016. An amount of Rs. 2,00,000/- has been approved for the above cited project for completing the initial phase of the work. Subsequent sanction will be made only after evaluating the progress of the project.

Item	1 <sup>st</sup> Year (Amount Rs.)
<b>Recurring:</b>	
1. Consumables	2,00,000
2. Micropipettes	
<b>Grant Total</b>	<b>2,00,000</b>

**Terms and conditions:**

1. No funds will be provided directly to the Principal Investigator, all the requests for the utilization of the sanctioned funds should be through proper channel.
2. Progress reports on the completion of every six months should be submitted to the Registrar through proper channel.
3. On the completion of the project, a detailed report should be prepared and submitted to the Registrar within one month from the date of completion of the project.
4. University has all the rights to terminate the project if the progress is not satisfactory.
5. This funding is given as startup grant for the PI and should use this grant to generate the preliminary findings useful for submitting projects for funding from the external agencies.

**Cc to:**

1. Co-Investigator
2. Finance Officer
3. Purchase and Stores
4. Deputy Director, YRC

**Dr. Shree Kumar Menon**  
**Registrar**

Dr. Gangadhara Somayaji K.S.  
Registrar  
Yenepoya (Deemed to be University)  
University Road, Deralakatte  
Mangalore- 575 018, Karnataka



Recognised under Sec 3(A) of UGC Act 1956  
Accredited by NAAC with 'A' Grade

22.09.2017

YU/YRC/Seed grant/055-2016

To

Dr. Suparna Laha  
Assistant Professor  
Yenepoya Research Centre  
Yenepoya University

Sub: Seed grant project No. YU/YRC/Seed grant/055-2016

Ref: i) First year progress report dtd: 26.08.2017

ii) Justification for the budget

With reference to your letter dated: 26.08.2017, for extension of the seed grant project titled: "Molecular mechanism of p53 mutations in cancer stem cells isolated from triple negative breast cancer cell lines", based on the progress you are granted extension of tenure by one year with a grant of Rs. 2,00,000/- in order to complete the pending work of the project. You should submit the final report after the completion of the project along with the statement of accounts.

A handwritten signature in black ink, appearing to be 'G. Menon', written over a horizontal line.

Dr. G. Shreekumar Menon  
Registrar  
Yenepoya University

ATTESTED

Dr. Gangadhara Somayaji K.S.  
Registrar  
Yenepoya (Deemed to be University)  
University Road, Deralakatte  
Mangalore- 575 018, Karnataka

YU/Seed grant/055-2016

04.04.2019

Dr. Suparna Laha  
Assistant Professor  
Yenepoya Research Centre  
Yenepoya (Deemed to be University)

Sub: Seed grant project No. YU/Seed grant/055-2016, Title: "Molecular mechanism of p53 mutations in cancer stem cells isolated from triple negative breast cancer cell lines"

Ref: i) Your report on work plan and activities to be carried out in the 2<sup>nd</sup> year dtd: 03.04.2019

ii) Recommendation by Dr. B.S. Rao.

\*\*\*\*\*

With reference to the above, based on the recommendation on the progress, third year grant of Rs. 2,00,000/- is sanctioned in order to complete the pending work of the project. You should submit the final report after the completion of the project along with the statement of accounts and copies of publications made from the project.



REGISTRAR

5/4

ATTESTED

Dr. Gangadhara Somayaji K.S.  
Registrar  
Yenepoya (Deemed to be University)  
University Road, Deralakatti  
Mangalore- 575 016, Karnataka



Recognized under Sec 3(A) of UGC Act 1956  
Accredited by NAAC with 'A' Grade

### SANCTION ORDER FOR THE SEED GRANT

YU/Seed grant/054-2016

Date: 05.08.2016

**Sub: R/P entitled** "Integrated metagenomic analysis of urine and their association with urolithiasis".

**Principle Investigator:** Dr. Rekha P.D., Professor and Deputy Director, Yenepoya Research Centre

On the recommendation of the Yenepoya Research Committee Meeting held on 14.07.2016, An amount of **Rs. 3,75,000/-** has been approved for the above cited project for one year from the date of sanction of this letter.


Items	1 <sup>st</sup> year (Rs.)
Next Generation sequencing	3,60,000
Travel	5,000
Contingency	10,000
<b>Total</b>	<b>3,75,000/-</b>

#### Terms and conditions:

1. No funds will be provided directly to the Principal Investigator, all the requests for the utilization of the sanctioned funds should be through proper channel.
2. Progress reports on the completion of **every six months** should be submitted to the Registrar through proper channel.
3. On the completion of the project, a detailed report should be prepared and submitted to the Registrar within one month from the date of completion of the project.
4. University has all the rights to terminate the project if the progress is not satisfactory.
5. This funding is given as startup grant for the PI and should use this grant to generate the preliminary findings useful for submitting projects for funding from the external agencies.

#### Cc to:

1. Finance Officer
2. Purchase and Stores
3. Deputy Director, YRC

  
**Dr. Shreekumar Menon**  
Registrar

Registrar  
Yenepoya University  
**ATTESTED**

Dr. Gangadhara Somayaji K.S.  
Registrar  
Yenepoya (Deemed to be University)  
University Road, Derbhatkatta  
Mangalore- 575 018



Recognised under Sec 3(A) of UGC Act 1956  
Accredited by NAAC with 'A' Grade

YU/YRC/Seed grant/054-2016

18.09.2017

To

Dr. Rekha P.D  
Professor & Deputy Director  
Yenepoya Research Centre  
Yenepoya University

Sub: Seed grant project No. YU/YRC/Seed grant/054-2016

Ref: Your report on work plan and activities to be carried out in the 2<sup>nd</sup> year  
dtd: 07.08.2017

With reference to your letter dated: 07.08.2017, for extension of the seed grant project titled: "Integrated metagenomic analysis of urine microbiome and their association with urolithiasis", based on the progress you are granted extension of tenure by one year with a grant of Rs. 1,30,000/- in order to complete the pending work of the project. You should submit the final report after the completion of the project along with the statement of accounts.

Dr. G. Shreekumar Menon  
Registrar  
Yenepoya University

ATTESTED

Dr. Gangadhara Somayaji K.S.  
Registrar  
Yenepoya (Deemed to be University)  
University Road, Deralakatte  
Mangalore- 575 018, Karnataka



16.08.2018

YU/YRC/Seed grant/054-2016

To,

Dr. Rekha P.D.  
Professor & Deputy Director,  
Yenepoya Research Centre  
Yenepoya (Deemed to be University)

**Sub:** Seed grant project No. YU/YRC/Seed grant/054-2016

**Ref:** i) Your report on work plan and activities to be carried out in the 3<sup>rd</sup> year  
dtd: 09.08.2018


ii) Recommendation by Dr. B.S. Rao

With reference to your letter dated: 09.08.2018, for extension of the seed grant project titled: "Integrated metagenomic analysis of urine microbiome and their association with urolithiasis", based on the progress you are granted extension of tenure by one year with a grant of Rs. 1,00,000/- in order to complete the pending work of the project. You should submit the final report after the completion of the project along with the statement of accounts.



Dr. G. Shreekumar Menon  
Registrar

**ATTESTED**

  
Dr. Gangadhara Somayaji K.S.  
Registrar  
Yenepoya (Deemed to be University)  
University Road, Dornakal  
Mangalore- 575 018, Karnataka



Recognized under Sec 3(A) of UGC Act 1956  
Accredited by NAAC with 'A' Grade

### SANCTION ORDER FOR THE SEED GRANT

YU/Seed grant/052-2016

Date: 05.08.2016

**Sub: R/P entitled** "A prospective study of detection of fluoroquinolone drug resistance in clinical isolates in clinical isolates of *Klebsiella species* from patients attending tertiary care hospital".

**Principle Investigator:** Dr. Sateesh K. Malkappa, Associate Professor, Dept. of Microbiology, Yenepoya Medical College

On the recommendation of the Yenepoya Research Committee Meeting held on 14.07.2016, an amount of Rs. 2,70,000/- has been approved for the above cited project for two years from the date of sanction of this letter. Second year grant will be released only after the successful completion of the first year objectives.

Sl. no	Item	1 <sup>st</sup> Year (Amount Rs)	2 <sup>nd</sup> Year (Amount Rs)
1	<b>Recurring:</b> 1. PCR kit, Primers and Probes for Multiplex PCR 2. Antibiotics	90,000	1,70,000
2	<b>Non – Recurring:</b> Equipment: micropipette (10-100 µl), accessories, micropipette tips, glassware.	10,000	
3	Year wise total amount (Rs.)	1,00,000	1,70,000
<b>Grant Total (A+B)</b>		<b>2,70,000</b>	

**Terms and conditions:**

1. No funds will be provided directly to the Principal Investigator, all the requests for the utilization of the sanctioned funds should be through proper channel.
2. Progress reports on the completion of every six months should be submitted to the Registrar through proper channel.
3. On the completion of the project, a detailed report should be prepared and submitted to the Registrar within one month from the date of completion of the project.
4. University has all the rights to terminate the project if the progress is not satisfactory.
5. This funding is given as startup grant for the PI and should use this grant to generate the preliminary findings useful for submitting projects for funding from the external agencies.

**Cc to:**

1. Dean, Yenepoya Medical College
2. Finance Officer
3. Purchase and Stores
4. Deputy Director, YRC

**Dr. Shree Kumar Menon**  
Registrar

ATTESTED

Dr. Gangadhara Somayaji K.S.  
Registrar  
Yenepoya (Deemed to be University)  
University Road, Deralakatte  
Mangalore- 575 018, Karnataka



Recognized under Sec 3(A) of UGC Act 1956  
Accredited by NAAC with 'A' Grade

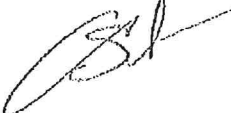
05.08.2016

To


Dr. Bipasha Bose  
Assistant Professor  
Yenepoya Research Centre

**Sub: Seed Grant Project No./YU/Seed Grant/2015-041**

On the recommendation of the Yenepoya Research Committee Meeting held on 14.07.2016, with reference to your ongoing seed grant project titled: "Evaluation for the presence of CD34<sup>+</sup>/45<sup>-</sup> adult stem cells from all three germ-layers, ectoderm, mesoderm and endoderm and use of such CD34<sup>+</sup>/45<sup>-</sup> cells in ameliorating muscular dystrophy in mouse model system", an amount of **Rs. 2,00,000/-** has been approved to complete the proposed objectives.

  
**Dr. Shreekumar Menon**  
Registrar

**ATTESTED**

  
Dr. Gangadhara Somayaji K.S.  
Registrar  
Yenepoya (Deemed to be University)  
University Road, Derlakatte  
Mangalore- 575 018, Karnataka

**Cc to:**

1. Finance Officer
2. Purchase and stores
3. Director R& F
4. Academic Section
5. Dy. Director. YRC

16.08.2018

YU/YRC/Seed grant/041-2015

To,

Dr. Bipasha Bose  
Associate Professor  
Yenepoya Research Centre  
Yenepoya (Deemed to be University)

Sub: Seed grant project No. YU/YRC/Seed grant/041-2015

Ref: i) Your report on work plan and activities to be carried out in the 3<sup>rd</sup> year  
dtd: 31.07.2018

ii) Recommendation by Dr. B.S. Rao

With reference to your letter dated: 31.07.2018, for extension of the seed grant project titled: "Evaluation for the presence of CD34<sup>+</sup>/45<sup>-</sup> adult stem cells from all three germ-layers, ectoderm, mesoderm and endoderm and use of such CD34<sup>+</sup>/45<sup>-</sup> in ameliorating muscular dystrophy in mouse model system", based on the progress you are granted extension of tenure by one year with a grant of Rs. 2,00,000/- in order to complete the pending work of the project. You should submit the final report after the completion of the project along with the statement of accounts.



Dr. G. Shreekumar Menon  
Registrar

**ATTESTED**  


Dr. Gangadhara Somayaji K.S.  
Registrar  
Yenepoya (Deemed to be University)  
University Road, Deralakatte  
Mangalore- 575 018, Karnataka



YENEPOYA  
(DEEMED TO BE UNIVERSITY)  
Recognised under Sec.3(A) of the UGC Act 1956  
Accredited by NAAC with 'A' Grade

23.09.2019

YU/Seed grant/041-2015

To,

Dr. Bipasha Bose  
Associate Professor  
Yenepoya Research Centre  
Yenepoya (Deemed to be University)

Sub: Seed grant project No. YU/Seed grant/041-2015, Title: "Evaluation for the presence of CD34<sup>+</sup>/45<sup>-</sup> adult stem cells from all three germ-layers, ectoderm mesoderm and endoderm and use of such CD34<sup>+</sup>/45<sup>-</sup> in ameliorating muscular dystrophy in mouse model system"

Ref:

- i) Seed grant number: YU/Seed grant/041-2015
- ii) Your report on work plan and activities to be carried out in the 3<sup>rd</sup> year dtd: 22.08.2019
- iii) Recommendation by Dr. B.S. Rao

\*\*\*\*\*

With reference to the above, based on the recommendation on the progress, Fourth year grant of Rs. 75,000/- is sanctioned in order to complete the pending work of the project. You should submit the final report after the completion of the project along with the statement of accounts and copies of publications made from the project. No further extension will be given for this project.

  
REGISTRAR

24/9  
ATTESTED  


Dr.Gangadhara Somayaji K.S.  
Registrar  
Yenepoya(Deemed to be University)  
University Road, Derlakatti,  
Mangalore- 575 013, Karnataka



Recognized under Sec 3(A) of UGC Act 1956  
Accredited by NAAC with 'A' Grade

**SANCTION ORDER FOR THE SEED GRANT**

YU/Seed grant/053-2016

Date: 05.08.2016

**Sub: R/P entitled** "A study on typing and detection of oncoproteins of human papilloma virus among sexually active women attending tertiary care hospital".

**Principle Investigator:** Dr. Vidya Pai, Professor and Head, Dept. of Microbiology, Yenepoya Medical College

On the recommendation of the Yenepoya Research Committee Meeting held on 14.07.2016. An amount of Rs. 2,50,000/- has been approved for the above cited project for two years from the date of sanction of this letter. Second year grant will be released only after the successful completion of the first year objectives.

Item	1 <sup>st</sup> Year (Amount Rs.)	2 <sup>nd</sup> Year (Amount Rs.)
<b>Recurring:</b> PCR reagents, Primers and Probes for Multiplex PCR	80,000	1,50,000
<b>Non - Recurring:</b> Micropipette (10-100 µl)	10,000	10,000
Year wise total amount (Rs.)	90,000	1,60,000
<b>Grant Total (A+B)</b>	<b>2,50,000</b>	

**Terms and conditions:**

1. No funds will be provided directly to the Principal Investigator, all the requests for the utilization of the sanctioned funds should be through proper channel.
2. Progress reports on the completion of every six months should be submitted to the Registrar through proper channel failing which further sanctions will not be made.
3. On the completion of the project, a detailed report should be prepared and submitted to the Registrar within one month from the date of completion of the project.
4. University has all the rights to terminate the project if the progress is not satisfactory.
5. This funding is given as startup grant for the PI and should use this grant to generate the preliminary findings useful for submitting projects for funding from the external agencies.

**Cc to:**

1. Dean, Yenepoya Medical College
2. Finance Officer
3. Purchase and Stores
4. Deputy Director, YRC

**Dr. Shreekumar Meun**  
Registrar

Dr. Gangadhara Somayaji K.S.  
Registrar  
Yenepoya (Deemed to be University)  
University Road, Deralakatte,  
Mangalore-575 018, Karnataka



Recognized under Sec 3(A) of UGC Act 1956  
Accredited by NAAC with 'A' Grade

22.09.2016

To

Dr. Riaz Abdulla  
Professor  
Dept. of Oral Pathology  
Yenepoya Dental College

Sub: Request for extension of the seed grant project  
Ref: i. No./YU/Seed Grant/2013-027  
ii. No. 1933 letter dated 21.09.2016

With reference to your request letter dated 21.09.2016, for extension of the seed grant project titled: "Genetic investigation of non syndromic cleft lip and palate (NSCLP) in the Indian population", and you are granted extension of the tenure by six months and utilization of the second year grant (Rs. 85,000/-) in order to complete the pending work of the project. You should submit the final report after the completion of the project along with the statement of accounts.

Dr. G. Shreekumar Menon  
Registrar  
Yenepoya University

ATTESTED

A handwritten signature in green ink, appearing to be "G", is written over the word "ATTESTED".

Dr.Gangadhara Somayaji K.S.  
Registrar  
Yenepoya(Deemed to be University)  
University Road, Derlakatte  
Mangalore- 575 018, Karnataka

Cc to:

1. Finance Officer
2. Purchase and stores
3. Director R& F
4. Academic Section
5. Dy. Director, YRC



Recognized under Sec 3(A) of UGC Act 1956  
Accredited by NAAC with 'A' Grade

**SANCTION ORDER FOR THE SEED GRANT**

No./YU/Seed Grant/050-2015

Date: 23.03.2016

**Sub: R/P entitled "Role of inflammatory cytokines and p53 –fibronolytic systems in smokers with or without COPD" under Seed Grant for Research for the Faculty of Yenepoya University.**

**Principle Investigator:** Dr. Yashodhar Bhandary, Assistant Professor, Yenepoya Research Centre

**Co Investigator:** Dr. Deepu Chengappa, Assistant Professor, Dept. of Respiratory Medicine, YMC

**Dr. Ashwini Shetty, Assistant Professor, Dept. of Anatomy, YMC**

On the recommendation of the Research Committee Meeting held on 16.03.2016, I am pleased to convey the administrative approval and sanction of the captioned project for three years from the date of this order with a grant of **Rs. 2, 00,000 /-** for the first phase of the project.


1. No funds will be provided directly to the Principal Investigator, all the requests for the utilization of the sanctioned funds should be through proper channel.
2. Progress reports on the completion of every six months shall be submitted to the Registrar through proper channel.
3. For the release of second year grant, a detailed expenditure certificate should be submitted to the Registrar, Yenepoya University duly verified by the Finance Officer, Yenepoya University.
4. On the completion of the project, a detailed report should be prepared and submitted to the Registrar within one month from the date of completion of the project.
5. University has all the rights to terminate the project if the progress is not satisfactory.
6. This funding is given as startup grant for the PI and based on the preliminary findings from the study the investigators should submit a detailed proposal for funding from the external agencies.

Cc to:

1. All Co-Investigators
2. Dean, Yenepoya Medical College
3. Finance Officer
4. Purchase and Stores
5. Deputy Director, YRC

  
Registrar

ATTESTED

  
Dr.Gangadhara Somayaji K.S.  
Registrar  
Yenepoya(Deemed to be University)  
University Road, Derlakatte  
Mangalore- 575 018, Karnataka





Recognized under Sec 3(A) of UGC Act 1956  
Accredited by NAAC with 'A' Grade

07.07.2017

To

Dr. Yashodhar P Bhandary  
Assistant Professor  
Yenepoya Research centre

**Sub: Seed grant project No.YU/Seed grant/050-2015**

**Ref: Your report on work plan and activities to be carried out in the 2<sup>nd</sup> year dtd:  
27.03.2017 and 18.04.2016**

With reference to your request letter dated 27.03.2017 and 18.04.2016, for extension of the seed grant project titled: "Role of inflammatory cytokines and p53 – fibronolytic systems in smokers with or without COPD", based on the progress you are granted extension of the tenure by one year with grant of Rs. 2,00,000/- in order to complete the pending work of the project. You should submit the final report after the completion of the project along with the statement of accounts.

Dr. G. Shreekumar Menon  
Registrar  
Yenepoya University

ATTESTED

Dr.Gangadhara Somayaji K.S.  
Registrar  
Yenepoya(Deemed to be University)  
University Road, Deralakatte  
Mangalore- 575 018, Karnataka



Recognized under Sec 3(A) of UGC Act 1956  
Accredited by NAAC with 'A' Grade

**SANCTION ORDER FOR THE SEED GRANT**

No./YU/Seed Grant/049-2015

Date: 23.03.2016

**Sub: R/P entitled** "Oxidative damage to limbal stem cells of eye in response to bright and ultraviolet light and its associated mechanisms" under Seed Grant for Research for the Faculty of Yenepoya University.

**Principle Investigator:** Dr. Cynthia Arunachalam., Professor and Head, Dept. of Ophthalmology, YMC

**Co Investigator:** Dr. Bipasha Bose, Assistant Professor, Yenepoya Research Centre

On the recommendation of the Research Committee Meeting held on 16.03.2016, I am pleased to convey the administrative approval and sanction of the captioned project for two years from the date of this order with a grant of **Rs. 2, 00,000/-** towards the first phase of the project.

1. No funds will be provided directly to the Principal Investigator, all the requests for the utilization of the sanctioned funds should be through proper channel.
2. Progress reports on the completion of every six months should be submitted to the Registrar through proper channel.
3. For the release of second year grant, a detailed expenditure certificate should be submitted to the Registrar, Yenepoya University duly verified by the Finance Officer, Yenepoya University.
4. On the completion of the project, a detailed report should be prepared and submitted to the Registrar within one month from the date of completion of the project.
5. University has all the rights to terminate the project if the progress is not satisfactory.
6. This funding is given as startup grant and based on the preliminary findings from the study the investigators should submit a detailed proposal for funding from the external agencies.

Cc to:

1. Co-Investigator
2. Dean, Yenepoya Medical College
3. Finance Officer
4. Purchase and Stores
5. Deputy Director, YRC

  
Registrar  
**ATTESTED**

Dr.Gangadhara Somayaji K.S.  
Registrar  
Yenepoya(Deemed to be University)  
University Road, Derai,  
Mangalore- 575 018, Karnataka

02.08.2018

YU/YRC/Seed grant/046-2015

To,

Dr. R.M. Shenoy  
Professor & HOD,  
Dept. of Orthopedics  
Yenepoya (Deemed to be University)

Sub: Seed grant project No. YU/YRC/Seed grant/046-2015


Ref: Your report on work plan and activities to be carried out in the 2<sup>nd</sup> year dtd:  
11.12.2017

With reference to your letter dated: 11.12.2017, for extension of the seed grant project titled: "Isolation, purification and characterization of mesenchymal stem cells from fracture hematoma", based on the progress you are granted extension of tenure by one year with a grant of Rs. 2,00,000/- in order to complete the pending work of the project. You should submit the final report after the completion of the project along with the statement of accounts.



Dr. G. Shreekumar Menon  
Registrar

ATTESTED

  
Dr. Gangadhara Somayaji K.S.  
Registrar  
Yenepoya (Deemed to be University)  
University Road, Deralakatte  
Mangalore- 575 018, Karnataka



Recognized under Sec 3 (A) of UGC Act 1956  
Accredited by NAAC with 'A' Grade

### SANCTION ORDER FOR THE SEED GRANT

No: YU/Seed grant/046-2015

Date: 05.07.2017

R/P titled: "Isolation, purification and characterization of mesenchymal stem cells from fracture hematoma"

**Principal Investigator:** Dr. R M Shenoy, Professor Dept. of Orthopedics, Yenepoya Medical College.

**Co-PIs:** Dr. Sudheer Shenoy, Assistant Professor, Yenepoya Research Centre

With reference to the above, based on the recommendation on the progress, a grant of Rs. 1,00,000/- is sanctioned in order to complete the proposed objectives of the project.

You should submit the progress report along with statement of accounts and copies of publications, presentations and patents if any made from the project.

#### ***Terms and Conditions***


1. No funds will be provided directly to the Principal Investigator, all the requests for the utilization of the sanctioned funds should be through proper channel.
2. Progress reports should be submitted to the Registrar through proper channel.
3. For the release of second year grant, a detailed expenditure certificate should be submitted to the Registrar, Yenepoya University duly verified by the Finance Officer.
4. On the completion of the project, a detailed report should be prepared and submitted to the Registrar within one month from the date of completion of the project.
5. University has all the rights to terminate the project if the progress is not satisfactory.
6. This funding is given as startup grant and based on the preliminary findings from the study the investigators should submit a detailed proposal for funding from the external agencies.

#### **Cc to:**

1. Co-Investigator
2. Dean, Yenepoya Medical College
3. Finance Officer
4. Purchase and Stores
5. Deputy Director, YRC

  
Registrar

**ATTESTED**

  
Dr. Gangadhara Somayaji K.S.  
Registrar  
Yenepoya (Deemed to be University)  
University Road, Deralakatte  
Mangalore- 575 018, Karnataka



Recognized under Sec 3 (A) of UGC Act 1956  
Accredited by NAAC with 'A' Grade

### SANCTION ORDER FOR THE SEED GRANT

No: YU/Seed grant/046-2015

Date: 15.07.2016

R/P titled: "Isolation, purification and characterization of mesenchymal stem cells from fracture hematoma"

**Principal-Investigator:** Dr. R.M Shenoy, Professor Dept. of Orthopedics, Yenepoya Medical College.

**Co-PIs:** Dr. Sudheer Shenoy, Assistant Professor, Yenepoya Research Centre

An amount of Rs. 1,00,000 has been approved towards consumables for the above cited project for the year 2016-17 with the terms and conditions listed herein.

**Terms and conditions:**

1. This funding is given as startup grant and based on the preliminary findings from the study the investigators should submit a detailed proposal for funding from the external agencies.
2. No funds will be provided directly to the Principal Investigator, all the requests for the utilization of the sanctioned funds should be through proper channel.
3. Progress reports on the completion of every six months shall be submitted to the Registrar through proper channel.
4. On the completion of the project, a detailed report should be prepared and submitted to the Registrar within one month from the date of completion of the project.
5. University has all the rights to terminate the project if the progress is not satisfactory.

**Cc to:**

1. Co-Investigator
2. Dean, Yenepoya Medical College
3. Finance Officer
4. Purchase and Stores
5. Director R&F
6. Academic Section
7. Deputy Director, YRC

Registrar

ATTESTED

Dr.Gangadhara Somayaji K.S.  
Registrar  
Yenepoya(Deemed to be University)  
University Road, Derlakatte  
Mangalore- 575 018, Karnataka



Recognized under Sec 3 (A) of UGC Act 1956  
Accredited by NAAC with 'A' Grade

### SANCTION ORDER FOR THE SEED GRANT

Date: 21.09.2016

R/P titled: "Dynamics of birth and death of N-glycosylation sites in viral proteins"

**Principal Investigator:** Dr. Shyama Prasad Rao, Assistant Professor, Yenepoya Research Centre.

**Ref:** YU/seedgrant/2014-040

An amount of **Rs. 1,00,000/-** has been approved towards consumables for the above cited project for the year 2016-17 with the terms and conditions listed herein.

#### *Terms and Conditions*

1. No funds will be provided directly to the Principal Investigator, all the requests for the utilization of the sanctioned funds should be through proper channel.
2. Progress reports on the completion of every six months should be submitted to the Registrar through proper channel.
3. For the release of second year grant, a detailed expenditure certificate should be submitted to the Registrar, Yenepoya University duly verified by the Finance Officer, Yenepoya University.
4. On the completion of the project, a detailed report should be prepared and submitted to the Registrar within one month from the date of completion of the project.
5. University has all the rights to terminate the project if the progress is not satisfactory.
6. This funding is given as startup grant and based on the preliminary findings from the study the investigators should submit a detailed proposal for funding from the external agencies.

#### **Cc to:**

1. Dean, Yenepoya Medical College
2. Finance Officer
3. Purchase and Stores
4. Deputy Director, YRC

Registrar

ATTESTED

Dr.Gangadhara Somayaji K.S.  
Registrar  
Yenepoya(Deemed to be University)  
University Road, Deralakatte  
Mangalore- 575 018, Karnataka



YENEPOYA  
UNIVERSITY

Recognized under Sec 3 (A) of UGC Act 1956  
Accredited by NAAC with 'A' Grade

### SANCTION ORDER FOR THE SEED GRANT

No: YU/seedgrant/2014-040

Date: 12.10.2017

R/P titled: Dynamics of birth and death of N-glycosylation sites in viral proteins.

**Principal Investigator:** Dr. Shyama Prasad Rao, Assistant Professor, Yenepoya Research Centre.

---


An amount of Rs. 50,000 has been approved towards consumables for the above cited project for the year 2017-18 with the terms and conditions listed herein.

**Terms and conditions:**


1. This funding is given as startup grant and based on the preliminary findings from the study the investigators should submit a detailed proposal for funding from the external agencies.
2. No funds will be provided directly to the Principal Investigator, all the requests for the utilization of the sanctioned funds should be through proper channel.
3. Progress reports on the completion of every six months shall be submitted to the Registrar through proper channel.
4. On the completion of the project, a detailed report should be prepared and submitted to the Registrar within one month from the date of completion of the project.
5. University has all the rights to terminate the project if the progress is not satisfactory.

**Cc to:**

1. Co-Investigator
2. Principal, Yenepoya Medical College
3. Finance Officer
4. Purchase and Stores
5. Director R&F
6. Academic Section
7. Deputy Director, YRC

  
Registrar

ATTESTED

  
Dr.Gangadhara Somayaji K.S.  
Registrar  
Yenepoya(Deemed to be University)  
University Road, Devalakatte  
Mangalore- 575 018, Karnataka



Recognized under Sec 3 (A) of UGC Act 1956  
Accredited by NAAC with 'A' Grade

### SANCTION ORDER FOR THE SEED GRANT

No: YU/Seedgrant/036-2014

Date: 29.11.2016

R/P titled: "Triglyceride levels in the blood as a risk for hypertension in the general population of Ullal town municipal council in D.K district."

**Principal Investigator:** Dr. R.N. Sujeer, Director, Dept of Rural Health care and Development, Yenepoya Medical College Hospital.

**Co-PI:** Dr. Mukhtarahmed B. Professor, Dept. of Internal Medicine, Yenepoya Medical College Hospital.

An amount of Rs. 37,000 has been approved towards consumables for the above cited project for the year 2017-18 with the terms and conditions listed herein.

**Terms and conditions:**

1. This funding is given as startup grant and based on the preliminary findings from the study the investigators should submit a detailed proposal for funding from the external agencies.
2. No funds will be provided directly to the Principal Investigator, all the requests for the utilization of the sanctioned funds should be through proper channel.
3. Progress reports on the completion of every six months shall be submitted to the Registrar through proper channel.
4. On the completion of the project, a detailed report should be prepared and submitted to the Registrar within one month from the date of completion of the project.
5. University has all the rights to terminate the project if the progress is not satisfactory.

**Cc to:**

1. Co-Investigator
2. Principal, Yenepoya Medical College
3. Finance Officer
4. Purchase and Stores
5. Director R&F
6. Academic Section
7. Deputy Director, YRC

  
Registrar

ATTESTED

  
Dr.Gangadhara Somayaji K.S.  
Registrar  
Yenepoya(Deemed to be University)  
University Road, Deralakatte  
Mangalore- 575 018, Karnataka